Computational Discovery of Salt Hydrates for Thermal Energy Storage

by

Steven Kiyabu

A dissertation submitted in partial fulfillment
of the requirements for the degree of
Doctor of Philosophy
(Mechanical Engineering and Scientific Computing)
in the University of Michigan
2022

Doctoral Committee:

Professor Donald J. Siegel, Chair
Assistant Professor Rohini Bala Chandran
Assistant Professor Bryan Goldsmith
Associate Professor Andrej Lenert

Steven Kiyabu

kiyabus@umich.edu

ORCID iD: 0000-0002-2653-5412

Dedication

To Jesus Christ, my Lord and Savior. May He find joy in this work that He has enabled and the journey that He has brought me on.

Acknowledgements

First, I wish to thank my adviser, Prof. Donald Siegel, for supporting and investing in me, first as an undergraduate researcher, then as a Ph.D. student. Rather than a burden, it has been such a great joy for me to go through this Ph.D. program, which is a testament to his kindness and support throughout these past five years. I have also been pleased to see how I've grown as an independent researcher, which again is a credit to his mentorship. My hope is that I can bless future mentees in the same way that he has blessed me.

I would also like to thank my committee members: Prof. Rohini Bala Chandran, Prof. Bryan Goldsmith, and Prof. Andrej Lenert. I greatly appreciate the time and effort they have taken to serve on my thesis committee, their helpful feedback on my project, and their support in my post-graduation job search. Additionally, I wish to thank the mentors that shaped the researcher I have become: Dr. Jeffrey Lowe for his mentorship when I was an undergraduate researcher in Prof. Siegel's lab, Dr. Alauddin Ahmed for his mentorship throughout my time in Prof. Siegel's lab, and Dr. Nicholas Wimer for his mentorship during my internship at NREL. I would also like to extend my appreciation to my lab mates in the Energy Storage and Materials Simulation Lab. I have learned so much from them, and they have made it a joy to come into lab each day.

There have been so many people who have walked alongside me during this journey whose support has been invaluable. I owe my deepest gratitude to Edith, my bride and the love of my life, for making these years the happiest years in my life. She has been so incredibly supportive, even following me to Ohio (of all places) after graduation. I also wish to thank Mom, Dad, mi suegra y suegro, Timothy, Paul, Carolina, Gregory H., Chuck R., Kyle Z., Kurt R., Ashley H., Steve W.,

Rolando A., Josh K., Xander D., Aaron C., Ian O., Young C., Daniel W., Ritz R., Andrew C., Clarence P., Joseph L., Pete S., and all the men and women in GradCru. Even during the pandemic, I never walked alone, and for that I am incredibly grateful.

Finally, I wish to express gratitude for the support that I have received through a variety of funding sources over the past seven years, including the University of Michigan's Summer Undergraduate Research in Engineering program, the University of Michigan Energy Institute Undergraduate Research Opportunity Program summer fellowship, the Michigan Institute for Computational Discovery & Engineering fellowship, the U.S. National Science Foundation Grant CBET-1351482, the Automotive Research Center, Cooperative Agreement W56HZV-19-2-0001 U.S. Army DEVCOM GVSC, the University of Michigan Graham Sustainability Institute's Carbon Neutrality Acceleration Program, and the J. Robert Beyster Computational Innovation Graduate Fellows program.

Table of Contents

List of Tables

List of Figures

List of Appendices

Abstract

Thermal energy storage (TES) has the potential to improve the efficiency of many applications, but has not been widely deployed. The viability of a TES system depends upon the performance and stability of its underlying storage material; improving the energy density of TES materials is an important step in accelerating the adoption of TES systems. Salt hydrates are a promising class of TES materials due to their relatively high energy densities and their reversibility. Despite their promise, relatively few salt hydrates have been characterized by a handful of experimental screening studies, presenting the possibility that new hydrate compositions with superior properties may exist. These new hydrates may be salt hydrates that have been observed experimentally, but have not been studied for TES, or they may be 'hypothetical' salt hydrates that have not yet been synthesized. Furthermore, current understanding of salt hydrate thermodynamics is limited to an approximation that thermodynamic properties of salt hydrates are additive and uniform. This study uses first-principles calculations, machine learning, and numerical system models to characterize new salt hydrates and identify TES materials that can out-perform known compounds, as well as develop deeper understanding about the features that affect the thermodynamics of salt hydration.

Focusing first on experimentally known, but under-characterized salt hydrates, high-throughput density functional theory calculations were performed on metal halide hydrates and hydroxides mined from the Inorganic Crystal Structure Database. In total, 265 hydration reactions were characterized with respect to their thermodynamic properties, gravimetric and volumetric energy densities, and operating temperatures. Promising reactions were identified for three

temperature ranges: low (< 100°C), medium (100–300°C), and high (> 300°C). Several high energy density reactions were identified, including the dehydration of $CrF_3 \cdot 9H_2O$, a compound which appears to be unexplored for TES. Correlations linking TES performance with dozens of chemical features for salt hydrates were quantified using a Pearson correlation matrix. These analyses reveal property-performance relationships involving energy densities, but were less successful in explaining the thermodynamics of hydration. In salt hydrates, the energy densities depend strongly on the water capacity of the hydrate, although no strong correlations were found for the enthalpy of dehydration. Based on these correlations, design rules for hydration-based TES systems are proposed.

Subsequently, the focus of this study turned to hypothetical salt hydrates. The energy densities, turning temperatures, and thermodynamic stabilities of 5292 hypothetical halide salt hydrates, 1779 hypothetical chalcogenide salt hydrates, and 5233 hypothetical complex anion salt hydrates are predicted using high-throughput density functional theory calculations. Several salt hydrates from each of these classes are identified as new, stable TES materials with class-leading energy densities and operating temperatures suitable for use in domestic heating and intermediate-temperature applications. The promising performance of these materials is demonstrated at the system level by parameterizing an operating model of a solar thermal TES system with data from the new hydrates and predicting system-level energy densities. Finally, machine learning models for salt hydrate thermodynamics are developed for each of the salt hydrate classes and used to identify design guidelines for maximizing energy density. In total, the new materials and design rules reported here are expected to foster the adoption of TES systems.

Chapter 1 Introduction

1.1 Thermal Energy Storage

Over two-thirds of the energy produced in the U.S. does no useful work and is ultimately lost as heat.[1] This heat loss occurs over a variety of systems and temperatures. Although some heat loss is expected due to the second law of thermodynamics, such a large fraction of energy loss indicates the room for improvement in energy efficiency. As a result, technologies such as thermal energy storage (TES) that can minimize these losses via heat capture, storage, and reuse have the potential to significantly improve energy efficiency. **Figure 1.1** shows common TES applications. At low temperatures (< 100°C),[2,3] thermal energy storage (TES) can be used to regulate the temperature of buildings,[2,4,5] textiles,[6,7] food,[8] electronics,[8,9] and vehicles.[10,11] Acting as a heat sink, TES adds thermal inertia to the system, reducing the temperature change caused by a given heat input. At medium temperatures (100–300°C),[12] TES can be used to capture waste heat, such as that produced from an internal combustion engine or during the production of metals,[12,13] for later use. At high temperatures (> 300°C),[14] TES can be applied in solar energy plants to store excess energy, as it is more economical to store heat than it is to store electricity.[15,16] These applications have the potential to significantly increase energy efficiency,[17–19] including: a 7.5% energy savings estimated in the European Union,[20] a global reduction of energy costs by 5–15% and peak electrical power demand by 13–33%,[21] and an increase in the annual capacity factor for concentrated solar plants from 30% up to 55%.[22] TES is also one of the few technologies that can decarbonize multiple sectors of the global economy.[23]

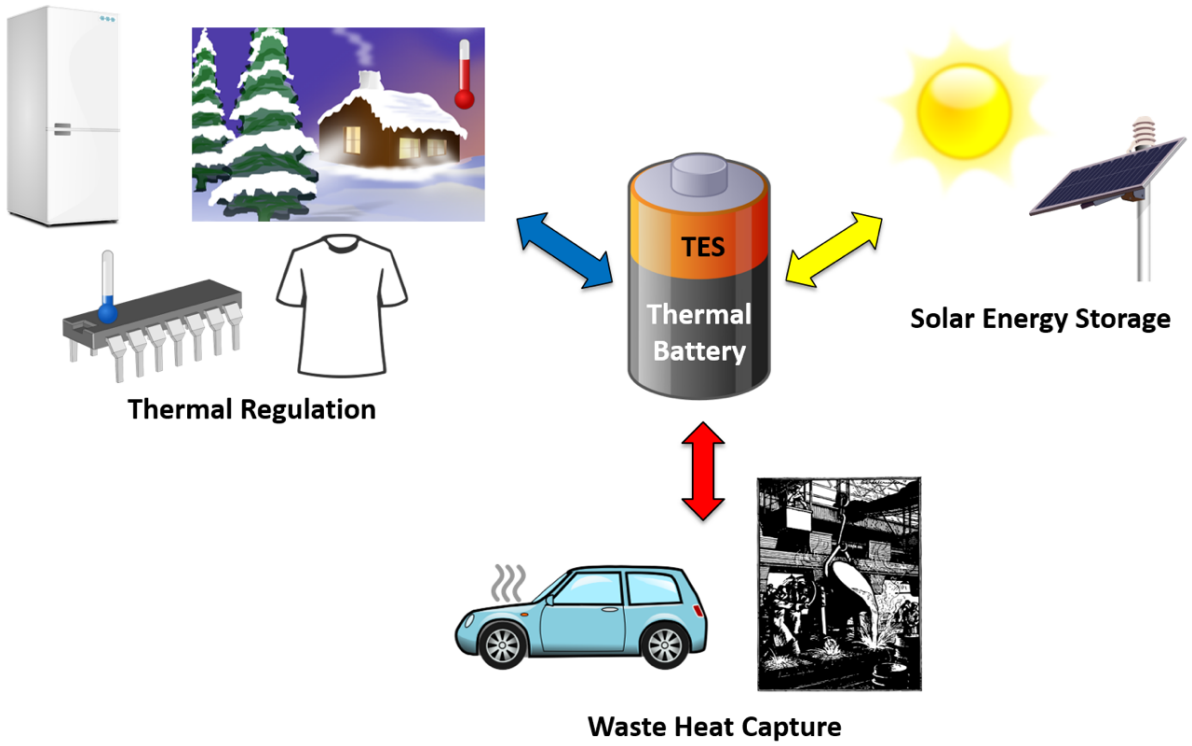

Figure 1.1 Common applications of thermal energy storage.

1.1.1 Examples of Thermal Energy Storage Applications

One advantage that TES systems can offer is an increase in thermal inertia. In general, as the thermal inertia of a system increases, it becomes less prone to temperature variations. Furthermore, it takes a longer time to change temperature given heat flow to or from the surrounding environment. Since TES systems are designed to capture heat more effectively than ordinary materials, they tend to offer a greater resistance to changing temperature when they are heated or cooled. This feature has been exploited in a variety of applications. For example, TES can be added to the structures of buildings to reduce the effect of thermal fluctuations throughout the day.[2,5,24] As a result, the HVAC systems can run more efficiently as they run less frequently for longer periods of time, reducing the amount of time spent during the inefficient warming up stage. TES can also be used to keep food and other perishables at low temperatures. A common everyday example is the use of ice as a phase change material, but containers with even greater

thermal inertia have been designed. For example, the Greenbox Thermal Management System has been used to keep vaccines and other temperature sensitive medical supplies cool during long periods of transportation.[25]

TES can also be used to protect sensitive electronics.[8,9] As electricity flows, the electrical resistance in the circuit results in energy loss through heat. This heat can physically damage fragile components in a circuit. As such, either cooling or a heat sink (a TES system) is required to maintain acceptable temperatures. TES can also be used in vehicles to keep the engine warm.[26,27] When a vehicle starts up from cold start, it takes several minutes of operation before the engine is warmed to steady operating temperature. Before that, the engine operates less efficiently, and the exhaust gas from the engine is lower in temperature, resulting in a less effective catalytic converter. Indeed, most of the pollution of a car occurs during the first several minutes of activity. It is quite common for car trips around town to only last a few minutes, so a large fraction of automotive use is performed under less than ideal conditions. A TES system can surround the engine, capturing waste heat from the engine, and keeping the engine warm for much longer times, reducing the inefficiencies of cold-start.

Another way that a TES system can be leveraged is as a thermal battery. The system captures and stores heat that can be later reused. TES has been used to capture waste heat from industrial processes, operating in the range of 100–300°C.[12,13] This captured heat is then used in a cogeneration scheme, increasing the overall efficiency of the process. TES can also be used in conjunction with solar energy generation.[15,16] The generation of solar energy fluctuates due to weather conditions as well as daily and seasonal cycles. Without an ancillary storage system, solar storage can only be used to cover baseline energy demand while the remainder of the energy is generated using fossil fuels. However, when TES is used, the solar plant can be allowed to run at

higher production levels. Excess energy is stored in the TES system and is later used during periods when the energy demand exceeds the energy supply. This heat can be stored at lower temperatures when directly used for a particular application (e.g., building heating), but is also often stored at higher temperatures (i.e., hundreds of degrees Celsius), especially when using concentrating solar collectors, to later drive high efficiency power generation cycles.

1.2 Thermal Energy Storage Materials

Given the advantages offered by TES systems, it is desirable to develop optimized materials for heat storage, since the storage medium is often a limiting factor in TES systems.[2,15] Materials that can reversibly store large amounts of heat for extended periods of time are preferred. TES materials operate in one of three ways: (*i.*) sensible heat storage (through a temperature change), (*ii.*) latent heat storage (via a phase change), or (*iii.*) thermochemical heat storage (through a chemical reaction or sorption process).[14]

1.2.1 Sensible Heat Storage

TES systems can take a variety of forms, but at its core, each system has a material that stores the thermal energy. The heat can be stored in one of three ways: as sensible heat, as latent heat, or as thermochemical heat. All materials store sensible heat. As heat is applied to the material, the material stores the heat as atomic kinetic energy (i.e., sensible heat), macroscopically indicated by a rise in temperature. Materials with higher specific heat capacities store more sensible heat for a given temperature increase; as such, these materials tend to store heat with higher energy densities. Liquid water, with its high specific heat capacity, tends to be a common medium for sensible heat storage. Other materials such as concrete, alcohols, plastic, and metal have also seen use in sensible heat storing systems.[2] Generally, sensible heat storage is the simplest type of TES.

Unless the operating temperature varies significantly, the material does not change drastically, avoiding issues of irreversibility. However, among all TES materials, sensible heat storage tends to have relatively low energy densities. Thus, they are not suitable for applications where lightweight and/or compact TES systems are required. Furthermore, insulation is a significant concern as sensible heat storing materials will tend to lose stored energy if the system is not well insulated. This is especially true in the case of long-term storage.

1.2.2 Latent Heat Storage

Another category of heat-storing materials is the class of phase change materials (PCMs). PCMs store heat as the latent heat of phase change. A common everyday example of this is an ice cube that slowly melts in order to keep a drink cool. These phase changes tend to occur at a specific temperature, which dictates the temperature at which the material will store or release latent heat. While this places constraints on the system design, constant temperature heating can be advantageous when designing the system to optimize heat transfer. Due to their ability to store both sensible and latent heat, PCMs tend to have slightly higher energy densities than sensible heat-storing materials. However, the change in the material during phase change can lead to practical issues, such as irreversible transformation and volume change. More on PCMs can be found in these reviews.[2,4]

1.2.3 Thermochemical Heat Storage

Arguably the most promising TES materials store thermochemical heat, which have reported the highest energy densities among TES materials.[28] The typical energy density ranges for the three methods of heat storage are shown in **Figure 1.2**.[3,6,14–16,29–33]

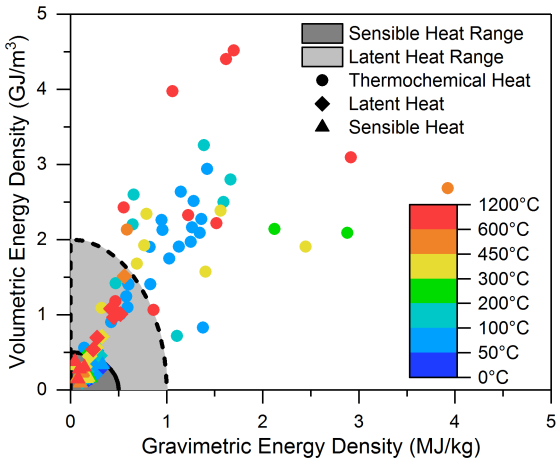

Figure 1.2 Volumetric energy density of TES materials as a function of gravimetric energy density for the three primary types of heat storage. Data are compiled from tabulated values from several sources.[3,6,14–16,29–33] Sensible heat energy densities were calculated from an 80°C temperature span (a range applicable for liquid water, a commonly used material).

Thermochemical heat is stored in reversible chemical reactions that take the following form:

$$Heat + A \leftrightarrow B + C \tag{1.1}$$

Heat is stored when compound *A* decomposes in the forward, endothermic reaction into products *B* and *C*. Heat is then released through the reverse, exothermic process, by allowing *B* & *C* to react. Unlike sensible or latent heat storage, which stores heat in a single material, in a thermochemical reaction heat can be stored indefinitely by keeping compounds *B* and *C* separate.

For a given pressure (e.g., 1 atm), the temperature at which the reaction in equation (1.1) is in equilibrium is commonly referred to as the turning temperature, T_{turn}, with $T_{turn} = {}^{\Delta H}/_{\Delta S}$, where ΔH is the change in enthalpy and ΔS is the change in entropy.[33–36] T_{turn} defines the thermodynamic threshold between the forward or the reverse reaction being favored:[33–36] For temperatures above T_{turn} the forward reaction is favored, and heat is stored; below T_{turn} the reverse reaction is favored, and heat is liberated. Neglecting kinetic effects, the magnitude of T_{turn} establishes the temperature

at which a given reaction can reversibly store and release heat. Thus T_{turn} can be used to categorize reactions into low, medium, and high temperature operating regimes.

1.3 Comparison of Low Temperature Thermochemical Heat Storage Materials

For low temperature thermochemical heat storage, there are three general classes of materials. In the first class, a solid chemically reacts with a gas, forming another solid. The most common low temperature materials in this class are salt hydrates, although ammoniates and methanolates operate analogously. The second class consists of the sorption of a gas by porous media, such as silica gel, zeolites, and MOFs. Finally, the third class is the absorption of a gas by a liquid. The different material families have different properties, which are summarized in **Table 1.1**.

Table 1.1 Overview of low temperature thermochemical heat storage materials.

Class	Material	Energy Density	Stability	Power Output	Non-technical Attributes	Maturity
1	Salt Hydrates	Up to 3.8 GJ/m^3 and 2.3 MJ/kg[37]	Issues with melting, deliquescence, and hydrolysis	Up to 0.7 MW/m^3 and 0.5 kW/kg[38,39]	Rarity and toxicity vary by salt	Laboratory and prototype scale
1	Salt Ammoniates	Up to 2.1 GJ/m^3 and 1.6 MJ/kg[40,41]	Issues with decomposition	Up to 1.5 kW/kg[41]	Rarity varies by salt, ammonia is toxic	Laboratory scale
1	Salt Methanolates	Up to 1.3 MJ/kg[42]	Not much data available	Up to 0.4 kW/kg[43]	Methanol is flammable	Laboratory scale
2	Silica Gel	Up to 0.8 GJ/m^3 and 1.4 MJ/kg[30]	Good stability	Up to 0.01 kW/kg (prototype)[44]	Cheaper	Commercial scale
2	Zeolites	Up to 0.7 GJ/m^3 and 1.1 MJ/kg[30]	Good stability	Up to 0.03 kW/kg (prototype)[45]	Can be expensive	Commercial scale
2	MOFs	Up to 1.3 MJ/kg[46]	Issues with decomposition in water	Up to 2.1 kW/kg[46]	Can be expensive	Laboratory scale

3	Liquid Dilution	Up to 1.4 GJ/m^3[47]	Good stability	Up to 0.03 MW/m^3 (prototype)[48]	Can be cheaper	Commercial scale

1.3.1 Thermochemical Reactions

In the first class of materials, heat is stored in the endothermic decomposition of the more complex solid into another simpler solid and a gas. The heat is released during the reverse synthesis reaction. In the case of salt hydrates (i.e., salt with water molecules incorporated into the crystal structure), the reaction formula looks like this: $Heat + MX \cdot nH_2O_{(s)} \leftrightarrow MX_{(s)} + nH_2O_{(g)}$, where $MX_{(s)}$ is a salt, $MX \cdot nH_2O_{(s)}$ is the salt hydrate, and $H_2O_{(g)}$ is water vapor. The choice of water as the reactive fluid carries several benefits for low temperature TES, including the safety and abundance of water, as well as the favorable thermodynamic properties that allow the (de)hydration reactions to be reversed at relatively low temperatures. Thermodynamically speaking, a first approximation for a salt hydrate is ice bound in the crystal structure of the salt. Many properties of salt hydrates seem to be higher temperature variations of the sublimation of ice to water vapor. Thus, salt hydrates capitalize on water's excellent heat storage properties. Of all the low temperature thermochemical heat storing materials, hydrates tend to have the highest energy densities on the material level. However, many salt hydrates display issues when implemented in practical systems. Some hydrates melt readily when heated too quickly. Others deliquesce when the water vapor pressure is too large. Still others will experience side reactions, such as the well-known hydrolysis of $MgCl_2$ hydrates, which forms gaseous HCl. All of these introduce irreversibilities into the system, reducing the amount of material that can effectively store heat over time. Furthermore, the complexities of heat and mass transfer in salt hydrates tends to lead to lower power densities, as salt hydrates tend to have low thermal conductivities as well

as kinetic barriers to water transport through the hydrate. In addition to these technical issues, some salts are also impractical due to their high cost or toxicity. Given these practical complications, much research is being done to characterize and understand these materials, though recently some large-scale prototypes using salt hydrates have been built.[49]

Similar to salt hydrates, salt ammoniates are salts with ammonia molecules held in the crystal structure. Salt ammoniates were originally proposed decades ago for thermochemical heat storage, but only recently have drawn more attention.[40,50] The ammoniates are analogues of salt hydrates as they are defined by the reaction $Heat + MX \cdot nNH_3 \leftrightarrow MX + nNH_{3(g)}$, where the reactive fluid is ammonia rather than water. This ammonia formation poses a significant practical challenge for many applications as ammonia is toxic. Even still, they may be of interest to specific applications. Recently, Müller et al. characterized many ammoniates according to their energy density.[40] The values of 2.1 GJ/m^3 and 1.6 MJ/kg recorded in **Table 1.1** have been adjusted to maintain consistency with the rest of the table, where energy densities are reported in terms of the volume and/or mass of the more complex material. Here, it can be seen that ammoniates have comparable, although slightly smaller energy densities than hydrates. Similar to hydrates, ammoniates may experience irreversible side reactions[40] and may be cost prohibitive. However, one potential advantage of ammoniates over hydrates is their faster discharging rates. This is demonstrated by the power value calculated from data reported by Yan et al. on the reaction of $MnCl_2$ with ammonia.[41] Finally, since ammoniates have not drawn as much attention as salt hydrates, most ammoniate studies are on the laboratory scale.

Another minor family of materials in the first class of materials are salt methanolates, which store methanol molecules in the salt crystal structure. Their reaction is defined as $Heat + MX \cdot nCH_3OH \leftrightarrow MX + nCH_3OH_{(g)}$. The literature on methanolates for TES is sparse. They are

mainly of interest for refrigeration applications, given methanol's favorable properties for refrigeration.[51] From the data available in the literature, it seems they have similar (perhaps slightly smaller) energy and power densities as salt hydrates.[42,43] One main drawback to their use is the flammability of methanol.

1.3.2 Porous Materials

The second class of low temperature thermochemical heat storing materials are porous media that adsorb a reactive gas to the surface of their internal pores. In most cases, this reactive gas is water, as water has many favorable properties mentioned previously. The size of these pores ranges from the nano-scale to the meso-scale. One of the more mature thermochemical heat storage materials is silica gel, which is amorphous silicon dioxide with nanopores. These pores readily absorb water from the environment, leading to its common use as a desiccant. Advantages of silica gel include its relatively lower cost and its low complexity, leading to good cycle stability.[52] As a result, it has been developed to commercial scale quicker than other thermochemical materials. However, its lower energy density, as shown in **Table 1.1**, limits its potential in compact applications. It should be noted that the small power cited is from a study on a large-scale prototype involving 350 kg of silica gel.[44]

Another type of material that falls in the second class is the family of zeolites. Zeolites are aluminosilicates that can adsorb water into their nanopores. Like silica gel, zeolites are less complex than other thermochemical heat storing materials and have been developed to the commercial scale. They tend to be stable, but are costlier than silica gel. They possess slightly smaller gravimetric energy densities than silica gels due to their weight, but higher power densities at prototype scale than silica gels. One characteristic of zeolites is their hydrophilicity, resulting in

high desorption temperatures for water.[52] As such, depending on the maximum charging temperature available, the reversible capacity of zeolites at low temperatures is often limited.

A third type of porous material that is of interest for low temperature TES is the family of metal-organic frameworks (MOFs). MOFs are porous structures consisting of metal clusters connected by organic linkers. The size of the pores in MOFs varies greatly. Given the many degrees of freedom in the MOF structure and composition, the potential chemical space for MOFs is astronomically large, which attracts the interest of materials designers. In addition to their cost, the main disadvantage of MOFs is that many MOFs will decompose irreversibly in the presence of water, making reversible water capture and release an impossibility.[53] However, some water-stable MOFs show promise, such as MIL-101. Ehrenmann et al. characterized the water adsorption of MIL-101, from which energy density and power were calculated in **Table 1.1**.[46] The energy density is similar to other types of materials, but the main advantage is the high power density of the material (2.1 kW/kg).

1.3.3 Liquid Dilution

The third class of low temperature thermochemical heat storing materials is liquid absorption. During the discharge process, the liquid absorbs the reactive gas, which tends to be the solvent in the liquid solution. As a result, the solution dilutes and releases heat. During the charging process, the reverse occurs and some of the solvent is desorbed from the liquid solution. Given its simplicity, it tends to have good stability and thus has reached commercial scale. Also, depending on the solute chosen, the material cost can be relatively inexpensive. Regarding its energy density and prototype-scale power density, its performance is rather average compared to other types of materials.

1.4 Hydration Reactions

In addition to energy density and operating temperature, many other factors influence whether a given TES material is of practical value. In the case of thermochemical storage, practical limitations include: cost, corrosivity, toxicity, cyclability, stability (with respect to phase changes/side reactions), and rates of heat and mass transfer.[2,3,32,54] To overcome some of these limitations, materials that store water—either through adsorption or chemical reaction (hydration/dehyration)—have received increasing attention.[3,12,32,33,35,36,55,56] In equation (1.1), a water-based thermochemical reaction would have hydratable material as compound *A*, compound *B* is the dehydrated version of *A*, and *C* is water vapor. Such reactions can be thought of as a phase change involving an ice-like phase stored within the host material, *A*.[57,58] Common hydratable materials used for TES include salt hydrates,[3,35,36,55] hydroxides,[12,33,35,36,59] zeolites,[60–62] and metal organic frameworks (MOFs).[63–65] The use of water as the working fluid in TES is motivated by the fact that it is abundant, non-toxic, light, and can reversibly store and discharge heat through sublimation at moderate temperatures. Thus, the use of water minimizes some of the practical limitations that affect many thermochemical systems. Furthermore, the sublimation of water from a solid, hydrated compound to water vapor involves both a high change in enthalpy, which is advantageous for its heat storage capacity, as well as a significant entropy change, that allows the reaction to be reversed at reasonable temperatures (see definition of T_{turn}).

1.4.1 Previous Salt Hydrate Studies

A small number of studies have characterized salt hydrates for TES. Wentworth et al.[33] screened several types of gas-forming decomposition reactions, including the decomposition of several hydroxides. Visscher et al.[36] focused on compounds containing lighter cations and reactions that could be charged below 250°C, including salt hydrates and hydroxides. N'Tsoukpoe

et al. experimentally screened 125 salt hydrates, emphasizing practical constraints.[3] Deutsch et al. characterized 506 hydration reactions using the HSC Chemistry[66] database.[35] Donkers et al.[55] screened 563 hydration reactions, extracting thermodynamic data from Glasser's salt hydrate database[67] and the International Critical Tables.[68] Richter et al.[69] applied a multistep approach to screen hydrates of 308 salts for thermochemical heat transformation, leveraging a variety of databases.[66,70–72] Afflerbach and Trettin experimentally characterized 29 complex salt hydrates formed from the hydration of minerals.[73] Clark et al. experimentally screened 41 salt hydrates for building heating applications under various operating conditions.[74]

Glasser and Jenkins investigated the thermodynamic properties of salt hydrates, and proposed the Thermodynamic Difference Rules.[75–77] These rules approximate the change in a given thermodynamic quantity (e.g., enthalpy, entropy) as constant for each added water of hydration, regardless of the salt's composition or state of hydration. The enthalpy of (de)hydration is important because it affects many aspects of TES performance, including energy density and operating conditions (described later in equations (3.2), (3.3), (4.1), and (4.2)). This model—although a helpful approximation for energy density—is less useful for predicting the operating conditions of salt hydrates, which are sensitive to variations in the enthalpy. Furthermore, Glasser and Jones point out that the Thermodynamic Difference Rules are unable to predict the relative stability of salt hydrates, which depends on differences in the enthalpy and entropy of dehydration among hydrates in the same salt family.[57] Hence the development of thermodynamic guidelines aimed at optimizing the TES performance of hydrates will be aided by knowledge that goes beyond average properties.

1.5 Goals and Scope of Dissertation

As illustrated by the previous discussion, salt hydrates demonstrate great potential for long duration, high-capacity thermochemical heat storage. Given the vast number of salts and the varying levels of hydration possible, the chemical space for salt hydrates is vast. However, only a few hundred salt hydrate compositions have been characterized for TES, either experimentally or using tabulated thermodynamic data. Many salt hydrates are experimentally known, but have not been examined for their TES utility due to a lack of thermodynamic and/or physical data. Furthermore, it has been hypothesized by Glasser and Jones that, due to the approximate homogeneity of salt hydrate thermodynamic properties, many stable or metastable salt hydrates that have not yet been synthesized may exist.[57]

The goal of this dissertation is to explore a wide composition space of salt hydrates using first principles calculations and machine learning. First principles calculations provide an accurate, efficient, and systematic way to predict and compare salt hydrate properties that are relevant for heat storage. By leveraging a high throughput computational approach, thousands of salt hydrates can be explored, many more than what would be possible experimentally over similar timescales. The benefit of exploring a large number of salt hydrates is two-fold. First, the probability of finding optimal materials increases as the number of salt hydrates screened increases. Second, the large number of salt hydrates characterized provides data for statistical analysis and machine learning, which can be used to identify property-performance trends among the salt hydrates.

The dissertation is structured as follows. In Chapter 3, a computational screening workflow is developed to predict the properties of known salt hydrates. Even within the pool of known salt hydrates, a few promising overlooked materials are identified for TES. A set of initial design rules for the energy density of salt hydrates are proposed after statistically analyzing the dataset of

known salt hydrates for linear correlations linking elementary properties with performance. In Chapter 4, the computational screening workflow from Chapter 3 is expanded to screen thousands of hypothetical halide salt hydrates. This component of the study includes hypothetical structure generation, a more rigorous thermodynamic stability analysis, and prediction of system-level energy properties for the new materials uncovered by the screening. Promising hypothetical halide hydrates are identified. Additionally, non-linear structure-property-performance trends are identified via machine learning, leading to more nuanced design rules for tuning the thermodynamic properties of halide salt hydrates. Chapter 5 further extends the analysis of Chapter 4 to hypothetical hydrates of salts containing chalcogenides and complex anions. More promising hypothetical hydrates are identified and design rules for these classes of hydrates are proposed. Finally, Chapter 6 takes a preliminary look into how the present study can be extended to the broad chemical space of mixed-metal salt hydrates.

Chapter 2 Methodology

2.1 First Principles Calculations

2.1.1 Schrödinger Equation

The behavior of materials can be modeled in a variety of ways, ranging from atomistic to continuum-level simulations. However, in order to model a material from first principles (i.e., without empirical data), one must turn to quantum mechanics. This level of theory allows for accurate modeling of a material's electronic structure, which fundamentally affects the material's macroscopic behavior. The Schrödinger equation relates the electronic wave function (i.e., the wave function describing the behavior of a system's electrons) to the total energy of the electrons. In this formalism, when calculating the electronic wave function, the atomic nuclei are assumed to be stationary particles under the Born Oppenheimer approximation.[78] The rationale for this assumption is that massive atomic nuclei (with each nucleon weighing more than 1800 electrons) will move on much longer time scales than do the electrons. Coupling the Born Oppenheimer approximation with non-relativistic and time-independent assumptions, the multi-body Schrödinger equation can be expressed as[79]

$$\left[\frac{h^2}{2m}\sum_{i=1}^{N}\nabla_i^2 + \sum_{i=1}^{N}V(\boldsymbol{r}_i) + \sum_{i=1}^{N}\sum_{j<i}U(\boldsymbol{r}_i,\boldsymbol{r}_j)\right]\Psi = E\Psi \qquad (2.1)$$

where h is Planck's constant, m is the mass of an electron, N is the number of electrons, V is the nuclei-electron potential energy function, U is the electron-electron potential energy function, $\boldsymbol{r}_i$ is the position of the ith electron, Ψ is the electronic wave function, and E is the ground state energy.

The three terms on the left-hand side of Equation (2.1) correspond to the kinetic energy of the electrons, the electron-nuclei interactions, and the electron-electron interactions. Unfortunately, Equation (2.1) can only be solved analytically in the simplest of cases. The electronic wave function has a dimension of 3*N*, corresponding to three spatial dimensions of *N* electrons. In the case of $MgCl_2 \cdot 6H_2O$ (a common salt hydrate that we may wish to model from first principles), a single formula unit contains 106 electrons, which correspond to a 318-dimensional wave function. This high dimensionality is computationally intractable for even the most advanced computing systems.

2.1.2 Density Functional Theory

A major breakthrough occurred when Hohenberg and Kohn proved two mathematical theorems that vastly simplified the many-body problem. These theorems state that 1) "The full many-particle ground state is a unique functional of [the electronic density in the ground state]" and 2) "[The energy functional] assumes its minimum value for the correct [electronic density in the ground state]".[80] In other words, there exists a unique functional of the electron density that, when minimized, yields the true ground state energy of the system consistent with the Schrödinger equation. If that functional were known, the intractable problem of solving for a 3*N*-dimensional wave function would be transformed into the tractable problem of solving for the 3-dimensional electron density.

The electron density functional has been formulated as

$$E[n(\boldsymbol{r})] = T_0[n(\boldsymbol{r})] + \int V(\boldsymbol{r})n(\boldsymbol{r})d\boldsymbol{r} + E_H[n(\boldsymbol{r})] + E_{XC}[n(\boldsymbol{r})] \quad (2.2)$$

where, T_0 is the kinetic energy of the electrons (using the simplifying assumption of non-interaction), E_H is the Hartree energy, E_{XC} is the exchange-correlation energy, and $n(\boldsymbol{r})$ is the electron density, defined by

$$n(\boldsymbol{r}) = 2\sum_{i=1}^{N} \psi_i^*(\boldsymbol{r})\psi_i(\boldsymbol{r}) \quad (2.3)$$

where ψ_i is the individual wave function of the i[th] electron. Similar to Equation (2.1), Equation (2.2) accounts for the kinetic energy of the electrons, electron-nuclei interactions, and electron-electron interactions (with E_H accounting for electron-electron repulsion and E_{XC} accounting for the quantum mechanical phenomena of electron exchange and electron correlation).

Algorithmically, Equation (2.2) is minimized by self-consistently solving the Kohn-Sham equations,[81] which are given by

$$\left[\frac{h^2}{2m}\nabla^2 + V(\boldsymbol{r}) + V_H(\boldsymbol{r}) + V_{XC}(\boldsymbol{r})\right]\psi_i(\boldsymbol{r}) = \varepsilon_i\psi_i(\boldsymbol{r}) \quad (2.4)$$

where ε_i is the i[th] eigenvalue, V_H is the Hartree potential defined by

$$V_H(\boldsymbol{r}) = e^2 \int \frac{n(\boldsymbol{r}')}{|\boldsymbol{r} - \boldsymbol{r}'|} d\boldsymbol{r}' \quad (2.5)$$

and V_{XC} is the exchange-correlation term defined by

$$V_{XC}(\boldsymbol{r}) = \frac{\delta E_{XC}(\boldsymbol{r})}{\delta n(\boldsymbol{r})}. \quad (2.6)$$

The Kohn Sham equations are similar to Equation (2.1), but apply to the wave function of a single electron rather than the entire electronic wave function. Given an initial electron density, Equation (2.4) can be solved to find ψ_i for each electron. From these wave functions, the electron density is recomputed via Equation (2.3). This process is repeated until the electron density converges.[79]

2.1.3 Exchange-Correlation Functional

Although most terms of the energy density functional in Equation (2.4) can be calculated, the exact form of the exchange-correlation functional is unknown in all but the simplest case: a uniform electron gas. Various approximations for the exchange-correlation functional have been developed. One of the simplest approximations for the exchange-correlation functional is the local density approximation (LDA), which approximates the exchange-correlation energy at every position to be the exchange-correlation energy of a uniform electron gas possessing an electron density equal to the local electron density. This is formulated as[79]

$$V_{XC}(\boldsymbol{r}) = V_{XC}^{electron\ gas}[n(\boldsymbol{r})]. \qquad (2.7)$$

Another common approximation in the generalized gradient approximation (GGA), which not only accounts for the local electron density, but also the gradient of the electron density. Common GGA exchange correlation functionals include the functional of Perdew-Burke-Ernzerhof (PBE)[82] and the Perdew-Wang functional (PW-91).[83]

Another family of exchange-correlation functionals was proposed by Dion et al.[84] These 'van der Waals aware' exchange-correlation functionals combine a semi-local exchange-correlation functional with a non-local correlation functional that models dispersion interactions. Various formulations of these functionals include vdW-DF2, optPBE-vdW, optB88-vdW, and optB86b-vdW.[84–89] Beyond this family of functionals, other exchange-correlation functionals have also been proposed to handle dispersion correction using a semiempirical approach (e.g., DFT-D2, DFT-D3, DFT-TS).[90–92]

2.1.4 Implementation

The relaxed geometries of all compounds, and their associated reaction energies, were evaluated using DFT, as implemented in the Vienna Ab-initio Simulation Package (VASP).[93]

Core-valence electron interactions were modeled with Blöchl's projector augmented wave method.[94,95] All structures were relaxed using the van der Waals aware exchange-correlation functional optPBE-vdW,[85] using an increasingly dense Monkhorst-Pack[96] k-point mesh, until convergence was reached. For most compounds, convergence was reached with a $6 \times 6 \times 6$ mesh. Atomic positions and all six lattice parameters were relaxed until all atomic forces were less than 0.02 eV/Å. After the relaxed structure was determined, a single point energy calculation was performed with the GGA functional of Perdew-Wang 91 (PW-91)[83] in order to determine the ground state energy. All calculations were performed with a 500 eV plane-wave cutoff energy, and all calculations were spin polarized. Since hydration reactions involve water vapor, DFT calculations on a single water molecule in a 10 Å × 10 Å × 10 Å simulation cell were also performed.

2.2 Machine Learning

Inspired by the ability of humans to learn and develop intuition from experiences, machine learning (ML) is an analogous technique wherein computer algorithms are employed to quantitatively learn from data. Common goals of this learning are to make predictions for new datasets and/or to understand what factors (or 'features') are needed by the algorithms to make accurate predictions. The former use of ML can accelerate (often dramatically) the screening of large datasets of materials, while the latter use allows one to understand *why* a given material exhibits a desired property, thus improving one's chemical intuition, and perhaps further accelerating the discovery process. The data can take any number of forms, including numerical data, discrete categories, graphs, images, audio, and text.

2.2.1 Supervised Learning

One major division in the field of machine learning is the division between supervised learning and unsupervised learning. The supervised learning task attempts to find some functional relationship between input properties and output behavior. In contrast, unsupervised learning does not consider any output behavior and only focuses on relationships between the properties. Assuming there is a (non-trivial) functional relationship between the input properties (X) and the output behavior (Y) defined by

$$Y = f(X) + \varepsilon_{noise} \tag{2.8}$$

where ε_{noise} accounts for the variation in Y that is independent of X, the supervised learning problem is formulated as finding $\hat{f}$ such that

$$\hat{f} = \underset{g}{\operatorname{argmin}} \left(L\big(Y, g(X)\big) \right) \tag{2.9}$$

given a loss function L between the true and predicted values of the output behavior a set of functions g, whose functional form is determined by the architecture of the ML algorithm. The identified function can then be used to make predictions ($\hat{Y}_{new}$) on new data (X_{new}), as shown below.

$$\hat{Y}_{new} = \hat{f}(X_{new}) \tag{2.10}$$

In theory, given enough degrees of freedom, a function can fit the data well, even fitting the data exactly. However, the utility of such a function is low as it overfits the data, reducing its ability to make predictions on data that it hasn't seen. To remedy this, a division in the data is made between the training set and the unseen test set. The ML model is only trained on the training data and not on the test set data. After training, the model's predictive accuracy is not determined by how well it fits the data in the training set, but on how accurately it can predict the data in the unseen test set. Data partitioning techniques like k-fold cross validation[97] are common to generate statistics on different training set/test set splits.

2.2.2 Hyperparameter Optimization

In many cases, ML algorithms possess adjustable hyperparameters that tune the learning behavior of the algorithm. Unlike the learned model weights, the hyperparameters are set by the human user. Since these hyperparameters affect the ML model that is ultimately learned, equation (2.9) can be expanded to include the hyperparameters (θ) as follows.

$$\hat{f} = \underset{g}{\operatorname{argmin}} \Big(L\big(Y, g(X, \theta)\big) \Big) \tag{2.11}$$

In many cases, the optimal hyperparameters are not known a priori. Rather, these hyperparameters are optimized empirically using a validation set. In the same way that a test set is withheld from the training set to evaluate the predictive performance of a ML model, a validation set is withheld from the training set to optimize the hyperparameters. Models using different hyperparameters are trained on the training data and evaluated using the validation data. The hyperparameters that minimize the error in the validation set are determined to be the optimal hyperparameters. Similar data partitioning schemes used for creating multiple test sets from the same dataset are commonly used to create multiple validation sets. It is important to note that during hyperparameter optimization, the withheld test set should be completely separate from the training set and validation set in order to maintain the integrity of the test set as a fair test of the model's performance on unseen data. Only after the optimal hyperparamaters have been identified and the model has been retrained using these hyperparameters and the combined training and validation data can the model be evaluated on the test set.

2.2.3 Regression Algorithms

Supervised learning can further be partitioned into two types of problems based on the nature of the predicted output *Y*. If *Y* is a discrete category (e.g., classes of animals like 'dog' or

'pig'), the supervised learning problem is a classification task. If, on the other hand, *Y* is a continuous numeric variable (e.g., 0.7, 5.2), the supervised learning problem is a regression task. Each task requires its own set of algorithms (although many algorithms have analogues for both types of supervised learning tasks). Below are several common algorithms that can be used for regression ML.

Ordinary Least Squares (OLS). OLS regression is a basic linear regression. In practice, variations of OLS are often preferred, but OLS offers a starting point for understanding linear regression. For OLS, there are no hyperparameters and *g(X)* is defined as

$$g(X) = Xw \tag{2.12}$$

where *w* is a vector of weights with a length equal to the number of columns (i.e., number of features) in *X*. Note that Equation (2.12) assumes that both *X* and *Y* are centered (i.e., with the mean of each column equaling zero), but can easily be modified if not. OLS also defines the loss function *L* as

$$L = \|Y - Xw\|_2^2 \tag{2.13}$$

where $\|...\|_2$ is the L2 norm.

Combining Equations (2.9), (2.10), (2.12), and (2.13), the closed form solution of the model becomes

$$\hat{Y}_{new} = \hat{f}_{OLS}(X_{new}) = X_{new}(X^T X)^{-1} X^T Y \tag{2.14}$$

Ridge Regression. Ridge regression[98] is a modified version of OLS that includes a regularization parameter (α). This regularization is useful for numerical stability when the columns of *X* are highly correlated (making $X^T X$ difficult to invert). Equation (2.12) holds for ridge regression, but the loss function is modified, as shown below.

$$L = \|Y - Xw\|_2^2 + \alpha\|w\|_2^2 \quad (2.15)$$

The ridge regression model can then be expressed as

$$\hat{Y}_{new} = \hat{f}_{ridge}(X_{new}) = X_{new}(X^T X + \alpha I)^{-1} X^T Y \quad (2.16)$$

where I is the identity matrix.

k-Nearest Neighbors (k-NN). Rather than generating a parameterized model fit to the training data, the k-NN algorithm[99] creates a non-parameterized model that stores the training data. When making predictions for a new data point, k-NN finds the k closest data points (i.e., the k nearest neighbors) in the training set to the predicted data point and then predicts the $\hat{Y}_{new}$ of the new data point to be the average of the Y values among the nearest neighbor data in the training set. k-NN uses several hyperparameters. The first hyperparameter (k) determines the number of nearest neighbors selected during prediction. The second hyperparmeter is the weighting scheme used when averaging the nearest neighbors. Two common values include a uniform weighting, where $\hat{Y}_{new}$ is computed as the unweighted average across the nearest neighbors, and a distance weighting, where a weighted average is computed across the nearest neighbors weighted by the inverse of the distance to the predicted point. In the former case, each nearest neighbor has an equal vote, whereas in the latter case, closer neighbors have greater influence than further neighbors. Finally, a third hyperparameter (p) determines how the distance between two data points is computed. Specifically, p is the power of the Minkowski distance ($D_{Minkowski}$), computed as

$$D_{Minkowski} = \left(\sum_{i=1}^{n} |u_i - v_i|^p\right)^{\frac{1}{p}} \quad (1)$$

where u_i and v_i are the i^{th} components of data points u and v with dimension n. Two common cases are $p = 1$ (L1 distance) and $p = 2$ (Euclidean distance).

Support Vector Machine (SVM). The SVM algorithm[100] identifies a hyperplane defined by the distribution of the training data. In the case of regression tasks, this hyperplane serves as the line of best fit, similar to linear regression models. Specifically, the SVM regression task is formulated as

$$\min_{w} \frac{1}{2}\|w\|_2^2 + C\sum_{i=1}^{n}|\xi_i| \tag{2.17}$$

constrained by

$$|Y_i - (Xw)_i| \leq \varepsilon + |\xi_i| \tag{2.18}$$

where w is the weight vector (analogous to OLS), Y_i is the Y value of i^{th} data point, $(Xw)_i$ is the i^{th} value of the matrix product Xw (i.e., the predicted Y_{pred} for the i^{th} data point), n is the number of data points in the training set, ξ_i is the slack variable for the i^{th} data point, and ε and C are hyperparameters. Ultimately, Equation (2.17) regularizes the model coefficients (first term) and minimizes the slack variables (second term) while Equation (2.18) constrains the hyperplane to fit the training data to within a given tolerance. This tolerance is determined by a global tolerance (ε) as well as an additional individual tolerance for each training data point (ξ_i). The global tolerance is set as a hyperparameter, while the individual tolerances are minimized by the SVM algorithm. The weight that the slack variables are given during minimization is determined by the hyperparameter C.

The SVM can leverage the 'kernel trick' by reformulating Equations (2.17) and (2.18) into the dual form. In doing so, the optimization task becomes a function of the inner products of the data points (i.e., $X_i^T X_j$ for data points X_i and X_j) rather than the data points themselves. Thus, if a non-linear kernel function $K(X_i, X_j)$ that holds to the properties of an inner product space were to replace the linear inner product $X_i^T X_j$, a corresponding non-linear hyperplane could be used.

The choice of kernel is thus another hyperparameter for the SVM algorithm. Besides the linear kernel,

$$K_{lin}(X_i, X_j) = X_i^T X_j \tag{2.19}$$

common kernels include the polynomial kernel

$$K_{poly}(X_i, X_j) = (a + X_i^T X_j)^b \tag{2.20}$$

with hyperparameters *a* and *b*, the radial basis function (a.k.a. Gaussian) kernel

$$K_{rbf}(X_i, X_j) = e^{-\gamma \|X_i - X_j\|_2^2} \tag{2.21}$$

with hyperparameter γ, and the sigmoid kernel

$$K_{sigm}(X_i, X_j) = \tanh(\gamma X_i^T X_j + r) \tag{2.22}$$

with hyperparameters γ and *r*.

Decision Tree. Decision trees[99] are tree structures consisting of decision nodes and leaves. Beginning with the starting node, a single feature is used to split the training data pool into two categories. The decision tree recursively unfolds, using a single feature as a binary discriminator at each decision node for the reduced training data that it receives. Eventually, when the reduced training data pool that a node receives is approximately homogeneous in *Y*, the branch terminates in a leaf rather than another decision node. When the decision tree is used to make predictions on new data, each predicted data point follows the appropriate decision path of the tree until it reaches a leaf. The predicted data point is then predicted to a have a $\hat{Y}_{new}$ equal to the average of the *Y* values of the training data associated with that leaf.

Several hyperparameter control the learning of the decision tree. Various loss metrics, such as mean squared error or mean absolute error, can be used to determine the optimal split at each decision node. The decision tree will learn the split that minimizes the loss function using the simplifying assumption that the two decision paths from the split will immediately terminate in

leaves. Another hyperparameter constrains the learning of the optimal split at each decision node by specifying the minimum number of samples that can constitute a leaf when determining the optimal split. Various hyperparameters determine the criteria for branch termination. Some examples are the maximum depth of the tree (i.e., a branch will automatically terminate after a set number of decision nodes if it has not already terminated) and the minimum number of samples to warrant a decision node.

Random Forest (RF). While individual decision trees may tend to overfit the training data, the RF algorithm[101] corrects this by creating an ensemble of many decision trees. These trees are bootstrap aggregated, meaning that each tree is trained on a subset of k data points selected randomly from the training data with replacement. Furthermore, at each decision node, only a randomly selected subset of features is considered for the best split. The prediction of each tree is then averaged when the RF predicts a new data point. By creating an ensemble of many diverse decision trees, a more general model with reduced overfitting and often higher predictive accuracy is produced. Common hyperparameters of the RF include the number of decision trees, the number of data points selected for training each tree, and the number of features randomly considered at each decision node. Hyperparameters inherited from decision trees can also be considered, although the ensembling of the RF reduces the need to tune these hyperparameters.

Extra Trees (ET). Also known as Extremely Randomized Trees, the ET algorithm[102] also creates an ensemble of decision trees. Unlike RFs, each decision tree in an ET model is trained on the entire training dataset without bootstrap aggregation. Additionally, when RFs and decision trees learn decision nodes, they determine the optimal split point for each considered feature and then select the optimal feature to split. In contrast, at each decision node in an ET tree, the algorithm computes a random split point for each considered feature and then select the optimal

feature to split. This creates great diversity among the ET trees. Like RFs, this ensembling of decision trees tends to reduce overfitting and increase predictive accuracy. Common hyperparameters of the ET include the number of decision trees and the number of features randomly considered at each decision node. Hyperparameters inherited from decision trees can also be considered, but like RFs, this tends to be less necessary.

Chapter 3 Screening of Known Salt Hydrates for Thermal Energy Storage

3.1 Introduction

Building on earlier screening studies, the present investigation employs a different approach—high-throughput first-principles computation—to identify promising TES materials. Such an approach allows for the characterization of hydrated compounds whose structures are known, but for which tabulated thermodynamic data is absent. Indeed, our analysis of the Inorganic Crystal Structure Database (ICSD)[103] has identified dozens of hydrated compounds that remain unexplored for thermochemical heat storage due to missing thermodynamic information. Similarly, other compounds have been omitted from prior analyses due to a lack of thermophysical data, such as density. First-principles calculations can provide this missing information with high accuracy and with reasonable computational effort.

In addition to its ability to accurately predict the thermodynamics of a given hydration reaction, first-principles computation also yields valuable information on the chemical, electronic, and structural properties of TES materials.[104–106] These data allow for the investigation of property-performance relationships. Such relationships can yield design rules, ultimately leading to the discovery of even better TES materials.

Here we report an exhaustive computational search for promising TES materials based on known hydrates of metal fluorides, chlorides, bromides, and hydroxides drawn from the ICSD. 265 hydration reactions were screened over a large range of temperatures; many of these reactions have not been characterized before. The reactions are characterized according to their gravimetric and volumetric energy density, as well as by their operating temperature. Promising hydration

reactions were identified as a function of temperature range, including one reaction that appears to be new to TES: the dehydration of $CrF_3 \bullet 9H_2O$.

To reveal trends linking TES performance with the chemical features of the storage materials, two property-performance databases were created: one for salt hydrates (108 hydrates, 50 properties) and one for hydroxides (27 hydroxides, 33 properties). These databases combine the calculated structural, thermodynamic, and TES data with tabulated data for ionic properties. Correlations linking TES performance with chemical features were quantified using a Pearson correlation matrix. These analyses reveal trends involving the thermodynamics of hydration. In hydrates, the thermodynamics depend strongly on the water capacity of the hydrate. In hydroxides, thermodynamic properties are largely determined by the ionicity of the cation-hydroxide bond; the ionicity of this bond is, in turn, influenced by the cation's electronegativity, polarizing power, ionic radius, and by the volumetric water capacity. Based on these correlations, design rules for hydration-based TES systems are proposed.

3.2 Methodology

3.2.1 Compilation of Materials for Screening

TES compounds were identified from a search of the ICSD[103] for hydrates of metal fluorides (30), chlorides (79), and bromides (38), as well as hydroxides (40 hydroxides, 16 hydroxide hydrates). Ten additional anhydrous salts were collected from the Landolt-Börnstein (LB) database.[107] A complete list of all these compounds can be found in **Table 3.1**. In sum, 163 hydrates and 40 hydroxides, as well as their respective anhydrous salts and oxides, were extracted from these databases. This yielded a large, yet computationally feasible, set of crystal structures for analysis via first-principles calculations.

Table 3.1 Complete list of compounds screened in this study. Compounds marked with an * are from the LB database,[107] while all other compounds are from the ICSD.[103]

$BaBr_2$	$UBr_4•9H_2O$	$KCdCl_3$	$SnCl_4•8H_2O$	$NaNiF_3$	$KOH•4H_2O$
$BaBr_2•2H_2O$	VBr_3*	$KCdCl_3•H_2O$	$SrCl_2$	$NaNiF_3•3H_2O$	$KOH•H_2O$
$BaBr_2•H_2O$	$VBr_3•6H_2O$	$KMnCl_3$	$SrCl_2•2H_2O$	RbF	$La(OH)_3$
$CaBr_2$	YBr_3*	$KMnCl_3•2H_2O$	$SrCl_2•6H_2O$	$RbF•H_2O$	La_2O_3
$CaBr_2•6H_2O$	$YBr_3•10H_2O$	$LaCl_3$	$SrCl_2•H_2O$	UF_4	Li_2O
$CaBr_2•9H_2O$	$YBr_3•8H_2O$	$LaCl_3•3H_2O$	$TlCl_3$*	$UF_4•2H_2O$	$Li_2Sn(OH)_6$
$CdBr_2$	$ZnBr_2$	$LaCl_3•7H_2O$	$TlCl_3•4H_2O$	VF_3	$Li_2Sn(OH)_6•2H_2O$
$CdBr_2•4H_2O$	$ZnBr_2•2H_2O$	Li_2ZnCl_4	UCl_3	$VF_3•2H_2O$	Li_2SnO_3
$CeBr_3$	$AlCl_3$	$Li_2ZnCl_4•2H_2O$	$UCl_3•6H_2O$	$VF_3•3H_2O$	LiOH
$CeBr_3•7H_2O$	$AlCl_3•6H_2O$	LiCl	$UCl_3•7H_2O$	ZnF_2	$LiOH•H_2O$
$CoBr_2$	$BaCl_2$	$LiCl•H_2O$	VCl_3	$ZnF_2•2H_2O$	$Lu(OH)_3$
$CoBr_2•2H_2O$	$BaCl_2•2H_2O$	$MgCl_2$	$VCl_3•4H_2O$	$ZnF_2•4H_2O$	Lu_2O_3
$CoBr_2•4H_2O$	$BaCl_2•H_2O$	$MgCl_2•2H_2O$	$VCl_3•6H_2O$	ZrF_4	$Mg(OH)_2$
$CoBr_2•6H_2O$	$BeCl_2$	$MgCl_2•4H_2O$	YCl_3	$ZrF_4•3H_2O$	MgO
$CuBr_2$	$BeCl_2•4H_2O$	$MgCl_2•6H_2O$	$YCl_3•6H_2O$	$ZrF_4•H_2O$	$Mn(OH)_2$
$CuBr_2•4H_2O$	$BiCl_3$	$MgCl_2•H_2O$	$ZnCl_2$	$Al(OH)_3$	MnO
$EuBr_3$*	$BiCl_3•H_2O$	$MgCsCl_3$	$ZnCl_2•1.33H_2O$	Al_2O_3	$Na_2Cu(OH)_4$
$EuBr_3•6H_2O$	$CaCl_2$	$MgCsCl_3•6H_2O$	$ZnCl_2•2.5H_2O$	$Ba(OH)_2$	Na_2CuO_2
$FeBr_2$	$CaCl_2•2H_2O$	$MgRbCl_3$	$ZnCl_2•3H_2O$	$Ba(OH)_2•3H_2O$	Na_2O
$FeBr_2•4H_2O$	$CaCl_2•4H_2O$	$MgRbCl_3•6H_2O$	$ZnCl_2•4.5H_2O$	$Ba(OH)_2•8H_2O$	$Na_2Pt(OH)_6$
K_2PtBr_4	$CaCl_2•6H_2O$	$MnCl_2$	AlF_3	$Ba(OH)_2•H_2O$	Na_2PtO_3
$K_2PtBr_4•2H_2O$	$CdCl_2$	$MnCl_2•2H_2O$	$AlF_3•3H_2O$	BaO	$Na_2Zn(OH)_4$
$KAuBr_4$	$CdCl_2•2.5H_2O$	$MnCl_2•4H_2O$	$AlF_3•9H_2O$	$Be(OH)_2$	$Na_2Zn_2O_3$
$KAuBr_4•2H_2O$	$CdCl_2•4H_2O$	$MnCl_2•H_2O$	$AlF_3•H_2O$	BeO	Na_2ZnO_2
$KInBr_4$	$CdCl_2•H_2O$	$MoCl_2$*	Ca_2AlF_7	$Ca(OH)_2$	NaOH
$KInBr_4•2H_2O$	$CeCl_3$	$MoCl_2•1.33H_2O$	$Ca_2AlF_7•H_2O$	CaO	$NaOH•3.5H_2O$
$LaBr_3$	$CeCl_3•6H_2O$	Na_2ZnCl_4	CrF_3	$CaPb(OH)_6$	$NaOH•4H_2O$
$LaBr_3•7H_2O$	$CeCl_3•7H_2O$	$Na_2ZnCl_4•3H_2O$	$CrF_3•3H_2O$	$CaPbO_3$	$NaOH•7H_2O$
LiBr	$CoCl_2$	NaCl	$CrF_3•5H_2O$	$CaPt(OH)_6$	$NaOH•H_2O$
$LiBr•H_2O$	$CoCl_2•2H_2O$	$NaCl•2H_2O$	$CrF_3•9H_2O$	$CaPtO_3$	$NaZn(OH)_3$
$LuBr_3$*	$CoCl_2•4H_2O$	$NaHgCl_3$	CuF_2	$CaSn(OH)_6$	$NaZn(OH)_3•3H_2O$
$LuBr_3•8H_2O$	$CoCl_2•6H_2O$	$NaHgCl_3•2H_2O$	$CuF_2•2H_2O$	$CaSnO_3$	$Nd(OH)_3$
$MgBr_2$	$CoCl_2•H_2O$	$NdCl_3$	FeF_3	$Cd(OH)_2$	Nd_2O_3
$MgBr_2•2H_2O$	$CrCl_2$	$NdCl_3•6H_2O$	$FeF_3•3H_2O$	CdO	$Ni(OH)_2$
$MgBr_2•4H_2O$	$CrCl_2•4H_2O$	$NiCl_2$	HfF_4	$Ce(OH)_3$	NiO
$MgBr_2•6H_2O$	$CrCl_3$	$NiCl_2•2H_2O$	$HfF_4•3H_2O$	Ce_2O_3	$Pr(OH)_3$
$MgBr_2•9H_2O$	$CrCl_3•6H_2O$	$NiCl_2•4H_2O$	HgF_2	$Co(OH)_2$	Pr_2O_3
$MgBr_2•H_2O$	$CuCl_2$	$NiCl_2•6H_2O$	$HgF_2•2H_2O$	CoO	Rb_2O
$MnBr_2$	$CuCl_2•2H_2O$	$PrCl_3$	InF_3	$Cu(OH)_2$	RbOH
$MnBr_2•2H_2O$	$ErCl_3$*	$PrCl_3•6H_2O$	$InF_3•3H_2O$	CuO	$RbOH•H_2O$

$MnBr_2•4H_2O$	$ErCl_3•6H_2O$	$PtCl_4$	K_2AlF_5	$Dy(OH)_3$	$Sc(OH)_3$
NaBr	$EuCl_2$	$PtCl_4•3.5H_2O$	$K_2AlF_5•H_2O$	Dy_2O_3	Sc_2O_3
$NaBr•2H_2O$	$EuCl_2•2H_2O$	$PtCl_4•5H_2O$	K_2FeF_5	$Eu(OH)_3$	$Sr(OH)_2$
$PrBr_3$	$FeCl_2$	$ReCl_3$	$K_2FeF_5•H_2O$	Eu_2O_3	$Sr(OH)_2•8H_2O$
$PrBr_3•6H_2O$	$FeCl_2•2H_2O$	$ReCl_3•1.67H_2O$	$KAlF_4$	$Ga(OH)_3$	$Sr(OH)_2•H_2O$
$PuBr_3$	$FeCl_2•4H_2O$	$ScCl_3$	$KAlF_4•0.33H_2O$	Ga_2O_3	SrO
$PuBr_3•6H_2O$	$FeCl_3$	$ScCl_3•7H_2O$	KF	$Gd(OH)_3$	$Te(OH)_6$
$ScBr_3$*	$FeCl_3•2.5H_2O$	$SmCl_3$*	$KF•2H_2O$	Gd_2O_3	TeO_3
$ScBr_3•7H_2O$	$FeCl_3•6H_2O$	$SmCl_3•6H_2O$	$KF•4H_2O$	$In(OH)_3$	Tl_2O
$SnBr_4$	$GdCl_3$	$SnCl_2$	$KSnF_3$	In_2O_3	TlOH
$SnBr_4•5H_2O$	$GdCl_3•6H_2O$	$SnCl_2•1.5H_2O$	$KSnF_3•0.5H_2O$	K_2O	$Y(OH)_3$
$SrBr_2$	$InCl_3$*	$SnCl_2•2H_2O$	Li_2TiF_6	$K_2Pb(OH)_6$	Y_2O_3
$SrBr_2•6H_2O$	$InCl_3•3H_2O$	$SnCl_4$	$Li_2TiF_6•2H_2O$	K_2PbO_3	$Zn(OH)_2$
$SrBr_2•H_2O$	K_2HgCl_4	$SnCl_4•2H_2O$	$LiMnF_4$	$K_2Sn(OH)_6$	ZnO
$TlBr_3$	$K_2HgCl_4•H_2O$	$SnCl_4•3H_2O$	$LiMnF_4•H_2O$	K_2SnO_3	
$TlBr_3•4H_2O$	$KAuCl_4$	$SnCl_4•4H_2O$	MnF_3	KOH	
UBr_4	$KAuCl_4•2H_2O$	$SnCl_4•5H_2O$	$MnF_3•3H_2O$	$KOH•2H_2O$	

3.2.2 Preparation of Materials for DFT Calculations

Density functional theory (DFT) calculations require crystal structures with integer atomic occupancies. Thus, structures with partial atomic occupancies were expanded into supercells where all atomic occupancies were unity or zero, while maintaining consistency with the prescribed overall stoichiometry. Hydrogen atoms were positioned within hydrogen-deficient unit cells by performing simulated annealing[108] classical molecular dynamics (MD) simulations to find low-energy structures. Initial configurations were generated using the Forcite module in Materials Studio (MS) 8.0[109] with fixed unit cell parameters and with all non-hydrogen atoms constrained to their perfect-lattice positions. MD calculations were run successively at 400 K, 300 K, 200 K, and 100 K, followed by geometry optimization at 0 K.[109] These structures were then relaxed using DFT (see section 2.1.4 for implementation details). All MD calculations employed the Universal Force Field,[110] and were run with a 1 fs timestep for 10 ps at each temperature. An NVT ensemble was used along with a Nose thermostat with a Q ratio of 10^{-5}. An Ewald sum was used to calculate the

electrostatic interactions between the atoms using the formal charge of each ion. Relaxation was performed using Forcite's 'Smart' algorithm until all forces on the hydrogen atoms were less than 10^{-3} kcal/mol/Å.

3.2.3 Thermodynamic Framework

The enthalpy of dehydration (ΔH) Equation (3.1) for each hydration reaction was evaluated from the ground state energies of the compounds using

$$\Delta H = \frac{E_{dehyd} - E_{hyd} + nE_{H2O}}{n} \tag{3.1}$$

where n is the number of moles of water liberated in the dehydration reaction, E_{dehyd} is the energy of the dehydrated compound, E_{hyd} is the energy of the hydrated compound, and E_{H2O} is the energy of the water vapor. The volumetric energy density (*VED*) and the gravimetric energy density (*GED*) were calculated using[3,33,35,36,55]

$$VED = \frac{n\Delta H}{V_{hyd}} \tag{3.2}$$

$$GED = \frac{n\Delta H}{MM_{hyd}} \tag{3.3}$$

where V_{hyd} and MM_{hyd} are the molar volume (calculated from the DFT-relaxed crystal structure) and the molar mass of the hydrated compound, respectively. This definition of V_{hyd} assumes that the storage medium adopts a single-crystal morphology, which will provide an upper-bound to the practically-achievable *VED*. (For example, a TES system that employs a hydrate in powdered form will have a lower *VED* due to imperfect packing of the powder particles.)

The change in the Gibbs free energy (ΔG) of a reaction is related to the enthalpy of dehydration via

$$\Delta G = \Delta H - T\Delta S \quad (3.4)$$

where T is the temperature and ΔS is the entropy of dehydration. When the system is in equilibrium (i.e., ΔG=0), T can be considered as T_{turn}, the turning temperature.[33–36] The entropy of dehydration per mole of water for all reactions was assumed to be uniform, 146 J/(K-mol H_2O).[57,67,76] Indeed, Glasser showed that the change in entropy in a salt dehydration reaction is approximately a constant 146 J/(K-mol H_2O), and is similar to the entropy of sublimation for ice, 140.5 J/(K-mol H_2O).[67]

3.2.4 Selection of an Appropriate Density Functional for Ab-Initio Calculations

The choice of exchange-correlation functional is important when modeling water-bonding systems. For example, Fischer suggested that functionals that include a dispersion correction would likely outperform GGA functionals when optimizing the structure of zeolites containing water.[111] Therefore, in the present study the performance of two conventional GGA functionals (PW-91 and PBE),[82,83] four nonempirical van der Waals functionals (vdW-DF2, optPBE-vdW, optB88-vdW, and optB86b-vdW),[84–89] and three semiempirical van der Waals functionals (DFT-D2, DFT-D3, DFT-TS)[90–92] were assessed for a test set of well-studied TES reactions.[56,112] The test reactions included $MgCl_2$ hydration (both from $MgCl_2$ to $MgCl_2 \bullet H_2O$ and from $MgCl_2 \bullet H_2O$ to $MgCl_2 \bullet 2H_2O$), and MgO hydration to $Mg(OH)_2$. The functionals were assessed with respect to their geometric and energetic accuracy. Geometric accuracy was measured based on the error in the calculated lattice parameters a, b, c, α, β, and γ compared to experimental values[113–116] from the ICSD. Similarly, energetic accuracy was characterized by the percent error in the enthalpy of dehydration relative to experiment.[67,117]

Figure 3.1 illustrates the relative accuracies of the exchange-correlation functionals. The maximum and average geometric and energetic errors are shown across the set of five compounds

for the geometric comparison, and across the three reactions for the energetic comparison. **Table 3.2** and **Table 3.3** summarize the calculated and experimental values. The data show that the nonempirical van der Waals exchange-correlation functionals are generally more accurate than the GGA functionals at reproducing the measured structure data, but worse at replicating the enthalpy of dehydration: the most accurate structural predictions were made by the optPBE-vdW functional, whereas the best enthalpies of dehydration were produced by the PW-91 functional. Combining the optPBE-vdW functional for geometry relaxation with the PW-91 for energies produced the most accurate predictions of structure and energy. This combination was adopted for the remainder of this study.

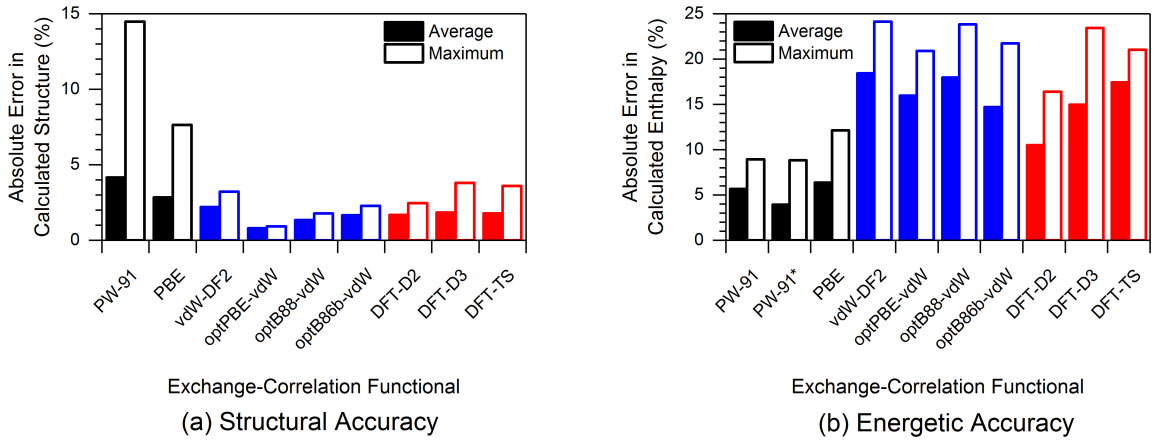

Figure 3.1 Comparison of exchange-correlation functionals for the hydration of $MgCl_2$ to $MgCl_2•H_2O$, the hydration from $MgCl_2•H_2O$ to $MgCl_2•2H_2O$, and the hydration of MgO to $Mg(OH)_2$. a) Average and maximum geometric errors of the five structures with respect to measured structure data from the ICSD. Maxima are determined by the largest error in a single lattice parameter. b) Average and maximum energetic errors with respect to experiment for the enthalpy of dehydration for the three hydration reactions. *Indicates a single point energy calculation using the geometry from an optPBE-vdW calculation. GGA functionals are shown in black, nonempirical van der Waals functionals are shown in blue, and semiempirical van der Waals functionals are shown in red.

Table 3.2 Structural comparison of five benchmarking compounds to experiment.

Method	$MgCl_2•2H_2O$				$MgCl_2•H_2O$			$MgCl_2$		$Mg(OH)_2$		MgO
	a (Å)	b (Å)	c (Å)	β (°)	a (Å)	b (Å)	c (Å)	a (Å)	c (Å)	a (Å)	c (Å)	a (Å)
PW-91	7.68	8.46	3.68	102.1	8.91	3.67	11.50	3.66	20.22	3.17	4.72	4.24
PBE	7.69	8.47	3.69	102.3	8.92	3.67	11.50	3.66	19.02	3.18	4.72	4.24
vdW-DF2	7.67	8.56	3.72	100.8	9.02	3.71	11.50	3.72	17.74	3.21	4.83	4.29
optPBE-vdW	7.42	8.51	3.67	99.2	8.94	3.65	11.41	3.67	17.79	3.18	4.73	4.25

optB88-vdW	7.37	8.42	3.66	99.2	8.87	3.64	11.29	3.65	17.47	3.16	4.70	4.24
optB86b-vdW	7.26	8.41	3.63	98.4	8.85	3.61	11.26	3.63	17.41	3.16	4.66	4.23
DFT-D2	7.28	8.38	3.63	98.8	8.84	3.61	11.26	3.62	18.03	3.13	4.66	4.19
DFT-D3	7.30	8.39	3.64	99.5	8.82	3.62	11.24	3.64	17.81	3.15	4.59	4.20
DFT-TS	7.31	8.37	3.65	99.3	8.85	3.64	11.27	3.65	17.65	3.14	4.60	4.19
Experiment	7.43 [113]	8.57 [113]	3.65 [113]	98.6 [113]	8.92 [113]	3.63 [113]	11.48 [113]	3.64 [114]	17.67 [114]	3.15 [115]	4.77 [115]	4.21 [116]

Table 3.3 Energetic comparison of the three benchmarking reactions to experiment.

Method	$MgCl_2 \cdot H_2O \rightarrow MgCl_2 + H_2O_{(g)}$ ΔH (kJ/mol)	$MgCl_2 \cdot 2H_2O \rightarrow MgCl_2 \cdot H_2O + H_2O_{(g)}$ ΔH (kJ/mol)	$Mg(OH)_2 \rightarrow MgO + H_2O_{(g)}$ ΔH (kJ/mol)
PW-91	79.8	73.9	74.3
PW-91*	82.1	72.2	74.4
PBE	77.9	71.5	71.7
PBE*	79.3	69.6	71.7
vdW-DF2	94.2	84.4	101.3
vdW-DF2*	94.0	84.1	100.5
optPBE-vdW	94.6	86.2	92.8
optPBE-vdW*	94.6	86.2	92.8
optB88-vdW	96.0	88.3	93.9
optB88-vdW*	96.0	88.4	93.9
optB86b-vdW	94.2	86.8	89.4
optB86b-vdW*	94.2	87.0	89.2
DFT-D2	91.2	83.0	76.8
DFT-D2*	91.3	83.1	77.0
DFT-D3	94.3	88.0	88.6
DFT-D3*	94.1	88.0	88.4
DFT-TS	92.3	86.3	64.7
DFT-TS*	92.0	86.3	64.9
Experiment	83.5[67]	71.3[67]	81.6[117]

3.2.5 Screening Method

A multi-step approach was used to identify the most promising reactions and to categorize them based on their operating temperature range, as illustrated in **Figure 3.2**. The main steps of this screening work-flow are described below.

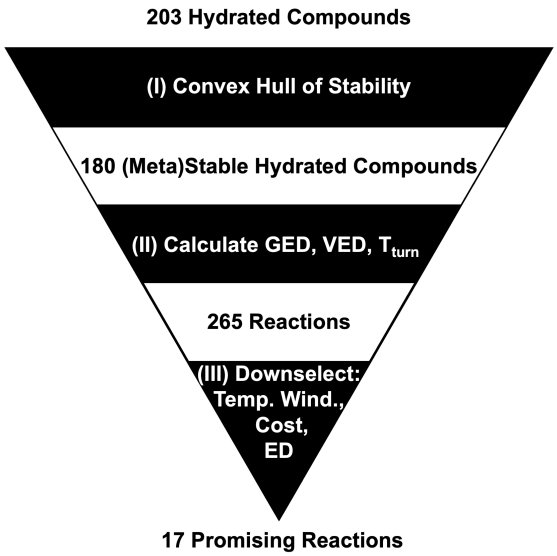

Figure 3.2 Screening procedure used to identify promising hydration reactions.

1. *Elimination of Unstable Compounds.* A thermodynamic filter was applied to identify and remove unstable hydrates. The convex hull concept was used to determine the thermodynamic stability of a given compound.[118,119] To apply this analysis to a system consisting of two distinct 'units'—i.e. salt formula units and water molecules—the enthalpy of formation is normalized on a per 'unit' basis. Hydrates that lie above the convex hull were deemed either metastable or unstable, since under these circumstances it is energetically favorable for the compound to decompose into a combination of the nearest stable phases on the hull. For instance, as seen in **Figure 3.3**, a combination of half $CaCl_2$ and $CaCl_2 \bullet 4H_2O$ has a lower enthalpy of formation than $CaCl_2 \bullet 2H_2O$, indicating that $CaCl_2 \bullet 2H_2O$ is not a stable phase. The convention in literature for the threshold between metastable and unstable compounds is ~50 meV/atom;[120–122] the same convention is adopted here. Compounds with distances less than 50 meV/atom are considered metastable and advance to the next step in the screening protocol; the others are considered unstable and removed. In total, 23 unstable compounds were identified.

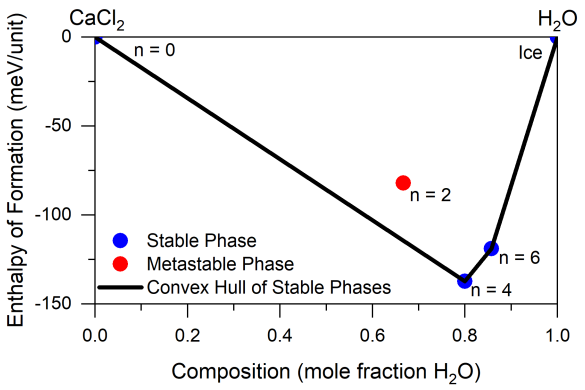

Figure 3.3 Convex hull illustrating the relative stability of various $CaCl_2$ hydrates. As the formation enthalpy of $CaCl_2 \bullet 2H_2O$ (red dot) lies above the convex hull by less than 50 meV/atom, it is classified as being metastable. A 'unit' refers to a water molecule or a $CaCl_2$ formula unit.

2. *Characterization of Reactions by Energy Density and Operating Temperature Range.* The energy densities and turning temperatures of the remaining 265 hydration reactions were evaluated using DFT. Some of these reactions consist of multiple steps due to the presence of stable intermediate hydrates. As such, these reactions possess a set of turning temperatures, which incur a temperature window. The temperature range between the maximum and minimum T_{turn} must be accessible to make full use of a given hydrate (i.e., access all the intermediate phases). If the highest and lowest turning temperatures of a given reaction were not in the same or adjacent temperature categories (defined below), that reaction was marked as having a 'wide temperature window.' Otherwise, the reaction was categorized by the temperature range in which the mean of the maximum and minimum turning temperature fell.
3. *Downselect Promising Reactions.* The three reactions exhibiting the largest root mean square of the *GED* and *VED* were identified for each temperature category. Several additional constraints were then placed on this list. For example, the temperature window could not be larger than 50°C, and high cost materials such as $BeCl_2 \bullet 4H_2O$, $Sc(OH)_3$, and $PtCl_4 \bullet 5H_2O$ were omitted. Specifically, salts containing metals that are more expensive

than lithium according to the U.S. Geological Survey[123] were removed. (Lithium was chosen as the cutoff point as it is an expensive material, yet commonly used in battery applications.) Of the identified promising reactions, the reactions with the highest root mean square of the *GED* and *VED* for low temperatures (< 100°C), medium temperatures (100–300°C), and high temperatures (> 300°C) were examined in the context of the existing literature.

3.2.6 Structure-Property Relationship Database

Two databases were compiled for the stable and metastable compounds. In the first database, 50 geometrical, ionic, and thermodynamic parameters for the 108 stable/metastable hydrates were compiled. These parameters included water content, ionic properties, changes in the structure from the anhydrous salt to the hydrate, structural properties of the anhydrous salt, hydrate, and fictitious expanded anhydrous salt (i.e. the hydrate structure with the water molecules removed), thermodynamic properties of the hydration reaction, and the energy storage capacity of the reaction. The second database consisted of 27 hydroxides characterized by 33 properties, which included the same types of properties as the salt hydrate database with the exception of anionic and structural properties of the expanded anhydrous salt (these properties are not physically meaningful for hydroxides). The division into two databases allowed for the inclusion of hydrate-specific properties as well as a comparison between these distinct types of hydration reactions. These two databases (and ancillary tables) can be found in Appendix A.

3.2.7 Property-Performance Relationships

Pearson correlation coefficient matrices were calculated to identify the most significant positive and negative correlations between pairs of features for both the salt hydrate and hydroxide

datasets. Correlation matrices were generated using the pandas 0.20.2 software package.[124] Feature pairs were rank-ordered based on correlation coefficients. In this way, physically meaningful property-performance trends can be revealed, which can aid in the identification of promising thermal storage materials. The goal is to identify elementary properties that correlate with the three primary TES performance metrics: enthalpy of dehydration, gravimetric energy density, and volumetric energy density. (The turning temperature was not included in this analysis since it is proportional to the enthalpy of dehydration.)

3.3 Results and Discussion

3.3.1 Screening Results

Figure 3.4 plots the calculated *GED*, *VED*, and temperature category for each of the 265 hydration reactions examined. Similar to the materials identified in the literature (**Figure 1.2**), the present hydration reactions exhibit a positive correlation between their gravimetric and volumetric energy densities, as $VED = GED \times \rho$, where ρ is the crystallographic (i.e., single-crystal) density. (Thus, the present estimate of *VED* represents an upper bound, if, for example, the storage medium was a loosely packed powder.) Furthermore, **Figure 3.4** also shows that higher temperature reactions tend to possess higher energy densities, and *vice versa*, due to their generally higher enthalpies of dehydration. A compilation of data for all reactions can be found in Appendix B.

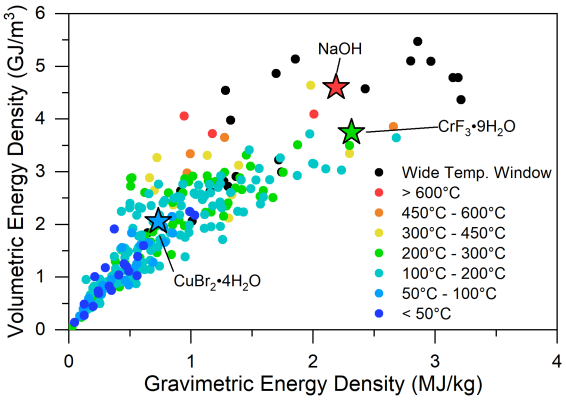

Figure 3.4 Volumetric energy density as a function of gravimetric energy density and temperature category for the 265 hydration reactions examined in the present study. Stars indicate the top-performing reactions identified for low, medium, and high temperature applications.

Out of the 265 reactions, 17 promising reactions according to energy density, cost, and temperature window were identified. These reactions are summarized in **Figure 3.5**. Three reactions are listed for each of 6 distinct temperature categories. Reactions that did not meet the temperature window constraint were excluded. Notably, since all reactions below 50°C had a temperature window greater than 50°C, all were excluded. Only two promising reactions were identified between 450°C and 600°C because the other reactions in that range contained expensive platinum and were therefore excluded. Of these 17 reactions, more than a third appear to be absent from the TES literature. These potentially new reactions involve the following six compounds: $AlF_3 \bullet 9H_2O$, $CrF_3 \bullet 9H_2O$, $FeBr_2 \bullet 4H_2O$, $Na_2Cu(OH)_4$, $NaOH \bullet 7H_2O$, and $ZnCl_2 \bullet 3H_2O$.

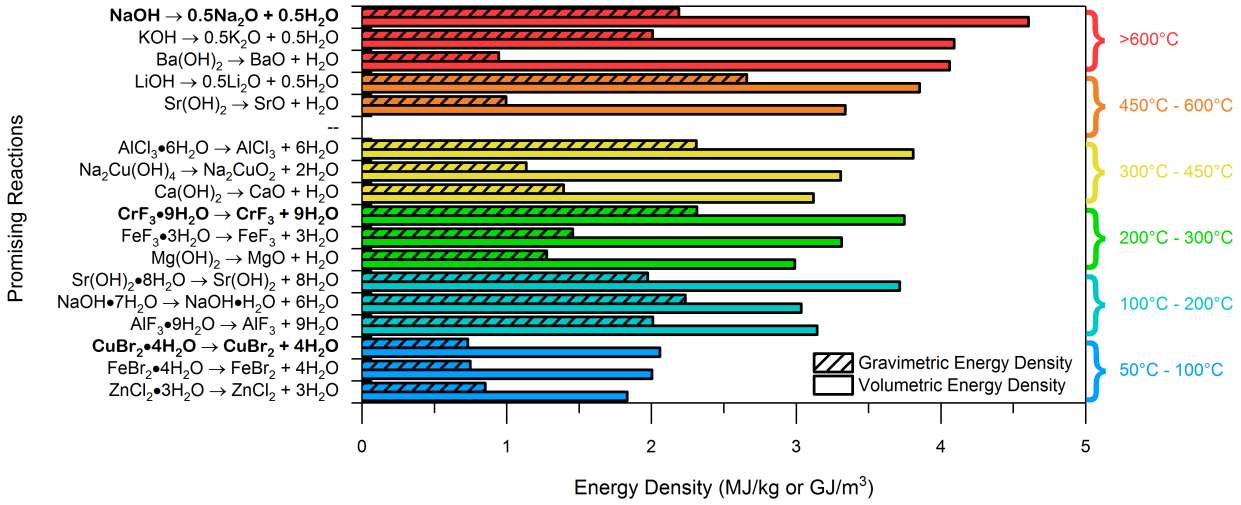

Figure 3.5 Promising TES reactions identified in the present study. Reactions are sorted by temperature, with their respective gravimetric and volumetric energy densities indicated by horizontal bars. Top-performing reactions for low (< 100°C), medium (100–300°C), and high-temperature (> 300°C) applications are indicated in bold.

These candidates can be further distilled into top-performing reactions within three generalized temperature ranges: $CuBr_2•4H_2O$ for low temperatures (< 100°C), $CrF_3•9H_2O$ for medium temperatures (100–300°C), and NaOH for high temperatures (> 300°C). The energy densities, operating temperatures, and DFT-optimized crystal structures of the hydrated/dehydrated compounds participating in these reactions are summarized in **Figure 3.6**.

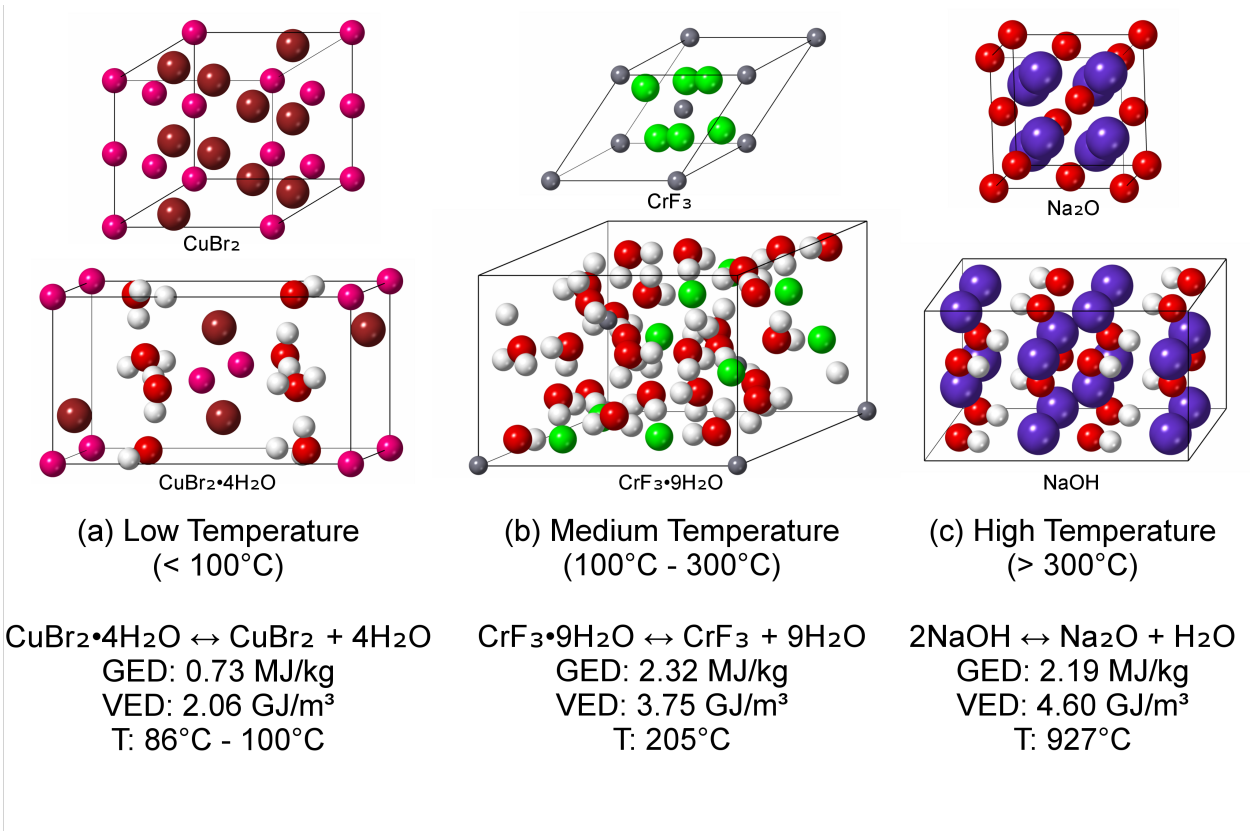

Figure 3.6 DFT-relaxed crystal structures of the top-performing dehydrated-hydrated compounds for a) low, b) medium, and c) high temperature heat storage. Dehydrated compounds are shown in the top row; hydrated compounds are shown in the bottom row. Hydrogen atoms are shown as white, oxygen atoms as red, bromine atoms as dark red, fluorine atoms as green, copper atoms as pink, chromium atoms as silver, and sodium atoms as violet. All atoms are visually represented by their van der Waals radii.

Top-Performing Reaction for Low Temperatures. As previously mentioned, copper (II) bromide tetrahydrate ($CuBr_2 \bullet 4H_2O$) was identified as a promising salt hydrate for low temperature TES. This dehydration reaction occurs in two steps. The first step occurs at a turning temperature of 86°C, where $CuBr_2 \bullet 4H_2O$ dehydrates into $CuBr_2$ and liquid water. The second step occurs at 100°C when the liquid water evaporates. The first step has a ΔH of 13.3 kJ/mol H_2O, while the second step has a ΔH of 40.7 kJ/mol H_2O, storing a total of 0.73 MJ/kg and 2.06 GJ/m^3. This compound is unique on account of its enthalpy of dehydration being low enough such that the average of the turning temperature range (86–100°C) is less than 100°C, but not so low that it is

unstable. Additionally, it has a high water capacity for this temperature range (four moles per formula unit), which is relevant to energy density in salt hydrates, as will be discussed later.

$CuBr_2 \bullet 4H_2O$ has not been identified as a promising compound in the experimental TES literature, but it has been discussed in recent screening studies. In their screening for low temperature salt hydration reactions, N'Tsoukpoe et al. removed this reaction from consideration on the basis of toxicity, since $CuBr_2$ has a health hazard rating of 2 (significant exposure can result in injury) according to NFPA 704.[3] The thermodynamic screenings of Deutsch et al.[35] and Donkers et al.[55] report similar energy densities to what was calculated here. However, both databases list other low temperature hydration reactions with higher gravimetric and volumetric energy densities than the hydration of $CuBr_2$. This is due to subtle differences in temperature classification. For example, some reactions with higher energy densities that we identified as occurring above 100°C were classified as occurring below 100°C in those studies.

Top-Performing Reaction for Medium Temperatures. Chromium (III) fluoride nonahydrate ($CrF_3 \bullet 9H_2O$) was identified by our screening protocol as a promising compound at medium temperatures. Chromium is a relatively small and light transition metal, while fluorine is the smallest and lightest halogen. Furthermore, the nonahydrate has a very high water capacity of 9 water molecules per formula unit. These factors combine to yield a high energy density of 2.32 MJ/kg and 3.75 GJ/m^3. An additional favorable feature of the nonahydrate phase is its highly exothermic formation energy (-69.4 meV/atom). This causes its location on the convex hull to fall below the lower hydrates of CrF_3. Thus, our calculations predict that there are no stable intermediate phases between the nonahydrate and the anhydrous salt. Hence, there is no temperature window: the reaction proceeds in a single step at a turning temperature of 205°C and an enthalpy of dehydration of 69.7 kJ/mol H_2O.

Recent screening and experimental TES studies appear to have overlooked $CrF_3 \bullet 9H_2O$. The database compiled by Donkers et al.[55] does not contain any medium temperature reactions that have both a higher gravimetric and volumetric energy density. Deutsch et al.[35] identified two hydration reactions with higher energy densities: the dehydration of $LiOH \bullet H_2O$ to Li_2O, and the dehydration of $AlCl_3 \bullet 6H_2O$. Both reactions were characterized in the present study. However, our calculations predict that the former reaction has a wide temperature window, while the latter reaction has a much smaller volumetric energy density, consistent with the data of Donkers et al.[55] Thus, $CrF_3 \bullet 9H_2O$ appears to be a novel TES material with very favorable heat storage properties.

Top-Performing Reaction for High Temperatures. At high temperatures, NaOH was identified by our screening as the most promising hydroxide for TES. No intermediates exist between NaOH and Na_2O, so the reaction occurs in a single step. Heat is stored at a turning temperature of 927°C, with an enthalpy of dehydration of 175.2 kJ/mol H_2O. Although NaOH only stores half a mole of water per mole of hydroxide, this limited capacity is offset by the small size, mass, and polarizing power of the sodium ion. The former reduces volume and mass of the compound, while, as discussed later, the small polarizing power increases the enthalpy of dehydration. Together, these features allow NaOH to store a great deal of heat on a gravimetric and volumetric basis: 2.19 MJ/kg and 4.60 GJ/m^3.

The dehydration of sodium hydroxide (NaOH) hasn't been identified as a promising reaction in the experimental literature, but has been discussed in previous studies that use tabulated thermodynamic data.[33,35] Our results are similar to the energy densities found in Deutsch et al.'s[35] screening, and to the enthalpy of dehydration found in Wentworth et al.'s[33] screening. The screening studies of Deutsch et al. and Donkers et al. identified four high temperature hydration reactions that have gravimetric and volumetric energy densities that exceed those of NaOH.[35,55]

Deutsch et al.[35] proposes three reactions: the dehydration of $LiCl•H_2O$ into Li_2Cl_2, the dehydration of $MnSO_4•7H_2O$ into the pentahydrate, and the dehydration of $Al_4C_3•6H_2O$. However, the promise of these reactions is questionable. First, Li_2Cl_2 is about 620 meV/atom higher in energy than LiCl,[35] thus $LiCl•H_2O$ will rather dehydrate to LiCl than the unstable Li_2Cl_2. Second, there is significant disagreement between the two databases concerning the dehydration of $MnSO_4•7H_2O$ to $MnSO_4•5H_2O$. Deutsch et al. cites the enthalpy of hydration to be 370 kJ/mol H_2O,[35] while Donkers et al. cites an enthalpy of 51 kJ/mol H_2O.[55] The two databases show more agreement on the very high enthalpy for $Al_4C_3•6H_2O$ (215 kJ/mol H_2O[35] and 170.9 kJ/mol H_2O[55]), indicating that it is a reaction of interest for high temperature applications, although Donkers at al. indicated that this reaction appears to be unrealistic.[55] Donkers et al. identified one high temperature reaction that outperformed NaOH in both gravimetric and volumetric energy densities: the dehydration of $Ce(SO_4)_2•5H_2O$.[55] This reaction has a *GED* of 4.55 MJ/kg and a *VED* of 7.08 GJ/m^3, but is charged at a temperature of 2261°C. As such, NaOH is still promising in the context of high temperature hydration reactions.

3.3.2 Comparison with Other Screening Studies

As previously mentioned, two recent studies[35,55] each screened over 500 hydration reactions using tabulated thermodynamic data collected from several (typically experimental) sources. Out of the 265 reactions that were characterized in the present study, 112 were partially or completely characterized by at least one of these earlier studies. To our knowledge, the other 153 reactions have not been investigated previously.

Figure 3.7 compares our DFT predictions to the data reported in those earlier studies. Regarding *GED* and *VED* (**Figure 3.7a**–**b**), our study agrees very well with the tabulated data: The mean absolute deviation between our calculations and the tabulated data is 0.12 MJ/kg and 0.27

GJ/m^3 for *GED* and *VED*, respectively. Exceptions to this agreement exist for a few reactions in the database of Deutsch et al.;[35] these discrepancies appear to arise from differences in the crystallographic densities.

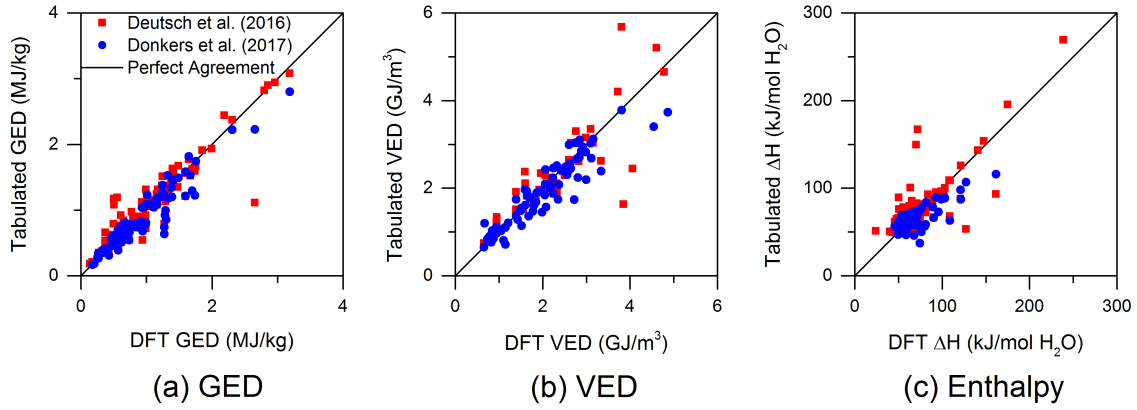

Figure 3.7 Comparison of TES properties from two recent studies using tabulated thermodynamic data (Deutsch et al.[35] and Donkers et al.[55]) with DFT data from the present study. a) Gravimetric energy density, b) volumetric energy density, and c) enthalpy of dehydration.

Regarding the enthalpies of dehydration, the present calculations exhibit a mean absolute deviation of 10.0 kJ/mol H_2O from the tabulated data. This deviation is comparable to the deviations between the two tabulations themselves,[35,55] MAD = 7.5 kJ/mol H_2O, for the reactions investigated here. The degree of agreement between DFT and the tabulated enthalpies is slightly better than that reported for hydrides.[125] Our DFT calculations show reasonable agreement with the enthalpies of dehydration reported by Deutsch et al.[35] (MAD = 11.1 kJ/mol H_2O). Stronger agreement is obtained with the data of Donkers et al. (MAD = 8.7 kJ/mol H_2O);[55] nevertheless, the DFT enthalpies are systematically larger than those reported by Donkers et al.

The agreement between each pair of screening studies is also assessed by the Pearson correlation coefficient. The Pearson correlation coefficient (r) of X and Y is calculated as follows, where $E[]$ is the expected value, μ_i is the mean value of property i, and σ_i is the standard deviation of property i.

$$r_{X,Y} = \frac{E[(X - \mu_X)(Y - \mu_Y)]}{\sigma_X \sigma_Y} \quad (3.5)$$

Study pairs with higher Pearson correlation coefficients demonstrate greater agreement. As shown in **Table 3.4**, given the level of agreement between the screenings of Deutsch et al.[35] and Donkers et al.[55] as a benchmark, this study shows good agreement with the data in these other two screenings.

Table 3.4 Pearson correlation coefficients for the agreement between the three studies.

Study Pair	GED	VED	ΔH
This Study – Deutsch et al.	0.933	0.840	0.794
This Study – Donkers et al.	0.951	0.932	0.784
Deutsch et al. – Donkers et al.	0.935	0.928	0.633

When comparing the studies, every reaction contained in both studies was included. The number of reactions compared for each thermodynamic quantity is shown in **Table 3.5**. For each pair of studies, the number of reactions compared is less for *VED* than *GED* or ΔH due to a lack of density information in the other studies necessary for calculating the *VED*.

Table 3.5 Number of reactions compared.

Study Pair	GED	VED	ΔH
This Study – Deutsch et al.	106	43	106
This Study – Donkers et al.	86	78	86
Deutsch et al. – Donkers et al.	82	29	82

3.3.3 Property-Performance Trends

The design of improved TES materials will be aided by the identification of elementary materials properties that correlate with (or control) TES performance. **Figure 3.8** shows the calculated Pearson correlation coefficients (*r*) between 50 salt hydrate properties (1225 correlations) and between 33 hydroxide properties (528 correlations). To simplify the analysis,

each property was subsequently categorized into one of 4 categories: (*i.*) water content properties (e.g. gravimetric water capacity), (*ii.*) ionic properties (e.g. cation electronegativity), (*iii.*) structural properties (e.g. density of the salt hydrate), or, (*iv.*) capacity or thermodynamic properties (e.g. *GED*, *VED*, enthalpy of dehydration). The properties assigned to each category are listed in Appendix A.

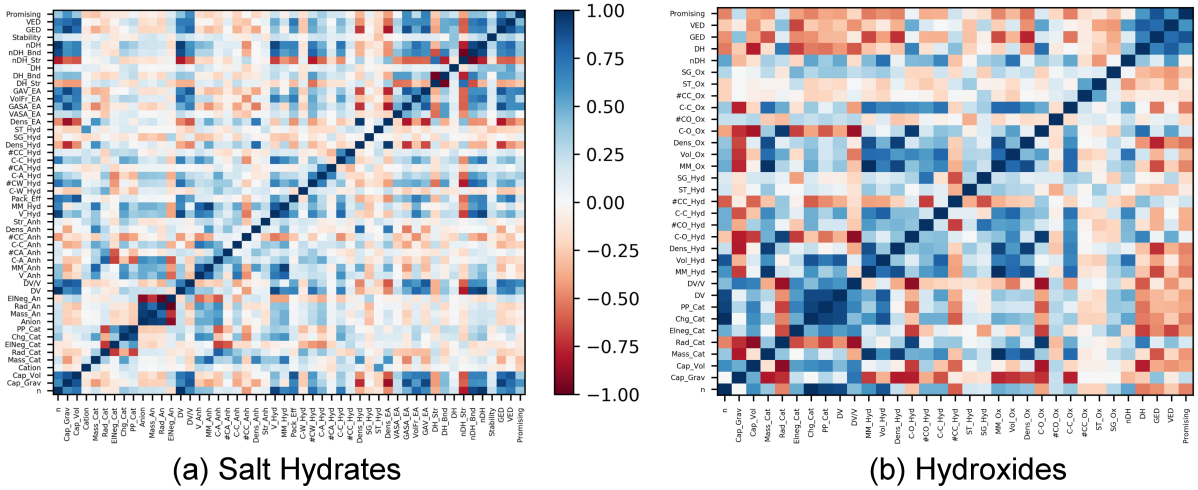

Figure 3.8 Color map of the Pearson correlation coefficient matrix for the a) 50 properties of the salt hydrate database, and the b) 33 properties of the hydroxide database. -1 represents perfect negative correlation, 0 represents no correlation, and 1 represents perfect positive correlation.

The correlation coefficients depicted in **Figure 3.8** allow one to identify the elementary properties that most strongly correlate (positively or negatively) with the properties of interest for TES. **Figure 3.9** shows the strongest correlations in three of the property categories (categories (*i.)* through (*iii.)* above) with four TES performance metrics: *GED*, *VED*, total enthalpy (*nΔH*), and enthalpy of dehydration per mole H_2O (*ΔH*). From **Figure 3.9a**, it is evident that water content and structural properties strongly affect the energy densities and *nΔH* in salt hydrates; on the other hand, no properties strongly correlate with *ΔH* in these compounds. Regarding hydroxides, **Figure 3.9b** shows that all three property categories have a weak-to-moderate effect on nearly all the TES properties of interest.

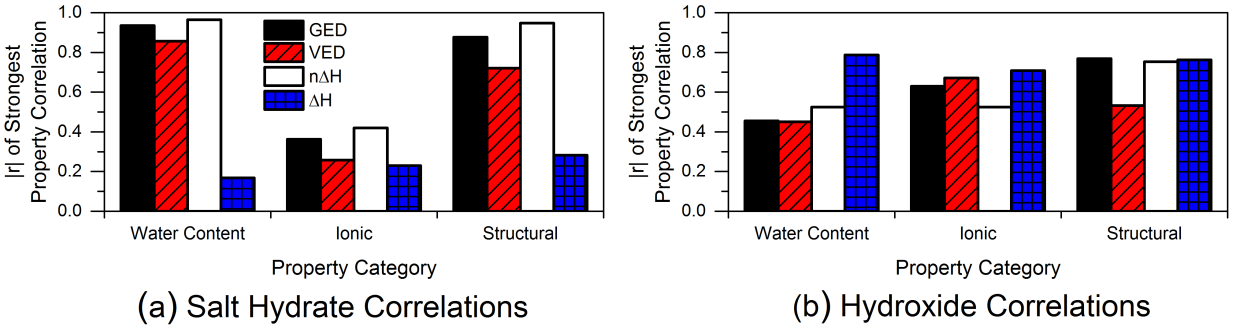

Figure 3.9 Absolute value of the Pearson correlation coefficient of the strongest correlating property from each property category (water content, ionic properties, structural properties) with TES-relevant properties of a) salt hydrates and b) hydroxides. Values are reported on a scale of 0 to 1, where 1 indicates perfect correlation (positive or negative) for a given property. Total enthalpy (nΔH) is in on a per mole of hydrated compound basis, while the enthalpy of dehydration (ΔH) is on a per mole of water basis.

Salt Hydrate Trends. As expected, the water content in salt hydrates strongly correlates with energy density and the total enthalpy of dehydration. **Figure 3.10** shows that *GED* correlates strongly with the gravimetric water capacity, *VED* correlates strongly with the volumetric water capacity, and the total enthalpy correlates strongly with the molar water capacity. These trends arise from the thermodynamics of hydration in salt hydrates being roughly additive: ΔH does not vary significantly between hydrates of the same salt. Furthermore, ΔH is largely independent of composition, as the thermodynamics of hydration do not vary significantly between hydrates of different salts.[57] Thus, *GED*, *VED*, and *nΔH* can be straightforwardly approximated based on the amount of water in the unit cell.

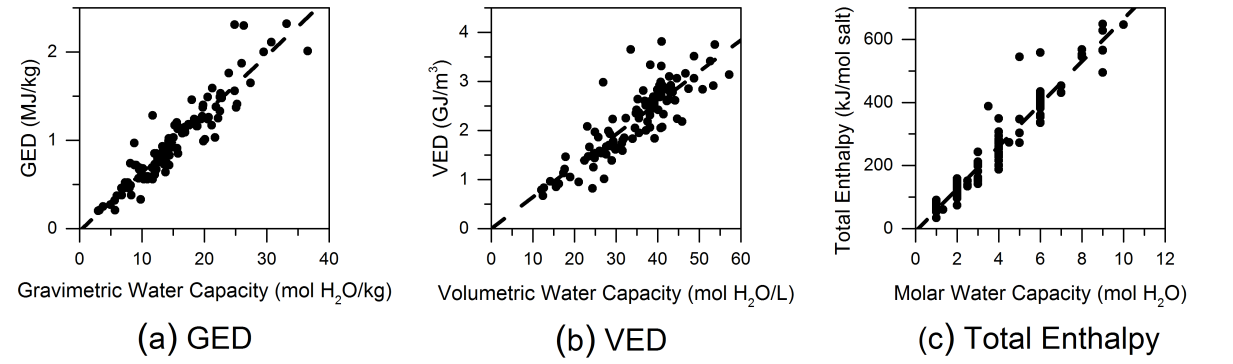

Figure 3.10 Correlations of water content in salt hydrates with a) gravimetric energy density [r = 0.935], b) volumetric energy density [r = 0.856], and c) total enthalpy [r = 0.964].

Ionic properties do not strongly correlate with the performance of salt hydrates, as shown in **Figure 3.9a**. A much stronger correlation is found, however, with structural properties. For $n\Delta H$, the strongest correlation ($r = 0.948$) among structural properties is with the absolute volume change upon hydration/dehydration. Similar to the behavior of thermodynamic properties (ΔH, ΔS), the volume change has been shown by Jenkins et al. to be roughly constant on a per mole H_2O basis.[75] Indeed, our analysis reveals that the absolute volume change and the molar water capacity are highly correlated ($r = 0.984$). *Thus, for each water molecule stored in a hydrate, a roughly constant amount of heat is released and a roughly constant volume change occurs*.

VED and *GED* also exhibit strong correlations with structural properties, as evidenced by **Figure 3.9a**. This relationship can, however, be traced to the dependence of structural properties on water content. For *VED*, the strongest correlation among structural properties is with the packing efficiency[126] of water in the unit cell ($r = 0.720$), which in turn is strongly correlated with the volumetric water capacity ($r = 0.855$). For *GED*, the strongest correlation among structural properties is with gravimetric surface area in the expanded anhydrous salt ($r = 0.877$). Surface area is itself strongly correlated with the gravimetric water capacity ($r = 0.884$). This latter relationship is reminiscent of the Chahine rule, which relates hydrogen uptake in adsorbents with their surface area.[127–129]

Hydroxide Trends. **Figure 3.9b** shows that several properties of the hydroxides exhibit moderately strong correlations with ΔH. Ionic properties, in particular the electronegativity of the cation (χ_C), represents one useful descriptor for ΔH. **Figure 3.11a** shows that ΔH initially decreases rapidly as χ_C increases. Subsequently, ΔH plateaus for $\chi_C > \sim 1.2$. This behavior can be traced to the ionicity of the cation-hydroxide bond. Ionicity is related to the difference in the electronegativity between a cation and anion (in this case, a hydroxide). Typically, a bond is

considered ionic if the electronegativity difference is approximately 2 or greater. Assuming an effective electronegativity of OH that is similar to that of oxygen, ~3.5, then ionic behavior is expected for χ_C < ~1.5. Indeed, this value is close to the value, χ_C = 1.2, below which large increases to ΔH are observed, **Figure 3.11a**. Thus, the onset of ionic bonding coincides with an increase in ΔH.

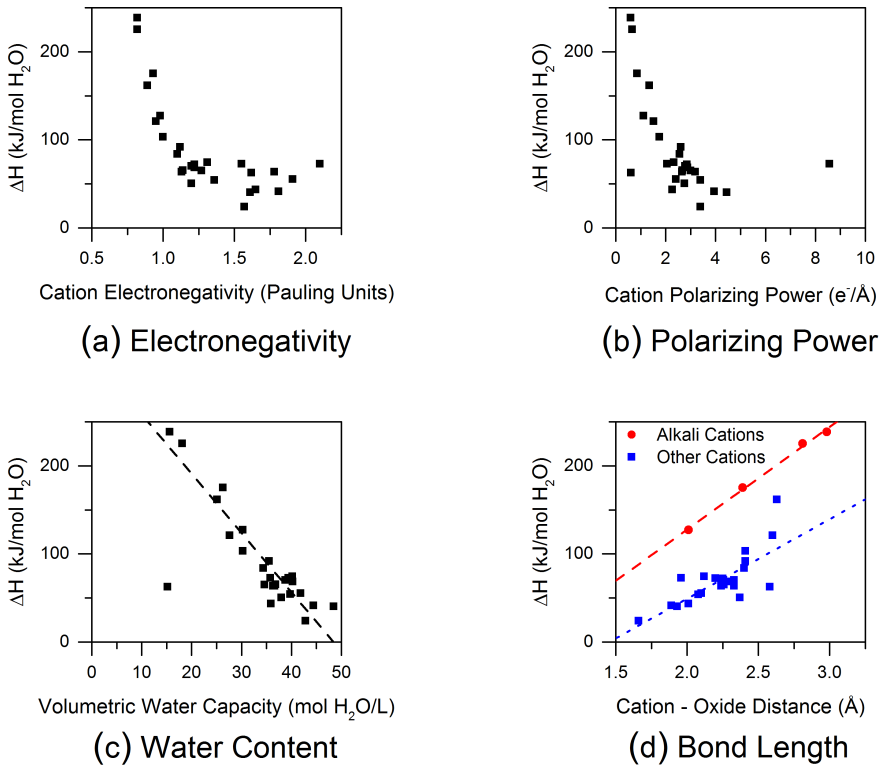

Figure 3.11 Correlations between enthalpy of dehydration in hydroxides with a) cation electronegativity [r = -0.692], b) cation polarizing power [r = -0.544] c) volumetric water capacity [r = -0.787], and d) cation-oxygen bond length in oxide [r = 0.762].

Figure 3.11b shows that ΔH decreases as the polarizing power of the cation increases. The polarizing power is given by the quotient of the cation's charge and its radius, q_c/r_c. As the polarizing power decreases, the ionicity of the cation-oxygen bond increases, according to Fajan's rules.[130,131] This correlation is reminiscent of the trend shown in **Figure 3.11a**, where ΔH decreases with increasing χ_C (equivalently, with decreasing ionicity of the hydroxide-cation bond).

While the polarizing power of the cation yields a moderate anti-correlation with ΔH (r = -0.544), a much stronger relation (r = -0.787) can be seen in **Figure 3.11c** between ΔH and n_v, the volumetric water capacity ($n_v = {}^{n}/_{V_{hyd}}$). To balance the chemical reaction associated with water storage in hydroxides, $M(OH)_{2n} \leftrightarrow MO_n + nH_2O$, n must be exactly half of the cation's (M) formal charge. Thus, n_v can be equivalently expressed as the ratio of half the cation's charge and V_{hyd}. This ratio is reminiscent of the definition of polarizing power (q_c/r_c), as V_{hyd} is correlated with the cation radius, r_C. Thus, n_v is a useful descriptor for ΔH in hydroxides, with the correlation reflecting the ionicity of the cation/hydroxide bond.

Figure 3.11d shows that ΔH for hydroxides is also correlated (r = 0.762) with crystallographic properties, such as the cation-oxygen distance in the oxide, $d_{C\text{-}O}$. More specifically, ΔH increases with $d_{C\text{-}O}$, with most of the hydroxides showing a single linear trend between ΔH and $d_{C\text{-}O}$. The four hydroxides with alkali cations (Li^+, Na^+, K^+, Rb^+), appear to exhibit a separate, but still linear trend, with larger ΔH values. These linear trends can be explained in terms of the electronegativity of the cation, χ_C. Cations with smaller χ_C are more likely to be oxidized and tend to have larger ionic radii. Naturally, a larger cationic radius is correlated with a larger $d_{C\text{-}O}$ (r = 0.957). As a result, $d_{C\text{-}O}$ exhibits an anti-correlation with χ_C (r = -0.685). Thus, smaller χ_C implies both a larger $d_{C\text{-}O}$ as well as larger ΔH. Regarding the alkali metal cations (red data in **Figure 3.11d**), we note that these cations tend to have smaller χ_C than other cations with similar radii. As such, the alkali hydroxides have generally larger ΔH compared to the other hydroxides with similar $d_{C\text{-}O}$.

Returning to **Figure 3.9b**, it is evident that the energy densities and $n\Delta H$ for hydroxides do not exhibit extremely strong correlations ($|r| < 0.8$) with any of the elementary properties examined

here. The strongest relation amongst this group is between *GED* and the density of the oxide, ρ_{ox} (r = -0.768). This relationship is plausible since $GED = n\Delta H/(\rho_{hyd}V_{hyd})$, where ρ_{hyd} is the density of the hydroxide. A larger ρ_{ox} generally corresponds to a larger ρ_{hyd} (r = 0.937), resulting in a lower *GED*. Another prominent correlation is between $n\Delta H$ and the volume of the hydroxide (r = 0.753). This trend occurs because a larger volume of the hydroxide is correlated with larger molar water content, n, and/or cationic radius. (Larger n leads to larger volume due to more hydroxide anions in the unit cell.) Higher water content naturally increases $n\Delta H$, and larger cationic radius is correlated with a smaller electronegativity (discussed previously), leading to an increased ΔH.

3.3.4 Design Rules

The trends revealed by the preceding correlation analyses suggest the following design rules for maximizing the performance of hydration-based TES materials.

- Enthalpy of dehydration: In salt hydrates, the total enthalpy, $n\Delta H$, correlates linearly with water capacity: $n\Delta H$ can be increased by increasing the number of water molecules, n, stored in the hydrate unit cell. In hydroxides, the thermodynamics are largely determined by the ionicity of the cation-hydroxide bond. Thus, ΔH can be increased by selecting cations having smaller electronegativity, lower polarizing power, larger ionic radius, and/or smaller volumetric water capacity.
- Operating temperature: The turning temperature, T_{turn}, is determined by the thermodynamics of hydration ($T_{turn} = {}^{\Delta H}/_{\Delta S}$). Therefore, T_{turn} can be tuned via the same chemical features that influence ΔH. This tuning can be achieved in hydroxides, for example, by cation substitution.

- Energy density: Maximizing *GED* in salt hydrates can be achieved by identifying compounds having high gravimetric water capacity. In hydroxides, compounds having smaller densities maximize *GED*. *VED* (= $n_v \Delta H$) can be maximized in the hydrates by maximizing the volumetric water capacity. In hydroxides, a moderate volumetric water capacity ($n_v \sim 24$ mol H_2O/L) is desirable (as achieved, for example, in NaOH, where n_v = 26.3), as it optimizes both n_v and ΔH.

3.4 Conclusions

Hydration reactions have demonstrated the potential to reversibly store heat with high energy densities, making them promising candidates for TES. The present study aims to accelerate the development of TES systems by predicting the performance of a large database of mostly-overlooked hydration reactions. In total, 265 reactions were screened using density functional theory calculations; more than half of these reactions appear to be new to the TES literature. Out of these candidates, the most promising reactions were identified in three distinct temperature ranges. These include: $CuBr_2 \bullet 4H_2O$ for low temperatures, $CrF_3 \bullet 9H_2O$ for medium temperatures, and NaOH for high temperatures.

Correlations linking TES performance with dozens of chemical features for hydrates and hydroxides were quantified using a Pearson correlation matrix. These analyses revealed several trends involving the thermodynamics of hydration. In salt hydrates, the thermodynamics depend strongly on the water capacity of the hydrate. In hydroxides, thermodynamic properties are largely determined by the ionicity of the cation-hydroxide bond, which is in turn influenced by the cation's electronegativity and polarizing power. Based on these correlations, design rules for hydration-based TES systems were proposed.

Chapter 4 Screening of Hypothetical Halide Salt Hydrates for Thermal Energy Storage

4.1 Introduction

As discussed earlier, literature reports focusing on the discovery/evaluation of salt hydrates for TES have been limited in scale, with only a few hundred compounds explored thus far. In contrast, 10^{5-6} ion-insertion compounds have been explored as cathode materials in batteries[132] or as adsorbents for gas capture/storage.[133] It is therefore reasonable to hypothesize that many promising salt hydrates may exist, but have not yet been synthesized. We refer to these new materials as 'hypothetical hydrates.'

Hypothetical materials based on new compositions can be generated from the crystal structures of known materials using atomic substitution. Subsequently, first-principles calculations can assess their thermodynamic stability. This approach has been applied to hydrides,[125] borohydrides,[134] anti-perovskites,[135] metal organic frameworks,[136,137] 18-electron ABX compositions,[119] and cubic perovskites.[121] Additionally, first-principles calculations have shown good agreement with experiment in predicting reaction enthalpies. It was shown in Chapter 3 that the uncertainty of density functional theory calculations with respect to experiment in calculating the enthalpies of dehydration for salt hydrates is ~10 kJ/mol H_2O, which is comparable to the uncertainty between experiments (7.5 kJ/mol H_2O).

Building on the computational protocol developed in Chapter 3, this study characterizes new hypothetical hydrates for their utility in TES. Adopting the crystal structures of known salt hydrates as templates, atomic substitution was used to generate 5,292 hypothetical hydrates. The energy densities, operating temperatures, and stabilities of the hydrates were evaluated using first-

principles calculations. Several new and stable TES materials with class-leading energy densities were identified, with operating temperatures suitable for domestic heating and intermediate temperature applications. Additionally, a numerical model[138] was used to project the system energy densities offered by these new materials when deployed within a recent thermochemical heat storage prototype.[49,138,139] Several hydrates were found to surpass the U.S. Department of Energy's system energy density target of 200 kWh/m^3.[140]

Subsequently, machine learning models were trained on the resulting database of computed hydrate properties and used to reveal non-linear structure-property-performance trends related to the thermodynamics of hydration. These analyses reveal that optimal performance is obtained for salt hydrates consisting of cations with small electronegativities and with crystal structures having small cation-water distances. In total, the new materials and design rules identified here are expected to accelerate the adoption of TES systems.

4.2 Methodology

4.2.1 Screening Method

Figure 4.1 shows the procedure used to identify promising TES reactions involving hypothetical hydrates (HH). This procedure was adapted from one used in Chapter 3, which focused on experimentally-known salt hydrates. The main components of the adapted procedure are described below.

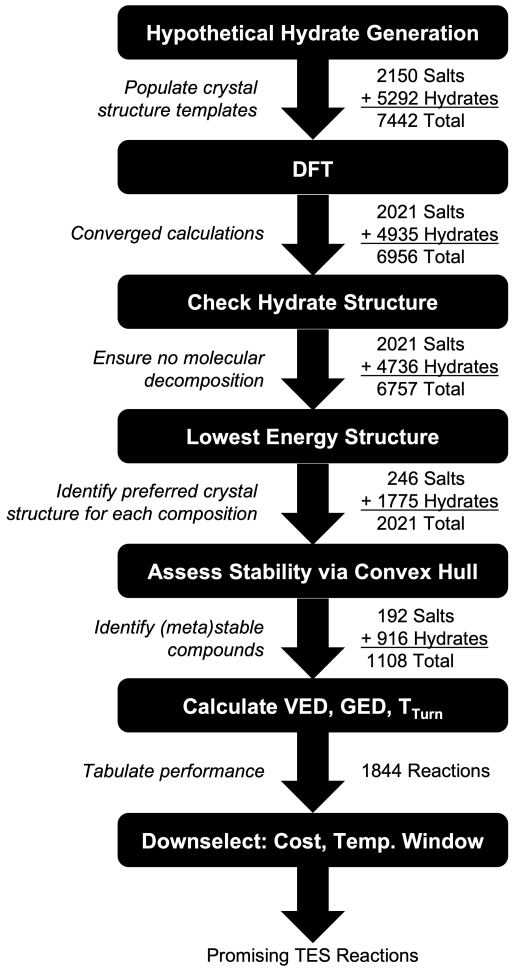

Figure 4.1 Screening procedure for identifying promising hypothetical salt hydrates.

Generation of Hypothetical Salt Hydrates. As an initial step, experimentally-known metal halide hydrates were identified within the ICSD.[103] This search yielded 76 distinct hydrate crystal structures. These structures were adopted as templates for the generation of HH. A full list of the templates can be found in **Table 4.1**. These templates were further divided into four categories according to the oxidation state of the cation from the hydrate composition that had populated the structure template. This approach is equivalent to categorizing the crystal structures as hydrates of binary salts, MX, MX_2, MX_3, or MX_4, where M represents a (metal) cation and X a (monovalent) halogen anion. Thus, in order to maintain charge neutrality, the structures of hydrates of MX_n salts

must be populated by *n*-valent cations, where *n* refers to a mono-, di-, tri-, or tetra-valent oxidation state.

Table 4.1 Complete list of the 76 experimental crystal structures from the ICSD[103] used as crystal structure templates for generation of hypothetical hydrates in this study. Seven apply to monovalent cations, 29 to divalent cations, 28 to trivalent cations, and 12 to tetravalent cations.

$LiCl•H_2O$	$RbF•H_2O$	$KF•2H_2O$	$NaCl•2H_2O$	$NaI•2H_2O$	$LiI•3H_2O$
$KF•4H_2O$	$SrCl_2•H_2O$	$CdCl_2•H_2O$	$BaCl_2•2H_2O$	$CaCl_2•2H_2O$	$CoCl_2•2H_2O$
$HgF_2•2H_2O$	$SnCl_2•2H_2O$	$SrCl_2•2H_2O$	$SrI_2•2H_2O$	$ZnF_2•2H_2O$	$BaBr_2•2H_2O$
$CaCl_2•4H_2O$	$CdBr_2•4H_2O$	$CuBr_2•4H_2O$	$FeCl_2•4H_2O$	$FeF_2•4H_2O$	$MnCl_2•4H_2O$
$ZnF_2•4H_2O$	$BeCl_2•4H_2O$	$CaCl_2•6H_2O$	$MgCl_2•6H_2O$	$NiCl_2•6H_2O$	$CaI_2•7H_2O$
$CaI_2•8H_2O$	$MgCl_2•8H_2O$	$MgI_2•8H_2O$	$CaBr_2•9H_2O$	$MgBr_2•9H_2O$	$MgCl_2•12H_2O$
$AlF_3•H_2O$	$BF_3•H_2O$	$BiCl_3•H_2O$	$BF_3•2H_2O$	$VF_3•2H_2O$	$AlF_3•3H_2O$
$CeCl_3•3H_2O$	$InCl_3•3H_2O$	$LaCl_3•3H_2O$	$VF_3•3H_2O$	$CrF_3•3H_2O$	$FeF_3•3H_2O$
$InF_3•3H_2O$	$MnF_3•3H_2O$	$TlBr_3•4H_2O$	$VCl_3•4H_2O$	$AlCl_3•6H_2O$	$GdCl_3•6H_2O$
$VCl_3•6H_2O$	$LaCl_3•7H_2O$	$ScCl_3•7H_2O$	$HoBr_3•8H_2O$	$ScI_3•8H_2O$	$AlF_3•9H_2O$
$CrF_3•9H_2O$	$SmI_3•9H_2O$	$LuI_3•10H_2O$	$YBr_3•10H_2O$	$ZrF_4•H_2O$	$PtI_4•2H_2O$
$SnCl_4•2H_2O$	$UF_4•2H_2O$	$SnCl_4•3H_2O$	$ZrF_4•3H_2O$	$SnCl_4•4H_2O$	$PtCl_4•5H_2O$
$SnCl_4•5H_2O$	$SnCl_4•8H_2O$	$UBr_4•9H_2O$	$ThBr_4•10H_2O$		

Figure 4.2 identifies the 38 elements (corresponding to 66 ions due to multiple oxidation states) that were explored as compositional components of the HH. A total of 10 monovalent cations (Li^{1+}, Na^{1+}, K^{1+}, Rb^{1+}, Cs^{1+}, Sc^{1+}, Y^{1+}, La^{1+}, Zr^{1+}, Cu^{1+}), 21 divalent cations (Be^{2+}, Mg^{2+}, Ca^{2+}, Sr^{2+}, Ba^{2+}, La^{2+}, Ti^{2+}, Zr^{2+}, V^{2+}, Cr^{2+}, Mo^{2+}, Mn^{2+}, Fe^{2+}, Co^{2+}, Ni^{2+}, Cu^{2+}, Zn^{2+}, Si^{2+}, Ge^{2+}, Sn^{2+}, Pb^{2+}), 17 trivalent cations (Sc^{3+}, Y^{3+}, La^{3+}, Ti^{3+}, Zr^{3+}, Hf^{3+}, V^{3+}, Nb^{3+}, Ta^{3+}, Cr^{3+}, Mo^{3+}, Mn^{3+}, Fe^{3+}, Co^{3+}, Ni^{3+}, Al^{3+}, Ga^{3+}), and 14 tetravalent cations (Ti^{4+}, Zr^{4+}, Hf^{4+}, V^{4+}, Nb^{4+}, Ta^{4+}, Cr^{4+}, Mo^{4+}, W^{4+}, Mn^{4+}, Si^{4+}, Ge^{4+}, Sn^{4+}, Pb^{4+}) were selected for cation substitution. With the exception of the precious metals (which were excluded based on their high cost), the selected cations achieve a broad sampling of the periodic table. This diversity is useful in the generation of generalized ML models, as discussed below. In addition to these cation substitutions, 4 halogens (F^-, Cl^-, Br^-, I^-) were used for anion substitution. Accounting for all possible substitutions of cations and anions into each of the 76 hydrate templates, a total of 5292 HH were generated, as shown in **Figure 4.3**.

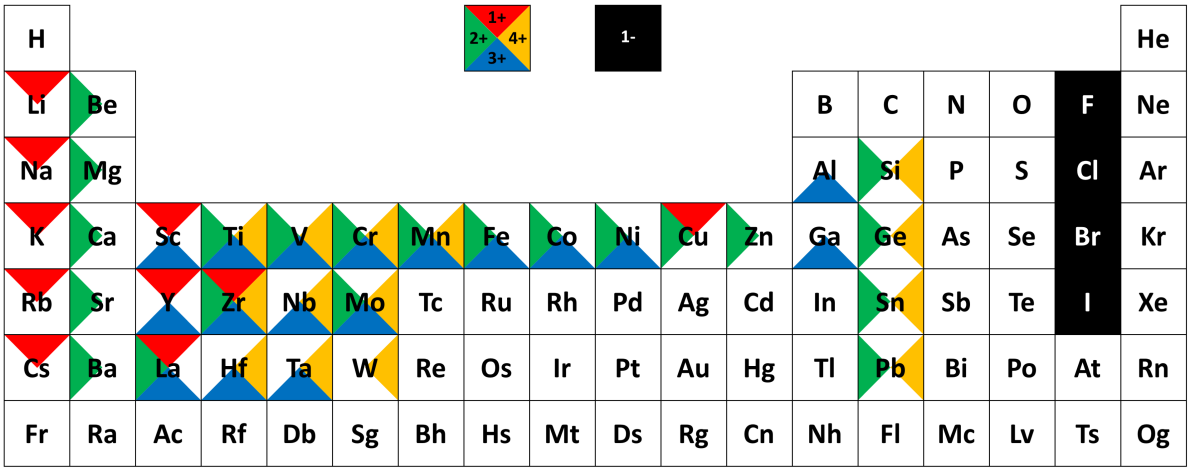

Figure 4.2 Periodic table highlighting the cations and anions used for ionic substitution into hydrate or salt crystal structure templates. The colored triangles indicate the oxidation states used for the metals.

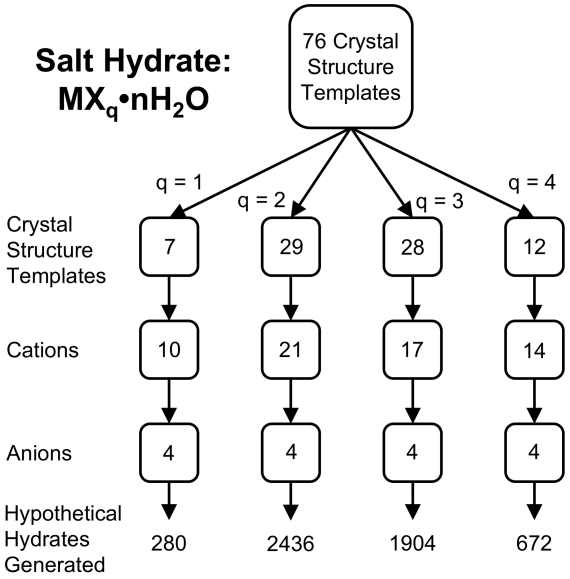

Figure 4.3 Schematic depicting generation of hypothetical hydrates via systematic variation of hydrate crystal structure, cation, and anion, constrained by the oxidation state of the cation.

To predict the performance of the HH, it is also necessary to characterize their respective anhydrous salts. When available, the crystal structure of a given salt composition was extracted from the ICSD.[103] In cases where the crystal structure of the anhydrate was not known (listed in **Table 4.2**), ionic substitution into crystal structure templates of known salts was performed, similar to the procedure used for the generation of HH. A total of 17, 37, 31, and 31 salt crystal

structures were used for MX, MX_2, MX_3, and MX_4 salts, respectively. These crystal structures are listed in **Table 4.3**. In total, 2150 experimentally known or hypothetical anhydrates were examined computationally.

Table 4.2 Complete list of the salt compositions missing from the ICSD.[103] Hypothetical crystal structure generation was performed for these compositions.

LaF	ScBr	ScF	ScI	YBr	YF	YI	ZrF	ZrI	CuI_2	$GeCl_2$	$LaCl_2$
LaF_2	$MoBr_2$	$MoCl_2$	MoF_2	$SiBr_2$	SiF_2	SiI_2	TiI_2	$ZrBr_2$	ZrF_2	$CoBr_3$	$CoCl_3$
CoI_3	FeI_3	$HfBr_3$	$HfCl_3$	HfF_3	$MnBr_3$	$MnCl_3$	MnI_3	$NbBr_3$	$NbCl_3$	$NiBr_3$	$NiCl_3$
NiI_3	$ScBr_3$	ScI_3	$TaBr_3$	$TaCl_3$	TaI_3	VBr_3	VI_3	YBr_3	ZrF_3	$CrBr_4$	$CrCl_4$
CrI_4	$HfBr_4$	$MnBr_4$	$MnCl_4$	MnI_4	$MoBr_4$	MoF_4	MoI_4	$PbBr_4$	PbI_4	$TaBr_4$	TaF_4
VBr_4	VI_4	WF_4	WI_4	$ZrBr_4$							

Table 4.3 Complete list of the 116 experimental crystal structures from the ICSD[103] used as crystal structure templates for generation of hypothetical anhydrous salts in this study. 17 correspond to monovalent cations, 37 to divalent cations, 31 to trivalent cations, and 31 to tetravalent cations.

AgCl	AuCl	AuI	BiI	CoO	CsCl	CuBr	CuCl	CuI	InCl	LaI	NaCl
TeI	TlI	ZnS – Sphalerite	ZnS – Wurtzite	ZrCl	AgF_2	$AuTe_2$	$BaCl_2$	$BeBr_2$	BeF_2	CaF_2	$CdCl_2$
CdI_2	CsI_2	$CuCl_2$	$CuZr_2$	$GeBr_2$	$HgBr_2$	$HgCl_2$	HgI_2	MoI_2	MoS_2	$MoTe_2$	$PbCl_2$
PbO_2	$PdBr_2$	$PdCl_2$	PrI_2	PtI_2	$SiCl_2$	SmF_2	SnF_2	SnI_2	$SrBr_2$	SrI_2	TaS_2
ThI_2	TiO_2	WTe_2	$YbCl_2$	$ZnBr_2$	$ZnCl_2$	$AlBr_3$	AlF_3	AlI_3	$AsBr_3$	$AuCl_3$	$BiCl_3$
BiI_3	$CrBr_3$	CsI_3	FeF_3	$GaCl_3$	LaF_3	MnF_3	$MoBr_3$	$MoCl_3$	$NdBr_3$	$PtBr_3$	PuF_3
$ReCl_3$	ReO_3	$RhBr_3$	$SbCl_3$	SbF_3	SbI_3	ScF_3	$SiCr_3$	ThI_3	TiI_3	UCl_3	YF_3
$ZrCl_3$	CrF_4	$HfCl_4$	MnF_4	$MoCl_4$	$NbCl_4$	NbI_4	$OsBr_4$	$OsCl_4$	$PbCl_4$	PdF_4	$ReCl_4$
$SeBr_4$	$SeCl_4$	$SiCl_4$	SiF_4	SnF_4	SnI_4	TaI_4	TeF_4	TeI_4	ThI_4	TiF_4	TiI_4
UBr_4	UCl_4	UF_4	WBr_4	WCl_4	XeF_4	$ZrCl_4$	ZrI_4				

DFT Calculations. The ground state energies and relaxed geometries of all 5292 HH and 2150 anhydrates (7442 total) were evaluated using density functional theory (VASP code).[93] The same computational protocol that was shown to be effective for experimentally-known salt hydrates in Chapter 3 was adopted. Spin polarized calculations were performed with a 500 eV planewave cutoff energy. Blöchl's projector augmented wave method was used to model interactions between core and valence electrons.[94,95] The crystal structure of each system was

optimized using the van der Waals aware optPBE-vdW[84–86,88] exchange-correlation functional, as well as a Monkhorst-Pack[96] k-point mesh of increasing density until convergence was achieved. Relaxation stopped when all atomic forces were less than 0.02 eV/Å. Subsequently, the ground state energy was determined (without additional relaxation) using the Perdew-Wang 91 (PW-91)[83] exchange-correlation functional. This two-step process was shown to yield good agreement with both the measured lattice constants and energetics of known hydrates (see **Figure 3.1**). A recent study confirmed that the optPBE-vdW functional was an appropriate choice for determining salt hydrate geometries.[141] Of the 7442 density functional theory (DFT) calculations attempted, 93.5% of the calculations converged, suggesting that the structure templates adopted here are reasonable initial approximations to the true structures. The resulting energies represent upper-bounds to the 'true' energies of the actual ground-state structures.

Removal of Non-Hydrates. A structural check was performed for each HH to verify that the optimized crystal structure was indeed a hydrate (i.e., that the water molecules in the HH did not dissociate). This structural check was accomplished by inspecting the local environment of the oxygen atoms to ensure that each oxygen was coordinated by two hydrogen atoms at a distance less than 1.1 Å. In this manner, 199 non-hydrates were identified; these systems were excluded from further scrutiny.

Determination of Lowest Energy Structures. As previously described, for each salt or hydrate composition several crystal structures were evaluated as possible ground-state structures. For example, for $NiF_3 \bullet 6H_2O$ the crystal structures corresponding to those of $AlCl_3 \bullet 6H_2O$, $GdCl_3 \bullet 6H_2O$, and $VCl_3 \bullet 6H_2O$ were explored. The structure with the lowest computed total energy was adopted as the best approximation to the stable crystal structure for that composition. Higher-energy structures were discarded.

Elimination of Unstable Compounds. To exclude unstable hydrates and salts, a thermodynamic filter was applied via a convex hull analysis.[119] Pymatgen[142] was used to compute the convex hull for each salt hydrate (i.e., metal, halogen, oxygen, and hydrogen) and for its associated salt. Stability was examined with respect to all solids in the Materials Project[143] that fall within the quaternary chemical space of a given hydrate. To ensure compatibility with the Materials Project database, additional single point energy calculations using the Materials Project calculation protocol were performed on all 1775 lowest energy HH structures. The free energies of 16 common gases formed between the halogens, oxygen, and hydrogen were also included in the analysis. These gases include Br_2, Cl_2O, Cl_2, ClO_2, ClO, F_2, H_2O_2, H_2, HBr, HCl, HF, HI, HOF, I_2, O_2, and OF_2. The free energies of the gases were estimated by adding an entropy term ($-T\Delta S_{gas}$) at 298 K to the energy, as done by Hummelshøj et al.[144] ΔS_{gas} was assumed to be the entropy of formation at standard conditions, as reported in the NIST-JANAF tables.[145] As done earlier in Chapter 3, unstable compounds located more than 50 meV/atom above the convex hull were removed from the analysis. 1108 stable/metastable hydrates and salts exhibited sufficient (meta)stability to warrant additional investigation.

Characterization of Reactions according to Stability, Energy Density, and Operating Temperature. Potential TES reactions were then characterized from the 1108 stable/metastable hydrates and salts. The enthalpy of dehydration (ΔH) per mole H_2O for each reaction was calculated using Equation (3.1). The volumetric and gravimetric energy densities were subsequently calculated using Equation (3.2) and Equation (3.3), respectively. Equilibrium between a salt hydrate, its dehydrated salt (or lower hydrate), and water vapor is described by[55]

$$-RT_{turn} \ln\left(\frac{p}{p_0}\right) = \Delta H - T_{turn}\Delta S \quad (4.1)$$

where p is the water vapor pressure, p_0 is atmospheric pressure (1 atm), T_{turn} is the turning temperature, ΔS is the entropy of dehydration, and R is the ideal gas constant. As done in Chapter 3, a uniform ΔS of 146 J/(K mol H_2O) was assumed. This value is based on the average entropy change reported in Glasser's salt hydrate database,[67,76] and assumes additivity and uniformity of the entropy of dehydration. When p = 1 atm., Equation (4.1) simplifies to

$$T_{turn} = \frac{\Delta H}{\Delta S} \quad (4.2)$$

which defines T_{turn} and allows its use as a simple metric to classify reactions according to their equilibrium temperature.[33,34] Additional details about salt hydration thermodynamics can be found in previous studies.[55,67]

In many cases, an overall hydration reaction will proceed as a sequence of two or more reactions involving intermediate hydrates (e.g., the hydration of $MgCl_2$).[38] These multiple step reactions exhibit multiple turning temperatures, one for each reaction step. The full range of turning temperatures must be accessed to access the full reaction.

The 1108 hydrates and salts whose energetics were less than 50 meV/atom above the convex hull were divided into four stability categories: those that are stable (i.e., on the hull), and those that were within 10, 25, and 50 meV of the hull, respectively. Reactions involving these hydrates and salts were similarly categorized: for example, for a reaction categorized as being within 10 meV of the hull, all reactants, products, and intermediates (if present) must also be within 10 meV of the hull.

Based on these criteria, a total of 238, 742, 1393, and 1844 reactions were characterized (based on the stability of their products and reactants) for stability thresholds of 0, <10, <25, and

<50 meV/atom, respectively. Based on their turning temperatures, these reactions were further categorized into one of several temperature categories (<50°C, 50–100°C, 100–200°C, 200–300°C, 300–450°C, 450–600°C, >600°C, and 'wide temperature window'). All reactions are detailed in Appendix C. Multi-step reactions are categorized as follows: For example, the hydration of $AlCl_3$ to $AlCl_3 \bullet 9H_2O$ occurs in 2 steps, with T_{turn} = 202°C for the nonahydrate-hexahydrate reaction, and T_{turn} = 361°C for the hexahydrate-salt reaction. Since the average T_{turn} is 282°C and all temperatures fall within two adjacent temperature categories (i.e., 200–300°C and 300–450°C), this reaction is classified according to the average T_{turn} (i.e., 200–300°C). In contrast, the overall reaction $AlBr_3$ / $AlBr_3 \bullet 9H_2O$ occurs via a hexahydrate intermediate with respective T_{turn} values of 183°C and 387°C. This reaction is labeled as having a 'wide temperature window' since the T_{turn} are not in adjacent temperature categories. More details about the temperature classification scheme can be found in Chapter 3.

Identify Promising Reactions. Of the candidate reactions, several promising reactions were identified for various stability criteria. Criteria for cost and temperature window (see Chapter 3) were used to eliminate hydrates that are expensive and reactions that require a very large temperature window (i.e., > 50°C).

4.2.2 Machine Learning

As shown by Equations (3.2), (3.3), (4.1), and (4.2), ΔH is a critical parameter for the TES performance of salt hydrates. Thus, models that can accurately and efficiently predict ΔH for these materials would be helpful. More importantly, these models can be used to establish design rules for hydrates by quantifying the impact of various input data (i.e., 'features') upon ΔH. Toward these goals, machine learning (ML) models were trained to predict ΔH using the DFT-

generated data for the 4736 HH. Here, ΔH corresponds to that of the complete dehydration reaction, resulting in the formation of the anhydrous salt and water vapor.

Four ML algorithms were examined: ridge regression,[98] k-nearest neighbors (k-NN),[99] support vector machine regression (SVM),[100] and random forest regression (RF).[101] All algorithms except for k-NN were used as implemented in Matlab.[146] The k-NN algorithm was based on an in-house Matlab code. For each algorithm, a feature selection process was performed. The main components of the process (**Figure 4.4**) are described below, including four ML 'steps'.

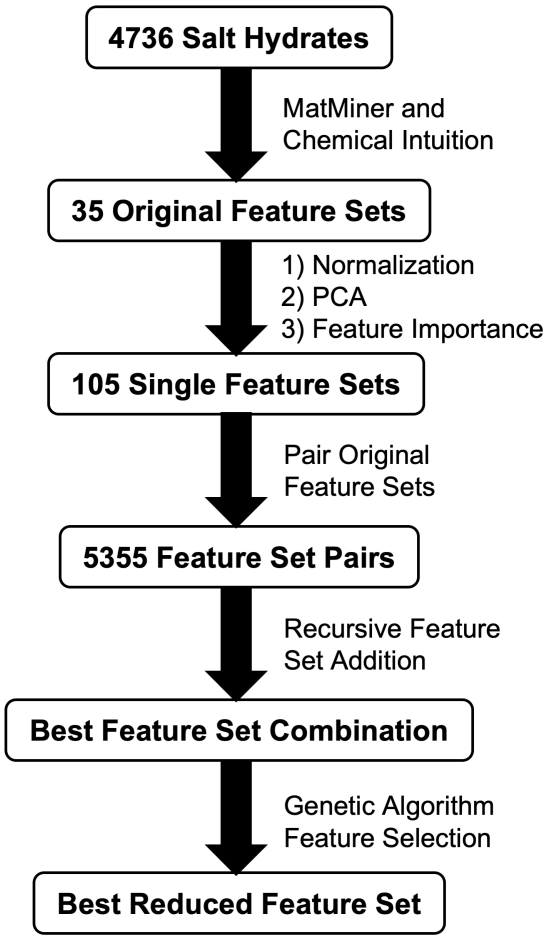

Figure 4.4 Schematic depicting the screening procedure for machine learning models.

Model Evaluation. For each ML model, 50% of the HH DFT data was randomly withheld as an unseen test set. This set was used to evaluate the performance of the model. Another

randomized 10% of the data was used as a validation set to optimize a given model's hyperparameters, which can be found in **Table 4.4**. To evaluate the test error of the model, many iterations of train/validation/test set splits were performed (minimum of five) until the standard deviation of the mean test error was no larger than 0.1 kJ/mol H_2O.

Table 4.4 ML algorithms are listed with their relevant hyperparameters, as well as the hyperparameter values tested during model validation.

Algorithm	Hyperparameters (Range of Values)
Ridge Reg.	Alpha (10^{-6}, 10^{-5}, …, 10^{6})
k-NN	k (1, 2, …, 20), weight (uniform, distance), power (1, 2)
SVM	Kernel (Gaussian, linear, polynomial)
RF	Trees (200)

Feature Set Generation. 35 feature sets (hereafter referred to as original feature sets) were explored to determine the set(s) that yielded the most accurate predictions, as well as the most interpretable trends. Of these, 33 were based on composition and structure featurizers from Matminer,[147] another employed a simple categorical representation of the HH, and the last was a custom feature set developed using the authors' chemical intuition. The categorical representation used three categories of features that describe the HH: the identity of the cation, the identity of the anion, and the identity of its crystal structure template. A one hot encoding scheme was used to represent the three categorical features, resulting in 142 Boolean features (62 cations + 4 anions + 76 structures). The 'chemical intuition' original feature set contained 18 features (listed in **Table 4.5**), including fundamental cation and anion features (e.g., ionic radius, electronegativity, mass) as well as structural features of the computed crystal structure (e.g., nearest neighbor distances, coordination numbers). The 35 original feature sets are summarized in **Table 4.6**.

Table 4.5 Description of the 18 salt hydrate features from the authors' chemical intuition. Structural features were computed from the DFT-optimized crystal structures of the hypothetical hydrates.

Feature	Units	Range	Description
n	-	1–12	Hydrate number (i.e., for $MgCl_2 \cdot 6H_2O$, n = 6)
MM_{cat}	g/mol	6.94–207.2	Molar mass of the cation[148]

r_{cat}	Å	0.54–1.81	Ionic radius of cation assuming coordination number of 6[149]
χ_{cat}	Pauling units	0.79–2.36	Electronegativity of cation according to Pauling Scale[148]
Z_{cat}	e	1–4	Formal charge of cation
$Z_{eff,cat}$	e	1.3–7.85	Effective nuclear charge of cation
PP_{cat}	e/Å	0.55–7.41	Polarizing power of the cation, equal to the formal charge divided by the ionic radius[149]
$e_{d,cat}$	e	0–10	Number of d orbital electrons in cation
CN_{cat}	-	4–8	Preferred coordination number of the cation[150] (assume CN_{cat} = 6 for cations missing from reference)
MM_{an}	g/mol	19–126.9	Molar mass of the anion[148]
r_{an}	Å	1.19–2.06	Ionic radius of anion assuming coordination number of 6[149]
χ_{an}	Pauling units	2.66–3.98	Electronegativity of anion according to Pauling Scale[148]
r_{CW}	Å	1.55–4.77	Distance between nearest neighbor cations and water molecules in the hydrate
CN_{CW}	-	1–10	Number of nearest neighbor water molecules coordinating the cation in the hydrate
r_{CA}	Å	1.52–5.68	Distance between nearest neighbor cations and anions in the hydrate
CN_{CA}	-	1–16	Number of nearest neighbor anions coordinating the cation in the hydrate
r_{CC}	Å	2.17–8.74	Distance between nearest neighbor cations in the hydrate
CN_{CC}	-	1–12	Number of nearest neighbor cations coordinating the cation in the hydrate

Table 4.6 List of all 35 original feature sets used in ML screening. The first two feature sets were designed by the authors while the others were implemented from Matminer and are listed by their class names.[147] Note that for the site featurizers, the mean, standard deviation, minimum, maximum, average deviation, range, and mode were used as features. Feature sets that are used in the predictive model are indicated by an X, while feature sets used in the interpretable model are indicated by a *.

Feature Set	SVM	RF	k-NN	Ridge
Salt Hydrate Ionic and Structural Features		X*	X*	
Salt Hydrate Categorical Representation	X*	X		X
composition.ElementProperty (matminer)		X		
composition.ElementProperty (matscholar_el)				X*
composition.ElementProperty (megnet_el)	X			
composition.Stoichiometry			X	
site.GaussianSymmFunc		X		
structure.BondFractions				X
structure.MaximumPackingEfficiency	X			
structure.OrbitalFieldMatrix		X	X	X
structure.StructuralHeterogeneity			X	
composition.AtomicOrbitals				
composition.BandCenter				
composition.ElementFraction				
composition.ElementProperty (magpie)				
composition.IonProperty				
composition.Meredig				

composition.OxidationStates
composition.TMetalFraction
composition.ValenceOrbital
composition.YangSolidSolution
site.CoordinationNumber
site.ElementalProperty
site.LocalPropertyDifference
site.VoronoiFingerprint
structure.ChemicalOrdering
structure.CoulombMatrix
structure.DensityFeatures
structure.Dimensionality
structure.EwaldEnergy
structure.GlobalSymmetryFeatures
structure. JarvisCFID
structure.SineCoulombMatrix
structure.StructuralComplexity
structure.XRDPowderPattern

Step 1: Feature Set Representations. Each original feature set (i.e., one of the 35 feature sets collected from Matminer[147] or created from chemical intuition) was represented in 3 ways, resulting in a total of 105 distinct feature set representations available to each ML algorithm. First, a model was trained with and without normalizing the data. (Normalized data has a mean of 0 and a standard deviation of 1.) Whichever approach had the lower test error was adopted as the first representation for that original feature set. For the second representation, Principal Component Analysis[151] was performed on the original feature set. Seven models were then trained on subsets of the principal components representing 5%, 10%, 25%, 50%, 75%, 90%, and 95% of the explained variance. The principal component subset with the lowest test error was selected for the second representation, favoring lower percentages of the explained variance in the case of ties. For the third representation, seven models were trained on the subset of the 5%, 10%, 25%, 50%, 75%, 90%, and 95% most important features, as determined by the magnitude of the coefficients from ordinary least squares regression performed on the normalized original feature set to predict ΔH. The feature subset with the lowest test error (favoring small feature sets in the case of ties) was

chosen for the third representation. In all cases, a feature set was considered to have a lower test error than another if the test error of the former was at least one standard deviation of the mean (0.1 kJ/mol H_2O) lower than the latter. The end result of this step was 105 feature representations of the 35 original feature sets that were combined and tuned in subsequent steps for higher accuracy.

Step 2: Feature Set Combination. A search for the best feature set pair was performed. Here, a feature set pair is defined as the combination of 2 of the 35 original feature sets, resulting in a total of 595 unique feature set pairs. Accounting for the 3^2 ways to represent each feature set yields a total of 5355 sets. ML models were trained on all of these feature sets and the top performing models were identified. The best models demonstrated both high accuracy (within two standard deviations of the mean of the lowest test error) as well as significant improvement compared to models developed for their constituent feature subsets (at least two standard deviations of the mean). In some cases, one of the 595 unique feature set pairs would have multiple representations appear among the most accurate models. In such cases, redundant entries were removed. While it would be computationally expensive to systematically test every combination of three original feature sets (6545 unique feature triplets x 3^3 representations = 176715 models), the best triplets likely are combinations of one of the top performing feature set pairs with another feature set. Thus, each top performing feature pair was systematically combined with each of the remaining feature set representations. After these models were evaluated, top performing feature set triplets were identified in the same way. This process was repeated, each time adding another feature set, until the best test error converged.

Step 3: Genetic Algorithm Feature Selection. A genetic algorithm[152] (GA), as implemented in Matlab,[153] was used to perform feature selection on the most accurate feature set. Use of a GA

to select the best features has been employed in previous studies.[154,155] The GA created multiple generations of populations of ML models. Each individual in the GA population was a ML model trained using a distinct subset of features. The fitness of each individual was the test error. Each generation consisted of 100 individuals (i.e., ML models trained on a subset of features). For each generation after the first, the 5 best individuals were kept from the previous generation, while the other 95 were generated (76 from scattered crossover and 19 from Gaussian mutation) using a stochastic uniform selection process for the parents. The genetic algorithm was terminated when convergence was reached (i.e., when the relative change in the optimal test error is less than 1e-6 over 50 generations) or after 200 generations, whichever occurred first.

Step 4: Evaluating the Final Model. The final model for each of the four ML algorithms was trained on the optimal feature set identified for that algorithm. Unlike the previous model evaluations during feature selection, which essentially used a 2-fold cross validation split to expedite the speed of statistical convergence, the test accuracy of the final model was evaluated using 10-fold cross validation (i.e., 10% test set). This 10-fold cross validation was done to estimate the model's accuracy when trained on nearly all of the dataset.

4.3 Results and Discussion

4.3.1 Materials Project Compatibility

In order to compare the energies of the HH and the materials in the Materials Project,[143] single point energy calculations were performed on all 1775 low energy salt hydrate structures, as well as 43 hypothetical salt structures not found in the Materials Project, using input files generated by Pymatgen to ensure compatibility. Energies for the gas molecules were computed in a similar way, although the ionic positions were allowed to relax during the calculation. Energy corrections were then applied in accordance with Wang et al.[156] to maintain compatibility with the Materials

Project database, with the exception of transition metal oxides. The Materials Project classifies a transition metal oxide as a compound having both a particular transition metal (V, Cr, Mn, Fe, Co, Ni, W, Mo) and oxygen in the composition. In this case, the Materials Project protocol specifies that GGA+U calculations should be performed and a correction factor applied for the specific transition metal. In most cases, this leads to improved accuracy. However, this led to systematic errors for salt hydrates containing transition metals. Although oxygen is present in the water molecule, the bonding of the transition metal in a salt hydrate is chemically distinct from that in a transition metal oxide: the former possesses coordinate covalent bonds to the water, while in the latter polar covalent bonds link the transition metal and the oxygen anion. While GGA+U calculations may potentially increase the accuracy of the calculation, the correction factor to make GGA+U calculations compatible with GGA calculations is not appropriate for salt hydrates as it was fit only from data of actual transition metal oxides (and not to hydrates).

To demonstrate that standard GGA calculations perform better than GGA+U calculations with the existing corrections, a comparison was made using the enthalpy of dehydration for the 74 salt hydrates found both in the present study and the Materials Project database. Experimental data is available for 42 of these hydrates.[35,55] While the hydrates containing the relevant transition metals would be classified as "transition metal oxides" by the Materials Project, the respective anhydrous salts would not, as they lack water molecules. Therefore, the effect of the transition metal oxide treatment will be reflected in the enthalpy.

Of the 74 hydrates present in the current study and in the Materials Project, 23 contained relevant transition metals while 51 did not. Among the 51 hydrates where the Materials Project did not apply the transition metal oxide scheme, the calculated enthalpies of dehydration differed by an average of 9.5 kJ/mol H_2O. However, the disagreement between this study and the Materials

Project doubled to 19.6 kJ/mol H_2O among the 23 transition metal hydrates. This demonstrates that greater disagreement occurs between the two DFT protocols for the transition metal hydrates. To determine which protocol was more accurate, the 42 hydrates with experimental data were compared. Among these 42 hydrates, 12 contained relevant transition metals while 30 did not. The Materials Project calculated enthalpies of dehydration differed from experiment by 10.4 kJ/mol H_2O and 21.9 kJ/mol H_2O for non-transition metal hydrates and transition metal hydrates respectively. This demonstrates that the Materials Project protocol for transition metal oxides is less accurate for transition metal salt hydrates as the error is double that of non-transition metal salt hydrates. In contrast, the present study's calculations more closely matched experimental data, with errors of 5.0 kJ/mol H_2O for non-transition metal hydrates and 5.2 kJ/mol H_2O for transition metal hydrates. This demonstrates that it is more appropriate to perform GGA calculations for transition metal hydrates without +U and energy corrections. It also validates the computational protocol used for calculating the enthalpy of dehydration of salt hydrates developed in Chapter 3.

As a result, transition metal salt hydrates were calculated using standard GGA calculations without correction, in contrast to the Materials Project protocol. Furthermore, salt hydrate entries in the Materials Project database that utilized this correction were omitted from the stability analysis.

Additionally, the energy of ice in the Materials Project was adjusted to match the experimental sublimation enthalpy, ΔH_{subl} = 51.1 kJ/mol H_2O. Using the authors' preferred DFT protocol (i.e., using PW-91 to calculate the energy), ΔH_{subl} = 67.1 kJ/mol H_2O. This value is similar to that obtained with the Materials Project protocol, ΔH_{subl} = 64.3 kJ/mol H_2O. The discrepancy between the calculated and experimental ΔH_{subl} is problematic for the stability analysis of salt hydrates. A salt hydrate whose ΔH is less than ΔH_{subl} will be metastable with respect to a mixture

of ice and the dehydrated phase. This metastability is why experimentally known salt hydrates generally do not exhibit ΔH less than ~50 kJ/mol H_2O. However, if this threshold for ΔH is artificially raised to 64–67 kJ/mol H_2O, many experimentally-known hydrates are incorrectly predicted to be metastable. As such, the energy of the ice phase found in the Materials Project was adjusted to be 51.1 kJ/mol H_2O lower in energy than that of water vapor.

The stability of each hydrate was then calculated using the convex hull. Twenty experimentally-known hydrates with existing entries in the Materials Project database were found to have slightly lower energies (a few meV/atom) than those generated by the authors' structural relaxation procedure. In these cases, the lower energy models were adopted.

4.3.2 Screening Results

Using four different stability criteria, **Figure 4.5** plots the (de)hydration reactions according to their *VED*, *GED*, and temperature. **Figure 4.5a** illustrates the 238 reactions predicted to lie on the convex hull. **Figure 4.5b–d** are similar to 4a, but relax the stability criterion to show all reactions (including those in stricter stability categories) within 10 meV/atom (742 reactions), 25 meV/atom (1393 reactions), and 50 meV/atom (1844 reactions) of the convex hull, respectively. For each stability criterion in **Figure 4.5**, the most promising reaction in terms of energy density, cost, and temperature window is highlighted for each temperature category. All reactions are summarized in Appendix C.

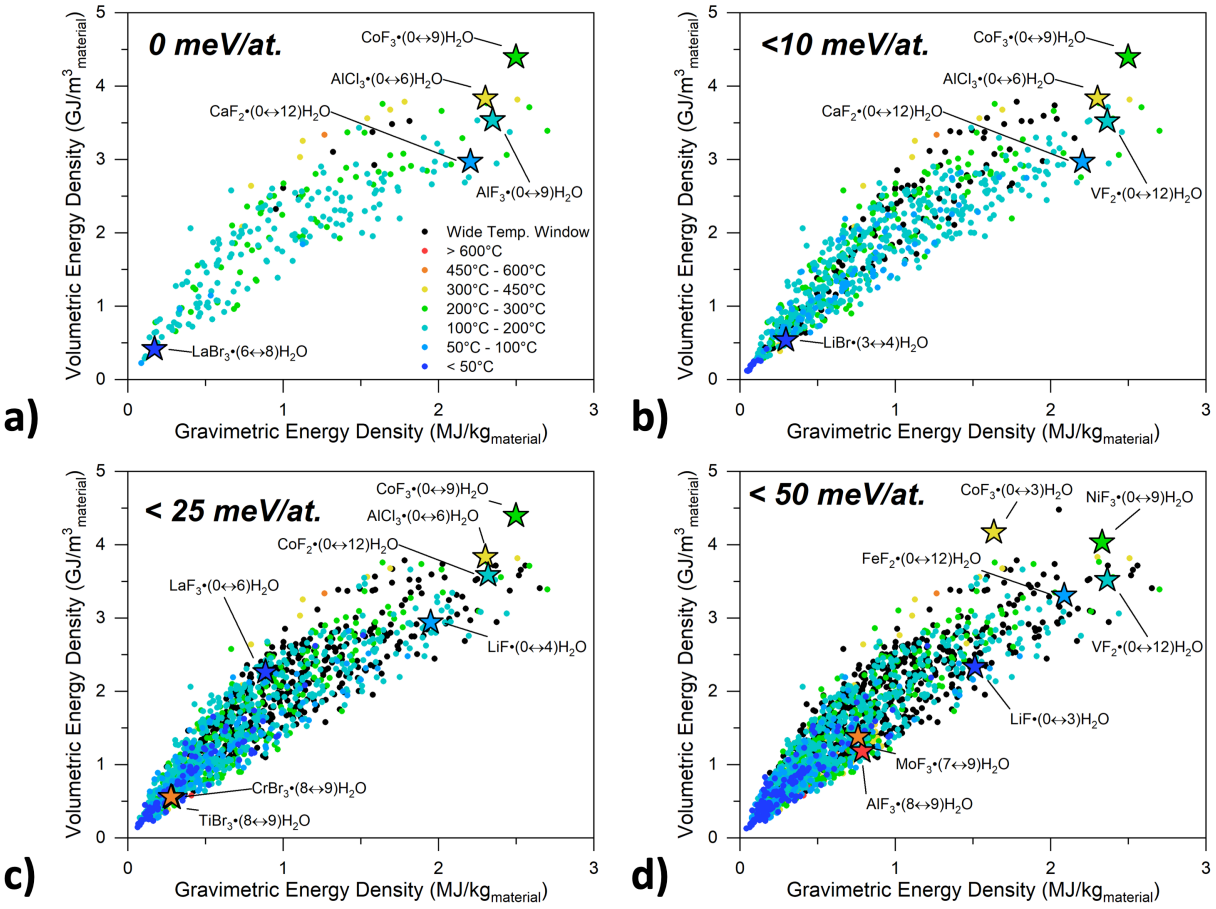

Figure 4.5 Volumetric energy density, gravimetric energy density, and temperature category for a) the 238 reactions predicted to lie on the convex hull, b) 742 reactions that are predicted to be within 10 meV/atom of the convex hull, c) the 1393 reactions predicted to be within 25 meV/atom of the convex hull, and d) 1844 reactions that are predicted to be within 50 meV/atom of the convex hull Promising reactions are shown as stars.

While no promising reactions were found for temperatures above 450°C for stricter stability criteria (i.e., on the convex hull and < 10 meV/atom), relaxing these criteria resulted in the emergence of additional promising reactions at high temperatures. Similarly, for reactions below 50°C, relaxing the criteria resulted in the addition of several reactions with significantly larger energy densities. For intermediate temperatures between 50–450°C, more relaxed stability criteria did not significantly expand the number of promising reactions. In general, relaxing the stability criteria increased the number of intermediate hydrates that were considered 'stable'. The presence of more intermediate hydrates results in more reaction steps, leading to wider temperature

windows. In some cases, the increased temperature windows disqualified some reactions that were considered promising using stricter stability criteria.

Table 4.7 summarizes 12 promising reactions identified by this screening using stricter stability criteria (i.e., on the convex hull and < 10 meV/atom). The reactions are categorized according to their predicted turning temperatures, with additional details provided for each reaction regarding T_{turn}, energy density, and stability. Regarding stability, the table includes predictions of the distance to the convex hull, as well as the expected decomposition reaction, if one is predicted to occur. Finally, **Table 4.7** indicates whether the hypothetical reaction is new to the TES literature, to the best of the authors' knowledge. **Table 4.8** shows promising hydrates using relaxed stability criteria (e.g., 25 meV/atom and 50 meV/atom).

Table 4.7 Details of promising salt (de)hydration reactions.

Temperature Category	Reaction	T_{turn} (°C)	GED (MJ/kg)	VED (GJ/m^3)	Dist. To Conv. Hull (meV/atom)	Decomposition Reaction	New to TES
< 50°C	$LaBr_3$•(6↔8)H_2O	32	0.17	0.42	0	-	Novel
	LiBr•(3↔4)H_2O	48	0.30	0.54	6.9	LiBr•4H_2O → LiBr•2H_2O + 2$H_2O_{(s)}$	Novel
50–100°C	CaF_2•(0↔12)H_2O	97	2.20	2.97	0	-	Novel
	SrF_2•(0↔12)H_2O	54 & 94	1.84	2.75	4.0	SrF_2•12H_2O → SrF_2 + 12$H_2O_{(s)}$	Novel
	SnF_2•(0↔12)H_2O	73 & 84 & 115	1.67	2.76	7.8	SnF_2•12H_2O → SnF_2•2H_2O + 10$H_2O_{(s)}$	Novel
100–200°C	AlF_3•(0↔9)H_2O	156 & 190	2.35	3.54	0	-	Chapter 3
	VF_2•(0↔12)H_2O	139	2.36	3.52	0	-	Novel
	MgF_2•(0↔12)H_2O	116 & 121	2.46	3.38	0	-	Novel
200–300°C	CoF_3•(0↔9)H_2O	256	2.50	4.40	0	-	Novel
	MoF_3•(0↔9)H_2O	211	2.02	3.66	0	-	Novel
300–450°C	$AlCl_3$•(0↔6)H_2O	361	2.30	3.83	0	-	Deutsch et al.[35]

	$AlBr_3•(0↔6)H_2O$	387	1.54	3.56	0	-	N'tsoukpoe et al.[3]

Table 4.8 Details of promising salt (de)hydration reactions with relaxed stability criteria (i.e., less than 50 meV/atom above the convex hull).

Temperature Category	Reaction	T_{turn} (°C)	GED (MJ/kg)	VED (GJ/m^3)	Dist. To Conv. Hull (meV/atom)	Decomposition Reaction	New to TES
< 50°C	$LaF_3•(0↔6)H_2O$	28 & 40	0.89	2.26	24.6	$LaF_3•6H_2O \rightarrow LaF_3 + 6H_2O_{(s)}$	Novel
	$LiF•(0↔3)H_2O$	-12 & 34	1.51	2.33	35.5	$LiF•3H_2O \rightarrow LiF + 3H_2O_{(s)}$	Novel
50–100°C	$LiF•(0↔4)H_2O$	54	1.95	2.94	15.6	$LiF•4H_2O \rightarrow LiF + 4H_2O_{(s)}$	Novel
	$FeF_2•(0↔12)H_2O$	96	2.09	3.31	38.9	$FeF_2•12H_2O \rightarrow FeF_2 + 12H_2O_{(s)}$	Novel
100–200°C	$CoF_2•(0↔12)H_2O$	141	2.32	3.59	17.5	$CoF_2•12H_2O \rightarrow CoF_2 + 12H_2O_{(s)}$	Novel
	$VF_2•(0↔12)H_2O$	139	2.36	3.52	0.0	-	Novel
200–300°C	$CoF_3•(0↔9)H_2O$	256	2.50	4.40	0.0	-	Novel
	$NiF_3•(0↔9)H_2O$	220	2.33	4.03	29.3	$NiF_3•9H_2O \rightarrow NiF_2•4H_2O + H_3OF + (7/2)H_2O_{(s)} + (1/4)O_{2(g)}$	Novel
300–450°C	$AlCl_3•(0↔6)H_2O$	361	2.30	3.83	0.0	-	Deutsch et al.[35]
	$CoF_3•(0↔3)H_2O$	361	1.63	4.17	37.6	$CoF_3•3H_2O \rightarrow (4/7)CoF_2 + (3/7)CoHO_2 + (13/7)H_3OF + (1/7)O_{2(g)}$	Novel
450–600°C	$CrBr_3•(8↔9)H_2O$	590	0.28	0.56	22.3	$CrBr_3•8H_2O \rightarrow (1/9)CrBr_3 + (8/9)CrBr_3•9H_2O$	Novel
	$MoF_3•(7↔9)H_2O$	547	0.76	1.38	41.4	$MoF_3•7H_2O \rightarrow (2/9)MoF_3 + (7/9)MoF_3•9H_2O$	Novel
> 600°C	$TiBr_3•(8↔9)H_2O$	611	0.29	0.55	15.0	$TiBr_3•9H_2O \rightarrow TiO_2 + (7/4)H_9BrO_4 + (5/4)HBr_{(g)} + (1/2)H_{2(g)}$	Novel
	$AlF_3•(8↔9)H_2O$	1054	0.79	1.19	48.0	$AlF_3•8H_2O \rightarrow (1/6)AlF_3•3H_2O + (5/6)AlF_3•9H_2O$	Novel

To place the promising hypothetical hydrates in context with respect to known salt hydrates, **Figure 4.6a** compiles the most promising reactions from both known (de)hydration reactions in the literature and hypothetical hydrates from the present study. Known (de)hydration reactions are taken from the DFT calculations from Chapter 3, while the hypothetical hydrates are taken from the 742 reactions in **Figure 4.5b** (i.e., hydrates within 10 meV/atom of the convex hull). The three most promising (de)hydration reactions for each temperature category are shown. Eight new hypothetical hydrates are found to surpass the performance of known hydration reactions (Chapter 3) below 450°C.

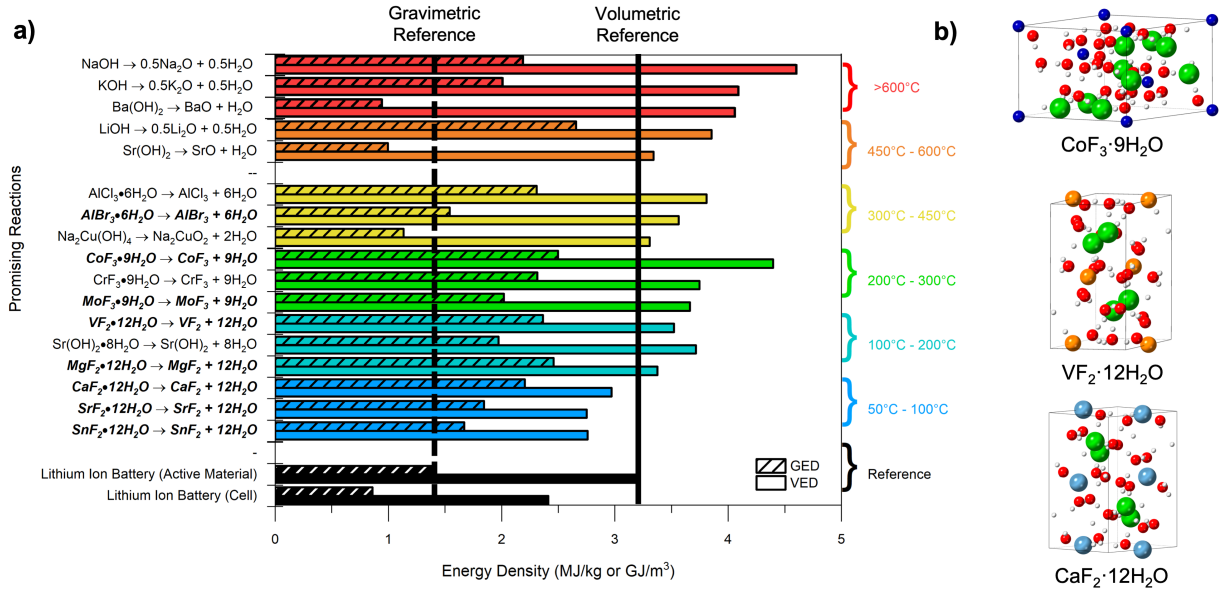

Figure 4.6 a) Energy densities for promising salt (de)hydration reactions as a function of operating temperature. The data includes known hydrates from Chapter 3 and hypothetical hydrates that are 10 meV/atom or less above the convex hull. (Hypothetical hydrates are highlighted in bold italics.) Gravimetric and volumetric energy densities are depicted by striped and solid horizontal bars, respectively. The energy densities of a lithium ion battery are shown for reference. b) Crystal structures of three promising hypothetical hydrates are shown on the right, where hydrogen atoms are shown as white, oxygen atoms as red, fluorine atoms as green, cobalt atoms as dark blue, vanadium atoms as orange, and calcium atoms as light blue.

Three novel hypothetical hydrates were found to have class-leading energy densities for their respective temperature ranges. Their crystal structures are shown in **Figure 4.6b**. For temperatures between 200–300°C, the hydration of CoF_3 to $CoF_3•9H_2O$ is predicted to occur in a

single step at 256°C with a *GED* of 2.50 MJ/kg and a *VED* of 4.40 GJ/m^3. For temperatures between 100–200°C, the hydration of VF_2 to VF_2•$12H_2O$ is predicted to occur in a single step at 139°C (*GED*: 2.36 MJ/kg, *VED*: 3.52 GJ/m^3). These energy densities are very similar to those of AlF_3, which operates via a two-step reaction at temperatures of 156 and 190°C. Finally, for temperatures between 50–100°C, the hydration of CaF_2 to CaF_2•$12H_2O$ is predicted to occur in a single step at 97°C (*GED*: 2.20 MJ/kg, *VED*: 2.97 GJ/m^3). All three hydration reactions are predicted to be stable and, to the best of the authors' knowledge, are new to TES. The energy densities of CaF_2 and CoF_3 are the largest of any reported TES reaction in their respective temperature categories.

To place the energy densities in broader context, **Figure 4.6a** also shows the energy densities of a lithium ion battery (Panasonic NCR18650B). This battery has a cell-level *GED* of 0.86 MJ/kg and a *VED* of 2.41 GJ/m^3.[157] On a materials basis, the active materials (i.e., anode and cathode) in the cell consume 12.6 cm^3 with a mass of 28.8 g, resulting in a *GED* of 1.4 MJ/kg and *VED* of 3.2 GJ/m^3.[157] Importantly, many of the promising salt hydrates (e.g., CoF_3•$9H_2O$) exceed the materials-only values of the battery. Although not an "apples to apples" comparison—batteries store electrical rather than thermal energy—these promising hydrates can generally store heat as effectively, if not more effectively, than batteries store electricity on a materials level. Furthermore, when energy is available in the form of heat, it is more efficient to store heat directly via hydration reactions than to convert the heat to electricity for storage in batteries. The disadvantage of the latter strategy is due to the low conversion inefficiencies of thermoelectric generators, which transform heat to electriticy with an efficiency of only 5–15%.[158,159] Finally, while Li-ion batteries operate most efficiently near room temperature, some salt hydrates can operate at moderately high temperatures (i.e., 200–450°C).

Figure 4.7 illustrates the calculated quaternary phase diagrams for three of the promising hypothetical hydrates with class-leading energy densities identified in this study (i.e., CoF_3•$9H_2O$, VF_2•$12H_2O$, and CaF_2•$12H_2O$). Each of the 4 vertices of the tetrahedron corresponds to an element in the salt hydrate composition, i.e., metal, non-metal, oxygen, and hydrogen. All compounds that are predicted to lie on the convex hull are plotted at their respective compositional coordinates within the tetrahedron.

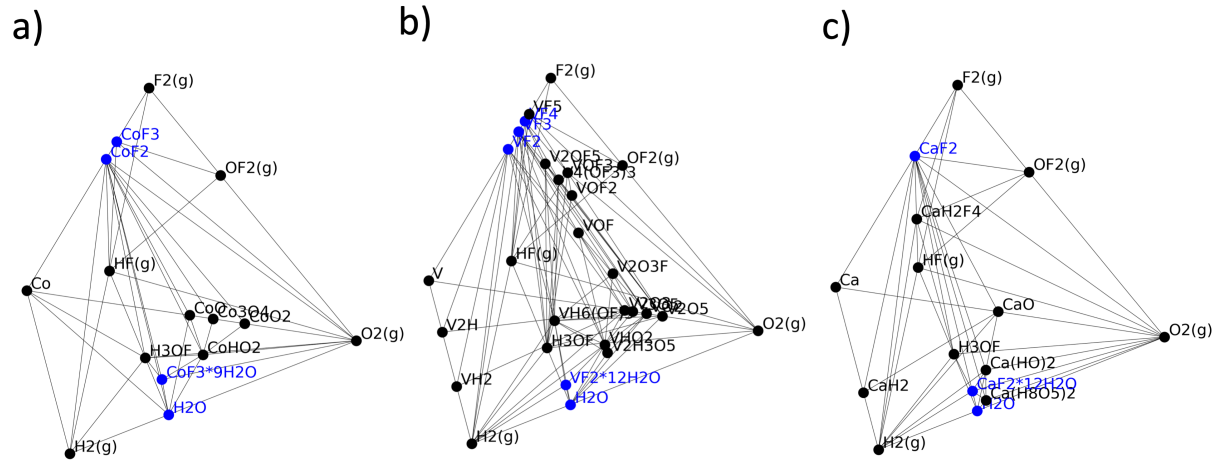

Figure 4.7 Quaternary phase diagrams computed from the thermodynamic stability analysis. The respective phase diagrams are shown for the promising salt hydrates of a) CoF_3•$9H_2O$, b) VF_2•$12H_2O$, and c) CaF_2•$12H_2O$. Salts, hydrates, and water are shown in blue, while other phases are shown in black.

Additionally, pressure-temperature phase diagrams were calculated for CoF_3•$9H_2O$, VF_2•$12H_2O$, and CaF_2•$12H_2O$. These are plotted in **Figure 4.8**. Equation (4.1) shows the thermodynamic equilibrium relation between water vapor pressure and temperature for a (de)hydration reaction. To more accurately predict thermodynamic properties, i.e., ΔS and ΔH, vibrational contributions to the entropy and enthalpy were calculated for CoF_3•$9H_2O$, CoF_3, VF_2•$12H_2O$, VF_2, CaF_2•$12H_2O$, and CaF_2, under the quasi-harmonic approximation using the Phonopy code.[160,161] Constant pressure properties were evaluated using 11 volumes for each salt and hydrate, scaling the lattice parameters by −2.5% to 2.5% in 0.5% increments. Supercells containing approximately 100 atoms and/or possessing lattice vectors of approximately 10 Å in

length were used for the calculations.[162] The enthalpy of water vapor was determined by a combination of the DFT computed energy of water vapor and the IAPWS steam tables.[163] The standard entropy of water was taken to be 188.84 J/K-mol.[145] ΔH and ΔS were then calculated for each (de)hydration reaction at 298 K. The dehydration of CoF_3•$9H_2O$ possessed a ΔH of 79.9 kJ/mol H_2O and ΔS of 161 J/K-mol H_2O. The dehydration of VF_2•$12H_2O$ possessed a ΔH of 61.1 kJ/mol H_2O and ΔS of 154 J/K-mol H_2O. The dehydration of CaF_2•$12H_2O$ possessed a ΔH of 54.9 kJ/mol H_2O and ΔS of 153 J/K-mol H_2O. In all three cases, ΔH (including temperature and vibrational contributions) was within 3 kJ/mol H_2O of the ΔH calculated using the simpler, 0 K procedure that does not account for vibrational contributions. The phase diagrams in **Figure 4.8** are plotted in terms of relative humidity, which is defined as $RH = \frac{p}{p_{sat}}$, where p is the water vapor pressure and p_{sat} is the temperature-dependent saturation pressure for water vapor.

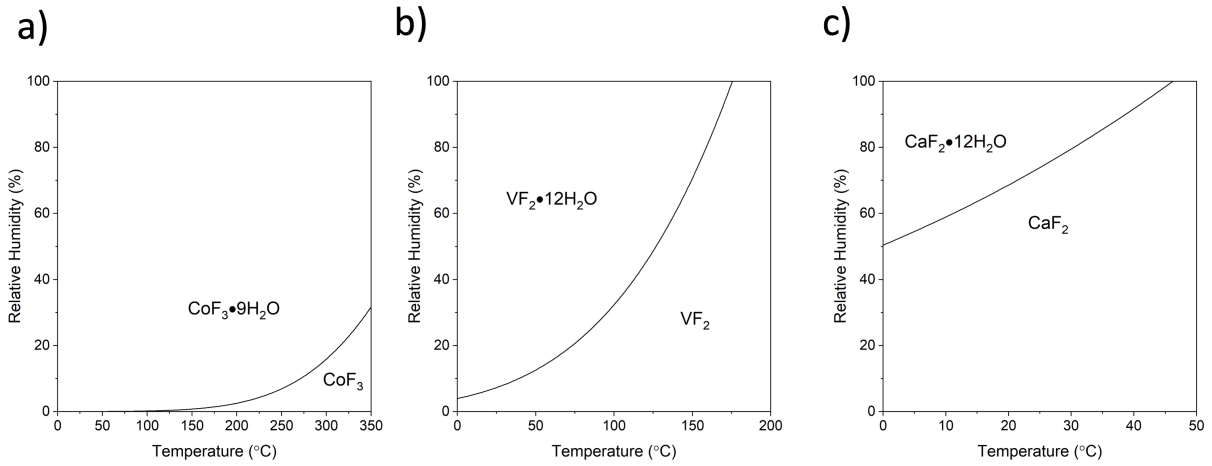

Figure 4.8 Phase diagrams illustrating the thermodynamic equilibrium for the dehydration reactions of a) CoF_3•$9H_2O$, b) VF_2•$12H_2O$, and c) CaF_2•$12H_2O$.

4.3.3 System Analysis

It is helpful to quantify the impact that the HH identified here would have on the performance of a TES system. To this end, system-level energy densities were estimated for the MERITS (More Effective use of Renewables Including compact seasonal Thermal energy Storage)

prototype system.[49,138,139] The MERITS system is a closed, modular system that stores solar energy for use in domestic heating applications. The original MERITS system was formulated using $Na_2S•5H_2O$ as the storage medium and operates within a temperature range of 65–80°C, which is sufficient for building applications that operate below 100°C.[55] The system is capable of a power output of 600–700 W, and has a projected energy density of ~0.8 GJ/m^3_{system}.[49,139]

De-Jong et al. developed a numerical model that predicts the MERITS system energy density as a function of the storage material and system geometry.[138] The model accounts for losses arising from heat transfer to/from the ambient and for the mass and volume of the hydrate/salt, heat exchanger, evaporator/condenser, insulation, and reactor materials used within each module. Additional details can be found in Appendix D.

Figure 4.9 shows the predicted system-level energy densities for the MERITS prototype wherein the HH examined here substitute for $Na_2S•5H_2O$. The operating temperatures of the HH were re-evaluated using Equation (4.1), assuming water vapor pressures consistent with the operation of the MERITS evaporator (12 mbar) and condenser (23 mbar). Given the lower vapor pressures, the HH operate at lower temperatures than those listed in **Table 4.7**, which assumed a water vapor pressure of 1 atm. This change in operating conditions excludes some low temperature reactions (e.g., $CaF_2•12H_2O$) from consideration as the MERITS system required a discharge temperature greater than 25°C. Reactions with expensive hydrates or a temperature window greater than 50°C were not included in the analysis.

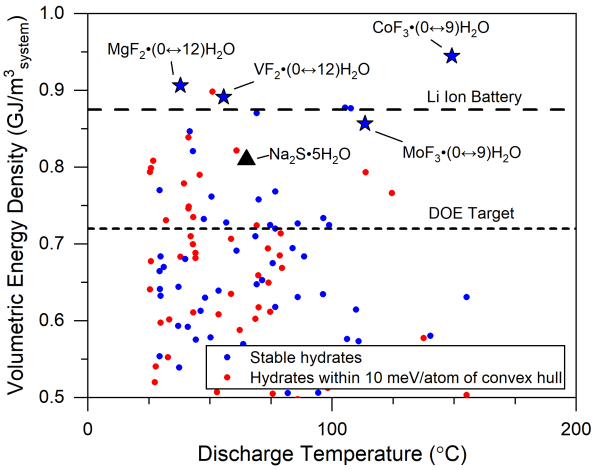

Figure 4.9 Projected system-level volumetric energy density and discharging temperature for the MERITS[49,138,139] TES system based on the hypothetical hydrates described in the present study. Hydrates are colored according to their reaction stability. Several promising reactions are shown as stars. For reference, the triangle depicts the salt hydrate used by the MERITS system, while the lines show the energy density of a lithium ion battery pack (long dash) and the DOE energy density target (short dash).

Figure 4.9 demonstrates that several of the newly identified, stable HH are predicted to out-perform the baseline $Na_2S•5H_2O$ material. For example, the hydration of CoF_3 to $CoF_3•9H_2O$ is projected to have a system-level energy density of 0.94 GJ/m^3 (18% larger than $Na_2S•5H_2O$). Other reactions with high projected system-level energy densities are the hydration of MgF_2 to $MgF_2•12H_2O$ (0.91 GJ/m^3, +13% vs. $Na_2S•5H_2O$) and the hydration of VF_2 to $VF_2•12H_2O$ (0.89 GJ/m^3, +11% vs. $Na_2S•5H_2O$). **Table 4.9** summarizes the properties of all HH that surpass the performance of the $Na_2S•5H_2O$-based system.

Table 4.9 Promising reactions that outperform $Na_2S•5H_2O$ in volumetric system energy densities.

Salt	n_{low}	n_{high}	Dist. to Convex Hull (meV/atom)	T_S (°C)	T_D (°C)	VED_{sys} (GJ/m^3)	VED_{sys} Improvement (%)
CoF_3	0	9	0.0	149	162	0.94	16.6%
MgF_2	0	12	0.0	38	51	0.91	11.9%
CuF_2	0	12	1.4	51	61	0.90	10.9%
VF_2	0	12	0.0	56	66	0.89	10.1%
NiF_2	0	4	0.0	105	117	0.88	8.3%
CrF_3	0	9	0.0	108	119	0.88	8.2%
ZnF_2	0	4	0.0	69	110	0.87	7.4%
MoF_3	0	9	0.0	113	125	0.86	5.8%
NaF	0	4	0.0	42	51	0.85	4.5%
MgF_2	0	4	3.2	41	51	0.84	3.5%

$AlCl_3$	0	6	0.0	233	249	0.83	2.0%
TiF_3	0	9	6.8	61	71	0.82	1.5%
$ZnCl_2$	0	12	0.0	43	72	0.82	1.4%

Finally, **Figure 4.9** also compares the energy densities of TES systems based on HH to that of a lithium ion battery pack (0.875 GJ/m^3)[164] as well as the DOE system-level energy density target for thermochemical heat storage systems (0.72 GJ/m^3).[140] Several salt hydrates demonstrate improvements in *VED* relative to battery storage, while even more exceed the DOE system-level energy density target.

4.3.4 Predictive Machine Learning

ML models were trained to maximize the accuracy in predicting ΔH for salt hydrates (assuming a full dehydration reaction). This approach is referred to as *predictive* machine learning; the goal is to determine how accurate ML can be in making these predictions, using the database of properties calculated in the present study. The ability to predict ΔH is crucial for predicting TES performance, as the energy density, T_{turn}, and stability are all dependent on the enthalpy. Unlike *interpretable* machine learning models where fewer features are used in order maximize understanding and minimize complexity, predictive machine learning models were trained without restrictions on the number of features or model complexity.

The multi-step strategy increased the accuracy of the models, as shown in **Table 4.10**. For each ML algorithm examined, combining feature sets (Step 2) led to a reduction in test error. The GA feature selection (Step 3) also yielded a reduction in test error. Finally, an increase in the amount of training data from 50% to 90% (Step 4) further increased the accuracy of the model. The optimal set of features also varied with the ML algorithm, ranging from 69 features for the k-NN model to 752 for ridge regression. At every step in the ML training procedure the SVM model

was the most accurate. Additionally, the interpretable ML models are shown in the last column of **Table 4.10**. Out of the 4 algorithms investigated, RF, k-NN, and SVM yielded similar MAE ranging from 6.2 to 6.7 kJ/mol H_2O. These errors are slightly larger than for the predictive models, which ranged from 4.4 to 5.9 kJ/mol H_2O. The interpretable ridge regression model was an outlier with a larger MAE of 9.7 kJ/mol H_2O.

Table 4.10 Mean absolute error (MAE, in kJ/mol H_2O) for predicting ΔH for the best predictive ML model as a function of different "steps" in the training process. Step 1 refers to the best ML model after identifying optimal feature representations. Step 2 corresponds to feature set pairing and subsequent feature set addition. Step 3 corresponds to the genetic algorithm feature selection, representing the test error of the final model when 50% of the data is in the test set. Step 4 corresponds to the model from Step 3 when trained on 90% of the data. For comparison, the MAE of the interpretable ML model is shown in the last column.

ML Algorithm	Predictive model test MAE				Interpretable model test MAE
	Step 1	Step 2	Step 3	Step 4	
RF	7.5	6.7	6.5	5.7	6.7
k-NN	8.5	7.6	6.8	5.9	6.3
Ridge Reg.	10.3	6.9	6.5	6.1	9.7
SVM	7.4	6.0	5.5	4.4	6.2

The predictive SVM model was trained on 127 features from the principal components of the MEGNet feature set,[165] the categorical salt hydrate representation, and the packing efficiency.[166] The RF model was trained on 203 features from Pymatgen's elemental properties,[142] orbital field properties,[167] the Gaussian symmetry function,[168,169] the salt hydrate categorical features, and the chemically intuited salt hydrate feature set. The k-NN model was trained on 69 features from the orbital field,[167] the chemically intuited salt hydrate features, the stoichiometry,[170] and the structure heterogeneity.[166] The ridge regression model was trained on 752 features from Matscholar's elemental properties,[171] the orbital field,[167] the principal components of the bond fraction,[172] and the salt hydrate categorical features.

For the most accurate predictive ML models (**Table 4.10**, Step 4), the errors between the ML predictions and DFT calculations range from 4.4 kJ/mol H_2O for SVM to 6.1 kJ/mol H_2O for ridge regression. A scatterplot demonstrating the accuracy of the corresponding SVM model is

shown in **Figure 4.10a**. To put the magnitude of these errors into context, the error in the prediction of ΔH for salt hydrates was estimated in Chapter 3 to be 10.0 kJ/mol H_2O between DFT and experiments, while the error between different experimental measurements of ΔH was estimated to be 7.5 kJ/mol H_2O. **Figure 4.10b** shows the test accuracy of the interpretable SVM model, which was only trained on the categorical salt hydrate representation.

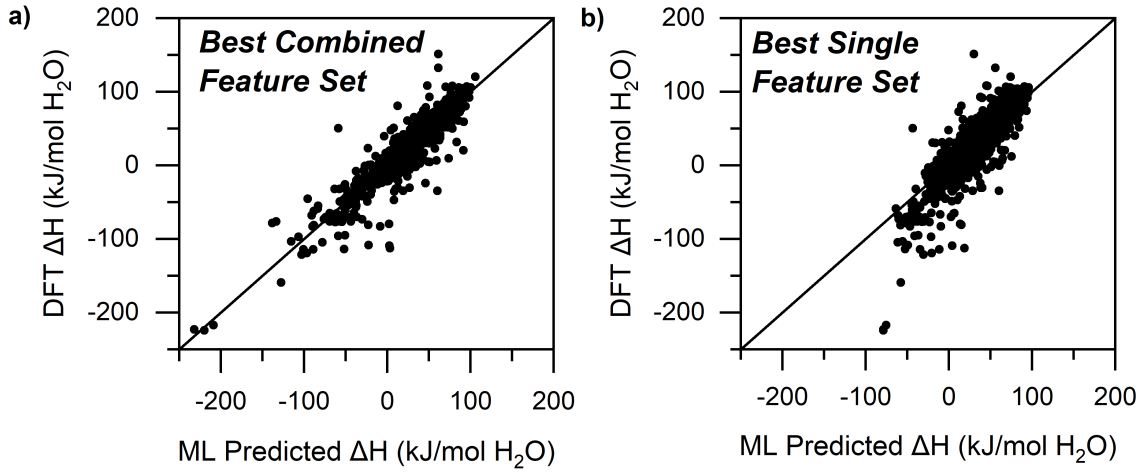

Figure 4.10 Scatterplots comparing the ML-predicted and DFT-calculated enthalpies of dehydration for a) the best combined feature set (MAE: 4.4 kJ/mol H_2O, R^2: 0.89) and b) the best single feature set (MAE: 6.2 kJ/mol H_2O, R^2: 0.79). In both cases, the SVM model was used as it possessed the smallest test error.

The predictive ML models demonstrate that ML can satisfactorily predict ΔH for salt hydrates. However, the large number of features these models employ—ranging from dozens to hundreds, depending on the algorithm—make it difficult to develop one's chemical intuition about which features are the most important for predicting TES performance. For this goal, we turn to interpretable ML.

4.3.5 Design Rules from Interpretable Machine Learning.

ML offers a pathway to extract property-performance trends from material datasets, yielding design rules.[173] To create interpretable ML models, the same process used for developing

predictive models was applied, with the exception that the feature set combination step was omitted (Step 2 in **Table 4.10**). GA feature selection was performed on the best feature representation, assuming a single feature set. Hence, the best feature subset for each ML algorithm was identified subject to the simplifying constraint that only a single feature set was available as input to that algorithm. In most cases, the GA achieved a test error reduction of between 0.3 kJ/mol H_2O (SVM) and 1.4 kJ/mol H_2O (k-NN) by removing a minimum of 7 features (k-NN) and a maximum of 505 features (ridge regression). However, in the case of RF, the GA removed only 1 feature with no significant change in the test error.

Figure 4.11 shows partial dependence plots (PDPs) that illustrate how the k-NN and RF ML models' predictions for ΔH vary with respect to changes in the value of a single feature.[174–176] Specifically, a PDP illustrates the predicted value of a ML model, averaged across the entire dataset, when the feature of interest is artificially varied in the dataset. This can highlight non-linear relationships with respect to isolated features. The k-NN (MAE = 6.3 kJ/mol H_2O) and RF (6.7 kJ/mol H_2O) models were both optimized when trained on the salt hydrate features compiled by the authors' chemical intuition. The high accuracy achieved when using this "chemistry-rich" feature set supports the notion that domain knowledge (i.e., chemical intuition) is helpful for feature set design. Six noteworthy feature trends identified by ML are highlighted in **Figure 4.11**.

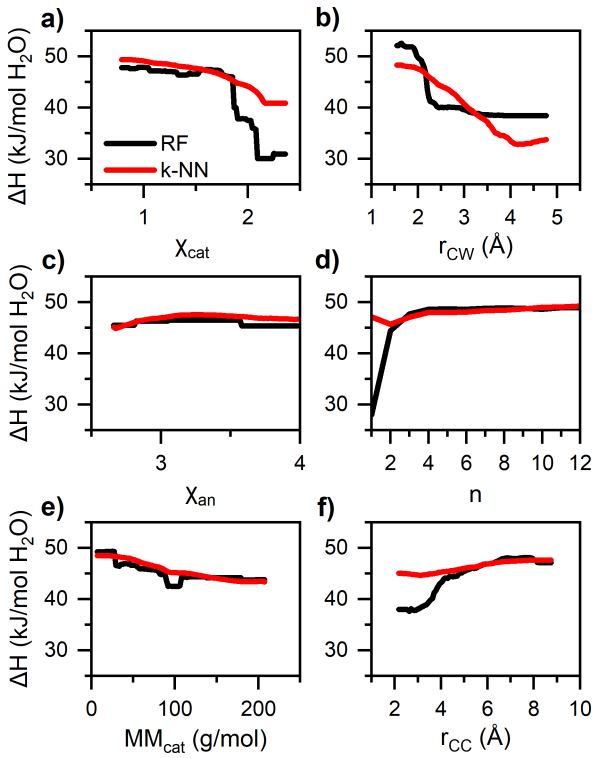

Figure 4.11 Partial dependence plots for ΔH with respect to variations in: a) the cation's electronegativity, b) cation-water distance, c) the anion's electronegativity, d) hydrate number, e) molar mass of the cation, and f) cation-cation distance. The black line shows the PDP for the RF model, while the red line shows the PDP for the k-NN model.

Strong Trends. The most important features exhibit a large variation in their PDP for Δ*H*. **Figure 4.11a–b** show that Δ*H* depends strongly on the cation electronegativity and on the cation-water distance. Regarding cation electronegativity, both the RF and k-NN models demonstrate a decrease in Δ*H* for HH containing cations with larger electronegativities. Similarly, **Figure 4.11b** shows that HH with larger distances between the cation and coordinating water molecules have smaller Δ*H*. The relevance of electronegativity and bond distance point to the importance of the cation-water bond. In a salt hydrate, water molecules coordinate around one or two cations, forming coordinate-covalent bonds with the cation(s), until the coordination shells of the cations are saturated. The trends in **Figure 4.11a–b** suggest that cations with higher electronegativities and larger water bond distances don't bond with water molecules as strongly, resulting in a lower Δ*H*.

Weak Trends. **Figure 4.11c–d** show that ΔH is weakly dependent on both the anion electronegativity and the hydrate number (i.e., the number of water molecules per formula unit). **Figure 4.11c** shows the PDP for the anion electronegativity. Both the RF and k-NN models indicate that the anions with moderate electronegativities between 2.9 and 3.2 (i.e., Cl^{1-} and Br^{1-}) have only slightly higher ΔH. Overall, ΔH is nearly constant across the range of relevant anion electronegativities. **Figure 4.11d** shows the PDP for the hydrate number. The RF and k-NN models disagree on whether monohydrates have low ΔH, but agree that ΔH is roughly constant for all hydrates with n >= 2.

Intermediate Trends. ΔH shows an intermediate dependence on both the cation molar mass and the distance between cations in the hydrate. **Figure 4.11e** shows the PDP for the cation molar mass. For both the RF and k-NN models, ΔH slowly decreases as the cation mass increases. Lighter—and therefore smaller—cations tend to bond more strongly with the coordinating water molecules, resulting in a higher ΔH. **Figure 4.11f** shows the PDP for the distance between nearest neighbor cations in the salt hydrate. In both cases, ΔH generally increases as the cation-cation distance in the HH increases. This observed trend may be related to the ordering of water-coordinated cation clusters within the salt hydrate, indicating that more energetically favorable structures have greater distances between cation clusters.

Design Rules. Tuning ΔH is crucial for controlling the heat storage performance of the salt hydrate. As discussed previously in Chapter 3, higher energy densities can be achieved by increasing ΔH and the number of water molecules stored per mass and per volume of the hydrate (i.e., the water capacity of the hydrate). The interpretable ML models reveal that increased energy densities via increased ΔH can be achieved by: 1) selecting compositions that contain cations that exhibit small electronegativities and molar masses (e.g., Na^{1+}, K^{1+}), and 2) crystal structures with

small cation-water distances (i.e., less than 2 Å) and large cation-cation distances (i.e., greater than 4 Å). Since ΔH is also proportional to a reaction's turning temperature, as shown in Equation (4.2), the above strategies are also effective in targeting higher temperature reactions.

Alternative Design Perspective. Regarding the other ML algorithms, the SVM model's accuracy (MAE: 6.2 kJ/mol H_2O) was maximized when trained on the salt hydrate categorical feature representation, while the best ridge regression model was trained on the Matscholar[171] elemental property feature set, although this model showed significantly higher test error (9.7 kJ/mol H_2O). The SVM interpretable model showed the highest predictive accuracy and was trained on a one hot encoding of the compositon of the cation, the anion, and on the crystal structure template used to generate the HH. The reason for the model's high predictive accuracy is the polynomial kernel. This kernel, when applied to a one hot encoding, will implicitly produce features corresponding to the categories for the cation-anion pair, the cation-structure pair, and the anion-structure pair. This leads to another design perspective. Without detailed knowledge of the composition or features of the crystal structure, one can still estimate ΔH simply by looking at other salt hydrates that share the same cation, anion, and/or crystal structure.

To illustrate this, **Figure 4.12** shows the average ΔH as a function of the cation identity (bottom plot), the anion (top left plot), and the cation-anion pair (top-right). Regarding the cation identity, the bottom plot shows that HH containing Al^{3+} possess the highest average ΔH, while those with Zr^{1+} exhibit the lowest average ΔH. Regarding the anion identity, the left plot shows that HH containing Cl^{1-} possess the highest average ΔH, while those with I^{1-} exhibit the lowest average ΔH. However, more detailed information is shown in the heatmap. Although the general ionic trends hold across the heatmap, there are noticeable deviations. For instance, the hydrates

with the highest average ΔH don't belong to $AlCl_3$, but rather the salt families of MnF_4, SnI_4, GeF_4, and CuF. Similar plots involving the structure can be found in **Figure 4.13** and **Figure 4.14**.

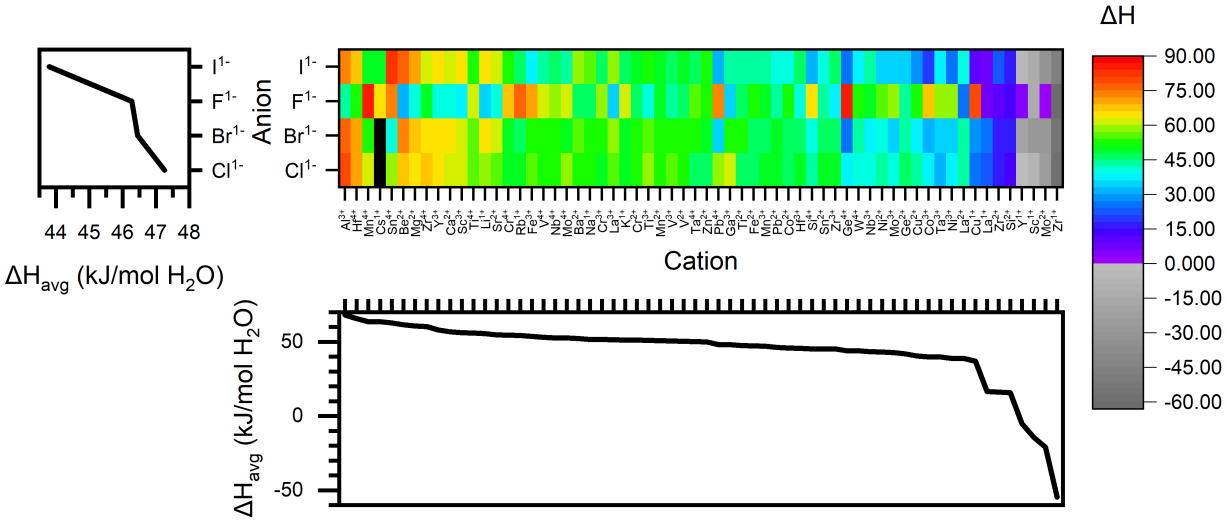

Figure 4.12 Heatmap showing the average enthalpy of dehydration for each ion and salt family. Black entries indicate missing values.

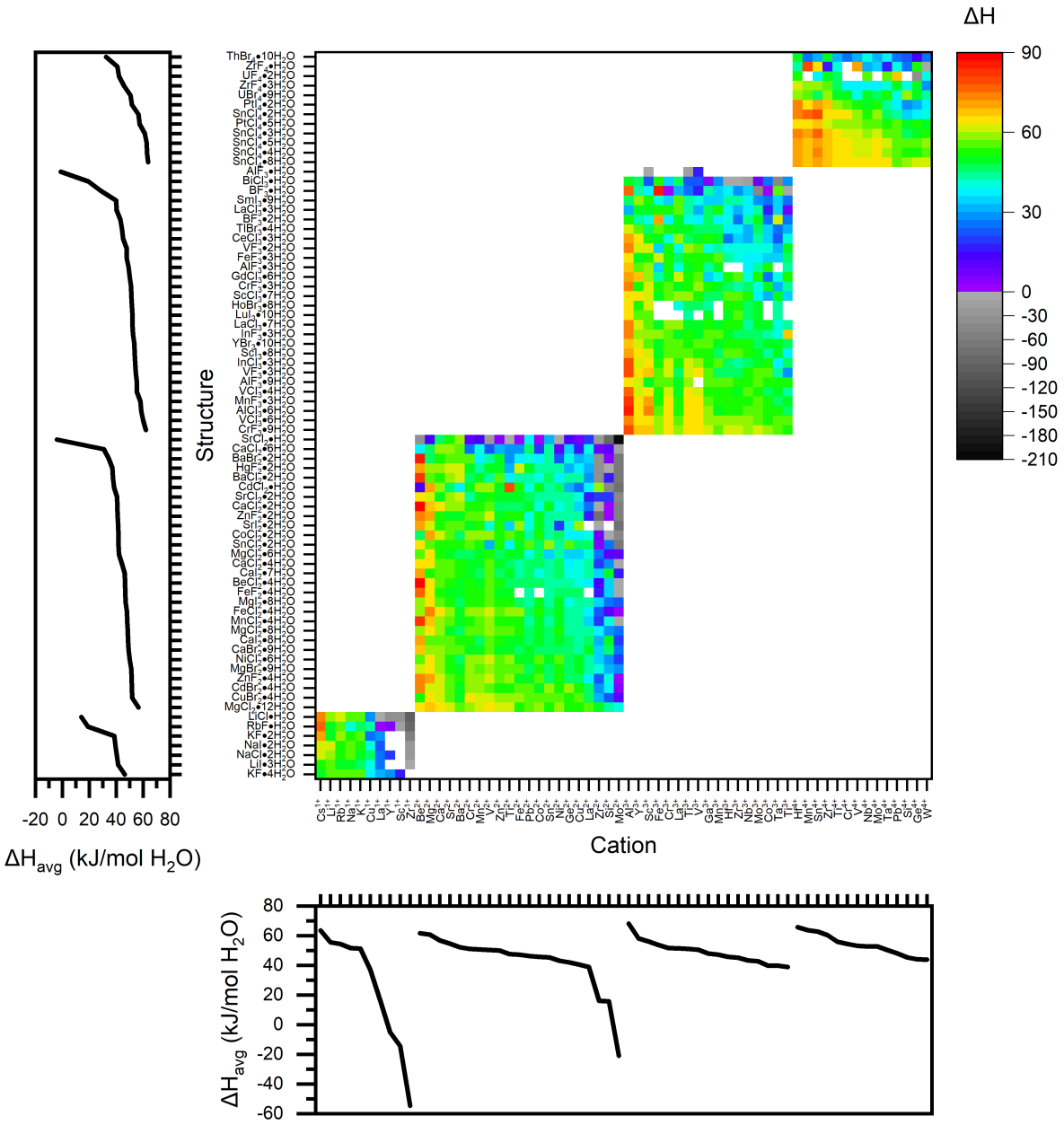

Figure 4.13 Heatmap showing the average enthalpy of dehydration for each cation, crystal structure template, and cation-structure pair. White entries indicate missing values or not applicable pairs (i.e., when the oxidation states of the cation and structure don't match).

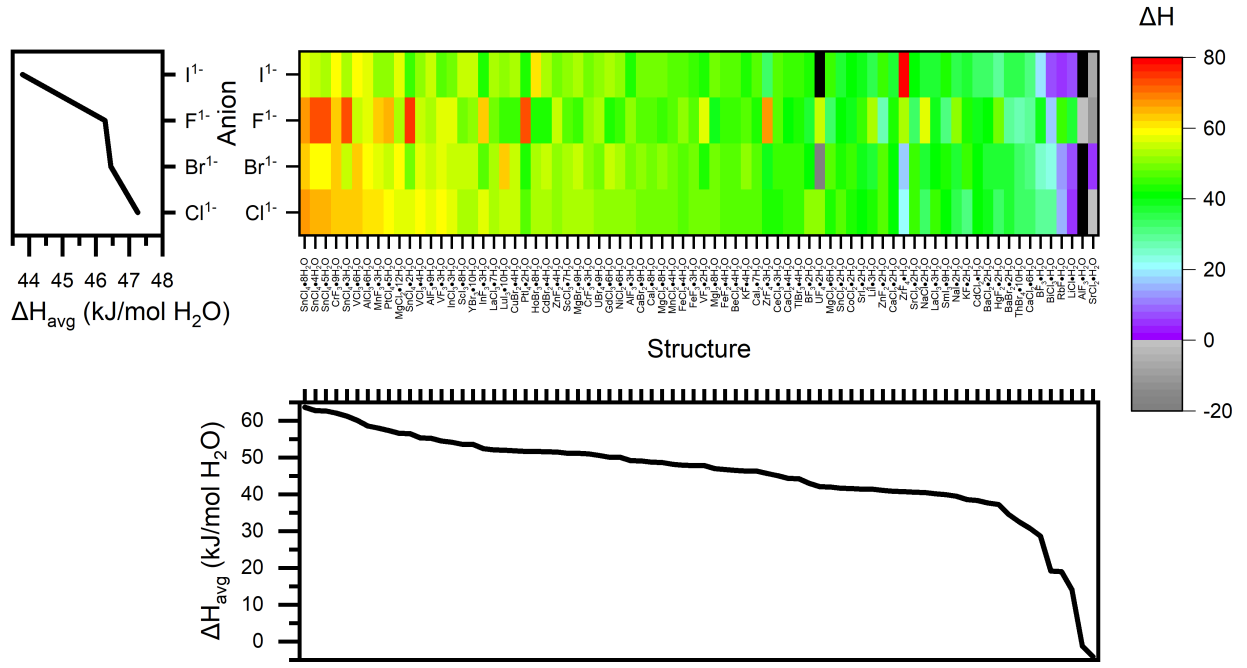

Figure 4.14 Heatmap showing the average enthalpy of dehydration for each anion, crystal structure template, and anion-structure pair. Black entries indicate missing values.

4.4 Conclusions

Salt hydrates demonstrate promise for TES due to their high energy densities and reversibility at moderate temperatures. Here, the energy densities, turning temperatures, and thermodynamic stabilities of 5292 hypothetical salt hydrates were predicted using high throughput density functional theory calculations. Several hydrates of metal-fluorides, including CoF_3•$9H_2O$, VF_2•$12H_2O$, and CaF_2•$12H_2O$ were identified as new, stable TES materials with class-leading energy densities and operating temperatures suitable for use in domestic heating and intermediate-temperature applications. These hydrates showed comparable or superior energy densities compared to the active material of a lithium ion battery. Additionally, a numerical model[138] was used to project the system energy densities offered by these new materials when deployed within a thermochemical heat storage prototype,[49,138,139] with several hydrates surpassing the U.S. Department of Energy's system energy density target.[140]

The hydrate dataset was used to train machine learning models of salt hydrate thermodynamics and to identify design guidelines for maximizing energy density. These analyses reveal that optimal performance is obtained for salt hydrates consisting of cations with small electronegativities and with crystal structures having small cation-water distances. The new materials and design rules identified here are expected to accelerate the adoption of TES systems.

Chapter 5 Screening of Hypothetical Chalcogenide and Complex Anion Salt Hydrates for Thermal Energy Storage

5.1 Introduction

Chapter 3 and Chapter 4 focused on the computational characterization and discovery of hydrates of halide salts. While halide salt hydrates have demonstrated promise for TES, they are not the only interesting salt hydrates. Other salt hydrates, such as $MgSO_4 \cdot 7H_2O$,[74,177] $K_2CO_3 \cdot 1.5H_2O$,[55,178] $Na_3PO_4 \cdot 12H_2O$,[74] and $Na_2S \cdot 5H_2O$[49] have been highlighted as promising for TES. The first three are examples of hydrates of complex anion salts, while the last is an example of a chalcogenide salt hydrate. In their screening of salt hydrates for TES, Donkers et al. listed 420 different salt hydrate compositions.[55] Of these, 27% were hydrates of halide salts, while 69% were hydrates of complex anion salts and 4% were hydrates of chalcogenide salts. Both the chemical spaces of complex anion salt hydrates and chalcogenide salt hydrates prove interesting for exploration. In the former case, the complex anion salt hydrates are shown to be the largest class of experimentally known salt hydrates, thus warranting a thorough screening. In the latter case, the chalcogenide salt hydrates are particularly rare, indicating that potentially promising materials might be hidden in this under-explored space.

The computational protocol developed in Chapter 4 generated and characterized hypothetical halide hydrates for TES. In this chapter, this protocol was adapted for hypothetical salt hydrates containing chalcogenides or complex anions. Specifically, a total of 1779 hypothetical chalcogenide salt hydrates and 5233 hypothetical complex anion salt hydrates were generated via atomic substitution into relevant crystal structure templates mined from the

Inorganic Crystal Structure Database.[103] First principles calculations were performed on all of these hypothetical hydrates to characterize their thermodynamic and heat storage properties. Promising reactions involving both chalcogenide salt hydrates and complex anion salt hydrates were identified for operating temperatures below 200ºC. System-level energy densities were projected using an adapted model of a thermochemical heat storage prototype,[49,138,139] revealing many hydrates with system-level energy densities that exceed the U.S. Department of Energy's target of 200 kWh/m^3.[140]

Interpretable machine learning models were trained separately on the resulting databases of chalcogenide salt hydrates and complex anion salt hydrates to identify the features that affect the thermodynamics of salt (de)hydration. Chalcogenide salt hydrates were found to possess a distribution of dehydration enthalpies that is lower and flatter than the distributions of halide salt hydrates and complex anion salt hydrates. Furthermore, general trends across the chalcogenide salt hydrates were identified with several features, such as the elemental embeddings from Matscholar.[171] In contrast, the complex anion salt hydrates proved to be a more heterogeneous class of salt hydrates. Rather than identifying general trends across the complex anion salt hydrates, the optimal model used 70 features to effectively partition the chemical space of complex anion salt hydrates. The promising materials and design insights identified in this study are anticipated to catalyze the development of effective TES systems.

5.2 Methodology

5.2.1 Screening Method

The computational protocol from Chapter 4 for screening hypothetical salt hydrates for TES was adapted for salt hydrates containing chalcogens and complex anions. The main components of the protocol are summarized below.

Generation of Hypothetical Salt Hydrates. Hypothetical chalcogenide hydrates were generated in the same manner as the hypothetical halide hydrates were generated in Chapter 4. The chalcogenide salts of interest possess a stoichiometry of M_2X, MX, M_2X_3, or MX_2, where M is a mono-, di-, tri-, or tetravalent cation, respectively, and X is a (divalent) chalcogen. After searching the Inorganic Crystal Structure Database[103] (ICSD) for experimentally known hydrates of these four salt hydrate stoichiometries, 40 distinct crystal structures were identified, although no hydrates were found for M_2X_3 salts. These 40 crystal structures served as templates for cation and anion substitution. The same 62 cations used in Chapter 4 for substitution in hypothetical halide hydrates were used to generate the hypothetical chalcogenide hydrates. Three chalcogens (O^{2-}, S^{2-}, Se^{2-}) were used for anion substitution. Accounting for all possible substitutions that obey charge neutrality, a total of 1779 hypothetical chalcogenide hydrates were generated. In addition to the hydrates, the respective anhydrous salts were also characterized. Hypothetical crystal structures were only generated for anhydrous salts that did not possess an experimentally known crystal structure in the ICSD. Otherwise, the experimentally known crystal structure was used. A total of 64, 17, and 37 crystal structure templates were used for hypothetical M_2X, MX, and MX_2 salts, respectively. In total, 966 experimental and hypothetical chalcogenide salts were gathered or generated.

Hypothetical hydrates were also generated for salts containing complex anions (i.e., ionized molecular structures). 43 complex anions were considered, which are listed in **Table 5.1**. A search through the ICSD for salt hydrates containing complex anions yielded 413 distinct crystal structures, which were used as templates for atomic substitution. In order to limit the number of hypothetical structures generated, hypothetical hydrates were only generated for salt compositions that 1) possessed an experimental crystal structure for the anhydrous salt in the ICSD, and 2)

contained an inexpensive cation (i.e., no more expensive than lithium[123]). This resulted in a total of 354 salt compositions. Stoichiometric compatibility was checked between the 354 salt compositions and 413 crystal structure templates, resulting in a total of 5233 hypothetical salt hydrates. For example, $MgSO_4$ could substitute for $NaClO_4$. Experimental crystal structures for the 354 anhydrous salts were also extracted from the ICSD and characterized.

Table 5.1 Complex anions used during hypothetical hydrate generation.

$As_2O_7^{4-}$	AsO_3^{3-}	AsO_4^{3-}	$B_4O_7^{2-}$	BrO_3^-	$C_2H_3O_2^-$	$C_2O_4^{2-}$
$C_4O_4^{2-}$	ClO_2^-	ClO_3^-	ClO_4^-	CN^-	CO_3^{2-}	$Cr_2O_7^{2-}$
CrO_4^{2-}	$H_2PO_4^-$	$HAsO_4^{2-}$	HCO_2^-	HPO_4^{2-}	HSO_4^-	IO_3^-
IO_4^-	MnO_4^-	MoO_4^{2-}	N_3^-	NO_2^-	NO_3^-	O_2^{2-}
OH^-	$P_2O_7^{4-}$	$P_3O_9^{3-}$	$P_4O_{12}^{4-}$	$P_6O_{18}^{6-}$	PO_4^{3-}	$S_2O_3^{2-}$
$S_2O_6^{2-}$	$S_4O_6^{2-}$	SCN^-	SiF_6^{2-}	SiO_4^{4-}	SO_3^{2-}	SO_4^{2-}
WO_4^{2-}						

DFT Calculations. Density functional theory (DFT) calculations were performed on the 7012 hypothetical salt hydrates and 1320 anhydrous salts via VASP.[93] All calculations were spin polarized and used a planewave cutoff energy of 500 eV. Core-valence electronic interactions were modeled via Blöchl's projector augmented wave method.[94,95] The crystal structure geometry (i.e., ionic positions and cell lattice) was relaxed using a van der Waals aware exchange-correlation functional (optPBE-vdW)[84–86,88] until all ionic forces were less than 0.02 eV/Å. An increasingly dense Monkhorst-Pack[96] k-point mesh was used until convergence was achieved. Following relaxation, the ground state energy of each crystal structure was calculated via a single point energy calculation (i.e., without further relaxation) using the PW-91[83] exchange-correlation functional. 7887 of the 8332 attempted DFT calculations converged.

Determination of Lowest Energy Structures. In many cases, multiple hypothetical hydrate crystal structures for a single chemical composition were generated and computationally characterized. The crystal structure with the lowest computed ground state energy was taken to be

the best prediction of the salt hydrate's true crystal structure, and the remaining high energy crystal structures were discarded.

Removal of Non-Hydrates. In order to identify water decomposition in the hypothetical hydrates, the distribution of the number of hydrogen atoms coordinating oxygen atoms was tabulated for each crystal structure (using a cutoff distance of 1.1 Å). This distribution was compared against the expected distribution for the given composition. For example, in $MgO{\bullet}4H_2O$, one would expect to find four 2-coordinated oxygen atoms and one 0-coordinated oxygen atom per formula unit. Crystal structures that exhibited deviation from the expected coordination distribution were considered to have experienced water decomposition and were thus discarded as non-hydrates. A total of 271 hypothetical chalcogenide hydrates and 53 hypothetical complex anion hydrates were removed in this fashion. The large number of hypothetical chalcogenide hydrates removed is not surprising as many oxide hydrates decomposed into hydroxides.

Elimination of Unstable Compounds. Thermodynamic convex hulls were computed via Pymatgen[142] to characterize the stability of the hypothetical hydrates. As done previously in Chapter 4, single point energy DFT calculations were performed for each of the remaining hypothetical hydrates using the Materials Project[143] computational protocol. Entries from the Materials Project were also included in the analysis, as were a number of common gases. Free energy terms ($-T\Delta S_{gas}$) were added to the gas energy to approximate a room temperature (T = 298 K) stability analysis. ΔS_{gas} was assumed to be the experimental entropy of formation listed in the NIST-JANAF tables.[145] **Table 5.2** shows the full list of 67 gases. Hypothetical hydrates that were found to be more than 50 meV/atom above the convex hull were discarded as unstable. A

total of 214 chalcogenide salts and hydrates remained as either stable or metastable, while 1269 complex anion salts and hydrates were characterized as stable or metastable.

Table 5.2 List of gases used in stability analysis.

Br	Br_2	Cl_2	Cl_2O	ClO	ClO_2	F_2
H_2	H_2O_2	HBr	HCl	HF	HI	HOF
I	I_2	O_2	OF_2	H_2S	SO_2	SO_3
S	H_2SO_4	H_3N	HNO_3	N_2	NO_2	NO_3
HN	HNO	N_2O	N_2O_3	N_2O_5	NO	C
CO_2	H_4C	C_3O_2	CO	H_2C	H_2CO	H_2CO_2
H_4C_2O	$H_8C_3O_2$	H_8C_5	HC	HC_2	HCO	P
PH_3	B	BH_3O_3	BH_3	BH	SiH_4	SiH
Si	SiO	SiO_2	HCNO	CN	CN_2	HCN
CS	CS_2	CSO	SN			

Characterization of Reactions by Stability, Energy Density, and Operating Temperature. Hypothetical (de)hydration reactions were characterized from the 214 (meta)stable chalcogenide salts/hydrates and 1269 (meta)stable complex anion salts/hydrates. The relative stability of each reaction was determined by the maximum distance to the convex hull between the hydrated and dehydrated phase. Various cutoffs for stability were used for screening (i.e., on the convex hull and < 10 meV/atom).

For each reaction, the enthalpy of dehydration (ΔH) per mole of H_2O was calculated using Equation (3.1). The energy densities were computed using Equations (3.2) and (3.3). The operating conditions of the (de)hydration reaction are governed by the thermodynamic equilibrium relation in Equation (4.1). Turning temperatures were characterized according to the simplified case of Equation (4.2). As done in Chapter 3 and Chapter 4, ΔS was assumed to be 146 J/mol H_2O-K, which is the average experimental entropy of dehydration for salt hydrates in Glasser's database.[67] The turning temperature (or set of turning temperatures in the case of multi-step (de)hydration reactions) was then used to categorize each reaction into one of several temperature categories: < 50°C, 50–100°C, 100–200°C, 200–300°C, 300–450°C, 450–600°C, > 600°C, and

wide temperature window. More details about reaction characterization can be found in Chapter 4.

Identify Promising Reactions. Promising reactions with optimal *GED* and *VED* were identified for each temperature category. As done in Chapter 3 and Chapter 4, promising reactions were subject to constraints of cost (i.e., no more expensive than lithium[123]), stability, and operating temperature window (i.e., < 50°C).

5.2.2 Machine Learning.

Machine learning (ML) models were trained to identify property-performance relations for ΔH among salt hydrates of various anion classes (i.e., chalcogenides and complex anions). Five algorithms were used: ridge regression,[98] k-nearest neighbors (k-NN),[99] support vector machine (SVM),[100] random forest (RF),[101] and extra trees (ET).[102] Models were trained using the Scikit-Learn library.[179]

Salt Hydrate Databases. Separate databases were compiled for 1) the hypothetical chalcogenide hydrates, and 2) the hypothetical complex anion hydrates. Each hydrate was characterized by the DFT-computed ΔH corresponding to complete dehydration (i.e., ΔH for the dehydration reaction of the given hydrate to the anhydrous salt). To focus on observing trends among realistic salt hydrates, only the lowest-energy salt hydrate crystal structures with $\Delta H > 0$ were included. The two databases consisted of 297 chalcogenide hydrates and 1626 complex anion hydrates, respectively.

Salt Hydrate Features. 34 'featurizers' from Matminer[147] were used to automatically generate compatible feature sets for the salt hydrate databases. Of these, 14 features sets were derived from the chemical composition of the salt hydrate, while the other 20 feature sets were derived from the crystal structure of the salt hydrate. Models using different feature sets were

trained and evaluated. All features were normalized to have a mean of 0 and a standard deviation of 1 before training.

Model Evaluation. Models were evaluated according to the mean absolute error of the test set. The test sets were generated via 5-fold cross validation (i.e., 20% of the data withheld as the unseen test set during each iteration). Furthermore, 3-fold cross validation was used within each training fold to optimize the hyperparameters of the ML algorithm with an exhaustive grid search for ridge regression, k-NN, and SVM models. Hyperparameter optimization was not performed for RF and ET, which used only a single hyperparameter to reduce computational cost. **Table 5.3** lists the hyperparameters that were optimized for each algorithm, as well as the possible values for each hyperparameter.

Table 5.3 Relevant hyperparameters and possible values for each of the five tested ML algorithms.

Algorithm	Hyperparameters (Range of Values)
Ridge Reg.	Alpha (10^{-6}, 10^{-5}, …, 10^{6})
k-NN	k (1, 2, …, 20), weight (uniform, distance), power (1, 2)
SVM	Kernel (radial basis function, sigmoid, linear, polynomial)
RF	Trees (200)
ET	Trees (200)

Recursive Feature Reduction. When determining the most significant features, recursive feature reduction was performed. A random forest was trained on the feature set and the feature importances were calculated. The features with lowest feature importances (i.e., those with feature importances within 0.001 of the minimum feature importance) were removed. This process was repeated until only one feature remained.

5.3 Results and Discussion

5.3.1 Screening Results

Figure 5.1 depicts the energy densities and temperature ranges of the hypothetical chalcogenide hydrates and complex anion hydrates using two different stability criteria. In the first stability case, salt hydrates must lie on the convex hull. This results in 19 reactions for the chalcogenides (**Figure 5.1a**) and 149 reactions for the complex anions (**Figure 5.1b**). When the stability requirement is relaxed to include hydrates within 10 meV/atom of the convex hull, the screening results in 32 chalcogenide reactions (**Figure 5.1c**) and 820 complex anion reactions (**Figure 5.1d**). Notably, the chalcogenide salt (de)hydration reactions are significantly more sparse than the complex anion salt (de)hydration reactions or the halide salt (de)hydration reactions studied earlier (Chapter 4). The observed sparsity, both here and in the experimental database of Donkers et al.,[55] is due to the lower stability of chalcogenides. While 386 of the 1650 complex anion salt hydrate compositions are found to be within 10 meV/atom of the convex hull (23%), only 22 of the 396 chalcogenide salt hydrate compositions are found to be within 10 meV/atom of the convex hull (6%). These reactions are listed in Appendix E.

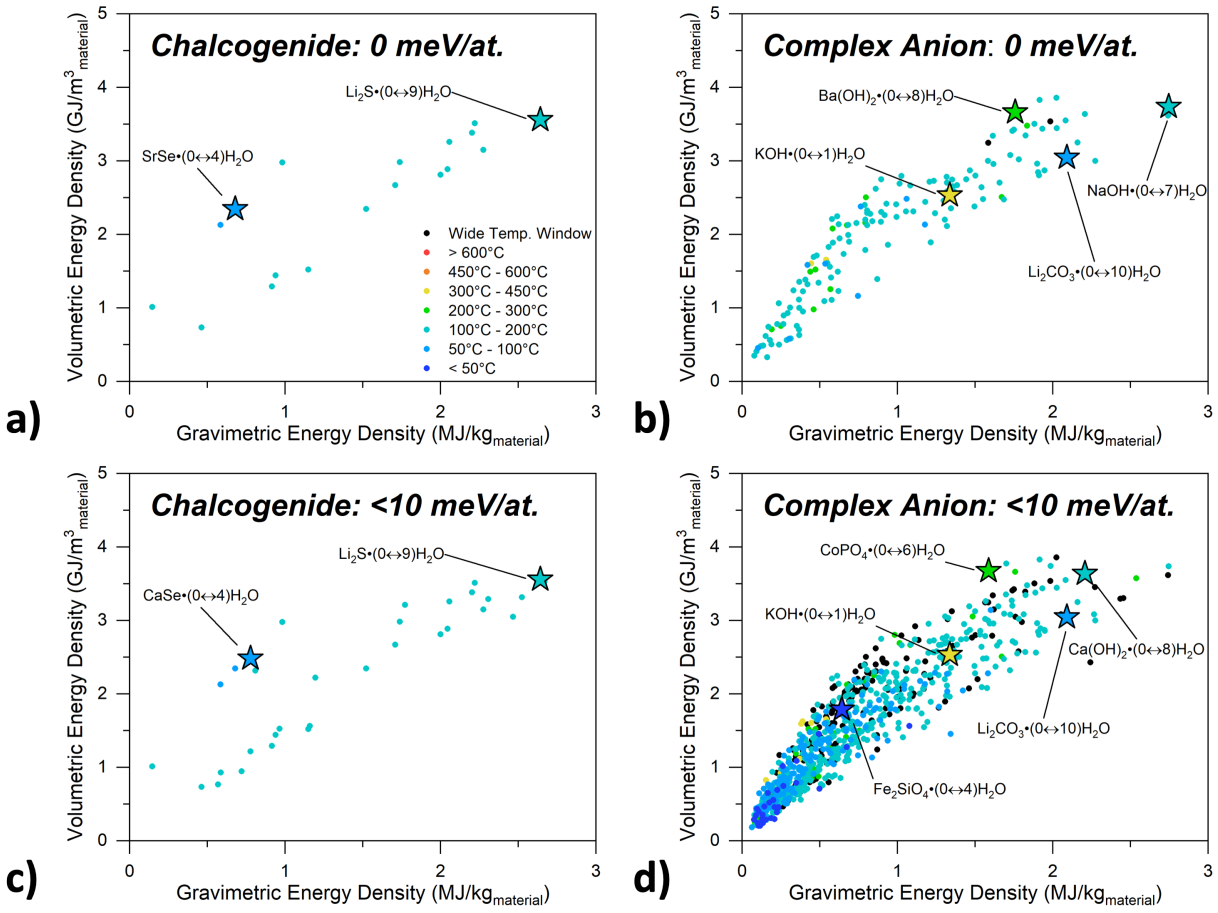

Figure 5.1 Gravimetric and volumetric energy densities and operating temperatures shown for a) the 19 chalcogenide salt (de)hydration reactions predicted to lie on the convex hull, b) the 149 complex anion salt (de)hydration reactions predicted to lie on the convex hull, c) the 32 chalcogenide salt (de)hydration reactions that are predicted to be within 10 meV/atom of the convex hull, and d) the 820 complex anion salt (de)hydration reactions that are predicted to be within 10 meV/atom of the convex hull. Promising reactions are shown as stars.

Table 5.4 summarizes the promising reactions identified among the chalcogenide salt hydrates. Reactions are categorized according to their operating temperature. Details regarding the turning temperature(s), energy densities, and stability of the (de)hydration reaction are listed for each reaction. The stability details consist of the maximum distance to the convex hull among the hydrated and dehydrated phase, as well as the thermodynamically favored decomposition reaction that is expected if the reaction is metastable. Finally, **Table 5.4** indicates whether each salt (de)hydration reaction is new to TES literature, to the best of the authors' knowledge. **Table 5.5**

is similar to **Table 5.4**, but summarizes the promising complex anion salt (de)hydration reactions identified in this screening.

Table 5.4 Details of promising chalcogenide salt (de)hydration reactions.

Temperature Category	Reaction	T_{turn} (°C)	GED (MJ/kg)	VED (GJ/m^3)	Dist. To Conv. Hull (meV/atom)	Decomposition Reaction	New to TES
50–100°C	$SrSe•(0↔4)H_2O$	96	0.68	2.35	0	-	Novel
	$CaSe•(0↔4)H_2O$	87	0.78	2.48	5.9	$CaSe•4H_2O \rightarrow CaSe + 4H_2O_{(s)}$	Novel
100–200°C	$Li_2S•(0↔9)H_2O$	131	2.64	3.56	0	-	Novel
	$Na_2S•(0↔9)H_2O$	154 & 180	2.67	3.53	0	-	N'tsoukpoe et al.[3]

Table 5.5 Details of promising complex anion salt (de)hydration reactions.

Temperature Category	Reaction	T_{turn} (°C)	GED (MJ/kg)	VED (GJ/m^3)	Dist. To Conv. Hull (meV/atom)	Decomposition Reaction	New to TES
< 50°C	$Fe_2SiO_4•(0↔4)H_2O$	30	0.64	1.79	5.7	$Fe_2SiO_4•4H_2O \rightarrow Fe_2SiO_4 + 4H_2O_{(s)}$	Novel
50–100°C	$Li_2CO_3•(0↔10)H_2O$	91	1.06	3.05	0	-	Novel
100–200°C	$NaOH•(0↔7)H_2O$	173	2.75	3.74	0	-	Richter et al.[69]
	$Ca(OH)_2•(0↔8)H_2O$	139	2.21	3.64	0	-	Novel
200–300°C	$Ba(OH)_2•(0↔8)H_2O$	202	1.76	3.66	0	-	Deutsch et al.[35]
	$CoPO_4•(0↔6)H_2O$	201	1.59	3.68	7.2	$CoPO_4•4H_2O \rightarrow (3/13)CoPO_4•9H_2O + (5/13)P_2H_8O_9 + (10/13)CoHO_2$	Novel
300–450°C	$KOH•(0↔1)H_2O$	405	1.34	2.53	0	-	Deutsch et al.[35]

When hypothetical halide salt (de)hydration reactions were screened in Chapter 4, promising reactions were compiled by temperature category and placed in the context of both known (de)hydration reactions and the material-level energy density of lithium ion battery[157] electrodes. As the current study is an extension of Chapter 4, **Figure 5.2a** shows the promising chalcogenide and complex anion salt (de)hydration reactions in the context of the most promising

reactions shown in Chapter 4. Two chalcogenide salt (de)hydration reactions and two complex anion salt (de)hydration reactions were found to be promising below 200°C. Notably, while the top performers between 50–450°C generally tend to be halide salt hydrates, the temperature range of 100–200°C proves to be an exception as all three promising materials are hydrates of chalcogenide salts or complex anion salts. The appearance of two promising chalcogenide salt hydrates is also significant considering the sparsity of stable chalcogenide salt hydrates discussed previously.

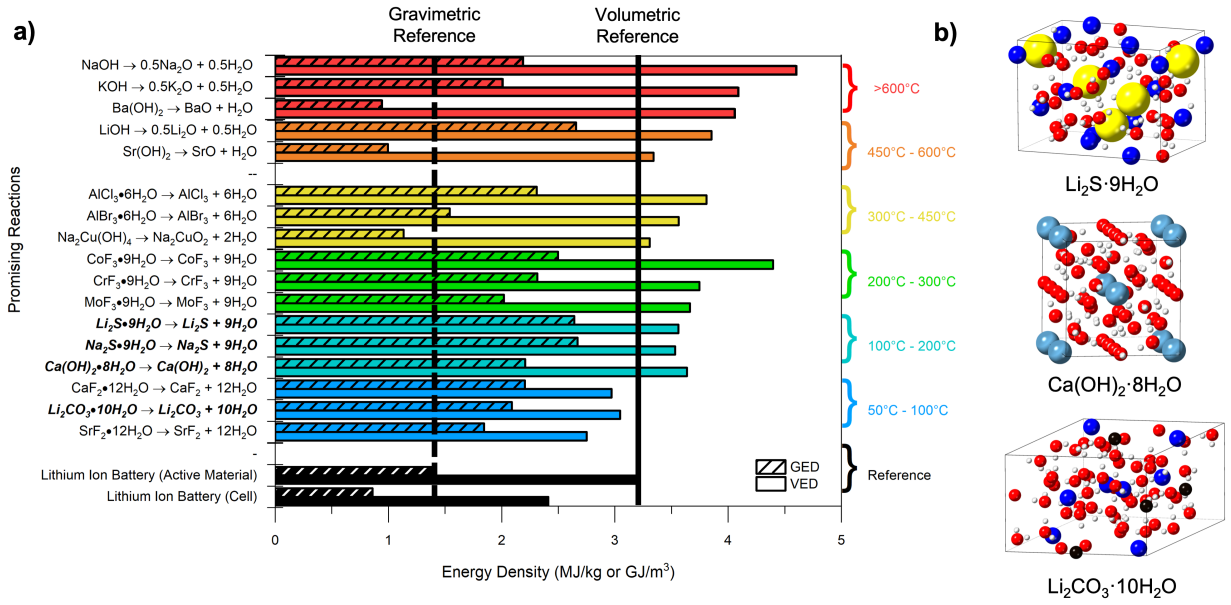

Figure 5.2 a) Gravimetric and volumetric energy densities of promising salt (de)hydration reactions, depicted by striped and solid horizontal bars, respectively. Reactions taken from earlier studies (Chapter 3 and Chapter 4) are shown in normal font, while chalcogenide and complex anion salt (de)hydration reactions are highlighted in bold italics. The energy densities of a lithium ion battery are shown for reference. b) Crystal structures of three promising hypothetical hydrates are shown on the right, where hydrogen atoms are shown as white, oxygen atoms as red, lithium atoms as dark blue, calcium atoms as light blue, sulfur atoms as yellow, and carbon atoms as black.

Of the four promising chalcogenide/complex anion salt hydrates listed in **Figure 5.2a**, only one has been studied before in the TES literature, to the best of the authors' knowledge. N'tsoukpoe et al., highlighted $Na_2S•9H_2O$ for its high energy density, but ultimately discarded it from their screening due to its toxicity.[3] The crystal structures of the other three new salt hydrates are shown in **Figure 5.2b**. $Li_2S•9H_2O$ is predicted to dehydrate to Li_2S in a single reaction step at 131°C with

a *GED* of 2.64 MJ/kg and a *VED* of 3.56 GJ/m^3. $Ca(OH)_2$•$8H_2O$ is predicted to dehydrate to $Ca(OH)_2$ in a single step at 139°C with a *GED* of 2.21 MJ/kg and a *VED* of 3.64 GJ/m^3. Li_2CO_3•$10H_2O$ is predicted to dehydrate to Li_2CO_3 in a single step at 91°C with a *GED* of 1.06 MJ/kg and a *VED* of 3.05 GJ/m^3. All three (de)hydration reactions are predicted to be thermodynamically stable.

As done for the hypothetical halide salt hydrates studied in Chapter 4, system-level energy densities (i.e., energy density calculated based on the volume of the entire heat storage system) were estimated for the hypothetical chalcogenide/complex anion salt hydrates within the MERITS (More Effective use of Renewables Including compact seasonal Thermal energy Storage) prototype TES system.[49,138,139] The numerical model for system-level energy density prediction originated from De-Jong et al.[138] for Na_2S•$5H_2O$ (i.e., the salt hydrate used in the MERITS prototype) and was adapted to include other hypothetical halide salt hydrates (Chapter 4). **Figure 5.3** shows the projected system-level volumetric energy density and discharging temperature for the hypothetical hydrates in the present study. Operating conditions were re-calculated via Equation (4.1) using the water vapor pressures of the MERITS evaporator (12 mbar) and condenser (23 mbar). Salt hydrates that are expensive or required a temperature window greater than 50°C were omitted. For reference, **Figure 5.3** also shows Na_2S•$5H_2O$, the energy density of a lithium ion battery pack,[164] and the Department of Energy's target energy density for thermochemical heat storage systems.[140]

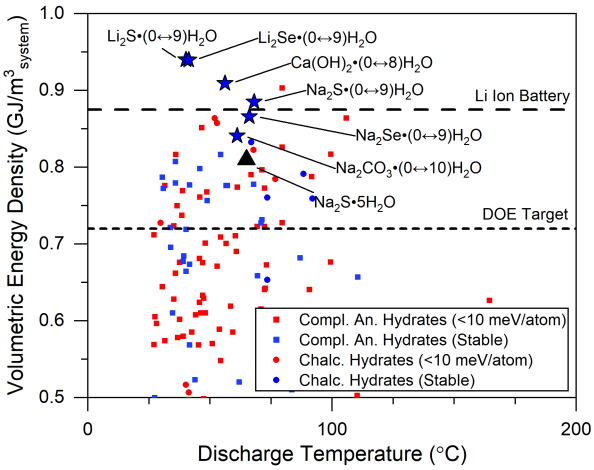

Figure 5.3 System-level volumetric energy densities and discharge temperature were predicted for hypothetical chalcogenide (circles) and complex anion (squares) salt (de)hydration reactions in the MERITS prototype.[49,138,139] Several promising reactions are highlighted (stars). The salt hydrate originally used in the MERITS prototype (triangle), lithium ion battery pack energy density[164] (long dashed line), and Department of Energy target for thermochemical heat storage[140] (short dashed line) are shown for reference.

Several promising (de)hydration reactions were found to have system-level volumetric energy densities greater than the DOE target, $Na_2S•5H_2O$, and even a lithium ion battery. The complete dehydration of $Li_2S•9H_2O$ and $Li_2Se•9H_2O$ were both projected to have system-level volumetric energy densities of 0.94 GJ/m^3 (16% greater than $Na_2S•5H_2O$). The dehydration of $Ca(OH)_2•8H_2O$ to $Ca(OH)_2$ was projected to have a system-level energy density of 0.91 GJ/m^3 (12% greater than $Na_2S•5H_2O$). The dehydration of $Na_2S•9H_2O$ to Na_2S was projected to have a system-level energy density of 0.89 GJ/m^3 (9% greater than $Na_2S•5H_2O$). All four of these reactions are predicted to be thermodynamically stable. **Table 5.6** lists all (de)hydration reactions predicted to outperform $Na_2S•5H_2O$.

Table 5.6 Promising chalcogenide and complex anion reactions that outperform $Na_2S•5H_2O$ in volumetric system energy densities.

Salt	n_{low}	n_{high}	Dist. to Convex Hull (meV/atom)	T_S (°C)	T_D (°C)	VED_{sys} (GJ/m^3)	VED_{sys} Improvement (%)
Li_2S	0	9	0.0	40	63	0.94	16.0%
Li_2Se	0	9	0.0	41	78	0.94	16.0%
$Ca(OH)_2$	0	8	0.0	56	66	0.91	12.2%
$Sr(OH)_2$	0	8	0.2	80	102	0.90	11.5%

Na_2S	0	9	0.0	68	99	0.89	9.3%
Na_2Se	0	9	0.0	66	103	0.87	6.9%
$CoPO_4$	0	6	7.2	106	117	0.86	6.7%
Li_2S	0	7	1.1	52	63	0.86	6.6%
Li_2S	0	5	9.1	53	63	0.86	5.9%
$AlPO_4$	0	7	8.0	47	56	0.85	5.1%
Na_2CO_3	0	10	0.0	61	111	0.84	3.8%
Li_2Se	0	7	0.0	67	78	0.83	2.8%
$Sr(OH)_2$	1	8	2.6	80	102	0.83	2.0%
Li_2Se	0	5	0.7	68	78	0.82	1.5%
$NiSO_4$	0	7	8.5	100	111	0.82	0.9%
$MgCO_3$	0	5	0.0	54	96	0.82	0.8%
Li_2SO_4	0	10	3.1	36	45	0.82	0.8%

5.3.2 Machine Learning.

Figure 5.4 shows the distribution of the enthalpies of dehydration across the two salt hydrate datasets (i.e., chalcogenides and complex anions), as well as the 1736 lowest energy hypothetical halide salt hydrates with $\Delta H > 0$ taken from Chapter 4 for reference. The chalcogenide hydrates are broadly distributed with a mean of 35 kJ/mol H_2O and a standard deviation of 18 kJ/mol H_2O, while the complex anion hydrates and halide hydrates possess much sharper distributions of 54 ± 14 kJ/mol H_2O and 54 ± 16 kJ/mol H_2O, respectively. The lower ΔH distribution of chalcogenide salt hydrates offers insight into the lower occurance of stable chalcogenide salt hydrates mentioned earlier. As discussed earlier in Chapter 4, salt hydrates with $\Delta H < \Delta H_{subl} = 51.1$ kJ/mol H_2O (i.e., the enthalpy of sublimation for water vapor) are determined by the convex hull stability analysis to be higher in energy than the dehydrated salt and ice. **Figure 5.4** shows that only a few of the chalcogenide salt hydrates possess $\Delta H > \Delta H_{subl}$, while a much larger number of complex anion salt hydrates and halide salt hydrates sit above ΔH_{subl}.

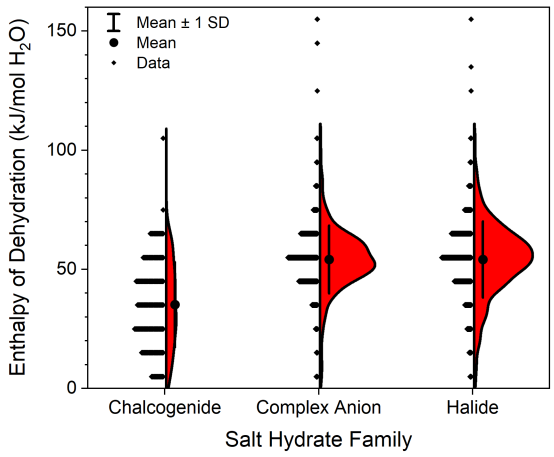

Figure 5.4 Half violin plots show the distribution of the enthalpy of dehydration by salt hydrate family. The dots on the left half of each plot show the data organized in a histogram, while the right half of the violin plot shows the smoothed distribution as well as the mean and standard deviation of the distribution.

Given the differing enthalpy distribution of the chalcogenide salt hydrates from the other salt hydrates, ML models were trained separately on the different salt hydrate family databases. To identify the most interesting feature sets, 340 distinct ML models were trained (2 salt hydrate families × 5 ML algorithms × 34 feature sets). The top-performing feature set (i.e., corresponding to the ML model with the lowest test error) was identified for each of the 10 salt hydrate family/ML algorithm pairs. A total of four compositional feature sets (Element Fractions, Ion Properties,[180] Matminer Element Properties,[142] and Matscholar Element Properties[171]) and one structural feature set (Jarvis CFID[181]) were identified, as shown in **Table 5.7**. These feature sets were further investigated.

Table 5.7 Top-performing Matminer[147] feature sets for each salt hydrate family/ML algorithm pair. Mean absolute test errors (kJ/mol H_2O) are also listed. Matminer featurizers are labelled as follows. ElementFraction: composition.ElementFraction, IonProperty: composition.IonProperty, Jarvis: structure.JarvisCFID, Matminer: composition.ElementProperty(Matminer), Matscholar: composition.ElementProperty(matscholar).

	Ridge Regr.	k-NN	SVM	RF	ET
Chalcogenide	Matscholar (7.6)	IonProperty (7.6)	Matscholar (7.8)	Matminer (6.9)	Matminer (6.1)
Complex Anion	Matscholar (8.1)	Jarvis (7.9)	Matscholar (7.6)	ElementFraction (7.2)	Jarvis (6.9)

The top-performing feature sets for each salt hydrate family were combined. Notably, the Matscholar Element Properties[171] feature set appeared in both combined feature sets, indicating some similarity among the salt hydrate families. Additionally, it should be noted that the combined chalcogenide feature set only included compositional features, while the complex anions included both compositional and structural features. This indicates that the chalcogenide hydrates tend to depend more on the composition of the hydrate, while both the composition and the structure play a critical role in the behavior of complex anion salt hydrates.

Recursive feature reduction was performed for each salt hydrate family to identify the most important features. **Figure 5.5** shows the performance of the 5 ML algorithms as a function of the number of features included. In both cases, the k-NN, RF, and ET models performed well with only a few features, while the inclusion of more features reduced the model's predictive accuracy. In contrast, the ridge regression and SVM models tended to perform better with more features, although they also tended to possess higher test errors than the k-NN, RF, and ET models. As such, the ridge regression and SVM models were disregarded when determining the optimal feature subset.

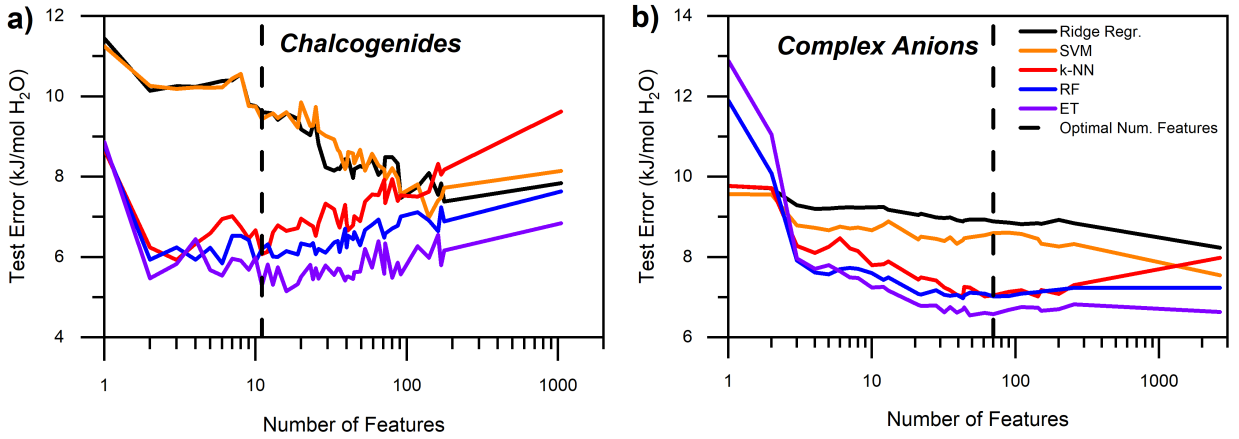

Figure 5.5 ML test error as a function of the number of features included for a) the chalcogenide salt hydrates, and b) the complex anion salt hydrates. The specific features for each given number of features is determined by recursive feature reduction. The optimal number of features is shown by the vertical dashed line.

Chalcogenide Salt Hydrates. The optimal chalcogenide feature subset included 11 features from the Matscholar Element Properties,[171] Matminer Element Properties,[142] and Ion Properties.[180] **Figure 5.6a–c** show the partial dependence plots (PDPs) of the three features that have the greatest effect on ΔH. These plots show how the average model prediction varies as a function of these features. **Figure 5.6a** shows the chalcogenide PDP for the standard deviation of the 72nd embedding of the Matscholar feature set. In the Matscholar feature set, every element on the periodic table has a distinct 200 feature embedding determined from natural language processing models trained in an unsupervised manner on abstracts of materials science journal articles. A standard deviation is taken over the elements in the composition of the salt hydrate, weighted by their atomic fractions. Regarding the 72nd embedding, S and Se have the lowest embeddings (-0.07), while metals like Cs, Mn, Sn, Li, and Ni have the highest embeddings (0.08–0.12). Like the other chalcogens, O falls on the lower end (-0.03), while H has an above average 72nd embedding (0.06). In **Figure 5.6a**, all three ML algorithms show the same trend: higher ΔH can be achieved with large standard deviations of the 72nd embedding, while hydrates with a standard deviation between 0.055–0.060 tend to have particularly small ΔH. Notably, as the hydrate number increases, the standard deviation will move towards the standard deviation of H_2O (0.060), which generally results in a lower ΔH.

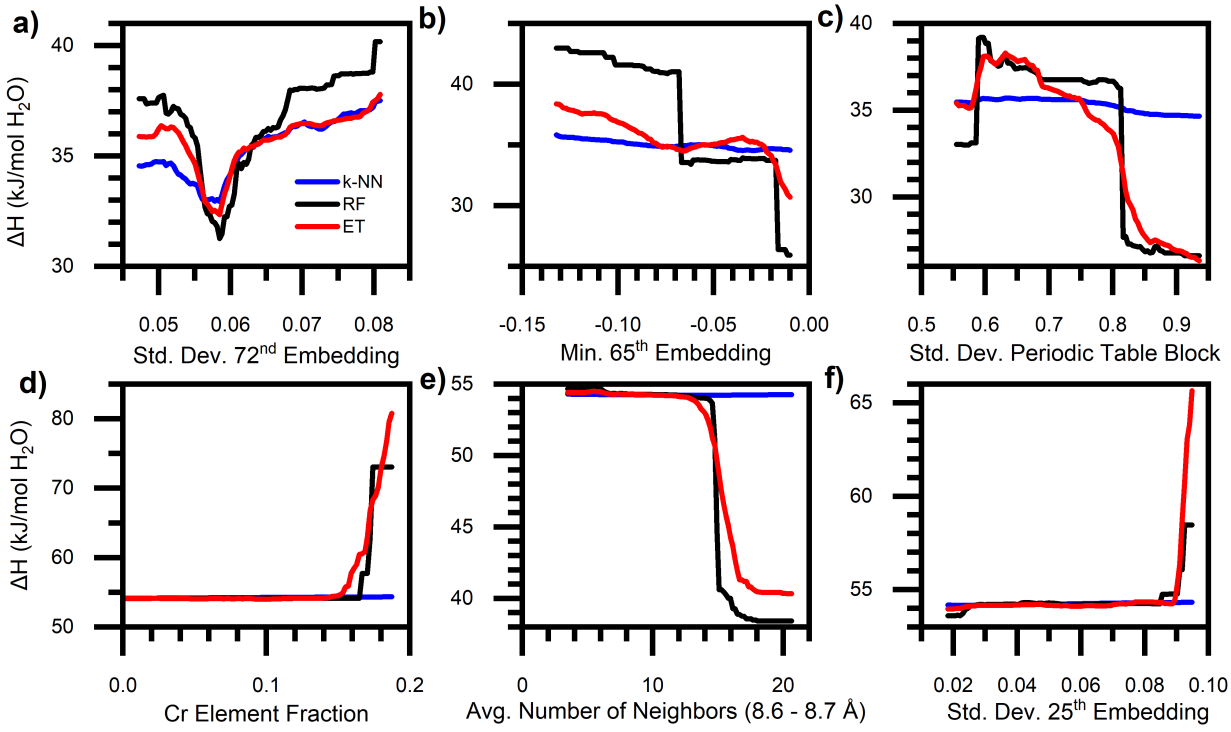

Figure 5.6 Partial dependence plots show the dependence of the optimal chalcogenide salt hydrate model (a–c) and the optimal complex anion salt hydrate model (d–f) on the three respective features that most significantly affect Δ*H*. The PDPs are a) chalcogenide: standard deviation of the 72nd Matscholar[171] embedding, b) chalcogenide: minimum of the 65th Matscholar[171] embedding, c) chalcogenide: standard deviation of the periodic table block number, d) complex anion: Cr element fraction, e) complex anion: average number of neighbors between 8.6–8.7 Å for each atom in the crystal structure, and f) complex anion: standard deviation of the 25th Matscholar[171] embedding.

Figure 5.6b shows the chalcogenide PDP of the minimum of the 65th Matscholar embedding. All three algorithms show that the predicted Δ*H* tends to decrease as the minimum 65th embedding increases. The minimum 65th embedding is usually determined by the metal; thus this PDP shows a direct dependence on the metal. In particular, metals with low 65th embeddings (e.g., Hf, Sc, Zr, Ti) tend to have higher Δ*H*, while metals with high 65th embeddings (e.g., Li, Na, W, Fe) tend to have lower Δ*H*.

Figure 5.6c shows the chalcogenide PDP of the standard deviation of the periodic table block. The periodic table blocks are assigned the following numbers based on their periodic table group number, with Groups 1–2 in block 1, Groups 13–18 in block 2, and Groups 3–12 in block 3. **Figure 5.6c** shows that Δ*H* tends to be higher for standard deviations between 0.59–0.81, and

that ΔH tends to decrease as the standard deviation increases. Since H is in block 1 and O and the other chalcogens are in block 2, the standard deviation can be reduced by choosing a metal from blocks 1 or 2 (i.e., not a transition metal), generally resulting in a higher ΔH. It should be noted that there is a slight difference in the standard deviation of the oxides as compared with analogous sulphides or selenides due to the weighting scheme used by Matminer in calculating the standard deviation. Furthermore, for any given salt, as the hydrate number increases, the standard deviation moves towards the standard deviation of H_2O (i.e., 0.71). For block 3 metals, this tends to increase ΔH.

Similar to the halide salt hydrates studied in Chapter 4, the thermodynamics of the chalcogenide hydrates depends significantly on the identity of the cation in the salt (which affects all three PDPs), while the dependence on the anion is less significant (which only slightly affects the first and third PDP). Unlike the halide hydrates in Chapter 4, dependencies on the crystal structure were not found for the chalcogenides. The trends are complex and at times contradictory, but optimal hydrates that meet the criteria for high ΔH (i.e., 72nd embedding standard deviation outside the range 0.055–0.065, minimum 65th embedding less than -0.07, block standard deviation less than 0.81) do exist. These hydrates are $HfS_2 \cdot H_2O$, $HfSe_2 \cdot H_2O$, $SrO \cdot H_2O$, and $ZrSe_2 \cdot H_2O$.

Complex Anion Salt Hydrates. The optimal complex anion feature subset included 70 features from the Matscholar Element Properties,[171] Jarvis CFID,[181] and Element Fractions. **Figure 5.6d–f** show the PDPs of the three features that have the greatest effect on ΔH for complex anion hydrates. **Figure 5.6d** shows the complex anion PDP for the element fraction of Cr. Both decision tree-based algorithms show a rapid rise in the predicted ΔH for large fractions of Cr (> 16%). Although it is much less noticeable for the k-NN model due to the large number of features, the rise in the k-NN PDP is very large compared to the other 69 features in the k-NN model. Thus, all

models agree that complex anion salt hydrates that contain about 1 Cr for every 6 atoms will tend to have higher ΔH.

Figure 5.6e shows the complex anion PDP for the 87th feature of the nearest neighbor distribution. The Jarvis CFID (Classical Force-field Inspired Descriptors) feature set contains features structural descriptors such as nearest neighbor distributions, radial distribution functions, and angle/dihedral distributions. The 87th nearest neighbor feature (out of 100 nearest neighbor features) corresponds to the 8.6–8.7 Å bin of the nearest neighbor distribution (i.e., the average number of atoms located between 8.6–8.7 Å away from a given atom in the crystal structure). **Figure 5.6e** shows that complex anion salt hydrates with 15 or more neighbors between 8.6–8.7 Å tend to have lower ΔH.

Figure 5.6f shows the complex anion PDP for the standard deviation of the 25th Matscholar embedding. Elements like Cr, Co, Cs, F, and Fe tend to have low 25th embeddings (-0.16 to -0.10), while elements like P, Ca, La, N tend to have high 25th embeddings (0.04–0.09). H has an embedding of -0.04, while O has an embedding of 0.00. **Figure 5.6f** shows that hydrates with high standard deviations of the 25th embedding (e.g., chromium phosphate hydrates) tend to have significantly higher ΔH. Additionally, salt hydrates with very small standard deviations of the 25th embedding tend to have slightly lower ΔH. It should be noted that as the hydrate number increases for a given salt, the standard deviation will move in the direction of the standard deviation of H_2O (0.026), which will increase ΔH for salts with lower 25th embedding standard deviations and greatly decrease ΔH for salts with very high 25th embedding standard deviations.

The PDPs of the three features that have the greatest effect on ΔH for complex anions show regimes of high and low ΔH. Unlike the optimal chalcogenide ML models, which used 11 features to predict general trends in ΔH across the chalcogenides, the optimal complex anion ML models

leveraged the most important of their 70 features to partition the space of complex anion salt hydrates into binary regimes of higher and lower ΔH. Given the greater heterogeneity of complex anion salt hydrates than chalcogenide salt hydrates, this is not surprising.

Predictions Across Salt Hydrate Families. To study the compatibility of the different salt hydrate families, the optimal models for the chalcogenide hydrates and complex anion hydrates were retrained leveraging the other salt hydrate database and/or the 1736 halide hydrates from Chapter 4 as additional training/validation data. Note that the test set was still only taken from either the chalcogenide hydrates or complex anion hydrates. The test errors are shown in **Table 5.8**. The predictive ability of the optimal chalcogenide hydrate ML models generally diminished when data from other salt hydrate families were added to the training set, especially in the case of complex anion hydrates. This is unsurprising as the chalcogenide hydrates were shown earlier to be distinct from the other salt hydrate families in **Figure 5.4**. Furthermore, the halide hydrates are chemically closer to chalcogenide hydrates than the diverse group of complex anion hydrates. The one exception to the trend of diminished predictive accuracy is seen in the RF model, where the addition of halide hydrates to the training set increased the predictive accuracy of the chalcogenide model.

Table 5.8 Predictive accuracy of optimal ML models when trained on additional data from other salt hydrate families.

Predicted Salt Hydrate Family	Additional Training Data	k-NN Test Error (kJ/mol H_2O)	RF Test Error (kJ/mol H_2O)	ET Test Error (kJ/mol H_2O)
Chalcogenide	None	6.2	6.2	5.5
	Complex Anion	8.4	6.8	6.2
	Halide	6.8	5.9	5.4
	Complex Anion & Halide	7.9	6.4	6.3
Complex Anion	None	7.3	7.1	6.7
	Chalcogenide	7.0	7.0	6.6
	Halide	7.1	7.1	6.7
	Complex Anion & Chalcogenide	7.1	7.1	6.6

In contrast to the optimal chalcogenide models, the optimal complex anion models did not significantly vary in their ability to predict complex anion hydrates when chalcogenide and/or halide data was added to the training set. As discussed before, the complex anion model is accustomed to the heterogeneity of complex anion salt hydrates, and thus is unaffected or perhaps slightly aided by more data from different salt hydrate families.

5.4 Conclusions

In this study, the computational protocol developed in Chapter 4 was adapted for hypothetical salt hydrates containing chalcogenides or complex anions. First principles calculations were performed on a total of 1779 hypothetical chalcogenide salt hydrates and 5233 hypothetical complex anion salt hydrates that were generated via atomic substitution into relevant crystal structure templates. The energy densities, operating conditions, and thermodynamic stability of (de)hydration reactions involving these hypothetical hydrates were predicted. Promising reactions involving both chalcogenide salt hydrates and complex anion salt hydrates were identified for operating temperatures below 200ºC. System-level energy densities were projected using an adapted model of a thermochemical heat storage prototype,[49,138,139] revealing many hydrates with system-level energy densities that exceed the U.S. Department of Energy's target of 200 kWh/m^3.[140]

Interpretable machine learning models were trained separately on the resulting databases of chalcogenide salt hydrates and complex anion salt hydrates to identify the features that affect the thermodynamics of salt (de)hydration. Chalcogenide salt hydrates were found to possess a distribution of dehydration enthalpies that is lower and flatter than the distributions of halide salt hydrates and complex anion salt hydrates. Furthermore, general trends across the chalcogenide salt hydrates were identified with several features, such as the elemental embeddings from

Matscholar.[171] In contrast, the complex anion salt hydrates proved to be a more heterogeneous class of salt hydrates. Rather than identifying general trends across the complex anion salt hydrates, the optimal model used 70 features to effectively partition the chemical space of complex anion salt hydrates. The promising materials and design insights identified in this study are anticipated to catalyze the development of effective TES systems.

Chapter 6 Discussion on Mixed Metal Salt Hydrates for Thermal Energy Storage

6.1 Introduction

One particularly interesting TES materials space is the class of mixed metal salt hydrates. Unlike the salt hydrates studied so far in this dissertation, whose salts contain a single cation and anion, mixed metal salt hydrates contain multiple cations. Many mixed metal salt hydrates have been observed experimentally. In the TES screening of Donkers et al.,[55] 20% of the 420 salt hydrates considered were mixed metal salt hydrates. Mixed anion salt hydrates are also possible, but less common. Recently, mixed metal salt hydrates have attracted interest for TES. Several experimental studies have found that mixtures of salt hydrates (e.g., $MgCl_2$-$CaCl_2$,[182] $MgSO_4$-$ZnSO_4$,[183] $MgSO_4$-$SrCl_2$[184]) demonstrate greater cyclability, energy densities, and reaction kinetics than their respective pure salts. Additionally, Heijmans et al.[185] computationally showed that the doping of $MgCl_2$ hydrates with Ca could reduce the formation of toxic HCl gas, a commonly observed irreversibility during the dehydration of $MgCl_2$ hydrates.[186] However, mixed metal salt hydrates still have their own limitations. A molecular dynamics study performed by Huinink et al.[187] found that Ca doping of $MgCl_2$ hydrates failed to increase the diffusivity of H_2O through the salt hydrate. Furthermore, mixing involves more complexity in the preparation of the material. Sutton et al.[188] investigated the effect that mixing technique had on the performance of mixed salt hydrates. A 20-fold difference in the energy density was noticed for hydrates of a $CaCl_2$-$LiNO_3$ mixture depending on whether or not the mixing technique prevented interactions between deliquesced salts. Even still, the literature seems to indicate the great potential of mixed metal salt hydrates for TES.

Another reason mixed metal salt hydrates are interesting for TES is the size of the available chemical space. A single metal salt hydrate possesses the general form $M_pX_q \bullet nH_2O$, where M is a cation, X in an anion, n is the hydrate number, and p and q are stoichiometric coefficients that enforce charge neutrality. There are three degrees of freedom within the chemical composition space of these hydrates: 1) the cation, 2) the anion, and 3) the hydrate number. The stoichiometric coefficients p and q are fixed based on the ratio of the oxidation states of the cation and anion. In contrast, a mixed metal salt hydrate with two cations possesses the general form $M_pM'_rX_q \bullet nH_2O$, where M' is another cation and r is a third stoichiometric coefficient. There are five degrees of freedom associated with this type of salt hydrate: 1) the first cation, 2) the second cation, 3) the cation mixing ratio (i.e., r/p), 4) the anion, and 5) the hydrate number. Unlike the single metal salt hydrates, where the stoichiometric coefficients are set by the charge neutrality constraint, mixed metal salt hydrates have an additional degree of freedom among the three stoichiometric coefficients. These extra two degrees of freedom not only greatly increase the size of the chemical space, but also increase the chemical space in a strategic direction for property tuning. As shown in Chapter 4 for the hypothetical halide salt hydrates and Chapter 5 for the hypothetical chalcogenide and complex anion salt hydrates, the choice of cation is crucial in tuning the thermodynamics of the salt hydrate. While single metal salt hydrates have a discrete set of choices for the cation, a practically infinite combination of cation pairs and mixing ratios is possible for mixed metal salt hydrates. Thus, an enlarged design space can be accessed by tapping into the extremely wide composition space of mixed metal salt hydrates.

This short chapter consists of a preliminary computational study of hypothetical mixed metal salt hydrates, investigating the thermodynamic effect of mixing and the effectiveness of ML

in predicting the performance of mixed metal salt hydrates. A discussion regarding future directions for a screening of mixed metal salt hydrates is also provided.

6.2 Methodology

First principles calculations were performed on a subset of hypothetical mixed metal salt hydrates. Given the vast chemical space of the mixed metal salt hydrates, a thorough screening was not attempted; nevertheless important critical thermodynamic properties of the mixed metal salt hydrates were computed, as done in previous chapters.

6.2.1 Hypothetical Hydrate Generation

Crystal structure templates were compiled for hypothetical mixed metal halide salt hydrates. The 76 crystal structure templates used in Chapter 4 for the hypothetical halide salt hydrates were adapted to include two distinct metal sites, thus transforming them into templates for mixed metal salt hydrates. In each case, 50% of the original metal sites were occupied by the first cation, while the other 50% were occupied by the second cation. Additionally, 311 experimentally known mixed metal halide salt hydrates (listed in Appendix F) were extracted from the ICSD,[103] resulting in a total of 387 crystal structure templates for hypothetical mixed metal halide salt hydrates. Accounting for the 62 cations used in Chapter 4, the 4 halides, and the constraint of charge neutrality, a total of 786,236 possible hypothetical mixed metal halide salt hydrates can be generated. Given the large number of structures, only a small fraction of these were characterized.

6.2.2 DFT Calculations

DFT calculations were performed on two subsets of generated hypothetical mixed metal salt hydrates, although no calculations were performed on known mixed metal salt hydrates in this

study. In both cases, relaxed crystal structure geometries and ground state energies were calculated using the VASP[93] code in the same manner as done in previous chapters. Specifically, all calculations used a 500 eV planewave cutoff energy, the projector augmented wave method of Blöchl,[94,95] spin polarization, and a converged Monkhorst-Pack[96] k-point mesh. The optPBE-vdW[84–86,88] exchange-correlation functional was used to optimize the crystal structure geometry (until the atomic forces were less than 0.02 eV/Å), while the Perdew-Wang 91[83] exchange correlation functional was used to calculate the final ground state energy.

6.2.3 Thermodynamics of Mixing

The first subset of investigated hypothetical mixed metal salt hydrates consisted of metal substitution into 28 hypothetical $MgCl_2$•nH_2O crystal structures calculated in Chapter 4. The $MgCl_2$•7H_2O structure was omitted due to its large size. Given the 20 other divalent cations, DFT calculations were performed on 560 hypothetical mixed metal salt hydrates of the form $Mg_{0.5}M_{0.5}Cl_2$•nH_2O. Of these, 86.8% of the calculations converged.

The enthalpy of mixing (ΔH_{mix}) was calculated for each salt hydrate in this subset as

$$\Delta H_{mix} = E_{mixed} - \frac{1}{2}E_{MgCl_2} - \frac{1}{2}E_{MCl_2} \quad (6.1)$$

where E_{mixed} is the energy of $Mg_{0.5}M_{0.5}Cl_2$•nH_2O, E_{MgCl_2} is the energy of $MgCl_2$•nH_2O, and E_{MCl_2} is the energy of MCl_2•nH_2O. When calculating the enthalpy of mixing, the crystal structures of all three salt hydrates are assumed to be identical. Note that a negative ΔH_{mix} indicates that mixing is thermodynamically favored relative to the unmixed salt hydrates.

6.2.4 Machine Learning Prediction of Mixed Metal Salt Hydrates

ML models were trained on a combination of single metal salt hydrates and mixed metal salt hydrates to determine how accurately ML could predict the properties of mixed metal salt hydrates.

Data. 4145 single metal salt hydrates (lowest energy structures) from the preceding chapters were adopted. Additionally, DFT calculations were performed on 1176 randomly selected hypothetical mixed metal salt hydrates generated from crystal structure templates of experimentally known mixed metal salt hydrates found in the ICSD.[103] (Note: the stability of the experimentally known mixed metal salt hydrate templates was not evaluated.) ML models were trained to predict ΔH for the complete dehydration of the salt hydrates (i.e., dehydrated to the anhydrous salt). In the case of the mixed metal salt hydrates, ΔH was calculated according to Equation (3.1), where E_{dehyd} was taken to be a linear combination of the energies of the respective anhydrous single metal salts.

Model Evaluation. Chapter 5 demonstrated that the Extra Trees (ET) ML algorithm performed the best for predicting ΔH for single metal salt hydrates. ET models were trained with 100 trees and evaluated on an unseen test set consisting of 20% of the salt hydrates of interest.

Feature Selection. 1499 features were compiled for the 4145 single metal salt hydrates using compositional featurizers from Matminer.[147] These features were also compiled for the 1176 mixed metal salt hydrates, but the mixed metal salt hydrate data was only considered after the feature selection process. Structural features were not considered as these are not generally known *a priori* for hypothetical salt hydrates and are therefore unhelpful when making predictions of new hypothetical salt hydrates. Redundant features (i.e., features that possessed a correlation coefficient with a previous feature greater than 0.8) and uninformative features (i.e., features that possessed a Pearson correlation coefficient with ΔH less than 0.2) were removed resulting in 201 features.

Recursive feature addition was then performed. When determining the best combination of *m+1* features, the 10 best performing models using *m* features were chosen. Each of these 10 models was then paired with each of the remaining features, trained, and evaluated. The test error of the best model plateaued after 18 features, so the best 18 feature model was selected as the optimal ML model.

6.3 Results and Discussion

6.3.1 Thermodynamics of Mixing

Figure 6.1 summarizes the DFT-calculated thermodynamics of mixing for the lowest energy structures of the hypothetical $Mg_{0.5}M_{0.5}Cl_2 \bullet nH_2O$ hydrates. Red boxes show hydrates where mixing is thermodynamically favorable relative to the single metal salt hydrates in that crystal structure. White boxes indicate that mixing is not particularly favorable or unfavorable, but rather behaves like a linear mixture of the two single metal salt hydrates (in that crystal structure). Blue boxes show hydrates where mixing is thermodynamically unfavorable. In this case, the mixed metal salt hydrate is predicted to phase separate into a mixture of the single metal salt hydrates (or possibly decompose into some other lower energy phase). As shown in **Figure 6.1**, the energetics of mixing are neutral or unfavorable in most cases.

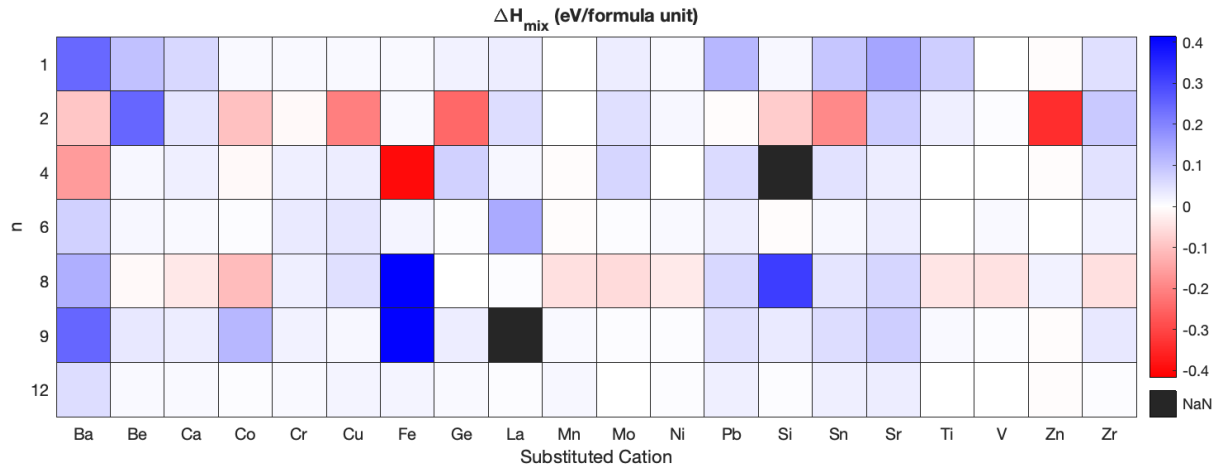

Figure 6.1 Heatmap of the enthalpy of mixing for the lowest energy $Mg_{0.5}M_{0.5}Cl_2 \bullet nH_2O$ hydrates. Negative values (red) indicate thermodynamically favorable mixing.

It is interesting to note that favorable mixing compositions tend to appear in particular rows corresponding to specific values of *n*: i.e., the dihydrate, tetrahydrate, and octohydrate. Although for a given hydrate number the lowest energy crystal structure varies across the different substituted cations, there seems to be a correlation between the hydrate number and whether or not any metals will favorably substitute for Mg. Although this trend is found specifically for hypothetical $Mg_{0.5}M_{0.5}Cl_2 \bullet nH_2O$ hydrates, this trend may indicate a potential strategy for screening mixed metal salt hydrates. A systematic DFT screening through the almost 800,000 hypothetical mixed metal salt hydrates is not feasible, so approximate-but-efficient algorithms such as ML would be useful in determining where to perform subsequent expensive DFT calculations. Hypothetically, if one were to know which mixed metal salt hydrates are 'red' *a priori*, DFT calculations would only need to be performed on those salt hydrates. DFT calculations would not be necessary for 'blue' or 'white' mixed metal salt hydrates because their thermodynamic behavior (i.e., stability and enthalpy of dehydration) is determined by the linear mixture of the respective single metal salt hydrates. Unfortunately, this knowledge is not known *a priori*. However, if the previous trend were to be true of mixed metal salt hydrates generally, 'red' mixed metal salt

hydrates would appear in clusters. Practically, this means that when a mixed metal salt hydrate is found to have lower energy than a linear mixture of the respective single metal salt hydrates in the same crystal structure, then one should perform systematic DFT calculations on metal substitutions within that mixed metal salt hydrate.

Figure 6.2 shows an interesting trend regarding the crystal structure of the mixed metal salt hydrates. Each of the 28 crystal structure templates used in generating the $Mg_{0.5}M_{0.5}Cl_2 \bullet nH_2O$ hydrates is represented by a datapoint, which are plotted according to their normalized cation-cation distance as well as the average of the absolute value of ΔH_{mix} across the 20 substituted metals. The absolute value of ΔH_{mix} shows the magnitude of non-linearity in mixing; mixed metal salt hydrates with low absolute values of ΔH_{mix} demonstrate linear mixing (i.e., neutral mixing energetics). The normalized cation-cation distance (R_{cc}) is calculated as

$$R_{cc} = \frac{r_{cc}}{r_{cw}} \tag{6.2}$$

where r_{cc} is the cation-cation distance in the respective $Mg_{0.5}M_{0.5}Cl_2 \bullet nH_2O$ crystal structure template, and r_{cw} is the cation-water bond distance in the respective $Mg_{0.5}M_{0.5}Cl_2 \bullet nH_2O$ crystal structure. **Figure 6.2** shows that as R_{cc} increases, the average magnitude of the enthalpy of mixing tends to decrease. This makes intuitive sense: when cations are further apart in the crystal structure, they will interact less with each other, reducing the effect (favorable or unfavorable) of mixing.

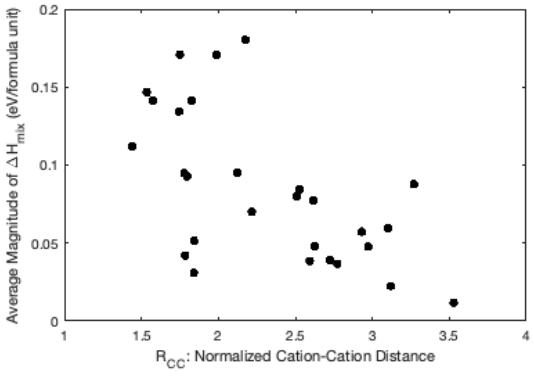

Figure 6.2 The average magnitude of the enthalpy of mixing tends to decrease across the 28 crystal structures as the respective $MgCl_2$•nH_2O structure's cation-cation distance increases. The cation-cation distance is normalized by the cation-water bond distance.

This leads to another strategy for screening mixed metal salt hydrates. Crystal structures that possess larger R_{cc} will tend to be 'white' hydrates discussed previously that exhibit nearly linear mixing behavior. As such, DFT calculations should focus on mixed metal salt hydrates with low values of R_{cc}. For example, consider a strategy where a linear mixing for all mixed salt hydrates with $n \geq 4$ and $R_{cc} \geq 2.25$ is assumed rather than performing DFT calculations. For $R_{cc} \geq 2.25$, the average magnitude of the enthalpy of mixing is less than 0.1 eV/formula unit (9.6 kJ/mol hydrate), while the average magnitude can be much greater for $R_{cc} < 2.25$. If n is 4, any given salt hydrate will have a minimum of 14 atoms per formula unit (i.e., 12 in the water, 1 cation fractionally split between multiple metals, and 1 anion). If we assume completely linear mixing (i.e., neutral mixing energetics), then the average error in this assumption is equal to the average magnitude of the mixing enthalpy, which in this case is at most 0.1 eV/formula unit or 9.6 kJ/mol hydrate. Assuming the limiting case of a salt hydrate with 4 water molecules and 14 atoms per formula unit, the average error in the energy predicted by a linear mixing approximation is at most 2.4 kJ/mol H_2O or 7.1 meV/atom. This average error in the energy directly translates into error in the enthalpy of dehydration or stability. An average error of 2.4 kJ/mol H_2O in the enthalpy of dehydration and

7.1 meV/atom in the thermodynamic stability is acceptable, and these average error values will decrease as the number of water molecules and atoms in the salt hydrate increases.

6.3.2 Machine Learning Prediction of Mixed Metal Salt Hydrates

The optimal 18 feature ET model was trained and tested on various datasets. **Figure 6.3a** shows the predictive accuracy of the optimal model when it is trained on 80% of the single metal salt hydrate data and tested on the remaining 20% of the single metal salt hydrates. It possesses a test mean absolute error (MAE) of 9.3 kJ/mol H_2O. This MAE is higher than the test errors seen in the models trained in Chapter 5. Since the purpose of the current model is to accurately predict ΔH (i.e., the enthalpy of dehydration) for unknown hypothetical hydrates rather than identify trends in the salt hydrate thermodynamics, it was only trained on compositional features. Furthermore, salt hydrates with low ΔH were also included in the data here, while Chapter 5 ignored salt hydrates with negative ΔH as these unstable hydrates were not interesting for understanding the trends in the thermodynamics of typical salt hydrates. Even still, this error with DFT is in the same range as the error between DFT and experiments calculated for salt hydrates in Chapter 3 (10.0 kJ/mol H_2O) or the uncertainty of experiments (7.5 kJ/mol H_2O).

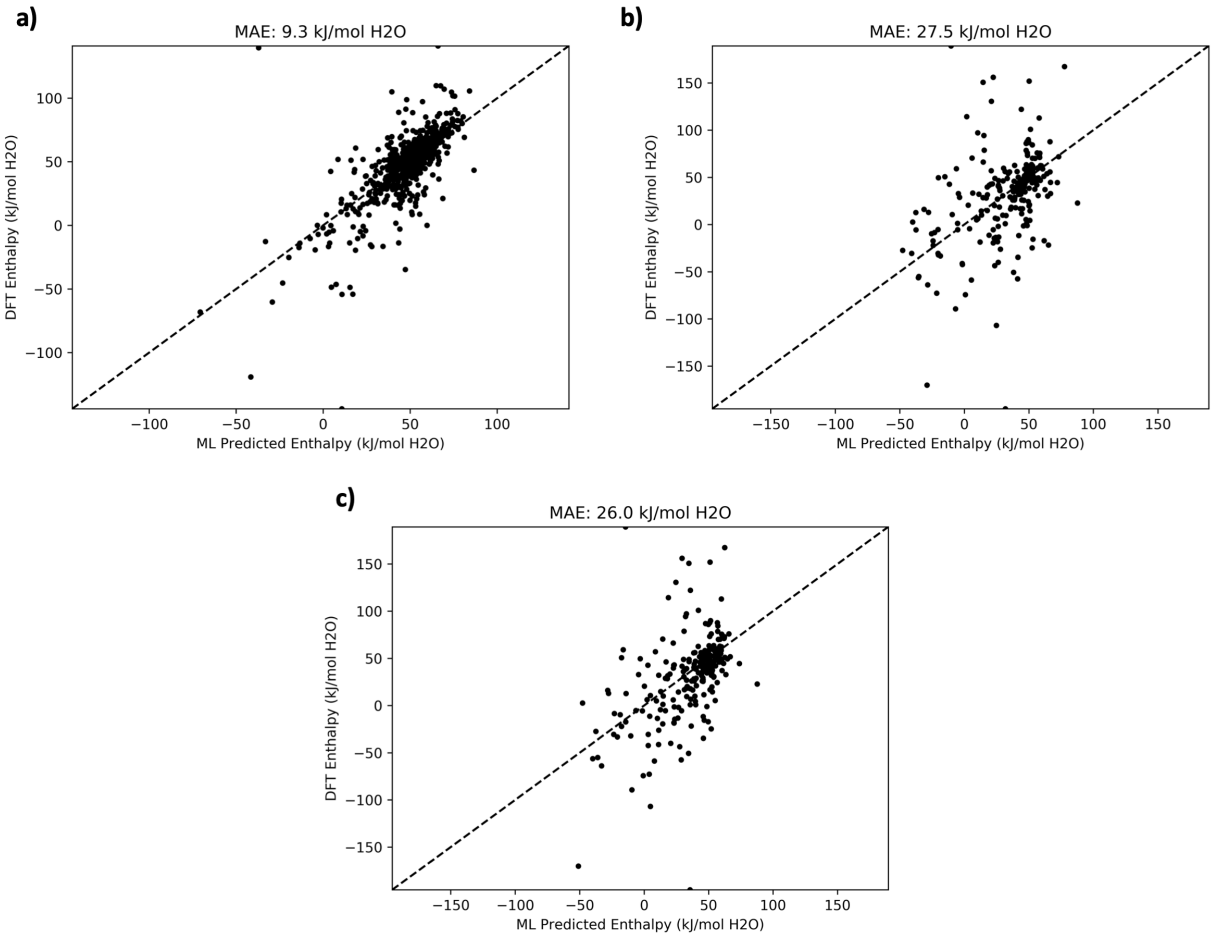

Figure 6.3 Predictive accuracy of the optimal model a) trained and tested on single metal salt hydrate data, b) trained and tested on mixed metal salt hydrate data, and c) trained on single and mixed metal salt hydrate data, tested on mixed metal salt hydrate data. Dashed lines show perfect agreement between ML and DFT.

Figure 6.3b shows the predictive performance of the optimal model when it is instead trained on 80% of the mixed metal salt hydrate data and tested on the remaining 20% of the mixed metal salt hydrate data. The predictive performance of the mixed metal salt hydrate ML model is much worse (MAE 27.5 kJ/mol H_2O) than the single metal salt hydrate ML model. This could be due to a variety of reasons. First, the features were selected to optimize the performance of the single metal salt hydrate model. Second, the mixed metal salt hydrate dataset was about 28% of the size of the single metal salt hydrates. However, with 940 training data points, this is less likely to be the dominating factor. Third, and perhaps most importantly, the mixed metal salt hydrate

data shows significantly greater range of ΔH values. The single metal salt hydrates have a ΔH distribution of 49 ± 24 kJ/mol H_2O, while the mixed metal salt hydrates have a ΔH distribution of 30 ± 46 kJ/mol H_2O. This wider distribution of ΔH proves difficult to predict for the ML model.

Figure 6.3c shows the predictive performance of a third model. This model is similar to that of **Figure 6.3b**, but also includes all of the single metal salt hydrates in the training set. The test error (on the 20% of mixed metal salt hydrates) is slightly lower than before (MAE 26.0 kJ/mol H_2O), indicating that the inclusion of the single metal salt hydrate data only slightly facilitated the model's learning. Although smaller, this degree of error is unacceptable for predicting the thermodynamics of hypothetical mixed metal salt hydrates.

6.4 Future Directions

The screening analysis presented in earlier chapters is absent here and should be employed to more carefully characterize mixed metal hydrates. The determination of the lowest energy structure requires several crystal structures of the same chemical composition to be calculated with DFT. Furthermore, a complete thermodynamic stability analysis requires calculation of the various hydrates (with different water contents) across the same (constant) salt family. This stability analysis affects which salt hydrates meet the various stability criteria, but also affects the set of reactions that occur in the salt family. For example, if the tetrahydrate and anhydrous salt were characterized, one could calculate the energy density of the reaction going from the salt to the tetrahydrate. However, if the stability of the mono-, di-, or tri-hydrate are unknown, one does not know whether the reaction will occur in a single reaction or multiple reaction steps. This leads to two potential pathways forward. 1) High-throughput DFT calculations could be performed for all hydrates in a few mixed metal salt families of interest. 2) A surrogate model (such as a ML algorithm) is developed to predict either the energy or stability with reasonable accuracy for all

hypothetical mixed metal salt hydrates. DFT calculations would be necessary to conduct on a subset of compositions to inform this surrogate model and then later to validate the interesting hypothetical mixed metal salt hydrates identified by the surrogate. Naturally, the latter option would be preferred if it is possible.

As demonstrated earlier, ML demonstrated difficulty predicting the enthalpy of dehydration for the class of mixed metal salt hydrates included in the training set. There are several ways to potentially increase predictive accuracy. 1) Accuracy may be increased by more rigorous calculation of ΔH. First, ΔH is currently calculated with respect to the linear combination of constituent single metal salts. However, a more accurate way to characterize the dehydrated phase would be to find the lowest energy phase(s) for the anhydrous composition using the Materials Project,[143] and then calculating the energy of these phases using the DFT calculation protocol used in this study. Additionally, every hypothetical crystal structure for a given salt hydrate composition should be characterized and the lowest energy structure taken to more rigorously predict ΔH. 2) Rather than predicting energy, a ML model can be trained on salt hydrate features to predict a mixed metal salt hydrate's thermodynamic stability. DFT calculations using the Materials Project[143] computational protocol would be performed on each calculated hypothetical mixed metal salt hydrate, and Pymatgen[142] would be used to calculate the energy to the convex hull. Given the distribution of energies to the convex hull, it is likely that a classification approach (e.g., predicting stability categories of 0 meV/atom, 0–10 meV/atom, 10–25 meV/atom, 25–50 meV/atom, and >50 meV/atom above the convex hull) would be more accurate than a regression approach. 3) Predictive accuracy may be increased by leveraging an active learning[189] strategy, where ML not only predicts the energy or thermodynamic stability, but performs an uncertainty

analysis to identify the next hypothetical mixed metal salt hydrates to perform DFT calculations on that will maximize the ML algorithm's predictive accuracy.

A high predictive accuracy is required for ML to serve as a surrogate for DFT. For example, given the uncertainty of experimental ΔH quantified in Chapter 3 (7.5 kJ/mol H_2O), the test error of predicting DFT-calculated ΔH should be at least similar in magnitude to 7.5 kJ/mol H_2O, if not lower. Since current ML models have not yet demonstrated this level of accuracy for mixed metal salt hydrates, other algorithms may help facilitate a targeted screening. For example, the previous discussion about the thermodynamics of mixing offers a starting point for both identifying the hypothetical hydrates that warrant DFT calculations and those that don't. It would be advisable to conduct a follow up study on more mixed metal salt hydrates to verify and build off of the insights developed earlier. For example, if the trend in **Figure 6.2** is shown to hold more generally for hypothetical mixed metal salt hydrates, it can be leveraged to determine when one can assume linear mixing.

Additionally, the gravimetric water capacity (n_g) is a critical feature that can be easily calculated for any hypothetical salt hydrate and it has been shown in Chapter 3 to correlate well with the gravimetric energy density (when fully dehydrated). The gravimetric water capacity is calculated as

$$n_g = \frac{n}{MM_{hyd}} \tag{6.3}$$

where n is the hydrate number and MM_{hyd} is the molar mass of the salt hydrate. This metric can be used to evaluate whether or not a hypothetical mixed metal salt hydrate has the potential to have a large gravimetric energy density. This may highlight particularly interesting salt hydrate families, where systematic DFT calculations could be performed. However, this metric should be used with caution as many single metal salt hydrates have possessed high n_g, but were not promising because

many reaction steps were required to fully (de)hydrate, resulting in a wide temperature window. Other strategies, especially those with an emphasis on the thermodynamic stability, should be used in conjunction with considerations of gravimetric water capacity.

6.5 Conclusions

Mixed metal salt hydrates show great potential for TES due to their superior experimental performance and a large chemical space. A total of 786,236 hypothetical mixed metal halide salt hydrates can be generated from plausible crystal structure templates. DFT calculations were performed on 560 $Mg_{0.5}M_{0.5}Cl_2 \bullet nH_2O$ hydrates and 1176 randomly selected mixed metal salt hydrates. Enthalpies of mixing were calculated for the $Mg_{0.5}M_{0.5}Cl_2 \bullet nH_2O$ hydrates, revealing clusters of hydrates with thermodynamically favorable mixing around particular hydrate numbers. Additionally, an inverse correlation was identified between the normalized cation-cation distance in the hydrate and the energetic effect of mixing. Both of these insights offer potential strategies for targeted screening of mixed metal salt hydrates.

A machine learning model was trained to predict the enthalpy of dehydration of the 1176 mixed metal salt hydrates, but its predictive accuracy was poor compared to a similar model developed for single metal salt hydrates. When the single metal salt hydrates were added to the training set of mixed metal salt hydrates, the predictive accuracy on the mixed metal salt hydrates slightly increased, but remained far from the level of accuracy required to guide DFT calculations. Future research directions were discussed. The effectiveness of ML could be increased by increasing the rigor of the calculated ΔH for mixed metal salt hydrates, predicting thermodynamic stability using classification ML, and by applying active learning strategies. Additional screening strategies could also be implemented by leveraging trends in simple features, such as the normalized cation-cation distance and gravimetric water capacity.

Chapter 7 Conclusions and Next Steps

Salt hydrates demonstrate great potential for thermal energy storage applications due to their high energy densities, reversibility at moderate temperatures, and capacity for long duration storage. However, a large number of practical complexities, such as issues with cyclability, cost, irreversible side reactions, and slow kinetics, have kept many salt hydrates from reaching their full potential as heat storage materials. While much research has gone into developing a few common salt hydrates, less research has focused on the discovery of other (new) salt hydrates with potentially superior performance. Together, these prior studies have characterized only a few hundred salt hydrates using tabulated thermodynamic data and relatively few experiments.[3,35,55,69] A broader search will be helpful in identifying optimal materials. The need for more promising materials is also heightened by the temperature dependence of TES systems. Since salt hydrates store heat under specific operating conditions, TES applications will benefit from the knowledge of a variety of promising salt hydrates which presumably will widen the space of available operating temperatures.

The present study has significantly expanded the field's knowledge of the salt hydrate chemical space. First principles calculations were performed to characterize the thermodynamic and heat storage properties of 4145 known and hypothetical salt hydrates. These calculations showed good agreement with tabulated data for known salt hydrates. A rigorous thermodynamic stability analysis revealed that 1594 (de)hydration reactions were predicted to be stable or nearly stable (within 10 meV/atom of the convex hull). Among these, several novel, promising reactions were identified from a variety of salt hydrate families over a wide range of temperatures. Such

reactions include the dehydration of $CrF_3 \bullet 9H_2O$, $CoF_3 \bullet 9H_2O$, $VF_2 \bullet 12H_2O$, $CaF_2 \bullet 12H_2O$, $Li_2S \bullet 9H_2O$, $Ca(OH)_2 \bullet 8H_2O$, and $Li_2CO_3 \bullet 10H_2O$. The materials-level energy densities of these salt hydrates were shown to exceed the materials-level energy density of lithium ion batteries. Additionally, when system-level energy densities were projected for their use in an experimental TES prototype,[49,138,139] a handful of these promising salt hydrates were found to have projected system-level energy densities greater than a lithium ion battery at the cell level. An even larger collection of materials were found to exceed the Department of Energy's system-level energy density target of 200 kWh/m^3.[140]

In addition to generating a large database of salt hydrates for TES and highlighting promising materials, this work expanded the knowledge of salt hydrate thermodynamics. Previous understanding of salt hydrate thermodynamics was driven by the Thermodynamic Difference Rules of Glasser and Jenkins,[75–77] which approximate the thermodynamic and physical changes during salt (de)hydration as uniform and additive. The present study has developed a more nuanced understanding of the enthalpy of dehydration for salt hydrates. This contribution is noteworthy given the importance that the enthalpy of dehydration (ΔH) has upon a salt hydrate's energy density and operating temperature. Among known halide salt hydrates, no strong linear correlations could be found between common salt hydrate properties and ΔH. However, ML revealed several non-linear trends in the enthalpy of dehydration for hypothetical salt hydrates. Notably, the different families of salt hydrates (i.e., halides, chalcogenides, and complex anions) were found to exhibit distinct behaviors. ΔH for halide salt hydrates was found to depend on the nature of the cation-water bond in the hydrate, as well as on the distance between cations in the crystal structure. Like the halide salt hydrates, ML revealed that ΔH for the chalcogenide salt hydrates depends primarily on the properties of the cation and less on the anion. However, unlike

the other two families, the thermodynamics of chalcogenide salt hydrates was found to not depend strongly on crystal structure properties. Furthermore, chalcogenide salt hydrates were found to have a lower and broader distribution of ΔH than the other two families. Finally, complex anion salt hydrates were shown to be a heterogeneous chemical space as these hydrates were best described by a ML model that partitioned the chemical space into subspaces of high and low ΔH. Unlike the other two salt hydrate families, complex anion salt hydrates were best modeled by partitioning the chemical space rather than learning general trends across the entire salt hydrate family. This knowledge of ΔH can be used to optimize heat storage properties of salt hydrates.

By understanding property-performance relationships in salt hydrates, the behavior of salt hydrates can be optimized. Both the energy density and operating temperature are correlated to ΔH and can thus be controlled by strategic tuning of ΔH. Mixed metal salt hydrates offer a pathway to leverage this new knowledge to tune the behavior of salt hydrates. Preliminary work indicates that many mixed metal salt hydrates demonstrate linear mixing behavior, which offers a starting point for strategic tuning of salt hydrate properties to achieve optimal performance. However, more work is required to identify effective strategies for a targeted and/or ML-catalyzed screening of mixed metal salt hydrates. This is the suggested next step for future endeavors building off this work, which is thoroughly discussed in section 6.4.

Another suggested future direction is a more detailed study on the entropy of dehydration. The present study assumed a constant value for the entropy of dehydration per mole of water, which aligns with the Thermodynamic Difference Rules approximation.[75–77] Vibrational entropy values were calculated from first principles for only a few promising salt hydrates. This entropy is necessary for the construction of phase diagrams, which are helpful for TES system designers as they show the possible range of operating conditions of the salt hydrate. Although vibrational

entropies are more expensive to calculate, calculations can be performed on a subset of salt hydrates whose expected performance warrant this additional effort. Computational prediction of the entropy of dehydration would offer a systematic way to generate data that can be used for training predictive ML models, which in turn may be used as a more accurate approximation of the entropy. Experimental data could also be used in training the ML model, although the uncertainty of reported experimental entropies is large. Using 60 duplicate data entries from the salt hydrate database of Donkers et al.,[55] the uncertainty in the entropy of dehydration was calculated to be 18.3 J/K-mol H_2O with a weak correlation coefficient of -0.08.

Another suggested avenue of computational research is the study of salt hydration and dehydration reaction kinetics. One crucial aspect of the reaction kinetics is water transport through the salt hydrate. It has been shown that water transport is the rate-limiting step of the dehydration of $MgSO_4 \cdot 7H_2O$.[190,191] The diffusivity and energy barriers associated with water transport can be predicted via first principles calculations using methods such as ab initio molecular dynamics[192] and the Nudged Elastic Band[193] method. These methods can also be used to study the interaction of water vapor at the surface of the salt or salt hydrate. This can be used to validate the existence of a wetting layer, which was hypothesized by Sögütoglu et al. to occur in salt hydrates during hydration to facilitate the nucleation and growth of the hydrated phase.[194] Studies that explore water storage in porous crystalline materials such as metal-organic frameworks (MOFs)[63–65] are recommended, as these materials may be less sensitive to the mass transport limitations expected to exist in the bulk hydrates examined here.

Experimental validation is highly desirable for the promising salt hydrates identified in this work. In addition to the synthesis of hypothetical salt hydrates, experimentally determined phase diagrams would be extremely helpful to validate the present calculations. Furthermore,

experiments are required to test the deliquescence, melting, kinetics, thermal conductivity, and cycling behavior of these promising salt hydrates; these properties are crucial for TES but are difficult or impossible for computation to predict. Deliquescence is of particular interest as it may limit or disqualify some of the promising salt hydrates identified here that contain a large amount of water. This follow up experimental work will be required to realize the benefits predicted for these newly identified heat storage materials.

Appendices

Appendix A. Compiled Database of Properties for Known Salt Hydrates and Hydroxides

Table A.1 Description of salt hydrate properties, denoted by the following categories: water content (WC), ionic properties (Ion), structural properties (Str), and thermodynamic/energy density properties (Thermo). All thermodynamic properties correspond to the reaction between the hydrate and its respective anhydrous salt. Some properties are numerically represented categories that are not of interest when examining correlations, but may be useful for clustering analysis. The expanded anhydrous salt refers to the fictitious crystal structure of the salt hydrate with the water molecules removed from the structure.

Variable	Category	Units	Description
Compound	-	-	Chemical formula of the salt hydrate
n	WC	H_2O/f.u.	Number of water molecules in the salt hydrate (i.e. for $MgCl_2 \cdot 6H_2O$, n = 6)
Cap_Grav	WC	mol H_2O/kg hydrate	Gravimetric Water Capacity, this multiplied by DH yields the *GED*
Cap_Vol	WC	mol H_2O/L hydrate	Volumetric Water Capacity, this multiplied by DH yields the *VED*
Cation	Ion	-	ID # for cation (see Table A.9)
Mass_Cat	Ion	g/mol	Molar mass of the cation[148]
Rad_Cat	Ion	pm	Ionic radius of cation assuming coordination number of 6[149]
ElNeg_Cat	Ion	Pauling units	Electronegativity of cation according to Pauling Scale[148]
Chg_Cat	Ion	e	Formal charge of cation
PP_Cat	Ion	e/Å	Polarizing power of the cation, equal to the formal charge divided by the ionic radius[149]
Anion	Ion	-	ID # for anion (see Table A.10)
Mass_An	Ion	g/mol	Molar mass of the anion[148]
Rad_An	Ion	pm	Ionic radius of anion assuming coordination number of 6[149]
ElNeg_An	Ion	Pauling units	Electronegativity of anion according to Pauling Scale[148]
DV	Str	$Å^3$/f.u.	Difference in hydrate and anhydrous salt volume
DV/V	Str	-	Relative change in volume from anhydrous salt to hydrate
V_Anh	Str	$Å^3$/f.u.	Volume of anhydrous salt
MM_Anh	Str	g/mol	Molar mass of anhydrous salt[148]
C-A_Anh	Str	Å	Distance between nearest neighbor cations and anions in the anhydrous salt

#CA_Anh	Str	-	Number of nearest neighbor anions coordinating the cation in the anhydrous salt
C-C_Anh	Str	Å	Distance between nearest neighbor cations in the anhydrous salt
#CC_Anh	Str	-	Number of nearest neighbor cations coordinating the cation in the anhydrous salt
Dens_Anh	Str	g/cm^3	Density of the anhydrous salt[103]
Str_Anh	Str	-	ID # for structure type and commonly associated space group of the anhydrous salt (see Table A.11)[103]
V_Hyd	Str	$Å^3$/f.u.	Volume of hydrate
MM_Hyd	Str	g/mol	Molar mass of hydrate[148]
Pack_Eff	Str	-	Measure of how efficiently water is packed into hydrate relative to ice[126]
C-W_Hyd	Str	Å	Distance between nearest neighbor cations and water molecules in the hydrate
#CW_Hyd	Str	-	Number of nearest neighbor water molecules coordinating the cation in the hydrate
C-A_Hyd	Str	Å	Distance between nearest neighbor cations and anions in the hydrate
#CA_Hyd	Str	-	Number of nearest neighbor anions coordinating the cation in the hydrate
C-C_Hyd	Str	Å	Distance between nearest neighbor cations in the hydrate
#CC_Hyd	Str	-	Number of nearest neighbor cations coordinating the cation in the hydrate
Dens_Hyd	Str	g/cm^3	Density of the hydrate[103]
SG_Hyd	Str	-	ID # for space group of hydrate (see Table A.12)[103]
ST_Hyd	Str	-	ID # for structure type of the hydrate (see Table A.13)[103]
Dens_EA	Str	g/cm^3	Density of the expanded anhydrous salt[195–197]
VASA_EA	Str	m^2/cm^3	Volumetric accesible surface area in the expanded anhydrous salt (using a He probe of radius 0.31 Å)[195–197]
GASA_EA	Str	m^2/g	Gravimetric accesible surface area in the expanded anhydrous salt (using a He probe of radius 0.31 Å)[195–197]
VolFr_EA	Str	-	Volume fraction of the accessible volume in the expanded anhydrous salt (using a probe radius of 0 Å)[195–197]
GAV_EA	Str	cm^3/g	Gravimetric accessible volume in the expanded anhydrous salt (using a probe radius of 0 Å)[195–197]
DH_Str	Thermo	kJ/mol H_2O	Structural enthalpy change - This is the energy difference between the expanded anhydrous salt and the anhydrous salt
DH_Bnd	Thermo	kJ/mol H_2O	Water bonding enthalpy change - This is the energy difference between the hydrate and expanded anhydrous salt
DH	Thermo	kJ/mol H_2O	Dehydration Enthalpy - This is the energy difference between the hydrate and the anhydrous salt, it is used to calculate the energy densities
nDH_Str	Thermo	kJ/mol salt	Structural enthalpy change - This is the energy difference between the expanded anhydrous salt and the anhydrous salt
nDH_Bnd	Thermo	kJ/mol salt	Water bonding enthalpy change - This is the energy difference between the hydrate and expanded anhydrous salt
nDH	Thermo	kJ/mol salt	Total enthalpy change - This is the energy difference between the hydrate and the anhydrous salt, it is used to calculate the energy densities
Stability	Thermo	-	Stable componds (1) vs. metastable compounds (0) as determined by distance above the convex hull
GED	Thermo	MJ/kg	Gravimetric energy density
VED	Thermo	GJ/m^3	Volumetric energy density

Promising	Thermo	-	Promising reactions (1) have VED > 3 and GED > 1.5, non-promising reactions (0) do not

Table A.2 (Part 1) Database of 50 salt hydrate features for all stable or metastable hydrates with well-defined properties (i.e. excluding hydrates with multiple cations or cations with missing ionic parameters).

Compound	n	Cap_Grav	Cap_Vol	Cation	Mass_Cat	Rad_Cat	ElNeg_Cat
$AlCl_3•6H_2O$	6	24.85	40.97	1	26.982	67.5	1.61
$AlF_3•3H_2O$	3	21.74	45.87	1	26.982	67.5	1.61
$AlF_3•9H_2O$	9	36.57	57.23	1	26.982	67.5	1.61
$AlF_3•H_2O$	1	9.80	24.36	1	26.982	67.5	1.61
$BaBr_2•2H_2O$	2	6.00	22.43	2	137.327	149	0.89
$BaBr_2•H_2O$	1	3.17	12.68	2	137.327	149	0.89
$BaCl_2•2H_2O$	2	8.19	24.87	2	137.327	149	0.89
$BeCl_2•4H_2O$	4	26.32	38.27	3	9.012	59	1.57
$BiCl_3•H_2O$	1	3.00	12.03	4	208.980	117	2.02
$CaBr_2•6H_2O$	6	19.48	43.60	5	40.078	114	1
$CaBr_2•9H_2O$	9	24.86	48.77	5	40.078	114	1
$CaCl_2•2H_2O$	2	13.60	28.74	5	40.078	114	1
$CaCl_2•4H_2O$	4	21.85	35.53	5	40.078	114	1
$CaCl_2•6H_2O$	6	27.39	47.44	5	40.078	114	1
$CdBr_2•4H_2O$	4	11.62	34.54	6	112.411	109	1.69
$CdCl_2•2.5H_2O$	2.5	10.95	29.86	6	112.411	109	1.69
$CdCl_2•4H_2O$	4	15.66	37.58	6	112.411	109	1.69
$CdCl_2•H_2O$	1	4.97	15.61	6	112.411	109	1.69
$CeBr_3•7H_2O$	7	13.84	39.16	7	140.116	115	1.12
$CeCl_3•6H_2O$	6	16.92	38.30	7	140.116	115	1.12
$CeCl_3•7H_2O$	7	18.79	42.73	7	140.116	115	1.12
$CoBr_2•2H_2O$	2	7.85	26.47	8	58.933	88.5	1.88
$CoBr_2•4H_2O$	4	13.76	39.30	8	58.933	88.5	1.88
$CoCl_2•2H_2O$	2	12.06	30.46	8	58.933	88.5	1.88
$CoCl_2•H_2O$	1	6.76	18.96	8	58.933	88.5	1.88
$CrCl_2•4H_2O$	4	20.52	40.16	9	51.996	94	1.66
$CrCl_3•6H_2O$	6	22.52	40.51	9	51.996	75.5	1.66
$CrF_3•3H_2O$	3	18.40	43.19	9	51.996	75.5	1.66
$CrF_3•5H_2O$	5	25.12	53.39	9	51.996	75.5	1.66
$CrF_3•9H_2O$	9	33.20	53.72	9	51.996	75.5	1.66
$CuBr_2•4H_2O$	4	13.54	38.15	10	63.546	87	1.9
$CuCl_2•2H_2O$	2	11.73	28.97	10	63.546	87	1.9
$CuF_2•2H_2O$	2	14.54	43.07	10	63.546	87	1.9
$ErCl_3•6H_2O$	6	15.72	40.47	11	167.259	103	1.24
$FeBr_2•4H_2O$	4	13.90	37.19	13	55.845	92	1.83
$FeCl_2•2H_2O$	2	12.29	29.99	13	55.845	92	1.83
$FeCl_2•4H_2O$	4	20.12	41.13	13	55.845	92	1.83
$FeCl_3•2.5H_2O$	2.5	12.06	26.05	13	55.845	78.5	1.83
$FeCl_3•6H_2O$	6	22.20	41.37	13	55.845	78.5	1.83
$FeF_3•3H_2O$	3	17.98	40.90	13	55.845	78.5	1.83
$GdCl_3•6H_2O$	6	16.14	39.93	14	157.250	107.8	1.2

$HfF_4•3H_2O$	3	9.72	38.25	15	178.490	85	1.3
$HgF_2•2H_2O$	2	7.28	40.57	16	200.590	116	2
$InCl_3•3H_2O$	3	10.90	24.53	17	114.818	94	1.78
$InF_3•3H_2O$	3	13.28	36.90	17	114.818	94	1.78
$KF•2H_2O$	2	21.25	35.24	18	39.098	152	0.82
$KF•4H_2O$	4	30.73	44.61	18	39.098	152	0.82
$LaBr_3•7H_2O$	7	13.87	38.64	19	138.905	117.2	1.1
$LaCl_3•3H_2O$	3	10.02	27.64	19	138.905	117.2	1.1
$LaCl_3•7H_2O$	7	18.85	42.23	19	138.905	117.2	1.1
$LiBr•H_2O$	1	9.54	25.77	20	6.941	90	0.98
$LuBr_3•8H_2O$	8	14.32	41.08	21	174.967	100.1	1.27
$MgBr_2•2H_2O$	2	9.09	24.95	22	24.305	86	1.31
$MgBr_2•4H_2O$	4	15.61	36.58	22	24.305	86	1.31
$MgBr_2•6H_2O$	6	20.53	42.83	22	24.305	86	1.31
$MgBr_2•9H_2O$	9	25.99	48.75	22	24.305	86	1.31
$MgBr_2•H_2O$	1	4.95	12.46	22	24.305	86	1.31
$MgCl_2•2H_2O$	2	15.24	29.17	22	24.305	86	1.31
$MgCl_2•4H_2O$	4	23.91	40.70	22	24.305	86	1.31
$MgCl_2•6H_2O$	6	29.51	46.66	22	24.305	86	1.31
$MgCl_2•H_2O$	1	8.83	17.89	22	24.305	86	1.31
$MnBr_2•2H_2O$	2	7.98	24.82	23	54.938	97	1.55
$MnCl_2•2H_2O$	2	12.36	28.29	23	54.938	97	1.55
$MnCl_2•H_2O$	1	6.95	17.32	23	54.938	97	1.55
$NaBr•2H_2O$	2	14.40	32.02	24	22.990	116	0.93
$NaCl•2H_2O$	2	21.17	35.49	24	22.990	116	0.93
$NiCl_2•2H_2O$	2	12.08	31.52	25	58.693	83	1.91
$NiCl_2•4H_2O$	4	19.84	44.72	25	58.693	83	1.91
$NiCl_2•6H_2O$	6	25.24	50.79	25	58.693	83	1.91
$PrBr_3•6H_2O$	6	12.28	34.92	26	140.908	113	1.13
$PrCl_3•6H_2O$	6	16.88	38.53	26	140.908	113	1.13
$PtCl_4•3.5H_2O$	3.5	8.75	26.88	27	195.084	76.5	2.28
$PtCl_4•5H_2O$	5	11.71	33.51	27	195.084	76.5	2.28
$PuBr_3•6H_2O$	6	10.14	35.38	28	244.000	114	1.28
$RbF•H_2O$	1	8.16	23.06	29	85.468	166	0.82
$SmCl_3•6H_2O$	6	16.45	39.18	30	150.360	109.8	1.17
$SnBr_4•5H_2O$	5	9.46	29.32	31	118.710	83	1.96
$SnCl_4•2H_2O$	2	6.74	17.63	31	118.710	83	1.96
$SnCl_4•3H_2O$	3	9.54	23.60	31	118.710	83	1.96
$SnCl_4•4H_2O$	4	12.03	28.19	31	118.710	83	1.96
$SnCl_4•5H_2O$	5	14.26	32.36	31	118.710	83	1.96
$SnCl_4•8H_2O$	8	19.77	38.95	31	118.710	83	1.96
$SrBr_2•H_2O$	1	3.77	14.22	32	87.620	132	0.95
$SrCl_2•2H_2O$	2	10.28	27.63	32	87.620	132	0.95
$SrCl_2•6H_2O$	6	22.50	44.20	32	87.620	132	0.95
$SrCl_2•H_2O$	1	5.66	16.22	32	87.620	132	0.95
$TlBr_3•4H_2O$	4	7.75	28.50	33	204.383	102.5	1.62
$TlCl_3•4H_2O$	4	10.45	31.64	33	204.383	102.5	1.62
$UBr_4•9H_2O$	9	12.50	39.04	34	238.029	103	1.38
$UCl_3•6H_2O$	6	13.26	38.47	34	238.029	116.5	1.38

$UCl_3•7H_2O$	7	14.88	42.75	34	238.029	116.5	1.38
$UF_4•2H_2O$	2	5.71	27.15	34	238.029	103	1.38
$VBr_3•6H_2O$	6	15.05	38.00	35	50.942	78	1.63
$VCl_3•4H_2O$	4	17.44	34.79	35	50.942	78	1.63
$VCl_3•6H_2O$	6	22.61	41.96	35	50.942	78	1.63
$VF_3•2H_2O$	2	13.89	35.53	35	50.942	78	1.63
$VF_3•3H_2O$	3	18.52	40.87	35	50.942	78	1.63
$YBr_3•10H_2O$	10	19.66	43.61	36	88.906	104	1.22
$YBr_3•8H_2O$	8	16.92	40.51	36	88.906	104	1.22
$YCl_3•6H_2O$	6	19.78	40.71	36	88.906	104	1.22
$ZnBr_2•2H_2O$	2	7.66	23.31	37	65.380	88	1.65
$ZnCl_2•1.33H_2O$	1.33	8.30	21.05	37	65.380	88	1.65
$ZnCl_2•2.5H_2O$	2.5	13.79	31.42	37	65.380	88	1.65
$ZnCl_2•3H_2O$	3	15.76	33.94	37	65.380	88	1.65
$ZnCl_2•4.5H_2O$	4.5	20.70	38.15	37	65.380	88	1.65
$ZnF_2•2H_2O$	2	14.35	40.72	37	65.380	88	1.65
$ZnF_2•4H_2O$	4	22.80	52.67	37	65.380	88	1.65
$ZrF_4•3H_2O$	3	13.56	37.16	38	91.224	86	1.33

Table A.3 (Part 2) Database of 50 salt hydrate features for all stable or metastable hydrates with well-defined properties (i.e. excluding hydrates with multiple cations or cations with missing ionic parameters).

Compound	Chg_Cat	PP_Cat	Anion	Mass_An	Rad_An	ElNeg_An	DV
$AlCl_3•6H_2O$	3	4.44	2	35.453	167	3.16	151.723
$AlF_3•3H_2O$	3	4.44	1	18.998	119	3.98	64.232
$AlF_3•9H_2O$	3	4.44	1	18.998	119	3.98	216.763
$AlF_3•H_2O$	3	4.44	1	18.998	119	3.98	23.795
$BaBr_2•2H_2O$	2	1.34	3	79.904	182	2.96	41.818
$BaBr_2•H_2O$	2	1.34	3	79.904	182	2.96	24.718
$BaCl_2•2H_2O$	2	1.34	2	35.453	167	3.16	42.495
$BeCl_2•4H_2O$	2	3.39	2	35.453	167	3.16	106.283
$BiCl_3•H_2O$	3	2.56	2	35.453	167	3.16	27.362
$CaBr_2•6H_2O$	2	1.75	3	79.904	182	2.96	129.190
$CaBr_2•9H_2O$	2	1.75	3	79.904	182	2.96	207.128
$CaCl_2•2H_2O$	2	1.75	2	35.453	167	3.16	31.900
$CaCl_2•4H_2O$	2	1.75	2	35.453	167	3.16	103.287
$CaCl_2•6H_2O$	2	1.75	2	35.453	167	3.16	126.352
$CdBr_2•4H_2O$	2	1.83	3	79.904	182	2.96	100.220
$CdCl_2•2.5H_2O$	2	1.83	2	35.453	167	3.16	61.023
$CdCl_2•4H_2O$	2	1.83	2	35.453	167	3.16	98.746
$CdCl_2•H_2O$	2	1.83	2	35.453	167	3.16	28.365
$CeBr_3•7H_2O$	3	2.61	3	79.904	182	2.96	171.770
$CeCl_3•6H_2O$	3	2.61	2	35.453	167	3.16	155.205
$CeCl_3•7H_2O$	3	2.61	2	35.453	167	3.16	167.080
$CoBr_2•2H_2O$	2	2.26	3	79.904	182	2.96	56.935
$CoBr_2•4H_2O$	2	2.26	3	79.904	182	2.96	100.485
$CoCl_2•2H_2O$	2	2.26	2	35.453	167	3.16	46.175
$CoCl_2•H_2O$	2	2.26	2	35.453	167	3.16	24.725

$CrCl_2•4H_2O$	2	2.13	2	35.453	167	3.16	96.245
$CrCl_3•6H_2O$	3	3.97	2	35.453	167	3.16	154.282
$CrF_3•3H_2O$	3	3.97	1	18.998	119	3.98	68.368
$CrF_3•5H_2O$	3	3.97	1	18.998	119	3.98	108.534
$CrF_3•9H_2O$	3	3.97	1	18.998	119	3.98	231.240
$CuBr_2•4H_2O$	2	2.30	3	79.904	182	2.96	93.815
$CuCl_2•2H_2O$	2	2.30	2	35.453	167	3.16	46.865
$CuF_2•2H_2O$	2	2.30	1	18.998	119	3.98	41.850
$ErCl_3•6H_2O$	3	2.91	2	35.453	167	3.16	126.368
$FeBr_2•4H_2O$	2	2.17	3	79.904	182	2.96	101.205
$FeCl_2•2H_2O$	2	2.17	2	35.453	167	3.16	46.165
$FeCl_2•4H_2O$	2	2.17	2	35.453	167	3.16	96.950
$FeCl_3•2.5H_2O$	3	3.82	2	35.453	167	3.16	74.452
$FeCl_3•6H_2O$	3	3.82	2	35.453	167	3.16	155.972
$FeF_3•3H_2O$	3	3.82	1	18.998	119	3.98	79.358
$GdCl_3•6H_2O$	3	2.78	2	35.453	167	3.16	150.240
$HfF_4•3H_2O$	4	4.71	1	18.998	119	3.98	69.370
$HgF_2•2H_2O$	2	1.72	1	18.998	119	3.98	36.780
$InCl_3•3H_2O$	3	3.19	2	35.453	167	3.16	91.656
$InF_3•3H_2O$	3	3.19	1	18.998	119	3.98	75.302
$KF•2H_2O$	1	0.66	1	18.998	119	3.98	59.530
$KF•4H_2O$	1	0.66	1	18.998	119	3.98	114.180
$LaBr_3•7H_2O$	3	2.56	3	79.904	182	2.96	172.850
$LaCl_3•3H_2O$	3	2.56	2	35.453	167	3.16	72.235
$LaCl_3•7H_2O$	3	2.56	2	35.453	167	3.16	167.250
$LiBr•H_2O$	1	1.11	3	79.904	182	2.96	22.610
$LuBr_3•8H_2O$	3	3.00	3	79.904	182	2.96	187.530
$MgBr_2•2H_2O$	2	2.33	3	79.904	182	2.96	50.020
$MgBr_2•4H_2O$	2	2.33	3	79.904	182	2.96	98.480
$MgBr_2•6H_2O$	2	2.33	3	79.904	182	2.96	149.535
$MgBr_2•9H_2O$	2	2.33	3	79.904	182	2.96	223.478
$MgBr_2•H_2O$	2	2.33	3	79.904	182	2.96	50.190
$MgCl_2•2H_2O$	2	2.33	2	35.453	167	3.16	44.950
$MgCl_2•4H_2O$	2	2.33	2	35.453	167	3.16	94.295
$MgCl_2•6H_2O$	2	2.33	2	35.453	167	3.16	144.615
$MgCl_2•H_2O$	2	2.33	2	35.453	167	3.16	23.905
$MnBr_2•2H_2O$	2	2.06	3	79.904	182	2.96	50.735
$MnCl_2•2H_2O$	2	2.06	2	35.453	167	3.16	47.375
$MnCl_2•H_2O$	2	2.06	2	35.453	167	3.16	25.852
$NaBr•2H_2O$	1	0.86	3	79.904	182	2.96	50.593
$NaCl•2H_2O$	1	0.86	2	35.453	167	3.16	49.516
$NiCl_2•2H_2O$	2	2.41	2	35.453	167	3.16	44.079
$NiCl_2•4H_2O$	2	2.41	2	35.453	167	3.16	87.222
$NiCl_2•6H_2O$	2	2.41	2	35.453	167	3.16	134.877
$PrBr_3•6H_2O$	3	2.65	3	79.904	182	2.96	161.125
$PrCl_3•6H_2O$	3	2.65	2	35.453	167	3.16	155.270
$PtCl_4•3.5H_2O$	4	5.23	2	35.453	167	3.16	73.679
$PtCl_4•5H_2O$	4	5.23	2	35.453	167	3.16	105.199

$PuBr_3•6H_2O$	3	2.63	3	79.904	182	2.96	159.247
$RbF•H_2O$	1	0.60	1	18.998	119	3.98	31.098
$SmCl_3•6H_2O$	3	2.73	2	35.453	167	3.16	152.920
$SnBr_4•5H_2O$	4	4.82	3	79.904	182	2.96	91.640
$SnCl_4•2H_2O$	4	4.82	2	35.453	167	3.16	28.822
$SnCl_4•3H_2O$	4	4.82	2	35.453	167	3.16	51.540
$SnCl_4•4H_2O$	4	4.82	2	35.453	167	3.16	76.041
$SnCl_4•5H_2O$	4	4.82	2	35.453	167	3.16	97.032
$SnCl_4•8H_2O$	4	4.82	2	35.453	167	3.16	181.494
$SrBr_2•H_2O$	2	1.52	3	79.904	182	2.96	17.160
$SrCl_2•2H_2O$	2	1.52	2	35.453	167	3.16	33.378
$SrCl_2•6H_2O$	2	1.52	2	35.453	167	3.16	138.580
$SrCl_2•H_2O$	2	1.52	2	35.453	167	3.16	15.585
$TlBr_3•4H_2O$	3	2.93	2	35.453	167	3.16	83.407
$TlCl_3•4H_2O$	3	2.93	2	35.453	167	3.16	91.158
$UBr_4•9H_2O$	4	3.88	3	79.904	182	2.96	205.052
$UCl_3•6H_2O$	3	2.58	2	35.453	167	3.16	155.420
$UCl_3•7H_2O$	3	2.58	2	35.453	167	3.16	168.310
$UF_4•2H_2O$	4	3.88	1	18.998	119	3.98	43.291
$VBr_3•6H_2O$	3	3.85	3	79.904	182	2.96	150.203
$VCl_3•4H_2O$	3	3.85	2	35.453	167	3.16	99.905
$VCl_3•6H_2O$	3	3.85	2	35.453	167	3.16	146.405
$VF_3•2H_2O$	3	3.85	1	18.998	119	3.98	44.861
$VF_3•3H_2O$	3	3.85	1	18.998	119	3.98	73.263
$YBr_3•10H_2O$	3	2.88	3	79.904	182	2.96	237.778
$YBr_3•8H_2O$	3	2.88	3	79.904	182	2.96	184.938
$YCl_3•6H_2O$	3	2.88	2	35.453	167	3.16	121.240
$ZnBr_2•2H_2O$	2	2.27	3	79.904	182	2.96	62.140
$ZnCl_2•1.33H_2O$	2	2.27	2	35.453	167	3.16	28.315
$ZnCl_2•2.5H_2O$	2	2.27	2	35.453	167	3.16	55.546
$ZnCl_2•3H_2O$	2	2.27	2	35.453	167	3.16	70.193
$ZnCl_2•4.5H_2O$	2	2.27	2	35.453	167	3.16	119.302
$ZnF_2•2H_2O$	2	2.27	1	18.998	119	3.98	44.949
$ZnF_2•4H_2O$	2	2.27	1	18.998	119	3.98	89.492
$ZrF_4•3H_2O$	4	4.65	1	18.998	119	3.98	71.917

Table A.4 (Part 3) Database of 50 salt hydrate features for all stable or metastable hydrates with well-defined properties (i.e. excluding hydrates with multiple cations or cations with missing ionic parameters).

Compound	DV/V	V_Anh	MM_Anh	C-A_Anh	#CA_Anh	C-C_Anh	#CC_Anh
$AlCl_3•6H_2O$	1.659	91.48	133.34	2.35	6	3.46	3
$AlF_3•3H_2O$	1.448	44.37	83.98	1.83	6	3.54	6
$AlF_3•9H_2O$	4.886	44.37	83.98	1.83	6	3.54	6
$AlF_3•H_2O$	0.536	44.37	83.98	1.83	6	3.54	6
$BaBr_2•2H_2O$	0.394	106.24	297.14	3.36	7	5.22	8
$BaBr_2•H_2O$	0.233	106.24	297.14	3.36	7	5.22	8
$BaCl_2•2H_2O$	0.467	91.05	208.23	3.19	7	4.96	8
$BeCl_2•4H_2O$	1.579	67.30	79.92	2.04	4	2.64	2

$BiCl_3•H_2O$	0.247	110.69	315.34	2.6	3	4.86	6
$CaBr_2•6H_2O$	1.300	99.34	199.89	2.92	6	4.33	2
$CaBr_2•9H_2O$	2.085	99.34	199.89	2.92	6	4.33	2
$CaCl_2•2H_2O$	0.381	83.67	110.98	2.76	6	4.18	2
$CaCl_2•4H_2O$	1.234	83.67	110.98	2.76	6	4.18	2
$CaCl_2•6H_2O$	1.510	83.67	110.98	2.76	6	4.18	2
$CdBr_2•4H_2O$	1.088	92.11	272.22	2.84	6	4.07	6
$CdCl_2•2.5H_2O$	0.783	77.98	183.32	2.69	6	3.9	6
$CdCl_2•4H_2O$	1.266	77.98	183.32	2.69	6	3.9	6
$CdCl_2•H_2O$	0.364	77.98	183.32	2.69	6	3.9	6
$CeBr_3•7H_2O$	1.374	125.05	379.83	3.12	9	4.44	2
$CeCl_3•6H_2O$	1.479	104.93	246.48	2.95	9	4.31	2
$CeCl_3•7H_2O$	1.592	104.93	246.48	2.95	9	4.31	2
$CoBr_2•2H_2O$	0.831	68.51	218.74	2.51	6	3.64	6
$CoBr_2•4H_2O$	1.467	68.51	218.74	2.51	6	3.64	6
$CoCl_2•2H_2O$	0.735	62.85	129.84	2.44	6	3.52	6
$CoCl_2•H_2O$	0.393	62.85	129.84	2.44	6	3.52	6
$CrCl_2•4H_2O$	1.392	69.14	122.90	2.41	4	3.51	2
$CrCl_3•6H_2O$	1.683	91.68	158.36	2.37	6	3.48	3
$CrF_3•3H_2O$	1.455	46.98	108.99	1.94	6	3.62	6
$CrF_3•5H_2O$	2.310	46.98	108.99	1.94	6	3.62	6
$CrF_3•9H_2O$	4.922	46.98	108.99	1.94	6	3.62	6
$CuBr_2•4H_2O$	1.169	80.28	223.35	2.45	4	3.53	2
$CuCl_2•2H_2O$	0.691	67.79	134.45	2.31	4	3.35	2
$CuF_2•2H_2O$	1.187	35.26	101.54	2.05	6	3.18	2
$ErCl_3•6H_2O$	1.055	119.81	273.62	2.65	6	3.95	3
$FeBr_2•4H_2O$	1.308	77.39	215.65	2.64	6	3.75	6
$FeCl_2•2H_2O$	0.715	64.56	126.75	2.48	6	3.54	6
$FeCl_2•4H_2O$	1.502	64.56	126.75	2.48	6	3.54	6
$FeCl_3•2.5H_2O$	0.877	84.89	162.20	2.28	6	3.38	3
$FeCl_3•6H_2O$	1.837	84.89	162.20	2.28	6	3.38	3
$FeF_3•3H_2O$	1.870	42.43	112.84	1.88	6	3.5	6
$GdCl_3•6H_2O$	1.514	99.27	263.61	2.88	9	4.13	2
$HfF_4•3H_2O$	1.139	60.88	254.48	2.1	8	4.15	8
$HgF_2•2H_2O$	0.816	45.09	238.59	2.45	8	4	12
$InCl_3•3H_2O$	0.822	111.44	221.18	2.58	6	3.76	3
$InF_3•3H_2O$	1.262	59.69	171.81	2.13	6	3.93	6
$KF•2H_2O$	1.715	34.72	58.10	2.83	8	3.26	6
$KF•4H_2O$	3.289	34.72	58.10	2.83	8	3.26	6
$LaBr_3•7H_2O$	1.351	127.97	378.62	3.15	9	4.54	2
$LaCl_3•3H_2O$	0.669	107.99	245.26	2.97	9	4.4	2
$LaCl_3•7H_2O$	1.549	107.99	245.26	2.97	9	4.4	2
$LiBr•H_2O$	0.540	41.84	86.85	2.76	6	3.9	12
$LuBr_3•8H_2O$	1.381	135.84	414.68	2.77	6	4.03	3
$MgBr_2•2H_2O$	0.602	83.10	184.11	2.7	6	3.88	6
$MgBr_2•4H_2O$	1.185	83.10	184.11	2.7	6	3.88	6
$MgBr_2•6H_2O$	1.799	83.10	184.11	2.7	6	3.88	6
$MgBr_2•9H_2O$	2.689	83.10	184.11	2.7	6	3.88	6

$MgBr_2•H_2O$	0.604	83.10	184.11	2.7	6	3.88	6
$MgCl_2•2H_2O$	0.652	68.91	95.21	2.52	6	3.66	6
$MgCl_2•4H_2O$	1.368	68.91	95.21	2.52	6	3.66	6
$MgCl_2•6H_2O$	2.099	68.91	95.21	2.52	6	3.66	6
$MgCl_2•H_2O$	0.347	68.91	95.21	2.52	6	3.66	6
$MnBr_2•2H_2O$	0.611	83.08	214.75	2.71	6	3.88	6
$MnCl_2•2H_2O$	0.677	70.00	125.84	2.56	6	3.7	6
$MnCl_2•H_2O$	0.369	70.00	125.84	2.56	6	3.7	6
$NaBr•2H_2O$	0.953	53.11	102.89	2.98	6	4.22	12
$NaCl•2H_2O$	1.124	44.06	58.44	2.8	6	3.96	12
$NiCl_2•2H_2O$	0.719	61.29	129.60	2.41	6	3.5	6
$NiCl_2•4H_2O$	1.423	61.29	129.60	2.41	6	3.5	6
$NiCl_2•6H_2O$	2.201	61.29	129.60	2.41	6	3.5	6
$PrBr_3•6H_2O$	1.297	124.23	380.62	3.11	9	4.4	2
$PrCl_3•6H_2O$	1.503	103.29	247.27	2.93	9	4.28	2
$PtCl_4•3.5H_2O$	0.517	142.57	336.90	2.28	4	4.42	1
$PtCl_4•5H_2O$	0.738	142.57	336.90	2.28	4	4.42	1
$PuBr_3•6H_2O$	1.301	122.38	483.71	3.03	8	4.06	2
$RbF•H_2O$	0.760	40.92	104.47	2.98	8	3.45	6
$SmCl_3•6H_2O$	1.509	101.37	256.72	2.91	9	4.26	2
$SnBr_4•5H_2O$	0.479	191.50	438.33	2.5	4	5.73	3
$SnCl_4•2H_2O$	0.181	159.58	260.52	2.33	4	5.39	3
$SnCl_4•3H_2O$	0.323	159.58	260.52	2.33	4	5.39	3
$SnCl_4•4H_2O$	0.477	159.58	260.52	2.33	4	5.39	3
$SnCl_4•5H_2O$	0.608	159.58	260.52	2.33	4	5.39	3
$SnCl_4•8H_2O$	1.137	159.58	260.52	2.33	4	5.39	3
$SrBr_2•H_2O$	0.172	99.62	247.43	3.19	7	4.75	3
$SrCl_2•2H_2O$	0.384	86.82	158.53	3.04	8	4.97	12
$SrCl_2•6H_2O$	1.596	86.82	158.53	3.04	8	4.97	12
$SrCl_2•H_2O$	0.180	86.82	158.53	3.04	8	4.97	12
$TlBr_3•4H_2O$	0.557	149.62	310.74	2.87	4	4.28	2
$TlCl_3•4H_2O$	0.768	118.75	310.74	2.68	6	3.88	3
$UBr_4•9H_2O$	1.154	177.76	557.64	2.87	6	4.64	3
$UCl_3•6H_2O$	1.501	103.58	344.39	2.93	9	4.28	2
$UCl_3•7H_2O$	1.625	103.58	344.39	2.93	9	4.28	2
$UF_4•2H_2O$	0.548	79.05	314.02	2.3	8	4.54	8
$VBr_3•6H_2O$	1.341	112.01	290.65	2.55	6	3.72	3
$VCl_3•4H_2O$	1.097	91.03	157.30	2.39	6	3.47	3
$VCl_3•6H_2O$	1.608	91.03	157.30	2.39	6	3.47	3
$VF_3•2H_2O$	0.923	48.62	107.94	1.95	6	3.66	6
$VF_3•3H_2O$	1.507	48.62	107.94	1.95	6	3.66	6
$YBr_3•10H_2O$	1.663	142.96	328.62	2.82	6	4.12	3
$YBr_3•8H_2O$	1.294	142.96	328.62	2.82	6	4.12	3
$YCl_3•6H_2O$	0.982	123.47	195.26	2.66	6	3.98	3
$ZnBr_2•2H_2O$	0.774	80.33	225.19	2.67	6	3.82	6
$ZnCl_2•1.33H_2O$	0.370	76.58	136.29	2.31	4	3.78	4
$ZnCl_2•2.5H_2O$	0.725	76.58	136.29	2.31	4	3.78	4
$ZnCl_2•3H_2O$	0.917	76.58	136.29	2.31	4	3.78	4

$ZnCl_2$•4.5H_2O	1.558	76.58	136.29	2.31	4	3.78	4
ZnF_2•2H_2O	1.228	36.61	103.38	2.07	6	3.2	2
ZnF_2•4H_2O	2.444	36.61	103.38	2.07	6	3.2	2
ZrF_4•3H_2O	1.157	62.14	167.22	2.13	8	3.59	1

Table A.5 (Part 4) Database of 50 salt hydrate features for all stable or metastable hydrates with well-defined properties (i.e. excluding hydrates with multiple cations or cations with missing ionic parameters).

Compound	Dens_Anh	Str_Anh	V_Hyd	MM_Hyd	Pack_Eff	C-W_Hyd	#CW_Hyd
$AlCl_3$•6H_2O	2.51	19	243.20	241.43	0.805	1.9	6
AlF_3•3H_2O	3.19	12	108.60	138.02	0.947	1.96	3
AlF_3•9H_2O	3.19	12	261.13	246.11	0.923	1.96	3
AlF_3•H_2O	3.19	12	68.16	101.99	0.468	1.87	2
$BaBr_2$•2H_2O	4.84	16	148.06	333.17	0.697	2.88	4
$BaBr_2$•H_2O	4.84	16	130.96	315.15	0.499	2.88	2
$BaCl_2$•2H_2O	3.94	16	133.54	244.26	0.700	2.88	4
$BeCl_2$•4H_2O	1.91	22	173.58	151.98	0.763	1.66	3
$BiCl_3$•H_2O	4.75	2	138.05	333.35	0.408	2.53	1
$CaBr_2$•6H_2O	3.38	4	228.53	307.98	0.892	2.55	9
$CaBr_2$•9H_2O	3.38	4	306.47	362.02	0.919	2.48	8
$CaCl_2$•2H_2O	2.23	17	115.57	147.01	0.764	2.52	2
$CaCl_2$•4H_2O	2.23	17	186.96	183.05	0.783	2.35	4
$CaCl_2$•6H_2O	2.23	17	210.02	219.08	0.909	2.54	9
$CdBr_2$•4H_2O	5.23	7	192.33	344.28	0.795	2.42	2
$CdCl_2$•2.5H_2O	4.08	5	139.01	228.36	0.717	2.37	1
$CdCl_2$•4H_2O	4.08	5	176.73	255.38	0.799	2.39	2
$CdCl_2$•H_2O	4.08	5	106.35	201.33	0.465	2.29	1
$CeBr_3$•7H_2O	5.18	26	296.82	505.93	0.841	2.56	7
$CeCl_3$•6H_2O	3.95	26	260.14	354.57	0.799	2.51	6
$CeCl_3$•7H_2O	3.95	26	272.01	372.58	0.851	2.56	7
$CoBr_2$•2H_2O	5.02	6	125.45	254.77	0.608	2.02	2
$CoBr_2$•4H_2O	5.02	6	169.00	290.80	0.791	1.97	4
$CoCl_2$•2H_2O	3.41	5	109.03	165.87	0.693	2.02	2
$CoCl_2$•H_2O	3.41	5	87.58	147.85	0.498	2.01	1
$CrCl_2$•4H_2O	2.94	4	165.38	194.96	0.810	2.06	4
$CrCl_3$•6H_2O	2.95	19	245.96	266.45	0.798	1.99	6
CrF_3•3H_2O	3.81	8	115.35	163.04	0.810	2.02	4
CrF_3•5H_2O	3.81	8	155.51	199.07	1.004	2.06	3
CrF_3•9H_2O	3.81	8	278.22	271.13	0.781	1.98	6
$CuBr_2$•4H_2O	4.83	10	174.09	295.42	0.816	2.03	2
$CuCl_2$•2H_2O	3.39	10	114.66	170.48	0.685	1.96	2
CuF_2•2H_2O	4.91	11	77.11	137.57	0.896	1.93	2
$ErCl_3$•6H_2O	3.78	1	246.18	381.71	0.863	2.38	6
$FeBr_2$•4H_2O	4.66	6	178.60	287.71	0.789	2.11	4
$FeCl_2$•2H_2O	3.21	5	110.73	162.78	0.692	2.08	2
$FeCl_2$•4H_2O	3.21	5	161.51	198.81	0.807	2.17	4
$FeCl_3$•2.5H_2O	2.92	3	159.34	207.24	0.566	4.06	5
$FeCl_3$•6H_2O	2.92	3	240.86	270.30	0.789	2.11	4

$FeF_3•3H_2O$	3.61	12	121.79	166.89	0.515	2.14	2
$GdCl_3•6H_2O$	4.54	26	249.51	371.70	0.811	2.42	6
$HfF_4•3H_2O$	7.11	27	130.25	308.53	0.722	2.2	2
$HgF_2•2H_2O$	9.32	13	81.87	274.62	0.869	2.39	2
$InCl_3•3H_2O$	3.48	1	203.10	275.22	0.622	2.27	3
$InF_3•3H_2O$	4.70	12	134.99	225.86	0.675	2.17	2
$KF•2H_2O$	3.37	9	94.25	94.13	0.609	2.78	4
$KF•4H_2O$	3.37	9	148.90	130.16	0.734	2.79	6
$LaBr_3•7H_2O$	5.07	26	300.82	504.72	0.839	2.59	7
$LaCl_3•3H_2O$	3.84	26	180.22	299.31	0.699	2.51	3
$LaCl_3•7H_2O$	3.84	26	275.24	371.37	0.851	2.58	7
$LiBr•H_2O$	3.47	14	64.45	104.86	0.631	2.07	2
$LuBr_3•8H_2O$	5.17	3	323.37	558.80	0.870	2.34	8
$MgBr_2•2H_2O$	3.29	6	133.12	220.14	0.662	2.04	2
$MgBr_2•4H_2O$	3.29	6	181.58	256.17	0.800	2.07	4
$MgBr_2•6H_2O$	3.29	6	232.64	292.20	0.852	2.09	6
$MgBr_2•9H_2O$	3.29	6	306.58	346.25	0.896	2.08	6
$MgBr_2•H_2O$	3.29	6	133.29	202.13	0.281	2	1
$MgCl_2•2H_2O$	2.34	5	113.86	131.24	0.699	2.04	2
$MgCl_2•4H_2O$	2.34	5	163.21	167.27	0.819	2.07	4
$MgCl_2•6H_2O$	2.34	5	213.53	203.30	0.867	2.08	6
$MgCl_2•H_2O$	2.34	5	92.82	113.23	0.508	2.02	1
$MnBr_2•2H_2O$	4.39	6	133.82	250.78	0.658	2.13	2
$MnCl_2•2H_2O$	2.99	5	117.38	161.87	0.680	2.14	2
$MnCl_2•H_2O$	2.99	5	95.85	143.86	0.486	2.12	1
$NaBr•2H_2O$	3.22	14	103.71	138.92	0.741	2.4	4
$NaCl•2H_2O$	2.14	14	93.58	94.47	0.747	2.39	4
$NiCl_2•2H_2O$	3.53	5	105.37	165.63	0.713	2.13	2
$NiCl_2•4H_2O$	3.53	5	148.52	201.66	0.861	2.1	4
$NiCl_2•6H_2O$	3.53	5	196.17	237.69	0.907	2.09	4
$PrBr_3•6H_2O$	5.34	26	285.35	488.71	0.791	2.49	6
$PrCl_3•6H_2O$	4.05	26	258.56	355.36	0.798	2.49	6
$PtCl_4•3.5H_2O$	3.92	23	216.25	399.95	0.717	2.13	3
$PtCl_4•5H_2O$	3.92	23	247.77	426.97	0.794	2.12	2
$PuBr_3•6H_2O$	6.78	15	281.63	591.80	0.795	2.49	6
$RbF•H_2O$	4.96	9	72.02	122.48	0.494	2.9	1
$SmCl_3•6H_2O$	4.34	26	254.29	364.81	0.804	2.46	6
$SnBr_4•5H_2O$	3.92	21	283.14	528.40	0.802	2.19	2
$SnCl_4•2H_2O$	2.71	21	188.40	296.55	0.624	2.22	2
$SnCl_4•3H_2O$	2.71	21	211.12	314.57	0.710	2.21	2
$SnCl_4•4H_2O$	2.71	21	235.62	332.58	0.761	2.18	2
$SnCl_4•5H_2O$	2.71	21	256.61	350.60	0.805	2.16	2
$SnCl_4•8H_2O$	2.71	21	341.07	404.64	0.850	2.15	2
$SrBr_2•H_2O$	4.25	24	116.78	265.44	0.550	2.69	2
$SrCl_2•2H_2O$	3.07	13	120.20	194.56	0.751	2.67	4
$SrCl_2•6H_2O$	3.07	13	225.40	266.62	0.878	2.68	9
$SrCl_2•H_2O$	3.07	13	102.41	176.54	0.572	2.66	2
$TlBr_3•4H_2O$	4.93	1	233.02	382.80	0.782	2.58	2

$TlCl_3•4H_2O$	4.70	1	209.91	382.80	0.771	2.5	2
$UBr_4•9H_2O$	5.45	25	382.81	719.78	0.862	2.47	8
$UCl_3•6H_2O$	5.51	26	259.00	452.48	0.798	2.51	6
$UCl_3•7H_2O$	5.51	26	271.89	470.49	0.849	2.56	7
$UF_4•2H_2O$	6.73	27	122.34	350.05	0.616	2.66	2
$VBr_3•6H_2O$	4.41	3	262.21	398.75	0.812	2.02	4
$VCl_3•4H_2O$	2.89	3	190.94	229.36	0.744	2.01	4
$VCl_3•6H_2O$	2.89	3	237.44	265.39	0.822	2.02	4
$VF_3•2H_2O$	3.46	12	93.48	143.97	0.710	2.04	4
$VF_3•3H_2O$	3.46	12	121.88	161.98	0.703	2.02	3
$YBr_3•10H_2O$	3.95	3	380.74	508.77	0.891	2.38	8
$YBr_3•8H_2O$	3.95	3	327.90	472.74	0.873	2.38	8
$YCl_3•6H_2O$	2.61	19	244.71	303.36	0.871	2.38	6
$ZnBr_2•2H_2O$	4.50	5	142.47	261.22	0.589	4.19	6
$ZnCl_2•1.33H_2O$	2.98	28	104.90	160.25	0.607	3.75	3
$ZnCl_2•2.5H_2O$	2.98	28	132.13	181.32	0.747	2.12	5
$ZnCl_2•3H_2O$	2.98	28	146.78	190.33	0.767	3.86	2
$ZnCl_2•4.5H_2O$	2.98	28	195.88	217.35	0.788	2.12	6
$ZnF_2•2H_2O$	4.95	20	81.56	139.41	0.785	2.13	2
$ZnF_2•4H_2O$	4.95	20	126.10	175.44	0.948	2.13	4
$ZrF_4•3H_2O$	4.61	29	134.06	221.26	0.675	2.22	2

Table A.6 (Part 5) Database of 50 salt hydrate features for all stable or metastable hydrates with well-defined properties (i.e. excluding hydrates with multiple cations or cations with missing ionic parameters).

Compound	C-A_Hyd	#CA_Hyd	C-C_Hyd	#CC_Hyd	Dens_Hyd	SG_Hyd	ST_Hyd
$AlCl_3•6H_2O$	4.44	12	5.93	2	1.67	33	1
$AlF_3•3H_2O$	1.80	3	4.65	2	2.01	34	2
$AlF_3•9H_2O$	1.8	3	6.1	2	1.44	34	3
$AlF_3•H_2O$	1.85	4	3.69	5	3.6	27	53
$BaBr_2•2H_2O$	3.5	6	4.47	2	3.84	1	50
$BaBr_2•H_2O$	3.41	7	4.66	2	4.18	29	51
$BaCl_2•2H_2O$	3.26	5	5.03	5	3.1	16	5
$BeCl_2•4H_2O$	2	1	4.76	3	1.55	15	37
$BiCl_3•H_2O$	2.78	5	4.48	3	4.05	2	6
$CaBr_2•6H_2O$	5.12	12	3.96	2	2.21	18	9
$CaBr_2•9H_2O$	4.95	7	6.03	2	1.96	16	7
$CaCl_2•2H_2O$	2.82	4	4.45	4	1.84	24	8
$CaCl_2•4H_2O$	2.76	2	5.89	6	1.55	15	20
$CaCl_2•6H_2O$	4.96	12	3.9	2	1.71	18	9
$CdBr_2•4H_2O$	2.8	4	4.05	2	3	32	10
$CdCl_2•2.5H_2O$	2.68	5	4.01	3	2.75	16	11
$CdCl_2•4H_2O$	2.66	4	3.82	2	2.41	17	12
$CdCl_2•H_2O$	2.68	5	3.91	4	3.22	31	51
$CeBr_3•7H_2O$	3.08	2	4.84	1	2.8	11	32
$CeCl_3•6H_2O$	2.88	2	6.62	6	2.28	13	13
$CeCl_3•7H_2O$	2.92	2	4.64	1	2.3	11	32
$CoBr_2•2H_2O$	2.64	4	3.76	2	3.41	2	14

$CoBr_2•4H_2O$	2.74	2	5.47	4	2.72	14	20
$CoCl_2•2H_2O$	2.48	4	3.54	2	2.48	2	14
$CoCl_2•H_2O$	2.47	5	3.57	4	2.78	31	51
$CrCl_2•4H_2O$	2.8	2	5.62	6	1.91	15	20
$CrCl_3•6H_2O$	4.48	12	5.75	2	1.81	33	1
$CrF_3•3H_2O$	1.91	2	5.11	4	2.22	36	23
$CrF_3•5H_2O$	1.9	3	5.54	4	1.98	24	67
$CrF_3•9H_2O$	4.07	6	6.83	6	1.63	34	15
$CuBr_2•4H_2O$	2.47	2	4.18	2	2.81	14	16
$CuCl_2•2H_2O$	2.32	2	3.79	2	2.5	30	17
$CuF_2•2H_2O$	1.95	2	3.33	2	2.96	7	14
$ErCl_3•6H_2O$	2.77	2	6.52	6	2.62	13	24
$FeBr_2•4H_2O$	2.7	2	5.81	6	2.63	14	20
$FeCl_2•2H_2O$	2.51	4	3.52	2	2.39	2	14
$FeCl_2•4H_2O$	2.46	2	5.42	4	1.97	15	20
$FeCl_3•2.5H_2O$	2.23	4	5.91	8	2.04	22	21
$FeCl_3•6H_2O$	2.31	2	6.04	2	1.81	2	22
$FeF_3•3H_2O$	1.94	4	3.68	2	2.32	19	2
$GdCl_3•6H_2O$	2.81	2	6.55	6	2.48	13	24
$HfF_4•3H_2O$	2.11	6	3.54	2	3.86	15	26
$HgF_2•2H_2O$	2.49	4	4.03	4	5.75	24	27
$InCl_3•3H_2O$	2.5	3	5.7	3	2.46	16	29
$InF_3•3H_2O$	2.12	4	4.27	2	2.88	20	2
$KF•2H_2O$	2.75	2	4.1	2	1.67	28	4
$KF•4H_2O$	4.74	7	4.04	1	1.44	15	30
$LaBr_3•7H_2O$	3.11	2	4.88	1	2.77	11	32
$LaCl_3•3H_2O$	3.01	6	4.48	2	2.75	21	31
$LaCl_3•7H_2O$	2.94	2	4.67	1	2.17	11	32
$LiBr•H_2O$	2.8	4	3.15	2	2.67	27	42
$LuBr_3•8H_2O$	4.81	7	6.05	1	2.85	16	28
$MgBr_2•2H_2O$	2.73	4	3.91	2	2.76	2	14
$MgBr_2•4H_2O$	2.75	2	5.74	5	2.27	4	33
$MgBr_2•6H_2O$	4.16	2	6.27	6	2.03	2	36
$MgBr_2•9H_2O$	4.8	6	6.6	6	1.86	1	34
$MgBr_2•H_2O$	2.63	4	3.69	2	3.11	31	51
$MgCl_2•2H_2O$	2.54	4	3.65	2	1.9	2	14
$MgCl_2•4H_2O$	2.57	2	5.63	6	1.65	24	35
$MgCl_2•6H_2O$	4.04	2	6.09	6	1.59	2	36
$MgCl_2•H_2O$	2.54	5	3.72	4	2.02	31	51
$MnBr_2•2H_2O$	2.73	4	3.87	2	3.1	2	14
$MnCl_2•2H_2O$	2.56	4	3.67	2	2.26	2	14
$MnCl_2•H_2O$	2.57	5	3.75	4	2.49	31	51
$NaBr•2H_2O$	2.97	2	3.67	3	2.16	15	38
$NaCl•2H_2O$	2.8	2	3.56	3	1.65	15	38
$NiCl_2•2H_2O$	2.4	4	3.44	2	2.6	7	39
$NiCl_2•4H_2O$	2.4	2	5.72	8	2.21	16	37
$NiCl_2•6H_2O$	2.42	2	6.45	10	1.85	15	40
$PrBr_3•6H_2O$	3.04	2	6.86	6	2.87	13	24

$PrCl_3•6H_2O$	2.87	2	6.62	6	2.3	13	24
$PtCl_4•3.5H_2O$	2.29	3	6.12	5	2.99	24	43
$PtCl_4•5H_2O$	2.33	4	6.94	10	2.87	3	44
$PuBr_3•6H_2O$	3	2	6.82	6	3.52	13	24
$RbF•H_2O$	2.89	4	4.35	4	2.9	31	41
$SmCl_3•6H_2O$	2.82	2	6.58	6	2.4	13	24
$SnBr_4•5H_2O$	2.61	4	6.8	6	3.18	1	48
$SnCl_4•2H_2O$	2.43	4	5.82	6	2.66	24	45
$SnCl_4•3H_2O$	2.43	4	6.16	6	2.49	15	46
$SnCl_4•4H_2O$	2.44	4	6.53	6	2.36	3	47
$SnCl_4•5H_2O$	2.44	4	6.58	6	2.27	1	48
$SnCl_4•8H_2O$	2.44	4	6.67	2	1.94	1	49
$SrBr_2•H_2O$	3.25	6	4.31	2	3.88	31	51
$SrCl_2•2H_2O$	3.27	6	4.21	2	2.7	8	50
$SrCl_2•6H_2O$	5.06	12	4.06	2	1.96	18	9
$SrCl_2•H_2O$	3.07	6	4.18	2	2.92	31	51
$TlBr_3•4H_2O$	2.64	3	6.51	8	3.64	26	52
$TlCl_3•4H_2O$	2.52	3	6.3	8	2.98	26	52
$UBr_4•9H_2O$	2.81	1	7.4	3	3.24	11	54
$UCl_3•6H_2O$	2.89	2	6.61	6	2.91	13	24
$UCl_3•7H_2O$	2.91	2	4.62	1	2.88	11	32
$UF_4•2H_2O$	2.18	3	3.94	2	6.31	6	55
$VBr_3•6H_2O$	2.55	2	6.74	8	2.58	15	57
$VCl_3•4H_2O$	2.37	2	6.07	6	1.97	2	56
$VCl_3•6H_2O$	2.39	2	6.52	8	1.84	15	57
$VF_3•2H_2O$	1.93	2	3.81	2	2.47	15	18
$VF_3•3H_2O$	1.96	3	4.98	6	2.14	35	58
$YBr_3•10H_2O$	4.74	6	7.14	3	2.2	11	59
$YBr_3•8H_2O$	4.83	7	6.06	1	2.38	16	28
$YCl_3•6H_2O$	2.79	2	6.51	6	2.08	13	24
$ZnBr_2•2H_2O$	2.47	4	3.29	1	3.02	10	25
$ZnCl_2•1.33H_2O$	2.31	4	4.09	3	2.48	23	60
$ZnCl_2•2.5H_2O$	2.51	1	4.2	1	2.3	16	61
$ZnCl_2•3H_2O$	2.3	4	5.24	4	2.15	11	62
$ZnCl_2•4.5H_2O$	4.58	7	5.55	3	1.81	17	63
$ZnF_2•2H_2O$	2.08	4	3.07	2	3	5	64
$ZnF_2•4H_2O$	2.08	2	5.16	6	2.31	25	65
$ZrF_4•3H_2O$	2.13	6	3.57	2	2.74	15	66

Table A.7 (Part 6) Database of 50 salt hydrate features for all stable or metastable hydrates with well-defined properties (i.e. excluding hydrates with multiple cations or cations with missing ionic parameters).

Compound	Dens_EA	VASA_EA	GASA_EA	VolFr_EA	GAV_EA	DH_Str	DH_Bnd
$AlCl_3•6H_2O$	0.91	9120	10017	0.58532	0.642909	-150.6	243.5
$AlF_3•3H_2O$	1.28	7104	5532	0.49036	0.38188	-163.4	210.9
$AlF_3•9H_2O$	0.53	3854	7218	0.78632	1.47248	-50.5	105.4
$AlF_3•H_2O$	2.05	5255	2568	0.35304	0.172563	-222.8	256.6
$BaBr_2•2H_2O$	3.33	6042	1813	0.42684	0.128085	-46.0	108.1

$BaBr_2•H_2O$	3.77	5071	1346	0.36912	0.0979731	-24.2	89.4
$BaCl_2•2H_2O$	2.59	6589	2545	0.44142	0.170477	-49.0	108.7
$BeCl_2•4H_2O$	0.76	7285	9528	0.59344	0.776208	-146.8	234.1
$BiCl_3•H_2O$	3.79	4830	1273	0.37442	0.0987141	-9.4	74.8
$CaBr_2•6H_2O$	1.45	7207	4962	0.62426	0.429809	-110.9	174.5
$CaBr_2•9H_2O$	1.08	6001	5541	0.71832	0.663238	-77.7	140.4
$CaCl_2•2H_2O$	1.59	6095	3822	0.40398	0.253331	-72.0	130.5
$CaCl_2•4H_2O$	0.99	7026	7127	0.60564	0.614392	-67.3	130.5
$CaCl_2•6H_2O$	0.88	7471	8514	0.62884	0.71663	-126.2	186.3
$CdBr_2•4H_2O$	2.35	4560	1940	0.65982	0.28073	-13.3	72.7
$CdCl_2•2.5H_2O$	2.19	5195	2372	0.59298	0.270785	-25.1	78.9
$CdCl_2•4H_2O$	1.72	4652	2701	0.67504	0.391909	-15.7	73.6
$CdCl_2•H_2O$	2.86	5919	2068	0.47182	0.164834	-32.0	86.6
$CeBr_3•7H_2O$	2.12	6617	3114	0.6305	0.29671	-88.0	152.5
$CeCl_3•6H_2O$	1.57	7134	4535	0.6289	0.399721	-89.9	154.5
$CeCl_3•7H_2O$	1.50	6735	4476	0.64248	0.426997	-87.9	149.5
$CoBr_2•2H_2O$	2.90	6409	2213	0.43546	0.150392	-35.4	93.7
$CoBr_2•4H_2O$	2.15	7741	3601	0.52898	0.246113	-72.4	119.3
$CoCl_2•2H_2O$	1.98	6531	3303	0.43482	0.219875	-43.2	97.5
$CoCl_2•H_2O$	2.46	5294	2151	0.34788	0.141305	-47.7	103.1
$CrCl_2•4H_2O$	1.23	7873	6380	0.55214	0.447426	-97.7	158.1
$CrCl_3•6H_2O$	1.07	8972	8392	0.5901	0.551967	-154.5	220.7
$CrF_3•3H_2O$	1.57	7882	5024	0.50048	0.318978	-117.7	185.3
$CrF_3•5H_2O$	1.16	6374	5477	0.63188	0.54296	-74.4	128.9
$CrF_3•9H_2O$	0.65	6583	10120	0.7354	1.13051	-178.8	248.6
$CuBr_2•4H_2O$	2.13	5109	2398	0.64754	0.303943	-25.1	79.0
$CuCl_2•2H_2O$	1.95	7083	3637	0.53372	0.274089	-50.6	98.7
$CuF_2•2H_2O$	2.19	7744	3542	0.55346	0.253104	-75.9	140.1
$ErCl_3•6H_2O$	1.85	7403	4011	0.61074	0.330916	-108.3	180.5
$FeBr_2•4H_2O$	2.01	7491	3736	0.55662	0.277603	-69.4	123.3
$FeCl_2•2H_2O$	1.90	6393	3363	0.4385	0.230683	-39.0	93.5
$FeCl_2•4H_2O$	1.30	7525	5774	0.5665	0.434705	-64.1	114.3
$FeCl_3•2.5H_2O$	1.69	6793	4018	0.4787	0.28319	-45.5	106.0
$FeCl_3•6H_2O$	1.12	6797	6078	0.62498	0.558885	-53.3	109.5
$FeF_3•3H_2O$	1.54	5715	3715	0.561	0.364637	-29.1	110.1
$GdCl_3•6H_2O$	1.75	7321	4173	0.61408	0.350023	14.2	56.6
$HfF_4•3H_2O$	3.24	5941	1831	0.52328	0.161292	-70.1	137.6
$HgF_2•2H_2O$	4.84	7436	1537	0.51538	0.1065	-97.7	168.7
$InCl_3•3H_2O$	1.81	6649	3677	0.57554	0.318264	-60.0	111.0
$InF_3•3H_2O$	2.11	5942	2812	0.59082	0.279552	-78.3	148.7
$KF•2H_2O$	1.02	2433	2377	0.15374	0.150198	-47.0	122.0
$KF•4H_2O$	0.65	6289	9706	0.37948	0.585713	-74.8	143.3
$LaBr_3•7H_2O$	2.09	6562	3140	0.63476	0.30371	-101.2	165.9
$LaCl_3•3H_2O$	2.26	6069	2686	0.49018	0.216902	-40.5	101.0
$LaCl_3•7H_2O$	1.48	6689	4520	0.6459	0.436497	-103.6	165.2
$LiBr•H_2O$	2.24	4970	2221	0.32044	0.143205	-49.6	121.8
$LuBr_3•8H_2O$	2.13	7302	3429	0.65306	0.306679	-136.8	207.8
$MgBr_2•2H_2O$	2.30	6524	2841	0.49446	0.215298	-38.2	117.4

$MgBr_2•4H_2O$	1.68	7188	4269	0.6109	0.36283	-64.2	141.1
$MgBr_2•6H_2O$	1.31	6860	5220	0.67672	0.514933	-103.7	176.2
$MgBr_2•9H_2O$	1.00	5531	5546	0.75634	0.758444	-76.6	148.7
$MgBr_2•H_2O$	2.29	6258	2729	0.50446	0.21994	-69.9	123.8
$MgCl_2•2H_2O$	1.39	6576	4736	0.49168	0.354092	-39.9	116.4
$MgCl_2•4H_2O$	0.97	7325	7562	0.61426	0.634093	-69.8	143.2
$MgCl_2•6H_2O$	0.74	7135	9636	0.68528	0.925498	-119.1	186.8
$MgCl_2•H_2O$	1.70	5555	3261	0.40414	0.237255	-48.2	130.0
$MnBr_2•2H_2O$	2.66	6229	2337	0.455	0.170745	-35.4	93.5
$MnCl_2•2H_2O$	1.78	6325	3553	0.4576	0.25703	-35.4	95.6
$MnCl_2•H_2O$	2.18	5522	2533	0.37484	0.171935	-37.3	102.6
$NaBr•2H_2O$	1.65	5620	3411	0.37976	0.230496	-56.4	114.0
$NaCl•2H_2O$	1.04	5527	5329	0.36926	0.356049	-61.6	116.6
$NiCl_2•2H_2O$	2.04	5947	2912	0.4859	0.237919	-41.1	91.6
$NiCl_2•4H_2O$	1.45	6920	4775	0.60212	0.415529	-74.5	124.5
$NiCl_2•6H_2O$	1.10	5836	5320	0.6996	0.637729	-45.0	100.9
$PrBr_3•6H_2O$	2.21	7076	3195	0.61538	0.277829	-77.5	146.7
$PrCl_3•6H_2O$	1.59	7180	4522	0.62406	0.39298	-86.5	152.4
$PtCl_4•3.5H_2O$	2.59	6902	2668	0.53848	0.208156	-51.3	162.0
$PtCl_4•5H_2O$	2.26	5048	2236	0.60764	0.269127	3.6	105.3
$PuBr_3•6H_2O$	2.85	7079	2482	0.61346	0.215089	-107.1	173.7
$RbF•H_2O$	2.41	6055	2514	0.39816	0.165302	-18.2	108.4
$SmCl_3•6H_2O$	1.68	7249	4324	0.62028	0.369997	-57.6	123.4
$SnBr_4•5H_2O$	2.57	6002	2335	0.55092	0.214313	-25.9	86.5
$SnCl_4•2H_2O$	2.30	6184	2693	0.423	0.184217	-64.3	133.0
$SnCl_4•3H_2O$	2.05	5907	2882	0.48122	0.234841	-44.8	115.3
$SnCl_4•4H_2O$	1.84	6167	3359	0.53608	0.291976	-31.0	101.6
$SnCl_4•5H_2O$	1.69	6045	3586	0.57152	0.33901	-28.3	97.7
$SnCl_4•8H_2O$	1.27	4616	3640	0.67998	0.536105	-17.5	86.6
$SrBr_2•H_2O$	3.52	4449	1265	0.31578	0.0897531	-32.1	99.7
$SrCl_2•2H_2O$	2.19	5621	2567	0.37868	0.172909	-70.1	124.8
$SrCl_2•6H_2O$	1.17	7262	6218	0.654	0.559998	-119.0	177.9
$SrCl_2•H_2O$	2.57	4224	1643	0.31178	0.121289	-41.6	98.1
$TlBr_3•4H_2O$	3.16	5211	1647	0.57212	0.180783	-3.0	70.7
$TlCl_3•4H_2O$	2.46	5447	2216	0.58514	0.238034	-21.9	78.8
$UBr_4•9H_2O$	2.42	6714	2776	0.65814	0.27208	-104.0	166.8
$UCl_3•6H_2O$	2.21	7030	3184	0.64408	0.2917	-97.6	162.5
$UCl_3•7H_2O$	2.10	6610	3143	0.66152	0.314507	-108.3	169.9
$UF_4•2H_2O$	4.26	6011	1410	0.47094	0.110495	-84.6	121.7
$VBr_3•6H_2O$	1.84	6727	3655	0.59898	0.325412	-78.1	146.2
$VCl_3•4H_2O$	1.15	7421	6472	0.59568	0.519559	-126.2	193.7
$VCl_3•6H_2O$	1.10	6935	6304	0.61132	0.555695	-86.6	154.4
$VF_3•2H_2O$	1.92	7236	3774	0.43112	0.224846	-128.3	194.8
$VF_3•3H_2O$	1.47	7730	5257	0.51924	0.353094	-132.3	198.4
$YBr_3•10H_2O$	1.43	6243	4356	0.7073	0.493506	-111.7	176.3
$YBr_3•8H_2O$	1.66	7213	4334	0.65778	0.39526	-137.4	205.4
$YCl_3•6H_2O$	1.33	7441	5616	0.60922	0.459787	-102.8	173.7
$ZnBr_2•2H_2O$	2.62	7126	2715	0.57512	0.219113	-73.8	136.6

$ZnCl_2$•1.33H_2O	2.16	7163	3320	0.5085	0.235679	-93.3	138.6
$ZnCl_2$•2.5H_2O	1.71	6895	4025	0.60234	0.351644	-95.8	151.0
$ZnCl_2$•3H_2O	1.54	6440	4176	0.63948	0.414712	-98.0	152.0
$ZnCl_2$•4.5H_2O	1.16	5237	4533	0.72768	0.629806	-67.6	128.3
ZnF_2•2H_2O	2.10	6689	3178	0.5928	0.281623	-52.7	103.1
ZnF_2•4H_2O	1.36	6699	4921	0.7189	0.528053	-76.6	141.4
ZrF_4•3H_2O	2.07	5840	2820	0.53202	0.256853	-65.1	132.7

Table A.8 (Part 7) Database of 50 salt hydrate features for all stable or metastable hydrates with well-defined properties (i.e. excluding hydrates with multiple cations or cations with missing ionic parameters).

Compound	DH	nDH_Str	nDH_Bnd	nDH	Stability	GED	VED	Promising
$AlCl_3$•6H_2O	92.9	-903.5	1461.2	557.7	1	2.31	3.81	1
AlF_3•3H_2O	47.4	-490.2	632.6	142.3	0	1.03	2.18	0
AlF_3•9H_2O	54.9	-454.6	949.0	494.4	1	2.01	3.14	1
AlF_3•H_2O	33.8	-222.8	256.6	33.8	0	0.33	0.82	0
$BaBr_2$•2H_2O	62.1	-92.1	216.2	124.1	1	0.37	1.39	0
$BaBr_2$•H_2O	65.2	-24.2	89.4	65.2	1	0.21	0.83	0
$BaCl_2$•2H_2O	59.7	-98.0	217.3	119.3	1	0.49	1.48	0
$BeCl_2$•4H_2O	87.4	-587.0	936.5	349.5	1	2.30	3.34	1
$BiCl_3$•H_2O	65.4	-9.4	74.8	65.4	1	0.20	0.79	0
$CaBr_2$•6H_2O	63.7	-665.3	1047.3	382.0	1	1.24	2.78	0
$CaBr_2$•9H_2O	62.7	-699.1	1263.5	564.4	1	1.56	3.06	1
$CaCl_2$•2H_2O	58.6	-144.0	261.1	117.1	0	0.80	1.68	0
$CaCl_2$•4H_2O	63.3	-269.0	522.0	253.0	1	1.38	2.25	0
$CaCl_2$•6H_2O	60.1	-757.4	1118.0	360.6	1	1.65	2.85	0
$CdBr_2$•4H_2O	59.5	-53.2	291.0	237.8	1	0.69	2.05	0
$CdCl_2$•2.5H_2O	53.8	-62.7	197.2	134.5	0	0.59	1.61	0
$CdCl_2$•4H_2O	57.9	-62.7	294.4	231.8	1	0.91	2.18	0
$CdCl_2$•H_2O	54.7	-32.0	86.6	54.7	0	0.27	0.85	0
$CeBr_3$•7H_2O	64.5	-615.8	1067.4	451.6	1	0.89	2.53	0
$CeCl_3$•6H_2O	64.6	-539.5	927.1	387.6	1	1.09	2.47	0
$CeCl_3$•7H_2O	61.6	-615.6	1046.6	430.9	0	1.16	2.63	0
$CoBr_2$•2H_2O	58.3	-70.7	187.4	116.7	1	0.46	1.54	0
$CoBr_2$•4H_2O	46.8	-289.7	477.0	187.4	0	0.64	1.84	0
$CoCl_2$•2H_2O	54.3	-86.5	195.0	108.5	1	0.65	1.65	0
$CoCl_2$•H_2O	55.5	-47.7	103.1	55.5	1	0.38	1.05	0
$CrCl_2$•4H_2O	60.4	-390.8	632.3	241.5	1	1.24	2.42	0
$CrCl_3$•6H_2O	66.2	-927.1	1324.0	396.9	1	1.49	2.68	0
CrF_3•3H_2O	67.6	-353.1	555.8	202.7	0	1.24	2.92	0
CrF_3•5H_2O	54.5	-371.8	644.5	272.5	0	1.37	2.91	0
CrF_3•9H_2O	69.7	-1609.3	2237.0	627.7	1	2.32	3.75	1
$CuBr_2$•4H_2O	54.0	-100.3	316.2	215.9	1	0.73	2.06	0
$CuCl_2$•2H_2O	48.0	-101.3	197.3	96.0	1	0.56	1.39	0
CuF_2•2H_2O	64.2	-151.7	280.1	128.4	1	0.93	2.77	0
$ErCl_3$•6H_2O	72.2	-650.0	1083.1	433.1	1	1.13	2.92	0
$FeBr_2$•4H_2O	53.9	-277.6	493.1	215.5	1	0.75	2.00	0
$FeCl_2$•2H_2O	54.6	-77.9	187.1	109.1	1	0.67	1.64	0

$FeCl_2•4H_2O$	50.2	-256.4	457.4	201.0	0	1.01	2.07	0
$FeCl_3•2.5H_2O$	60.5	-113.7	264.9	151.2	1	0.73	1.58	0
$FeCl_3•6H_2O$	56.2	-319.7	657.1	337.5	1	1.25	2.33	0
$FeF_3•3H_2O$	81.0	-87.3	330.3	243.0	1	1.46	3.31	0
$GdCl_3•6H_2O$	70.8	85.2	339.6	424.7	1	1.14	2.83	0
$HfF_4•3H_2O$	67.4	-210.4	412.7	202.3	1	0.66	2.58	0
$HgF_2•2H_2O$	71.1	-195.4	337.5	142.1	1	0.52	2.88	0
$InCl_3•3H_2O$	51.0	-180.0	333.0	153.0	1	0.56	1.25	0
$InF_3•3H_2O$	70.4	-235.0	446.1	211.1	1	0.93	2.60	0
$KF•2H_2O$	75.0	-93.9	243.9	150.0	1	1.59	2.64	0
$KF•4H_2O$	68.5	-299.0	573.1	274.1	1	2.11	3.06	1
$LaBr_3•7H_2O$	64.7	-708.1	1161.1	453.0	1	0.90	2.50	0
$LaCl_3•3H_2O$	60.5	-121.6	303.1	181.5	0	0.61	1.67	0
$LaCl_3•7H_2O$	61.6	-725.0	1156.3	431.3	1	1.16	2.60	0
$LiBr•H_2O$	72.2	-49.6	121.8	72.2	1	0.69	1.86	0
$LuBr_3•8H_2O$	71.0	-1094.6	1662.3	567.7	1	1.02	2.92	0
$MgBr_2•2H_2O$	79.1	-76.5	234.7	158.2	1	0.72	1.97	0
$MgBr_2•4H_2O$	76.9	-256.8	564.3	307.4	1	1.20	2.81	0
$MgBr_2•6H_2O$	72.5	-622.1	1057.0	434.8	0	1.49	3.10	0
$MgBr_2•9H_2O$	72.1	-689.3	1337.9	648.6	1	1.87	3.51	1
$MgBr_2•H_2O$	53.9	-69.9	123.8	53.9	0	0.27	0.67	0
$MgCl_2•2H_2O$	76.6	-79.7	232.8	153.1	1	1.17	2.23	0
$MgCl_2•4H_2O$	73.4	-279.3	572.9	293.6	1	1.76	2.99	0
$MgCl_2•6H_2O$	67.6	-714.8	1120.6	405.8	1	2.00	3.16	1
$MgCl_2•H_2O$	81.7	-48.2	130.0	81.7	1	0.72	1.46	0
$MnBr_2•2H_2O$	58.2	-70.7	187.0	116.3	1	0.46	1.44	0
$MnCl_2•2H_2O$	60.2	-70.8	191.2	120.5	1	0.74	1.70	0
$MnCl_2•H_2O$	65.3	-37.3	102.6	65.3	1	0.45	1.13	0
$NaBr•2H_2O$	57.6	-112.8	228.1	115.3	1	0.83	1.85	0
$NaCl•2H_2O$	55.1	-123.1	233.3	110.1	1	1.17	1.95	0
$NiCl_2•2H_2O$	50.6	-82.1	183.3	101.2	0	0.61	1.59	0
$NiCl_2•4H_2O$	50.1	-298.0	498.2	200.2	0	0.99	2.24	0
$NiCl_2•6H_2O$	56.0	-269.7	605.5	335.8	1	1.41	2.84	0
$PrBr_3•6H_2O$	69.2	-464.9	880.3	415.4	1	0.85	2.42	0
$PrCl_3•6H_2O$	65.9	-519.0	914.7	395.7	1	1.11	2.54	0
$PtCl_4•3.5H_2O$	110.7	-179.6	567.1	387.5	1	0.97	2.98	0
$PtCl_4•5H_2O$	108.9	18.0	526.4	544.5	1	1.28	3.65	0
$PuBr_3•6H_2O$	66.6	-642.7	1042.4	399.7	1	0.68	2.36	0
$RbF•H_2O$	90.2	-18.2	108.4	90.2	1	0.74	2.08	0
$SmCl_3•6H_2O$	65.7	-345.7	740.1	394.4	1	1.08	2.58	0
$SnBr_4•5H_2O$	60.6	-129.3	432.3	302.9	1	0.57	1.78	0
$SnCl_4•2H_2O$	68.8	-128.6	266.1	137.5	0	0.46	1.21	0
$SnCl_4•3H_2O$	70.5	-134.3	345.8	211.6	0	0.67	1.66	0
$SnCl_4•4H_2O$	70.6	-124.0	406.6	282.4	1	0.85	1.99	0
$SnCl_4•5H_2O$	69.4	-141.5	488.4	347.0	0	0.99	2.25	0
$SnCl_4•8H_2O$	69.1	-140.2	692.9	552.6	1	1.37	2.69	0
$SrBr_2•H_2O$	67.6	-32.1	99.7	67.6	1	0.25	0.96	0
$SrCl_2•2H_2O$	54.7	-140.2	249.6	109.5	0	0.56	1.51	0

$SrCl_2•6H_2O$	58.9	-713.9	1067.5	353.6	1	1.33	2.61	0
$SrCl_2•H_2O$	56.4	-41.6	98.1	56.4	0	0.32	0.91	0
$TlBr_3•4H_2O$	67.6	-12.2	282.6	270.5	1	0.52	1.93	0
$TlCl_3•4H_2O$	56.9	-87.4	315.0	227.6	1	0.59	1.80	0
$UBr_4•9H_2O$	62.8	-936.0	1501.5	565.5	1	0.79	2.45	0
$UCl_3•6H_2O$	64.8	-585.8	974.9	389.1	1	0.86	2.49	0
$UCl_3•7H_2O$	61.6	-758.1	1189.6	431.4	0	0.92	2.64	0
$UF_4•2H_2O$	37.1	-169.2	243.3	74.1	0	0.21	1.01	0
$VBr_3•6H_2O$	68.2	-468.5	877.5	409.0	1	1.03	2.59	0
$VCl_3•4H_2O$	67.5	-504.8	774.8	270.0	0	1.18	2.35	0
$VCl_3•6H_2O$	67.8	-519.8	926.4	406.5	1	1.53	2.84	0
$VF_3•2H_2O$	66.4	-256.7	389.5	132.8	1	0.92	2.36	0
$VF_3•3H_2O$	66.1	-396.9	595.2	198.2	1	1.22	2.70	0
$YBr_3•10H_2O$	64.6	-1116.7	1762.7	646.0	1	1.27	2.82	0
$YBr_3•8H_2O$	68.1	-1099.0	1643.6	544.6	1	1.15	2.76	0
$YCl_3•6H_2O$	70.9	-617.0	1042.3	425.3	1	1.40	2.89	0
$ZnBr_2•2H_2O$	62.8	-147.6	273.3	125.7	1	0.48	1.47	0
$ZnCl_2•1.33H_2O$	45.3	-124.1	184.4	60.3	0	0.38	0.95	0
$ZnCl_2•2.5H_2O$	55.3	-239.4	377.6	138.1	0	0.76	1.74	0
$ZnCl_2•3H_2O$	54.0	-294.1	456.0	161.9	0	0.85	1.83	0
$ZnCl_2•4.5H_2O$	60.6	-304.4	577.2	272.8	1	1.26	2.31	0
$ZnF_2•2H_2O$	50.4	-105.4	206.3	100.8	0	0.72	2.05	0
$ZnF_2•4H_2O$	64.8	-306.3	565.5	259.3	1	1.48	3.41	0
$ZrF_4•3H_2O$	67.5	-195.4	398.0	202.6	1	0.92	2.51	0

Table A.9 Salt hydrate cations.

Cation	Symbol
1	Al
2	Ba
3	Be
4	Bi
5	Ca
6	Cd
7	Ce
8	Co
9	Cr
10	Cu
11	Er
12	Eu
13	Fe
14	Gd
15	Hf
16	Hg
17	In
18	K
19	La
20	Li

21	Lu
22	Mg
23	Mn
24	Na
25	Ni
26	Pr
27	Pt
28	Pu
29	Rb
30	Sm
31	Sn
32	Sr
33	Tl
34	U
35	V
36	Y
37	Zn
38	Zr

Table A.10 Salt hydrate anions.

Anion	Symbol
1	F
2	Cl
3	Br

Table A.11 Anhydrous salt structure types and space groups.

Str_Anh	Structure Type	Common Space Group
1	AlCl3	C 1 2/m 1
2	BiCl3	P n 21 a
3	BiI3	R -3
4	CaCl2	P n n m
5	CdCl2(3R)	R -3 m H
6	CdI2	P -3 m 1
7	CdI2(hP6)	P 63 m c
8	CrF3	R -3 c R
9	CsCl	P m -3 m
10	CuCl2	C 1 2/m 1
11	CuF2	P 1 21/n 1
12	FeF3	R -3 c H
13	Fluorite-CaF2	F m -3 m
14	NaCl	F m -3 m
15	NdBr3	C c m m
16	PbCl2	P n m a
17	PbO2-alpha	P b c n
18	PuBr3	C m c m

19	RhBr3	C 1 2/m 1
20	Rutile-TiO2	P 42/m n m
21	SiCl4	P 1 21/c 1
22	SiS2(Ibam)	I b a m
23	SnI4	P a -3
24	SrBr2	P 4/n Z
25	UBr4	C 1 2/m 1
26	UCl3	P 63/m
27	UF4	C 1 2/c 1
28	ZnCl2	P n a 21
29	ZrF4	P 42/m

Table A.12 Salt hydrate space groups.

SG_Hyd	Space Group
1	C 1 2/c 1
2	C 1 2/m 1
3	C 1 c 1
4	C m c m
5	F d d d S
6	F m -3 m
7	I 1 2/m 1
8	I 1 c 1
9	I -4 2 d
10	I m m m
11	P -1
12	P 1 2/c 1
13	P 1 2/n 1
14	P 1 21/a 1
15	P 1 21/c 1
16	P 1 21/n 1
17	P 21 21 21
18	P 3 2 1
19	P 4/n S
20	P 4/n Z
21	P -6 2 m
22	P b c 21
23	P b c a
24	P b c n
25	P c a 21
26	P c m n
27	P m -3 m
28	P m c 21
29	P m c n
30	P m n a
31	P n m a
32	P n n m
33	R -3 c H

34	R -3 H
35	R 3 m H
36	R -3 m R

Table A.13 Salt hydrate structure types.

ST_Hyd	Structure Type
1	AlCl3(H2O)6
2	AlF3(H2O)3
3	AlF3(H2O)9
4	Ba(OH)2H2O
5	BaCl2(H2O)2
6	BiCl3(H2O)1
7	CaBr2(H2O)9
8	CaCl2(H2O)2
9	CaCl2(H2O)6
10	CdBr2(H2O)4
11	CdCl2(H2O)2.5
12	CdCl2(H2O)4
13	CeCl3(H2O)6
14	CoCl2(H2O)2
15	CrF3(H2O)9
16	CuBr2(H2O)4
17	CuCl2(H2O)2
18	CuZrF6(H2O)4
19	EuBr3(H2O)6
20	FeCl2(H2O)4
21	FeCl3(H2O)2.5
22	FeCl3(H2O)6
23	FeF3
24	GdCl3(H2O)6
25	H12MgZn2O6Br6
26	HfF4(H2O)3
27	HgF2(H2O)2
28	HoBr3(H2O)8
29	InCl3(H2O)3
30	KF(H2O)4
31	LaCl3(H2O)3
32	LaCl3(H2O)7
33	MgBr2(H2O)4
34	MgBr2(H2O)9
35	MgCl2(H2O)4
36	MgCl2(H2O)6
37	MnCl2(H2O)4
38	NaCl(H2O)2
39	NiCl2(H2O)2
40	NiCl2(H2O)6
41	PbO(H2O)

42	Perovskite-CaTiO3
43	PtCl4(H2O)3.5
44	PtCl4(H2O)5
45	SnCl4(H2O)2
46	SnCl4(H2O)3
47	SnCl4(H2O)4
48	SnCl4(H2O)5
49	SnCl4(H2O)8
50	SrCl2(H2O)2
51	SrCl2H2O
52	TlBr3(H2O)4
53	U4S3
54	UBr4(H2O)9
55	UF4(H2O)2
56	VCl3(H2O)4
57	VCl3(H2O)6
58	VF3(H2O)3
59	YBr3(H2O)10
60	ZnCl2(H2O)1.33
61	ZnCl2(H2O)2.5
62	ZnCl2(H2O)3
63	ZnCl2(H2O)4.5
64	ZnF2(H2O)2
65	ZnF2(H2O)4
66	ZrF4(H2O)3
67	(NH4)2AlF5(H2O)

Table A.14 Description of hydroxide properties, denoted by the following categories: water content (WC), ionic properties (Ion), structural properties (Str), and thermodynamic/energy density properties (Thermo). All thermodynamic properties correspond to the reaction between the hydroxide and its respective oxide. Some properties are numerically represented categories that are not of interest when examining correlations, but may be useful for clustering analysis.

Property	Category	Units	Description
Compound	-	-	Chemical formula of the hydroxide
n	WC	H_2O/f.u.	Number of water molecules involved in the hydration reaction
Cap_Grav	WC	mol H_2O/kg hydroxide	Gravimetric Water Capacity, this multiplied by DH yields the GED
Cap_Vol	WC	mol H_2O/L hydroxide	Volumetric Water Capacity, this multiplied by DH yields the VED
Mass_Cat	Ion	g/mol	Molar mass of the cation[148]
Rad_Cat	Ion	pm	Ionic radius of cation assuming coordination number of 6[149]
Elneg_Cat	Ion	Pauling Units	Electronegativity of cation according to Pauling Scale[148]
Chg_Cat	Ion	e	Formal charge of cation
PP_Cat	Ion	e/Å	Polarizing power of the cation, equal to the formal charge divided by the ionic radius[149]
DV	Str	$Å^3$/f.u.	Difference in hydroxide and oxide volume

DV/V	Str	-	Relative change in volume from oxide to hydroxide
MM_Hyd	Str	g/mol	Molar mass of the hydroxide[148]
Vol_Hyd	Str	$Å^3$/f.u.	Volume of the hydroxide
Dens_Hyd	Str	g/cm^3	Density of the hydroxide[103]
C-O_Hyd	Str	Å	Distance between nearest neighbor cations and oxygens in the hydroxide
#CO_Hyd	Str	-	Number of nearest neighbor oxygens coordinating the cation in the hydroxide
C-C_Hyd	Str	Å	Distance between nearest neighbor cations in the hydroxide
#CC_Hyd	Str	-	Number of nearest neighbor cations coordinating the cation in the hydroxide
ST_Hyd	Str	-	ID # for structure type of the hydroxide (see Table A.19)[103]
SG_Hyd	Str	-	ID # for space group of the hydroxide (see Table A.20)[103]
MM_Ox	Str	g/mol	Molar mass of the oxide[148]
Vol_Ox	Str	$Å^3$/f.u.	Volume of the oxide
Dens_Ox	Str	g/cm^3	Density of the oxide[103]
C-O_Ox	Str	Å	Distance between nearest neighbor cations and oxygens in the oxide
#CO_Ox	Str	-	Number of nearest neighbor oxygens coordinating the cation in the oxide
C-C_Ox	Str	Å	Distance between nearest neighbor cations in the oxide
#CC_Ox	Str	-	Number of nearest neighbor cations coordinating the cation in the oxide
ST_Ox	Str	-	ID # for structure type of the oxide (see Table A.21)[103]
SG_Ox	Str	-	ID # for space group of the oxide (see Table A.22)[103]
nDH	Thermo	kJ/mol oxide	Total enthalpy change - This is the energy difference between the hydroxide and the oxide, it is used to calculate the energy densities
DH	Thermo	kJ/mol H_2O	Dehydration Enthalpy - This is the energy difference between the hydroxide and the oxide, it is used to calculate the energy densities
GED	Thermo	MJ/kg	Gravimetric energy density
VED	Thermo	GJ/m^3	Volumetric energy density
Promising	Thermo	-	Promising reactions (1) have VED > 3 and GED > 1.5, non-promising reactions (0) do not

Table A.15 (Part 1) Database of 33 hydroxide properties for all stable or metastable hydroxides with well-defined properties (i.e. excluding hydroxides with multiple cations or cations with missing ionic parameters).

Compound	n	Cap_Grav	Cap_Vol	Mass_Cat	Rad_Cat	Elneg_Cat	Chg_Cat	PP_Cat	DV
$Al(OH)_3$	1.5	19.23	48.47	26.982	67.5	1.61	3	4.44	29.47
$Ba(OH)_2$	1	5.84	25.10	137.327	149	0.89	2	1.34	22.62
$Be(OH)_2$	1	23.24	42.83	9.012	59	1.57	2	3.39	24.66
$Ca(OH)_2$	1	13.50	30.25	40.078	114	1	2	1.75	26.80
$Ce(OH)_3$	1.5	7.85	35.56	140.116	115	1.12	3	2.61	16.45
$Dy(OH)_3$	1.5	7.03	39.92	162.500	105.2	1.22	3	2.85	27.80
$Eu(OH)_3$	1.5	7.39	37.97	151.964	108.7	1.2	3	2.76	27.37
$Ga(OH)_3$	1.5	12.42	44.45	69.723	76	1.81	3	3.95	28.05
$Gd(OH)_3$	1.5	7.20	38.80	157.250	107.8	1.2	3	2.78	27.22
$In(OH)_3$	1.5	9.04	36.64	114.818	94	1.78	3	3.19	35.20
KOH	0.5	8.91	18.15	39.098	152	0.82	1	0.66	11.40
$La(OH)_3$	1.5	7.90	34.37	138.905	117.2	1.1	3	2.56	30.65
LiOH	0.5	20.88	30.26	6.941	90	0.98	1	1.11	14.90
$Lu(OH)_3$	1.5	6.64	34.62	174.967	100.1	1.27	3	3.00	38.79

$Mg(OH)_2$	1	17.15	40.19	24.305	86	1.31	2	2.33	22.21
$Mn(OH)_2$	1	11.24	35.81	54.938	97	1.55	2	2.06	25.14
NaOH	0.5	12.50	26.30	22.990	116	0.93	1	0.86	10.52
$Nd(OH)_3$	1.5	7.68	36.80	144.242	112.3	1.14	3	2.67	29.68
$Ni(OH)_2$	1	10.79	41.82	58.693	83	1.91	2	2.41	21.19
$Pr(OH)_3$	1.5	7.82	36.32	140.908	113	1.13	3	2.65	30.52
RbOH	0.5	4.93	15.61	85.468	166	0.82	1	0.60	12.25
$Sc(OH)_3$	1.5	15.63	39.74	44.956	88.5	1.36	3	3.39	34.75
$Sr(OH)_2$	1	8.22	27.61	87.620	132	0.95	2	1.52	24.86
$Te(OH)_6$	3	13.06	39.38	127.600	70	2.1	6	8.57	78.38
TlOH	0.5	2.26	15.22	204.383	164	1.62	1	0.61	17.56
$Y(OH)_3$	1.5	10.72	40.25	88.906	104	1.22	3	2.88	26.83
$Zn(OH)_2$	1	10.06	35.92	65.380	88	1.65	2	2.27	21.27

Table A.16 (Part 2) Database of 33 hydroxide properties for all stable or metastable hydroxides with well-defined properties (i.e. excluding hydroxides with multiple cations or cations with missing ionic parameters).

Compound	DV/V	MM Hyd	Vol Hyd	Dens Hyd	C-O Hyd	#CO Hyd	C-C Hyd	#CC Hyd	ST Hyd
$Al(OH)_3$	1.34	78.002	51.39	2.52	1.93	6.00	2.86	3.00	1
$Ba(OH)_2$	0.52	171.341	66.15	4.30	2.94	8.00	3.96	2.00	2
$Be(OH)_2$	1.75	43.026	38.77	1.84	1.65	4.00	2.91	4.00	13
$Ca(OH)_2$	0.95	74.092	54.89	2.24	2.38	6.00	3.60	6.00	3
$Ce(OH)_3$	0.31	191.137	70.05	4.53	2.56	9.00	3.78	2.00	12
$Dy(OH)_3$	0.80	213.521	62.40	5.68	2.45	9.00	3.57	2.00	12
$Eu(OH)_3$	0.72	202.985	65.61	5.14	2.51	9.00	3.68	2.00	12
$Ga(OH)_3$	1.00	120.753	56.03	3.58	2.03	6.00	3.83	6.00	5
$Gd(OH)_3$	0.74	208.271	64.20	5.39	2.48	9.00	3.64	2.00	12
$In(OH)_3$	1.07	165.839	67.98	4.05	2.21	6.00	4.08	6.00	5
KOH	0.33	56.105	45.74	2.04	2.83	5.00	3.83	8.00	6
$La(OH)_3$	0.73	189.926	72.46	4.35	2.59	9.00	3.86	2.00	7
LiOH	1.19	23.948	27.44	1.45	1.98	4.00	2.52	4.00	8
$Lu(OH)_3$	1.17	225.988	71.94	5.22	2.25	6.00	4.16	6.00	5
$Mg(OH)_2$	1.16	58.319	41.32	2.34	2.11	6.00	3.17	6.00	3
$Mn(OH)_2$	1.18	88.952	46.37	3.19	2.21	6.00	3.35	6.00	3
NaOH	0.50	39.997	31.58	2.10	2.40	5.00	3.20	6.00	6
$Nd(OH)_3$	0.78	195.263	67.69	4.79	2.53	9.00	3.74	2.00	7
$Ni(OH)_2$	1.14	92.707	39.71	3.88	2.09	6.00	3.17	6.00	3
$Pr(OH)_3$	0.80	191.928	68.59	4.65	2.54	9.00	3.75	2.00	12
RbOH	0.30	101.475	53.19	3.17	2.98	5.00	4.08	10.00	6
$Sc(OH)_3$	1.24	95.977	62.67	2.54	2.12	6.00	3.97	6.00	5
$Sr(OH)_2$	0.70	121.634	60.14	3.36	2.62	7.00	4.00	8.00	9
$Te(OH)_6$	1.63	229.641	126.52	3.01	1.96	6.00	4.87	2.00	10
TlOH	0.47	221.387	54.56	6.74	2.59	3.00	4.09	9.00	11
$Y(OH)_3$	0.77	139.927	61.89	3.75	2.44	9.00	3.56	2.00	12
$Zn(OH)_2$	0.85	99.404	46.23	3.57	1.99	4.00	3.43	4.00	13

Table A.17 (Part 3) Database of 33 hydroxide properties for all stable or metastable hydroxides with well-defined properties (i.e. excluding hydroxides with multiple cations or cations with missing ionic parameters).

Compound	SG_Hyd	MM_Ox	Vol_Ox	Dens_Ox	C-O_Ox	#CO_Ox	C-C_Ox	#CC_Ox	ST_Ox
$Al(OH)_3$	5	50.980	21.92	3.86	1.93	6.00	2.79	4.00	3
$Ba(OH)_2$	12	153.326	43.53	5.85	2.63	4.00	3.88	10.00	1
$Be(OH)_2$	6	25.011	14.11	2.94	1.66	4.00	2.71	12.00	14
$Ca(OH)_2$	7	56.077	28.09	3.32	2.41	6.00	3.41	12.00	10
$Ce(OH)_3$	10	164.115	53.60	5.08	2.41	6.00	3.21	2.00	9
$Dy(OH)_3$	10	186.499	34.60	8.95	2.25	4.00	3.66	12.00	9
$Eu(OH)_3$	10	175.963	38.24	7.64	2.37	4.00	3.61	5.00	12
$Ga(OH)_3$	3	93.731	27.98	5.56	1.89	4.00	3.26	5.00	8
$Gd(OH)_3$	10	181.249	36.97	8.14	2.33	4.00	3.50	3.00	5
$In(OH)_3$	3	138.817	32.78	7.03	2.24	6.00	3.31	3.00	11
KOH	4	47.098	34.34	2.28	2.81	4.00	3.25	6.00	7
$La(OH)_3$	9	162.904	41.81	6.47	2.40	4.00	3.90	12.00	9
LiOH	8	14.941	12.54	1.98	2.01	4.00	2.32	6.00	7
$Lu(OH)_3$	3	198.965	33.16	9.97	2.26	4.00	3.35	3.00	2
$Mg(OH)_2$	7	40.304	19.11	3.50	2.12	6.00	3.00	12.00	10
$Mn(OH)_2$	7	70.937	21.24	5.55	2.20	6.00	3.11	12.00	10
NaOH	4	30.990	21.06	2.44	2.39	4.00	2.76	6.00	7
$Nd(OH)_3$	9	168.241	38.02	7.35	2.33	4.00	3.78	12.00	9
$Ni(OH)_2$	7	74.692	18.52	6.70	2.10	6.00	2.97	12.00	10
$Pr(OH)_3$	10	164.906	38.07	7.19	2.33	4.00	3.78	12.00	9
RbOH	4	92.468	40.94	3.75	2.98	4.00	3.45	6.00	7
$Sc(OH)_3$	3	68.954	27.92	4.10	2.08	3.00	3.14	3.00	2
$Sr(OH)_2$	11	103.619	35.28	4.88	2.60	6.00	3.68	12.00	10
$Te(OH)_6$	5	175.597	48.14	6.06	1.96	6.00	3.64	6.00	6
TlOH	1	212.380	37.01	9.53	2.58	3.00	3.64	9.00	13
$Y(OH)_3$	10	112.904	35.06	5.35	2.30	4.00	3.43	3.00	2
$Zn(OH)_2$	6	81.389	24.96	5.41	2.01	4.00	3.28	12.00	14

Table A.18 (Part 4) Database of 33 hydroxide properties for all stable or metastable hydroxides with well-defined properties (i.e. excluding hydroxides with multiple cations or cations with missing ionic parameters).

Compound	SG_Ox	nDH	DH	GED	VED	Promising
$Al(OH)_3$	10	60.6	40.4	0.777	1.959	0
$Ba(OH)_2$	7	161.7	161.7	0.944	4.059	0
$Be(OH)_2$	8	24.0	24.0	0.557	1.027	0
$Ca(OH)_2$	3	103.1	103.1	1.392	3.119	0
$Ce(OH)_3$	5	137.9	91.9	0.721	3.269	0
$Dy(OH)_3$	6	108.0	72.0	0.506	2.873	0
$Eu(OH)_3$	2	75.7	50.4	0.373	1.915	0
$Ga(OH)_3$	2	62.1	41.4	0.514	1.839	0
$Gd(OH)_3$	2	105.5	70.3	0.507	2.729	0
$In(OH)_3$	9	95.5	63.7	0.576	2.333	0
KOH	3	112.7	225.4	2.008	4.091	1
$La(OH)_3$	6	125.8	83.8	0.662	2.882	0

LiOH	3	63.7	127.3	2.658	3.853	1
$Lu(OH)_3$	4	97.3	64.9	0.431	2.246	0
$Mg(OH)_2$	3	74.4	74.4	1.276	2.991	0
$Mn(OH)_2$	3	72.5	72.5	0.815	2.595	0
NaOH	3	87.6	175.1	2.189	4.604	1
$Nd(OH)_3$	6	97.7	65.2	0.501	2.398	0
$Ni(OH)_2$	3	55.2	55.2	0.595	2.308	0
$Pr(OH)_3$	6	95.5	63.7	0.498	2.313	0
RbOH	3	119.3	238.6	1.176	3.725	0
$Sc(OH)_3$	4	81.1	54.1	0.845	2.149	0
$Sr(OH)_2$	3	121.0	121.0	0.995	3.340	0
$Te(OH)_6$	10	218.4	72.8	0.951	2.867	0
TlOH	11	31.3	62.6	0.141	0.953	0
$Y(OH)_3$	4	102.9	68.6	0.735	2.760	0
$Zn(OH)_2$	8	43.4	43.4	0.437	1.559	0

Table A.19 Hydroxide structure types.

ST_Hyd	Hydroxide Structure Type
1	Al(OH)3(gibbsite)
2	Ba(OH)2(Pnma)
3	Brucite-Mg(OH)2
4	Cu(OH)2
5	In(OH)3
6	KOH
7	LaHO
8	LiOH
9	Sr(OH)2
10	Te(OH)6
11	TlOH
12	UCl3
13	Zn(OH)2

Table A.20 Hydroxide space groups.

SG_Hyd	Hydroxide Space Group
1	C 1 2 1
2	C m c 21
3	I m -3
4	P 1 21/m 1
5	P 1 21/n 1
6	P 21 21 21
7	P -3 m 1
8	P 4/n m m S
9	P 4/n m m Z
10	P 63/m
11	P n a m

12	P n m a

Table A.21 Oxide structure types.

ST_Ox	Oxide Structure Type
1	BiIn
2	Bixbyite-Mn2O3
3	Corundum-Al2O3
4	CuO(mS8)
5	Er2O3(beta)
6	FeF3
7	Fluorite-CaF2
8	Ga2O3
9	La2O3
10	NaCl
11	Rh2S3
12	Sm2O3
13	Tl2O
14	Wurtzite-ZnS(2H)

Table A.22 Oxide space groups.

SG_Ox	Oxide Space Group
1	C 1 2/c 1
2	C 1 2/m 1
3	F m -3 m
4	I a -3
5	P 3 2 1
6	P -3 m 1
7	P 4/n m m S
8	P 63 m c
9	P b c n
10	R -3 c H
11	R -3 m H

Appendix B. Computed Database of Known Hydration Reactions

Table B.1 265 screened reactions listed by salt family, number of the higher (n_{high}) and lower (n_{low}) hydrate, distance of the least stable compound to the convex hull (E_{hull}), discharging (T_{low}) and charging (T_{high}) temperature, temperature window (T_{wind}), temperature category, enthalpy of dehydration (ΔH), gravimetric energy density (GED), and volumetric energy density (VED). In the case of hydroxide reactions, a negative number indicates the oxide while 0 indicates the hydroxide. Bolded and italicized hydrate numbers indicate metastability.

Salt	n_{high}	n_{low}	E_{hull} (meV/at)	T_{low} (°C)	T_{high} (°C)	T_{wind} (°C)	Temp. Category	ΔH (kJ/mol H_2O)	GED (MJ/kg)	VED (GJ/m^3)
$BaBr_2$	2	0	0	130	174	44	100°C - 200°C	62.1	0.373	1.391
$BaBr_2$	2	1	0	130	130	0	100°C - 200°C	58.9	0.177	0.660
$BaBr_2$	1	0	0	174	174	0	100°C - 200°C	65.2	0.207	0.827
$CaBr_2$	9	0	0	144	163	19	100°C - 200°C	62.7	1.559	3.060
$CaBr_2$	9	6	0	144	144	0	100°C - 200°C	60.8	0.504	0.988
$CaBr_2$	6	0	0	163	163	0	100°C - 200°C	63.7	1.241	2.777
$CdBr_2$	4	0	0	134	134	0	100°C - 200°C	59.5	0.691	2.053
$CeBr_3$	7	0	0	169	169	0	100°C - 200°C	64.5	0.893	2.526
$CoBr_2$	4	0	15.7	-31	127	158	Wide temperature window	46.9	0.644	1.841
$CoBr_2$	4	2	15.7	-31	100	131	< 50°C	35.4	0.243	0.695
$CoBr_2$	2	0	0	127	127	0	100°C - 200°C	58.4	0.458	1.546
$CuBr_2$	4	0	0	86	100	14	50°C - 100°C	54.0	0.731	2.059
$EuBr_3$	6	0	0	151	151	0	100°C - 200°C	62.0	0.744	2.173
$FeBr_2$	4	0	0	83	100	17	50°C - 100°C	53.9	0.749	2.004
$LaBr_3$	7	0	0	170	170	0	100°C - 200°C	64.7	0.898	2.501
LiBr	1	0	0	222	222	0	200°C - 300°C	72.2	0.689	1.860
$LuBr_3$	8	0	0	213	213	0	200°C - 300°C	71.0	1.016	2.915
$MgBr_2$	9	0	0	194	269	75	200°C - 300°C	72.1	1.873	3.513
$MgBr_2$	9	1	43.5	194	441	247	Wide temperature window	74.4	1.718	3.223
$MgBr_2$	9	2	0	194	238	44	200°C - 300°C	70.1	1.417	2.658
$MgBr_2$	9	4	0	194	194	0	100°C - 200°C	68.2	0.985	1.848
$MgBr_2$	9	6	4.4	215	215	0	200°C - 300°C	71.2	0.617	1.157
$MgBr_2$	6	0	4.4	163	269	106	200°C - 300°C	72.5	1.488	3.103
$MgBr_2$	6	1	43.5	163	441	278	Wide temperature window	76.2	1.303	2.721
$MgBr_2$	6	2	4.4	163	238	75	200°C - 300°C	69.2	0.947	1.976
$MgBr_2$	6	4	4.4	163	163	0	100°C - 200°C	63.7	0.436	0.909
$MgBr_2$	4	0	0	238	269	31	200°C - 300°C	76.9	1.200	2.811

$MgBr_2$	4	1	43.5	238	441	203	300°C - 450°C	84.6	1.981	4.640
$MgBr_2$	4	2	43.5	238	238	0	200°C - 300°C	74.6	0.582	1.364
$MgBr_2$	2	0	43.5	269	269	0	200°C - 300°C	79.1	0.719	1.973
$MgBr_2$	2	1	43.5	441	441	0	300°C - 450°C	104.3	0.258	0.650
$MgBr_2$	1	0	43.5	84	100	16	50°C - 100°C	53.9	0.267	0.671
$MnBr_2$	2	0	0	125	125	0	100°C - 200°C	58.2	0.464	1.443
NaBr	2	0	0	122	122	0	100°C - 200°C	57.7	0.830	1.846
$PrBr_3$	6	0	0	201	201	0	200°C - 300°C	69.2	0.850	2.417
$PuBr_3$	6	0	0	183	183	0	100°C - 200°C	66.6	0.675	2.357
$SnBr_4$	5	0	0	142	142	0	100°C - 200°C	60.6	0.573	1.776
$SrBr_2$	1	0	0	190	190	0	100°C - 200°C	67.6	0.255	0.961
$TlBr_3$	4	0	0	190	190	0	100°C - 200°C	67.6	0.524	1.928
UBr_4	9	0	0	157	157	0	100°C - 200°C	62.8	0.786	2.453
VBr_3	6	0	0	194	194	0	100°C - 200°C	68.2	1.026	2.590
YBr_3	10	0	0	-3	193	196	Wide temperature window	64.6	1.270	2.817
YBr_3	10	8	0	-3	100	103	< 50°C	50.8	0.200	0.443
YBr_3	8	0	0	193	193	0	100°C - 200°C	68.1	1.152	2.758
$ZnBr_2$	2	0	0	157	157	0	100°C - 200°C	62.9	0.481	1.465
K_2PtBr_4	2	0	0	0	100	100	50°C - 100°C	50.8	0.162	0.594
$KAuBr_4$	2	0	16.1	-17	100	117	< 50°C	37.4	0.126	0.489
$KInBr_4$	2	0	10.6	5	100	95	50°C - 100°C	40.6	0.159	0.500
$AlCl_3$	6	0	0	364	364	0	300°C - 450°C	93.0	2.310	3.808
$BaCl_2$	2	0	0	136	136	0	100°C - 200°C	59.7	0.488	1.483
$BeCl_2$	4	0	0	325	325	0	300°C - 450°C	87.4	2.300	3.344
$BiCl_3$	1	0	0	175	175	0	100°C - 200°C	65.4	0.196	0.787
$CaCl_2$	6	0	0	80	160	80	100°C - 200°C	60.1	1.646	2.851
$CaCl_2$	6	2	10.9	80	193	113	100°C - 200°C	60.9	1.111	1.924
$CaCl_2$	6	4	10.9	80	100	20	50°C - 100°C	53.8	0.491	0.850
$CaCl_2$	4	0	10.9	160	160	0	100°C - 200°C	63.3	1.382	2.247
$CaCl_2$	4	2	10.9	193	193	0	100°C - 200°C	68.0	0.743	1.208
$CaCl_2$	2	0	10.9	128	128	0	100°C - 200°C	58.6	0.797	1.682
$CdCl_2$	4	0	0	124	124	0	100°C - 200°C	58.0	0.908	2.178
$CdCl_2$	4	1	5.7	132	132	0	100°C - 200°C	59.1	0.603	1.274
$CdCl_2$	4	2.5	10.4	172	172	0	100°C - 200°C	65.0	0.249	0.525
$CdCl_2$	2.5	0	10.4	65	102	37	50°C - 100°C	53.8	0.589	1.607
$CdCl_2$	2.5	1	10.4	65	100	35	50°C - 100°C	53.2	0.349	0.953
$CdCl_2$	1	0	5.7	102	102	0	100°C - 200°C	54.7	0.272	0.854
$CeCl_3$	7	0	1.4	24	169	145	Wide temperature window	61.6	1.157	2.630
$CeCl_3$	7	6	1.4	24	100	76	50°C - 100°C	43.3	0.116	0.264
$CeCl_3$	6	0	0	169	169	0	100°C - 200°C	64.6	1.093	2.474
$CoCl_2$	2	0	0	59	107	48	50°C - 100°C	54.3	0.654	1.652
$CoCl_2$	2	1	0	59	100	41	50°C - 100°C	53.0	0.320	0.807
$CoCl_2$	1	0	0	107	107	0	100°C - 200°C	55.5	0.375	1.052
$CrCl_2$	4	0	0	141	141	0	100°C - 200°C	60.4	1.239	2.425

$CrCl_3$	6	0	0	180	180	0	100°C - 200°C	66.2	1.490	2.680
$CuCl_2$	2	0	0	-186	100	286	< 50°C	48.0	0.563	1.390
$ErCl_3$	6	0	0	221	221	0	200°C - 300°C	72.2	1.135	2.921
$EuCl_2$	2	0	0	103	103	0	100°C - 200°C	54.9	0.424	1.534
$FeCl_2$	4	0	1.1	41	101	60	Wide temperature window	50.3	1.011	2.067
$FeCl_2$	4	2	1.1	41	100	59	50°C - 100°C	45.9	0.462	0.944
$FeCl_2$	2	0	0	101	101	0	100°C - 200°C	54.6	0.670	1.636
$FeCl_3$	6	0	0	66	141	75	100°C - 200°C	56.3	1.249	2.327
$FeCl_3$	6	2.5	0	66	100	34	50°C - 100°C	53.2	0.689	1.284
$FeCl_3$	2.5	0	0	141	141	0	100°C - 200°C	60.5	0.730	1.576
$GdCl_3$	6	0	0	212	212	0	200°C - 300°C	70.8	1.143	2.826
$InCl_3$	3	0	0	5	100	95	50°C - 100°C	51.0	0.556	1.251
$LaCl_3$	7	0	0	149	149	0	100°C - 200°C	61.6	1.161	2.602
$LaCl_3$	7	3	2.6	155	155	0	100°C - 200°C	62.4	0.672	1.506
$LaCl_3$	3	0	2.6	141	141	0	100°C - 200°C	60.5	0.606	1.672
$MgCl_2$	6	0	0	111	287	176	100°C - 200°C	67.6	1.996	3.156
$MgCl_2$	6	1	0	111	216	105	100°C - 200°C	64.8	1.593	2.519
$MgCl_2$	6	2	0	111	208	97	100°C - 200°C	63.1	1.242	1.963
$MgCl_2$	6	4	0	111	111	0	100°C - 200°C	56.1	0.552	0.873
$MgCl_2$	4	0	0	208	287	79	200°C - 300°C	73.4	1.755	2.987
$MgCl_2$	4	1	0	208	216	8	200°C - 300°C	70.6	1.267	2.156
$MgCl_2$	4	2	0	208	208	0	200°C - 300°C	70.3	0.840	1.430
$MgCl_2$	2	0	0	216	287	71	200°C - 300°C	76.6	1.167	2.233
$MgCl_2$	2	1	0	216	216	0	200°C - 300°C	71.4	0.544	1.041
$MgCl_2$	1	0	0	287	287	0	200°C - 300°C	81.7	0.722	1.462
$MnCl_2$	2	0	0	104	174	70	100°C - 200°C	60.3	0.744	1.705
$MnCl_2$	2	1	0	104	104	0	100°C - 200°C	55.1	0.340	0.780
$MnCl_2$	1	0	0	174	174	0	100°C - 200°C	65.3	0.454	1.131
$MoCl_2$	1.33	0	0	103	103	0	100°C - 200°C	54.8	0.383	1.160
NaCl	2	0	0	104	104	0	100°C - 200°C	55.1	1.165	1.954
$NiCl_2$	6	0	0	110	110	0	100°C - 200°C	56.0	1.413	2.842
$NiCl_2$	6	2	12.4	129	129	0	100°C - 200°C	58.7	0.988	1.987
$NiCl_2$	6	4	16.4	191	191	0	100°C - 200°C	67.8	0.570	1.148
$NiCl_2$	4	0	16.4	-80	100	180	< 50°C	50.1	0.993	2.238
$NiCl_2$	4	2	16.4	-80	100	180	< 50°C	49.6	0.492	1.109
$NiCl_2$	2	0	12.4	-13	100	113	< 50°C	50.6	0.611	1.595
$PrCl_3$	6	0	0	179	179	0	100°C - 200°C	66.0	1.114	2.541
$PtCl_4$	5	0	0	444	485	41	450°C - 600°C	108.9	1.275	3.649
$PtCl_4$	5	3.5	0	444	444	0	300°C - 450°C	104.7	0.368	1.052
$PtCl_4$	3.5	0	0	485	485	0	450°C - 600°C	110.7	0.969	2.976
$ReCl_3$	1.67	0	0	82	100	18	50°C - 100°C	53.8	0.278	0.843
$SmCl_3$	6	0	0	177	177	0	100°C - 200°C	65.7	1.081	2.576
$SnCl_2$	2	0	0	169	169	0	100°C - 200°C	64.5	0.572	1.569
$SnCl_2$	2	1.5	19.3	360	360	0	300°C - 450°C	92.4	0.205	0.562
$SnCl_2$	1.5	0	19.3	105	105	0	100°C - 200°C	55.2	0.382	1.159

$SnCl_4$	8	0	0	190	211	21	200°C - 300°C	69.1	1.366	2.690
$SnCl_4$	8	2	3.5	190	233	43	200°C - 300°C	69.2	0.460	1.263
$SnCl_4$	8	3	0.1	190	213	23	200°C - 300°C	68.3	0.295	0.895
$SnCl_4$	8	4	0	190	190	0	100°C - 200°C	67.5	0.668	1.315
$SnCl_4$	8	5	1.6	197	197	0	100°C - 200°C	68.6	0.254	0.501
$SnCl_4$	5	0	1.6	168	211	43	100°C - 200°C	69.4	0.990	2.246
$SnCl_4$	5	2	3.5	168	233	65	200°C - 300°C	69.8	0.414	0.816
$SnCl_4$	5	3	1.6	168	213	45	100°C - 200°C	67.8	0.386	0.877
$SnCl_4$	5	4	1.6	168	168	0	100°C - 200°C	64.4	0.184	0.417
$SnCl_4$	4	0	0	211	211	0	200°C - 300°C	70.6	0.849	1.991
$SnCl_4$	4	2	3.5	213	233	20	200°C - 300°C	72.4	0.103	0.234
$SnCl_4$	4	3	0.1	213	213	0	200°C - 300°C	70.9	0.025	0.057
$SnCl_4$	3	0	0.1	210	210	0	200°C - 300°C	70.5	0.673	1.664
$SnCl_4$	3	2	3.5	233	233	0	200°C - 300°C	73.9	0.235	0.581
$SnCl_4$	2	0	3.5	198	198	0	100°C - 200°C	68.8	0.464	1.212
$SrCl_2$	6	0	0	131	131	0	100°C - 200°C	58.9	1.326	2.605
$SrCl_2$	6	1	4.3	134	134	0	100°C - 200°C	59.4	1.114	2.188
$SrCl_2$	6	2	9.6	144	144	0	100°C - 200°C	61.0	0.914	1.796
$SrCl_2$	2	0	9.6	102	102	0	100°C - 200°C	54.8	0.563	1.513
$SrCl_2$	2	1	9.6	65	100	35	50°C - 100°C	53.2	0.273	0.735
$SrCl_2$	1	0	4.3	113	113	0	100°C - 200°C	56.4	0.319	0.915
$TlCl_3$	4	0	0	117	117	0	100°C - 200°C	56.9	0.595	1.800
UCl_3	7	0	1.8	17	171	154	Wide temperature window	61.6	0.917	2.635
UCl_3	7	6	1.8	17	100	83	50°C - 100°C	42.4	0.090	0.259
UCl_3	6	0	0	171	171	0	100°C - 200°C	64.9	0.860	2.495
VCl_3	6	0	0	191	191	0	100°C - 200°C	67.8	1.532	2.843
VCl_3	6	4	0.8	195	195	0	100°C - 200°C	68.4	0.515	0.957
VCl_3	4	0	0.8	189	189	0	100°C - 200°C	67.5	1.177	2.348
YCl_3	6	0	0	213	213	0	200°C - 300°C	70.9	1.402	2.886
$ZnCl_2$	4.5	0	0	142	142	0	100°C - 200°C	60.6	1.255	2.313
$ZnCl_2$	4.5	1.33	22.6	175	175	0	100°C - 200°C	65.4	0.952	1.755
$ZnCl_2$	4.5	2.5	13.2	188	188	0	100°C - 200°C	67.4	0.620	1.142
$ZnCl_2$	4.5	3	17.2	232	232	0	200°C - 300°C	73.8	0.509	0.938
$ZnCl_2$	3	0	17.2	86	100	14	50°C - 100°C	54.0	0.851	1.832
$ZnCl_2$	3	1.33	22.6	-186	152	338	Wide temperature window	57.8	0.506	1.090
$ZnCl_2$	3	2.5	17.2	-186	100	286	< 50°C	48.0	0.126	0.272
$ZnCl_2$	2.5	0	13.2	105	105	0	100°C - 200°C	55.2	0.762	1.736
$ZnCl_2$	2.5	1.33	22.6	152	152	0	100°C - 200°C	62.0	0.399	0.909
$ZnCl_2$	1.33	0	22.6	-111	100	211	< 50°C	49.1	0.409	1.037

K_2HgCl_4	1	0	0	295	295	0	200°C - 300°C	83.0	0.189	0.621
$KAuCl_4$	2	0	0	-130	100	230	< 50°C	48.9	0.242	0.734
$KCdCl_3$	1	0	3.0	31	100	69	50°C - 100°C	44.4	0.161	0.462
$KMnCl_3$	2	0	0	142	142	0	100°C - 200°C	60.6	0.513	1.150
Li_2ZnCl_4	2	0	0	207	207	0	200°C - 300°C	70.1	0.545	1.193
$MgCsCl_3$	6	0	0	202	202	0	200°C - 300°C	69.4	1.120	2.231
$MgRbCl_3$	6	0	0	209	209	0	200°C - 300°C	70.3	1.305	2.407
Na_2ZnCl_4	3	0	0	128	128	0	100°C - 200°C	58.6	0.572	1.212
$NaHgCl_3$	2	0	0	203	203	0	200°C - 300°C	69.6	0.380	1.299
AlF_3	9	0	0	103	103	0	100°C - 200°C	54.9	2.009	3.144
AlF_3	9	1	31.2	121	121	0	100°C - 200°C	57.5	1.870	2.927
AlF_3	9	3	17.9	129	129	0	100°C - 200°C	58.7	1.430	2.238
AlF_3	3	0	17.9	-224	100	324	< 50°C	47.4	1.031	2.176
AlF_3	3	1	31.2	92	100	8	50°C - 100°C	54.2	0.785	1.657
AlF_3	1	0	31.2	-41	100	141	< 50°C	33.8	0.331	0.823
CrF_3	9	0	0	205	205	0	200°C - 300°C	69.7	2.315	3.746
CrF_3	9	3	5.1	212	212	0	200°C - 300°C	70.8	1.566	2.534
CrF_3	9	5	41.3	335	335	0	300°C - 450°C	88.7	1.309	2.118
CrF_3	5	0	41.3	-34	190	224	Wide temperature window	54.5	1.370	2.912
CrF_3	5	3	41.3	-34	100	134	< 50°C	34.9	0.350	0.744
CrF_3	3	0	5.1	190	190	0	100°C - 200°C	67.6	1.243	2.918
CuF_2	2	0	0	167	167	0	100°C - 200°C	64.2	0.933	2.765
FeF_3	3	0	0	282	282	0	200°C - 300°C	81.0	1.455	3.313
HfF_4	3	0	0	189	189	0	100°C - 200°C	67.4	0.656	2.579
HgF_2	2	0	0	214	214	0	200°C - 300°C	71.1	0.517	2.882
InF_3	3	0	0	209	209	0	200°C - 300°C	70.4	0.935	2.597
KF	4	0	0	152	241	89	100°C - 200°C	68.5	2.106	3.057
KF	4	2	0	152	152	0	100°C - 200°C	62.1	0.953	1.384
KF	2	0	0	241	241	0	200°C - 300°C	75.0	1.594	2.643
RbF	1	0	0	345	345	0	300°C - 450°C	90.2	0.736	2.080
UF_4	2	0	18.2	-19	100	119	< 50°C	37.1	0.212	1.006
VF_3	3	0	0	175	182	7	100°C - 200°C	66.1	1.224	2.700
VF_3	3	2	0	175	175	0	100°C - 200°C	65.4	0.404	0.891
VF_3	2	0	0	182	182	0	100°C - 200°C	66.4	0.922	2.359
ZnF_2	4	0	0	171	171	0	100°C - 200°C	64.8	1.478	3.415
ZnF_2	4	2	33.2	269	269	0	200°C - 300°C	79.2	0.903	2.086
ZnF_2	2	0	33.2	-26	100	126	< 50°C	50.4	0.723	2.052
ZrF_4	3	0	0	190	190	0	100°C - 200°C	67.5	0.916	2.510

Ca_2AlF_7	1	0	0.2	45	100	55	50°C - 100°C	46.4	0.180	0.520
K_2FeF_5	1	0	33.2	-194	100	294	< 50°C	11.5	0.047	0.138
$KAlF_4$	0.33	0	0	193	193	0	100°C - 200°C	68.1	0.153	0.391
$KSnF_3$	0.5	0	0	70	100	30	50°C - 100°C	53.4	0.119	0.393
Li_2TiF_6	2	0	0	-50	100	150	< 50°C	50.1	0.473	1.201
$LiMnF_4$	1	0	0	103	103	0	100°C - 200°C	54.9	0.352	1.015
$NaNiF_3$	3	0	0	195	195	0	100°C - 200°C	68.3	1.064	2.742
$Al(OH)_3$	0	-1.5	14.0	4	100	96	50°C - 100°C	40.4	0.777	1.958
$Ba(OH)_2$	3	-1	0	206	835	629	Wide temperature window	95.8	1.699	4.863
$Ba(OH)_2$	3	0	0	206	284	78	200°C - 300°C	73.8	0.983	2.813
$Ba(OH)_2$	3	1	0	206	206	0	200°C - 300°C	70.0	0.621	1.778
$Ba(OH)_2$	1	-1	0	284	835	551	Wide temperature window	121.5	1.283	4.541
$Ba(OH)_2$	1	0	0	284	284	0	200°C - 300°C	81.3	0.429	1.519
$Ba(OH)_2$	0	-1	0	835	835	0	> 600°C	161.7	0.944	4.059
$Be(OH)_2$	0	-1	47.1	-109	100	209	< 50°C	24.0	0.558	1.028
$Ca(OH)_2$	0	-1	0	433	433	0	300°C - 450°C	103.1	1.392	3.119
$CaPb(OH)_6$	0	-3	0	170	170	0	100°C - 200°C	64.7	0.555	2.172
$CaPt(OH)_6$	0	-3	29.2	-43	100	143	< 50°C	33.5	0.298	1.178
$CaSn(OH)_6$	0	-3	0	187	187	0	100°C - 200°C	67.1	0.772	2.408
$Ce(OH)_3$	0	-1.5	0	357	357	0	300°C - 450°C	91.9	0.721	3.269
$Dy(OH)_3$	0	-1.5	0	220	220	0	200°C - 300°C	72.0	0.506	2.874
$Eu(OH)_3$	0	-1.5	0	-22	100	122	< 50°C	50.5	0.373	1.916
$Ga(OH)_3$	0	-1.5	11.8	11	100	89	50°C - 100°C	41.4	0.514	1.841
$Gd(OH)_3$	0	-1.5	0	209	209	0	200°C - 300°C	70.3	0.507	2.729
$In(OH)_3$	0	-1.5	0	163	163	0	100°C - 200°C	63.7	0.576	2.333
$K_2Pb(OH)_6$	0	-3	0	346	346	0	300°C - 450°C	90.4	0.700	2.645

$K_2Sn(OH)_6$	0	-3	0	53	100	47	50°C - 100°C	52.8	0.530	1.118
KOH	2	-0.5	0	148	1271	1123	Wide temperature window	109.3	2.966	5.094
KOH	2	0	0	148	406	258	Wide temperature window	80.3	1.743	2.993
KOH	2	1	0	148	148	0	100°C - 200°C	61.5	0.668	1.146
KOH	1	-0.5	0	406	1271	865	Wide temperature window	141.2	2.858	5.471
KOH	1	0	0	406	406	0	300°C - 450°C	99.1	1.337	2.560
KOH	0	-0.5	0	1271	1271	0	> 600°C	225.4	2.009	4.092
$La(OH)_3$	0	-1.5	0	301	301	0	300°C - 450°C	83.9	0.662	2.883
$Li_2Sn(OH)_6$	2	-3	0	112	112	0	100°C - 200°C	56.2	1.039	2.566
$Li_2Sn(OH)_6$	2	0	43.4	327	327	0	300°C - 450°C	87.6	0.647	1.598
$Li_2Sn(OH)_6$	0	-3	43.4	-31	100	131	< 50°C	35.3	0.451	1.250
LiOH	1	-0.5	0	207	600	393	Wide temperature window	89.2	3.189	4.784
LiOH	1	0	0	207	207	0	200°C - 300°C	70.1	1.671	2.506
LiOH	0	-0.5	0	600	600	0	450°C - 600°C	127.4	2.660	3.856
$Lu(OH)_3$	0	-1.5	0	171	171	0	100°C - 200°C	64.9	0.431	2.246
$Mg(OH)_2$	0	-1	0	237	237	0	200°C - 300°C	74.4	1.276	2.990
$Mn(OH)_2$	0	-1	0	224	224	0	200°C - 300°C	72.5	0.815	2.597
$Na_2Cu(OH)_4$	0	-2	0	416	416	0	300°C - 450°C	100.7	1.134	3.307
$Na_2Pt(OH)_6$	0	-3	0	215	215	0	200°C - 300°C	71.3	0.623	2.606
NaOH	7	-0.5	0	137	927	790	Wide temperature window	71.1	3.213	4.364
NaOH	7	0	0	137	240	103	100°C - 200°C	63.7	2.683	3.645
NaOH	7	1	0	137	170	33	100°C - 200°C	61.8	2.232	3.033
NaOH	7	3.5	0	137	137	0	100°C - 200°C	59.8	1.261	1.713
NaOH	3.5	-0.5	0	170	927	757	Wide temperature window	81.1	3.146	4.785
NaOH	3.5	0	0	170	240	70	200°C - 300°C	67.7	2.298	3.495

NaOH	3.5	1	0	170	170	0	100°C - 200°C	64.7	1.569	2.387
NaOH	1	-0.5	0	240	927	687	Wide temperature window	108.3	2.801	5.102
NaOH	1	0	0	240	240	0	200°C - 300°C	74.9	1.291	2.352
NaOH	0	-0.5	0	927	927	0	> 600°C	175.2	2.189	4.604
$Nd(OH)_3$	0	-1.5	0	173	173	0	100°C - 200°C	65.1	0.500	2.397
$Ni(OH)_2$	0	-1	0	105	105	0	100°C - 200°C	55.2	0.595	2.309
$Pr(OH)_3$	0	-1.5	0	163	163	0	100°C - 200°C	63.7	0.498	2.312
RbOH	1	-0.5	0	428	1361	933	Wide temperature window	147.7	1.855	5.136
RbOH	1	0	0	428	428	0	300°C - 450°C	102.3	0.856	2.371
RbOH	0	-0.5	0	1361	1361	0	> 600°C	238.6	1.176	3.725
$Sc(OH)_3$	0	-1.5	0	88	100	12	50°C - 100°C	54.1	0.845	2.149
$Sr(OH)_2$	8	-1	0	176	556	380	Wide temperature window	71.7	2.428	4.572
$Sr(OH)_2$	8	0	0	176	176	0	100°C - 200°C	65.5	1.973	3.715
$Sr(OH)_2$	8	1	1.8	177	177	0	100°C - 200°C	65.8	1.732	3.262
$Sr(OH)_2$	1	-1	1.8	165	556	391	Wide temperature window	92.5	1.325	3.975
$Sr(OH)_2$	1	0	1.8	165	165	0	100°C - 200°C	64.0	0.458	1.375
$Sr(OH)_2$	0	-1	0	556	556	0	450°C - 600°C	121.0	0.995	3.341
$Te(OH)_6$	0	-3	0	226	226	0	200°C - 300°C	72.8	0.951	2.867
TlOH	0	-0.5	0	156	156	0	100°C - 200°C	62.6	0.141	0.953
$Y(OH)_3$	0	-1.5	0	197	197	0	100°C - 200°C	68.6	0.735	2.761
$Zn(OH)_2$	0	-1	6.8	24	100	76	50°C - 100°C	43.4	0.437	1.559

Table B.2 23 unstable compounds listed by their distance to the convex hull (E_{hull}) and calculated enthalpy of dehydration to the dehydrated compound (ΔH).

Compound	E_{hull} (meV/atom)	ΔH (kJ/mol H2O)
$CoBr_2•6H_2O$	523.4	-126.2
$MnBr_2•4H_2O$	137.4	2.7
$ScBr_3•7H_2O$	774.9	-220.3
$SrBr_2•6H_2O$	906.9	-256.1
$BaCl_2•H_2O$	634.5	-307.6
$CoCl_2•6H_2O$	65.9	27.0
$CoCl_2•4H_2O$	114.6	9.0

$LiCl•H_2O$	849.7	-363.2
$MnCl_2•4H_2O$	124.4	8.5
$NdCl_3•6H_2O$	1442.9	-463.8
$ScCl_3•7H_2O$	353.1	-75.0
$MnF_3•3H_2O$	127.5	-6.6
$ZrF_4•H_2O$	65.0	17.3
$K_2AlF_5•H_2O$	544.2	-530.9
$Ba(OH)_2•8H_2O$	1020.0	-248.6
$Cd(OH)_2$	295.2	-95.7
$Co(OH)_2$	56.2	19.6
$Cu(OH)_2$	67.8	14.0
$KOH•4H_2O$	129.1	40.0
$NaOH•4H_2O$	724.2	-154.2
$Na_2Zn(OH)_4$	292.8	-108.7
$NaZn(OH)_3•3H_2O$	397.4	-98.2
$NaZn(OH)_3$	232.2	-72.8

Appendix C. Computed Database of Hypothetical Halide Salt Hydration Reactions

Table C.1 238 hypothetical (de)hydration reactions that are predicted to lie on the convex hull are characterized by the number of water molecules per formula unit in the dehydrated (n_{low}) and hydrated (n_{high}) states, volumetric (VED) and gravimetric (GED) energy densities, maximum distance to the convex hull (E_{hull}), whether the hydrate contains an expensive metal, minimum ($T_{turn,min}$) and maximum ($T_{turn,max}$) turning temperatures of the (de)hydration reaction(s), and temperature category. Reactions are ordered by descending $ED_{RMS} = \sqrt{VED^2 + GED^2}$.

Salt	n_{low}	n_{high}	VED (GJ/m^3)	GED (MJ/kg)	E_{hull} (meV/at)	Expensive Metal	$T_{turn,min}$ (°C)	$T_{turn,max}$ (°C)	Temp. Categ.
CoF3	0	9	4.397	2.498	0.0	No	256	256	200°C - 300°C
BeCl2	0	4	3.816	2.508	0.0	Yes	380	380	300°C - 450°C
AlCl3	0	9	3.714	2.585	0.0	No	202	361	200°C - 300°C
AlCl3	0	6	3.833	2.302	0.0	No	361	361	300°C - 450°C
CrF3	0	9	3.765	2.311	0.0	No	204	204	200°C - 300°C
MgCl2	0	12	3.392	2.701	0.0	No	194	288	200°C - 300°C
AlF3	0	9	3.537	2.349	0.0	No	156	190	100°C - 200°C
VF2	0	12	3.522	2.364	0.0	No	139	139	100°C - 200°C
ZnF2	0	12	3.533	2.249	0.0	No	119	174	100°C - 200°C
GeF4	0	5	3.789	1.782	0.0	Yes	223	440	300°C - 450°C
MoF3	0	9	3.662	2.019	0.0	No	211	211	200°C - 300°C
MgF2	0	12	3.375	2.459	0.0	No	118	118	100°C - 200°C
NiF2	0	4	3.759	1.640	0.0	No	201	201	200°C - 300°C
BeBr2	0	4	3.681	1.688	0.0	Yes	423	423	300°C - 450°C
AlBr3	0	9	3.524	1.813	0.0	No	183	387	Wide Temp. Window
MgBr2	0	12	3.290	2.153	0.0	No	200	257	200°C - 300°C
MgCl2	1	12	3.062	2.438	0.0	No	194	245	200°C - 300°C
AlBr3	0	6	3.564	1.542	0.0	No	387	387	300°C - 450°C
SnF4	0	8	3.482	1.700	0.0	No	124	354	Wide Temp. Window
GaF3	0	9	3.301	1.906	0.0	Yes	105	166	100°C - 200°C
TiF4	0	8	3.219	1.993	0.0	No	121	222	100°C - 200°C
CaCl2	0	12	2.944	2.375	0.0	No	169	187	100°C - 200°C
ZnF2	0	4	3.433	1.487	0.0	No	174	174	100°C - 200°C
BeI2	0	8	3.377	1.574	0.0	Yes	99	452	Wide Temp. Window
NaF1	0	4	3.103	2.019	0.0	No	121	121	100°C - 200°C
CaF2	0	12	2.971	2.205	0.0	No	97	97	50°C - 100°C
MgI2	0	9	3.365	1.525	0.0	No	209	274	200°C - 300°C
SnF4	0	5	3.371	1.413	0.0	No	227	354	200°C - 300°C
ScCl3	0	9	2.935	2.081	0.0	Yes	215	240	200°C - 300°C
ZnCl2	0	12	2.926	2.047	0.0	No	139	139	100°C - 200°C
BeI2	0	4	3.336	1.265	0.0	Yes	452	452	450°C - 600°C
ScF3	0	9	2.970	1.976	0.0	Yes	124	124	100°C - 200°C
MgI2	0	12	3.077	1.773	0.0	No	195	274	200°C - 300°C
MgCl2	2	12	2.757	2.196	0.0	No	194	202	100°C - 200°C

TiF4	0	5	3.058	1.689	0.0	No	222	222	200°C - 300°C
CaCl2	1	12	2.689	2.170	0.0	No	169	170	100°C - 200°C
KF1	0	4	2.834	1.971	0.0	No	157	176	100°C - 200°C
GeF4	0	2	3.254	1.127	0.0	Yes	440	440	300°C - 450°C
GaCl3	0	9	2.911	1.822	0.0	Yes	187	267	200°C - 300°C
CaBr2	0	12	2.844	1.924	0.0	No	178	245	200°C - 300°C
CrCl3	0	9	2.861	1.897	0.0	No	190	190	100°C - 200°C
MgCl2	0	4	2.875	1.770	0.0	No	202	288	200°C - 300°C
AlI3	0	9	3.103	1.322	0.0	No	142	379	Wide Temp. Window
RbF1	0	4	2.923	1.586	0.0	Yes	155	344	Wide Temp. Window
SrCl2	0	12	2.662	1.957	0.0	No	140	172	100°C - 200°C
AlF3	0	3	2.932	1.468	0.0	No	190	190	100°C - 200°C
ScCl3	0	6	2.798	1.690	0.0	Yes	215	240	200°C - 300°C
MnCl4	0	8	2.833	1.615	0.0	No	187	256	200°C - 300°C
ZnBr2	0	12	2.804	1.654	0.0	No	144	144	100°C - 200°C
AlI3	0	6	3.034	1.108	0.0	No	379	379	300°C - 450°C
YCl3	0	6	2.887	1.406	0.0	Yes	214	214	200°C - 300°C
ZrF4	0	8	2.805	1.542	0.0	Yes	108	189	100°C - 200°C
CoBr2	0	12	2.743	1.633	0.0	No	132	132	100°C - 200°C
HfF4	0	8	2.906	1.245	0.0	Yes	119	196	100°C - 200°C
YF3	0	9	2.695	1.647	0.0	Yes	113	113	100°C - 200°C
YCl3	0	9	2.619	1.737	0.0	Yes	171	214	100°C - 200°C
ScBr3	0	9	2.763	1.468	0.0	Yes	193	243	200°C - 300°C
CaBr2	1	12	2.575	1.743	0.0	No	178	179	100°C - 200°C
VCl4	0	8	2.679	1.556	0.0	No	176	176	100°C - 200°C
CaI2	0	12	2.657	1.581	0.0	No	181	219	200°C - 300°C
VF3	0	3	2.822	1.259	0.0	No	193	193	100°C - 200°C
SrBr2	0	12	2.586	1.635	0.0	No	153	191	100°C - 200°C
MgBr2	0	4	2.803	1.208	0.0	No	257	257	200°C - 300°C
SnCl4	0	8	2.723	1.368	0.0	No	196	204	200°C - 300°C
LiCl1	0	2	2.578	1.599	0.0	No	140	173	100°C - 200°C
GaCl3	1	9	2.539	1.589	0.0	Yes	187	187	100°C - 200°C
CrBr3	0	9	2.600	1.294	0.0	No	174	174	100°C - 200°C
BaCl2	0	12	2.389	1.620	0.0	No	113	152	100°C - 200°C
ZnI2	0	12	2.544	1.336	0.0	No	135	135	100°C - 200°C
BeF2	0	2	2.485	1.430	0.0	Yes	134	134	100°C - 200°C
YBr3	0	6	2.675	1.002	0.0	Yes	227	227	200°C - 300°C
ScBr3	0	6	2.593	1.151	0.0	Yes	243	243	200°C - 300°C
PbCl2	0	12	2.478	1.378	0.0	No	106	144	100°C - 200°C
GaBr3	0	9	2.555	1.227	0.0	Yes	151	225	100°C - 200°C
CaBr2	2	12	2.341	1.584	0.0	No	178	178	100°C - 200°C
MgCl2	4	12	2.198	1.750	0.0	No	194	194	100°C - 200°C
MnI2	0	9	2.568	1.120	0.0	No	128	128	100°C - 200°C
YI3	0	9	2.612	1.001	0.0	Yes	100	234	Wide Temp. Window
SrI2	0	12	2.433	1.379	0.0	No	160	187	100°C - 200°C
YBr3	0	9	2.468	1.284	0.0	Yes	166	227	100°C - 200°C
HfF4	0	5	2.604	0.929	0.0	Yes	119	196	100°C - 200°C
PbCl4	0	8	2.545	1.077	0.0	No	182	182	100°C - 200°C

LiBr1	0	2	2.524	1.126	0.0	No	180	222	200°C - 300°C
SnF4	0	2	2.641	0.794	0.0	No	354	354	300°C - 450°C
AlF3	3	9	2.297	1.526	0.0	No	156	156	100°C - 200°C
CuCl2	0	4	2.463	1.183	0.0	No	145	145	100°C - 200°C
ScI3	0	9	2.486	1.111	0.0	Yes	170	251	200°C - 300°C
SrCl2	2	12	2.191	1.611	0.0	No	140	140	100°C - 200°C
RbF1	0	2	2.485	1.103	0.0	Yes	171	344	Wide Temp. Window
KF1	0	2	2.301	1.393	0.0	No	176	176	100°C - 200°C
BaBr2	0	12	2.310	1.369	0.0	No	122	172	100°C - 200°C
LaCl3	0	6	2.450	1.098	0.0	No	170	170	100°C - 200°C
YI3	0	8	2.503	0.941	0.0	Yes	181	234	200°C - 300°C
ZrF4	0	3	2.509	0.915	0.0	Yes	189	189	100°C - 200°C
ZnF2	4	12	2.250	1.433	0.0	No	119	119	100°C - 200°C
HfF4	0	3	2.581	0.666	0.0	Yes	196	196	100°C - 200°C
GaF3	3	9	2.308	1.333	0.0	Yes	166	166	100°C - 200°C
MgI2	0	4	2.486	0.912	0.0	No	274	274	200°C - 300°C
SnF4	2	8	2.375	1.160	0.0	No	124	227	100°C - 200°C
CaCl2	0	4	2.177	1.427	0.0	No	170	187	100°C - 200°C
VBr4	0	8	2.390	0.973	0.0	No	156	156	100°C - 200°C
SrI2	1	12	2.221	1.258	0.0	No	160	171	100°C - 200°C
YI3	0	7	2.402	0.858	0.0	Yes	189	234	200°C - 300°C
CaI2	2	12	2.184	1.300	0.0	No	181	181	100°C - 200°C
LaI3	0	9	2.375	0.884	0.0	No	141	208	100°C - 200°C
MgBr2	4	12	2.108	1.379	0.0	No	200	200	100°C - 200°C
SrBr2	2	12	2.124	1.343	0.0	No	153	153	100°C - 200°C
LaBr3	0	8	2.324	0.952	0.0	No	32	194	Wide Temp. Window
CaCl2	4	12	1.954	1.576	0.0	No	169	169	100°C - 200°C
SrI2	0	6	2.352	0.866	0.0	No	167	187	100°C - 200°C
KCl1	0	4	2.000	1.509	0.0	No	106	106	100°C - 200°C
MgCl2	0	2	2.186	1.200	0.0	No	245	288	200°C - 300°C
BaI2	0	12	2.190	1.180	0.0	No	125	226	100°C - 200°C
LaBr3	0	6	2.339	0.840	0.0	No	194	194	100°C - 200°C
GaF3	0	3	2.308	0.916	0.0	Yes	105	105	100°C - 200°C
YI3	0	6	2.356	0.768	0.0	Yes	234	234	200°C - 300°C
ScI3	0	6	2.312	0.860	0.0	Yes	251	251	200°C - 300°C
MnCl4	2	8	2.142	1.221	0.0	No	191	256	200°C - 300°C
SnCl4	0	5	2.247	0.993	0.0	No	204	204	200°C - 300°C
MgCl2	1	4	2.080	1.281	0.0	No	202	245	200°C - 300°C
BaBr2	1	12	2.097	1.243	0.0	No	122	146	100°C - 200°C
LiI1	0	2	2.268	0.855	0.0	No	225	225	200°C - 300°C
BaCl2	2	12	1.958	1.328	0.0	No	113	113	100°C - 200°C
ScCl3	3	9	1.924	1.364	0.0	Yes	215	216	200°C - 300°C
CrI3	0	9	2.171	0.904	0.0	No	136	136	100°C - 200°C
PbCl2	2	12	2.035	1.131	0.0	No	106	127	100°C - 200°C
SrI2	2	12	2.015	1.142	0.0	No	160	167	100°C - 200°C
NaCl1	0	2	1.949	1.172	0.0	No	106	106	100°C - 200°C
SnCl2	0	4	2.059	0.943	0.0	No	129	169	100°C - 200°C
MgI2	4	12	1.956	1.127	0.0	No	195	209	200°C - 300°C

RbF1	1	4	1.982	1.075	0.0	Yes	155	171	100°C - 200°C
BaI2	1	12	1.967	1.060	0.0	No	125	135	100°C - 200°C
ScCl3	0	3	1.948	1.095	0.0	Yes	240	240	200°C - 300°C
CuBr2	0	4	2.093	0.753	0.0	No	108	108	100°C - 200°C
GaI3	0	9	2.052	0.838	0.0	Yes	118	118	100°C - 200°C
RbF1	0	1	2.085	0.736	0.0	Yes	344	344	300°C - 450°C
LaI3	0	6	2.099	0.671	0.0	No	208	208	200°C - 300°C
BaBr2	2	12	1.895	1.124	0.0	No	122	122	100°C - 200°C
RbCl1	0	4	1.866	1.147	0.0	Yes	106	106	100°C - 200°C
LiCl1	0	1	1.904	1.078	0.0	No	173	173	100°C - 200°C
GeBr2	0	4	2.016	0.787	0.0	Yes	137	137	100°C - 200°C
KBr1	0	4	1.846	1.126	0.0	No	95	95	50°C - 100°C
BaI2	0	6	2.029	0.730	0.0	No	125	226	100°C - 200°C
GeF4	2	5	1.935	0.910	0.0	Yes	223	223	200°C - 300°C
CsF1	0	2	1.993	0.735	0.0	Yes	151	249	100°C - 200°C
GaBr3	2	9	1.912	0.918	0.0	Yes	151	151	100°C - 200°C
PbCl2	0	4	1.991	0.681	0.0	No	127	144	100°C - 200°C
PbF2	0	2	2.061	0.403	0.0	No	115	115	100°C - 200°C
SrI2	1	6	1.946	0.716	0.0	No	167	171	100°C - 200°C
BaI2	2	12	1.785	0.962	0.0	No	125	129	100°C - 200°C
NaBr1	0	2	1.831	0.838	0.0	No	126	126	100°C - 200°C
MnCl4	3	8	1.744	0.994	0.0	No	191	191	100°C - 200°C
BaF2	0	2	1.914	0.583	0.0	No	149	149	100°C - 200°C
MnCl4	0	3	1.809	0.844	0.0	No	187	256	200°C - 300°C
SnF4	2	5	1.836	0.770	0.0	No	227	227	200°C - 300°C
LiBr1	0	1	1.859	0.689	0.0	No	222	222	200°C - 300°C
SnBr2	0	4	1.863	0.671	0.0	No	120	139	100°C - 200°C
PbBr2	0	4	1.871	0.549	0.0	No	140	140	100°C - 200°C
SnF2	0	2	1.848	0.588	0.0	No	115	115	100°C - 200°C
MgI2	4	9	1.765	0.799	0.0	No	209	209	200°C - 300°C
CaCl2	1	4	1.618	1.061	0.0	No	170	170	100°C - 200°C
SnBr4	0	5	1.778	0.575	0.0	No	143	143	100°C - 200°C
ZrF4	3	8	1.623	0.892	0.0	Yes	108	108	100°C - 200°C
HfF4	3	8	1.702	0.729	0.0	Yes	119	129	100°C - 200°C
PbCl2	4	12	1.610	0.895	0.0	No	106	106	100°C - 200°C
SrCl2	0	2	1.710	0.667	0.0	No	172	172	100°C - 200°C
NaI1	0	2	1.668	0.658	0.0	No	146	146	100°C - 200°C
BaI2	1	6	1.624	0.584	0.0	No	125	135	100°C - 200°C
KF1	2	4	1.386	0.964	0.0	No	157	157	100°C - 200°C
SnCl2	0	2	1.579	0.573	0.0	No	169	169	100°C - 200°C
SrBr2	0	2	1.593	0.478	0.0	No	191	191	100°C - 200°C
SrI2	2	6	1.554	0.572	0.0	No	167	167	100°C - 200°C
CaBr2	0	2	1.529	0.601	0.0	No	179	245	200°C - 300°C
MgCl2	0	1	1.464	0.723	0.0	No	288	288	200°C - 300°C
SnI2	0	4	1.552	0.492	0.0	No	102	102	100°C - 200°C
CsF1	0	1	1.556	0.449	0.0	Yes	249	249	200°C - 300°C
ScCl3	3	6	1.363	0.823	0.0	Yes	215	215	200°C - 300°C
MgCl2	2	4	1.346	0.829	0.0	No	202	202	200°C - 300°C

BaCl2	0	2	1.458	0.508	0.0	No	152	152	100°C - 200°C
PbCl2	0	2	1.461	0.387	0.0	No	144	144	100°C - 200°C
RbF1	2	4	1.305	0.708	0.0	Yes	155	155	100°C - 200°C
LiCl1	1	2	1.239	0.769	0.0	No	140	140	100°C - 200°C
MnCl4	0	2	1.318	0.577	0.0	No	187	187	100°C - 200°C
BaBr2	0	2	1.338	0.379	0.0	No	146	172	100°C - 200°C
SnBr2	0	2	1.329	0.383	0.0	No	139	139	100°C - 200°C
SrI2	6	12	1.201	0.681	0.0	No	160	160	100°C - 200°C
BaI2	2	6	1.292	0.465	0.0	No	125	125	100°C - 200°C
SrI2	0	2	1.296	0.350	0.0	No	171	187	100°C - 200°C
GaBr3	0	2	1.255	0.421	0.0	Yes	225	225	200°C - 300°C
LiBr1	1	2	1.206	0.538	0.0	No	180	180	100°C - 200°C
BaI2	0	2	1.277	0.310	0.0	No	135	226	100°C - 200°C
CaI2	0	2	1.231	0.436	0.0	No	219	219	200°C - 300°C
BeI2	4	8	1.144	0.533	0.0	Yes	99	99	50°C - 100°C
AlCl3	6	9	1.013	0.705	0.0	No	202	202	200°C - 300°C
TiF4	5	8	1.041	0.645	0.0	No	121	121	100°C - 200°C
GeCl2	2	4	1.081	0.571	0.0	Yes	149	149	100°C - 200°C
BaI2	6	12	1.076	0.580	0.0	No	129	129	100°C - 200°C
MnCl2	0	1	1.131	0.454	0.0	No	174	174	100°C - 200°C
MgCl2	1	2	1.049	0.576	0.0	No	245	245	200°C - 300°C
ScCl3	6	9	0.963	0.683	0.0	Yes	216	216	200°C - 300°C
SnF4	5	8	1.050	0.513	0.0	No	124	124	100°C - 200°C
RbF1	1	2	1.040	0.462	0.0	Yes	171	171	100°C - 200°C
SnCl4	5	8	1.010	0.508	0.0	No	196	196	100°C - 200°C
HfF4	5	8	1.031	0.442	0.0	Yes	129	129	100°C - 200°C
CaCl2	0	1	0.983	0.521	0.0	No	187	187	100°C - 200°C
VCl3	6	9	0.919	0.619	0.0	No	179	179	100°C - 200°C
SnCl2	2	4	0.980	0.449	0.0	No	129	129	100°C - 200°C
CaBr2	0	1	0.975	0.347	0.0	No	245	245	200°C - 300°C
PbCl2	2	4	0.975	0.333	0.0	No	127	127	100°C - 200°C
AlBr3	6	9	0.906	0.466	0.0	No	183	183	100°C - 200°C
NiCl2	0	1	0.959	0.337	0.0	No	67	67	50°C - 100°C
GaCl3	0	1	0.922	0.406	0.0	Yes	267	267	200°C - 300°C
HfF4	3	5	0.932	0.332	0.0	Yes	119	119	100°C - 200°C
YCl3	6	9	0.820	0.544	0.0	Yes	171	171	100°C - 200°C
ScBr3	6	9	0.859	0.456	0.0	Yes	193	193	100°C - 200°C
SnBr2	2	4	0.910	0.328	0.0	No	120	120	100°C - 200°C
CsF1	1	2	0.893	0.329	0.0	Yes	151	151	100°C - 200°C
YBr3	6	9	0.754	0.392	0.0	Yes	166	166	100°C - 200°C
BaBr2	0	1	0.823	0.206	0.0	No	172	172	100°C - 200°C
YI3	6	9	0.777	0.298	0.0	Yes	100	189	100°C - 200°C
MgI2	9	12	0.720	0.415	0.0	No	195	195	100°C - 200°C
SrI2	0	1	0.793	0.187	0.0	No	187	187	100°C - 200°C
AlI3	6	9	0.749	0.319	0.0	No	142	142	100°C - 200°C
ScI3	6	9	0.738	0.330	0.0	Yes	170	170	100°C - 200°C
BaI2	0	1	0.780	0.178	0.0	No	226	226	200°C - 300°C
CaBr2	1	2	0.713	0.280	0.0	No	179	179	100°C - 200°C

LaI3	6	9	0.715	0.266	0.0	No	141	141	100°C - 200°C
VI3	6	9	0.675	0.287	0.0	No	116	116	100°C - 200°C
MnCl4	2	3	0.660	0.308	0.0	No	256	256	200°C - 300°C
BaBr2	1	2	0.650	0.184	0.0	No	146	146	100°C - 200°C
SrI2	1	2	0.637	0.172	0.0	No	171	171	100°C - 200°C
YI3	6	8	0.579	0.218	0.0	Yes	181	189	100°C - 200°C
BaI2	1	2	0.574	0.139	0.0	No	135	135	100°C - 200°C
YI3	7	9	0.499	0.191	0.0	Yes	100	181	100°C - 200°C
LaBr3	6	8	0.416	0.170	0.0	No	32	32	< 50°C
YI3	6	7	0.317	0.113	0.0	Yes	189	189	100°C - 200°C
YI3	7	8	0.287	0.108	0.0	Yes	181	181	100°C - 200°C
YI3	8	9	0.225	0.086	0.0	Yes	100	100	50°C - 100°C

Table C.2 742 hypothetical (de)hydration reactions that are predicted to lie within 10 meV/atom of the convex hull are characterized by the number of water molecules per formula unit in the dehydrated (n_{low}) and hydrated (n_{high}) states, volumetric (VED) and gravimetric (GED) energy densities, maximum distance to the convex hull (E_{hull}), whether the hydrate contains an expensive metal, minimum ($T_{turn,min}$) and maximum ($T_{turn,max}$) turning temperatures of the (de)hydration reaction(s), and temperature category. Reactions are ordered by descending $ED_{RMS} = \sqrt{VED^2 + GED^2}$.

Salt	n_{low}	n_{high}	VED (GJ/m^3)	GED (MJ/kg)	E_{hull} (meV/at)	Expensive Metal	$T_{turn,min}$ (°C)	$T_{turn,max}$ (°C)	Temp. Categ.
CoF3	0	9	4.397	2.498	0.0	No	256	256	200°C - 300°C
BeCl2	0	4	3.816	2.508	0.0	Yes	380	380	300°C - 450°C
AlCl3	0	9	3.714	2.585	0.0	No	202	361	200°C - 300°C
AlCl3	0	6	3.833	2.302	0.0	No	361	361	300°C - 450°C
CrF3	0	9	3.765	2.311	0.0	No	204	204	200°C - 300°C
NiF2	0	12	3.716	2.367	9.4	No	124	201	100°C - 200°C
MgCl2	0	12	3.392	2.701	0.0	No	168	288	200°C - 300°C
MgCl2	0	9	3.560	2.401	7.5	No	168	288	200°C - 300°C
GeF4	0	8	3.738	2.025	1.9	Yes	110	440	Wide Temp. Window
AlF3	0	9	3.537	2.349	0.0	No	156	234	100°C - 200°C
VF2	0	12	3.522	2.364	0.0	No	139	139	100°C - 200°C
ZnF2	0	12	3.533	2.249	0.0	No	119	192	100°C - 200°C
GeF4	0	5	3.789	1.782	0.0	Yes	183	440	Wide Temp. Window
MoF3	0	9	3.662	2.019	0.0	No	211	211	200°C - 300°C
MgF2	0	12	3.375	2.459	0.0	No	116	121	100°C - 200°C
CuF2	0	12	3.515	2.238	1.4	No	133	133	100°C - 200°C
NiF2	0	4	3.759	1.640	0.0	No	201	201	200°C - 300°C
BeBr2	0	9	3.553	2.040	6.6	Yes	78	423	Wide Temp. Window
BeBr2	0	8	3.595	1.954	9.5	Yes	78	423	Wide Temp. Window
BeBr2	0	4	3.681	1.688	0.0	Yes	423	423	300°C - 450°C
MgBr2	0	9	3.519	1.873	2.0	No	157	314	Wide Temp. Window
AlBr3	0	9	3.524	1.813	0.0	No	183	387	Wide Temp. Window
SiF4	0	8	3.344	2.089	5.8	No	103	211	100°C - 200°C
MgBr2	0	12	3.290	2.153	0.0	No	157	314	Wide Temp. Window
MgCl2	1	12	3.062	2.438	0.0	No	168	245	200°C - 300°C
GeF4	0	4	3.565	1.591	1.3	Yes	183	440	Wide Temp. Window

AlBr3	0	6	3.564	1.542	0.0	No	387	387	300°C - 450°C
SnF4	0	8	3.482	1.700	0.0	No	124	354	Wide Temp. Window
VF4	0	8	3.290	1.991	1.2	No	129	225	100°C - 200°C
GaF3	0	9	3.301	1.906	0.0	Yes	105	166	100°C - 200°C
TiF4	0	8	3.219	1.993	0.0	No	121	243	100°C - 200°C
CaCl2	0	12	2.944	2.375	0.0	No	165	187	100°C - 200°C
TiF3	0	9	3.156	2.058	6.8	No	145	145	100°C - 200°C
SiF4	0	5	3.273	1.821	5.0	No	211	211	200°C - 300°C
ZnF2	0	4	3.433	1.487	0.0	No	156	192	100°C - 200°C
BeI2	0	8	3.377	1.574	0.0	Yes	86	452	Wide Temp. Window
MgCl2	1	9	3.088	2.083	7.5	No	168	245	200°C - 300°C
BeI2	0	7	3.401	1.494	2.4	Yes	86	452	Wide Temp. Window
NaF1	0	4	3.103	2.019	0.0	No	121	121	100°C - 200°C
CaF2	0	12	2.971	2.205	0.0	No	72	106	50°C - 100°C
MgI2	0	9	3.365	1.525	0.0	No	183	298	200°C - 300°C
VF3	0	6	3.296	1.667	9.0	No	84	193	100°C - 200°C
SnF4	0	5	3.371	1.413	0.0	No	195	354	Wide Temp. Window
GeF4	0	3	3.388	1.355	4.5	Yes	183	440	Wide Temp. Window
BeI2	0	9	3.293	1.568	9.7	Yes	-96	452	Wide Temp. Window
BeF2	0	4	3.134	1.852	4.8	Yes	76	134	100°C - 200°C
ScCl3	0	9	2.935	2.081	0.0	Yes	105	269	100°C - 200°C
BeI2	0	12	3.137	1.737	6.3	Yes	-96	452	Wide Temp. Window
ZnCl2	0	12	2.926	2.047	0.0	No	123	147	100°C - 200°C
VF4	0	5	3.153	1.675	5.0	No	225	225	200°C - 300°C
BeI2	0	4	3.336	1.265	0.0	Yes	452	452	450°C - 600°C
ScF3	0	9	2.970	1.976	0.0	Yes	123	125	100°C - 200°C
MgBr2	1	12	2.979	1.949	8.2	No	157	314	Wide Temp. Window
MgI2	0	12	3.077	1.773	0.0	No	183	298	200°C - 300°C
MgCl2	2	12	2.757	2.196	0.0	No	168	237	200°C - 300°C
MgF2	0	4	3.052	1.711	3.2	No	121	121	100°C - 200°C
TiF4	0	5	3.058	1.689	0.0	No	173	243	200°C - 300°C
MgBr2	1	9	3.077	1.637	8.2	No	157	314	Wide Temp. Window
ZnF2	2	12	2.918	1.858	7.9	No	119	192	100°C - 200°C
CaCl2	1	12	2.689	2.170	0.0	No	165	173	100°C - 200°C
KF1	0	4	2.834	1.971	0.0	No	157	194	100°C - 200°C
MgBr2	0	8	2.992	1.714	8.9	No	157	285	200°C - 300°C
GeF4	0	2	3.254	1.127	0.0	Yes	440	440	300°C - 450°C
MnCl2	0	9	2.931	1.805	6.4	No	103	174	100°C - 200°C
GaCl3	0	9	2.911	1.822	0.0	Yes	137	267	200°C - 300°C
MgBr2	0	6	3.094	1.489	6.1	No	157	285	200°C - 300°C
CaBr2	0	12	2.844	1.924	0.0	No	142	245	100°C - 200°C
CrCl3	0	9	2.861	1.897	0.0	No	190	190	100°C - 200°C
LiCl1	0	4	2.800	1.982	3.8	No	67	173	100°C - 200°C
MgCl2	0	4	2.875	1.770	0.0	No	202	288	200°C - 300°C
AlI3	0	9	3.103	1.322	0.0	No	142	379	Wide Temp. Window
CuCl2	0	12	2.756	1.903	2.4	No	89	145	100°C - 200°C
SnF4	0	4	3.115	1.221	2.4	No	195	354	Wide Temp. Window
RbF1	0	4	2.923	1.586	0.0	Yes	155	344	Wide Temp. Window

MgI2	0	8	3.015	1.403	2.9	No	183	298	200°C - 300°C
SrF2	0	12	2.750	1.845	4.0	No	54	94	50°C - 100°C
SrCl2	0	12	2.662	1.957	0.0	No	110	172	100°C - 200°C
AlF3	2	9	2.750	1.827	7.5	No	156	234	100°C - 200°C
CaBr2	0	9	2.878	1.586	9.7	No	142	245	100°C - 200°C
AlF3	0	3	2.932	1.468	0.0	No	167	234	200°C - 300°C
ScCl3	0	6	2.798	1.690	0.0	Yes	105	269	100°C - 200°C
MnCl4	0	8	2.833	1.615	0.0	No	187	256	200°C - 300°C
MgI2	1	9	2.967	1.344	8.6	No	183	298	200°C - 300°C
ZnBr2	0	12	2.804	1.654	0.0	No	126	195	100°C - 200°C
AlI3	0	6	3.034	1.108	0.0	No	379	379	300°C - 450°C
MgI2	1	12	2.799	1.612	8.6	No	183	298	200°C - 300°C
SnF2	0	12	2.759	1.668	7.8	No	73	115	50°C - 100°C
YCl3	0	8	2.818	1.558	9.6	Yes	22	217	Wide Temp. Window
YCl3	0	6	2.887	1.406	0.0	Yes	210	217	200°C - 300°C
ZrF4	0	8	2.805	1.542	0.0	Yes	75	189	100°C - 200°C
MgCl2	2	9	2.653	1.789	7.5	No	168	202	100°C - 200°C
MgBr2	2	12	2.677	1.751	0.5	No	157	314	Wide Temp. Window
MnCl2	0	6	2.812	1.519	3.6	No	124	174	100°C - 200°C
CoBr2	0	12	2.743	1.633	0.0	No	132	132	100°C - 200°C
YBr3	0	10	2.920	1.289	7.9	Yes	-94	245	Wide Temp. Window
ZrCl4	0	8	2.792	1.514	1.7	Yes	216	216	200°C - 300°C
HfCl4	0	8	2.898	1.270	7.1	Yes	232	232	200°C - 300°C
NiCl2	0	6	2.826	1.422	7.2	No	67	122	50°C - 100°C
HfF4	0	8	2.906	1.245	0.0	Yes	119	281	100°C - 200°C
LiCl1	0	3	2.588	1.815	3.2	No	67	173	100°C - 200°C
YF3	0	9	2.695	1.647	0.0	Yes	113	113	100°C - 200°C
ZnBr2	0	9	2.846	1.355	9.8	No	126	126	100°C - 200°C
YCl3	0	7	2.787	1.461	8.8	Yes	22	217	Wide Temp. Window
CaCl2	2	12	2.447	1.974	2.5	No	169	173	100°C - 200°C
YCl3	0	9	2.619	1.737	0.0	Yes	22	357	Wide Temp. Window
NiBr2	0	12	2.716	1.577	9.7	No	118	118	100°C - 200°C
MnBr2	0	9	2.803	1.403	3.3	No	103	162	100°C - 200°C
ScBr3	0	9	2.763	1.468	0.0	Yes	193	249	200°C - 300°C
CaF2	2	12	2.510	1.863	7.4	No	101	106	100°C - 200°C
TiF4	0	4	2.758	1.459	3.1	No	173	241	200°C - 300°C
CaBr2	1	12	2.575	1.743	0.0	No	142	244	100°C - 200°C
VCl4	0	8	2.679	1.556	0.0	No	162	198	100°C - 200°C
CaI2	0	12	2.657	1.581	0.0	No	124	229	100°C - 200°C
VF3	0	3	2.822	1.259	0.0	No	193	193	100°C - 200°C
GaCl3	0	6	2.735	1.426	7.1	Yes	137	267	200°C - 300°C
SrBr2	0	9	2.785	1.320	9.4	No	101	192	100°C - 200°C
LiBr1	0	4	2.702	1.482	6.9	No	48	222	Wide Temp. Window
PbF2	0	12	2.750	1.365	5.1	No	75	115	50°C - 100°C
MgI2	0	6	2.828	1.189	0.6	No	206	298	200°C - 300°C
SrBr2	0	12	2.586	1.635	0.0	No	101	223	100°C - 200°C
MgBr2	0	4	2.803	1.208	0.0	No	237	285	200°C - 300°C
SnCl4	0	8	2.723	1.368	0.0	No	177	214	100°C - 200°C

LiCl1	0	2	2.578	1.599	0.0	No	140	173	100°C - 200°C
CaI2	0	9	2.738	1.304	4.4	No	124	229	100°C - 200°C
SnF4	0	3	2.855	1.011	3.9	No	195	354	Wide Temp. Window
CoCl3	0	9	2.569	1.586	6.0	No	121	123	100°C - 200°C
MnCl2	1	9	2.563	1.578	6.4	No	103	124	100°C - 200°C
MgBr2	2	9	2.647	1.408	2.0	No	157	314	Wide Temp. Window
GaCl3	1	9	2.539	1.589	0.0	Yes	137	209	100°C - 200°C
SnCl2	0	12	2.485	1.666	1.0	No	95	169	100°C - 200°C
NaCl1	0	4	2.456	1.685	1.2	No	101	106	100°C - 200°C
YBr3	0	8	2.715	1.173	3.7	Yes	96	236	Wide Temp. Window
MgBr2	1	8	2.559	1.466	8.9	No	157	270	200°C - 300°C
SrCl2	0	6	2.599	1.326	7.8	No	110	172	100°C - 200°C
LiBr1	0	3	2.579	1.339	2.3	No	71	222	Wide Temp. Window
CrBr3	0	9	2.600	1.294	0.0	No	174	174	100°C - 200°C
MgI2	2	12	2.506	1.444	0.8	No	183	267	200°C - 300°C
BaCl2	0	12	2.389	1.620	0.0	No	87	152	100°C - 200°C
MgI2	1	8	2.611	1.215	8.6	No	183	298	200°C - 300°C
SrI2	0	9	2.646	1.121	4.3	No	9	235	Wide Temp. Window
ZnI2	0	12	2.544	1.336	0.0	No	121	179	100°C - 200°C
BeF2	0	2	2.485	1.430	0.0	Yes	134	134	100°C - 200°C
YBr3	0	7	2.645	1.081	3.9	Yes	96	236	Wide Temp. Window
YBr3	0	6	2.675	1.002	0.0	Yes	217	236	200°C - 300°C
CaBr2	1	9	2.499	1.377	9.7	No	142	179	100°C - 200°C
LaCl3	0	7	2.601	1.161	4.6	No	23	176	Wide Temp. Window
CoCl3	0	6	2.541	1.269	4.6	No	123	123	100°C - 200°C
ScBr3	0	6	2.593	1.151	0.0	Yes	237	249	200°C - 300°C
PbCl2	0	12	2.478	1.378	0.0	No	106	144	100°C - 200°C
GaBr3	0	9	2.555	1.227	0.0	Yes	120	225	100°C - 200°C
CaBr2	2	12	2.341	1.584	0.0	No	142	244	100°C - 200°C
ZnF2	0	2	2.679	0.898	7.9	No	156	156	100°C - 200°C
CaI2	1	12	2.425	1.444	4.0	No	124	229	100°C - 200°C
YI3	0	10	2.613	1.041	2.9	Yes	31	234	Wide Temp. Window
MgCl2	4	12	2.198	1.750	0.0	No	168	237	200°C - 300°C
ZnI2	0	9	2.588	1.075	9.9	No	121	121	100°C - 200°C
MnI2	0	9	2.568	1.120	0.0	No	128	128	100°C - 200°C
TiF4	0	3	2.525	1.210	4.0	No	173	241	200°C - 300°C
MgI2	2	9	2.550	1.155	0.8	No	183	267	200°C - 300°C
YI3	0	9	2.612	1.001	0.0	Yes	100	234	Wide Temp. Window
SrI2	0	12	2.433	1.379	0.0	No	9	235	Wide Temp. Window
MgBr2	1	6	2.515	1.210	8.2	No	157	270	200°C - 300°C
SrBr2	1	12	2.355	1.489	3.6	No	101	223	100°C - 200°C
YBr3	0	9	2.468	1.284	0.0	Yes	96	245	Wide Temp. Window
ScI3	0	8	2.594	0.998	6.3	Yes	25	251	Wide Temp. Window
SrBr2	0	6	2.565	1.061	2.7	No	110	192	100°C - 200°C
MgF2	4	12	2.242	1.633	3.2	No	116	116	100°C - 200°C
WCl4	0	8	2.550	1.080	5.0	No	161	161	100°C - 200°C
GeBr2	0	12	2.353	1.456	9.8	Yes	81	137	100°C - 200°C
CaF2	0	4	2.380	1.409	2.2	No	72	106	50°C - 100°C

HfF4	0	5	2.604	0.929	0.0	Yes	119	281	100°C - 200°C
PbCl4	0	8	2.545	1.077	0.0	No	155	190	100°C - 200°C
LiBr1	0	2	2.524	1.126	0.0	No	180	222	200°C - 300°C
NiF2	4	12	2.327	1.483	9.4	No	124	124	100°C - 200°C
GeF4	2	8	2.426	1.315	1.9	Yes	110	251	100°C - 200°C
SnF4	0	2	2.641	0.794	0.0	No	354	354	300°C - 450°C
AlF3	3	9	2.297	1.526	0.0	No	156	156	100°C - 200°C
SrF2	2	12	2.283	1.531	4.0	No	54	93	50°C - 100°C
AlF3	0	2	2.525	1.071	7.5	No	167	167	100°C - 200°C
LaBr3	0	10	2.521	1.080	7.6	No	-35	213	Wide Temp. Window
CuCl2	0	4	2.463	1.183	0.0	No	145	145	100°C - 200°C
ScI3	0	9	2.486	1.111	0.0	Yes	25	305	Wide Temp. Window
TiF4	2	8	2.314	1.432	0.7	No	121	243	100°C - 200°C
ZrBr4	0	8	2.531	0.999	7.4	Yes	202	202	200°C - 300°C
SrCl2	2	12	2.191	1.611	0.0	No	110	161	100°C - 200°C
RbF1	0	2	2.485	1.103	0.0	Yes	171	344	Wide Temp. Window
ZrF4	0	5	2.441	1.182	4.7	Yes	75	189	100°C - 200°C
NiCl2	1	6	2.411	1.213	7.2	No	122	122	100°C - 200°C
SrBr2	1	9	2.436	1.155	9.4	No	101	191	100°C - 200°C
KF1	0	2	2.301	1.393	0.0	No	158	194	100°C - 200°C
BaBr2	0	12	2.310	1.369	0.0	No	106	172	100°C - 200°C
LaCl3	0	6	2.450	1.098	0.0	No	164	176	100°C - 200°C
NiCl3	0	6	2.378	1.226	2.3	No	109	109	100°C - 200°C
CaI2	1	9	2.414	1.150	4.4	No	124	229	100°C - 200°C
YI3	0	8	2.503	0.941	0.0	Yes	181	234	200°C - 300°C
ZrF4	0	3	2.509	0.915	0.0	Yes	189	189	100°C - 200°C
ZnF2	4	12	2.250	1.433	0.0	No	119	119	100°C - 200°C
HfF4	0	3	2.581	0.666	0.0	Yes	154	281	200°C - 300°C
GaF3	3	9	2.308	1.333	0.0	Yes	166	166	100°C - 200°C
GaCl3	2	9	2.256	1.412	4.5	Yes	183	209	100°C - 200°C
SnBr2	0	12	2.304	1.331	2.6	No	90	139	100°C - 200°C
LaBr3	0	7	2.503	0.897	4.2	No	30	197	Wide Temp. Window
MgI2	0	4	2.486	0.912	0.0	No	263	298	200°C - 300°C
LaF3	0	9	2.311	1.289	8.6	No	78	78	50°C - 100°C
LiI1	0	3	2.433	1.033	7.9	No	61	243	Wide Temp. Window
SnF4	2	8	2.375	1.160	0.0	No	124	252	100°C - 200°C
MnCl4	0	5	2.352	1.206	0.4	No	187	256	200°C - 300°C
ScI3	0	7	2.474	0.911	7.7	Yes	25	251	Wide Temp. Window
SnF2	2	12	2.256	1.364	7.8	No	73	84	50°C - 100°C
NaBr1	0	4	2.302	1.249	5.7	No	77	127	100°C - 200°C
ZnCl2	0	4	2.369	1.110	8.7	No	123	123	100°C - 200°C
MnCl2	1	6	2.295	1.239	3.6	No	124	124	100°C - 200°C
KF1	1	4	2.138	1.487	8.7	No	157	194	100°C - 200°C
CaCl2	0	4	2.177	1.427	0.0	No	165	187	100°C - 200°C
SrI2	0	8	2.399	1.010	8.9	No	9	203	Wide Temp. Window
ScCl3	0	4	2.265	1.253	9.9	Yes	105	240	100°C - 200°C
PbBr2	0	12	2.316	1.154	0.9	No	97	148	100°C - 200°C
VBr4	0	8	2.390	0.973	0.0	No	111	199	100°C - 200°C

LaCl3	0	9	2.194	1.342	1.8	No	23	176	Wide Temp. Window
SrI2	1	12	2.221	1.258	0.0	No	9	235	Wide Temp. Window
YI3	0	7	2.402	0.858	0.0	Yes	189	234	200°C - 300°C
GaBr3	0	6	2.382	0.898	9.4	Yes	120	225	100°C - 200°C
CaI2	2	12	2.184	1.300	0.0	No	124	211	100°C - 200°C
MgI2	1	6	2.339	0.984	8.6	No	206	298	200°C - 300°C
LaI3	0	9	2.375	0.884	0.0	No	22	247	Wide Temp. Window
SrI2	1	9	2.331	0.988	4.3	No	9	235	Wide Temp. Window
LaI3	0	10	2.360	0.907	0.9	No	-52	247	Wide Temp. Window
MoBr4	0	8	2.355	0.896	4.3	No	156	156	100°C - 200°C
MgBr2	4	12	2.108	1.379	0.0	No	157	314	Wide Temp. Window
PbF2	2	12	2.255	1.119	5.1	No	75	82	50°C - 100°C
BaI2	0	9	2.329	0.950	4.6	No	94	226	Wide Temp. Window
SrBr2	2	12	2.124	1.343	0.0	No	101	223	100°C - 200°C
ScF3	0	3	2.249	1.119	1.3	Yes	125	125	100°C - 200°C
LaBr3	0	8	2.324	0.952	0.0	No	30	197	Wide Temp. Window
CaCl2	4	12	1.954	1.576	0.0	No	169	169	100°C - 200°C
SrI2	0	6	2.352	0.866	0.0	No	131	203	100°C - 200°C
KCl1	0	4	2.000	1.509	0.0	No	86	117	100°C - 200°C
BaCl2	0	6	2.261	1.057	6.7	No	87	152	100°C - 200°C
CaF2	4	12	2.003	1.486	2.2	No	101	101	100°C - 200°C
MgCl2	0	2	2.186	1.200	0.0	No	245	288	200°C - 300°C
MnBr2	0	4	2.329	0.885	0.7	No	162	162	100°C - 200°C
SrI2	0	7	2.314	0.921	9.0	No	9	203	Wide Temp. Window
BaI2	0	12	2.190	1.180	0.0	No	94	226	Wide Temp. Window
LaBr3	0	6	2.339	0.840	0.0	No	190	197	100°C - 200°C
GaCl3	1	6	2.203	1.148	7.1	Yes	137	183	100°C - 200°C
GaF3	0	3	2.308	0.916	0.0	Yes	105	105	100°C - 200°C
YI3	0	6	2.356	0.768	0.0	Yes	234	234	200°C - 300°C
CaBr2	2	9	2.168	1.195	9.7	No	142	170	100°C - 200°C
CaBr2	0	4	2.261	0.996	1.2	No	170	245	200°C - 300°C
ScI3	0	6	2.312	0.860	0.0	Yes	251	251	200°C - 300°C
MnCl4	2	8	2.142	1.221	0.0	No	187	256	200°C - 300°C
MgBr2	2	8	2.138	1.225	8.9	No	157	237	100°C - 200°C
SnCl4	0	5	2.247	0.993	0.0	No	177	214	100°C - 200°C
LiCl1	1	4	1.997	1.414	3.8	No	67	140	100°C - 200°C
MgCl2	1	4	2.080	1.281	0.0	No	202	245	200°C - 300°C
BaBr2	1	12	2.097	1.243	0.0	No	106	146	100°C - 200°C
SnF2	0	4	2.240	0.952	1.7	No	84	115	50°C - 100°C
CaI2	0	6	2.228	0.972	9.4	No	124	229	100°C - 200°C
VCl4	0	5	2.153	1.124	6.3	No	162	162	100°C - 200°C
ZnCl2	4	12	1.989	1.391	8.7	No	147	147	100°C - 200°C
LiI1	0	2	2.268	0.855	0.0	No	207	243	200°C - 300°C
SnCl2	2	12	2.011	1.348	1.0	No	95	129	100°C - 200°C
MgI2	2	8	2.187	1.018	2.9	No	183	263	200°C - 300°C
TiF4	0	2	2.189	0.939	0.7	No	241	241	200°C - 300°C
ScF3	3	9	1.976	1.315	1.3	Yes	123	123	100°C - 200°C
HfF4	2	8	2.176	0.932	9.5	Yes	119	281	100°C - 200°C

BaCl2	2	12	1.958	1.328	0.0	No	87	131	100°C - 200°C
LaBr3	0	9	2.113	1.052	1.6	No	30	213	Wide Temp. Window
ScCl3	3	9	1.924	1.364	0.0	Yes	105	269	100°C - 200°C
CrI3	0	9	2.171	0.904	0.0	No	136	137	100°C - 200°C
BaBr2	0	6	2.175	0.858	3.5	No	106	172	100°C - 200°C
LaI3	0	8	2.189	0.794	5.9	No	22	208	Wide Temp. Window
PbCl2	2	12	2.035	1.131	0.0	No	106	127	100°C - 200°C
SrI2	2	12	2.015	1.142	0.0	No	9	235	Wide Temp. Window
SrBr2	2	9	2.087	0.990	9.4	No	101	171	100°C - 200°C
SrF2	0	4	2.067	1.026	8.7	No	54	94	50°C - 100°C
CaI2	2	9	2.077	0.989	4.4	No	124	193	100°C - 200°C
CaF2	0	2	2.122	0.882	7.4	No	72	72	50°C - 100°C
PbF2	0	4	2.194	0.677	3.0	No	75	115	50°C - 100°C
SnI2	0	12	2.033	1.059	7.6	No	73	127	100°C - 200°C
GeF4	3	8	2.006	1.087	4.5	Yes	110	251	100°C - 200°C
SrBr2	1	6	2.104	0.870	3.6	No	110	191	100°C - 200°C
NaCl1	0	2	1.949	1.172	0.0	No	106	106	100°C - 200°C
CaBr2	4	12	1.881	1.273	1.2	No	142	244	100°C - 200°C
SnCl2	0	4	2.059	0.943	0.0	No	129	169	100°C - 200°C
TiF4	3	8	1.921	1.189	4.0	No	121	243	100°C - 200°C
MgI2	4	12	1.956	1.127	0.0	No	183	267	200°C - 300°C
RbF1	1	4	1.982	1.075	0.0	Yes	155	171	100°C - 200°C
MgBr2	1	4	2.065	0.890	8.2	No	237	270	200°C - 300°C
SrF2	4	12	1.866	1.252	8.7	No	93	93	50°C - 100°C
SrI2	1	8	2.071	0.872	8.9	No	9	203	Wide Temp. Window
MgCl2	4	9	1.854	1.251	7.5	No	168	168	100°C - 200°C
BaI2	1	12	1.967	1.060	0.0	No	94	164	100°C - 200°C
ScCl3	0	3	1.948	1.095	0.0	Yes	240	240	200°C - 300°C
NaCl1	1	4	1.838	1.261	4.4	No	101	106	100°C - 200°C
CuBr2	0	4	2.093	0.753	0.0	No	108	108	100°C - 200°C
PbI2	0	12	2.017	0.933	6.1	No	86	90	50°C - 100°C
GaI3	0	9	2.052	0.838	0.0	Yes	83	153	100°C - 200°C
RbF1	0	1	2.085	0.736	0.0	Yes	344	344	300°C - 450°C
LaI3	0	6	2.099	0.671	0.0	No	208	208	200°C - 300°C
BaBr2	2	12	1.895	1.124	0.0	No	106	133	100°C - 200°C
SrI2	2	9	2.027	0.859	4.3	No	9	235	Wide Temp. Window
NiBr3	0	6	2.051	0.768	4.9	No	83	83	50°C - 100°C
RbCl1	0	4	1.866	1.147	0.0	Yes	90	113	100°C - 200°C
LiCl1	0	1	1.904	1.078	0.0	No	173	173	100°C - 200°C
LaI3	0	7	2.064	0.719	7.7	No	22	208	Wide Temp. Window
PbCl4	0	5	2.052	0.749	6.6	No	155	183	100°C - 200°C
SnF4	3	8	1.962	0.958	3.9	No	124	252	100°C - 200°C
SnBr2	2	12	1.883	1.088	2.6	No	90	120	100°C - 200°C
BaI2	1	9	2.006	0.818	4.6	No	94	135	100°C - 200°C
SnCl4	0	4	1.993	0.850	2.6	No	202	214	200°C - 300°C
MgBr2	2	6	1.952	0.939	6.1	No	157	237	100°C - 200°C
GeBr2	0	4	2.016	0.787	0.0	Yes	137	137	100°C - 200°C
KBr1	0	4	1.846	1.126	0.0	No	79	105	50°C - 100°C

BaI2	0	6	2.029	0.730	0.0	No	116	226	100°C - 200°C
YBr3	3	10	1.964	0.867	7.9	Yes	-94	245	Wide Temp. Window
GeF4	2	5	1.935	0.910	0.0	Yes	183	251	200°C - 300°C
LiBr1	1	4	1.873	1.028	6.9	No	48	180	Wide Temp. Window
CrI3	0	6	2.031	0.663	3.8	No	136	136	100°C - 200°C
CsF1	0	2	1.993	0.735	0.0	Yes	151	249	100°C - 200°C
CuCl2	4	12	1.748	1.207	2.4	No	89	89	50°C - 100°C
GaBr3	2	9	1.912	0.918	0.0	Yes	120	192	100°C - 200°C
PbBr2	2	12	1.893	0.943	0.9	No	97	132	100°C - 200°C
WF4	3	8	1.955	0.798	7.6	No	168	168	100°C - 200°C
PbCl2	0	4	1.991	0.681	0.0	No	127	144	100°C - 200°C
SrI2	1	7	1.953	0.777	9.0	No	9	203	Wide Temp. Window
PbF2	0	2	2.061	0.403	0.0	No	115	115	100°C - 200°C
SnF2	4	12	1.793	1.084	7.8	No	73	73	50°C - 100°C
MgBr2	4	9	1.839	0.978	2.0	No	157	314	Wide Temp. Window
VI4	0	8	1.974	0.658	8.9	No	123	123	100°C - 200°C
MgBr2	0	2	1.944	0.730	0.5	No	270	285	200°C - 300°C
SrI2	1	6	1.946	0.716	0.0	No	131	203	100°C - 200°C
ScBr3	3	9	1.822	0.968	8.8	Yes	193	249	200°C - 300°C
SrBr2	4	12	1.743	1.102	8.2	No	101	223	100°C - 200°C
YCl3	3	9	1.713	1.136	0.9	Yes	22	357	Wide Temp. Window
ScCl3	4	9	1.675	1.188	9.9	Yes	216	269	200°C - 300°C
SrBr2	0	4	1.901	0.774	8.2	No	110	192	100°C - 200°C
CaI2	0	4	1.904	0.751	1.1	No	176	229	200°C - 300°C
SrF2	0	2	1.935	0.663	0.8	No	94	94	50°C - 100°C
TiF4	2	5	1.787	0.987	0.7	No	173	243	200°C - 300°C
CaI2	4	12	1.752	1.043	1.1	No	124	211	100°C - 200°C
GaCl3	2	6	1.799	0.938	7.1	Yes	183	183	100°C - 200°C
BaI2	2	12	1.785	0.962	0.0	No	94	164	100°C - 200°C
PbF2	4	12	1.812	0.899	5.1	No	82	82	50°C - 100°C
NaBr1	0	2	1.831	0.838	0.0	No	124	127	100°C - 200°C
MnCl4	3	8	1.744	0.994	0.0	No	187	194	100°C - 200°C
PbBr4	0	8	1.900	0.633	3.6	No	91	91	50°C - 100°C
BaF2	0	2	1.914	0.583	0.0	No	149	149	100°C - 200°C
MnCl4	0	3	1.809	0.844	0.0	No	187	256	200°C - 300°C
CaI2	1	6	1.827	0.797	9.4	No	124	229	100°C - 200°C
SnF4	2	5	1.836	0.770	0.0	No	195	252	200°C - 300°C
MgI2	1	4	1.869	0.685	8.6	No	263	298	200°C - 300°C
LiCl1	1	3	1.625	1.140	3.2	No	67	140	100°C - 200°C
LiBr1	0	1	1.859	0.689	0.0	No	222	222	200°C - 300°C
MgI2	2	6	1.826	0.768	0.8	No	206	263	200°C - 300°C
SnBr2	0	4	1.863	0.671	0.0	No	120	139	100°C - 200°C
PbBr2	0	4	1.871	0.549	0.0	No	132	148	100°C - 200°C
GaI3	1	9	1.803	0.736	2.7	Yes	83	145	100°C - 200°C
ZnF2	2	4	1.786	0.774	7.9	No	192	192	100°C - 200°C
MgBr2	6	12	1.629	1.066	6.1	No	164	314	Wide Temp. Window
GaI3	0	6	1.850	0.591	6.7	Yes	83	153	100°C - 200°C
RbBr1	0	4	1.734	0.873	5.0	Yes	76	85	50°C - 100°C

SnF2	0	2	1.848	0.588	0.0	No	115	115	100°C - 200°C
MgI2	4	9	1.765	0.799	0.0	No	183	267	200°C - 300°C
CaCl2	1	4	1.618	1.061	0.0	No	165	173	100°C - 200°C
VBr4	0	5	1.817	0.639	8.9	No	111	135	100°C - 200°C
NaBr1	1	4	1.687	0.916	5.7	No	77	124	100°C - 200°C
SnI2	2	12	1.701	0.886	8.7	No	73	127	100°C - 200°C
YCl3	3	8	1.674	0.926	9.6	Yes	22	210	Wide Temp. Window
KCl1	1	4	1.525	1.151	5.7	No	104	117	100°C - 200°C
PbCl4	0	4	1.800	0.632	7.1	No	183	183	100°C - 200°C
YCl3	0	3	1.699	0.861	0.9	Yes	217	217	200°C - 300°C
SrI2	2	8	1.753	0.738	8.9	No	9	203	Wide Temp. Window
BaBr2	1	6	1.769	0.698	3.5	No	106	146	100°C - 200°C
SnCl2	4	12	1.579	1.059	1.0	No	95	95	50°C - 100°C
SrI2	4	12	1.642	0.930	6.7	No	9	235	Wide Temp. Window
BaI2	2	9	1.742	0.710	4.6	No	94	133	100°C - 200°C
HfF4	0	2	1.825	0.429	9.5	Yes	154	154	100°C - 200°C
SnCl4	3	8	1.674	0.841	5.1	No	177	202	100°C - 200°C
SnBr4	0	5	1.778	0.575	0.0	No	134	171	100°C - 200°C
CaCl2	0	2	1.642	0.892	2.5	No	165	187	100°C - 200°C
KI1	0	4	1.650	0.869	4.4	No	72	89	50°C - 100°C
ZrF4	3	8	1.623	0.892	0.0	Yes	75	129	100°C - 200°C
HfF4	3	8	1.702	0.729	0.0	Yes	119	129	100°C - 200°C
SrCl2	2	6	1.645	0.839	7.8	No	110	110	100°C - 200°C
PbCl2	4	12	1.610	0.895	0.0	No	106	106	100°C - 200°C
ScBr3	0	3	1.720	0.660	8.8	Yes	237	237	200°C - 300°C
SrCl2	0	2	1.710	0.667	0.0	No	172	172	100°C - 200°C
YBr3	3	9	1.627	0.846	4.8	Yes	96	245	Wide Temp. Window
KF1	0	1	1.625	0.827	8.7	No	158	158	100°C - 200°C
LaBr3	3	10	1.675	0.717	7.6	No	-35	213	Wide Temp. Window
YBr3	3	8	1.663	0.718	4.8	Yes	96	236	Wide Temp. Window
BaI2	0	4	1.728	0.531	2.4	No	116	226	100°C - 200°C
SnCl4	0	3	1.671	0.678	5.1	No	214	214	200°C - 300°C
LaCl3	0	3	1.685	0.639	2.3	No	164	164	100°C - 200°C
LiBr1	1	3	1.592	0.826	2.3	No	71	180	100°C - 200°C
NaI1	0	2	1.668	0.658	0.0	No	143	148	100°C - 200°C
CaBr2	1	4	1.630	0.718	1.2	No	170	179	100°C - 200°C
SrBr2	2	6	1.644	0.679	2.7	No	110	171	100°C - 200°C
BeI2	4	12	1.540	0.852	6.3	Yes	-96	135	Wide Temp. Window
TiF4	4	8	1.496	0.926	3.1	No	121	243	100°C - 200°C
GeBr2	4	12	1.489	0.922	9.8	Yes	81	81	50°C - 100°C
SrI2	0	4	1.636	0.605	6.7	No	131	187	100°C - 200°C
CaBr2	4	9	1.520	0.838	9.7	No	142	142	100°C - 200°C
GeF4	4	8	1.524	0.826	1.9	Yes	110	234	100°C - 200°C
SrI2	2	7	1.604	0.638	9.0	No	9	203	Wide Temp. Window
BaI2	1	6	1.624	0.584	0.0	No	116	135	100°C - 200°C
KCl1	0	2	1.413	0.972	4.0	No	86	104	50°C - 100°C
SrCl2	6	12	1.379	1.014	7.8	No	161	161	100°C - 200°C
SnBr2	4	12	1.482	0.856	2.6	No	90	90	50°C - 100°C

MgI2	0	2	1.628	0.518	0.8	No	270	298	200°C - 300°C
YCl3	3	7	1.513	0.793	8.8	Yes	22	210	Wide Temp. Window
VBr4	0	4	1.604	0.539	7.2	No	135	135	100°C - 200°C
MgI2	6	12	1.465	0.844	0.6	No	183	267	200°C - 300°C
LiI1	1	3	1.556	0.660	7.9	No	61	243	Wide Temp. Window
KF1	2	4	1.386	0.964	0.0	No	157	157	100°C - 200°C
HfF4	2	5	1.589	0.567	9.5	Yes	119	281	100°C - 200°C
SnF4	4	8	1.514	0.739	2.4	No	124	252	100°C - 200°C
BeF2	2	4	1.447	0.855	4.8	Yes	76	76	50°C - 100°C
SnCl2	0	2	1.579	0.573	0.0	No	169	169	100°C - 200°C
SrBr2	4	9	1.512	0.717	9.4	No	101	171	100°C - 200°C
LaCl3	3	9	1.426	0.872	2.3	No	23	176	Wide Temp. Window
RbCl1	1	4	1.420	0.872	5.1	Yes	107	113	100°C - 200°C
SrBr2	0	2	1.593	0.478	0.0	No	191	192	100°C - 200°C
PbBr2	4	12	1.486	0.740	0.9	No	97	97	50°C - 100°C
SrI2	2	6	1.554	0.572	0.0	No	131	203	100°C - 200°C
LaBr3	0	3	1.581	0.468	0.6	No	190	190	100°C - 200°C
KBr1	1	4	1.405	0.857	4.6	No	92	105	50°C - 100°C
CaBr2	0	2	1.529	0.601	0.0	No	179	245	200°C - 300°C
BaI2	4	12	1.438	0.775	2.4	No	94	164	100°C - 200°C
MgCl2	0	1	1.464	0.723	0.0	No	288	288	200°C - 300°C
CaI2	4	9	1.474	0.702	4.4	No	124	193	100°C - 200°C
BeBr2	4	9	1.413	0.811	6.6	Yes	78	162	100°C - 200°C
MnBr2	4	9	1.457	0.729	3.3	No	103	103	100°C - 200°C
SnI2	0	4	1.552	0.492	0.0	No	76	127	100°C - 200°C
CsF1	0	1	1.556	0.449	0.0	Yes	249	249	200°C - 300°C
YBr3	0	3	1.516	0.561	4.8	Yes	217	217	200°C - 300°C
MnCl4	2	5	1.438	0.738	0.4	No	187	256	200°C - 300°C
YBr3	3	7	1.489	0.609	4.8	Yes	96	236	Wide Temp. Window
VF3	3	6	1.429	0.723	9.0	No	84	84	50°C - 100°C
SrI2	4	9	1.474	0.625	6.7	No	9	235	Wide Temp. Window
SnBr4	0	4	1.526	0.476	4.0	No	134	171	100°C - 200°C
CaI2	6	12	1.370	0.816	9.4	No	193	211	200°C - 300°C
YCl3	3	6	1.433	0.698	0.9	Yes	210	210	200°C - 300°C
ScCl3	3	6	1.363	0.823	0.0	Yes	105	269	100°C - 200°C
GeF4	2	4	1.453	0.649	1.3	Yes	183	251	200°C - 300°C
LaCl3	3	7	1.447	0.646	4.6	No	23	176	Wide Temp. Window
MgCl2	2	4	1.346	0.829	0.0	No	202	202	200°C - 300°C
GaCl3	0	2	1.435	0.654	4.5	Yes	137	267	200°C - 300°C
GaI3	1	6	1.501	0.480	6.7	Yes	83	102	50°C - 100°C
BaCl2	2	6	1.421	0.664	6.7	No	87	87	50°C - 100°C
GaBr3	2	6	1.458	0.549	9.4	Yes	120	120	100°C - 200°C
LiI1	0	1	1.486	0.461	5.4	No	207	207	200°C - 300°C
MgBr2	4	8	1.346	0.771	8.9	No	157	164	100°C - 200°C
BaCl2	0	2	1.458	0.508	0.0	No	152	152	100°C - 200°C
SrBr2	6	12	1.300	0.822	2.7	No	101	223	100°C - 200°C
CaI2	2	6	1.409	0.614	9.4	No	124	176	100°C - 200°C
LiCl1	2	4	1.253	0.887	3.8	No	67	82	50°C - 100°C

MgI2	4	8	1.390	0.647	2.9	No	183	206	100°C - 200°C
PbI2	0	4	1.472	0.398	4.5	No	90	90	50°C - 100°C
CaI2	1	4	1.416	0.558	4.0	No	176	229	200°C - 300°C
LaBr3	3	9	1.360	0.677	1.6	No	30	213	Wide Temp. Window
PbCl2	0	2	1.461	0.387	0.0	No	144	144	100°C - 200°C
NaCl1	0	1	1.321	0.724	4.4	No	106	106	100°C - 200°C
GaI3	3	9	1.388	0.567	5.1	Yes	102	145	100°C - 200°C
SnCl4	4	8	1.333	0.670	2.6	No	177	196	100°C - 200°C
BaBr2	2	6	1.386	0.547	3.5	No	106	106	100°C - 200°C
SrBr2	1	4	1.380	0.562	8.2	No	110	191	100°C - 200°C
LaBr3	3	8	1.378	0.565	0.6	No	30	197	Wide Temp. Window
SnI2	4	12	1.319	0.687	7.6	No	73	73	50°C - 100°C
RbF1	2	4	1.305	0.708	0.0	Yes	155	155	100°C - 200°C
BaCl2	6	12	1.228	0.833	6.7	No	131	131	100°C - 200°C
GeF4	3	5	1.342	0.631	4.5	Yes	234	251	200°C - 300°C
TiF4	2	4	1.309	0.693	3.1	No	173	211	100°C - 200°C
NaCl1	2	4	1.220	0.837	1.2	No	101	101	100°C - 200°C
PbI2	4	12	1.340	0.620	6.1	No	86	86	50°C - 100°C
LaBr3	3	7	1.383	0.496	4.2	No	30	197	Wide Temp. Window
MgBr2	2	4	1.348	0.581	0.5	No	237	237	200°C - 300°C
RbCl1	0	2	1.293	0.691	2.9	Yes	90	107	50°C - 100°C
SnF4	2	4	1.363	0.534	2.4	No	195	235	200°C - 300°C
RbBr1	1	4	1.308	0.658	5.8	Yes	82	85	50°C - 100°C
LiCl1	1	2	1.239	0.769	0.0	No	140	140	100°C - 200°C
YBr3	3	6	1.362	0.510	4.8	Yes	236	236	200°C - 300°C
CaF2	2	4	1.247	0.738	7.4	No	106	106	100°C - 200°C
MnCl4	0	2	1.318	0.577	0.0	No	187	187	100°C - 200°C
ScBr3	3	6	1.311	0.582	8.8	Yes	249	249	200°C - 300°C
KBr1	0	2	1.252	0.676	3.6	No	79	92	50°C - 100°C
TiF4	3	5	1.236	0.683	4.0	No	211	243	200°C - 300°C
KI1	1	4	1.248	0.657	5.2	No	74	89	50°C - 100°C
KF1	1	2	1.196	0.724	8.7	No	194	194	100°C - 200°C
BaBr2	0	2	1.338	0.379	0.0	No	146	172	100°C - 200°C
SnBr2	0	2	1.329	0.383	0.0	No	139	139	100°C - 200°C
SrI2	6	12	1.201	0.681	0.0	No	9	235	Wide Temp. Window
PbCl4	4	8	1.270	0.538	7.1	No	155	190	100°C - 200°C
BaI2	2	6	1.292	0.465	0.0	No	116	133	100°C - 200°C
BeBr2	4	8	1.205	0.655	9.5	Yes	78	78	50°C - 100°C
SnF4	3	5	1.263	0.529	3.9	No	235	252	200°C - 300°C
PbBr2	0	2	1.333	0.305	0.6	No	148	148	100°C - 200°C
MgBr2	8	12	1.142	0.747	8.9	No	214	314	200°C - 300°C
LaCl3	3	6	1.241	0.556	2.3	No	176	176	100°C - 200°C
BaBr2	6	12	1.167	0.692	3.5	No	133	133	100°C - 200°C
VBr4	4	8	1.253	0.510	7.2	No	111	199	100°C - 200°C
SrI2	0	2	1.296	0.350	0.0	No	171	187	100°C - 200°C
BaI2	4	9	1.239	0.505	4.6	No	94	133	100°C - 200°C
BeI2	4	9	1.200	0.571	9.7	Yes	-96	135	Wide Temp. Window
GaBr3	0	2	1.255	0.421	0.0	Yes	225	225	200°C - 300°C

NaBr1	0	1	1.231	0.483	3.0	No	127	127	100°C - 200°C
LiBr1	1	2	1.206	0.538	0.0	No	180	180	100°C - 200°C
BaI2	0	2	1.277	0.310	0.0	No	135	226	100°C - 200°C
MgBr2	0	1	1.249	0.403	8.2	No	285	285	200°C - 300°C
MgBr2	6	9	1.158	0.616	6.1	No	164	314	Wide Temp. Window
CaI2	0	2	1.231	0.436	0.0	No	209	229	200°C - 300°C
MgI2	2	4	1.219	0.447	0.8	No	263	263	200°C - 300°C
CaCl2	2	4	1.085	0.711	2.5	No	173	173	100°C - 200°C
KCl1	2	4	1.028	0.776	4.0	No	117	117	100°C - 200°C
SrI2	1	4	1.197	0.442	6.7	No	131	171	100°C - 200°C
SrI2	4	8	1.176	0.495	8.9	No	9	203	Wide Temp. Window
BaI2	1	4	1.216	0.374	2.4	No	116	135	100°C - 200°C
LiBr1	2	4	1.115	0.612	6.9	No	48	71	50°C - 100°C
SnBr4	0	3	1.216	0.362	9.8	No	134	134	100°C - 200°C
BeI2	4	8	1.144	0.533	0.0	Yes	86	135	100°C - 200°C
LiI1	1	2	1.175	0.443	5.4	No	243	243	200°C - 300°C
VF4	5	8	1.074	0.650	5.0	No	129	129	100°C - 200°C
SiF4	5	8	1.063	0.664	5.8	No	103	103	100°C - 200°C
LaBr3	3	6	1.179	0.423	0.6	No	197	197	100°C - 200°C
RbBr1	0	2	1.126	0.510	5.8	Yes	76	82	50°C - 100°C
AlCl3	6	9	1.013	0.705	0.0	No	202	202	200°C - 300°C
SrI2	7	12	1.071	0.607	9.0	No	139	235	100°C - 200°C
TiF4	5	8	1.041	0.645	0.0	No	121	121	100°C - 200°C
NaBr1	2	4	1.076	0.584	5.7	No	77	77	50°C - 100°C
GeCl2	2	4	1.081	0.571	0.0	Yes	149	149	100°C - 200°C
BaI2	6	12	1.076	0.580	0.0	No	94	164	100°C - 200°C
VCl4	5	8	1.054	0.612	6.3	No	198	198	100°C - 200°C
KI1	0	2	1.111	0.500	5.7	No	72	74	50°C - 100°C
MnCl2	0	1	1.131	0.454	0.0	No	174	174	100°C - 200°C
MnCl4	5	8	1.053	0.600	0.4	No	194	194	100°C - 200°C
GeF4	5	8	1.057	0.573	1.9	Yes	110	110	100°C - 200°C
AlF3	2	3	1.071	0.536	7.5	No	234	234	200°C - 300°C
MgCl2	1	2	1.049	0.576	0.0	No	245	245	200°C - 300°C
ScCl3	4	6	1.011	0.611	9.9	Yes	269	269	200°C - 300°C
ScCl3	6	9	0.963	0.683	0.0	Yes	216	216	200°C - 300°C
CaBr2	2	4	1.079	0.476	1.2	No	170	170	100°C - 200°C
GaCl3	6	9	0.997	0.624	7.1	Yes	209	209	200°C - 300°C
ZrF4	5	8	1.029	0.566	4.7	Yes	129	129	100°C - 200°C
SnF4	5	8	1.050	0.513	0.0	No	124	124	100°C - 200°C
MgI2	6	9	1.063	0.482	0.6	No	183	267	200°C - 300°C
SnF2	2	4	1.074	0.456	1.7	No	84	84	50°C - 100°C
MoCl4	5	8	1.029	0.539	3.1	No	197	197	100°C - 200°C
MgCl2	9	12	0.900	0.717	7.5	No	237	237	200°C - 300°C
MgI2	8	12	0.997	0.574	2.9	No	195	267	200°C - 300°C
RbF1	1	2	1.040	0.462	0.0	Yes	171	171	100°C - 200°C
NaCl1	1	2	0.974	0.586	4.4	No	106	106	100°C - 200°C
NaI1	0	1	1.074	0.362	2.3	No	143	143	100°C - 200°C
SnCl4	5	8	1.010	0.508	0.0	No	196	196	100°C - 200°C

HfF4	5	8	1.031	0.442	0.0	Yes	129	129	100°C - 200°C
RbCl1	2	4	0.952	0.585	2.9	Yes	113	113	100°C - 200°C
CaCl2	0	1	0.983	0.521	0.0	No	187	187	100°C - 200°C
KBr1	2	4	0.947	0.578	3.6	No	105	105	100°C - 200°C
VCl3	6	9	0.919	0.619	0.0	No	179	179	100°C - 200°C
GaI3	0	3	1.049	0.329	5.1	Yes	83	153	100°C - 200°C
MnCl2	6	9	0.928	0.571	6.4	No	103	103	100°C - 200°C
SrF2	2	4	0.975	0.484	8.7	No	54	54	50°C - 100°C
KCl1	0	1	0.928	0.567	5.7	No	86	86	50°C - 100°C
PbF2	2	4	1.036	0.320	3.0	No	75	75	50°C - 100°C
BeI2	7	12	0.946	0.524	6.3	Yes	-96	135	Wide Temp. Window
SnCl2	2	4	0.980	0.449	0.0	No	129	129	100°C - 200°C
VBr4	5	8	0.986	0.402	8.9	No	199	199	100°C - 200°C
YBr3	6	10	0.972	0.429	7.9	Yes	-94	245	Wide Temp. Window
PbCl4	5	8	0.971	0.411	6.6	No	190	190	100°C - 200°C
HfF4	2	3	1.015	0.262	9.5	Yes	281	281	200°C - 300°C
SrI2	4	7	0.969	0.386	9.0	No	9	203	Wide Temp. Window
CaI2	6	9	0.940	0.447	9.4	No	193	193	100°C - 200°C
CaBr2	0	1	0.975	0.347	0.0	No	245	245	200°C - 300°C
PbCl2	2	4	0.975	0.333	0.0	No	127	127	100°C - 200°C
MnCl4	3	5	0.913	0.468	0.4	No	187	187	100°C - 200°C
MgBr2	1	2	0.959	0.360	8.2	No	270	270	200°C - 300°C
MgI2	0	1	0.988	0.268	8.6	No	270	270	200°C - 300°C
AlBr3	6	9	0.906	0.466	0.0	No	183	183	100°C - 200°C
NiCl2	0	1	0.959	0.337	0.0	No	67	67	50°C - 100°C
SrI2	8	12	0.881	0.499	8.9	No	193	235	200°C - 300°C
GaCl3	0	1	0.922	0.406	0.0	Yes	267	267	200°C - 300°C
BeI2	4	7	0.922	0.405	2.4	Yes	86	86	50°C - 100°C
NaBr1	1	2	0.913	0.418	3.0	No	124	124	100°C - 200°C
CoCl3	6	9	0.853	0.526	6.0	No	121	121	100°C - 200°C
SnI2	0	2	0.970	0.249	8.7	No	76	76	50°C - 100°C
SrBr2	0	1	0.965	0.255	3.6	No	192	192	100°C - 200°C
GaBr3	6	9	0.899	0.431	9.4	Yes	192	192	100°C - 200°C
MgBr2	4	6	0.893	0.430	6.1	No	157	157	100°C - 200°C
HfF4	3	5	0.932	0.332	0.0	Yes	119	119	100°C - 200°C
YCl3	6	9	0.820	0.544	0.0	Yes	22	357	Wide Temp. Window
RbBr1	2	4	0.874	0.440	5.8	Yes	85	85	50°C - 100°C
CaI2	2	4	0.908	0.358	1.1	No	176	176	100°C - 200°C
MgBr2	9	12	0.815	0.533	2.0	No	214	214	200°C - 300°C
ScBr3	6	9	0.859	0.456	0.0	Yes	193	193	100°C - 200°C
CaBr2	9	12	0.804	0.544	9.7	No	244	244	200°C - 300°C
SnBr2	2	4	0.910	0.328	0.0	No	120	120	100°C - 200°C
YI3	6	10	0.898	0.358	2.9	Yes	31	189	Wide Temp. Window
GaI3	3	6	0.920	0.294	6.7	Yes	102	102	100°C - 200°C
PbBr2	2	4	0.917	0.269	0.6	No	132	132	100°C - 200°C
SrBr2	4	6	0.883	0.365	8.2	No	171	171	100°C - 200°C
KI1	2	4	0.844	0.444	5.7	No	89	89	50°C - 100°C
SnCl4	3	5	0.871	0.385	5.1	No	177	202	100°C - 200°C

CsF1	1	2	0.893	0.329	0.0	Yes	151	151	100°C - 200°C
MgI2	4	6	0.862	0.362	0.6	No	206	206	200°C - 300°C
SrBr2	6	9	0.843	0.400	9.4	No	101	101	100°C - 200°C
SrBr2	2	4	0.859	0.350	8.2	No	110	110	100°C - 200°C
RbCl1	0	1	0.837	0.381	5.1	Yes	90	90	50°C - 100°C
ZnBr2	9	12	0.788	0.465	9.8	No	195	195	100°C - 200°C
CaCl2	1	2	0.801	0.435	2.5	No	165	165	100°C - 200°C
ZrF4	3	5	0.816	0.395	4.7	Yes	75	75	50°C - 100°C
NaI1	1	2	0.839	0.331	2.3	No	148	148	100°C - 200°C
KBr1	0	1	0.814	0.375	4.6	No	79	79	50°C - 100°C
LiCl1	2	3	0.734	0.515	3.2	No	67	67	50°C - 100°C
SrI2	4	6	0.840	0.309	6.7	No	203	203	200°C - 300°C
SrI2	6	9	0.822	0.349	4.3	No	9	235	Wide Temp. Window
LaBr3	6	10	0.814	0.348	7.6	No	-35	213	Wide Temp. Window
GeF4	2	3	0.822	0.329	4.5	Yes	183	183	100°C - 200°C
KCl1	1	2	0.723	0.498	5.7	No	104	104	100°C - 200°C
SrBr2	9	12	0.742	0.469	9.4	No	223	223	200°C - 300°C
MgI2	1	2	0.834	0.265	8.6	No	298	298	200°C - 300°C
SnI2	2	4	0.829	0.263	8.7	No	127	127	100°C - 200°C
LaI3	6	10	0.795	0.305	0.9	No	-52	247	Wide Temp. Window
GeF4	3	4	0.777	0.347	4.5	Yes	251	251	200°C - 300°C
YBr3	6	9	0.754	0.392	0.0	Yes	96	245	Wide Temp. Window
BaBr2	0	1	0.823	0.206	0.0	No	172	172	100°C - 200°C
TiF4	2	3	0.763	0.366	4.0	No	173	173	100°C - 200°C
BaI2	2	4	0.798	0.245	2.4	No	116	116	100°C - 200°C
YI3	6	9	0.777	0.298	0.0	Yes	100	189	100°C - 200°C
MgI2	9	12	0.720	0.415	0.0	No	195	195	100°C - 200°C
SrBr2	1	2	0.796	0.239	3.6	No	191	191	100°C - 200°C
BeI2	8	12	0.721	0.399	6.3	Yes	-96	105	Wide Temp. Window
SrI2	2	4	0.773	0.286	6.7	No	131	131	100°C - 200°C
SnF4	2	3	0.776	0.275	3.9	No	195	195	100°C - 200°C
SrI2	0	1	0.793	0.187	0.0	No	187	187	100°C - 200°C
AlI3	6	9	0.749	0.319	0.0	No	142	142	100°C - 200°C
CaI2	9	12	0.698	0.416	4.4	No	211	211	200°C - 300°C
ScI3	6	9	0.738	0.330	0.0	Yes	25	305	Wide Temp. Window
YBr3	7	10	0.732	0.323	7.9	Yes	-94	245	Wide Temp. Window
BaI2	0	1	0.780	0.178	0.0	No	226	226	200°C - 300°C
ZnI2	9	12	0.703	0.370	9.9	No	179	179	100°C - 200°C
GaI3	6	9	0.731	0.299	6.7	Yes	145	145	100°C - 200°C
CaI2	0	1	0.756	0.226	4.0	No	209	209	200°C - 300°C
CrI3	6	9	0.725	0.302	3.8	No	137	137	100°C - 200°C
LiCl1	3	4	0.640	0.453	3.8	No	82	82	50°C - 100°C
MgBr2	6	8	0.678	0.389	8.9	No	164	164	100°C - 200°C
LiBr1	2	3	0.688	0.357	2.3	No	71	71	50°C - 100°C
RbBr1	0	1	0.722	0.278	5.8	Yes	76	76	50°C - 100°C
SnBr4	3	5	0.736	0.238	9.8	No	144	171	100°C - 200°C
TiF4	3	4	0.682	0.361	4.0	No	211	211	200°C - 300°C
BaI2	6	9	0.713	0.291	4.6	No	94	94	50°C - 100°C

YCl3	7	9	0.638	0.423	8.8	Yes	134	357	Wide Temp. Window
CaBr2	1	2	0.713	0.280	0.0	No	179	179	100°C - 200°C
LaI3	6	9	0.715	0.266	0.0	No	22	247	Wide Temp. Window
SnF4	3	4	0.709	0.278	3.9	No	235	235	200°C - 300°C
RbCl1	1	2	0.662	0.354	5.1	Yes	107	107	100°C - 200°C
MgI2	6	8	0.678	0.316	2.9	No	183	183	100°C - 200°C
LaCl3	6	9	0.638	0.390	1.8	No	23	123	Wide Temp. Window
SrI2	9	12	0.646	0.366	4.3	No	193	193	100°C - 200°C
KI1	0	1	0.683	0.274	5.2	No	72	72	50°C - 100°C
VI3	6	9	0.675	0.287	0.0	No	116	116	100°C - 200°C
GeF4	4	5	0.660	0.310	1.3	Yes	234	234	200°C - 300°C
TiF4	4	5	0.638	0.352	3.1	No	243	243	200°C - 300°C
MnCl4	2	3	0.660	0.308	0.0	No	256	256	200°C - 300°C
KBr1	1	2	0.638	0.344	4.6	No	92	92	50°C - 100°C
CaI2	4	6	0.662	0.289	9.4	No	124	124	100°C - 200°C
BeI2	9	12	0.624	0.345	9.7	Yes	105	105	100°C - 200°C
BaI2	4	6	0.660	0.238	2.4	No	133	133	100°C - 200°C
SnF4	4	5	0.642	0.269	2.4	No	252	252	200°C - 300°C
GaI3	1	3	0.656	0.206	5.1	Yes	83	83	50°C - 100°C
YI3	7	10	0.638	0.254	2.9	Yes	31	181	Wide Temp. Window
LaBr3	7	10	0.629	0.269	7.6	No	-35	213	Wide Temp. Window
SrI2	7	9	0.629	0.267	9.0	No	139	235	100°C - 200°C
GaCl3	1	2	0.619	0.282	4.5	Yes	137	137	100°C - 200°C
LaI3	7	10	0.634	0.244	7.7	No	-52	247	Wide Temp. Window
BaBr2	1	2	0.650	0.184	0.0	No	146	146	100°C - 200°C
CaI2	1	2	0.628	0.222	4.0	No	229	229	200°C - 300°C
LiI1	2	3	0.612	0.260	7.9	No	61	61	50°C - 100°C
LaBr3	6	9	0.595	0.296	1.6	No	30	213	Wide Temp. Window
BaI2	9	12	0.584	0.315	4.6	No	164	164	100°C - 200°C
SrI2	1	2	0.637	0.172	0.0	No	171	171	100°C - 200°C
RbI1	0	1	0.596	0.211	9.6	Yes	60	60	50°C - 100°C
ScI3	7	9	0.573	0.256	7.7	Yes	180	305	Wide Temp. Window
RbBr1	1	2	0.569	0.258	5.8	Yes	82	82	50°C - 100°C
YCl3	6	8	0.546	0.302	9.6	Yes	22	134	Wide Temp. Window
YBr3	6	8	0.572	0.247	3.7	Yes	96	157	100°C - 200°C
YI3	6	8	0.579	0.218	0.0	Yes	181	189	100°C - 200°C
LiBr1	3	4	0.538	0.295	6.9	No	48	48	< 50°C
YBr3	7	9	0.542	0.282	3.9	Yes	157	245	200°C - 300°C
KI1	1	2	0.557	0.251	5.7	No	74	74	50°C - 100°C
BaI2	1	2	0.574	0.139	0.0	No	135	135	100°C - 200°C
LaI3	7	9	0.545	0.203	7.7	No	155	247	200°C - 300°C
LaCl3	7	9	0.464	0.284	4.6	No	123	123	100°C - 200°C
SrI2	6	8	0.496	0.209	8.9	No	9	139	Wide Temp. Window
ScI3	6	8	0.500	0.192	6.3	Yes	25	180	Wide Temp. Window
YI3	7	9	0.499	0.191	0.0	Yes	100	181	100°C - 200°C
SnCl4	3	4	0.489	0.208	5.1	No	202	202	200°C - 300°C
MgBr2	8	9	0.465	0.248	8.9	No	314	314	300°C - 450°C
ScCl3	3	4	0.447	0.247	9.9	Yes	105	105	100°C - 200°C

GaI3	0	1	0.485	0.133	2.7	Yes	153	153	100°C - 200°C
YBr3	8	10	0.453	0.200	7.9	Yes	-94	245	Wide Temp. Window
LaBr3	7	9	0.430	0.214	4.2	No	34	213	Wide Temp. Window
LaBr3	8	10	0.442	0.189	7.6	No	-35	213	Wide Temp. Window
BeI2	7	9	0.422	0.201	9.7	Yes	-96	135	Wide Temp. Window
LaI3	6	8	0.439	0.159	5.9	No	22	155	Wide Temp. Window
YCl3	8	9	0.388	0.257	9.6	Yes	357	357	300°C - 450°C
SnCl4	4	5	0.424	0.187	2.6	No	177	177	100°C - 200°C
LaBr3	6	8	0.416	0.170	0.0	No	30	34	< 50°C
MgI2	8	9	0.395	0.179	2.9	No	267	267	200°C - 300°C
LaI3	8	10	0.402	0.155	5.9	No	-52	247	Wide Temp. Window
SnBr4	3	4	0.407	0.127	9.8	No	171	171	100°C - 200°C
PbCl4	4	5	0.390	0.142	7.1	No	155	155	100°C - 200°C
YI3	8	10	0.382	0.152	2.9	Yes	31	100	50°C - 100°C
BeBr2	8	9	0.334	0.192	9.5	Yes	162	162	100°C - 200°C
SrI2	8	9	0.348	0.147	8.9	No	235	235	200°C - 300°C
SnBr4	4	5	0.356	0.115	4.0	No	144	144	100°C - 200°C
VBr4	4	5	0.346	0.122	8.9	No	111	111	100°C - 200°C
YCl3	7	8	0.316	0.175	9.6	Yes	134	134	100°C - 200°C
ScI3	8	9	0.321	0.144	6.3	Yes	305	305	300°C - 450°C
BeI2	7	8	0.314	0.146	2.4	Yes	135	135	100°C - 200°C
YI3	6	7	0.317	0.113	0.0	Yes	189	189	100°C - 200°C
YBr3	7	8	0.307	0.133	3.9	Yes	157	157	100°C - 200°C
YBr3	8	9	0.296	0.154	3.7	Yes	245	245	200°C - 300°C
ScI3	7	8	0.302	0.116	7.7	Yes	180	180	100°C - 200°C
LaI3	8	9	0.299	0.111	5.9	No	247	247	200°C - 300°C
SrI2	7	8	0.294	0.124	9.0	No	139	139	100°C - 200°C
YBr3	6	7	0.290	0.119	3.9	Yes	96	96	50°C - 100°C
YI3	7	8	0.287	0.108	0.0	Yes	181	181	100°C - 200°C
LaBr3	8	9	0.264	0.131	1.6	No	213	213	200°C - 300°C
YCl3	6	7	0.255	0.134	8.8	Yes	22	22	< 50°C
LaCl3	6	7	0.261	0.117	4.6	No	23	23	< 50°C
LaI3	7	8	0.259	0.094	7.7	No	155	155	100°C - 200°C
LaBr3	6	7	0.245	0.088	4.2	No	30	30	< 50°C
YI3	8	9	0.225	0.086	0.0	Yes	100	100	50°C - 100°C
SrI2	6	7	0.221	0.088	9.0	No	9	9	< 50°C
ScI3	6	7	0.214	0.079	7.7	Yes	25	25	< 50°C
LaBr3	7	8	0.209	0.086	4.2	No	34	34	< 50°C
LaI3	6	7	0.192	0.067	7.7	No	22	22	< 50°C
YI3	9	10	0.172	0.068	2.9	Yes	31	31	< 50°C
LaBr3	9	10	0.145	0.062	7.6	No	-35	-35	< 50°C
BeI2	8	9	0.128	0.061	9.7	Yes	-96	-96	< 50°C
LaI3	9	10	0.120	0.046	0.9	No	-52	-52	< 50°C
YBr3	9	10	0.116	0.051	7.9	Yes	-94	-94	< 50°C

Table C.3 1393 hypothetical (de)hydration reactions that are predicted to lie within 25 meV/atom of the convex hull are characterized by the number of water molecules per formula unit in the dehydrated (n_{low}) and hydrated (n_{high}) states, volumetric (VED) and gravimetric (GED) energy densities, maximum distance to the convex hull (E_{hull}),

whether the hydrate contains an expensive metal, minimum ($T_{turn,min}$) and maximum ($T_{turn,max}$) turning temperatures of the (de)hydration reaction(s), and temperature category. Reactions are ordered by descending $ED_{RMS} = \sqrt{VED^2 + GED^2}$.

Salt	n_{low}	n_{high}	VED (GJ/m^3)	GED (MJ/kg)	E_{hull} (meV/at.)	Expensive Metal	$T_{turn,min}$ (°C)	$T_{turn,max}$ (°C)	Temp. Categ.
CoF3	0	9	4.397	2.498	0.0	No	256	256	200°C - 300°C
BeCl2	0	4	3.816	2.508	0.0	Yes	380	380	300°C - 450°C
AlCl3	0	9	3.714	2.585	0.0	No	202	361	200°C - 300°C
BeCl2	0	7	3.718	2.558	11.8	Yes	60	380	Wide Temp. Window
AlCl3	0	6	3.833	2.302	0.0	No	361	361	300°C - 450°C
BeCl2	0	9	3.660	2.529	18.6	Yes	-21	380	Wide Temp. Window
CrF3	0	9	3.765	2.311	0.0	No	178	256	200°C - 300°C
NiF2	0	12	3.716	2.367	9.4	No	33	215	Wide Temp. Window
BeCl2	0	8	3.584	2.517	17.6	Yes	-21	380	Wide Temp. Window
MgCl2	0	12	3.392	2.701	0.0	No	124	288	200°C - 300°C
BeCl2	0	12	3.407	2.651	13.4	Yes	-21	380	Wide Temp. Window
MgCl2	0	9	3.560	2.401	7.5	No	124	288	200°C - 300°C
CoF2	0	12	3.587	2.318	17.5	No	141	141	100°C - 200°C
GeF4	0	8	3.738	2.025	1.9	Yes	110	440	Wide Temp. Window
AlF3	0	9	3.537	2.349	0.0	No	63	248	Wide Temp. Window
VF2	0	12	3.522	2.364	0.0	No	139	139	100°C - 200°C
ZnF2	0	12	3.533	2.249	0.0	No	-16	286	Wide Temp. Window
MnF4	0	5	3.736	1.890	18.6	No	299	299	200°C - 300°C
GeF4	0	5	3.789	1.782	0.0	Yes	183	440	Wide Temp. Window
MoF3	0	9	3.662	2.019	0.0	No	181	270	200°C - 300°C
MgF2	0	12	3.375	2.459	0.0	No	9	224	Wide Temp. Window
CuF2	0	12	3.515	2.238	1.4	No	39	223	Wide Temp. Window
NiF2	0	4	3.759	1.640	0.0	No	201	201	200°C - 300°C
BeBr2	0	9	3.553	2.040	6.6	Yes	78	423	Wide Temp. Window
BeBr2	0	8	3.595	1.954	9.5	Yes	78	423	Wide Temp. Window
CrF3	0	6	3.664	1.819	21.2	No	178	178	100°C - 200°C
BeBr2	0	4	3.681	1.688	0.0	Yes	423	423	300°C - 450°C
CuF2	0	6	3.670	1.703	18.3	No	45	179	Wide Temp. Window
MgBr2	0	9	3.519	1.873	2.0	No	157	314	Wide Temp. Window
AlBr3	0	9	3.524	1.813	0.0	No	183	387	Wide Temp. Window
SiF4	0	8	3.344	2.089	5.8	No	103	232	100°C - 200°C
BeBr2	0	12	3.315	2.116	11.7	Yes	46	423	Wide Temp. Window
MgBr2	0	12	3.290	2.153	0.0	No	157	314	Wide Temp. Window
MgCl2	0	6	3.351	2.027	12.5	No	124	288	200°C - 300°C
MgCl2	1	12	3.062	2.438	0.0	No	124	254	100°C - 200°C
GeF4	0	4	3.565	1.591	1.3	Yes	183	440	Wide Temp. Window
CuF2	0	9	3.421	1.872	21.1	No	39	179	Wide Temp. Window
AlBr3	0	6	3.564	1.542	0.0	No	387	387	300°C - 450°C
SnF4	0	8	3.482	1.700	0.0	No	124	438	Wide Temp. Window
CuF2	0	4	3.549	1.522	15.2	No	179	179	100°C - 200°C
ZnF2	1	12	3.246	2.066	12.8	No	-16	286	Wide Temp. Window
VF4	0	8	3.290	1.991	1.2	No	129	254	100°C - 200°C
NiF2	0	8	3.337	1.892	16.1	No	33	201	Wide Temp. Window

BeF2	0	12	3.102	2.251	17.1	Yes	41	134	Wide Temp. Window
VCl2	0	12	3.083	2.272	23.2	No	165	165	100°C - 200°C
MgCl2	0	8	3.091	2.260	12.2	No	124	288	200°C - 300°C
AlF3	0	6	3.350	1.821	19.1	No	63	234	Wide Temp. Window
BeF2	0	9	3.128	2.176	14.0	Yes	41	134	Wide Temp. Window
MoF3	0	6	3.466	1.525	15.9	No	181	181	100°C - 200°C
TiF4	0	8	3.219	1.993	0.0	No	121	278	100°C - 200°C
CaCl2	0	12	2.944	2.375	0.0	No	67	270	Wide Temp. Window
TiF3	0	9	3.156	2.058	6.8	No	145	145	100°C - 200°C
SiF4	0	5	3.273	1.821	5.0	No	168	232	200°C - 300°C
ZnF2	0	4	3.433	1.487	0.0	No	127	192	100°C - 200°C
ZnF2	0	6	3.386	1.592	19.2	No	-14	192	Wide Temp. Window
BeI2	0	8	3.377	1.574	0.0	Yes	86	452	Wide Temp. Window
MgCl2	1	9	3.088	2.083	7.5	No	124	254	100°C - 200°C
BeF2	0	8	3.051	2.121	14.2	Yes	41	134	Wide Temp. Window
BeI2	0	7	3.401	1.494	2.4	Yes	86	452	Wide Temp. Window
ZnF2	0	9	3.248	1.786	25.0	No	-16	192	Wide Temp. Window
NaF1	0	4	3.103	2.019	0.0	No	87	156	100°C - 200°C
CaF2	0	12	2.971	2.205	0.0	No	0	203	Wide Temp. Window
MgI2	0	9	3.365	1.525	0.0	No	183	298	200°C - 300°C
SnF4	0	5	3.371	1.413	0.0	No	195	438	Wide Temp. Window
GeF4	0	3	3.388	1.355	4.5	Yes	183	440	Wide Temp. Window
BeF2	0	4	3.134	1.852	4.8	Yes	76	134	100°C - 200°C
BeF2	0	7	2.994	2.070	13.0	Yes	41	134	Wide Temp. Window
ZnF2	0	8	3.173	1.764	20.2	No	-14	192	Wide Temp. Window
CoCl2	0	12	2.951	2.078	17.3	No	137	137	100°C - 200°C
NiCl2	0	12	2.942	2.042	14.4	No	67	147	100°C - 200°C
ZnCl2	0	12	2.926	2.047	0.0	No	53	220	Wide Temp. Window
VF4	0	5	3.153	1.675	5.0	No	197	254	200°C - 300°C
BeI2	0	4	3.336	1.265	0.0	Yes	452	452	450°C - 600°C
ScF3	0	9	2.970	1.976	0.0	Yes	71	235	Wide Temp. Window
MgBr2	1	12	2.979	1.949	8.2	No	157	314	Wide Temp. Window
MgI2	0	12	3.077	1.773	0.0	No	183	298	200°C - 300°C
LiF1	0	4	2.944	1.949	15.6	No	54	54	50°C - 100°C
MgCl2	2	12	2.757	2.196	0.0	No	124	254	100°C - 200°C
MgF2	0	4	3.052	1.711	3.2	No	121	121	100°C - 200°C
TiF4	0	5	3.058	1.689	0.0	No	173	278	200°C - 300°C
MgBr2	1	9	3.077	1.637	8.2	No	157	314	Wide Temp. Window
CaCl2	0	9	2.868	1.973	15.7	No	67	187	100°C - 200°C
GeF2	0	12	2.893	1.912	14.8	Yes	64	153	100°C - 200°C
ZnF2	2	12	2.918	1.858	7.9	No	-16	286	Wide Temp. Window
CaCl2	1	12	2.689	2.170	0.0	No	67	270	Wide Temp. Window
KF1	0	4	2.834	1.971	0.0	No	157	194	100°C - 200°C
MgBr2	0	8	2.992	1.714	8.9	No	157	285	200°C - 300°C
VBr2	0	12	2.933	1.814	20.8	No	123	208	100°C - 200°C
MgF2	0	8	2.869	1.911	24.5	No	9	121	Wide Temp. Window
GeF4	0	2	3.254	1.127	0.0	Yes	440	440	300°C - 450°C
MnCl2	0	9	2.931	1.805	6.4	No	103	174	100°C - 200°C

GaCl3	0	9	2.911	1.822	0.0	Yes	100	267	100°C - 200°C
MgBr2	0	6	3.094	1.489	6.1	No	157	285	200°C - 300°C
CaBr2	0	12	2.844	1.924	0.0	No	48	268	Wide Temp. Window
CrCl3	0	9	2.861	1.897	0.0	No	190	190	100°C - 200°C
LiCl1	0	4	2.800	1.982	3.8	No	67	173	100°C - 200°C
TiCl3	0	9	2.800	1.952	13.8	No	197	197	100°C - 200°C
VBr2	0	9	3.033	1.512	12.8	No	123	173	100°C - 200°C
MgCl2	0	4	2.875	1.770	0.0	No	202	288	200°C - 300°C
ZnCl2	0	9	2.914	1.694	12.5	No	53	214	Wide Temp. Window
CuCl2	0	12	2.756	1.903	2.4	No	-40	185	Wide Temp. Window
SiF4	0	4	2.946	1.592	11.8	No	168	232	200°C - 300°C
SnF4	0	4	3.115	1.221	2.4	No	195	438	Wide Temp. Window
SnF4	1	8	3.002	1.466	19.9	No	124	438	Wide Temp. Window
NiCl2	1	12	2.735	1.898	14.4	No	115	147	100°C - 200°C
RbF1	0	4	2.923	1.586	0.0	Yes	155	344	Wide Temp. Window
MgI2	0	8	3.015	1.403	2.9	No	183	298	200°C - 300°C
SrF2	0	12	2.750	1.845	4.0	No	-1	173	Wide Temp. Window
AlF3	2	9	2.750	1.827	7.5	No	63	248	Wide Temp. Window
TiF4	1	8	2.798	1.732	10.5	No	121	278	100°C - 200°C
CaBr2	0	9	2.878	1.586	9.7	No	48	268	Wide Temp. Window
CaCl2	0	6	2.839	1.646	16.7	No	67	187	100°C - 200°C
AlF3	0	3	2.932	1.468	0.0	No	167	234	200°C - 300°C
ScCl3	0	6	2.798	1.690	0.0	Yes	105	361	Wide Temp. Window
MnCl4	0	8	2.833	1.615	0.0	No	187	256	200°C - 300°C
MgI2	1	9	2.967	1.344	8.6	No	183	298	200°C - 300°C
ZnBr2	0	12	2.804	1.654	0.0	No	27	320	Wide Temp. Window
MgCl2	1	8	2.623	1.918	12.2	No	124	245	100°C - 200°C
ZnF2	1	9	2.848	1.566	25.0	No	-16	192	Wide Temp. Window
AlI3	0	6	3.034	1.108	0.0	No	379	379	300°C - 450°C
MgI2	1	12	2.799	1.612	8.6	No	183	298	200°C - 300°C
SnF2	0	12	2.759	1.668	7.8	No	16	130	Wide Temp. Window
YCl3	0	8	2.818	1.558	9.6	Yes	22	283	Wide Temp. Window
YCl3	0	6	2.887	1.406	0.0	Yes	75	283	Wide Temp. Window
MgCl2	2	9	2.653	1.789	7.5	No	124	254	100°C - 200°C
MgBr2	2	12	2.677	1.751	0.5	No	157	314	Wide Temp. Window
MnCl2	0	6	2.812	1.519	3.6	No	124	174	100°C - 200°C
CoBr2	0	12	2.743	1.633	0.0	No	114	187	100°C - 200°C
CuCl2	0	9	2.764	1.574	16.0	No	-40	145	Wide Temp. Window
ZrCl4	0	8	2.792	1.514	1.7	Yes	183	238	200°C - 300°C
VF4	0	4	2.819	1.440	11.0	No	197	224	200°C - 300°C
HfCl4	0	8	2.898	1.270	7.1	Yes	201	251	200°C - 300°C
NiCl2	0	6	2.826	1.422	7.2	No	67	132	50°C - 100°C
HfF4	0	8	2.906	1.245	0.0	Yes	-29	281	Wide Temp. Window
LiCl1	0	3	2.588	1.815	3.2	No	67	173	100°C - 200°C
YF3	0	9	2.695	1.647	0.0	Yes	11	226	Wide Temp. Window
ZnBr2	0	9	2.846	1.355	9.8	No	27	320	Wide Temp. Window
SrF2	0	9	2.765	1.513	16.7	No	-1	94	< 50°C
TiCl4	0	8	2.707	1.612	14.0	No	188	188	100°C - 200°C

YCl3	0	7	2.787	1.461	8.8	Yes	22	283	Wide Temp. Window
ZnF2	1	8	2.748	1.528	20.2	No	-14	192	Wide Temp. Window
CaCl2	2	12	2.447	1.974	2.5	No	67	270	Wide Temp. Window
YCl3	0	9	2.619	1.737	0.0	Yes	22	357	Wide Temp. Window
NiBr2	0	12	2.716	1.577	9.7	No	118	118	100°C - 200°C
MgCl2	1	6	2.685	1.624	12.5	No	124	245	100°C - 200°C
MnBr2	0	9	2.803	1.403	3.3	No	103	162	100°C - 200°C
CaCl2	0	8	2.479	1.909	13.3	No	67	187	100°C - 200°C
BaF2	0	9	2.821	1.349	15.0	No	4	224	Wide Temp. Window
CaF2	2	12	2.510	1.863	7.4	No	0	203	Wide Temp. Window
TiF4	0	4	2.758	1.459	3.1	No	173	278	200°C - 300°C
CoBr2	0	9	2.810	1.336	13.3	No	114	114	100°C - 200°C
CaBr2	1	12	2.575	1.743	0.0	No	48	268	Wide Temp. Window
ZnCl2	0	6	2.770	1.388	11.2	No	97	123	100°C - 200°C
VCl4	0	8	2.679	1.556	0.0	No	120	214	100°C - 200°C
CaI2	0	12	2.657	1.581	0.0	No	115	296	200°C - 300°C
ZnF2	1	6	2.797	1.315	19.2	No	-14	192	Wide Temp. Window
VF3	0	3	2.822	1.259	0.0	No	193	193	100°C - 200°C
GaCl3	0	6	2.735	1.426	7.1	Yes	100	267	100°C - 200°C
LiBr1	0	4	2.702	1.482	6.9	No	48	222	Wide Temp. Window
MgI2	0	6	2.828	1.189	0.6	No	206	298	200°C - 300°C
BeF2	2	12	2.480	1.800	17.1	Yes	41	76	50°C - 100°C
CrCl4	0	8	2.653	1.522	23.7	No	167	167	100°C - 200°C
MgBr2	0	4	2.803	1.208	0.0	No	237	285	200°C - 300°C
VI2	0	12	2.678	1.463	16.3	No	146	178	100°C - 200°C
SnCl4	0	8	2.723	1.368	0.0	No	177	244	200°C - 300°C
CaCl2	1	9	2.510	1.727	15.7	No	67	173	100°C - 200°C
VBr2	0	6	2.800	1.180	22.8	No	123	173	100°C - 200°C
LiCl1	0	2	2.578	1.599	0.0	No	140	173	100°C - 200°C
CaI2	0	9	2.738	1.304	4.4	No	115	296	200°C - 300°C
CaBr2	0	6	2.764	1.241	12.1	No	108	245	100°C - 200°C
BaF2	0	12	2.580	1.587	10.5	No	4	224	Wide Temp. Window
SnF4	0	3	2.855	1.011	3.9	No	195	438	Wide Temp. Window
CaBr2	0	7	2.719	1.316	18.3	No	48	245	Wide Temp. Window
CoCl3	0	9	2.569	1.586	6.0	No	82	164	100°C - 200°C
MnCl2	1	9	2.563	1.578	6.4	No	103	124	100°C - 200°C
MgBr2	2	9	2.647	1.408	2.0	No	157	314	Wide Temp. Window
SnF2	0	8	2.708	1.285	18.5	No	16	115	Wide Temp. Window
GaCl3	1	9	2.539	1.589	0.0	Yes	100	247	100°C - 200°C
CaF2	0	8	2.474	1.669	22.6	No	0	106	Wide Temp. Window
SiF4	0	3	2.673	1.307	19.4	No	168	214	100°C - 200°C
NbCl4	0	8	2.613	1.393	21.9	No	179	179	100°C - 200°C
YBr3	0	8	2.715	1.173	3.7	Yes	96	314	Wide Temp. Window
ZnCl2	0	8	2.516	1.549	18.1	No	53	123	50°C - 100°C
TiBr3	0	9	2.614	1.371	15.0	No	144	611	Wide Temp. Window
MgBr2	1	8	2.559	1.466	8.9	No	157	270	200°C - 300°C
SnF4	1	5	2.705	1.134	19.9	No	195	438	Wide Temp. Window
SrCl2	0	6	2.599	1.326	7.8	No	88	230	Wide Temp. Window

LiBr1	0	3	2.579	1.339	2.3	No	71	222	Wide Temp. Window
CrBr3	0	9	2.600	1.294	0.0	No	-43	590	Wide Temp. Window
CuCl2	0	6	2.603	1.287	19.5	No	-40	145	Wide Temp. Window
ZnF2	1	4	2.664	1.154	12.8	No	184	192	100°C - 200°C
MgI2	2	12	2.506	1.444	0.8	No	183	267	200°C - 300°C
BaCl2	0	12	2.389	1.620	0.0	No	-40	222	Wide Temp. Window
SrF2	0	6	2.622	1.207	19.6	No	-1	94	< 50°C
ScF3	2	9	2.399	1.596	17.5	Yes	123	235	100°C - 200°C
MgI2	1	8	2.611	1.215	8.6	No	183	298	200°C - 300°C
SrI2	0	9	2.646	1.121	4.3	No	9	235	Wide Temp. Window
ZnI2	0	12	2.544	1.336	0.0	No	32	286	Wide Temp. Window
YF3	0	6	2.635	1.136	22.3	Yes	11	152	Wide Temp. Window
BeF2	0	2	2.485	1.430	0.0	Yes	134	134	100°C - 200°C
VF4	0	3	2.598	1.204	13.2	No	224	224	200°C - 300°C
SiF4	2	8	2.426	1.516	14.7	No	103	232	100°C - 200°C
YBr3	0	7	2.645	1.081	3.9	Yes	96	314	Wide Temp. Window
YBr3	0	6	2.675	1.002	0.0	Yes	110	314	Wide Temp. Window
CaBr2	1	9	2.499	1.377	9.7	No	48	268	Wide Temp. Window
LaCl3	0	7	2.601	1.161	4.6	No	23	298	Wide Temp. Window
YCl3	1	8	2.488	1.376	20.7	Yes	22	283	Wide Temp. Window
CoCl3	0	6	2.541	1.269	4.6	No	82	164	100°C - 200°C
ScBr3	0	6	2.593	1.151	0.0	Yes	128	309	Wide Temp. Window
PbCl2	0	12	2.478	1.378	0.0	No	-32	236	Wide Temp. Window
CaBr2	0	8	2.415	1.477	11.4	No	48	268	Wide Temp. Window
YCl3	1	9	2.358	1.564	20.7	Yes	22	357	Wide Temp. Window
BaF2	0	8	2.559	1.199	23.7	No	4	149	Wide Temp. Window
CaBr2	2	12	2.341	1.584	0.0	No	48	268	Wide Temp. Window
ZnF2	0	2	2.679	0.898	7.9	No	127	184	100°C - 200°C
ZnBr2	0	6	2.620	1.052	13.3	No	83	149	100°C - 200°C
CaI2	1	12	2.425	1.444	4.0	No	115	296	200°C - 300°C
TiF4	1	5	2.468	1.363	10.5	No	173	278	200°C - 300°C
BeF2	2	9	2.312	1.608	14.0	Yes	41	76	50°C - 100°C
YI3	0	10	2.613	1.041	2.9	Yes	31	312	Wide Temp. Window
MgCl2	4	12	2.198	1.750	0.0	No	124	254	100°C - 200°C
GeF2	0	4	2.506	1.264	12.1	Yes	92	153	100°C - 200°C
TiBr3	0	8	2.566	1.129	14.2	No	144	144	100°C - 200°C
ZnI2	0	9	2.588	1.075	9.9	No	32	286	Wide Temp. Window
HfBr4	0	8	2.654	0.899	16.9	Yes	221	221	200°C - 300°C
MnI2	0	9	2.568	1.120	0.0	No	128	128	100°C - 200°C
TiF4	0	3	2.525	1.210	4.0	No	173	278	200°C - 300°C
MgI2	2	9	2.550	1.155	0.8	No	183	267	200°C - 300°C
YI3	0	9	2.612	1.001	0.0	Yes	100	312	Wide Temp. Window
SrI2	0	12	2.433	1.379	0.0	No	9	235	Wide Temp. Window
MgBr2	1	6	2.515	1.210	8.2	No	157	270	200°C - 300°C
YBr3	0	9	2.468	1.284	0.0	Yes	96	314	Wide Temp. Window
GeCl4	0	8	2.440	1.336	13.9	Yes	137	137	100°C - 200°C
ScI3	0	8	2.594	0.998	6.3	Yes	25	251	Wide Temp. Window
BaF2	0	6	2.566	1.066	17.3	No	28	149	Wide Temp. Window

GeF2	2	12	2.317	1.531	14.8	Yes	64	92	50°C - 100°C
SrBr2	0	6	2.565	1.061	2.7	No	110	192	100°C - 200°C
MgF2	4	12	2.242	1.633	3.2	No	9	224	Wide Temp. Window
WCl4	0	8	2.550	1.080	5.0	No	92	203	Wide Temp. Window
GeBr2	0	12	2.353	1.456	9.8	Yes	81	155	100°C - 200°C
CaF2	0	4	2.380	1.409	2.2	No	72	106	50°C - 100°C
HfF4	0	5	2.604	0.929	0.0	Yes	-29	281	Wide Temp. Window
NaF1	0	2	2.413	1.348	13.0	No	87	87	50°C - 100°C
PbCl4	0	8	2.545	1.077	0.0	No	155	218	100°C - 200°C
LiBr1	0	2	2.524	1.126	0.0	No	180	222	200°C - 300°C
NiF2	4	12	2.327	1.483	9.4	No	33	215	Wide Temp. Window
GeF4	2	8	2.426	1.315	1.9	Yes	110	251	100°C - 200°C
SnF4	0	2	2.641	0.794	0.0	No	271	438	300°C - 450°C
AlF3	3	9	2.297	1.526	0.0	No	63	248	Wide Temp. Window
SrF2	2	12	2.283	1.531	4.0	No	-1	173	Wide Temp. Window
NiCl3	1	9	2.376	1.381	24.5	No	57	165	100°C - 200°C
CaI2	0	7	2.530	1.065	12.2	No	115	229	100°C - 200°C
YCl3	1	6	2.468	1.202	20.7	Yes	75	283	Wide Temp. Window
AlF3	0	2	2.525	1.071	7.5	No	167	167	100°C - 200°C
LaBr3	0	10	2.521	1.080	7.6	No	-35	278	Wide Temp. Window
BaCl2	0	9	2.420	1.271	15.5	No	-40	197	Wide Temp. Window
CuCl2	0	4	2.463	1.183	0.0	No	145	145	100°C - 200°C
YCl3	1	7	2.420	1.268	20.7	Yes	22	283	Wide Temp. Window
ZnF2	2	9	2.391	1.314	25.0	No	-16	192	Wide Temp. Window
ScI3	0	9	2.486	1.111	0.0	Yes	25	305	Wide Temp. Window
TiF4	2	8	2.314	1.432	0.7	No	121	243	100°C - 200°C
ZrBr4	0	8	2.531	0.999	7.4	Yes	150	219	100°C - 200°C
RbF1	0	2	2.485	1.103	0.0	Yes	171	344	Wide Temp. Window
PbCl2	0	9	2.509	1.040	19.5	No	-32	214	Wide Temp. Window
MgCl2	2	8	2.191	1.603	12.2	No	124	202	100°C - 200°C
NiCl2	1	6	2.411	1.213	7.2	No	115	132	100°C - 200°C
CaCl2	1	8	2.137	1.646	13.3	No	67	173	100°C - 200°C
VBr3	1	9	2.398	1.220	18.4	No	176	258	200°C - 300°C
KF1	0	2	2.301	1.393	0.0	No	158	194	100°C - 200°C
LaCl3	0	6	2.450	1.098	0.0	No	80	298	Wide Temp. Window
CaI2	1	9	2.414	1.150	4.4	No	115	296	200°C - 300°C
YI3	0	8	2.503	0.941	0.0	Yes	117	312	Wide Temp. Window
ZrF4	0	3	2.509	0.915	0.0	Yes	126	314	Wide Temp. Window
CaCl2	1	6	2.310	1.340	16.7	No	67	173	100°C - 200°C
LiI1	0	4	2.415	1.138	12.9	No	2	243	Wide Temp. Window
ZnF2	4	12	2.250	1.433	0.0	No	-16	286	Wide Temp. Window
HfF4	0	3	2.581	0.666	0.0	Yes	154	281	200°C - 300°C
GaCl3	2	9	2.256	1.412	4.5	Yes	100	247	100°C - 200°C
LaBr3	0	7	2.503	0.897	4.2	No	30	278	Wide Temp. Window
ZnBr2	0	8	2.374	1.186	21.6	No	27	149	Wide Temp. Window
MgI2	0	4	2.486	0.912	0.0	No	263	298	200°C - 300°C
LaF3	0	9	2.311	1.289	8.6	No	28	166	Wide Temp. Window
LiI1	0	3	2.433	1.033	7.9	No	61	243	Wide Temp. Window

SnF4	2	8	2.375	1.160	0.0	No	124	252	100°C - 200°C
MnCl4	0	5	2.352	1.206	0.4	No	187	256	200°C - 300°C
HfCl4	0	5	2.472	0.932	20.8	Yes	251	251	200°C - 300°C
BaCl2	1	12	2.184	1.481	11.3	No	-40	222	Wide Temp. Window
ScI3	0	7	2.474	0.911	7.7	Yes	25	251	Wide Temp. Window
SnF2	2	12	2.256	1.364	7.8	No	16	130	Wide Temp. Window
CaCl2	2	9	2.170	1.493	15.7	No	67	173	100°C - 200°C
BeF2	2	8	2.157	1.500	14.2	Yes	41	76	50°C - 100°C
TiBr4	0	8	2.425	1.008	17.8	No	169	169	100°C - 200°C
PbCl2	1	12	2.294	1.275	20.8	No	-32	236	Wide Temp. Window
VBr2	0	4	2.453	0.921	20.4	No	173	173	100°C - 200°C
CrBr3	0	8	2.396	1.059	22.3	No	-43	146	Wide Temp. Window
NaBr1	0	4	2.302	1.249	5.7	No	-20	173	Wide Temp. Window
CuF2	4	12	2.209	1.406	15.2	No	39	223	Wide Temp. Window
ZnCl2	0	4	2.369	1.110	8.7	No	123	123	100°C - 200°C
SiF4	0	2	2.407	1.016	14.7	No	214	214	200°C - 300°C
MnCl2	1	6	2.295	1.239	3.6	No	124	124	100°C - 200°C
KF1	1	4	2.138	1.487	8.7	No	157	194	100°C - 200°C
YF3	2	9	2.222	1.358	23.3	Yes	11	226	Wide Temp. Window
CaCl2	0	4	2.177	1.427	0.0	No	165	187	100°C - 200°C
SrI2	0	8	2.399	1.010	8.9	No	9	203	Wide Temp. Window
ZrCl4	0	5	2.335	1.131	12.2	Yes	183	238	200°C - 300°C
ZnF2	2	8	2.263	1.258	20.2	No	-14	192	Wide Temp. Window
ScCl3	0	4	2.265	1.253	9.9	Yes	105	361	Wide Temp. Window
PbBr2	0	12	2.316	1.154	0.9	No	-47	216	Wide Temp. Window
CrBr3	0	7	2.374	1.024	12.5	No	146	146	100°C - 200°C
VI2	0	6	2.425	0.888	22.0	No	146	146	100°C - 200°C
VBr4	0	8	2.390	0.973	0.0	No	81	199	100°C - 200°C
GeCl2	2	12	2.077	1.508	12.3	Yes	86	149	100°C - 200°C
SrI2	1	12	2.221	1.258	0.0	No	9	235	Wide Temp. Window
YI3	0	7	2.402	0.858	0.0	Yes	117	312	Wide Temp. Window
BaCl2	0	8	2.279	1.142	21.8	No	-40	172	Wide Temp. Window
NbBr4	0	8	2.376	0.922	23.5	No	166	166	100°C - 200°C
GaBr3	0	6	2.382	0.898	9.4	Yes	43	256	Wide Temp. Window
CaI2	2	12	2.184	1.300	0.0	No	115	296	200°C - 300°C
MgI2	1	6	2.339	0.984	8.6	No	206	298	200°C - 300°C
LaI3	0	9	2.375	0.884	0.0	No	22	263	Wide Temp. Window
SrI2	1	9	2.331	0.988	4.3	No	9	235	Wide Temp. Window
SnF4	1	4	2.356	0.923	19.9	No	195	438	Wide Temp. Window
CaI2	0	8	2.234	1.168	11.7	No	115	229	100°C - 200°C
MoBr4	0	8	2.355	0.896	4.3	No	71	193	100°C - 200°C
MgBr2	4	12	2.108	1.379	0.0	No	157	314	Wide Temp. Window
ScF3	0	3	2.249	1.119	1.3	Yes	71	235	Wide Temp. Window
LaBr3	0	8	2.324	0.952	0.0	No	30	278	Wide Temp. Window
CaCl2	4	12	1.954	1.576	0.0	No	67	270	Wide Temp. Window
LaCl3	1	7	2.290	1.022	18.6	No	23	298	Wide Temp. Window
PbBr2	0	9	2.353	0.867	18.6	No	-47	198	Wide Temp. Window
SrI2	0	6	2.352	0.866	0.0	No	131	203	100°C - 200°C

KCl1	0	4	2.000	1.509	0.0	No	86	117	100°C - 200°C
BaCl2	0	6	2.261	1.057	6.7	No	37	172	Wide Temp. Window
CaF2	4	12	2.003	1.486	2.2	No	0	203	Wide Temp. Window
MgCl2	0	2	2.186	1.200	0.0	No	245	288	200°C - 300°C
MnBr2	0	4	2.329	0.885	0.7	No	162	162	100°C - 200°C
SrI2	0	7	2.314	0.921	9.0	No	9	203	Wide Temp. Window
BaF2	0	4	2.339	0.853	13.1	No	28	149	Wide Temp. Window
NiCl2	0	4	2.238	1.089	13.9	No	67	115	50°C - 100°C
CaBr2	1	7	2.239	1.084	18.3	No	48	179	Wide Temp. Window
LaBr3	1	10	2.285	0.979	16.4	No	-35	278	Wide Temp. Window
GaF3	4	9	2.152	1.243	23.9	Yes	164	255	200°C - 300°C
LaBr3	0	6	2.339	0.840	0.0	No	114	278	100°C - 200°C
GaCl3	1	6	2.203	1.148	7.1	Yes	100	247	100°C - 200°C
GaF3	0	3	2.308	0.916	0.0	Yes	-42	400	Wide Temp. Window
YI3	0	6	2.356	0.768	0.0	Yes	117	312	Wide Temp. Window
CaBr2	2	9	2.168	1.195	9.7	No	48	268	Wide Temp. Window
ZnBr2	0	4	2.330	0.830	10.2	No	149	149	100°C - 200°C
CaBr2	0	4	2.261	0.996	1.2	No	170	245	200°C - 300°C
NiCl2	4	12	2.027	1.407	14.4	No	132	147	100°C - 200°C
ScI3	0	6	2.312	0.860	0.0	Yes	251	251	200°C - 300°C
YCl3	2	9	2.056	1.363	12.5	Yes	22	357	Wide Temp. Window
MnCl4	2	8	2.142	1.221	0.0	No	187	256	200°C - 300°C
MgBr2	2	8	2.138	1.225	8.9	No	157	237	100°C - 200°C
TiI3	0	9	2.250	0.992	11.1	No	173	173	100°C - 200°C
SnCl4	0	5	2.247	0.993	0.0	No	177	244	200°C - 300°C
NiCl3	1	6	2.182	1.125	24.5	No	137	165	100°C - 200°C
SrCl2	1	6	2.184	1.114	14.5	No	88	230	Wide Temp. Window
LiCl1	1	4	1.997	1.414	3.8	No	67	140	100°C - 200°C
MgCl2	1	4	2.080	1.281	0.0	No	202	245	200°C - 300°C
SnF2	0	4	2.240	0.952	1.7	No	84	115	50°C - 100°C
BeF2	2	7	2.002	1.384	13.0	Yes	41	76	50°C - 100°C
WBr4	0	8	2.309	0.763	12.6	No	120	200	100°C - 200°C
CaI2	0	6	2.228	0.972	9.4	No	124	229	100°C - 200°C
CaBr2	1	6	2.217	0.995	12.1	No	108	179	100°C - 200°C
BaF2	2	12	2.068	1.273	10.5	No	4	224	Wide Temp. Window
VCl4	0	5	2.153	1.124	6.3	No	120	214	100°C - 200°C
LaF3	0	6	2.261	0.885	24.6	No	28	40	< 50°C
ZnCl2	4	12	1.989	1.391	8.7	No	53	220	Wide Temp. Window
LiI1	0	2	2.268	0.855	0.0	No	207	243	200°C - 300°C
3-Feb	0	6	2.269	0.846	23.4	No	117	117	100°C - 200°C
MgCl2	2	6	2.071	1.252	12.5	No	124	202	100°C - 200°C
VCl4	2	8	2.092	1.215	22.0	No	158	214	100°C - 200°C
GaCl3	0	4	2.191	1.020	21.0	Yes	100	267	100°C - 200°C
PbCl2	1	9	2.232	0.925	20.8	No	-32	214	Wide Temp. Window
ZnI2	0	8	2.222	0.941	20.3	No	32	191	Wide Temp. Window
MgI2	2	8	2.187	1.018	2.9	No	183	263	200°C - 300°C
AlF3	2	6	2.118	1.152	19.1	No	63	234	Wide Temp. Window
CaBr2	1	8	2.055	1.257	11.4	No	48	268	Wide Temp. Window

YCl3	2	8	2.107	1.165	12.5	Yes	22	283	Wide Temp. Window
BeF2	4	12	1.947	1.413	17.1	Yes	41	68	50°C - 100°C
BaCl2	1	9	2.116	1.112	15.5	No	-40	197	Wide Temp. Window
TiF4	0	2	2.189	0.939	0.7	No	205	278	200°C - 300°C
PbBr2	1	12	2.129	1.061	18.8	No	-47	216	Wide Temp. Window
YF3	0	4	2.206	0.884	20.4	Yes	11	152	Wide Temp. Window
SrF2	2	9	2.084	1.141	16.7	No	-1	77	< 50°C
ScF3	3	9	1.976	1.315	1.3	Yes	123	123	100°C - 200°C
SiF4	3	8	2.012	1.256	19.4	No	103	232	100°C - 200°C
ZnI2	0	6	2.233	0.791	19.7	No	32	191	Wide Temp. Window
HfF4	2	8	2.176	0.932	9.5	Yes	-29	281	Wide Temp. Window
BaCl2	2	12	1.958	1.328	0.0	No	-40	222	Wide Temp. Window
LaBr3	0	9	2.113	1.052	1.6	No	30	278	Wide Temp. Window
TiF4	1	4	2.085	1.103	10.5	No	173	278	200°C - 300°C
GeF2	0	2	2.194	0.849	11.2	Yes	153	153	100°C - 200°C
CrI3	0	9	2.171	0.904	0.0	No	13	385	Wide Temp. Window
ZnF2	2	6	2.127	1.000	19.2	No	-14	192	Wide Temp. Window
MoCl4	2	8	2.080	1.090	12.6	No	162	230	100°C - 200°C
HfF4	0	4	2.229	0.739	12.0	Yes	-29	281	Wide Temp. Window
NiBr3	0	9	2.145	0.935	19.9	No	-3	144	Wide Temp. Window
BaBr2	0	6	2.175	0.858	3.5	No	23	190	Wide Temp. Window
LaI3	0	8	2.189	0.794	5.9	No	22	263	Wide Temp. Window
ZnI2	2	12	2.062	1.083	20.7	No	32	286	Wide Temp. Window
PbCl2	2	12	2.035	1.131	0.0	No	-32	236	Wide Temp. Window
LaCl3	1	6	2.124	0.952	18.6	No	113	298	200°C - 300°C
GaCl3	3	9	1.973	1.235	16.9	Yes	100	247	100°C - 200°C
LaBr3	1	7	2.191	0.785	16.4	No	30	278	Wide Temp. Window
GeI2	0	12	2.039	1.110	14.6	Yes	63	87	50°C - 100°C
SrI2	2	12	2.015	1.142	0.0	No	9	235	Wide Temp. Window
CaI2	1	7	2.132	0.898	12.2	No	115	229	100°C - 200°C
SrF2	0	4	2.067	1.026	8.7	No	54	94	50°C - 100°C
CaI2	2	9	2.077	0.989	4.4	No	115	296	200°C - 300°C
ZrCl4	0	4	2.080	0.979	16.9	Yes	238	238	200°C - 300°C
CaF2	0	2	2.122	0.882	7.4	No	72	72	50°C - 100°C
PbF2	0	4	2.194	0.677	3.0	No	75	115	50°C - 100°C
VF4	3	8	1.962	1.187	13.2	No	129	254	100°C - 200°C
SnCl4	2	8	2.045	1.028	14.2	No	177	244	200°C - 300°C
VBr2	4	12	1.946	1.203	20.8	No	123	208	100°C - 200°C
CaCl2	2	8	1.812	1.395	13.3	No	67	173	100°C - 200°C
ScCl3	2	6	1.954	1.180	19.9	Yes	105	361	Wide Temp. Window
BaF2	2	9	2.058	0.985	15.0	No	4	224	Wide Temp. Window
GeF4	3	8	2.006	1.087	4.5	Yes	110	251	100°C - 200°C
GeBr2	2	12	1.940	1.200	10.4	Yes	81	155	100°C - 200°C
NaI1	0	4	2.065	0.960	12.9	No	-13	148	Wide Temp. Window
SrBr2	1	6	2.104	0.870	3.6	No	110	191	100°C - 200°C
NaCl1	0	2	1.949	1.172	0.0	No	106	106	100°C - 200°C
CaBr2	4	12	1.881	1.273	1.2	No	48	268	Wide Temp. Window
YBr3	2	8	2.083	0.900	20.5	Yes	96	314	Wide Temp. Window

CoBr3	0	6	2.126	0.781	11.3	No	90	90	50°C - 100°C
SnCl2	0	4	2.059	0.943	0.0	No	129	169	100°C - 200°C
TiF4	3	8	1.921	1.189	4.0	No	121	243	100°C - 200°C
MgI2	4	12	1.956	1.127	0.0	No	183	267	200°C - 300°C
RbF1	1	4	1.982	1.075	0.0	Yes	155	171	100°C - 200°C
YCl3	2	7	1.995	1.045	12.5	Yes	22	283	Wide Temp. Window
PbCl2	0	6	2.105	0.800	19.3	No	-32	214	Wide Temp. Window
MgBr2	1	4	2.065	0.890	8.2	No	237	270	200°C - 300°C
SrF2	4	12	1.866	1.252	8.7	No	-1	173	Wide Temp. Window
SrI2	1	8	2.071	0.872	8.9	No	9	203	Wide Temp. Window
SiF4	2	5	1.956	1.089	14.7	No	168	232	200°C - 300°C
MgCl2	4	9	1.854	1.251	7.5	No	124	254	100°C - 200°C
ScCl3	0	3	1.948	1.095	0.0	Yes	180	361	Wide Temp. Window
ZnF2	6	12	1.879	1.196	19.2	No	-16	286	Wide Temp. Window
LaBr3	1	8	2.060	0.844	16.4	No	30	278	Wide Temp. Window
CuBr2	0	4	2.093	0.753	0.0	No	108	108	100°C - 200°C
BeCl2	4	12	1.753	1.363	13.4	Yes	-21	122	Wide Temp. Window
YF3	3	9	1.892	1.156	12.9	Yes	11	226	Wide Temp. Window
GaI3	0	9	2.052	0.838	0.0	Yes	83	153	100°C - 200°C
SrCl2	0	4	1.966	1.020	10.4	No	88	230	Wide Temp. Window
YBr3	2	9	1.963	1.021	20.5	Yes	96	314	Wide Temp. Window
MgCl2	6	12	1.730	1.378	12.5	No	168	254	200°C - 300°C
RbF1	0	1	2.085	0.736	0.0	Yes	344	344	300°C - 450°C
PbBr2	1	9	2.075	0.764	18.8	No	-47	198	Wide Temp. Window
YCl3	0	4	1.972	0.993	12.8	Yes	75	283	Wide Temp. Window
ScBr3	0	4	2.060	0.790	17.8	Yes	128	237	100°C - 200°C
YCl3	2	6	1.983	0.966	12.5	Yes	75	283	Wide Temp. Window
LaI3	0	6	2.099	0.671	0.0	No	153	263	200°C - 300°C
SrI2	2	9	2.027	0.859	4.3	No	9	235	Wide Temp. Window
ZrI4	0	8	2.081	0.698	17.6	Yes	171	171	100°C - 200°C
NiBr3	0	6	2.051	0.768	4.9	No	23	144	Wide Temp. Window
RbCl1	0	4	1.866	1.147	0.0	Yes	90	113	100°C - 200°C
TiI4	0	8	2.072	0.708	24.2	No	151	151	100°C - 200°C
LiCl1	0	1	1.904	1.078	0.0	No	173	173	100°C - 200°C
LaBr3	2	10	2.011	0.861	14.3	No	-35	278	Wide Temp. Window
GeF2	4	12	1.824	1.206	14.8	Yes	64	64	50°C - 100°C
LaI3	0	7	2.064	0.719	7.7	No	22	263	Wide Temp. Window
PbCl4	0	5	2.052	0.749	6.6	No	155	218	100°C - 200°C
SnF4	3	8	1.962	0.958	3.9	No	124	252	100°C - 200°C
BaCl2	1	8	1.944	0.974	21.8	No	-40	172	Wide Temp. Window
CaF2	2	8	1.802	1.216	22.6	No	0	106	Wide Temp. Window
CaI2	1	8	1.927	1.007	11.7	No	115	229	100°C - 200°C
SnCl4	0	4	1.993	0.850	2.6	No	199	244	200°C - 300°C
MgBr2	2	6	1.952	0.939	6.1	No	157	237	100°C - 200°C
GeBr2	0	4	2.016	0.787	0.0	Yes	120	155	100°C - 200°C
KBr1	0	4	1.846	1.126	0.0	No	79	105	50°C - 100°C
BaI2	0	6	2.029	0.730	0.0	No	116	226	100°C - 200°C
ZnBr2	4	12	1.857	1.095	10.2	No	27	320	Wide Temp. Window

ZrBr4	0	5	2.029	0.697	19.2	Yes	150	219	100°C - 200°C
CrI3	0	8	2.003	0.766	14.1	No	13	136	Wide Temp. Window
VCl4	0	4	1.915	0.963	19.3	No	120	214	100°C - 200°C
LaBr3	1	6	2.016	0.724	16.4	No	177	278	200°C - 300°C
GeF4	2	5	1.935	0.910	0.0	Yes	183	251	200°C - 300°C
LiBr1	1	4	1.873	1.028	6.9	No	48	180	Wide Temp. Window
CrI3	0	6	2.031	0.663	3.8	No	136	136	100°C - 200°C
LaCl3	2	7	1.950	0.870	22.8	No	23	298	Wide Temp. Window
LaBr3	1	9	1.903	0.947	16.4	No	30	278	Wide Temp. Window
NaBr1	0	3	1.887	0.977	19.0	No	-20	127	Wide Temp. Window
CsF1	0	2	1.993	0.735	0.0	Yes	151	249	100°C - 200°C
CuCl2	4	12	1.748	1.207	2.4	No	-40	185	Wide Temp. Window
SnF2	2	8	1.913	0.908	18.5	No	16	84	50°C - 100°C
PbBr2	2	12	1.893	0.943	0.9	No	-47	216	Wide Temp. Window
CoCl3	3	9	1.799	1.111	18.3	No	121	164	100°C - 200°C
WF4	3	8	1.955	0.798	7.6	No	168	168	100°C - 200°C
WCl4	0	5	1.983	0.719	18.9	No	92	203	Wide Temp. Window
YBr3	2	7	1.951	0.797	20.5	Yes	96	314	Wide Temp. Window
PbCl2	0	4	1.991	0.681	0.0	No	73	214	Wide Temp. Window
SrI2	1	7	1.953	0.777	9.0	No	9	203	Wide Temp. Window
PbF2	0	2	2.061	0.403	0.0	No	115	115	100°C - 200°C
SnF2	4	12	1.793	1.084	7.8	No	16	130	Wide Temp. Window
PbCl4	2	8	1.929	0.817	20.8	No	155	218	100°C - 200°C
CaCl2	2	6	1.807	1.048	16.7	No	67	173	100°C - 200°C
MgBr2	4	9	1.839	0.978	2.0	No	157	314	Wide Temp. Window
GaBr3	1	6	1.948	0.734	13.6	Yes	43	256	Wide Temp. Window
VI4	0	8	1.974	0.658	8.9	No	123	123	100°C - 200°C
MgBr2	0	2	1.944	0.730	0.5	No	270	285	200°C - 300°C
CuF2	6	12	1.750	1.114	18.3	No	39	223	Wide Temp. Window
SrI2	1	6	1.946	0.716	0.0	No	131	203	100°C - 200°C
SnF4	1	3	1.953	0.692	19.9	No	195	438	Wide Temp. Window
ZnI2	2	9	1.910	0.794	20.7	No	32	286	Wide Temp. Window
ZnI2	0	4	1.961	0.636	12.0	No	115	191	100°C - 200°C
YCl3	3	9	1.713	1.136	0.9	Yes	22	357	Wide Temp. Window
BaCl2	1	6	1.861	0.870	11.3	No	37	172	Wide Temp. Window
SrBr2	0	4	1.901	0.774	8.2	No	110	192	100°C - 200°C
PbBr2	0	6	1.943	0.647	20.6	No	-47	198	Wide Temp. Window
VBr4	2	8	1.896	0.772	20.2	No	111	199	100°C - 200°C
CaI2	0	4	1.904	0.751	1.1	No	176	229	200°C - 300°C
SrF2	0	2	1.935	0.663	0.8	No	94	94	50°C - 100°C
CaBr2	2	8	1.741	1.065	11.4	No	48	268	Wide Temp. Window
TiF4	2	5	1.787	0.987	0.7	No	173	243	200°C - 300°C
CaI2	4	12	1.752	1.043	1.1	No	115	296	200°C - 300°C
GaCl3	0	3	1.846	0.863	16.9	Yes	137	267	200°C - 300°C
GaCl3	2	6	1.799	0.938	7.1	Yes	100	247	100°C - 200°C
CaCl2	6	12	1.577	1.273	16.7	No	83	270	Wide Temp. Window
GaCl3	4	9	1.715	1.073	21.0	Yes	209	247	200°C - 300°C
CaBr2	2	7	1.821	0.882	18.3	No	48	170	Wide Temp. Window

SnI4	0	5	1.946	0.537	19.7	No	101	292	100°C - 200°C
MoBr4	2	8	1.883	0.717	11.6	No	177	193	100°C - 200°C
YBr3	2	6	1.887	0.707	20.5	Yes	110	314	Wide Temp. Window
NaBr1	0	2	1.831	0.838	0.0	No	124	127	100°C - 200°C
BaCl2	2	9	1.782	0.936	15.5	No	-40	197	Wide Temp. Window
NaF1	2	4	1.686	1.097	13.0	No	156	156	100°C - 200°C
MnCl4	3	8	1.744	0.994	0.0	No	187	194	100°C - 200°C
CuI2	2	12	1.783	0.921	17.3	No	-9	137	Wide Temp. Window
PbBr4	0	8	1.900	0.633	3.6	No	40	175	Wide Temp. Window
BaF2	0	2	1.914	0.583	0.0	No	149	149	100°C - 200°C
BaF2	4	12	1.703	1.048	13.1	No	4	224	Wide Temp. Window
VCl4	3	8	1.728	1.004	12.6	No	158	199	100°C - 200°C
MnCl4	0	3	1.809	0.844	0.0	No	187	256	200°C - 300°C
PbCl2	2	9	1.842	0.764	19.5	No	-32	127	Wide Temp. Window
CaI2	1	6	1.827	0.797	9.4	No	124	229	100°C - 200°C
SnF4	2	5	1.836	0.770	0.0	No	195	252	200°C - 300°C
MgI2	1	4	1.869	0.685	8.6	No	263	298	200°C - 300°C
LiCl1	1	3	1.625	1.140	3.2	No	67	140	100°C - 200°C
BaCl2	4	12	1.643	1.114	15.1	No	-40	222	Wide Temp. Window
GeCl2	4	12	1.606	1.166	12.3	Yes	86	86	50°C - 100°C
YF3	2	6	1.821	0.786	23.3	Yes	11	152	Wide Temp. Window
LiBr1	0	1	1.859	0.689	0.0	No	222	222	200°C - 300°C
BaCl2	0	4	1.827	0.766	15.1	No	37	172	Wide Temp. Window
MgI2	2	6	1.826	0.768	0.8	No	206	263	200°C - 300°C
SnBr2	0	4	1.863	0.671	0.0	No	120	139	100°C - 200°C
NiCl3	3	9	1.704	0.990	13.0	No	57	137	50°C - 100°C
BeBr2	4	12	1.660	1.060	11.7	Yes	46	162	Wide Temp. Window
BeF2	4	9	1.612	1.122	14.0	Yes	41	68	50°C - 100°C
YF3	4	9	1.672	1.022	20.4	Yes	56	226	Wide Temp. Window
PbBr2	0	4	1.871	0.549	0.0	No	98	198	100°C - 200°C
GaI3	1	9	1.803	0.736	2.7	Yes	83	145	100°C - 200°C
ZnF2	2	4	1.786	0.774	7.9	No	192	192	100°C - 200°C
MgBr2	6	12	1.629	1.066	6.1	No	164	314	Wide Temp. Window
GaI3	0	6	1.850	0.591	6.7	Yes	83	153	100°C - 200°C
LaBr3	2	7	1.828	0.655	14.3	No	30	278	Wide Temp. Window
RbBr1	0	4	1.734	0.873	5.0	Yes	-35	205	Wide Temp. Window
SnF2	0	2	1.848	0.588	0.0	No	115	115	100°C - 200°C
LaCl3	2	6	1.768	0.792	22.8	No	176	298	200°C - 300°C
NaI1	0	3	1.771	0.785	16.7	No	-13	148	Wide Temp. Window
MgI2	4	9	1.765	0.799	0.0	No	183	267	200°C - 300°C
VBr3	3	9	1.725	0.877	19.9	No	176	181	100°C - 200°C
CaCl2	1	4	1.618	1.061	0.0	No	165	173	100°C - 200°C
YBr3	0	4	1.811	0.675	14.1	Yes	110	314	Wide Temp. Window
VBr4	0	5	1.817	0.639	8.9	No	81	189	100°C - 200°C
NiCl2	1	4	1.731	0.842	13.9	No	115	115	100°C - 200°C
NaBr1	1	4	1.687	0.916	5.7	No	-20	173	Wide Temp. Window
BaF2	2	8	1.736	0.813	23.7	No	4	39	< 50°C
YI3	3	10	1.778	0.709	11.7	Yes	31	312	Wide Temp. Window

YCl3	3	8	1.674	0.926	9.6	Yes	22	278	Wide Temp. Window
WI4	0	8	1.838	0.527	11.8	No	104	104	100°C - 200°C
KCl1	1	4	1.525	1.151	5.7	No	104	117	100°C - 200°C
PbCl4	0	4	1.800	0.632	7.1	No	167	218	100°C - 200°C
CaBr2	2	6	1.740	0.781	12.1	No	108	170	100°C - 200°C
YCl3	0	3	1.699	0.861	0.9	Yes	151	283	200°C - 300°C
SrI2	2	8	1.753	0.738	8.9	No	9	203	Wide Temp. Window
BaBr2	1	6	1.769	0.698	3.5	No	23	190	Wide Temp. Window
WCl4	3	8	1.746	0.740	18.7	No	203	203	200°C - 300°C
MoBr4	0	5	1.802	0.588	15.5	No	71	177	100°C - 200°C
LaBr3	2	8	1.753	0.718	14.3	No	30	278	Wide Temp. Window
TiF4	1	3	1.707	0.818	10.5	No	173	278	200°C - 300°C
ZnCl2	6	12	1.550	1.085	11.2	No	53	220	Wide Temp. Window
YF3	0	3	1.731	0.756	12.9	Yes	32	152	Wide Temp. Window
ZrBr4	0	4	1.793	0.595	22.0	Yes	219	219	200°C - 300°C
SrI2	4	12	1.642	0.930	6.7	No	9	235	Wide Temp. Window
PbCl2	1	6	1.761	0.669	20.8	No	-32	214	Wide Temp. Window
HfF4	0	2	1.825	0.429	9.5	Yes	154	154	100°C - 200°C
ZnI2	4	12	1.659	0.872	12.0	No	32	286	Wide Temp. Window
SnCl4	3	8	1.674	0.841	5.1	No	177	202	100°C - 200°C
LiI1	1	4	1.693	0.798	12.9	No	2	243	Wide Temp. Window
SnBr4	0	5	1.778	0.575	0.0	No	134	171	100°C - 200°C
CaCl2	0	2	1.642	0.892	2.5	No	165	187	100°C - 200°C
NiCl2	6	12	1.534	1.065	14.4	No	147	147	100°C - 200°C
KI1	0	4	1.650	0.869	4.4	No	72	89	50°C - 100°C
CaI2	2	7	1.718	0.723	12.2	No	115	176	100°C - 200°C
LaF3	3	9	1.625	0.906	18.9	No	28	166	Wide Temp. Window
LaBr3	2	9	1.659	0.826	14.3	No	30	278	Wide Temp. Window
HfF4	3	8	1.702	0.729	0.0	Yes	-29	267	Wide Temp. Window
SrCl2	2	6	1.645	0.839	7.8	No	88	132	100°C - 200°C
PbCl2	4	12	1.610	0.895	0.0	No	-32	236	Wide Temp. Window
ScBr3	0	3	1.720	0.660	8.8	Yes	237	237	200°C - 300°C
YI3	3	9	1.719	0.658	11.7	Yes	100	312	Wide Temp. Window
SrCl2	0	2	1.710	0.667	0.0	No	113	230	100°C - 200°C
PbBr2	2	9	1.722	0.634	18.6	No	-47	132	Wide Temp. Window
YBr3	3	9	1.627	0.846	4.8	Yes	96	299	Wide Temp. Window
SrF2	6	12	1.520	1.020	19.6	No	77	173	100°C - 200°C
ZnCl2	4	9	1.581	0.919	12.5	No	53	214	Wide Temp. Window
KF1	0	1	1.625	0.827	8.7	No	158	158	100°C - 200°C
VBr2	4	9	1.631	0.813	20.4	No	123	155	100°C - 200°C
LaBr3	3	10	1.675	0.717	7.6	No	-35	213	Wide Temp. Window
CuF2	4	9	1.590	0.870	21.1	No	39	45	< 50°C
CaI2	2	8	1.606	0.840	11.7	No	115	176	100°C - 200°C
YBr3	3	8	1.663	0.718	4.8	Yes	96	299	Wide Temp. Window
SiF4	4	8	1.536	0.959	11.8	No	103	229	100°C - 200°C
VBr3	1	4	1.702	0.608	19.7	No	176	258	200°C - 300°C
BaI2	0	4	1.728	0.531	2.4	No	116	226	100°C - 200°C
SnI4	0	4	1.743	0.473	23.6	No	292	292	200°C - 300°C

VF4	4	8	1.543	0.934	11.0	No	129	254	100°C - 200°C
SnCl4	0	3	1.671	0.678	5.1	No	199	244	200°C - 300°C
LaCl3	0	3	1.685	0.639	2.3	No	80	298	Wide Temp. Window
YCl3	4	9	1.499	0.994	12.8	Yes	22	357	Wide Temp. Window
WBr4	0	5	1.731	0.484	21.1	No	120	120	100°C - 200°C
NiI2	4	12	1.593	0.830	20.7	No	5	302	Wide Temp. Window
CaBr2	6	12	1.486	1.006	12.1	No	48	268	Wide Temp. Window
CaCl2	4	9	1.477	1.017	15.7	No	67	160	100°C - 200°C
LiBr1	1	3	1.592	0.826	2.3	No	71	180	100°C - 200°C
NaI1	0	2	1.668	0.658	0.0	No	143	148	100°C - 200°C
SrF2	2	6	1.626	0.748	19.6	No	-1	54	< 50°C
ScF3	0	2	1.630	0.727	17.5	Yes	71	71	50°C - 100°C
CuCl2	6	12	1.467	1.013	19.5	No	80	185	100°C - 200°C
CaBr2	1	4	1.630	0.718	1.2	No	170	179	100°C - 200°C
SrBr2	2	6	1.644	0.679	2.7	No	110	171	100°C - 200°C
VBr2	6	12	1.508	0.933	22.8	No	155	208	100°C - 200°C
MgF2	8	12	1.431	1.042	24.5	No	224	224	200°C - 300°C
ZrF4	0	2	1.675	0.574	17.3	Yes	126	126	100°C - 200°C
BaCl2	2	8	1.576	0.789	21.8	No	-40	136	Wide Temp. Window
TiF4	4	8	1.496	0.926	3.1	No	121	243	100°C - 200°C
GeBr2	4	12	1.489	0.922	9.8	Yes	81	81	50°C - 100°C
LaI3	3	9	1.640	0.611	23.0	No	22	263	Wide Temp. Window
SrI2	0	4	1.636	0.605	6.7	No	131	187	100°C - 200°C
LaBr3	2	6	1.640	0.589	14.3	No	197	278	200°C - 300°C
LaF3	0	3	1.654	0.548	18.9	No	40	40	< 50°C
VCl4	0	3	1.568	0.754	12.6	No	120	214	100°C - 200°C
CaBr2	4	9	1.520	0.838	9.7	No	48	268	Wide Temp. Window
MgCl2	4	8	1.399	1.023	12.2	No	124	168	100°C - 200°C
GeF4	4	8	1.524	0.826	1.9	Yes	110	234	100°C - 200°C
CoCl3	0	3	1.575	0.710	18.3	No	82	82	50°C - 100°C
SrI2	2	7	1.604	0.638	9.0	No	9	203	Wide Temp. Window
BaI2	1	6	1.624	0.584	0.0	No	116	135	100°C - 200°C
PbCl4	3	8	1.586	0.671	10.4	No	155	190	100°C - 200°C
KCl1	0	2	1.413	0.972	4.0	No	86	104	50°C - 100°C
PbF2	6	12	1.534	0.762	23.2	No	70	163	100°C - 200°C
MgI2	0	2	1.628	0.518	0.8	No	270	298	200°C - 300°C
YCl3	3	7	1.513	0.793	8.8	Yes	22	278	Wide Temp. Window
CuI2	2	9	1.572	0.651	23.6	No	-9	137	Wide Temp. Window
VBr4	3	8	1.575	0.642	12.8	No	111	199	100°C - 200°C
RbI1	0	4	1.545	0.701	10.1	Yes	48	83	50°C - 100°C
NiF2	8	12	1.430	0.911	16.1	No	215	215	200°C - 300°C
ZrF4	4	8	1.485	0.817	19.2	Yes	129	262	100°C - 200°C
BeF2	4	8	1.391	0.967	14.2	Yes	41	50	< 50°C
YCl3	1	4	1.512	0.762	20.7	Yes	75	283	Wide Temp. Window
ZnBr2	6	12	1.458	0.860	13.3	No	27	320	Wide Temp. Window
VBr4	0	4	1.604	0.539	7.2	No	81	189	100°C - 200°C
MgI2	6	12	1.465	0.844	0.6	No	183	267	200°C - 300°C
LiI1	1	3	1.556	0.660	7.9	No	61	243	Wide Temp. Window

KF1	2	4	1.386	0.964	0.0	No	157	157	100°C - 200°C
ZnF2	0	1	1.618	0.482	12.8	No	127	127	100°C - 200°C
HfF4	2	5	1.589	0.567	9.5	Yes	-29	281	Wide Temp. Window
PbBr2	1	6	1.600	0.533	20.6	No	-47	198	Wide Temp. Window
SnF4	4	8	1.514	0.739	2.4	No	124	252	100°C - 200°C
GeI2	0	4	1.599	0.527	11.2	Yes	87	87	50°C - 100°C
SrF2	4	9	1.477	0.808	16.7	No	-1	77	< 50°C
SrCl2	1	4	1.494	0.776	14.5	No	88	230	Wide Temp. Window
BeF2	2	4	1.447	0.855	4.8	Yes	76	76	50°C - 100°C
SnCl2	0	2	1.579	0.573	0.0	No	169	169	100°C - 200°C
BeCl2	4	9	1.380	0.954	18.6	Yes	-21	60	< 50°C
BaF2	4	9	1.513	0.724	15.0	No	4	224	Wide Temp. Window
YI3	4	10	1.558	0.621	18.4	Yes	31	312	Wide Temp. Window
AlF3	6	9	1.397	0.928	19.1	No	248	248	200°C - 300°C
YI3	3	8	1.566	0.589	11.7	Yes	117	312	Wide Temp. Window
ZnBr2	4	9	1.508	0.718	10.2	No	27	320	Wide Temp. Window
ZnF2	4	9	1.460	0.803	25.0	No	-16	70	< 50°C
RbCl1	1	4	1.420	0.872	5.1	Yes	107	113	100°C - 200°C
GaCl3	1	4	1.508	0.702	21.0	Yes	100	138	100°C - 200°C
SrBr2	0	2	1.593	0.478	0.0	No	191	192	100°C - 200°C
ZnI2	2	8	1.531	0.648	20.7	No	32	115	Wide Temp. Window
BaBr2	0	4	1.560	0.576	18.7	No	23	172	Wide Temp. Window
GeI4	0	8	1.574	0.526	22.0	Yes	53	53	50°C - 100°C
PbBr2	4	12	1.486	0.740	0.9	No	-47	216	Wide Temp. Window
PbCl2	1	4	1.569	0.537	20.8	No	127	214	100°C - 200°C
SrI2	2	6	1.554	0.572	0.0	No	131	203	100°C - 200°C
SiF4	2	4	1.451	0.784	14.7	No	168	232	200°C - 300°C
YI3	0	4	1.570	0.504	18.4	Yes	117	220	100°C - 200°C
LaBr3	0	3	1.581	0.468	0.6	No	114	278	100°C - 200°C
BaF2	2	6	1.520	0.631	17.3	No	28	39	< 50°C
KBr1	1	4	1.405	0.857	4.6	No	92	105	50°C - 100°C
ZnF2	8	12	1.387	0.883	20.2	No	-16	286	Wide Temp. Window
CaBr2	0	2	1.529	0.601	0.0	No	179	245	200°C - 300°C
NiBr3	3	9	1.500	0.654	22.7	No	-3	144	Wide Temp. Window
CrF3	6	9	1.392	0.855	21.2	No	256	256	200°C - 300°C
MgCl2	0	1	1.464	0.723	0.0	No	288	288	200°C - 300°C
CaI2	4	9	1.474	0.702	4.4	No	115	296	200°C - 300°C
SnCl2	6	12	1.355	0.908	22.8	No	148	148	100°C - 200°C
BeBr2	4	9	1.413	0.811	6.6	Yes	78	162	100°C - 200°C
MnBr2	4	9	1.457	0.729	3.3	No	103	103	100°C - 200°C
NaI1	1	4	1.476	0.686	12.9	No	-13	148	Wide Temp. Window
SnI2	0	4	1.552	0.492	0.0	No	24	127	Wide Temp. Window
HfF4	4	8	1.493	0.640	12.0	Yes	129	267	100°C - 200°C
CsF1	0	1	1.556	0.449	0.0	Yes	249	249	200°C - 300°C
SrCl2	7	12	1.303	0.958	23.6	No	153	244	100°C - 200°C
GaBr3	0	3	1.530	0.527	10.2	Yes	43	256	Wide Temp. Window
YBr3	0	3	1.516	0.561	4.8	Yes	169	314	Wide Temp. Window
MnCl4	2	5	1.438	0.738	0.4	No	187	256	200°C - 300°C

VBr3	4	9	1.440	0.732	19.7	No	181	181	100°C - 200°C
YBr3	3	7	1.489	0.609	4.8	Yes	96	299	Wide Temp. Window
AlF3	3	6	1.409	0.766	19.1	No	63	63	50°C - 100°C
YCl3	4	8	1.403	0.776	12.8	Yes	22	278	Wide Temp. Window
GaF3	6	9	1.387	0.801	17.2	Yes	255	255	200°C - 300°C
SrI2	4	9	1.474	0.625	6.7	No	9	235	Wide Temp. Window
SnBr4	0	4	1.526	0.476	4.0	No	134	171	100°C - 200°C
CaI2	6	12	1.370	0.816	9.4	No	115	296	200°C - 300°C
YCl3	3	6	1.433	0.698	0.9	Yes	75	278	Wide Temp. Window
CaBr2	7	12	1.320	0.893	18.3	No	180	268	200°C - 300°C
ScCl3	3	6	1.363	0.823	0.0	Yes	105	269	100°C - 200°C
VCl4	4	8	1.376	0.799	19.3	No	158	198	100°C - 200°C
GeF4	2	4	1.453	0.649	1.3	Yes	183	251	200°C - 300°C
PbCl4	0	3	1.510	0.497	10.4	No	167	218	100°C - 200°C
YI3	4	9	1.484	0.568	18.4	Yes	100	312	Wide Temp. Window
YBr3	4	9	1.408	0.732	14.1	Yes	96	299	Wide Temp. Window
CaF2	8	12	1.273	0.944	22.6	No	203	203	200°C - 300°C
LaCl3	3	7	1.447	0.646	4.6	No	23	176	Wide Temp. Window
VI2	6	12	1.389	0.759	22.0	No	178	178	100°C - 200°C
ScCl3	0	2	1.417	0.706	19.9	Yes	180	180	100°C - 200°C
RbBr1	0	3	1.452	0.626	21.0	Yes	-35	82	< 50°C
MgCl2	2	4	1.346	0.829	0.0	No	202	202	200°C - 300°C
CsI1	0	4	1.458	0.607	14.5	Yes	72	72	50°C - 100°C
GaCl3	0	2	1.435	0.654	4.5	Yes	137	267	200°C - 300°C
GaI3	1	6	1.501	0.480	6.7	Yes	83	102	50°C - 100°C
GaCl3	3	6	1.394	0.727	16.9	Yes	100	247	100°C - 200°C
BaCl2	2	6	1.421	0.664	6.7	No	37	136	Wide Temp. Window
CuBr2	6	12	1.355	0.787	23.5	No	95	149	100°C - 200°C
CoCl3	3	6	1.401	0.700	18.3	No	164	164	100°C - 200°C
MoF3	6	9	1.370	0.755	15.9	No	270	270	200°C - 300°C
SnF4	1	2	1.496	0.450	19.9	No	438	438	300°C - 450°C
GaBr3	2	6	1.458	0.549	9.4	Yes	43	146	Wide Temp. Window
SiF4	3	5	1.361	0.757	19.4	No	229	232	200°C - 300°C
BaF2	6	12	1.325	0.815	17.3	No	4	224	Wide Temp. Window
LiI1	0	1	1.486	0.461	5.4	No	207	207	200°C - 300°C
VCl4	2	5	1.375	0.718	22.0	No	158	214	100°C - 200°C
MgBr2	4	8	1.346	0.771	8.9	No	157	164	100°C - 200°C
PbCl2	6	12	1.354	0.753	19.3	No	67	236	Wide Temp. Window
MgCl2	8	12	1.210	0.964	12.2	No	237	254	200°C - 300°C
BaCl2	0	2	1.458	0.508	0.0	No	132	172	100°C - 200°C
CaI2	2	6	1.409	0.614	9.4	No	124	176	100°C - 200°C
LiCl1	2	4	1.253	0.887	3.8	No	67	82	50°C - 100°C
MgI2	4	8	1.390	0.647	2.9	No	183	206	100°C - 200°C
MoCl4	2	5	1.388	0.642	12.6	No	162	230	100°C - 200°C
PbI2	0	4	1.472	0.398	4.5	No	54	126	50°C - 100°C
CaI2	1	4	1.416	0.558	4.0	No	176	229	200°C - 300°C
MoCl4	4	8	1.346	0.705	23.8	No	162	197	100°C - 200°C
LaBr3	3	9	1.360	0.677	1.6	No	30	213	Wide Temp. Window

CuI2	4	12	1.349	0.697	17.3	No	-9	136	Wide Temp. Window
ZnI2	6	12	1.343	0.705	19.7	No	63	286	Wide Temp. Window
CuCl2	4	9	1.318	0.750	16.0	No	-40	80	< 50°C
ZrCl4	4	8	1.332	0.723	16.9	Yes	183	197	100°C - 200°C
BeF2	7	12	1.226	0.890	17.1	Yes	41	68	50°C - 100°C
YBr3	4	8	1.389	0.600	14.1	Yes	96	299	Wide Temp. Window
PbBr2	1	4	1.451	0.426	18.8	No	132	198	100°C - 200°C
GeI2	4	12	1.328	0.723	14.6	Yes	63	63	50°C - 100°C
PbCl2	0	2	1.461	0.387	0.0	No	73	214	Wide Temp. Window
NaCl1	0	1	1.321	0.724	4.4	No	106	106	100°C - 200°C
NiF2	4	8	1.310	0.743	16.1	No	33	33	< 50°C
ZnF2	1	2	1.428	0.478	12.8	No	184	184	100°C - 200°C
LaI3	3	8	1.414	0.513	23.0	No	22	263	Wide Temp. Window
GaI3	3	9	1.388	0.567	5.1	Yes	102	145	100°C - 200°C
SnCl4	4	8	1.333	0.670	2.6	No	177	196	100°C - 200°C
BaBr2	2	6	1.386	0.547	3.5	No	23	190	Wide Temp. Window
SrBr2	1	4	1.380	0.562	8.2	No	110	191	100°C - 200°C
LaBr3	3	8	1.378	0.565	0.6	No	30	197	Wide Temp. Window
BaCl2	4	9	1.316	0.691	15.5	No	-40	197	Wide Temp. Window
SnCl4	2	5	1.358	0.600	14.2	No	177	244	200°C - 300°C
RbF1	2	4	1.305	0.708	0.0	Yes	155	155	100°C - 200°C
BaCl2	6	12	1.228	0.833	6.7	No	-40	222	Wide Temp. Window
GeF4	3	5	1.342	0.631	4.5	Yes	234	251	200°C - 300°C
TiF4	2	4	1.309	0.693	3.1	No	173	211	100°C - 200°C
YI3	3	7	1.387	0.496	11.7	Yes	117	312	Wide Temp. Window
GaF3	2	3	1.368	0.543	22.7	Yes	400	400	300°C - 450°C
LaBr3	3	7	1.383	0.496	4.2	No	30	197	Wide Temp. Window
MgBr2	2	4	1.348	0.581	0.5	No	237	237	200°C - 300°C
RbCl1	0	2	1.293	0.691	2.9	Yes	90	107	50°C - 100°C
SnF4	2	4	1.363	0.534	2.4	No	195	235	200°C - 300°C
RbBr1	1	4	1.308	0.658	5.8	Yes	-35	205	Wide Temp. Window
ZnF2	4	8	1.277	0.710	20.2	No	-14	70	< 50°C
LiCl1	1	2	1.239	0.769	0.0	No	140	140	100°C - 200°C
ZnI2	4	9	1.344	0.558	12.0	No	32	286	Wide Temp. Window
YBr3	3	6	1.362	0.510	4.8	Yes	110	299	200°C - 300°C
CaCl2	4	8	1.149	0.885	13.3	No	67	160	100°C - 200°C
SnBr2	6	12	1.255	0.725	20.7	No	46	227	Wide Temp. Window
CaF2	2	4	1.247	0.738	7.4	No	106	106	100°C - 200°C
MnCl4	0	2	1.318	0.577	0.0	No	187	187	100°C - 200°C
MgF2	4	8	1.197	0.797	24.5	No	9	9	< 50°C
BaCl2	1	4	1.324	0.555	15.1	No	37	172	Wide Temp. Window
ScBr3	3	6	1.311	0.582	8.8	Yes	128	309	Wide Temp. Window
NiCl3	3	6	1.274	0.657	12.6	No	137	137	100°C - 200°C
VF4	3	5	1.264	0.671	13.2	No	197	254	200°C - 300°C
MgCl2	6	9	1.186	0.800	12.5	No	168	254	200°C - 300°C
ZnF2	9	12	1.203	0.766	25.0	No	286	286	200°C - 300°C
KBr1	0	2	1.252	0.676	3.6	No	79	92	50°C - 100°C
SrBr2	7	12	1.202	0.760	16.4	No	144	234	100°C - 200°C

ZnCl2	8	12	1.165	0.815	18.1	No	214	220	200°C - 300°C
BeCl2	7	12	1.120	0.871	13.4	Yes	-21	122	Wide Temp. Window
BeCl2	4	8	1.161	0.815	17.6	Yes	-21	60	< 50°C
ZnI2	2	6	1.337	0.473	20.7	No	32	115	Wide Temp. Window
NiCl3	1	3	1.286	0.583	24.5	No	165	165	100°C - 200°C
TiF4	3	5	1.236	0.683	4.0	No	211	243	200°C - 300°C
CaCl2	8	12	1.099	0.886	13.3	No	83	270	Wide Temp. Window
KI1	1	4	1.248	0.657	5.2	No	74	89	50°C - 100°C
YI3	4	8	1.320	0.496	18.4	Yes	181	312	Wide Temp. Window
PbBr2	6	12	1.259	0.627	20.6	No	73	216	Wide Temp. Window
BeF2	4	7	1.151	0.796	13.0	Yes	41	41	< 50°C
KF1	1	2	1.196	0.724	8.7	No	194	194	100°C - 200°C
GeBr2	0	2	1.329	0.427	10.4	Yes	120	120	100°C - 200°C
BaBr2	0	2	1.338	0.379	0.0	No	146	172	100°C - 200°C
YCl3	0	2	1.265	0.577	12.5	Yes	151	217	100°C - 200°C
SnBr2	0	2	1.329	0.383	0.0	No	139	139	100°C - 200°C
ZnCl2	4	8	1.177	0.725	18.1	No	53	97	50°C - 100°C
SrI2	6	12	1.201	0.681	0.0	No	9	235	Wide Temp. Window
PbCl4	4	8	1.270	0.538	7.1	No	155	190	100°C - 200°C
SnF4	0	1	1.327	0.373	19.9	No	271	271	200°C - 300°C
CaI2	7	12	1.183	0.704	12.2	No	167	296	200°C - 300°C
BaI2	2	6	1.292	0.465	0.0	No	116	133	100°C - 200°C
BeBr2	4	8	1.205	0.655	9.5	Yes	78	78	50°C - 100°C
SnF4	3	5	1.263	0.529	3.9	No	235	252	200°C - 300°C
WCl4	0	3	1.302	0.421	18.7	No	92	92	50°C - 100°C
PbBr2	0	2	1.333	0.305	0.6	No	98	198	100°C - 200°C
YCl3	4	7	1.211	0.635	12.8	Yes	22	278	Wide Temp. Window
YF3	3	6	1.255	0.541	22.3	Yes	11	56	< 50°C
ScCl3	2	4	1.195	0.662	19.9	Yes	105	361	Wide Temp. Window
MoI4	3	8	1.300	0.415	11.6	No	120	172	100°C - 200°C
MgBr2	8	12	1.142	0.747	8.9	No	214	314	200°C - 300°C
PbCl2	2	6	1.276	0.485	19.3	No	-32	127	Wide Temp. Window
YI3	0	3	1.298	0.413	11.7	Yes	220	220	200°C - 300°C
YF3	6	9	1.162	0.710	22.3	Yes	226	226	200°C - 300°C
LaCl3	3	6	1.241	0.556	2.3	No	176	176	100°C - 200°C
YCl3	1	3	1.209	0.613	20.7	Yes	217	283	200°C - 300°C
VBr4	4	8	1.253	0.510	7.2	No	111	199	100°C - 200°C
VBr3	1	3	1.275	0.450	19.9	No	258	258	200°C - 300°C
NiI2	4	9	1.243	0.519	24.1	No	5	302	Wide Temp. Window
PbBr4	0	5	1.292	0.370	23.1	No	40	40	< 50°C
SrI2	0	2	1.296	0.350	0.0	No	171	187	100°C - 200°C
VF3	4	6	1.197	0.606	20.1	No	175	175	100°C - 200°C
ZnI2	0	2	1.282	0.382	20.7	No	191	191	100°C - 200°C
PbCl4	2	5	1.250	0.456	20.8	No	155	218	100°C - 200°C
TiF4	0	1	1.236	0.491	10.5	No	205	205	200°C - 300°C
VBr4	0	3	1.265	0.402	12.8	No	81	188	100°C - 200°C
GaBr3	0	2	1.255	0.421	0.0	Yes	195	256	200°C - 300°C
NaBr1	0	1	1.231	0.483	3.0	No	127	127	100°C - 200°C

CaBr2	4	8	1.127	0.689	11.4	No	48	268	Wide Temp. Window
LiBr1	1	2	1.206	0.538	0.0	No	180	180	100°C - 200°C
YF3	0	2	1.223	0.490	23.3	Yes	32	32	< 50°C
LaCl3	1	3	1.232	0.467	18.6	No	113	298	200°C - 300°C
NaBr1	1	3	1.169	0.605	19.0	No	-20	124	Wide Temp. Window
BaI2	0	2	1.277	0.310	0.0	No	135	226	100°C - 200°C
MgBr2	0	1	1.249	0.403	8.2	No	285	285	200°C - 300°C
MgBr2	6	9	1.158	0.616	6.1	No	164	314	Wide Temp. Window
ZrBr4	4	8	1.219	0.481	22.0	Yes	150	196	100°C - 200°C
LaI3	0	3	1.268	0.325	23.0	No	153	153	100°C - 200°C
SnF2	4	8	1.182	0.561	18.5	No	16	16	< 50°C
LaI3	3	7	1.235	0.430	23.0	No	22	263	Wide Temp. Window
CaI2	0	2	1.231	0.436	0.0	No	209	229	200°C - 300°C
SnI2	1	4	1.244	0.394	20.6	No	127	127	100°C - 200°C
SnCl4	0	2	1.218	0.465	14.2	No	199	199	100°C - 200°C
GaF3	4	6	1.184	0.544	23.9	Yes	164	164	100°C - 200°C
PbCl2	4	9	1.203	0.499	19.5	No	-32	67	< 50°C
ZnBr2	8	12	1.121	0.661	21.6	No	195	320	Wide Temp. Window
SrCl2	8	12	1.048	0.771	17.1	No	153	244	100°C - 200°C
MgI2	2	4	1.219	0.447	0.8	No	263	263	200°C - 300°C
GaF3	0	2	1.230	0.414	22.7	Yes	-42	-42	< 50°C
CaCl2	2	4	1.085	0.711	2.5	No	173	173	100°C - 200°C
GeF2	2	4	1.155	0.583	12.1	Yes	92	92	50°C - 100°C
KCl1	2	4	1.028	0.776	4.0	No	117	117	100°C - 200°C
LaCl3	0	2	1.228	0.384	22.8	No	80	113	50°C - 100°C
YBr3	4	7	1.189	0.486	14.1	Yes	96	299	Wide Temp. Window
RbI1	1	4	1.169	0.530	10.1	Yes	48	83	50°C - 100°C
CaF2	4	8	1.063	0.717	22.6	No	0	0	< 50°C
NiBr3	3	6	1.201	0.450	22.7	No	144	144	100°C - 200°C
YF3	2	4	1.186	0.475	23.3	Yes	11	152	Wide Temp. Window
SrI2	1	4	1.197	0.442	6.7	No	131	171	100°C - 200°C
TiF4	1	2	1.173	0.503	10.5	No	278	278	200°C - 300°C
SrI2	4	8	1.176	0.495	8.9	No	9	203	Wide Temp. Window
CuF2	9	12	1.074	0.684	21.1	No	223	223	200°C - 300°C
BaBr2	7	12	1.095	0.649	18.1	No	91	228	Wide Temp. Window
BaI2	1	4	1.216	0.374	2.4	No	116	135	100°C - 200°C
YI3	3	6	1.209	0.394	11.7	Yes	117	312	Wide Temp. Window
LiBr1	2	4	1.115	0.612	6.9	No	48	71	50°C - 100°C
SnBr4	0	3	1.216	0.362	9.8	No	134	134	100°C - 200°C
BaF2	4	8	1.148	0.538	23.7	No	4	39	< 50°C
BeI2	4	8	1.144	0.533	0.0	Yes	86	135	100°C - 200°C
SnI2	6	12	1.118	0.582	22.6	No	42	191	Wide Temp. Window
LiI1	1	2	1.175	0.443	5.4	No	243	243	200°C - 300°C
VF4	5	8	1.074	0.650	5.0	No	129	129	100°C - 200°C
MoBr4	2	5	1.193	0.389	15.5	No	177	177	100°C - 200°C
CaBr2	8	12	1.039	0.703	11.4	No	180	244	200°C - 300°C
SiF4	5	8	1.063	0.664	5.8	No	103	103	100°C - 200°C
LaBr3	3	6	1.179	0.423	0.6	No	197	197	100°C - 200°C

VBr4	2	5	1.178	0.414	20.2	No	111	189	100°C - 200°C
BeCl2	4	7	1.029	0.708	11.8	Yes	60	60	50°C - 100°C
PbI2	6	12	1.132	0.523	24.6	No	50	188	100°C - 200°C
GaBr3	3	6	1.165	0.439	10.2	Yes	146	146	100°C - 200°C
RbBr1	0	2	1.126	0.510	5.8	Yes	76	82	50°C - 100°C
AlCl3	6	9	1.013	0.705	0.0	No	202	202	200°C - 300°C
SrI2	7	12	1.071	0.607	9.0	No	139	235	100°C - 200°C
GaCl3	1	3	1.113	0.521	16.9	Yes	137	138	100°C - 200°C
PbBr2	2	6	1.165	0.388	20.6	No	-47	132	Wide Temp. Window
LaI3	3	6	1.169	0.374	23.0	No	263	263	200°C - 300°C
PbF2	8	12	1.097	0.545	20.8	No	155	163	100°C - 200°C
TiF4	5	8	1.041	0.645	0.0	No	121	121	100°C - 200°C
NaBr1	2	4	1.076	0.584	5.7	No	-20	173	Wide Temp. Window
VCl4	0	2	1.115	0.502	22.0	No	120	120	100°C - 200°C
GeCl2	2	4	1.081	0.571	0.0	Yes	149	149	100°C - 200°C
SnF2	8	12	1.045	0.632	18.5	No	130	130	100°C - 200°C
VCl4	5	8	1.054	0.612	6.3	No	198	198	100°C - 200°C
KI1	0	2	1.111	0.500	5.7	No	72	74	50°C - 100°C
MnCl2	0	1	1.131	0.454	0.0	No	174	174	100°C - 200°C
BeCl2	8	12	0.960	0.747	17.6	Yes	58	122	50°C - 100°C
YCl3	4	6	1.090	0.531	12.8	Yes	278	278	200°C - 300°C
MnCl4	5	8	1.053	0.600	0.4	No	194	194	100°C - 200°C
BeF2	8	12	0.980	0.711	17.1	Yes	41	68	50°C - 100°C
NiBr3	0	3	1.146	0.367	22.7	No	23	23	< 50°C
NaI1	1	3	1.100	0.488	16.7	No	-13	148	Wide Temp. Window
GeF4	5	8	1.057	0.573	1.9	Yes	110	110	100°C - 200°C
BaCl2	8	12	0.992	0.673	21.8	No	197	222	200°C - 300°C
AlF3	2	3	1.071	0.536	7.5	No	234	234	200°C - 300°C
MgCl2	1	2	1.049	0.576	0.0	No	245	245	200°C - 300°C
LaF3	3	6	1.109	0.434	24.6	No	28	28	< 50°C
YI3	4	7	1.120	0.400	18.4	Yes	189	312	Wide Temp. Window
LaBr3	1	3	1.140	0.338	16.4	No	177	278	200°C - 300°C
PbBr2	4	9	1.115	0.411	18.6	No	-47	73	< 50°C
BaCl2	4	8	1.062	0.532	21.8	No	-40	136	Wide Temp. Window
ScCl3	4	6	1.011	0.611	9.9	Yes	269	269	200°C - 300°C
CaBr2	2	4	1.079	0.476	1.2	No	170	170	100°C - 200°C
VCl4	2	4	1.052	0.529	22.0	No	199	214	200°C - 300°C
GaCl3	6	9	0.997	0.624	7.1	Yes	209	209	200°C - 300°C
SrBr2	8	12	0.994	0.629	14.9	No	223	234	200°C - 300°C
ZrF4	5	8	1.029	0.566	4.7	Yes	129	129	100°C - 200°C
SnF4	5	8	1.050	0.513	0.0	No	124	124	100°C - 200°C
MoCl4	2	4	1.068	0.474	23.8	No	230	230	200°C - 300°C
CaI2	4	8	1.034	0.541	11.7	No	115	167	100°C - 200°C
MgI2	6	9	1.063	0.482	0.6	No	183	267	200°C - 300°C
SnF2	2	4	1.074	0.456	1.7	No	84	84	50°C - 100°C
BaF2	8	12	0.990	0.609	23.7	No	106	224	100°C - 200°C
MoCl4	5	8	1.029	0.539	3.1	No	197	197	100°C - 200°C
ZnBr2	4	8	1.037	0.518	21.6	No	27	83	50°C - 100°C

CaCl2	9	12	0.902	0.728	15.7	No	270	270	200°C - 300°C
GaCl3	4	6	1.026	0.535	21.0	Yes	247	247	200°C - 300°C
BaBr2	1	4	1.083	0.400	18.7	No	23	146	Wide Temp. Window
CaCl2	6	9	0.949	0.653	16.7	No	83	160	100°C - 200°C
MgCl2	9	12	0.900	0.717	7.5	No	237	237	200°C - 300°C
MgI2	8	12	0.997	0.574	2.9	No	195	267	200°C - 300°C
PbI4	0	5	1.108	0.307	11.5	No	65	65	50°C - 100°C
ZrCl4	5	8	1.006	0.546	12.2	Yes	197	197	100°C - 200°C
PbCl4	0	2	1.092	0.334	20.8	No	167	167	100°C - 200°C
CoI2	8	12	1.008	0.529	23.4	No	206	206	200°C - 300°C
WCl4	5	8	1.048	0.444	18.9	No	203	203	200°C - 300°C
RbF1	1	2	1.040	0.462	0.0	Yes	171	171	100°C - 200°C
NaCl1	1	2	0.974	0.586	4.4	No	106	106	100°C - 200°C
HfF4	2	4	1.077	0.357	12.0	Yes	-29	281	Wide Temp. Window
NaI1	0	1	1.074	0.362	2.3	No	143	143	100°C - 200°C
NiI2	8	12	1.004	0.523	17.1	No	166	302	Wide Temp. Window
ZrF4	2	3	1.063	0.388	17.3	Yes	314	314	300°C - 450°C
CaI2	8	12	0.972	0.579	11.7	No	211	296	200°C - 300°C
SnCl4	5	8	1.010	0.508	0.0	No	196	196	100°C - 200°C
GeBr2	2	4	1.051	0.410	10.4	Yes	155	155	100°C - 200°C
VBr2	6	9	1.009	0.503	22.8	No	155	155	100°C - 200°C
ZnI2	8	12	0.994	0.522	20.3	No	179	286	200°C - 300°C
HfF4	5	8	1.031	0.442	0.0	Yes	129	129	100°C - 200°C
PbF2	6	9	1.046	0.402	23.2	No	70	163	100°C - 200°C
YBr3	0	2	1.060	0.354	20.5	Yes	169	169	100°C - 200°C
RbCl1	2	4	0.952	0.585	2.9	Yes	113	113	100°C - 200°C
BaI2	7	12	0.982	0.529	11.7	No	99	247	Wide Temp. Window
CaBr2	4	7	1.002	0.485	18.3	No	48	108	Wide Temp. Window
HfCl4	5	8	1.019	0.447	20.8	Yes	201	201	200°C - 300°C
CaCl2	0	1	0.983	0.521	0.0	No	187	187	100°C - 200°C
SrF2	6	9	0.974	0.533	19.6	No	77	77	50°C - 100°C
SnCl4	2	4	1.021	0.435	14.2	No	202	244	200°C - 300°C
KBr1	2	4	0.947	0.578	3.6	No	105	105	100°C - 200°C
VCl3	6	9	0.919	0.619	0.0	No	179	179	100°C - 200°C
NiCl2	4	6	0.990	0.498	13.9	No	132	132	100°C - 200°C
ZnCl2	6	9	0.958	0.557	12.5	No	53	214	Wide Temp. Window
LaF3	6	9	0.964	0.537	24.6	No	166	166	100°C - 200°C
MgCl2	4	6	0.943	0.570	12.5	No	124	124	100°C - 200°C
GaI3	0	3	1.049	0.329	5.1	Yes	83	153	100°C - 200°C
CaBr2	6	9	0.963	0.531	12.1	No	48	268	Wide Temp. Window
LaBr3	0	2	1.058	0.295	14.3	No	114	177	100°C - 200°C
YCl3	2	4	0.980	0.494	12.8	Yes	75	283	Wide Temp. Window
GaCl3	2	4	0.991	0.461	21.0	Yes	100	138	100°C - 200°C
YBr3	4	6	1.021	0.382	14.1	Yes	299	299	200°C - 300°C
MnCl2	6	9	0.928	0.571	6.4	No	103	103	100°C - 200°C
SrF2	2	4	0.975	0.484	8.7	No	54	54	50°C - 100°C
KCl1	0	1	0.928	0.567	5.7	No	86	86	50°C - 100°C
PbF2	2	4	1.036	0.320	3.0	No	75	75	50°C - 100°C

CuF2	6	9	0.948	0.519	21.1	No	39	39	< 50°C
SnCl2	2	4	0.980	0.449	0.0	No	129	129	100°C - 200°C
ZnF2	6	9	0.942	0.518	25.0	No	-16	70	< 50°C
BaBr2	8	12	0.920	0.546	17.6	No	199	228	200°C - 300°C
ZnCl2	9	12	0.877	0.613	12.5	No	220	220	200°C - 300°C
ScF3	2	3	0.956	0.475	17.5	Yes	235	235	200°C - 300°C
ScBr3	4	6	0.975	0.433	17.8	Yes	309	309	300°C - 450°C
VBr4	5	8	0.986	0.402	8.9	No	199	199	100°C - 200°C
CaI2	4	7	0.977	0.411	12.2	No	115	124	100°C - 200°C
MnBr4	5	8	0.982	0.397	12.8	No	198	198	100°C - 200°C
PbCl4	5	8	0.971	0.411	6.6	No	190	190	100°C - 200°C
BaF2	6	9	0.950	0.454	17.3	No	4	224	Wide Temp. Window
CuCl2	6	9	0.915	0.521	19.5	No	80	80	50°C - 100°C
RbI1	0	2	0.979	0.384	14.0	Yes	48	60	50°C - 100°C
CuF2	4	6	0.953	0.442	18.3	No	45	45	< 50°C
CuI2	4	9	0.969	0.402	23.6	No	-9	-9	< 50°C
HfF4	2	3	1.015	0.262	9.5	Yes	281	281	200°C - 300°C
ZnBr2	6	9	0.945	0.450	13.3	No	27	320	Wide Temp. Window
SrI2	4	7	0.969	0.386	9.0	No	9	203	Wide Temp. Window
NaCl1	3	4	0.859	0.590	24.0	No	254	254	200°C - 300°C
GaBr3	1	3	0.984	0.339	13.6	Yes	43	256	Wide Temp. Window
CuI2	2	4	0.994	0.307	15.1	No	137	137	100°C - 200°C
CaI2	6	9	0.940	0.447	9.4	No	115	296	200°C - 300°C
ScCl3	7	9	0.848	0.602	17.7	Yes	138	608	Wide Temp. Window
BaF2	2	4	0.975	0.356	13.1	No	28	28	< 50°C
SrCl2	1	2	0.966	0.377	14.5	No	230	230	200°C - 300°C
ZnI2	4	8	0.954	0.404	20.3	No	32	63	< 50°C
CaBr2	0	1	0.975	0.347	0.0	No	245	245	200°C - 300°C
PbCl2	2	4	0.975	0.333	0.0	No	127	127	100°C - 200°C
MnCl4	3	5	0.913	0.468	0.4	No	187	187	100°C - 200°C
MoBr4	5	8	0.959	0.365	15.5	No	193	193	100°C - 200°C
SrF2	9	12	0.851	0.571	16.7	No	173	173	100°C - 200°C
MgBr2	1	2	0.959	0.360	8.2	No	270	270	200°C - 300°C
MgI2	0	1	0.988	0.268	8.6	No	270	270	200°C - 300°C
SrCl2	9	12	0.822	0.605	14.7	No	244	244	200°C - 300°C
WBr4	5	8	0.967	0.320	21.1	No	200	200	100°C - 200°C
AlBr3	6	9	0.906	0.466	0.0	No	183	183	100°C - 200°C
MoCl3	6	9	0.868	0.531	11.9	No	168	168	100°C - 200°C
NiCl2	0	1	0.959	0.337	0.0	No	67	67	50°C - 100°C
LiI1	2	4	0.917	0.432	12.9	No	2	61	< 50°C
SrI2	8	12	0.881	0.499	8.9	No	193	235	200°C - 300°C
YBr3	2	4	0.948	0.353	20.5	Yes	110	314	Wide Temp. Window
VCl4	3	5	0.893	0.466	12.6	No	158	199	100°C - 200°C
GaCl3	0	1	0.922	0.406	0.0	Yes	267	267	200°C - 300°C
CuCl2	9	12	0.829	0.572	16.0	No	185	185	100°C - 200°C
ZrBr4	5	8	0.937	0.370	19.2	Yes	196	196	100°C - 200°C
BeI2	4	7	0.922	0.405	2.4	Yes	86	86	50°C - 100°C
NaBr1	1	2	0.913	0.418	3.0	No	124	124	100°C - 200°C

CoCl3	6	9	0.853	0.526	6.0	No	121	121	100°C - 200°C
SnI2	0	2	0.970	0.249	8.7	No	24	127	Wide Temp. Window
SrBr2	0	1	0.965	0.255	3.6	No	192	192	100°C - 200°C
RbBr1	1	3	0.914	0.394	21.0	Yes	-35	82	< 50°C
SrCl2	2	4	0.881	0.457	10.4	No	88	88	50°C - 100°C
MgBr2	4	6	0.893	0.430	6.1	No	157	157	100°C - 200°C
HfF4	3	5	0.932	0.332	0.0	Yes	-29	267	Wide Temp. Window
ZnCl2	4	6	0.882	0.442	11.2	No	97	97	50°C - 100°C
CuBr2	6	9	0.894	0.418	23.5	No	95	95	50°C - 100°C
PbCl4	2	4	0.930	0.327	20.8	No	178	218	100°C - 200°C
YCl3	6	9	0.820	0.544	0.0	Yes	22	357	Wide Temp. Window
BeBr2	8	12	0.827	0.528	11.7	Yes	46	162	Wide Temp. Window
WCl4	3	5	0.922	0.334	18.9	No	203	203	200°C - 300°C
RbBr1	2	4	0.874	0.440	5.8	Yes	-35	205	Wide Temp. Window
SrCl2	4	6	0.869	0.444	10.4	No	132	132	100°C - 200°C
CaI2	2	4	0.908	0.358	1.1	No	176	176	100°C - 200°C
MgBr2	9	12	0.815	0.533	2.0	No	214	214	200°C - 300°C
ZnI2	6	9	0.899	0.373	19.7	No	63	286	Wide Temp. Window
CaBr2	9	12	0.804	0.544	9.7	No	244	244	200°C - 300°C
NaI1	2	4	0.880	0.409	12.9	No	-13	89	< 50°C
SrCl2	0	1	0.916	0.320	14.5	No	113	113	100°C - 200°C
SnBr2	2	4	0.910	0.328	0.0	No	120	120	100°C - 200°C
YI3	6	10	0.898	0.358	2.9	Yes	31	189	Wide Temp. Window
GaI3	3	6	0.920	0.294	6.7	Yes	102	102	100°C - 200°C
VBr4	2	4	0.908	0.305	20.2	No	188	189	100°C - 200°C
PbBr2	2	4	0.917	0.269	0.6	No	132	132	100°C - 200°C
SrBr2	4	6	0.883	0.365	8.2	No	171	171	100°C - 200°C
YI3	4	6	0.907	0.296	18.4	Yes	312	312	300°C - 450°C
YF3	4	6	0.876	0.378	22.3	Yes	56	56	50°C - 100°C
KI1	2	4	0.844	0.444	5.7	No	89	89	50°C - 100°C
SnCl4	3	5	0.871	0.385	5.1	No	177	202	100°C - 200°C
CsF1	1	2	0.893	0.329	0.0	Yes	151	151	100°C - 200°C
BeCl2	9	12	0.750	0.584	18.6	Yes	122	122	100°C - 200°C
ZnI2	2	4	0.892	0.289	20.7	No	115	115	100°C - 200°C
VBr2	9	12	0.797	0.493	20.8	No	208	208	200°C - 300°C
MgI2	4	6	0.862	0.362	0.6	No	206	206	200°C - 300°C
VBr2	4	6	0.861	0.363	22.8	No	123	123	100°C - 200°C
PbCl2	9	12	0.812	0.451	19.5	No	236	236	200°C - 300°C
SrBr2	2	4	0.859	0.350	8.2	No	110	110	100°C - 200°C
BaI2	8	12	0.816	0.440	11.6	No	164	247	200°C - 300°C
SiF4	2	3	0.832	0.407	19.4	No	168	168	100°C - 200°C
PbBr4	5	8	0.879	0.293	23.1	No	175	175	100°C - 200°C
ScCl3	2	3	0.802	0.451	19.9	Yes	361	361	300°C - 450°C
RbCl1	0	1	0.837	0.381	5.1	Yes	90	90	50°C - 100°C
NiI2	4	8	0.847	0.355	20.7	No	5	5	< 50°C
SnI2	8	12	0.813	0.423	22.8	No	42	191	Wide Temp. Window
ZnBr2	9	12	0.788	0.465	9.8	No	195	195	100°C - 200°C
PbI2	8	12	0.830	0.384	24.2	No	124	188	100°C - 200°C

PbF2	9	12	0.819	0.407	15.3	No	155	155	100°C - 200°C
MgCl2	6	8	0.736	0.539	12.5	No	168	168	100°C - 200°C
CaCl2	1	2	0.801	0.435	2.5	No	165	165	100°C - 200°C
BaCl2	9	12	0.753	0.511	15.5	No	222	222	200°C - 300°C
PbI2	0	2	0.889	0.192	17.1	No	54	54	50°C - 100°C
BaBr2	4	6	0.846	0.334	18.7	No	190	190	100°C - 200°C
CoBr2	9	12	0.779	0.464	13.3	No	187	187	100°C - 200°C
CaCl2	4	6	0.782	0.454	16.7	No	67	67	50°C - 100°C
NaI1	1	2	0.839	0.331	2.3	No	148	148	100°C - 200°C
VBr4	0	2	0.865	0.255	20.2	No	81	81	50°C - 100°C
KBr1	0	1	0.814	0.375	4.6	No	79	79	50°C - 100°C
LiCl1	2	3	0.734	0.515	3.2	No	67	67	50°C - 100°C
SrI2	4	6	0.840	0.309	6.7	No	203	203	200°C - 300°C
SrI2	6	9	0.822	0.349	4.3	No	9	235	Wide Temp. Window
BaCl2	4	6	0.808	0.377	15.1	No	136	136	100°C - 200°C
GaBr3	7	9	0.802	0.385	24.6	Yes	125	573	Wide Temp. Window
BeF2	9	12	0.719	0.522	17.1	Yes	41	41	< 50°C
BaCl2	0	1	0.846	0.261	11.3	No	132	132	100°C - 200°C
LaBr3	6	10	0.814	0.348	7.6	No	-35	213	Wide Temp. Window
GeF4	2	3	0.822	0.329	4.5	Yes	183	183	100°C - 200°C
RbI1	2	4	0.806	0.365	14.0	Yes	83	83	50°C - 100°C
PbCl2	6	9	0.817	0.339	19.5	No	67	67	50°C - 100°C
SnBr2	9	12	0.766	0.442	22.0	No	227	227	200°C - 300°C
PbCl2	1	2	0.854	0.227	20.8	No	214	214	200°C - 300°C
CaBr2	4	6	0.804	0.361	12.1	No	108	108	100°C - 200°C
SiF4	3	4	0.775	0.419	19.4	No	232	232	200°C - 300°C
NiCl3	6	9	0.760	0.442	13.0	No	57	57	50°C - 100°C
KCl1	1	2	0.723	0.498	5.7	No	104	104	100°C - 200°C
SrBr2	9	12	0.742	0.469	9.4	No	223	223	200°C - 300°C
MgI2	1	2	0.834	0.265	8.6	No	298	298	200°C - 300°C
SnI2	2	4	0.829	0.263	8.7	No	127	127	100°C - 200°C
MnCl3	6	9	0.725	0.469	16.3	No	73	73	50°C - 100°C
MoI4	5	8	0.818	0.261	21.0	No	172	172	100°C - 200°C
YCl3	0	1	0.804	0.290	20.7	Yes	151	151	100°C - 200°C
PbCl4	3	5	0.802	0.292	10.4	No	155	178	100°C - 200°C
GeF4	3	4	0.777	0.347	4.5	Yes	251	251	200°C - 300°C
YBr3	6	9	0.754	0.392	0.0	Yes	96	245	Wide Temp. Window
BaBr2	0	1	0.823	0.206	0.0	No	172	172	100°C - 200°C
TiF4	2	3	0.763	0.366	4.0	No	173	173	100°C - 200°C
MoBr4	0	2	0.814	0.222	11.6	No	71	71	50°C - 100°C
ZnF2	4	6	0.761	0.358	19.2	No	-14	-14	< 50°C
PbI2	2	4	0.810	0.219	17.1	No	126	126	100°C - 200°C
CuBr2	9	12	0.724	0.420	15.5	No	149	149	100°C - 200°C
BaF2	4	6	0.773	0.321	17.3	No	39	39	< 50°C
MoBr3	6	9	0.755	0.360	13.5	No	136	136	100°C - 200°C
ZnBr2	4	6	0.776	0.312	13.3	No	83	83	50°C - 100°C
BaCl2	2	4	0.771	0.323	15.1	No	37	37	< 50°C
SrCl2	7	9	0.726	0.413	23.6	No	153	209	100°C - 200°C

BaI2	2	4	0.798	0.245	2.4	No	116	116	100°C - 200°C
YI3	6	9	0.777	0.298	0.0	Yes	100	189	100°C - 200°C
ZnF2	6	8	0.727	0.404	20.2	No	70	70	50°C - 100°C
MgI2	9	12	0.720	0.415	0.0	No	195	195	100°C - 200°C
SrBr2	1	2	0.796	0.239	3.6	No	191	191	100°C - 200°C
CaBr2	7	9	0.727	0.401	18.3	No	180	268	200°C - 300°C
PbBr2	6	9	0.777	0.286	20.6	No	73	73	50°C - 100°C
PbBr2	9	12	0.738	0.368	18.6	No	216	216	200°C - 300°C
SrI2	2	4	0.773	0.286	6.7	No	131	131	100°C - 200°C
SnF4	2	3	0.776	0.275	3.9	No	195	195	100°C - 200°C
ScBr3	7	9	0.722	0.384	15.7	Yes	165	463	Wide Temp. Window
PbCl2	0	1	0.799	0.171	20.8	No	73	73	50°C - 100°C
SrI2	0	1	0.793	0.187	0.0	No	187	187	100°C - 200°C
CaI2	9	12	0.698	0.416	4.4	No	211	211	200°C - 300°C
CaCl2	6	8	0.643	0.495	16.7	No	160	160	100°C - 200°C
SrF2	4	6	0.737	0.339	19.6	No	-1	-1	< 50°C
BeF2	7	9	0.666	0.463	14.0	Yes	50	68	50°C - 100°C
BaF2	9	12	0.689	0.424	15.0	No	106	106	100°C - 200°C
ScI3	6	9	0.738	0.330	0.0	Yes	25	305	Wide Temp. Window
BaCl2	1	2	0.764	0.266	11.3	No	172	172	100°C - 200°C
VBr4	3	5	0.762	0.268	12.8	No	111	189	100°C - 200°C
BaI2	0	1	0.780	0.178	0.0	No	226	226	200°C - 300°C
ZnI2	9	12	0.703	0.370	9.9	No	179	179	100°C - 200°C
SnBr2	6	9	0.728	0.317	22.0	No	46	46	< 50°C
BaCl2	6	9	0.702	0.369	15.5	No	-40	197	Wide Temp. Window
BaBr2	9	12	0.680	0.403	10.6	No	199	199	100°C - 200°C
GaI3	6	9	0.731	0.299	6.7	Yes	145	145	100°C - 200°C
CrBr3	7	9	0.706	0.352	12.5	No	-43	590	Wide Temp. Window
CaI2	0	1	0.756	0.226	4.0	No	209	209	200°C - 300°C
NiI2	9	12	0.699	0.364	24.1	No	166	166	100°C - 200°C
LaCl3	2	3	0.735	0.279	22.8	No	298	298	200°C - 300°C
CrI3	6	9	0.725	0.302	3.8	No	13	385	Wide Temp. Window
LiCl1	3	4	0.640	0.453	3.8	No	82	82	50°C - 100°C
MgBr2	6	8	0.678	0.389	8.9	No	164	164	100°C - 200°C
NaBr1	3	4	0.686	0.373	19.0	No	173	173	100°C - 200°C
AlI3	7	9	0.714	0.304	21.0	No	203	438	300°C - 450°C
YF3	2	3	0.711	0.311	23.3	Yes	152	152	100°C - 200°C
SiF4	4	5	0.678	0.377	11.8	No	229	229	200°C - 300°C
LiBr1	2	3	0.688	0.357	2.3	No	71	71	50°C - 100°C
RbBr1	0	1	0.722	0.278	5.8	Yes	76	76	50°C - 100°C
SnBr4	3	5	0.736	0.238	9.8	No	144	171	100°C - 200°C
TiF4	3	4	0.682	0.361	4.0	No	211	211	200°C - 300°C
SrBr2	7	9	0.695	0.329	16.4	No	144	234	100°C - 200°C
YCl3	7	9	0.638	0.423	8.8	Yes	134	357	Wide Temp. Window
CaBr2	1	2	0.713	0.280	0.0	No	179	179	100°C - 200°C
PbBr2	1	2	0.746	0.171	18.8	No	198	198	100°C - 200°C
LaI3	6	9	0.715	0.266	0.0	No	22	247	Wide Temp. Window
SnF4	3	4	0.709	0.278	3.9	No	235	235	200°C - 300°C

VF4	3	4	0.676	0.345	13.2	No	197	197	100°C - 200°C
VF4	4	5	0.668	0.355	11.0	No	254	254	200°C - 300°C
PbI2	6	9	0.714	0.245	24.6	No	50	124	50°C - 100°C
CaI2	7	9	0.678	0.323	12.2	No	167	296	200°C - 300°C
RbCl1	1	2	0.662	0.354	5.1	Yes	107	107	100°C - 200°C
MgI2	6	8	0.678	0.316	2.9	No	183	183	100°C - 200°C
SnI2	9	12	0.663	0.345	23.3	No	191	191	100°C - 200°C
YCl3	1	2	0.679	0.310	20.7	Yes	217	217	200°C - 300°C
SrI2	9	12	0.646	0.366	4.3	No	193	193	100°C - 200°C
PbF2	6	8	0.693	0.257	23.2	No	70	70	50°C - 100°C
KI1	0	1	0.683	0.274	5.2	No	72	72	50°C - 100°C
VI3	6	9	0.675	0.287	0.0	No	116	116	100°C - 200°C
CuI2	9	12	0.650	0.336	23.6	No	136	136	100°C - 200°C
GeF4	4	5	0.660	0.310	1.3	Yes	234	234	200°C - 300°C
TiF4	4	5	0.638	0.352	3.1	No	243	243	200°C - 300°C
MnCl4	2	3	0.660	0.308	0.0	No	256	256	200°C - 300°C
KBr1	1	2	0.638	0.344	4.6	No	92	92	50°C - 100°C
CaI2	4	6	0.662	0.289	9.4	No	124	124	100°C - 200°C
YCl3	2	3	0.643	0.326	12.5	Yes	283	283	200°C - 300°C
BeI2	9	12	0.624	0.345	9.7	Yes	105	105	100°C - 200°C
GaBr3	0	1	0.682	0.208	13.6	Yes	195	195	100°C - 200°C
SnI2	6	9	0.662	0.261	23.3	No	42	48	< 50°C
PbI2	9	12	0.645	0.298	21.1	No	188	188	100°C - 200°C
ScCl3	8	9	0.578	0.410	19.7	Yes	608	608	> 600°C
GaBr3	1	2	0.666	0.224	13.6	Yes	256	256	200°C - 300°C
BaI2	4	6	0.660	0.238	2.4	No	133	133	100°C - 200°C
CaBr2	6	8	0.598	0.366	12.1	No	48	268	Wide Temp. Window
ZrF4	4	5	0.627	0.304	19.2	Yes	262	262	200°C - 300°C
SnF4	4	5	0.642	0.269	2.4	No	252	252	200°C - 300°C
GaI3	1	3	0.656	0.206	5.1	Yes	83	83	50°C - 100°C
YI3	7	10	0.638	0.254	2.9	Yes	31	181	Wide Temp. Window
LaBr3	7	10	0.629	0.269	7.6	No	-35	213	Wide Temp. Window
SrI2	7	9	0.629	0.267	9.0	No	139	235	100°C - 200°C
HfF4	4	5	0.641	0.229	12.0	Yes	267	267	200°C - 300°C
GaCl3	1	2	0.619	0.282	4.5	Yes	137	137	100°C - 200°C
BaBr2	2	4	0.634	0.234	18.7	No	23	23	< 50°C
BaBr2	1	2	0.650	0.184	0.0	No	146	146	100°C - 200°C
BeBr2	9	12	0.568	0.363	11.7	Yes	46	46	< 50°C
LaCl3	1	2	0.642	0.200	22.8	No	113	113	100°C - 200°C
BaBr2	7	9	0.613	0.275	18.1	No	91	228	Wide Temp. Window
CaI2	1	2	0.628	0.222	4.0	No	229	229	200°C - 300°C
VCl4	2	3	0.600	0.288	22.0	No	214	214	200°C - 300°C
LiI1	2	3	0.612	0.260	7.9	No	61	61	50°C - 100°C
LaBr3	6	9	0.595	0.296	1.6	No	30	213	Wide Temp. Window
BaI2	9	12	0.584	0.315	4.6	No	164	164	100°C - 200°C
SrI2	1	2	0.637	0.172	0.0	No	171	171	100°C - 200°C
LaCl3	0	1	0.628	0.196	18.6	No	80	80	50°C - 100°C
LaBr3	2	3	0.627	0.186	14.3	No	278	278	200°C - 300°C

RbBr1	3	4	0.583	0.294	21.0	Yes	205	205	200°C - 300°C
PbBr2	0	1	0.633	0.141	18.8	No	98	98	50°C - 100°C
ZnCl2	6	8	0.551	0.339	18.1	No	53	53	50°C - 100°C
YBr3	2	3	0.605	0.224	20.5	Yes	314	314	300°C - 450°C
NiBr3	6	9	0.590	0.257	19.9	No	-3	-3	< 50°C
SnCl4	2	3	0.591	0.240	14.2	No	244	244	200°C - 300°C
CoBr3	7	9	0.574	0.269	22.0	No	151	151	100°C - 200°C
CuCl2	4	6	0.567	0.281	19.5	No	-40	-40	< 50°C
RbI1	0	1	0.596	0.211	9.6	Yes	60	60	50°C - 100°C
ScI3	7	9	0.573	0.256	7.7	Yes	180	305	Wide Temp. Window
FeI3	6	9	0.580	0.235	21.3	No	49	49	< 50°C
ZnI2	4	6	0.589	0.208	19.7	No	32	32	< 50°C
RbBr1	1	2	0.569	0.258	5.8	Yes	82	82	50°C - 100°C
MoI4	3	5	0.602	0.166	21.0	No	120	120	100°C - 200°C
BaI2	7	9	0.577	0.235	11.7	No	99	247	Wide Temp. Window
YCl3	6	8	0.546	0.302	9.6	Yes	22	134	Wide Temp. Window
CrBr3	8	9	0.558	0.278	22.3	No	590	590	450°C - 600°C
YBr3	6	8	0.572	0.247	3.7	Yes	96	157	100°C - 200°C
YI3	6	8	0.579	0.218	0.0	Yes	181	189	100°C - 200°C
BeCl2	7	9	0.509	0.351	18.6	Yes	-21	58	< 50°C
TiBr3	8	9	0.547	0.287	15.0	No	611	611	> 600°C
GaCl3	2	3	0.557	0.261	16.9	Yes	138	138	100°C - 200°C
LiBr1	3	4	0.538	0.295	6.9	No	48	48	< 50°C
LaBr3	0	1	0.596	0.143	16.4	No	114	114	100°C - 200°C
YBr3	7	9	0.542	0.282	3.9	Yes	157	245	200°C - 300°C
KI1	1	2	0.557	0.251	5.7	No	74	74	50°C - 100°C
GaBr3	8	9	0.545	0.262	23.2	Yes	573	573	450°C - 600°C
BaF2	6	8	0.540	0.253	23.7	No	4	4	< 50°C
CaI2	6	8	0.528	0.276	11.7	No	115	167	100°C - 200°C
BaI2	1	2	0.574	0.139	0.0	No	135	135	100°C - 200°C
LaBr3	1	2	0.568	0.158	16.4	No	177	177	100°C - 200°C
LaI3	7	9	0.545	0.203	7.7	No	155	247	200°C - 300°C
VCl4	3	4	0.518	0.260	19.3	No	199	199	100°C - 200°C
SnI2	1	2	0.557	0.143	20.6	No	127	127	100°C - 200°C
PbCl4	2	3	0.541	0.178	20.8	No	218	218	200°C - 300°C
NaI1	3	4	0.513	0.238	16.7	No	89	89	50°C - 100°C
ZnI2	6	8	0.500	0.212	20.3	No	63	63	50°C - 100°C
SrI2	6	8	0.496	0.209	8.9	No	9	139	Wide Temp. Window
VBr3	3	4	0.506	0.181	19.9	No	176	176	100°C - 200°C
ScI3	6	8	0.500	0.192	6.3	Yes	25	180	Wide Temp. Window
MgCl2	8	9	0.443	0.299	12.2	No	254	254	200°C - 300°C
YI3	7	9	0.499	0.191	0.0	Yes	100	181	100°C - 200°C
SnCl4	3	4	0.489	0.208	5.1	No	202	202	200°C - 300°C
ZnBr2	6	8	0.475	0.237	21.6	No	27	27	< 50°C
MgBr2	8	9	0.465	0.248	8.9	No	314	314	300°C - 450°C
VBr4	2	3	0.499	0.159	20.2	No	188	188	100°C - 200°C
GaCl3	3	4	0.472	0.220	21.0	Yes	100	100	100°C - 200°C
ZnBr2	8	9	0.470	0.224	21.6	No	320	320	300°C - 450°C

RbI1	1	2	0.481	0.189	14.0	Yes	48	48	< 50°C
PbCl2	4	6	0.480	0.182	19.3	No	-32	-32	< 50°C
ScBr3	8	9	0.453	0.241	13.8	Yes	463	463	450°C - 600°C
NaBr1	2	3	0.455	0.236	19.0	No	-20	-20	< 50°C
YF3	3	4	0.475	0.190	20.4	Yes	11	11	< 50°C
ScCl3	3	4	0.447	0.247	9.9	Yes	105	105	100°C - 200°C
GaI3	0	1	0.485	0.133	2.7	Yes	153	153	100°C - 200°C
BaF2	8	9	0.449	0.215	23.7	No	224	224	200°C - 300°C
SnI2	6	8	0.460	0.181	22.8	No	48	48	< 50°C
PbI2	6	8	0.462	0.156	24.6	No	50	50	50°C - 100°C
VCl4	4	5	0.426	0.223	19.3	No	158	158	100°C - 200°C
LaBr3	7	9	0.430	0.214	4.2	No	34	213	Wide Temp. Window
LaBr3	8	10	0.442	0.189	7.6	No	-35	213	Wide Temp. Window
SrCl2	7	8	0.419	0.232	23.6	No	209	209	200°C - 300°C
VBr4	3	4	0.454	0.153	12.8	No	189	189	100°C - 200°C
ZnCl2	8	9	0.410	0.238	18.1	No	214	214	200°C - 300°C
ZrCl4	4	5	0.426	0.206	16.9	Yes	183	183	100°C - 200°C
PbCl4	3	4	0.446	0.157	10.4	No	178	178	100°C - 200°C
LaI3	6	8	0.439	0.159	5.9	No	22	155	Wide Temp. Window
YCl3	8	9	0.388	0.257	9.6	Yes	357	357	300°C - 450°C
AlI3	8	9	0.428	0.182	15.8	No	438	438	300°C - 450°C
SnI2	0	1	0.451	0.111	20.6	No	24	24	< 50°C
SnCl4	4	5	0.424	0.187	2.6	No	177	177	100°C - 200°C
MoCl4	4	5	0.419	0.194	23.8	No	162	162	100°C - 200°C
NiI2	8	9	0.424	0.177	24.1	No	302	302	300°C - 450°C
NaI1	2	3	0.419	0.186	16.7	No	-13	-13	< 50°C
ScBr3	3	4	0.428	0.164	17.8	Yes	128	128	100°C - 200°C
LiI1	3	4	0.414	0.195	12.9	No	2	2	< 50°C
LaBr3	6	8	0.416	0.170	0.0	No	30	34	< 50°C
ZnI2	8	9	0.408	0.169	20.3	No	286	286	200°C - 300°C
CaBr2	7	8	0.375	0.229	18.3	No	268	268	200°C - 300°C
PbBr2	4	6	0.417	0.139	20.6	No	-47	-47	< 50°C
PbF2	8	9	0.407	0.156	20.8	No	163	163	100°C - 200°C
MgI2	8	9	0.395	0.179	2.9	No	267	267	200°C - 300°C
BeF2	7	8	0.355	0.247	14.2	Yes	50	50	< 50°C
BaCl2	6	8	0.386	0.193	21.8	No	-40	-40	< 50°C
SnBr4	3	4	0.407	0.127	9.8	No	171	171	100°C - 200°C
CaI2	8	9	0.383	0.182	11.7	No	296	296	200°C - 300°C
YCl3	3	4	0.377	0.190	12.8	Yes	75	75	50°C - 100°C
SrBr2	8	9	0.381	0.181	14.9	No	234	234	200°C - 300°C
CrI3	8	9	0.388	0.162	14.1	No	385	385	300°C - 450°C
BeF2	8	9	0.342	0.238	14.2	Yes	68	68	50°C - 100°C
PbCl4	4	5	0.390	0.142	7.1	No	155	155	100°C - 200°C
YI3	8	10	0.382	0.152	2.9	Yes	31	100	50°C - 100°C
CrI3	6	8	0.378	0.145	14.1	No	13	13	< 50°C
RbBr1	2	3	0.366	0.158	21.0	Yes	-35	-35	< 50°C
YBr3	3	4	0.374	0.139	14.1	Yes	110	110	100°C - 200°C
BaCl2	8	9	0.352	0.185	21.8	No	197	197	100°C - 200°C

ScCl3	7	8	0.340	0.203	19.7	Yes	138	138	100°C - 200°C
LaCl3	8	9	0.337	0.206	12.2	No	302	302	300°C - 450°C
SrCl2	8	9	0.341	0.194	17.1	No	153	153	100°C - 200°C
BaBr2	8	9	0.355	0.159	17.6	No	228	228	200°C - 300°C
GaBr3	2	3	0.368	0.127	10.2	Yes	43	43	< 50°C
BeBr2	8	9	0.334	0.192	9.5	Yes	162	162	100°C - 200°C
ZrBr4	4	5	0.359	0.123	22.0	Yes	150	150	100°C - 200°C
CaBr2	8	9	0.332	0.183	11.4	No	180	180	100°C - 200°C
SrI2	8	9	0.348	0.147	8.9	No	235	235	200°C - 300°C
SnBr4	4	5	0.356	0.115	4.0	No	144	144	100°C - 200°C
SrBr2	7	8	0.333	0.155	16.4	No	144	144	100°C - 200°C
VBr4	4	5	0.346	0.122	8.9	No	111	111	100°C - 200°C
BaI2	8	9	0.336	0.137	11.6	No	247	247	200°C - 300°C
ScBr3	7	8	0.331	0.149	15.7	Yes	165	165	100°C - 200°C
YCl3	7	8	0.316	0.175	9.6	Yes	134	134	100°C - 200°C
ScI3	8	9	0.321	0.144	6.3	Yes	305	305	300°C - 450°C
BeCl2	8	9	0.289	0.199	18.6	Yes	58	58	50°C - 100°C
CaI2	6	7	0.321	0.135	12.2	No	115	115	100°C - 200°C
HfF4	3	4	0.330	0.109	12.0	Yes	-29	-29	< 50°C
BeI2	7	8	0.314	0.146	2.4	Yes	135	135	100°C - 200°C
YI3	3	4	0.327	0.105	18.4	Yes	117	117	100°C - 200°C
AlI3	7	8	0.318	0.126	21.0	No	203	203	200°C - 300°C
YI3	6	7	0.317	0.113	0.0	Yes	189	189	100°C - 200°C
CaCl2	8	9	0.276	0.190	15.7	No	83	83	50°C - 100°C
YBr3	7	8	0.307	0.133	3.9	Yes	157	157	100°C - 200°C
YBr3	8	9	0.296	0.154	3.7	Yes	245	245	200°C - 300°C
CaBr2	6	7	0.297	0.144	18.3	No	48	48	< 50°C
GaBr3	7	8	0.302	0.128	24.6	Yes	125	125	100°C - 200°C
ScI3	7	8	0.302	0.116	7.7	Yes	180	180	100°C - 200°C
LaI3	8	9	0.299	0.111	5.9	No	247	247	200°C - 300°C
SrI2	7	8	0.294	0.124	9.0	No	139	139	100°C - 200°C
CaI2	7	8	0.280	0.147	12.2	No	167	167	100°C - 200°C
YBr3	6	7	0.290	0.119	3.9	Yes	96	96	50°C - 100°C
YI3	7	8	0.287	0.108	0.0	Yes	181	181	100°C - 200°C
BaBr2	7	8	0.275	0.120	18.1	No	91	91	50°C - 100°C
LaBr3	8	9	0.264	0.131	1.6	No	213	213	200°C - 300°C
ZnF2	8	9	0.257	0.141	25.0	No	-16	-16	< 50°C
YCl3	6	7	0.255	0.134	8.8	Yes	22	22	< 50°C
PbI2	8	9	0.272	0.093	24.2	No	124	124	100°C - 200°C
SnI4	4	5	0.276	0.076	23.6	No	101	101	100°C - 200°C
LaCl3	6	7	0.261	0.117	4.6	No	23	23	< 50°C
BeCl2	7	8	0.234	0.164	17.6	Yes	-21	-21	< 50°C
LaI3	7	8	0.259	0.094	7.7	No	155	155	100°C - 200°C
BaI2	7	8	0.252	0.102	11.7	No	99	99	50°C - 100°C
LaBr3	6	7	0.245	0.088	4.2	No	30	30	< 50°C
YI3	8	9	0.225	0.086	0.0	Yes	100	100	50°C - 100°C
SrI2	6	7	0.221	0.088	9.0	No	9	9	< 50°C
SnI2	8	9	0.218	0.086	23.3	No	42	42	< 50°C

ScI3	6	7	0.214	0.079	7.7	Yes	25	25	< 50°C
LaBr3	7	8	0.209	0.086	4.2	No	34	34	< 50°C
LaI3	6	7	0.192	0.067	7.7	No	22	22	< 50°C
CrBr3	7	8	0.174	0.077	22.3	No	-43	-43	< 50°C
YI3	9	10	0.172	0.068	2.9	Yes	31	31	< 50°C
LaBr3	9	10	0.145	0.062	7.6	No	-35	-35	< 50°C

Table C.4 1844 hypothetical (de)hydration reactions that are predicted to lie within 50 meV/atom of the convex hull are characterized by the number of water molecules per formula unit in the dehydrated (n_{low}) and hydrated (n_{high}) states, volumetric (VED) and gravimetric (GED) energy densities, maximum distance to the convex hull (E_{hull}), whether the hydrate contains an expensive metal, minimum ($T_{turn,min}$) and maximum ($T_{turn,max}$) turning temperatures of the (de)hydration reaction(s), and temperature category. Reactions are ordered by descending $ED_{RMS} = \sqrt{VED^2 + GED^2}$.

Salt	n_{low}	n_{high}	VED (GJ/m^3)	GED (MJ/kg)	E_{hull} (meV/at.)	Expensive Metal	$T_{turn,min}$ (°C)	$T_{turn,max}$ (°C)	Temp. Categ.
CoF3	0	6	4.480	2.053	29.0	No	143	361	Wide Temp. Window
NiF3	0	9	4.035	2.331	29.3	No	220	220	200°C - 300°C
BeCl2	0	4	3.816	2.508	0.0	Yes	380	380	300°C - 450°C
BeCl2	0	7	3.718	2.558	11.8	Yes	60	380	Wide Temp. Window
CoF3	0	3	4.171	1.635	37.6	No	361	361	300°C - 450°C
AlCl3	0	6	3.833	2.302	0.0	No	220	448	300°C - 450°C
BeCl2	0	9	3.660	2.529	18.6	Yes	-21	380	Wide Temp. Window
CrF3	0	9	3.765	2.311	0.0	No	178	256	200°C - 300°C
NiF2	0	12	3.716	2.367	9.4	No	1	286	Wide Temp. Window
BeCl2	0	8	3.584	2.517	17.6	Yes	-21	380	Wide Temp. Window
MgCl2	0	12	3.392	2.701	0.0	No	124	288	200°C - 300°C
BeCl2	0	12	3.407	2.651	13.4	Yes	-21	380	Wide Temp. Window
MgCl2	0	9	3.560	2.401	7.5	No	124	288	200°C - 300°C
GeF4	0	8	3.738	2.025	1.9	Yes	110	564	Wide Temp. Window
VF2	0	12	3.522	2.364	0.0	No	139	139	100°C - 200°C
ZnF2	0	12	3.533	2.249	0.0	No	-16	286	Wide Temp. Window
MnF4	0	5	3.736	1.890	18.6	No	299	299	200°C - 300°C
GeF4	0	5	3.789	1.782	0.0	Yes	183	564	Wide Temp. Window
CuF2	0	12	3.515	2.238	1.4	No	-18	223	Wide Temp. Window
NiF2	0	4	3.759	1.640	0.0	No	201	201	200°C - 300°C
BeBr2	0	9	3.553	2.040	6.6	Yes	78	423	Wide Temp. Window
BeBr2	0	8	3.595	1.954	9.5	Yes	78	423	Wide Temp. Window
CrF3	0	6	3.664	1.819	21.2	No	178	178	100°C - 200°C
NiF2	0	6	3.657	1.742	46.8	No	1	201	Wide Temp. Window
BeBr2	0	4	3.681	1.688	0.0	Yes	423	423	300°C - 450°C
CuF2	0	6	3.670	1.703	18.3	No	45	218	Wide Temp. Window
NiF2	0	9	3.455	1.915	40.8	No	1	201	Wide Temp. Window
SiF4	0	8	3.344	2.089	5.8	No	103	232	100°C - 200°C
BeBr2	0	12	3.315	2.116	11.7	Yes	46	423	Wide Temp. Window
CuF2	0	8	3.456	1.858	27.2	No	45	218	Wide Temp. Window
MgCl2	0	6	3.351	2.027	12.5	No	124	288	200°C - 300°C
MgCl2	1	12	3.062	2.438	0.0	No	124	254	100°C - 200°C

FeF2	0	12	3.310	2.086	38.9	No	96	96	50°C - 100°C
GeF4	0	4	3.565	1.591	1.3	Yes	183	564	Wide Temp. Window
CuF2	0	9	3.421	1.872	21.1	No	-18	218	Wide Temp. Window
AlBr3	0	6	3.564	1.542	0.0	No	323	513	300°C - 450°C
SnF4	0	8	3.482	1.700	0.0	No	124	438	Wide Temp. Window
CoF2	0	4	3.526	1.581	44.0	No	185	185	100°C - 200°C
CuF2	0	4	3.549	1.522	15.2	No	141	218	100°C - 200°C
ZnF2	1	12	3.246	2.066	12.8	No	-16	286	Wide Temp. Window
VF4	0	8	3.290	1.991	1.2	No	112	348	Wide Temp. Window
NiF2	0	8	3.337	1.892	16.1	No	1	201	Wide Temp. Window
BeF2	0	12	3.102	2.251	17.1	Yes	41	134	Wide Temp. Window
VCl2	0	12	3.083	2.272	23.2	No	88	231	Wide Temp. Window
MgCl2	0	8	3.091	2.260	12.2	No	124	288	200°C - 300°C
BeF2	0	9	3.128	2.176	14.0	Yes	41	134	Wide Temp. Window
MoF3	0	6	3.466	1.525	15.9	No	181	181	100°C - 200°C
TiF4	0	8	3.219	1.993	0.0	No	121	278	100°C - 200°C
CaCl2	0	12	2.944	2.375	0.0	No	67	270	Wide Temp. Window
CoF2	0	8	3.318	1.807	49.7	No	15	185	Wide Temp. Window
TiF3	0	9	3.156	2.058	6.8	No	83	204	Wide Temp. Window
SiF4	0	5	3.273	1.821	5.0	No	168	232	200°C - 300°C
ZnF2	0	4	3.433	1.487	0.0	No	127	192	100°C - 200°C
ZnF2	0	6	3.386	1.592	19.2	No	-14	192	Wide Temp. Window
BeI2	0	8	3.377	1.574	0.0	Yes	86	452	Wide Temp. Window
MgCl2	1	9	3.088	2.083	7.5	No	124	254	100°C - 200°C
MoF4	0	8	3.301	1.722	43.0	No	128	245	100°C - 200°C
BeF2	0	8	3.051	2.121	14.2	Yes	41	134	Wide Temp. Window
BeI2	0	7	3.401	1.494	2.4	Yes	86	452	Wide Temp. Window
ZnF2	0	9	3.248	1.786	25.0	No	-16	192	Wide Temp. Window
MgI2	0	9	3.365	1.525	0.0	No	183	298	200°C - 300°C
VCl2	0	9	3.118	1.927	47.9	No	88	195	100°C - 200°C
SnF4	0	5	3.371	1.413	0.0	No	195	438	Wide Temp. Window
GeF4	0	3	3.388	1.355	4.5	Yes	183	564	Wide Temp. Window
BeF2	0	4	3.134	1.852	4.8	Yes	76	134	100°C - 200°C
BeF2	0	7	2.994	2.070	13.0	Yes	41	134	Wide Temp. Window
GeF4	1	8	3.197	1.732	47.3	Yes	110	564	Wide Temp. Window
ZnF2	0	8	3.173	1.764	20.2	No	-14	192	Wide Temp. Window
CoCl2	0	12	2.951	2.078	17.3	No	96	152	100°C - 200°C
NiCl2	0	12	2.942	2.042	14.4	No	20	213	Wide Temp. Window
ZnCl2	0	12	2.926	2.047	0.0	No	26	220	Wide Temp. Window
VF4	0	5	3.153	1.675	5.0	No	112	348	Wide Temp. Window
BeI2	0	4	3.336	1.265	0.0	Yes	452	452	450°C - 600°C
MgI2	0	12	3.077	1.773	0.0	No	183	298	200°C - 300°C
AlCl3	0	4	3.107	1.681	38.1	No	220	351	200°C - 300°C
LiF1	0	4	2.944	1.949	15.6	No	-12	207	Wide Temp. Window
MgCl2	2	12	2.757	2.196	0.0	No	124	254	100°C - 200°C
MgF2	0	4	3.052	1.711	3.2	No	-4	184	Wide Temp. Window
TiF4	0	5	3.058	1.689	0.0	No	173	278	200°C - 300°C
CaCl2	0	9	2.868	1.973	15.7	No	67	187	100°C - 200°C

ZnF2	2	12	2.918	1.858	7.9	No	-16	286	Wide Temp. Window
CuF2	2	12	2.918	1.857	41.7	No	-18	223	Wide Temp. Window
CaCl2	1	12	2.689	2.170	0.0	No	67	270	Wide Temp. Window
VBr2	0	12	2.933	1.814	20.8	No	123	208	100°C - 200°C
GeF4	0	2	3.254	1.127	0.0	Yes	315	564	300°C - 450°C
MnCl2	0	9	2.931	1.805	6.4	No	103	174	100°C - 200°C
VCl2	0	6	3.033	1.624	28.1	No	123	168	100°C - 200°C
MgBr2	0	6	3.094	1.489	6.1	No	157	285	200°C - 300°C
CaBr2	0	12	2.844	1.924	0.0	No	48	268	Wide Temp. Window
CrCl3	0	9	2.861	1.897	0.0	No	127	410	Wide Temp. Window
LiCl1	0	4	2.800	1.982	3.8	No	67	173	100°C - 200°C
MoF4	0	5	3.109	1.408	43.0	No	224	245	200°C - 300°C
TiF3	0	6	3.010	1.599	29.7	No	83	149	100°C - 200°C
VCl3	0	9	2.826	1.904	34.2	No	47	237	Wide Temp. Window
VBr2	0	9	3.033	1.512	12.8	No	123	189	100°C - 200°C
MgCl2	0	4	2.875	1.770	0.0	No	202	288	200°C - 300°C
ZnCl2	0	9	2.914	1.694	12.5	No	26	214	Wide Temp. Window
NiCl2	0	9	2.903	1.695	31.3	No	20	213	Wide Temp. Window
ZnCl2	1	12	2.750	1.924	35.8	No	53	220	Wide Temp. Window
SiF4	0	4	2.946	1.592	11.8	No	168	232	200°C - 300°C
SnF4	0	4	3.115	1.221	2.4	No	195	438	Wide Temp. Window
GeF4	1	5	3.024	1.422	47.3	Yes	183	564	Wide Temp. Window
SnF4	1	8	3.002	1.466	19.9	No	124	438	Wide Temp. Window
VF4	1	8	2.857	1.729	42.2	No	112	348	Wide Temp. Window
NiCl2	1	12	2.735	1.898	14.4	No	20	213	Wide Temp. Window
MgI2	0	8	3.015	1.403	2.9	No	183	298	200°C - 300°C
TiF4	1	8	2.798	1.732	10.5	No	121	278	100°C - 200°C
CaBr2	0	9	2.878	1.586	9.7	No	48	268	Wide Temp. Window
CaCl2	0	6	2.839	1.646	16.7	No	67	187	100°C - 200°C
AlF3	0	3	2.932	1.468	0.0	No	167	234	200°C - 300°C
ScCl3	0	6	2.798	1.690	0.0	Yes	45	361	Wide Temp. Window
PbF4	0	5	3.104	1.020	33.3	No	223	255	200°C - 300°C
MnCl4	0	8	2.833	1.615	0.0	No	187	256	200°C - 300°C
MgI2	1	9	2.967	1.344	8.6	No	183	298	200°C - 300°C
VCl2	0	8	2.711	1.801	26.0	No	88	168	100°C - 200°C
MgCl2	1	8	2.623	1.918	12.2	No	124	245	100°C - 200°C
ZnF2	1	9	2.848	1.566	25.0	No	-16	192	Wide Temp. Window
AlI3	0	6	3.034	1.108	0.0	No	379	379	300°C - 450°C
MgI2	1	12	2.799	1.612	8.6	No	183	298	200°C - 300°C
CoCl2	0	6	2.880	1.458	46.6	No	96	136	100°C - 200°C
YCl3	0	8	2.818	1.558	9.6	Yes	22	283	Wide Temp. Window
YCl3	0	6	2.887	1.406	0.0	Yes	75	283	Wide Temp. Window
MgCl2	2	9	2.653	1.789	7.5	No	124	254	100°C - 200°C
MnCl2	0	6	2.812	1.519	3.6	No	124	174	100°C - 200°C
CoBr2	0	12	2.743	1.633	0.0	No	-23	367	Wide Temp. Window
ZrCl4	0	8	2.792	1.514	1.7	Yes	183	260	200°C - 300°C
TiCl3	0	6	2.765	1.561	30.0	No	195	195	100°C - 200°C
VBr2	1	12	2.696	1.667	39.4	No	123	208	100°C - 200°C

VF4	0	4	2.819	1.440	11.0	No	112	348	Wide Temp. Window
HfCl4	0	8	2.898	1.270	7.1	Yes	192	283	200°C - 300°C
NiCl2	0	6	2.826	1.422	7.2	No	67	137	100°C - 200°C
HfF4	0	8	2.906	1.245	0.0	Yes	-29	281	Wide Temp. Window
LiCl1	0	3	2.588	1.815	3.2	No	67	173	100°C - 200°C
VCl3	0	6	2.751	1.546	34.2	No	47	237	Wide Temp. Window
TiCl4	0	8	2.707	1.612	14.0	No	167	197	100°C - 200°C
YCl3	0	7	2.787	1.461	8.8	Yes	22	283	Wide Temp. Window
VCl3	1	9	2.609	1.758	41.6	No	179	237	200°C - 300°C
ZnF2	1	8	2.748	1.528	20.2	No	-14	192	Wide Temp. Window
CaCl2	2	12	2.447	1.974	2.5	No	67	270	Wide Temp. Window
YCl3	0	9	2.619	1.737	0.0	Yes	22	357	Wide Temp. Window
MgCl2	1	6	2.685	1.624	12.5	No	124	245	100°C - 200°C
MnBr2	0	9	2.803	1.403	3.3	No	103	162	100°C - 200°C
CaCl2	0	8	2.479	1.909	13.3	No	67	187	100°C - 200°C
TiF4	0	4	2.758	1.459	3.1	No	173	278	200°C - 300°C
CoBr2	0	9	2.810	1.336	13.3	No	-23	367	Wide Temp. Window
CaBr2	1	12	2.575	1.743	0.0	No	48	268	Wide Temp. Window
ZnCl2	0	6	2.770	1.388	11.2	No	26	188	Wide Temp. Window
VCl4	0	8	2.679	1.556	0.0	No	120	214	100°C - 200°C
ZnCl2	2	12	2.534	1.773	30.7	No	53	220	Wide Temp. Window
CaI2	0	12	2.657	1.581	0.0	No	115	296	200°C - 300°C
ZnF2	1	6	2.797	1.315	19.2	No	-14	192	Wide Temp. Window
VF3	0	3	2.822	1.259	0.0	No	179	220	100°C - 200°C
GaCl3	0	6	2.735	1.426	7.1	Yes	100	267	100°C - 200°C
LiBr1	0	4	2.702	1.482	6.9	No	48	222	Wide Temp. Window
ZnCl2	1	9	2.662	1.548	35.8	No	53	214	Wide Temp. Window
NiCl2	2	12	2.526	1.753	35.5	No	20	213	Wide Temp. Window
MgI2	0	6	2.828	1.189	0.6	No	206	298	200°C - 300°C
BeF2	2	12	2.480	1.800	17.1	Yes	41	76	50°C - 100°C
MoF4	0	4	2.818	1.202	43.0	No	224	245	200°C - 300°C
CrCl4	0	8	2.653	1.522	23.7	No	152	191	100°C - 200°C
MgBr2	0	4	2.803	1.208	0.0	No	237	285	200°C - 300°C
SnCl4	0	8	2.723	1.368	0.0	No	177	244	200°C - 300°C
CaCl2	1	9	2.510	1.727	15.7	No	67	173	100°C - 200°C
VBr2	0	6	2.800	1.180	22.8	No	123	189	100°C - 200°C
LiCl1	0	2	2.578	1.599	0.0	No	140	173	100°C - 200°C
CaI2	0	9	2.738	1.304	4.4	No	115	296	200°C - 300°C
CaBr2	0	6	2.764	1.241	12.1	No	108	245	100°C - 200°C
AlCl3	0	3	2.655	1.458	44.9	No	351	351	300°C - 450°C
SnF4	0	3	2.855	1.011	3.9	No	195	438	Wide Temp. Window
NiCl2	1	9	2.611	1.525	31.3	No	20	213	Wide Temp. Window
CaBr2	0	7	2.719	1.316	18.3	No	48	245	Wide Temp. Window
VBr2	1	9	2.696	1.344	39.4	No	123	189	100°C - 200°C
MnCl2	1	9	2.563	1.578	6.4	No	103	124	100°C - 200°C
PbF4	0	4	2.863	0.868	48.6	No	255	255	200°C - 300°C
SiF4	0	3	2.673	1.307	19.4	No	168	214	100°C - 200°C
NbCl4	0	8	2.613	1.393	21.9	No	164	203	100°C - 200°C

YF3	1	9	2.526	1.544	37.0	Yes	-22	693	Wide Temp. Window
NiCl2	0	8	2.521	1.547	40.0	No	20	137	Wide Temp. Window
YBr3	0	8	2.715	1.173	3.7	Yes	85	314	Wide Temp. Window
ZnCl2	0	8	2.516	1.549	18.1	No	26	188	Wide Temp. Window
FeCl3	0	6	2.631	1.341	31.0	No	141	141	100°C - 200°C
AlBr3	0	4	2.766	1.028	48.7	No	323	323	300°C - 450°C
GeF4	1	4	2.694	1.203	47.3	Yes	183	564	Wide Temp. Window
CuF2	2	9	2.583	1.414	41.7	No	-18	218	Wide Temp. Window
VCl2	0	4	2.626	1.330	31.4	No	168	168	100°C - 200°C
SnF4	1	5	2.705	1.134	19.9	No	195	438	Wide Temp. Window
ScCl3	1	6	2.502	1.511	46.3	Yes	105	361	Wide Temp. Window
SrCl2	0	6	2.599	1.326	7.8	No	88	230	Wide Temp. Window
LiBr1	0	3	2.579	1.339	2.3	No	71	222	Wide Temp. Window
CrBr3	0	9	2.600	1.294	0.0	No	-43	590	Wide Temp. Window
CuCl2	0	6	2.603	1.287	19.5	No	-40	219	Wide Temp. Window
ZnF2	1	4	2.664	1.154	12.8	No	184	192	100°C - 200°C
MgF2	1	4	2.530	1.418	46.1	No	118	184	100°C - 200°C
MgI2	2	12	2.506	1.444	0.8	No	183	267	200°C - 300°C
VBr2	2	12	2.457	1.519	35.3	No	123	208	100°C - 200°C
BaCl2	0	12	2.389	1.620	0.0	No	-40	222	Wide Temp. Window
SrF2	0	6	2.622	1.207	19.6	No	-1	94	< 50°C
VBr3	0	9	2.573	1.309	41.1	No	2	671	Wide Temp. Window
CuF2	2	8	2.541	1.366	41.7	No	45	218	Wide Temp. Window
HfF4	1	8	2.648	1.134	30.0	Yes	-29	281	Wide Temp. Window
MgI2	1	8	2.611	1.215	8.6	No	183	298	200°C - 300°C
SrI2	0	9	2.646	1.121	4.3	No	9	235	Wide Temp. Window
ZnI2	0	12	2.544	1.336	0.0	No	32	286	Wide Temp. Window
VF4	1	5	2.536	1.348	42.2	No	112	348	Wide Temp. Window
BeF2	0	2	2.485	1.430	0.0	Yes	134	134	100°C - 200°C
ZrCl3	0	9	2.406	1.555	47.2	Yes	153	153	100°C - 200°C
VF4	0	3	2.598	1.204	13.2	No	112	348	Wide Temp. Window
CrCl3	0	7	2.476	1.436	28.1	No	127	127	100°C - 200°C
SiF4	2	8	2.426	1.516	14.7	No	103	232	100°C - 200°C
YBr3	0	7	2.645	1.081	3.9	Yes	85	314	Wide Temp. Window
YBr3	0	6	2.675	1.002	0.0	Yes	85	314	Wide Temp. Window
CaBr2	1	9	2.499	1.377	9.7	No	48	268	Wide Temp. Window
YCl3	1	8	2.488	1.376	20.7	Yes	22	283	Wide Temp. Window
ScBr3	0	6	2.593	1.151	0.0	Yes	128	392	Wide Temp. Window
CaBr2	0	8	2.415	1.477	11.4	No	48	268	Wide Temp. Window
YCl3	1	9	2.358	1.564	20.7	Yes	22	357	Wide Temp. Window
CaBr2	2	12	2.341	1.584	0.0	No	48	268	Wide Temp. Window
ZnF2	0	2	2.679	0.898	7.9	No	127	184	100°C - 200°C
ZnBr2	0	6	2.620	1.052	13.3	No	83	201	Wide Temp. Window
CaI2	1	12	2.425	1.444	4.0	No	115	296	200°C - 300°C
TiF4	1	5	2.468	1.363	10.5	No	173	278	200°C - 300°C
BeF2	2	9	2.312	1.608	14.0	Yes	41	76	50°C - 100°C
TaCl4	0	8	2.586	1.115	50.0	Yes	173	173	100°C - 200°C
CoBr2	0	6	2.613	1.047	42.2	No	118	118	100°C - 200°C

YI3	0	10	2.613	1.041	2.9	Yes	31	322	Wide Temp. Window
MgCl2	4	12	2.198	1.750	0.0	No	124	254	100°C - 200°C
GeF2	0	4	2.506	1.264	12.1	Yes	92	153	100°C - 200°C
ZnI2	0	9	2.588	1.075	9.9	No	32	286	Wide Temp. Window
HfBr4	0	8	2.654	0.899	16.9	Yes	164	251	200°C - 300°C
MnI2	0	9	2.568	1.120	0.0	No	128	128	100°C - 200°C
TiF4	0	3	2.525	1.210	4.0	No	173	278	200°C - 300°C
MgI2	2	9	2.550	1.155	0.8	No	183	267	200°C - 300°C
VCl3	1	6	2.438	1.370	41.6	No	208	237	200°C - 300°C
YI3	0	9	2.612	1.001	0.0	Yes	100	322	Wide Temp. Window
SrI2	0	12	2.433	1.379	0.0	No	9	235	Wide Temp. Window
MgBr2	1	6	2.515	1.210	8.2	No	157	270	200°C - 300°C
YBr3	0	9	2.468	1.284	0.0	Yes	85	314	Wide Temp. Window
GeCl4	0	8	2.440	1.336	13.9	Yes	81	202	Wide Temp. Window
ScI3	0	8	2.594	0.998	6.3	Yes	25	322	Wide Temp. Window
LiF1	0	3	2.332	1.512	35.5	No	-12	34	< 50°C
BaF2	0	6	2.566	1.066	17.3	No	28	149	Wide Temp. Window
TiBr3	0	6	2.571	1.050	28.2	No	186	232	200°C - 300°C
SrBr2	0	6	2.565	1.061	2.7	No	110	192	100°C - 200°C
WCl4	0	8	2.550	1.080	5.0	No	92	244	Wide Temp. Window
CaF2	0	4	2.380	1.409	2.2	No	72	106	50°C - 100°C
HfF4	0	5	2.604	0.929	0.0	Yes	-29	281	Wide Temp. Window
NaF1	0	2	2.413	1.348	13.0	No	22	152	Wide Temp. Window
PbCl4	0	8	2.545	1.077	0.0	No	155	218	100°C - 200°C
LiBr1	0	2	2.524	1.126	0.0	No	180	222	200°C - 300°C
NiF2	4	12	2.327	1.483	9.4	No	1	286	Wide Temp. Window
GeF4	2	8	2.426	1.315	1.9	Yes	110	251	100°C - 200°C
SnF4	0	2	2.641	0.794	0.0	No	271	438	300°C - 450°C
CoCl2	0	4	2.490	1.184	49.5	No	136	136	100°C - 200°C
CuF2	0	2	2.606	0.879	41.7	No	141	141	100°C - 200°C
LaBr2	0	12	2.385	1.364	45.5	No	128	128	100°C - 200°C
CaI2	0	7	2.530	1.065	12.2	No	115	229	100°C - 200°C
YCl3	1	6	2.468	1.202	20.7	Yes	75	283	Wide Temp. Window
AlF3	0	2	2.525	1.071	7.5	No	167	167	100°C - 200°C
BaCl2	0	9	2.420	1.271	15.5	No	-40	197	Wide Temp. Window
CuCl2	0	4	2.463	1.183	0.0	No	71	219	Wide Temp. Window
YCl3	1	7	2.420	1.268	20.7	Yes	22	283	Wide Temp. Window
ZnF2	2	9	2.391	1.314	25.0	No	-16	192	Wide Temp. Window
ZnCl2	2	9	2.357	1.370	30.7	No	53	214	Wide Temp. Window
ScI3	0	9	2.486	1.111	0.0	Yes	25	322	Wide Temp. Window
TiF4	2	8	2.314	1.432	0.7	No	121	243	100°C - 200°C
ZrBr4	0	8	2.531	0.999	7.4	Yes	150	239	100°C - 200°C
RbF1	0	2	2.485	1.103	0.0	Yes	171	344	Wide Temp. Window
MgCl2	2	8	2.191	1.603	12.2	No	124	202	100°C - 200°C
ZnCl2	1	6	2.414	1.210	35.8	No	90	188	100°C - 200°C
TiF3	0	3	2.436	1.162	38.8	No	149	149	100°C - 200°C
NiCl2	1	6	2.411	1.213	7.2	No	70	137	100°C - 200°C
CaCl2	1	8	2.137	1.646	13.3	No	67	173	100°C - 200°C

VF4	2	8	2.304	1.395	35.0	No	112	254	100°C - 200°C
CrBr3	1	9	2.409	1.199	46.0	No	-43	590	Wide Temp. Window
VBr3	1	9	2.398	1.220	18.4	No	59	671	Wide Temp. Window
CrBr3	0	6	2.507	0.975	48.8	No	22	202	Wide Temp. Window
KF1	0	2	2.301	1.393	0.0	No	158	194	100°C - 200°C
NiBr2	0	6	2.496	0.994	37.8	No	21	148	Wide Temp. Window
NiCl2	2	9	2.317	1.353	35.5	No	20	213	Wide Temp. Window
YBr3	1	8	2.459	1.062	36.6	Yes	96	314	Wide Temp. Window
CuF2	2	6	2.427	1.126	41.7	No	45	218	Wide Temp. Window
CaI2	1	9	2.414	1.150	4.4	No	115	296	200°C - 300°C
YI3	0	8	2.503	0.941	0.0	Yes	117	322	Wide Temp. Window
ZrF4	0	3	2.509	0.915	0.0	Yes	126	314	Wide Temp. Window
CaCl2	1	6	2.310	1.340	16.7	No	67	173	100°C - 200°C
LiI1	0	4	2.415	1.138	12.9	No	2	243	Wide Temp. Window
ZnF2	4	12	2.250	1.433	0.0	No	-16	286	Wide Temp. Window
HfF4	0	3	2.581	0.666	0.0	Yes	29	281	Wide Temp. Window
ZnCl2	1	8	2.263	1.394	35.8	No	53	188	100°C - 200°C
MgI2	0	4	2.486	0.912	0.0	No	263	298	200°C - 300°C
VBr3	0	8	2.433	1.046	41.1	No	2	258	Wide Temp. Window
MoF4	0	3	2.465	0.963	43.2	No	224	224	200°C - 300°C
NiI2	0	12	2.346	1.222	32.6	No	-12	302	Wide Temp. Window
LiI1	0	3	2.433	1.033	7.9	No	61	243	Wide Temp. Window
SnF4	2	8	2.375	1.160	0.0	No	124	252	100°C - 200°C
MnCl4	0	5	2.352	1.206	0.4	No	187	256	200°C - 300°C
HfCl4	0	5	2.472	0.932	20.8	Yes	192	283	200°C - 300°C
BaCl2	1	12	2.184	1.481	11.3	No	-40	222	Wide Temp. Window
ScI3	0	7	2.474	0.911	7.7	Yes	25	322	Wide Temp. Window
CaCl2	2	9	2.170	1.493	15.7	No	67	173	100°C - 200°C
VBr2	2	9	2.357	1.175	35.3	No	123	189	100°C - 200°C
CrBr4	0	8	2.442	0.972	31.6	No	96	179	100°C - 200°C
BeF2	2	8	2.157	1.500	14.2	Yes	41	76	50°C - 100°C
TiBr4	0	8	2.425	1.008	17.8	No	128	199	100°C - 200°C
VCl3	0	4	2.345	1.178	46.7	No	47	237	Wide Temp. Window
VBr2	0	4	2.453	0.921	20.4	No	156	189	100°C - 200°C
CrBr3	0	8	2.396	1.059	22.3	No	-43	202	Wide Temp. Window
NaBr1	0	4	2.302	1.249	5.7	No	-20	173	Wide Temp. Window
CuF2	4	12	2.209	1.406	15.2	No	-18	223	Wide Temp. Window
ZnCl2	0	4	2.369	1.110	8.7	No	26	188	Wide Temp. Window
SiF4	0	2	2.407	1.016	14.7	No	214	214	200°C - 300°C
NiCl2	1	8	2.225	1.366	40.0	No	20	137	Wide Temp. Window
VF4	0	2	2.414	0.992	35.0	No	214	348	200°C - 300°C
MnCl2	1	6	2.295	1.239	3.6	No	124	124	100°C - 200°C
YF3	2	9	2.222	1.358	23.3	Yes	-22	693	Wide Temp. Window
CaCl2	0	4	2.177	1.427	0.0	No	165	187	100°C - 200°C
SrI2	0	8	2.399	1.010	8.9	No	9	203	Wide Temp. Window
ZrCl4	0	5	2.335	1.131	12.2	Yes	183	260	200°C - 300°C
ZnF2	2	8	2.263	1.258	20.2	No	-14	192	Wide Temp. Window
ScCl3	0	4	2.265	1.253	9.9	Yes	45	361	Wide Temp. Window

CrBr3	0	7	2.374	1.024	12.5	No	-11	202	Wide Temp. Window
VI2	0	6	2.425	0.888	22.0	No	146	146	100°C - 200°C
WF4	2	8	2.391	0.975	47.6	No	130	227	100°C - 200°C
VBr4	0	8	2.390	0.973	0.0	No	81	199	100°C - 200°C
YF3	1	6	2.345	1.012	37.0	Yes	11	152	Wide Temp. Window
YBr3	1	7	2.364	0.966	36.6	Yes	96	314	Wide Temp. Window
SrI2	1	12	2.221	1.258	0.0	No	9	235	Wide Temp. Window
YBr3	1	9	2.264	1.177	36.6	Yes	96	314	Wide Temp. Window
YI3	0	7	2.402	0.858	0.0	Yes	117	322	Wide Temp. Window
BaCl2	0	8	2.279	1.142	21.8	No	-40	172	Wide Temp. Window
NbBr4	0	8	2.376	0.922	23.5	No	145	203	100°C - 200°C
VCl2	4	12	2.048	1.509	31.4	No	88	231	Wide Temp. Window
CaI2	2	12	2.184	1.300	0.0	No	115	296	200°C - 300°C
MgI2	1	6	2.339	0.984	8.6	No	206	298	200°C - 300°C
LaI3	0	9	2.375	0.884	0.0	No	22	361	Wide Temp. Window
VBr2	1	6	2.334	0.983	39.4	No	123	189	100°C - 200°C
SrI2	1	9	2.331	0.988	4.3	No	9	235	Wide Temp. Window
CoBr2	0	8	2.257	1.144	30.7	No	-23	118	Wide Temp. Window
SnF4	1	4	2.356	0.923	19.9	No	195	438	Wide Temp. Window
GeCl2	0	4	2.231	1.179	25.9	Yes	36	315	Wide Temp. Window
CaI2	0	8	2.234	1.168	11.7	No	115	229	100°C - 200°C
MoBr4	0	8	2.355	0.896	4.3	No	71	211	Wide Temp. Window
VF3	0	2	2.347	0.917	31.5	No	179	179	100°C - 200°C
YBr3	1	6	2.356	0.883	36.6	Yes	110	314	Wide Temp. Window
ScF3	0	3	2.249	1.119	1.3	Yes	71	235	Wide Temp. Window
CaCl2	4	12	1.954	1.576	0.0	No	67	270	Wide Temp. Window
TiCl4	0	5	2.211	1.187	30.0	No	167	188	100°C - 200°C
GeF4	1	3	2.330	0.932	47.3	Yes	183	564	Wide Temp. Window
LiF1	0	2	2.186	1.230	37.1	No	-12	-12	< 50°C
SrI2	0	6	2.352	0.866	0.0	No	131	203	100°C - 200°C
TiF3	3	9	2.095	1.366	38.8	No	83	204	Wide Temp. Window
BaCl2	0	6	2.261	1.057	6.7	No	37	172	Wide Temp. Window
MgCl2	0	2	2.186	1.200	0.0	No	245	288	200°C - 300°C
ZrBr3	0	9	2.222	1.128	47.6	Yes	150	150	100°C - 200°C
MnBr2	0	4	2.329	0.885	0.7	No	162	162	100°C - 200°C
SrI2	0	7	2.314	0.921	9.0	No	9	203	Wide Temp. Window
BaF2	0	4	2.339	0.853	13.1	No	28	149	Wide Temp. Window
NiCl2	0	4	2.238	1.089	13.9	No	67	137	100°C - 200°C
CaBr2	1	7	2.239	1.084	18.3	No	48	179	Wide Temp. Window
GaCl3	1	6	2.203	1.148	7.1	Yes	100	247	100°C - 200°C
YF3	1	8	2.200	1.154	37.0	Yes	-22	152	Wide Temp. Window
GaF3	0	3	2.308	0.916	0.0	Yes	-42	400	Wide Temp. Window
NiI2	0	9	2.289	0.955	32.6	No	-12	302	Wide Temp. Window
YI3	0	6	2.356	0.768	0.0	Yes	117	322	Wide Temp. Window
CaBr2	2	9	2.168	1.195	9.7	No	48	268	Wide Temp. Window
ZnBr2	0	4	2.330	0.830	10.2	No	98	201	Wide Temp. Window
CaBr2	0	4	2.261	0.996	1.2	No	170	245	200°C - 300°C
NiCl2	4	12	2.027	1.407	14.4	No	20	213	Wide Temp. Window

ScI3	0	6	2.312	0.860	0.0	Yes	159	322	Wide Temp. Window
YCl3	2	9	2.056	1.363	12.5	Yes	22	357	Wide Temp. Window
MnCl4	2	8	2.142	1.221	0.0	No	187	256	200°C - 300°C
SnCl4	0	5	2.247	0.993	0.0	No	177	244	200°C - 300°C
SrCl2	1	6	2.184	1.114	14.5	No	88	230	Wide Temp. Window
LiCl1	1	4	1.997	1.414	3.8	No	67	140	100°C - 200°C
VF3	4	9	2.067	1.302	44.7	No	175	231	200°C - 300°C
MgCl2	1	4	2.080	1.281	0.0	No	202	245	200°C - 300°C
SnF2	0	4	2.240	0.952	1.7	No	-37	268	Wide Temp. Window
LaI2	0	12	2.157	1.127	48.2	No	119	119	100°C - 200°C
YF3	1	7	2.173	1.096	37.0	Yes	8	152	Wide Temp. Window
BeF2	2	7	2.002	1.384	13.0	Yes	41	76	50°C - 100°C
WBr4	0	8	2.309	0.763	12.6	No	7	237	Wide Temp. Window
CaI2	0	6	2.228	0.972	9.4	No	124	229	100°C - 200°C
CaBr2	1	6	2.217	0.995	12.1	No	108	179	100°C - 200°C
VCl4	0	5	2.153	1.124	6.3	No	120	214	100°C - 200°C
ZnCl2	4	12	1.989	1.391	8.7	No	53	220	Wide Temp. Window
LiI1	0	2	2.268	0.855	0.0	No	207	243	200°C - 300°C
3-Feb	0	6	2.269	0.846	23.4	No	117	117	100°C - 200°C
MgCl2	2	6	2.071	1.252	12.5	No	124	202	100°C - 200°C
VCl4	2	8	2.092	1.215	22.0	No	158	214	100°C - 200°C
GaCl3	0	4	2.191	1.020	21.0	Yes	100	267	100°C - 200°C
VBr3	1	8	2.218	0.953	40.8	No	59	258	Wide Temp. Window
ZnI2	0	8	2.222	0.941	20.3	No	32	191	Wide Temp. Window
MgI2	2	8	2.187	1.018	2.9	No	183	263	200°C - 300°C
CaBr2	1	8	2.055	1.257	11.4	No	48	268	Wide Temp. Window
CoCl2	4	12	1.970	1.387	49.5	No	96	152	100°C - 200°C
YCl3	2	8	2.107	1.165	12.5	Yes	22	283	Wide Temp. Window
BeF2	4	12	1.947	1.413	17.1	Yes	41	68	50°C - 100°C
CrBr3	1	6	2.230	0.867	48.8	No	202	202	200°C - 300°C
CrCl4	0	5	2.125	1.096	37.8	No	152	158	100°C - 200°C
BaCl2	1	9	2.116	1.112	15.5	No	-40	197	Wide Temp. Window
HfF4	1	5	2.245	0.801	30.0	Yes	-29	281	Wide Temp. Window
TiF4	0	2	2.189	0.939	0.7	No	205	278	200°C - 300°C
VF4	1	4	2.120	1.083	42.2	No	112	348	Wide Temp. Window
MgF2	6	12	1.921	1.400	25.1	No	-22	306	Wide Temp. Window
CrBr3	1	8	2.172	0.960	46.0	No	-43	202	Wide Temp. Window
SiF4	3	8	2.012	1.256	19.4	No	103	232	100°C - 200°C
ZnI2	0	6	2.233	0.791	19.7	No	32	191	Wide Temp. Window
HfF4	2	8	2.176	0.932	9.5	Yes	-29	281	Wide Temp. Window
BaCl2	2	12	1.958	1.328	0.0	No	-40	222	Wide Temp. Window
HfCl4	0	4	2.219	0.802	27.8	Yes	212	283	200°C - 300°C
TiF4	1	4	2.085	1.103	10.5	No	173	278	200°C - 300°C
GeF2	0	2	2.194	0.849	11.2	Yes	153	153	100°C - 200°C
CrI3	0	9	2.171	0.904	0.0	No	13	385	Wide Temp. Window
ZnF2	2	6	2.127	1.000	19.2	No	-14	192	Wide Temp. Window
MoCl4	2	8	2.080	1.090	12.6	No	162	235	100°C - 200°C
HfF4	0	4	2.229	0.739	12.0	Yes	-29	281	Wide Temp. Window

NiBr2	0	4	2.213	0.782	36.7	No	21	148	Wide Temp. Window
BaBr2	0	6	2.175	0.858	3.5	No	23	190	Wide Temp. Window
MgF2	0	2	2.117	0.981	29.1	No	-4	118	Wide Temp. Window
NiBr2	1	6	2.166	0.863	43.6	No	60	148	100°C - 200°C
LaI3	0	8	2.189	0.794	5.9	No	22	361	Wide Temp. Window
ZnI2	2	12	2.062	1.083	20.7	No	32	286	Wide Temp. Window
CrBr3	1	7	2.135	0.921	46.0	No	-11	202	Wide Temp. Window
SrI2	2	12	2.015	1.142	0.0	No	9	235	Wide Temp. Window
CaI2	1	7	2.132	0.898	12.2	No	115	229	100°C - 200°C
ZrCl4	2	8	2.032	1.102	43.9	Yes	183	228	200°C - 300°C
LaI3	1	9	2.166	0.806	35.7	No	22	361	Wide Temp. Window
SrF2	0	4	2.067	1.026	8.7	No	54	94	50°C - 100°C
NbCl4	0	5	2.084	0.982	42.6	No	164	164	100°C - 200°C
CaI2	2	9	2.077	0.989	4.4	No	115	296	200°C - 300°C
HfI4	0	8	2.203	0.657	31.5	Yes	194	194	100°C - 200°C
ZrCl4	0	4	2.080	0.979	16.9	Yes	207	260	200°C - 300°C
CaF2	0	2	2.122	0.882	7.4	No	72	72	50°C - 100°C
ZnCl2	2	8	1.956	1.205	30.7	No	53	188	100°C - 200°C
PbF2	0	4	2.194	0.677	3.0	No	75	115	50°C - 100°C
VF4	3	8	1.962	1.187	13.2	No	129	254	100°C - 200°C
SnCl4	2	8	2.045	1.028	14.2	No	177	244	200°C - 300°C
VBr2	4	12	1.946	1.203	20.8	No	123	208	100°C - 200°C
CaCl2	2	8	1.812	1.395	13.3	No	67	173	100°C - 200°C
NiF2	6	12	1.926	1.227	46.8	No	1	286	Wide Temp. Window
ScCl3	2	6	1.954	1.180	19.9	Yes	105	361	Wide Temp. Window
GeF4	3	8	2.006	1.087	4.5	Yes	110	251	100°C - 200°C
NaI1	0	4	2.065	0.960	12.9	No	-13	148	Wide Temp. Window
SrBr2	1	6	2.104	0.870	3.6	No	110	191	100°C - 200°C
YI3	2	10	2.114	0.842	32.3	Yes	31	322	Wide Temp. Window
NaCl1	0	2	1.949	1.172	0.0	No	106	106	100°C - 200°C
AlCl3	3	6	1.948	1.170	44.9	No	220	448	300°C - 450°C
CaBr2	4	12	1.881	1.273	1.2	No	48	268	Wide Temp. Window
YBr3	2	8	2.083	0.900	20.5	Yes	96	314	Wide Temp. Window
SnCl2	0	4	2.059	0.943	0.0	No	41	298	Wide Temp. Window
HfBr4	0	5	2.174	0.629	34.4	Yes	164	251	200°C - 300°C
NiCl2	2	8	1.927	1.183	40.0	No	20	137	Wide Temp. Window
TiF4	3	8	1.921	1.189	4.0	No	121	243	100°C - 200°C
MgI2	4	12	1.956	1.127	0.0	No	183	267	200°C - 300°C
YCl3	2	7	1.995	1.045	12.5	Yes	22	283	Wide Temp. Window
PbCl2	0	6	2.105	0.800	19.3	No	-32	214	Wide Temp. Window
MgBr2	1	4	2.065	0.890	8.2	No	237	270	200°C - 300°C
SrI2	1	8	2.071	0.872	8.9	No	9	203	Wide Temp. Window
SiF4	2	5	1.956	1.089	14.7	No	168	232	200°C - 300°C
MgCl2	4	9	1.854	1.251	7.5	No	124	254	100°C - 200°C
MoF4	3	8	1.981	1.034	43.2	No	128	245	100°C - 200°C
ScCl3	0	3	1.948	1.095	0.0	Yes	45	361	Wide Temp. Window
NiCl2	2	6	1.992	1.002	35.5	No	132	137	100°C - 200°C
ZnF2	6	12	1.879	1.196	19.2	No	-16	286	Wide Temp. Window

YI3	2	9	2.078	0.796	32.3	Yes	100	322	Wide Temp. Window
CuBr2	0	4	2.093	0.753	0.0	No	3	213	Wide Temp. Window
BeCl2	4	12	1.753	1.363	13.4	Yes	-21	122	Wide Temp. Window
YF3	3	9	1.892	1.156	12.9	Yes	-22	693	Wide Temp. Window
ZnCl2	2	6	1.981	0.993	30.7	No	97	188	100°C - 200°C
TiCl4	0	4	1.965	1.024	36.7	No	185	188	100°C - 200°C
SrCl2	0	4	1.966	1.020	10.4	No	88	230	Wide Temp. Window
YBr3	2	9	1.963	1.021	20.5	Yes	96	314	Wide Temp. Window
MgCl2	6	12	1.730	1.378	12.5	No	168	254	200°C - 300°C
RbF1	0	1	2.085	0.736	0.0	Yes	344	344	300°C - 450°C
YCl3	0	4	1.972	0.993	12.8	Yes	75	283	Wide Temp. Window
ScBr3	0	4	2.060	0.790	17.8	Yes	128	392	Wide Temp. Window
YCl3	2	6	1.983	0.966	12.5	Yes	75	283	Wide Temp. Window
LaI3	0	6	2.099	0.671	0.0	No	67	361	Wide Temp. Window
SrI2	2	9	2.027	0.859	4.3	No	9	235	Wide Temp. Window
ZrI4	0	8	2.081	0.698	17.6	Yes	164	182	100°C - 200°C
TiI4	0	8	2.072	0.708	24.2	No	151	151	100°C - 200°C
LiCl1	0	1	1.904	1.078	0.0	No	173	173	100°C - 200°C
LaI3	0	7	2.064	0.719	7.7	No	22	361	Wide Temp. Window
PbCl4	0	5	2.052	0.749	6.6	No	155	218	100°C - 200°C
NiBr3	1	9	2.002	0.873	42.4	No	-3	144	Wide Temp. Window
SnF4	3	8	1.962	0.958	3.9	No	124	252	100°C - 200°C
BaCl2	1	8	1.944	0.974	21.8	No	-40	172	Wide Temp. Window
CaI2	1	8	1.927	1.007	11.7	No	115	229	100°C - 200°C
TiI3	0	6	2.041	0.743	45.9	No	182	182	100°C - 200°C
VCl3	1	4	1.940	0.974	46.7	No	237	237	200°C - 300°C
SnCl4	0	4	1.993	0.850	2.6	No	199	244	200°C - 300°C
MgBr2	2	6	1.952	0.939	6.1	No	157	237	100°C - 200°C
GeBr2	0	4	2.016	0.787	0.0	Yes	29	211	Wide Temp. Window
ScCl3	1	4	1.890	1.046	46.3	Yes	105	361	Wide Temp. Window
BaI2	0	6	2.029	0.730	0.0	No	116	226	100°C - 200°C
ZrBr4	0	5	2.029	0.697	19.2	Yes	150	239	100°C - 200°C
CrI3	0	8	2.003	0.766	14.1	No	13	136	Wide Temp. Window
VCl4	0	4	1.915	0.963	19.3	No	120	214	100°C - 200°C
TiBr3	0	4	2.008	0.745	40.8	No	186	186	100°C - 200°C
ZrI3	0	9	1.965	0.850	42.6	Yes	137	137	100°C - 200°C
GeF4	2	5	1.935	0.910	0.0	Yes	183	251	200°C - 300°C
LiBr1	1	4	1.873	1.028	6.9	No	48	180	Wide Temp. Window
VBr3	0	4	2.012	0.719	41.1	No	2	258	Wide Temp. Window
CrI3	0	6	2.031	0.663	3.8	No	136	136	100°C - 200°C
NiI2	0	6	2.011	0.697	32.6	No	21	82	50°C - 100°C
NaBr1	0	3	1.887	0.977	19.0	No	-20	127	Wide Temp. Window
CsF1	0	2	1.993	0.735	0.0	Yes	151	249	100°C - 200°C
ZnCl2	1	4	1.922	0.901	35.8	No	90	188	100°C - 200°C
LiF1	2	4	1.769	1.172	37.1	No	34	207	Wide Temp. Window
WF4	3	8	1.955	0.798	7.6	No	130	227	100°C - 200°C
WCl4	0	5	1.983	0.719	18.9	No	92	244	Wide Temp. Window
CrCl4	0	4	1.891	0.934	44.9	No	152	152	100°C - 200°C

YBr3	2	7	1.951	0.797	20.5	Yes	96	314	Wide Temp. Window
PbCl2	0	4	1.991	0.681	0.0	No	73	214	Wide Temp. Window
SrI2	1	7	1.953	0.777	9.0	No	9	203	Wide Temp. Window
PbF2	0	2	2.061	0.403	0.0	No	115	115	100°C - 200°C
CuF2	2	4	1.926	0.826	41.7	No	218	218	200°C - 300°C
PbCl4	2	8	1.929	0.817	20.8	No	155	218	100°C - 200°C
LaI3	1	8	1.969	0.714	35.7	No	22	361	Wide Temp. Window
HfF4	1	3	2.028	0.523	30.0	Yes	280	281	200°C - 300°C
NiI2	0	8	1.930	0.809	32.6	No	-12	82	< 50°C
CaCl2	2	6	1.807	1.048	16.7	No	67	173	100°C - 200°C
VI4	0	8	1.974	0.658	8.9	No	47	180	Wide Temp. Window
MgBr2	0	2	1.944	0.730	0.5	No	270	285	200°C - 300°C
YI3	2	8	1.943	0.731	32.3	Yes	117	322	Wide Temp. Window
CuF2	6	12	1.750	1.114	18.3	No	-18	223	Wide Temp. Window
GeCl2	1	4	1.835	0.969	43.7	Yes	149	315	Wide Temp. Window
SrI2	1	6	1.946	0.716	0.0	No	131	203	100°C - 200°C
SnF4	1	3	1.953	0.692	19.9	No	195	438	Wide Temp. Window
ZnI2	2	9	1.910	0.794	20.7	No	32	286	Wide Temp. Window
CrBr4	2	8	1.917	0.763	31.6	No	171	179	100°C - 200°C
ZnI2	0	4	1.961	0.636	12.0	No	115	191	100°C - 200°C
YF3	2	8	1.822	0.956	30.7	Yes	-22	152	Wide Temp. Window
NbI4	0	8	1.954	0.639	28.0	No	135	135	100°C - 200°C
YCl3	3	9	1.713	1.136	0.9	Yes	22	357	Wide Temp. Window
BaCl2	1	6	1.861	0.870	11.3	No	37	172	Wide Temp. Window
SrBr2	0	4	1.901	0.774	8.2	No	110	192	100°C - 200°C
SnF2	1	4	1.886	0.802	41.7	No	84	268	Wide Temp. Window
PbBr2	0	6	1.943	0.647	20.6	No	-47	198	Wide Temp. Window
VBr4	2	8	1.896	0.772	20.2	No	111	199	100°C - 200°C
CaI2	0	4	1.904	0.751	1.1	No	176	229	200°C - 300°C
SrF2	0	2	1.935	0.663	0.8	No	94	94	50°C - 100°C
CaF2	7	12	1.642	1.218	37.0	No	-15	279	Wide Temp. Window
ScBr3	2	6	1.869	0.829	34.9	Yes	128	392	Wide Temp. Window
CaBr2	2	8	1.741	1.065	11.4	No	48	268	Wide Temp. Window
TiF4	2	5	1.787	0.987	0.7	No	173	243	200°C - 300°C
CaI2	4	12	1.752	1.043	1.1	No	115	296	200°C - 300°C
GeCl4	0	5	1.835	0.889	33.8	Yes	81	164	100°C - 200°C
GaCl3	0	3	1.846	0.863	16.9	Yes	137	267	200°C - 300°C
NbI3	0	9	1.872	0.790	48.1	No	109	109	100°C - 200°C
MgF2	2	4	1.772	0.993	29.1	No	184	184	100°C - 200°C
LaI3	2	9	1.903	0.708	29.8	No	22	361	Wide Temp. Window
WBr4	2	8	1.926	0.637	44.6	No	175	237	200°C - 300°C
GaCl3	2	6	1.799	0.938	7.1	Yes	100	247	100°C - 200°C
CaCl2	6	12	1.577	1.273	16.7	No	83	270	Wide Temp. Window
CaBr2	2	7	1.821	0.882	18.3	No	48	170	Wide Temp. Window
VBr2	2	6	1.865	0.785	35.3	No	123	189	100°C - 200°C
GeF4	1	2	1.912	0.662	47.3	Yes	564	564	450°C - 600°C
SnI4	0	5	1.946	0.537	19.7	No	93	451	Wide Temp. Window
MoBr4	2	8	1.883	0.717	11.6	No	116	211	100°C - 200°C

YBr3	2	6	1.887	0.707	20.5	Yes	110	314	Wide Temp. Window
NaBr1	0	2	1.831	0.838	0.0	No	124	127	100°C - 200°C
MoI4	0	8	1.918	0.612	26.4	No	63	172	100°C - 200°C
BaCl2	2	9	1.782	0.936	15.5	No	-40	197	Wide Temp. Window
MnCl4	3	8	1.744	0.994	0.0	No	187	194	100°C - 200°C
HfCl4	0	3	1.897	0.651	40.3	Yes	283	283	200°C - 300°C
HfBr4	0	4	1.933	0.536	41.0	Yes	251	251	200°C - 300°C
MoBr2	0	12	1.746	0.982	48.6	No	-8	-8	< 50°C
PbBr4	0	8	1.900	0.633	3.6	No	-21	175	Wide Temp. Window
TiBr4	0	5	1.885	0.676	35.0	No	128	173	100°C - 200°C
BaF2	0	2	1.914	0.583	0.0	No	149	149	100°C - 200°C
VCl4	3	8	1.728	1.004	12.6	No	158	199	100°C - 200°C
GeBr4	0	9	1.849	0.752	45.3	Yes	43	45	< 50°C
MnCl4	0	3	1.809	0.844	0.0	No	187	256	200°C - 300°C
CaI2	1	6	1.827	0.797	9.4	No	124	229	100°C - 200°C
SnF4	2	5	1.836	0.770	0.0	No	195	252	200°C - 300°C
MgI2	1	4	1.869	0.685	8.6	No	263	298	200°C - 300°C
VBr2	1	4	1.863	0.700	39.4	No	159	189	100°C - 200°C
NiBr3	1	6	1.863	0.698	42.4	No	72	144	100°C - 200°C
ZrBr4	2	8	1.849	0.730	46.6	Yes	150	207	100°C - 200°C
LiCl1	1	3	1.625	1.140	3.2	No	67	140	100°C - 200°C
BaCl2	4	12	1.643	1.114	15.1	No	-40	222	Wide Temp. Window
YF3	1	4	1.843	0.738	37.0	Yes	11	152	Wide Temp. Window
YF3	2	6	1.821	0.786	23.3	Yes	11	152	Wide Temp. Window
LiBr1	0	1	1.859	0.689	0.0	No	222	222	200°C - 300°C
VF4	2	5	1.750	0.930	35.0	No	112	254	100°C - 200°C
BaCl2	0	4	1.827	0.766	15.1	No	37	172	Wide Temp. Window
MgI2	2	6	1.826	0.768	0.8	No	206	263	200°C - 300°C
SnBr2	0	4	1.863	0.671	0.0	No	48	230	Wide Temp. Window
TiCl4	3	8	1.698	1.011	48.7	No	167	197	100°C - 200°C
BeBr2	4	12	1.660	1.060	11.7	Yes	46	162	Wide Temp. Window
CuCl2	2	6	1.765	0.873	45.0	No	-40	219	Wide Temp. Window
GeF2	6	12	1.643	1.086	42.6	Yes	-1	200	Wide Temp. Window
VCl2	6	12	1.584	1.167	28.1	No	88	231	Wide Temp. Window
YF3	2	7	1.755	0.885	26.2	Yes	8	152	Wide Temp. Window
BeF2	4	9	1.612	1.122	14.0	Yes	41	68	50°C - 100°C
YF3	4	9	1.672	1.022	20.4	Yes	-22	693	Wide Temp. Window
CoF3	3	6	1.774	0.813	37.6	No	143	143	100°C - 200°C
ZnBr2	2	6	1.811	0.727	41.2	No	83	201	Wide Temp. Window
PbBr2	0	4	1.871	0.549	0.0	No	98	198	100°C - 200°C
ZnF2	2	4	1.786	0.774	7.9	No	192	192	100°C - 200°C
MgBr2	7	12	1.626	1.064	33.8	No	214	595	Wide Temp. Window
RbBr1	0	4	1.734	0.873	5.0	Yes	-35	205	Wide Temp. Window
SnF2	0	2	1.848	0.588	0.0	No	-37	268	Wide Temp. Window
VCl2	4	9	1.649	1.019	47.9	No	88	195	100°C - 200°C
NaI1	0	3	1.771	0.785	16.7	No	-13	148	Wide Temp. Window
MgI2	4	9	1.765	0.799	0.0	No	183	267	200°C - 300°C
WF4	2	5	1.834	0.622	47.6	No	219	227	200°C - 300°C

LaI3	1	7	1.828	0.637	35.7	No	22	361	Wide Temp. Window
VBr3	3	9	1.725	0.877	19.9	No	59	671	Wide Temp. Window
CaCl2	1	4	1.618	1.061	0.0	No	165	173	100°C - 200°C
YBr3	0	4	1.811	0.675	14.1	Yes	85	314	Wide Temp. Window
MoCl4	3	8	1.710	0.896	30.4	No	162	225	100°C - 200°C
VF4	1	3	1.751	0.811	42.2	No	112	348	Wide Temp. Window
ZrCl4	0	3	1.756	0.797	26.5	Yes	228	260	200°C - 300°C
LaI3	1	6	1.835	0.587	35.7	No	67	361	Wide Temp. Window
VBr4	0	5	1.817	0.639	8.9	No	81	189	100°C - 200°C
MnBr4	3	8	1.785	0.722	46.2	No	109	499	Wide Temp. Window
NiCl2	1	4	1.731	0.842	13.9	No	70	137	100°C - 200°C
HfF4	1	4	1.822	0.604	30.0	Yes	-29	281	Wide Temp. Window
NaBr1	1	4	1.687	0.916	5.7	No	-20	173	Wide Temp. Window
YI3	3	10	1.778	0.709	11.7	Yes	31	312	Wide Temp. Window
YCl3	3	8	1.674	0.926	9.6	Yes	22	278	Wide Temp. Window
WI4	0	8	1.838	0.527	11.8	No	16	173	Wide Temp. Window
NbBr4	0	5	1.812	0.606	43.9	No	145	145	100°C - 200°C
PbCl4	0	4	1.800	0.632	7.1	No	167	218	100°C - 200°C
CaBr2	2	6	1.740	0.781	12.1	No	108	170	100°C - 200°C
YI3	2	7	1.795	0.642	32.3	Yes	117	322	Wide Temp. Window
YCl3	0	3	1.699	0.861	0.9	Yes	151	283	200°C - 300°C
ZrCl4	3	8	1.674	0.908	26.5	Yes	183	207	100°C - 200°C
NiBr2	1	4	1.795	0.635	43.6	No	148	148	100°C - 200°C
SrI2	2	8	1.753	0.738	8.9	No	9	203	Wide Temp. Window
BaBr2	1	6	1.769	0.698	3.5	No	23	190	Wide Temp. Window
WCl4	3	8	1.746	0.740	18.7	No	161	244	200°C - 300°C
MoBr4	0	5	1.802	0.588	15.5	No	71	211	Wide Temp. Window
VCl3	4	9	1.571	1.059	46.7	No	179	208	100°C - 200°C
TiF4	1	3	1.707	0.818	10.5	No	173	278	200°C - 300°C
ZnCl2	6	12	1.550	1.085	11.2	No	53	220	Wide Temp. Window
ZrBr4	0	4	1.793	0.595	22.0	Yes	193	239	200°C - 300°C
SrI2	4	12	1.642	0.930	6.7	No	9	235	Wide Temp. Window
PbCl2	1	6	1.761	0.669	20.8	No	-32	214	Wide Temp. Window
HfF4	0	2	1.825	0.429	9.5	Yes	29	280	Wide Temp. Window
ZnI2	4	12	1.659	0.872	12.0	No	32	286	Wide Temp. Window
SnCl4	3	8	1.674	0.841	5.1	No	177	202	100°C - 200°C
LiI1	1	4	1.693	0.798	12.9	No	2	243	Wide Temp. Window
NiCl2	4	9	1.614	0.942	31.3	No	20	213	Wide Temp. Window
SnBr4	0	5	1.778	0.575	0.0	No	90	223	Wide Temp. Window
CaCl2	0	2	1.642	0.892	2.5	No	165	187	100°C - 200°C
NiI2	0	4	1.789	0.539	32.6	No	82	82	50°C - 100°C
CoCl2	6	12	1.527	1.075	46.6	No	152	152	100°C - 200°C
NiCl2	6	12	1.534	1.065	14.4	No	20	213	Wide Temp. Window
CaI2	2	7	1.718	0.723	12.2	No	115	176	100°C - 200°C
CoI2	4	12	1.647	0.864	37.6	No	-6	340	Wide Temp. Window
HfCl4	3	8	1.701	0.745	40.3	Yes	192	212	200°C - 300°C
HfF4	3	8	1.702	0.729	0.0	Yes	-29	267	Wide Temp. Window
SrCl2	2	6	1.645	0.839	7.8	No	88	132	100°C - 200°C

SnCl2	1	4	1.677	0.767	37.9	No	129	298	200°C - 300°C
ScI3	0	4	1.752	0.573	25.4	Yes	159	235	100°C - 200°C
ScBr3	0	3	1.720	0.660	8.8	Yes	159	392	Wide Temp. Window
YI3	3	9	1.719	0.658	11.7	Yes	100	312	Wide Temp. Window
SrCl2	0	2	1.710	0.667	0.0	No	113	230	100°C - 200°C
YBr3	3	9	1.627	0.846	4.8	Yes	96	299	Wide Temp. Window
TiCl4	0	3	1.638	0.823	48.7	No	185	185	100°C - 200°C
CuCl2	7	12	1.505	1.039	30.1	No	185	323	Wide Temp. Window
ZnCl2	4	9	1.581	0.919	12.5	No	53	214	Wide Temp. Window
KF1	0	1	1.625	0.827	8.7	No	158	158	100°C - 200°C
VBr2	4	9	1.631	0.813	20.4	No	123	155	100°C - 200°C
GeCl2	0	2	1.670	0.730	25.9	Yes	36	315	Wide Temp. Window
WCl4	0	4	1.717	0.592	38.2	No	92	244	Wide Temp. Window
CuF2	4	9	1.590	0.870	21.1	No	-18	68	< 50°C
CaI2	2	8	1.606	0.840	11.7	No	115	176	100°C - 200°C
YBr3	3	8	1.663	0.718	4.8	Yes	96	299	Wide Temp. Window
SiF4	4	8	1.536	0.959	11.8	No	103	229	100°C - 200°C
VBr3	1	4	1.702	0.608	19.7	No	176	258	200°C - 300°C
BaI2	0	4	1.728	0.531	2.4	No	116	226	100°C - 200°C
SnI4	0	4	1.743	0.473	23.6	No	93	451	Wide Temp. Window
VF4	4	8	1.543	0.934	11.0	No	129	254	100°C - 200°C
SnCl4	0	3	1.671	0.678	5.1	No	199	244	200°C - 300°C
LaCl3	0	3	1.685	0.639	2.3	No	80	298	Wide Temp. Window
LaI3	2	8	1.691	0.613	29.8	No	22	361	Wide Temp. Window
YCl3	4	9	1.499	0.994	12.8	Yes	22	357	Wide Temp. Window
WBr4	0	5	1.731	0.484	21.1	No	7	237	Wide Temp. Window
NiI2	4	12	1.593	0.830	20.7	No	-12	302	Wide Temp. Window
ScI3	3	9	1.640	0.733	27.6	Yes	25	322	Wide Temp. Window
CaBr2	6	12	1.486	1.006	12.1	No	48	268	Wide Temp. Window
CaCl2	4	9	1.477	1.017	15.7	No	67	160	100°C - 200°C
LiBr1	1	3	1.592	0.826	2.3	No	71	180	100°C - 200°C
NaI1	0	2	1.668	0.658	0.0	No	143	148	100°C - 200°C
FeCl2	6	12	1.476	1.013	36.4	No	31	216	Wide Temp. Window
SrF2	2	6	1.626	0.748	19.6	No	-1	54	< 50°C
ScF3	0	2	1.630	0.727	17.5	Yes	71	71	50°C - 100°C
CaBr2	1	4	1.630	0.718	1.2	No	170	179	100°C - 200°C
SrBr2	2	6	1.644	0.679	2.7	No	110	171	100°C - 200°C
VBr2	6	12	1.508	0.933	22.8	No	155	208	100°C - 200°C
ScCl3	1	3	1.546	0.869	46.3	Yes	315	361	300°C - 450°C
MgF2	8	12	1.431	1.042	24.5	No	-22	306	Wide Temp. Window
ZrF4	0	2	1.675	0.574	17.3	Yes	126	126	100°C - 200°C
GeBr2	1	4	1.645	0.643	40.1	Yes	155	211	100°C - 200°C
BaCl2	2	8	1.576	0.789	21.8	No	-40	136	Wide Temp. Window
TiF4	4	8	1.496	0.926	3.1	No	121	243	100°C - 200°C
YI3	2	6	1.671	0.545	32.3	Yes	117	322	Wide Temp. Window
LaI3	3	9	1.640	0.611	23.0	No	22	361	Wide Temp. Window
GeF2	7	12	1.459	0.964	43.5	Yes	37	200	Wide Temp. Window
TiBr4	0	4	1.649	0.570	38.9	No	151	173	100°C - 200°C

SrI2	0	4	1.636	0.605	6.7	No	131	187	100°C - 200°C
NiF2	4	9	1.526	0.846	40.8	No	1	66	< 50°C
VCl4	0	3	1.568	0.754	12.6	No	120	214	100°C - 200°C
CaBr2	4	9	1.520	0.838	9.7	No	48	268	Wide Temp. Window
MgCl2	4	8	1.399	1.023	12.2	No	124	168	100°C - 200°C
GeF4	4	8	1.524	0.826	1.9	Yes	110	234	100°C - 200°C
NiCl2	0	2	1.620	0.602	35.5	No	67	70	50°C - 100°C
SrI2	2	7	1.604	0.638	9.0	No	9	203	Wide Temp. Window
BaI2	1	6	1.624	0.584	0.0	No	116	135	100°C - 200°C
PbCl4	3	8	1.586	0.671	10.4	No	155	190	100°C - 200°C
MoF4	4	8	1.522	0.794	29.1	No	128	244	100°C - 200°C
KCl1	0	2	1.413	0.972	4.0	No	86	104	50°C - 100°C
GeCl4	0	4	1.552	0.722	41.4	Yes	81	81	50°C - 100°C
MgI2	0	2	1.628	0.518	0.8	No	270	298	200°C - 300°C
YCl3	3	7	1.513	0.793	8.8	Yes	22	278	Wide Temp. Window
LaBr3	4	10	1.567	0.671	27.6	No	-35	345	Wide Temp. Window
CrBr4	0	4	1.617	0.535	33.4	No	96	171	100°C - 200°C
VBr3	0	3	1.605	0.566	41.1	No	2	258	Wide Temp. Window
VBr4	3	8	1.575	0.642	12.8	No	111	199	100°C - 200°C
NiF2	8	12	1.430	0.911	16.1	No	1	286	Wide Temp. Window
ZrF4	4	8	1.485	0.817	19.2	Yes	129	262	100°C - 200°C
BeF2	4	8	1.391	0.967	14.2	Yes	41	50	< 50°C
YCl3	1	4	1.512	0.762	20.7	Yes	75	283	Wide Temp. Window
AlCl3	4	6	1.452	0.872	38.1	No	448	448	300°C - 450°C
SrF2	7	12	1.406	0.943	29.1	No	59	267	Wide Temp. Window
ScI3	3	8	1.580	0.608	27.6	Yes	25	322	Wide Temp. Window
GeCl2	7	12	1.370	0.995	49.1	Yes	129	252	100°C - 200°C
VBr4	0	4	1.604	0.539	7.2	No	81	189	100°C - 200°C
MgI2	6	12	1.465	0.844	0.6	No	183	267	200°C - 300°C
LiI1	1	3	1.556	0.660	7.9	No	61	243	Wide Temp. Window
ZnF2	0	1	1.618	0.482	12.8	No	127	127	100°C - 200°C
HfF4	2	5	1.589	0.567	9.5	Yes	-29	281	Wide Temp. Window
PbBr2	1	6	1.600	0.533	20.6	No	-47	198	Wide Temp. Window
SnF4	4	8	1.514	0.739	2.4	No	124	252	100°C - 200°C
GeI2	0	4	1.599	0.527	11.2	Yes	6	168	Wide Temp. Window
SrCl2	1	4	1.494	0.776	14.5	No	88	230	Wide Temp. Window
TiBr4	3	8	1.553	0.645	49.7	No	128	199	100°C - 200°C
BeF2	2	4	1.447	0.855	4.8	Yes	76	76	50°C - 100°C
SnCl2	0	2	1.579	0.573	0.0	No	41	298	Wide Temp. Window
BeCl2	4	9	1.380	0.954	18.6	Yes	-21	60	< 50°C
YI3	4	10	1.558	0.621	18.4	Yes	31	312	Wide Temp. Window
YI3	3	8	1.566	0.589	11.7	Yes	117	312	Wide Temp. Window
ZrI4	0	5	1.608	0.463	44.8	Yes	164	164	100°C - 200°C
ZnBr2	7	12	1.439	0.849	34.7	No	195	320	Wide Temp. Window
ZnF2	4	9	1.460	0.803	25.0	No	-16	70	< 50°C
GeF4	0	1	1.585	0.515	47.3	Yes	315	315	300°C - 450°C
NaF1	0	1	1.504	0.717	31.2	No	22	22	< 50°C
GaCl3	1	4	1.508	0.702	21.0	Yes	100	138	100°C - 200°C

SrBr2	0	2	1.593	0.478	0.0	No	191	192	100°C - 200°C
ZnI2	2	8	1.531	0.648	20.7	No	32	115	Wide Temp. Window
WBr4	3	8	1.578	0.522	25.4	No	175	200	100°C - 200°C
BaBr2	0	4	1.560	0.576	18.7	No	23	172	Wide Temp. Window
VI4	2	8	1.576	0.526	31.3	No	71	180	100°C - 200°C
GeI4	0	8	1.574	0.526	22.0	Yes	53	53	50°C - 100°C
MoBr4	3	8	1.551	0.590	27.8	No	116	202	100°C - 200°C
PbCl2	1	4	1.569	0.537	20.8	No	127	214	100°C - 200°C
SrI2	2	6	1.554	0.572	0.0	No	131	203	100°C - 200°C
CoBr2	6	12	1.422	0.846	42.2	No	-23	367	Wide Temp. Window
CuF2	4	8	1.456	0.783	27.2	No	45	68	50°C - 100°C
SiF4	2	4	1.451	0.784	14.7	No	168	232	200°C - 300°C
YI3	0	4	1.570	0.504	18.4	Yes	117	322	Wide Temp. Window
LaBr3	0	3	1.581	0.468	0.6	No	114	278	100°C - 200°C
BaF2	2	6	1.520	0.631	17.3	No	28	39	< 50°C
ZnF2	8	12	1.387	0.883	20.2	No	-16	286	Wide Temp. Window
ZrBr4	3	8	1.529	0.604	31.1	Yes	150	196	100°C - 200°C
MoBr4	0	4	1.568	0.493	25.9	No	71	211	Wide Temp. Window
CaBr2	0	2	1.529	0.601	0.0	No	179	245	200°C - 300°C
CuCl2	0	2	1.533	0.590	45.0	No	71	71	50°C - 100°C
MoCl3	2	6	1.480	0.707	31.2	No	103	103	100°C - 200°C
CoF3	7	9	1.425	0.810	44.6	No	134	862	Wide Temp. Window
NiBr3	3	9	1.500	0.654	22.7	No	-3	144	Wide Temp. Window
CrF3	6	9	1.392	0.855	21.2	No	256	256	200°C - 300°C
MgCl2	0	1	1.464	0.723	0.0	No	288	288	200°C - 300°C
NaF1	1	2	1.425	0.796	31.2	No	152	152	100°C - 200°C
CaI2	4	9	1.474	0.702	4.4	No	115	296	200°C - 300°C
NiBr2	7	12	1.409	0.818	32.3	No	182	316	Wide Temp. Window
BeBr2	4	9	1.413	0.811	6.6	Yes	78	162	100°C - 200°C
MnBr2	4	9	1.457	0.729	3.3	No	103	103	100°C - 200°C
NaI1	1	4	1.476	0.686	12.9	No	-13	148	Wide Temp. Window
SnI2	0	4	1.552	0.492	0.0	No	24	127	Wide Temp. Window
CoF2	9	12	1.367	0.883	41.0	No	358	358	300°C - 450°C
HfF4	4	8	1.493	0.640	12.0	Yes	129	267	100°C - 200°C
GaF3	7	9	1.406	0.812	43.1	Yes	-40	1100	Wide Temp. Window
LaI3	2	7	1.531	0.534	29.8	No	22	361	Wide Temp. Window
CsF1	0	1	1.556	0.449	0.0	Yes	249	249	200°C - 300°C
SrCl2	7	12	1.303	0.958	23.6	No	153	244	100°C - 200°C
GaBr3	0	3	1.530	0.527	10.2	Yes	43	256	Wide Temp. Window
YBr3	0	3	1.516	0.561	4.8	Yes	85	314	Wide Temp. Window
MnCl4	2	5	1.438	0.738	0.4	No	187	256	200°C - 300°C
VBr3	4	9	1.440	0.732	19.7	No	59	671	Wide Temp. Window
VBr2	0	2	1.528	0.509	35.3	No	156	159	100°C - 200°C
YBr3	3	7	1.489	0.609	4.8	Yes	96	299	Wide Temp. Window
CuCl2	2	4	1.450	0.696	45.0	No	219	219	200°C - 300°C
YCl3	4	8	1.403	0.776	12.8	Yes	22	278	Wide Temp. Window
SrI2	4	9	1.474	0.625	6.7	No	9	235	Wide Temp. Window
CoI3	0	6	1.529	0.471	30.8	No	22	22	< 50°C

SnBr4	0	4	1.526	0.476	4.0	No	90	223	Wide Temp. Window
YF3	3	8	1.414	0.742	30.7	Yes	-22	56	< 50°C
CaI2	6	12	1.370	0.816	9.4	No	115	296	200°C - 300°C
YCl3	3	6	1.433	0.698	0.9	Yes	75	278	Wide Temp. Window
CaBr2	7	12	1.320	0.893	18.3	No	180	268	200°C - 300°C
ScCl3	3	6	1.363	0.823	0.0	Yes	105	269	100°C - 200°C
VCl4	4	8	1.376	0.799	19.3	No	158	198	100°C - 200°C
GeF4	2	4	1.453	0.649	1.3	Yes	183	251	200°C - 300°C
SnI4	0	3	1.537	0.407	28.7	No	175	451	Wide Temp. Window
PbCl4	0	3	1.510	0.497	10.4	No	167	218	100°C - 200°C
YI3	4	9	1.484	0.568	18.4	Yes	100	312	Wide Temp. Window
YBr3	4	9	1.408	0.732	14.1	Yes	96	299	Wide Temp. Window
SnBr2	1	4	1.492	0.537	26.0	No	120	230	100°C - 200°C
CaF2	8	12	1.273	0.944	22.6	No	-15	276	Wide Temp. Window
ScCl3	0	2	1.417	0.706	19.9	Yes	45	315	Wide Temp. Window
CrCl4	4	8	1.373	0.788	44.9	No	158	191	100°C - 200°C
TiCl4	4	8	1.359	0.810	36.7	No	167	197	100°C - 200°C
RbBr1	0	3	1.452	0.626	21.0	Yes	-35	82	< 50°C
MgCl2	2	4	1.346	0.829	0.0	No	202	202	200°C - 300°C
CsI1	0	4	1.458	0.607	14.5	Yes	72	72	50°C - 100°C
GeCl4	4	8	1.385	0.758	41.4	Yes	164	202	100°C - 200°C
GaCl3	0	2	1.435	0.654	4.5	Yes	137	267	200°C - 300°C
LaI3	2	6	1.502	0.480	29.8	No	67	361	Wide Temp. Window
MoF3	7	9	1.378	0.760	41.4	No	547	547	450°C - 600°C
GaCl3	3	6	1.394	0.727	16.9	Yes	100	247	100°C - 200°C
NaF1	3	4	1.316	0.856	38.7	No	396	396	300°C - 450°C
BaCl2	2	6	1.421	0.664	6.7	No	37	136	Wide Temp. Window
PbF2	7	12	1.402	0.696	30.1	No	155	204	100°C - 200°C
SnF4	1	2	1.496	0.450	19.9	No	438	438	300°C - 450°C
ZnCl2	0	2	1.457	0.561	30.7	No	26	90	50°C - 100°C
TiF3	3	6	1.378	0.732	38.8	No	83	83	50°C - 100°C
YBr3	1	4	1.462	0.545	36.6	Yes	110	314	Wide Temp. Window
SiF4	3	5	1.361	0.757	19.4	No	229	232	200°C - 300°C
2-Feb	6	12	1.352	0.773	28.2	No	108	108	100°C - 200°C
LiI1	0	1	1.486	0.461	5.4	No	207	207	200°C - 300°C
ZrBr4	0	3	1.479	0.472	31.1	Yes	207	239	200°C - 300°C
VCl4	2	5	1.375	0.718	22.0	No	158	214	100°C - 200°C
NiI3	0	6	1.477	0.464	30.6	No	17	17	< 50°C
MgF2	9	12	1.250	0.911	29.2	No	306	306	300°C - 450°C
MgCl2	8	12	1.210	0.964	12.2	No	237	254	200°C - 300°C
BaCl2	0	2	1.458	0.508	0.0	No	132	172	100°C - 200°C
AlBr3	4	6	1.416	0.612	48.7	No	513	513	450°C - 600°C
LaI3	4	9	1.444	0.538	29.9	No	22	361	Wide Temp. Window
CaI2	2	6	1.409	0.614	9.4	No	124	176	100°C - 200°C
LiCl1	2	4	1.253	0.887	3.8	No	67	82	50°C - 100°C
VF3	6	9	1.298	0.818	44.7	No	231	231	200°C - 300°C
MgI2	4	8	1.390	0.647	2.9	No	183	206	100°C - 200°C
ScI3	4	9	1.400	0.626	25.4	Yes	25	322	Wide Temp. Window

MoCl4	2	5	1.388	0.642	12.6	No	162	235	100°C - 200°C
SnCl2	7	12	1.268	0.850	33.1	No	49	278	Wide Temp. Window
PbI2	0	4	1.472	0.398	4.5	No	-16	126	Wide Temp. Window
ZnCl2	2	4	1.379	0.646	30.7	No	188	188	100°C - 200°C
CaI2	1	4	1.416	0.558	4.0	No	176	229	200°C - 300°C
ScI3	0	3	1.448	0.464	27.6	Yes	235	235	200°C - 300°C
MoCl4	4	8	1.346	0.705	23.8	No	162	197	100°C - 200°C
ZnI2	6	12	1.343	0.705	19.7	No	63	286	Wide Temp. Window
ZrCl4	4	8	1.332	0.723	16.9	Yes	183	197	100°C - 200°C
BeF2	7	12	1.226	0.890	17.1	Yes	41	68	50°C - 100°C
YBr3	4	8	1.389	0.600	14.1	Yes	96	299	Wide Temp. Window
GeBr4	0	5	1.434	0.481	47.0	Yes	45	45	< 50°C
PbBr2	1	4	1.451	0.426	18.8	No	132	198	100°C - 200°C
PbCl2	0	2	1.461	0.387	0.0	No	73	214	Wide Temp. Window
VBr3	3	8	1.388	0.597	40.8	No	59	176	100°C - 200°C
GeBr2	7	12	1.282	0.794	49.1	Yes	140	265	200°C - 300°C
NaCl1	0	1	1.321	0.724	4.4	No	106	106	100°C - 200°C
NiF2	4	8	1.310	0.743	16.1	No	1	66	< 50°C
ZnF2	1	2	1.428	0.478	12.8	No	184	184	100°C - 200°C
LaI3	3	8	1.414	0.513	23.0	No	22	361	Wide Temp. Window
VCl2	4	8	1.252	0.832	31.4	No	88	123	100°C - 200°C
GeF2	8	12	1.249	0.826	41.7	Yes	156	200	100°C - 200°C
YF3	1	3	1.368	0.598	37.0	Yes	120	152	100°C - 200°C
SnCl4	4	8	1.333	0.670	2.6	No	177	196	100°C - 200°C
CuF2	8	12	1.258	0.801	27.2	No	-18	223	Wide Temp. Window
BaBr2	2	6	1.386	0.547	3.5	No	23	190	Wide Temp. Window
SrBr2	1	4	1.380	0.562	8.2	No	110	191	100°C - 200°C
ZrCl4	2	5	1.341	0.649	43.9	Yes	183	228	200°C - 300°C
LaF3	1	3	1.413	0.469	44.1	No	128	128	100°C - 200°C
BaCl2	4	9	1.316	0.691	15.5	No	-40	197	Wide Temp. Window
SnCl4	2	5	1.358	0.600	14.2	No	177	244	200°C - 300°C
WCl4	4	8	1.367	0.579	38.2	No	161	203	100°C - 200°C
BaCl2	6	12	1.228	0.833	6.7	No	-40	222	Wide Temp. Window
GeF4	3	5	1.342	0.631	4.5	Yes	234	251	200°C - 300°C
PbBr4	3	8	1.406	0.468	40.3	No	115	175	100°C - 200°C
TiF4	2	4	1.309	0.693	3.1	No	173	211	100°C - 200°C
ZrCl4	0	2	1.363	0.578	43.9	Yes	260	260	200°C - 300°C
ScF3	7	9	1.232	0.820	39.4	Yes	-25	962	Wide Temp. Window
HfCl4	4	8	1.353	0.593	27.8	Yes	192	201	100°C - 200°C
YI3	3	7	1.387	0.496	11.7	Yes	117	312	Wide Temp. Window
GaF3	2	3	1.368	0.543	22.7	Yes	400	400	300°C - 450°C
VI2	7	12	1.292	0.706	29.5	No	183	303	Wide Temp. Window
VI4	0	5	1.414	0.408	25.2	No	47	143	Wide Temp. Window
ScI3	3	7	1.380	0.508	27.6	Yes	25	322	Wide Temp. Window
MgBr2	2	4	1.348	0.581	0.5	No	237	237	200°C - 300°C
RbCl1	0	2	1.293	0.691	2.9	Yes	90	107	50°C - 100°C
SnF4	2	4	1.363	0.534	2.4	No	195	235	200°C - 300°C
RbBr1	1	4	1.308	0.658	5.8	Yes	-35	205	Wide Temp. Window

VF4	1	2	1.353	0.556	42.2	No	348	348	300°C - 450°C
ZnF2	4	8	1.277	0.710	20.2	No	-14	70	< 50°C
CoF2	4	8	1.283	0.699	49.7	No	15	15	< 50°C
LiCl1	1	2	1.239	0.769	0.0	No	140	140	100°C - 200°C
YF3	3	7	1.302	0.656	26.2	Yes	8	56	< 50°C
PbCl2	7	12	1.274	0.708	31.6	No	86	238	Wide Temp. Window
NiF2	9	12	1.229	0.783	40.8	No	286	286	200°C - 300°C
CoI2	6	12	1.289	0.676	40.2	No	-6	340	Wide Temp. Window
ZnI2	4	9	1.344	0.558	12.0	No	32	286	Wide Temp. Window
YBr3	3	6	1.362	0.510	4.8	Yes	110	299	200°C - 300°C
CaCl2	4	8	1.149	0.885	13.3	No	67	160	100°C - 200°C
CoI2	4	9	1.336	0.562	37.6	No	-6	340	Wide Temp. Window
SnBr2	6	12	1.255	0.725	20.7	No	10	227	Wide Temp. Window
CaF2	2	4	1.247	0.738	7.4	No	106	106	100°C - 200°C
NiI2	6	12	1.281	0.667	29.2	No	-12	302	Wide Temp. Window
CuCl2	8	12	1.188	0.820	30.1	No	185	323	Wide Temp. Window
VCl2	8	12	1.160	0.855	26.0	No	195	231	200°C - 300°C
MnCl4	0	2	1.318	0.577	0.0	No	187	187	100°C - 200°C
SrF2	8	12	1.195	0.802	27.7	No	173	267	200°C - 300°C
BaCl2	1	4	1.324	0.555	15.1	No	37	172	Wide Temp. Window
ScBr3	3	6	1.311	0.582	8.8	Yes	128	309	Wide Temp. Window
NiCl2	8	12	1.177	0.817	40.0	No	210	213	200°C - 300°C
TiF3	6	9	1.200	0.782	29.7	No	204	204	200°C - 300°C
VF4	3	5	1.264	0.671	13.2	No	197	254	200°C - 300°C
MgCl2	6	9	1.186	0.800	12.5	No	168	254	200°C - 300°C
LaCl3	4	7	1.306	0.583	28.8	No	23	320	Wide Temp. Window
FeCl2	6	9	1.222	0.741	36.4	No	216	216	200°C - 300°C
BaF2	7	12	1.215	0.748	27.2	No	99	224	Wide Temp. Window
ZnF2	9	12	1.203	0.766	25.0	No	286	286	200°C - 300°C
NiCl2	4	8	1.214	0.745	40.0	No	20	132	Wide Temp. Window
MoI4	0	5	1.373	0.378	26.4	No	63	147	100°C - 200°C
KBr1	0	2	1.252	0.676	3.6	No	79	92	50°C - 100°C
AlF3	8	9	1.185	0.787	48.0	No	1054	1054	> 600°C
LaF3	4	7	1.320	0.528	49.6	No	-41	193	Wide Temp. Window
SrBr2	7	12	1.202	0.760	16.4	No	144	234	100°C - 200°C
ZnCl2	8	12	1.165	0.815	18.1	No	214	220	200°C - 300°C
CuBr2	2	4	1.335	0.480	45.2	No	213	213	200°C - 300°C
BeCl2	7	12	1.120	0.871	13.4	Yes	-21	122	Wide Temp. Window
BeCl2	4	8	1.161	0.815	17.6	Yes	-21	60	< 50°C
ZnI2	2	6	1.337	0.473	20.7	No	32	115	Wide Temp. Window
MnBr3	4	9	1.272	0.619	33.2	No	10	533	Wide Temp. Window
LaBr3	4	9	1.265	0.629	27.6	No	30	345	Wide Temp. Window
TiF4	3	5	1.236	0.683	4.0	No	211	243	200°C - 300°C
CaCl2	8	12	1.099	0.886	13.3	No	83	270	Wide Temp. Window
YI3	4	8	1.320	0.496	18.4	Yes	181	312	Wide Temp. Window
CoCl3	1	3	1.283	0.578	44.5	No	161	161	100°C - 200°C
BeF2	4	7	1.151	0.796	13.0	Yes	41	41	< 50°C
MoF4	3	5	1.274	0.577	43.2	No	244	245	200°C - 300°C

KF1	1	2	1.196	0.724	8.7	No	194	194	100°C - 200°C
TiBr4	0	3	1.326	0.440	49.7	No	151	151	100°C - 200°C
GeBr2	0	2	1.329	0.427	10.4	Yes	29	211	Wide Temp. Window
VF4	0	1	1.306	0.490	42.2	No	214	214	200°C - 300°C
ZnBr2	0	2	1.328	0.414	41.2	No	98	98	50°C - 100°C
BaBr2	0	2	1.338	0.379	0.0	No	146	172	100°C - 200°C
VI4	3	8	1.319	0.440	26.6	No	71	180	100°C - 200°C
YCl3	0	2	1.265	0.577	12.5	Yes	151	217	100°C - 200°C
ZnBr2	2	4	1.308	0.466	41.2	No	201	201	200°C - 300°C
GaF3	8	9	1.202	0.694	49.9	Yes	1100	1100	> 600°C
ScI3	4	8	1.292	0.497	25.4	Yes	25	322	Wide Temp. Window
CrBr4	4	8	1.286	0.512	33.4	No	179	179	100°C - 200°C
SnBr2	0	2	1.329	0.383	0.0	No	48	230	Wide Temp. Window
MgF2	1	2	1.254	0.581	46.1	No	118	118	100°C - 200°C
ZnCl2	4	8	1.177	0.725	18.1	No	53	97	50°C - 100°C
SrI2	6	12	1.201	0.681	0.0	No	9	235	Wide Temp. Window
PbCl4	4	8	1.270	0.538	7.1	No	155	190	100°C - 200°C
VF4	2	4	1.228	0.627	35.0	No	112	197	100°C - 200°C
SnF4	0	1	1.327	0.373	19.9	No	271	271	200°C - 300°C
CaI2	7	12	1.183	0.704	12.2	No	167	296	200°C - 300°C
BaI2	2	6	1.292	0.465	0.0	No	116	133	100°C - 200°C
BeBr2	4	8	1.205	0.655	9.5	Yes	78	78	50°C - 100°C
CaF2	9	12	1.100	0.817	26.3	No	276	276	200°C - 300°C
SnF4	3	5	1.263	0.529	3.9	No	235	252	200°C - 300°C
AlF3	4	6	1.203	0.654	26.1	No	157	157	100°C - 200°C
WCl4	0	3	1.302	0.421	18.7	No	92	92	50°C - 100°C
PbBr2	0	2	1.333	0.305	0.6	No	98	198	100°C - 200°C
YCl3	4	7	1.211	0.635	12.8	Yes	22	278	Wide Temp. Window
YF3	3	6	1.255	0.541	22.3	Yes	11	56	< 50°C
ScCl3	2	4	1.195	0.662	19.9	Yes	105	361	Wide Temp. Window
GeCl2	8	12	1.105	0.803	39.1	Yes	129	252	100°C - 200°C
MoI4	3	8	1.300	0.415	11.6	No	94	172	100°C - 200°C
MgBr2	8	12	1.142	0.747	8.9	No	214	314	200°C - 300°C
PbCl2	2	6	1.276	0.485	19.3	No	-32	127	Wide Temp. Window
WI4	3	8	1.310	0.375	36.9	No	132	173	100°C - 200°C
YI3	0	3	1.298	0.413	11.7	Yes	169	322	Wide Temp. Window
YF3	6	9	1.162	0.710	22.3	Yes	-22	693	Wide Temp. Window
LaBr3	4	8	1.258	0.515	27.6	No	30	345	Wide Temp. Window
NiCl2	2	4	1.221	0.594	35.5	No	137	137	100°C - 200°C
CuI2	6	12	1.206	0.623	32.8	No	-38	306	Wide Temp. Window
VBr2	2	4	1.269	0.477	35.3	No	189	189	100°C - 200°C
YCl3	1	3	1.209	0.613	20.7	Yes	217	283	200°C - 300°C
VBr4	4	8	1.253	0.510	7.2	No	111	199	100°C - 200°C
VBr3	1	3	1.275	0.450	19.9	No	258	258	200°C - 300°C
SnF2	1	2	1.288	0.410	41.7	No	268	268	200°C - 300°C
CoCl3	4	6	1.208	0.604	36.2	No	292	292	200°C - 300°C
TiBr4	4	8	1.246	0.518	38.9	No	128	199	100°C - 200°C
NiI2	4	9	1.243	0.519	24.1	No	-12	302	Wide Temp. Window

MnBr4	4	8	1.248	0.505	49.1	No	109	198	100°C - 200°C
LaI3	0	4	1.285	0.399	29.9	No	67	185	100°C - 200°C
PbBr4	0	5	1.292	0.370	23.1	No	-21	146	Wide Temp. Window
SrI2	0	2	1.296	0.350	0.0	No	171	187	100°C - 200°C
VF3	4	6	1.197	0.606	20.1	No	175	175	100°C - 200°C
ZnI2	0	2	1.282	0.382	20.7	No	191	191	100°C - 200°C
PbCl4	2	5	1.250	0.456	20.8	No	155	218	100°C - 200°C
TiF4	0	1	1.236	0.491	10.5	No	205	205	200°C - 300°C
VBr4	0	3	1.265	0.402	12.8	No	81	188	100°C - 200°C
PbBr2	7	12	1.188	0.592	33.1	No	60	291	Wide Temp. Window
AlCl3	7	9	1.089	0.758	34.6	No	169	819	Wide Temp. Window
CoBr2	8	12	1.140	0.678	30.7	No	187	367	Wide Temp. Window
WI4	0	5	1.286	0.313	34.2	No	16	132	Wide Temp. Window
GaBr3	0	2	1.255	0.421	0.0	Yes	195	256	200°C - 300°C
NaBr1	0	1	1.231	0.483	3.0	No	127	127	100°C - 200°C
CaBr2	4	8	1.127	0.689	11.4	No	48	268	Wide Temp. Window
LiBr1	1	2	1.206	0.538	0.0	No	180	180	100°C - 200°C
LaBr3	4	7	1.241	0.445	27.6	No	30	345	Wide Temp. Window
SnCl2	8	12	1.095	0.734	31.7	No	114	278	100°C - 200°C
HfBr4	4	8	1.248	0.423	41.0	Yes	164	201	100°C - 200°C
LaCl3	1	3	1.232	0.467	18.6	No	113	298	200°C - 300°C
NaBr1	1	3	1.169	0.605	19.0	No	-20	124	Wide Temp. Window
SnI4	0	2	1.276	0.319	47.6	No	451	451	450°C - 600°C
BaI2	0	2	1.277	0.310	0.0	No	135	226	100°C - 200°C
MgBr2	0	1	1.249	0.403	8.2	No	285	285	200°C - 300°C
MoBr4	4	8	1.226	0.467	25.9	No	116	193	100°C - 200°C
ZrBr4	4	8	1.219	0.481	22.0	Yes	150	196	100°C - 200°C
NiCl3	4	6	1.164	0.600	32.0	No	288	288	200°C - 300°C
LaI3	0	3	1.268	0.325	23.0	No	90	185	100°C - 200°C
LaI3	3	7	1.235	0.430	23.0	No	22	361	Wide Temp. Window
NiBr2	8	12	1.130	0.656	43.8	No	182	316	Wide Temp. Window
MgBr2	7	9	1.153	0.614	33.8	No	314	595	450°C - 600°C
CaI2	0	2	1.231	0.436	0.0	No	209	229	200°C - 300°C
SnI2	1	4	1.244	0.394	20.6	No	127	127	100°C - 200°C
SnCl4	0	2	1.218	0.465	14.2	No	199	199	100°C - 200°C
GaF3	4	6	1.184	0.544	23.9	Yes	164	164	100°C - 200°C
ZnBr2	8	12	1.121	0.661	21.6	No	195	320	Wide Temp. Window
SrCl2	8	12	1.048	0.771	17.1	No	153	244	100°C - 200°C
MgI2	2	4	1.219	0.447	0.8	No	263	263	200°C - 300°C
GaF3	0	2	1.230	0.414	22.7	Yes	-42	-42	< 50°C
WF4	3	5	1.229	0.417	43.7	No	227	227	200°C - 300°C
CaCl2	2	4	1.085	0.711	2.5	No	173	173	100°C - 200°C
LiF1	3	4	1.080	0.715	35.5	No	207	207	200°C - 300°C
GeF2	2	4	1.155	0.583	12.1	Yes	92	92	50°C - 100°C
YF3	4	8	1.142	0.599	30.7	Yes	-22	56	< 50°C
GeI2	6	12	1.131	0.616	31.9	Yes	-32	179	Wide Temp. Window
LaCl3	0	2	1.228	0.384	22.8	No	80	113	50°C - 100°C
WBr4	2	5	1.237	0.346	44.6	No	175	237	200°C - 300°C

LaI3	4	8	1.208	0.438	29.9	No	22	361	Wide Temp. Window
YBr3	4	7	1.189	0.486	14.1	Yes	96	299	Wide Temp. Window
NiBr3	3	6	1.201	0.450	22.7	No	144	144	100°C - 200°C
YF3	2	4	1.186	0.475	23.3	Yes	11	152	Wide Temp. Window
CuBr2	8	12	1.104	0.641	33.3	No	149	391	Wide Temp. Window
SrI2	1	4	1.197	0.442	6.7	No	131	171	100°C - 200°C
TiF4	1	2	1.173	0.503	10.5	No	278	278	200°C - 300°C
SrI2	4	8	1.176	0.495	8.9	No	9	203	Wide Temp. Window
MoBr4	0	3	1.222	0.365	27.8	No	71	211	Wide Temp. Window
CuF2	9	12	1.074	0.684	21.1	No	223	223	200°C - 300°C
BaBr2	7	12	1.095	0.649	18.1	No	91	228	Wide Temp. Window
VI4	0	4	1.227	0.340	39.9	No	47	143	Wide Temp. Window
ScI3	3	6	1.192	0.444	27.6	Yes	159	322	Wide Temp. Window
BaI2	1	4	1.216	0.374	2.4	No	116	135	100°C - 200°C
YI3	3	6	1.209	0.394	11.7	Yes	117	312	Wide Temp. Window
LiBr1	2	4	1.115	0.612	6.9	No	48	71	50°C - 100°C
SnBr4	0	3	1.216	0.362	9.8	No	90	223	Wide Temp. Window
KF1	3	4	1.037	0.721	31.1	No	370	370	300°C - 450°C
BeI2	4	8	1.144	0.533	0.0	Yes	86	135	100°C - 200°C
LiI1	1	2	1.175	0.443	5.4	No	243	243	200°C - 300°C
PbI2	1	4	1.212	0.327	32.6	No	124	126	100°C - 200°C
VF4	5	8	1.074	0.650	5.0	No	129	129	100°C - 200°C
MoBr4	2	5	1.193	0.389	15.5	No	116	211	100°C - 200°C
CaBr2	8	12	1.039	0.703	11.4	No	180	244	200°C - 300°C
SiF4	5	8	1.063	0.664	5.8	No	103	103	100°C - 200°C
VBr4	2	5	1.178	0.414	20.2	No	111	189	100°C - 200°C
BeCl2	4	7	1.029	0.708	11.8	Yes	60	60	50°C - 100°C
PbCl2	8	12	1.083	0.602	28.7	No	236	238	200°C - 300°C
RbBr1	0	2	1.126	0.510	5.8	Yes	76	82	50°C - 100°C
ScF3	8	9	1.026	0.683	43.9	Yes	962	962	> 600°C
SrI2	7	12	1.071	0.607	9.0	No	139	235	100°C - 200°C
GaCl3	1	3	1.113	0.521	16.9	Yes	137	138	100°C - 200°C
SnI2	7	12	1.090	0.567	39.3	No	42	309	Wide Temp. Window
PbBr2	2	6	1.165	0.388	20.6	No	-47	132	Wide Temp. Window
ZrBr4	2	5	1.161	0.399	46.6	Yes	150	207	100°C - 200°C
LaI3	3	6	1.169	0.374	23.0	No	67	361	Wide Temp. Window
LaF3	4	6	1.142	0.447	49.6	No	193	193	100°C - 200°C
PbF2	8	12	1.097	0.545	20.8	No	155	163	100°C - 200°C
TiF4	5	8	1.041	0.645	0.0	No	121	121	100°C - 200°C
NaBr1	2	4	1.076	0.584	5.7	No	-20	173	Wide Temp. Window
ScBr3	0	2	1.159	0.394	34.9	Yes	159	159	100°C - 200°C
YBr3	1	3	1.148	0.425	36.6	Yes	253	314	200°C - 300°C
VCl4	0	2	1.115	0.502	22.0	No	120	120	100°C - 200°C
GeCl2	2	4	1.081	0.571	0.0	Yes	149	149	100°C - 200°C
MgF2	0	1	1.119	0.489	46.1	No	-4	-4	< 50°C
VCl4	5	8	1.054	0.612	6.3	No	198	198	100°C - 200°C
ScBr3	2	4	1.137	0.436	34.9	Yes	128	392	Wide Temp. Window
KI1	0	2	1.111	0.500	5.7	No	72	74	50°C - 100°C

MnCl2	0	1	1.131	0.454	0.0	No	174	174	100°C - 200°C
SnBr4	2	5	1.159	0.375	25.4	No	144	223	100°C - 200°C
NbF4	5	8	1.070	0.583	32.4	No	143	143	100°C - 200°C
BeCl2	8	12	0.960	0.747	17.6	Yes	58	122	50°C - 100°C
HfF4	1	2	1.181	0.278	30.0	Yes	280	280	200°C - 300°C
YCl3	4	6	1.090	0.531	12.8	Yes	278	278	200°C - 300°C
MnCl4	5	8	1.053	0.600	0.4	No	194	194	100°C - 200°C
BeF2	8	12	0.980	0.711	17.1	Yes	41	68	50°C - 100°C
GeCl4	5	8	1.060	0.581	33.8	Yes	202	202	200°C - 300°C
CrCl4	5	8	1.049	0.602	37.8	No	191	191	100°C - 200°C
TiCl4	5	8	1.036	0.617	30.0	No	197	197	100°C - 200°C
CoF3	8	9	1.048	0.596	40.3	No	862	862	> 600°C
NaI1	1	3	1.100	0.488	16.7	No	-13	148	Wide Temp. Window
GeF4	5	8	1.057	0.573	1.9	Yes	110	110	100°C - 200°C
MoF4	5	8	1.065	0.555	29.1	No	128	128	100°C - 200°C
MoI4	0	4	1.160	0.309	32.2	No	63	147	100°C - 200°C
LaCl3	4	6	1.094	0.490	28.8	No	320	320	300°C - 450°C
BaCl2	8	12	0.992	0.673	21.8	No	197	222	200°C - 300°C
AlF3	2	3	1.071	0.536	7.5	No	234	234	200°C - 300°C
MgCl2	1	2	1.049	0.576	0.0	No	245	245	200°C - 300°C
GeCl2	1	2	1.094	0.478	43.7	Yes	315	315	300°C - 450°C
PbBr4	4	8	1.132	0.377	28.8	No	115	175	100°C - 200°C
CoBr3	0	3	1.136	0.363	34.2	No	19	19	< 50°C
YI3	4	7	1.120	0.400	18.4	Yes	189	312	Wide Temp. Window
LaBr3	1	3	1.140	0.338	16.4	No	177	278	200°C - 300°C
BaCl2	4	8	1.062	0.532	21.8	No	-40	136	Wide Temp. Window
PbI2	7	12	1.076	0.498	38.1	No	124	254	100°C - 200°C
ScCl3	4	6	1.011	0.611	9.9	Yes	269	269	200°C - 300°C
CaBr2	2	4	1.079	0.476	1.2	No	170	170	100°C - 200°C
VCl4	2	4	1.052	0.529	22.0	No	199	214	200°C - 300°C
SrBr2	8	12	0.994	0.629	14.9	No	223	234	200°C - 300°C
GeBr2	8	12	0.999	0.618	35.6	Yes	140	223	100°C - 200°C
ZrF4	5	8	1.029	0.566	4.7	Yes	129	129	100°C - 200°C
ZrBr4	0	2	1.123	0.335	46.6	Yes	239	239	200°C - 300°C
NbCl4	5	8	1.034	0.551	42.6	No	203	203	200°C - 300°C
SnF4	5	8	1.050	0.513	0.0	No	124	124	100°C - 200°C
MoCl4	2	4	1.068	0.474	23.8	No	225	235	200°C - 300°C
CaI2	4	8	1.034	0.541	11.7	No	115	167	100°C - 200°C
MgI2	6	9	1.063	0.482	0.6	No	183	267	200°C - 300°C
SnF2	2	4	1.074	0.456	1.7	No	84	84	50°C - 100°C
VCl2	6	9	0.990	0.612	47.9	No	88	195	100°C - 200°C
BaF2	8	12	0.990	0.609	23.7	No	106	224	100°C - 200°C
MoCl4	5	8	1.029	0.539	3.1	No	197	197	100°C - 200°C
CaCl2	9	12	0.902	0.728	15.7	No	270	270	200°C - 300°C
CoBr3	4	6	1.088	0.400	46.7	No	283	283	200°C - 300°C
GaCl3	4	6	1.026	0.535	21.0	Yes	247	247	200°C - 300°C
WF4	5	8	1.070	0.437	43.7	No	130	130	100°C - 200°C
BaBr2	1	4	1.083	0.400	18.7	No	23	146	Wide Temp. Window

GaCl3	7	9	0.978	0.612	31.1	Yes	151	721	Wide Temp. Window
CaCl2	6	9	0.949	0.653	16.7	No	83	160	100°C - 200°C
WBr4	0	3	1.117	0.280	25.4	No	7	237	Wide Temp. Window
GeF2	9	12	0.960	0.634	34.7	Yes	200	200	200°C - 300°C
MgCl2	9	12	0.900	0.717	7.5	No	237	237	200°C - 300°C
MgI2	8	12	0.997	0.574	2.9	No	195	267	200°C - 300°C
ZrCl4	5	8	1.006	0.546	12.2	Yes	197	197	100°C - 200°C
NiCl3	2	3	1.042	0.473	45.1	No	437	437	300°C - 450°C
PbCl4	0	2	1.092	0.334	20.8	No	167	167	100°C - 200°C
PbBr2	8	12	1.021	0.509	31.3	No	216	291	200°C - 300°C
ScI3	4	7	1.069	0.394	25.4	Yes	25	322	Wide Temp. Window
CoI2	8	12	1.008	0.529	23.4	No	162	340	Wide Temp. Window
WCl4	5	8	1.048	0.444	18.9	No	203	203	200°C - 300°C
RbF1	1	2	1.040	0.462	0.0	Yes	171	171	100°C - 200°C
NaCl1	1	2	0.974	0.586	4.4	No	106	106	100°C - 200°C
VI2	8	12	0.997	0.544	49.0	No	183	303	Wide Temp. Window
HfF4	2	4	1.077	0.357	12.0	Yes	-29	281	Wide Temp. Window
NaI1	0	1	1.074	0.362	2.3	No	143	143	100°C - 200°C
NiI2	8	12	1.004	0.523	17.1	No	166	302	Wide Temp. Window
ZrF4	2	3	1.063	0.388	17.3	Yes	314	314	300°C - 450°C
CaI2	8	12	0.972	0.579	11.7	No	211	296	200°C - 300°C
SnCl4	5	8	1.010	0.508	0.0	No	196	196	100°C - 200°C
VBr3	4	8	1.037	0.446	40.8	No	59	59	50°C - 100°C
GeBr2	2	4	1.051	0.410	10.4	Yes	155	155	100°C - 200°C
GeF2	6	9	0.990	0.541	42.6	Yes	-1	156	Wide Temp. Window
VBr2	6	9	1.009	0.503	22.8	No	155	155	100°C - 200°C
CrCl3	7	9	0.939	0.623	28.1	No	410	410	300°C - 450°C
ZnI2	8	12	0.994	0.522	20.3	No	179	286	200°C - 300°C
HfF4	5	8	1.031	0.442	0.0	Yes	129	129	100°C - 200°C
MgF2	6	9	0.941	0.606	29.2	No	-22	68	< 50°C
YF3	4	7	1.000	0.504	26.2	Yes	8	56	< 50°C
YBr3	0	2	1.060	0.354	20.5	Yes	85	253	Wide Temp. Window
VI4	4	8	1.060	0.354	39.9	No	71	180	100°C - 200°C
BaI2	7	12	0.982	0.529	11.7	No	99	247	Wide Temp. Window
SnBr2	8	12	0.966	0.558	25.8	No	119	227	100°C - 200°C
CuCl2	7	9	0.969	0.552	30.1	No	252	323	200°C - 300°C
CaBr2	4	7	1.002	0.485	18.3	No	48	108	Wide Temp. Window
HfCl4	5	8	1.019	0.447	20.8	Yes	201	201	200°C - 300°C
CaCl2	0	1	0.983	0.521	0.0	No	187	187	100°C - 200°C
GaBr3	4	6	1.040	0.392	40.7	Yes	287	287	200°C - 300°C
CuBr2	0	2	1.067	0.311	45.2	No	3	3	< 50°C
SnCl4	2	4	1.021	0.435	14.2	No	202	244	200°C - 300°C
VCl3	6	9	0.919	0.619	0.0	No	179	179	100°C - 200°C
NiCl2	4	6	0.990	0.498	13.9	No	132	132	100°C - 200°C
ZnCl2	6	9	0.958	0.557	12.5	No	53	214	Wide Temp. Window
AlBr3	7	9	0.984	0.507	34.3	No	277	665	Wide Temp. Window
NiF2	6	9	0.968	0.537	46.8	No	1	66	< 50°C
MnBr4	3	5	1.046	0.363	46.2	No	109	499	Wide Temp. Window

YF3	7	9	0.943	0.577	26.2	Yes	-22	693	Wide Temp. Window
MgCl2	4	6	0.943	0.570	12.5	No	124	124	100°C - 200°C
ZrCl4	2	4	0.997	0.469	43.9	Yes	207	228	200°C - 300°C
VCl2	9	12	0.886	0.653	47.9	No	231	231	200°C - 300°C
KCl1	3	4	0.878	0.663	38.4	No	392	392	300°C - 450°C
GaI3	0	3	1.049	0.329	5.1	Yes	83	153	100°C - 200°C
RbF1	3	4	0.966	0.524	27.9	Yes	361	361	300°C - 450°C
CaBr2	6	9	0.963	0.531	12.1	No	48	268	Wide Temp. Window
LaBr3	0	2	1.058	0.295	14.3	No	114	177	100°C - 200°C
YCl3	2	4	0.980	0.494	12.8	Yes	75	283	Wide Temp. Window
LaBr3	4	6	1.032	0.371	27.6	No	345	345	300°C - 450°C
CrI2	8	12	0.960	0.528	32.2	No	199	199	100°C - 200°C
MoI4	4	8	1.043	0.333	32.2	No	94	172	100°C - 200°C
GaCl3	2	4	0.991	0.461	21.0	Yes	100	138	100°C - 200°C
VF3	2	3	0.996	0.445	31.5	No	220	220	200°C - 300°C
YBr3	4	6	1.021	0.382	14.1	Yes	299	299	200°C - 300°C
MnCl2	6	9	0.928	0.571	6.4	No	103	103	100°C - 200°C
GeCl2	9	12	0.881	0.639	35.2	Yes	252	252	200°C - 300°C
SrF2	2	4	0.975	0.484	8.7	No	54	54	50°C - 100°C
KCl1	0	1	0.928	0.567	5.7	No	86	86	50°C - 100°C
NiCl3	7	9	0.938	0.545	40.3	No	338	338	300°C - 450°C
PbF2	2	4	1.036	0.320	3.0	No	75	75	50°C - 100°C
SnCl2	1	2	1.019	0.370	37.9	No	298	298	200°C - 300°C
SnF2	9	12	0.925	0.560	25.6	No	204	204	200°C - 300°C
CuF2	6	9	0.948	0.519	21.1	No	-18	68	< 50°C
VCl3	4	6	0.941	0.529	46.7	No	208	208	200°C - 300°C
SnCl2	2	4	0.980	0.449	0.0	No	129	129	100°C - 200°C
CuI2	8	12	0.957	0.494	37.7	No	136	306	Wide Temp. Window
ZnF2	6	9	0.942	0.518	25.0	No	-16	70	< 50°C
PbBr4	0	4	1.035	0.287	28.8	No	-21	146	Wide Temp. Window
LaI3	4	7	1.014	0.353	29.9	No	22	361	Wide Temp. Window
NiCl2	9	12	0.882	0.612	31.3	No	210	210	200°C - 300°C
BaBr2	8	12	0.920	0.546	17.6	No	199	228	200°C - 300°C
ZnCl2	9	12	0.877	0.613	12.5	No	220	220	200°C - 300°C
SnCl2	9	12	0.887	0.595	28.1	No	278	278	200°C - 300°C
ScF3	2	3	0.956	0.475	17.5	Yes	235	235	200°C - 300°C
ScBr3	4	6	0.975	0.433	17.8	Yes	309	309	300°C - 450°C
VCl2	4	6	0.939	0.503	31.4	No	123	123	100°C - 200°C
NiCl2	6	9	0.919	0.537	31.3	No	20	213	Wide Temp. Window
VBr4	5	8	0.986	0.402	8.9	No	199	199	100°C - 200°C
CaI2	4	7	0.977	0.411	12.2	No	115	124	100°C - 200°C
MnBr4	5	8	0.982	0.397	12.8	No	198	198	100°C - 200°C
PbCl4	5	8	0.971	0.411	6.6	No	190	190	100°C - 200°C
TiBr4	5	8	0.971	0.404	35.0	No	199	199	100°C - 200°C
RbI1	0	2	0.979	0.384	14.0	Yes	48	60	50°C - 100°C
CuF2	4	6	0.953	0.442	18.3	No	45	45	< 50°C
HfF4	2	3	1.015	0.262	9.5	Yes	281	281	200°C - 300°C
LaI3	1	4	0.997	0.310	35.7	No	67	185	100°C - 200°C

SrI2	4	7	0.969	0.386	9.0	No	9	203	Wide Temp. Window
NaCl1	3	4	0.859	0.590	24.0	No	254	254	200°C - 300°C
GaBr3	1	3	0.984	0.339	13.6	Yes	43	256	Wide Temp. Window
CuI2	2	4	0.994	0.307	15.1	No	137	137	100°C - 200°C
CaI2	6	9	0.940	0.447	9.4	No	115	296	200°C - 300°C
ScCl3	7	9	0.848	0.602	17.7	Yes	138	608	Wide Temp. Window
BaF2	2	4	0.975	0.356	13.1	No	28	28	< 50°C
SrCl2	1	2	0.966	0.377	14.5	No	230	230	200°C - 300°C
ZnI2	4	8	0.954	0.404	20.3	No	32	63	< 50°C
NbBr4	5	8	0.965	0.375	43.9	No	203	203	200°C - 300°C
CaBr2	0	1	0.975	0.347	0.0	No	245	245	200°C - 300°C
GeI2	2	4	0.979	0.323	42.4	Yes	168	168	100°C - 200°C
PbCl2	2	4	0.975	0.333	0.0	No	127	127	100°C - 200°C
LiF1	2	3	0.863	0.560	37.1	No	34	34	< 50°C
ScCl3	1	2	0.920	0.458	46.3	Yes	315	315	300°C - 450°C
MnCl4	3	5	0.913	0.468	0.4	No	187	187	100°C - 200°C
MoBr4	5	8	0.959	0.365	15.5	No	193	193	100°C - 200°C
SrF2	9	12	0.851	0.571	16.7	No	173	173	100°C - 200°C
MgBr2	1	2	0.959	0.360	8.2	No	270	270	200°C - 300°C
MgI2	0	1	0.988	0.268	8.6	No	270	270	200°C - 300°C
SrCl2	9	12	0.822	0.605	14.7	No	244	244	200°C - 300°C
WBr4	5	8	0.967	0.320	21.1	No	200	200	100°C - 200°C
CoBr2	6	9	0.920	0.437	42.2	No	-23	367	Wide Temp. Window
VBr2	0	1	0.980	0.274	39.4	No	156	156	100°C - 200°C
ZnBr2	7	9	0.919	0.437	34.7	No	294	320	300°C - 450°C
GeI2	8	12	0.893	0.486	38.8	Yes	178	179	100°C - 200°C
NiCl2	0	1	0.959	0.337	0.0	No	67	67	50°C - 100°C
LiI1	2	4	0.917	0.432	12.9	No	2	61	< 50°C
SrI2	8	12	0.881	0.499	8.9	No	193	235	200°C - 300°C
YBr3	2	4	0.948	0.353	20.5	Yes	110	314	Wide Temp. Window
HfBr4	5	8	0.955	0.323	34.4	Yes	201	201	200°C - 300°C
VCl4	3	5	0.893	0.466	12.6	No	158	199	100°C - 200°C
GaCl3	0	1	0.922	0.406	0.0	Yes	267	267	200°C - 300°C
CuCl2	9	12	0.829	0.572	16.0	No	185	185	100°C - 200°C
ZrBr4	5	8	0.937	0.370	19.2	Yes	196	196	100°C - 200°C
BeI2	4	7	0.922	0.405	2.4	Yes	86	86	50°C - 100°C
NaBr1	1	2	0.913	0.418	3.0	No	124	124	100°C - 200°C
CoCl2	4	6	0.895	0.453	49.5	No	96	96	50°C - 100°C
SnI2	0	2	0.970	0.249	8.7	No	24	127	Wide Temp. Window
SrBr2	0	1	0.965	0.255	3.6	No	192	192	100°C - 200°C
RbBr1	1	3	0.914	0.394	21.0	Yes	-35	82	< 50°C
TiCl4	3	5	0.876	0.470	48.7	No	167	188	100°C - 200°C
SrCl2	2	4	0.881	0.457	10.4	No	88	88	50°C - 100°C
MgBr2	4	6	0.893	0.430	6.1	No	157	157	100°C - 200°C
MoCl4	3	5	0.899	0.415	30.4	No	162	225	100°C - 200°C
ScF3	4	6	0.864	0.483	30.9	Yes	74	74	50°C - 100°C
MoCl3	7	9	0.844	0.516	33.9	No	371	371	300°C - 450°C
CoI2	4	8	0.910	0.388	37.6	No	-6	67	< 50°C

HfF4	3	5	0.932	0.332	0.0	Yes	-29	267	Wide Temp. Window
ZnCl2	4	6	0.882	0.442	11.2	No	97	97	50°C - 100°C
TiBr3	4	6	0.913	0.373	40.8	No	232	232	200°C - 300°C
PbCl4	2	4	0.930	0.327	20.8	No	178	218	100°C - 200°C
YCl3	6	9	0.820	0.544	0.0	Yes	22	357	Wide Temp. Window
BeBr2	8	12	0.827	0.528	11.7	Yes	46	162	Wide Temp. Window
WCl4	3	5	0.922	0.334	18.9	No	161	244	200°C - 300°C
CrBr4	0	2	0.944	0.264	25.5	No	96	96	50°C - 100°C
RbBr1	2	4	0.874	0.440	5.8	Yes	-35	205	Wide Temp. Window
CrBr3	6	9	0.875	0.436	48.8	No	-43	590	Wide Temp. Window
SrCl2	4	6	0.869	0.444	10.4	No	132	132	100°C - 200°C
CaI2	2	4	0.908	0.358	1.1	No	176	176	100°C - 200°C
MgBr2	9	12	0.815	0.533	2.0	No	214	214	200°C - 300°C
ZnI2	6	9	0.899	0.373	19.7	No	63	286	Wide Temp. Window
CaBr2	9	12	0.804	0.544	9.7	No	244	244	200°C - 300°C
VI4	0	3	0.938	0.251	26.6	No	47	139	Wide Temp. Window
NaI1	2	4	0.880	0.409	12.9	No	-13	89	< 50°C
ZrCl4	3	5	0.873	0.423	26.5	Yes	183	207	100°C - 200°C
SrCl2	0	1	0.916	0.320	14.5	No	113	113	100°C - 200°C
LaI3	4	6	0.922	0.295	29.9	No	361	361	300°C - 450°C
SnBr2	2	4	0.910	0.328	0.0	No	120	120	100°C - 200°C
YI3	6	10	0.898	0.358	2.9	Yes	31	189	Wide Temp. Window
CoCl3	7	9	0.816	0.504	25.8	No	292	292	200°C - 300°C
HfCl4	3	5	0.897	0.338	40.3	Yes	192	212	200°C - 300°C
VBr4	2	4	0.908	0.305	20.2	No	188	189	100°C - 200°C
MoBr4	2	4	0.913	0.287	25.9	No	202	211	200°C - 300°C
PbBr2	2	4	0.917	0.269	0.6	No	132	132	100°C - 200°C
SrBr2	4	6	0.883	0.365	8.2	No	171	171	100°C - 200°C
NiBr2	7	9	0.862	0.411	32.3	No	209	316	200°C - 300°C
YI3	4	6	0.907	0.296	18.4	Yes	312	312	300°C - 450°C
YF3	4	6	0.876	0.378	22.3	Yes	56	56	50°C - 100°C
VI4	2	5	0.915	0.264	31.3	No	71	143	100°C - 200°C
SnCl4	3	5	0.871	0.385	5.1	No	177	202	100°C - 200°C
CsF1	1	2	0.893	0.329	0.0	Yes	151	151	100°C - 200°C
MnBr3	4	8	0.873	0.376	33.2	No	10	10	< 50°C
BeCl2	9	12	0.750	0.584	18.6	Yes	122	122	100°C - 200°C
YI3	0	2	0.911	0.255	32.3	Yes	169	169	100°C - 200°C
AlCl3	8	9	0.775	0.540	32.8	No	819	819	> 600°C
ZnI2	2	4	0.892	0.289	20.7	No	115	115	100°C - 200°C
VBr2	9	12	0.797	0.493	20.8	No	208	208	200°C - 300°C
LaI3	1	3	0.908	0.233	35.7	No	184	185	100°C - 200°C
NiBr3	1	3	0.892	0.286	42.4	No	72	72	50°C - 100°C
MgI2	4	6	0.862	0.362	0.6	No	206	206	200°C - 300°C
RbCl1	3	4	0.796	0.489	35.6	Yes	374	374	300°C - 450°C
VBr2	4	6	0.861	0.363	22.8	No	123	123	100°C - 200°C
CaF2	7	9	0.794	0.492	37.0	No	-15	279	Wide Temp. Window
ScI3	4	6	0.875	0.326	25.4	Yes	322	322	300°C - 450°C
CrBr4	2	4	0.883	0.292	33.4	No	171	171	100°C - 200°C

PbCl2	9	12	0.812	0.451	19.5	No	236	236	200°C - 300°C
SrBr2	2	4	0.859	0.350	8.2	No	110	110	100°C - 200°C
BaI2	8	12	0.816	0.440	11.6	No	164	247	200°C - 300°C
SiF4	2	3	0.832	0.407	19.4	No	168	168	100°C - 200°C
PbBr4	5	8	0.879	0.293	23.1	No	175	175	100°C - 200°C
SrF2	7	9	0.808	0.442	29.1	No	59	267	Wide Temp. Window
ScCl3	2	3	0.802	0.451	19.9	Yes	361	361	300°C - 450°C
GeBr2	9	12	0.782	0.484	31.4	Yes	223	223	200°C - 300°C
RbCl1	0	1	0.837	0.381	5.1	Yes	90	90	50°C - 100°C
NiI2	4	8	0.847	0.355	20.7	No	-12	21	< 50°C
SnI2	8	12	0.813	0.423	22.8	No	42	191	Wide Temp. Window
ZnBr2	9	12	0.788	0.465	9.8	No	195	195	100°C - 200°C
PbI2	8	12	0.830	0.384	24.2	No	124	188	100°C - 200°C
PbF2	9	12	0.819	0.407	15.3	No	155	155	100°C - 200°C
TiCl3	8	9	0.749	0.522	47.0	No	859	859	> 600°C
NiBr2	9	12	0.790	0.459	29.4	No	182	182	100°C - 200°C
PbF2	7	9	0.852	0.327	30.1	No	163	204	100°C - 200°C
MgCl2	6	8	0.736	0.539	12.5	No	168	168	100°C - 200°C
CaCl2	1	2	0.801	0.435	2.5	No	165	165	100°C - 200°C
BaCl2	9	12	0.753	0.511	15.5	No	222	222	200°C - 300°C
SnI4	2	5	0.877	0.242	47.6	No	93	175	100°C - 200°C
CoI2	6	9	0.838	0.353	40.2	No	-6	340	Wide Temp. Window
PbI2	0	2	0.889	0.192	17.1	No	-16	124	Wide Temp. Window
BaBr2	4	6	0.846	0.334	18.7	No	190	190	100°C - 200°C
NiF2	4	6	0.820	0.391	46.8	No	1	1	< 50°C
ZrBr4	2	4	0.861	0.286	46.6	Yes	193	207	100°C - 200°C
CoBr2	9	12	0.779	0.464	13.3	No	187	187	100°C - 200°C
CaCl2	4	6	0.782	0.454	16.7	No	67	67	50°C - 100°C
SnBr4	2	4	0.862	0.269	25.4	No	171	223	100°C - 200°C
MoI4	0	3	0.874	0.224	26.4	No	63	63	50°C - 100°C
NaI1	1	2	0.839	0.331	2.3	No	148	148	100°C - 200°C
SnF2	6	8	0.815	0.387	28.1	No	29	222	Wide Temp. Window
VBr4	0	2	0.865	0.255	20.2	No	81	81	50°C - 100°C
VI2	7	9	0.826	0.360	33.4	No	302	303	300°C - 450°C
KBr1	0	1	0.814	0.375	4.6	No	79	79	50°C - 100°C
LiCl1	2	3	0.734	0.515	3.2	No	67	67	50°C - 100°C
GaI3	4	6	0.853	0.273	31.7	Yes	249	249	200°C - 300°C
SrI2	4	6	0.840	0.309	6.7	No	203	203	200°C - 300°C
KBr1	3	4	0.763	0.466	32.1	No	336	336	300°C - 450°C
SrI2	6	9	0.822	0.349	4.3	No	9	235	Wide Temp. Window
VI4	5	8	0.846	0.282	25.2	No	180	180	100°C - 200°C
BaCl2	4	6	0.808	0.377	15.1	No	136	136	100°C - 200°C
GaBr3	7	9	0.802	0.385	24.6	Yes	125	573	Wide Temp. Window
BeF2	9	12	0.719	0.522	17.1	Yes	41	41	< 50°C
BaCl2	0	1	0.846	0.261	11.3	No	132	132	100°C - 200°C
LaBr3	6	10	0.814	0.348	7.6	No	-35	213	Wide Temp. Window
GeF4	2	3	0.822	0.329	4.5	Yes	183	183	100°C - 200°C
GeBr4	5	9	0.819	0.333	47.0	Yes	43	43	< 50°C

SnBr2	9	12	0.766	0.442	22.0	No	227	227	200°C - 300°C
WF4	2	3	0.854	0.229	47.6	No	219	219	200°C - 300°C
PbCl2	1	2	0.854	0.227	20.8	No	214	214	200°C - 300°C
CaBr2	4	6	0.804	0.361	12.1	No	108	108	100°C - 200°C
SiF4	3	4	0.775	0.419	19.4	No	232	232	200°C - 300°C
MoBr3	7	9	0.793	0.379	41.1	No	119	626	Wide Temp. Window
YF3	8	9	0.749	0.458	30.7	Yes	693	693	> 600°C
KCl1	1	2	0.723	0.498	5.7	No	104	104	100°C - 200°C
SrBr2	9	12	0.742	0.469	9.4	No	223	223	200°C - 300°C
NiI2	6	9	0.809	0.338	29.2	No	-12	302	Wide Temp. Window
MgI2	1	2	0.834	0.265	8.6	No	298	298	200°C - 300°C
LaI3	0	2	0.844	0.216	29.8	No	90	185	100°C - 200°C
BaF2	7	9	0.785	0.376	27.2	No	99	224	Wide Temp. Window
SnI2	2	4	0.829	0.263	8.7	No	127	127	100°C - 200°C
MgF2	6	8	0.724	0.482	25.1	No	68	68	50°C - 100°C
PbI4	4	9	0.827	0.268	40.8	No	-45	399	Wide Temp. Window
YI3	2	4	0.827	0.266	32.3	Yes	117	322	Wide Temp. Window
NiCl2	1	2	0.813	0.302	35.5	No	70	70	50°C - 100°C
TiBr3	7	9	0.765	0.401	41.0	No	78	611	Wide Temp. Window
GeBr2	1	2	0.819	0.263	40.1	Yes	211	211	200°C - 300°C
MoI4	5	8	0.818	0.261	21.0	No	172	172	100°C - 200°C
ZnCl2	1	2	0.800	0.308	35.8	No	90	90	50°C - 100°C
CuF2	6	8	0.754	0.405	27.2	No	68	68	50°C - 100°C
YCl3	0	1	0.804	0.290	20.7	Yes	151	151	100°C - 200°C
PbCl4	3	5	0.802	0.292	10.4	No	155	178	100°C - 200°C
GeF4	3	4	0.777	0.347	4.5	Yes	251	251	200°C - 300°C
WI4	5	8	0.817	0.234	34.2	No	173	173	100°C - 200°C
YBr3	6	9	0.754	0.392	0.0	Yes	96	245	Wide Temp. Window
YF3	1	2	0.788	0.315	37.0	Yes	120	120	100°C - 200°C
GaI3	7	9	0.785	0.320	35.0	Yes	23	775	Wide Temp. Window
BaBr2	0	1	0.823	0.206	0.0	No	172	172	100°C - 200°C
TiF4	2	3	0.763	0.366	4.0	No	173	173	100°C - 200°C
MnCl3	8	9	0.709	0.459	44.5	No	744	744	> 600°C
HfF4	0	1	0.829	0.162	30.0	Yes	29	29	< 50°C
MoBr4	0	2	0.814	0.222	11.6	No	71	71	50°C - 100°C
GeI2	0	2	0.814	0.225	42.4	Yes	6	6	< 50°C
SnBr2	1	2	0.811	0.233	26.0	No	230	230	200°C - 300°C
ZrI4	5	8	0.800	0.268	44.8	Yes	182	182	100°C - 200°C
ZnF2	4	6	0.761	0.358	19.2	No	-14	-14	< 50°C
ZnCl2	0	1	0.791	0.283	35.8	No	26	26	< 50°C
PbI2	2	4	0.810	0.219	17.1	No	126	126	100°C - 200°C
CuBr2	9	12	0.724	0.420	15.5	No	149	149	100°C - 200°C
BaF2	4	6	0.773	0.321	17.3	No	39	39	< 50°C
ZnBr2	4	6	0.776	0.312	13.3	No	83	83	50°C - 100°C
BaCl2	2	4	0.771	0.323	15.1	No	37	37	< 50°C
SrCl2	7	9	0.726	0.413	23.6	No	153	209	100°C - 200°C
CuI2	6	9	0.771	0.320	32.8	No	-38	306	Wide Temp. Window
BaI2	2	4	0.798	0.245	2.4	No	116	116	100°C - 200°C

YI3	6	9	0.777	0.298	0.0	Yes	100	189	100°C - 200°C
NiF2	6	8	0.724	0.411	46.8	No	66	66	50°C - 100°C
ZnF2	6	8	0.727	0.404	20.2	No	70	70	50°C - 100°C
MgI2	9	12	0.720	0.415	0.0	No	195	195	100°C - 200°C
SrBr2	1	2	0.796	0.239	3.6	No	191	191	100°C - 200°C
CaBr2	7	9	0.727	0.401	18.3	No	180	268	200°C - 300°C
SnBr4	0	2	0.796	0.223	25.4	No	90	90	50°C - 100°C
GeF2	7	9	0.724	0.395	43.5	Yes	37	156	Wide Temp. Window
PbBr2	9	12	0.738	0.368	18.6	No	216	216	200°C - 300°C
SrI2	2	4	0.773	0.286	6.7	No	131	131	100°C - 200°C
SnF4	2	3	0.776	0.275	3.9	No	195	195	100°C - 200°C
WBr4	3	5	0.789	0.221	25.4	No	175	175	100°C - 200°C
ScBr3	7	9	0.722	0.384	15.7	Yes	165	463	Wide Temp. Window
PbCl2	0	1	0.799	0.171	20.8	No	73	73	50°C - 100°C
SrI2	0	1	0.793	0.187	0.0	No	187	187	100°C - 200°C
CaI2	9	12	0.698	0.416	4.4	No	211	211	200°C - 300°C
CaCl2	6	8	0.643	0.495	16.7	No	160	160	100°C - 200°C
SrF2	4	6	0.737	0.339	19.6	No	-1	-1	< 50°C
BeF2	7	9	0.666	0.463	14.0	Yes	50	68	50°C - 100°C
PbI4	4	8	0.777	0.231	40.8	No	-45	399	Wide Temp. Window
BaF2	9	12	0.689	0.424	15.0	No	106	106	100°C - 200°C
ScI3	6	9	0.738	0.330	0.0	Yes	25	305	Wide Temp. Window
GaCl3	8	9	0.685	0.429	29.2	Yes	721	721	> 600°C
BaCl2	1	2	0.764	0.266	11.3	No	172	172	100°C - 200°C
VBr4	3	5	0.762	0.268	12.8	No	111	189	100°C - 200°C
GeCl2	7	9	0.692	0.418	49.1	Yes	129	200	100°C - 200°C
VBr2	1	2	0.766	0.255	39.4	No	159	159	100°C - 200°C
MnBr4	3	4	0.766	0.252	49.1	No	499	499	450°C - 600°C
NiBr2	4	6	0.748	0.298	37.8	No	60	60	50°C - 100°C
MoBr4	3	5	0.765	0.250	27.8	No	116	202	100°C - 200°C
ScBr3	2	3	0.748	0.287	34.9	Yes	392	392	300°C - 450°C
TiBr4	3	5	0.753	0.270	49.7	No	128	173	100°C - 200°C
BaI2	0	1	0.780	0.178	0.0	No	226	226	200°C - 300°C
VI2	9	12	0.701	0.383	33.4	No	183	183	100°C - 200°C
ZrBr4	3	5	0.754	0.259	31.1	Yes	150	193	100°C - 200°C
ZnI2	9	12	0.703	0.370	9.9	No	179	179	100°C - 200°C
SnBr2	6	9	0.728	0.317	22.0	No	10	119	Wide Temp. Window
BaCl2	6	9	0.702	0.369	15.5	No	-40	197	Wide Temp. Window
BaBr2	9	12	0.680	0.403	10.6	No	199	199	100°C - 200°C
MoF4	3	4	0.727	0.310	43.2	No	245	245	200°C - 300°C
GeBr2	7	9	0.707	0.352	49.1	Yes	140	265	200°C - 300°C
CrBr3	7	9	0.706	0.352	12.5	No	-43	590	Wide Temp. Window
CaI2	0	1	0.756	0.226	4.0	No	209	209	200°C - 300°C
NiI2	9	12	0.699	0.364	24.1	No	166	166	100°C - 200°C
LaCl3	2	3	0.735	0.279	22.8	No	298	298	200°C - 300°C
CrI3	6	9	0.725	0.302	3.8	No	13	385	Wide Temp. Window
LiCl1	3	4	0.640	0.453	3.8	No	82	82	50°C - 100°C
VI3	4	6	0.739	0.264	31.6	No	214	214	200°C - 300°C

NaBr1	3	4	0.686	0.373	19.0	No	173	173	100°C - 200°C
MgBr2	7	8	0.674	0.386	33.8	No	595	595	450°C - 600°C
AlI3	7	9	0.714	0.304	21.0	No	203	438	300°C - 450°C
YF3	2	3	0.711	0.311	23.3	Yes	152	152	100°C - 200°C
SiF4	4	5	0.678	0.377	11.8	No	229	229	200°C - 300°C
LiBr1	2	3	0.688	0.357	2.3	No	71	71	50°C - 100°C
CoI2	9	12	0.686	0.360	33.2	No	162	162	100°C - 200°C
RbBr1	0	1	0.722	0.278	5.8	Yes	76	76	50°C - 100°C
SnBr4	3	5	0.736	0.238	9.8	No	144	171	100°C - 200°C
TiF4	3	4	0.682	0.361	4.0	No	211	211	200°C - 300°C
SrBr2	7	9	0.695	0.329	16.4	No	144	234	100°C - 200°C
YCl3	7	9	0.638	0.423	8.8	Yes	134	357	Wide Temp. Window
CaBr2	1	2	0.713	0.280	0.0	No	179	179	100°C - 200°C
SnF2	0	1	0.739	0.197	41.7	No	-37	-37	< 50°C
PbBr2	1	2	0.746	0.171	18.8	No	198	198	100°C - 200°C
WI4	0	3	0.745	0.170	36.9	No	16	16	< 50°C
GeCl2	0	1	0.711	0.279	43.7	Yes	36	36	< 50°C
GeI2	9	12	0.670	0.365	31.1	Yes	179	179	100°C - 200°C
LaI3	6	9	0.715	0.266	0.0	No	22	247	Wide Temp. Window
SnF4	3	4	0.709	0.278	3.9	No	235	235	200°C - 300°C
VF4	3	4	0.676	0.345	13.2	No	197	197	100°C - 200°C
PbBr4	0	3	0.734	0.190	40.3	No	-21	-21	< 50°C
VF4	4	5	0.668	0.355	11.0	No	254	254	200°C - 300°C
PbCl2	7	9	0.696	0.289	31.6	No	86	238	Wide Temp. Window
CaI2	7	9	0.678	0.323	12.2	No	167	296	200°C - 300°C
RbCl1	1	2	0.662	0.354	5.1	Yes	107	107	100°C - 200°C
MgI2	6	8	0.678	0.316	2.9	No	183	183	100°C - 200°C
SnI2	9	12	0.663	0.345	23.3	No	191	191	100°C - 200°C
YCl3	1	2	0.679	0.310	20.7	Yes	217	217	200°C - 300°C
SrI2	9	12	0.646	0.366	4.3	No	193	193	100°C - 200°C
VF4	2	3	0.670	0.310	35.0	No	112	112	100°C - 200°C
AlCl3	3	4	0.648	0.351	44.9	No	220	220	200°C - 300°C
KI1	0	1	0.683	0.274	5.2	No	72	72	50°C - 100°C
NiBr2	0	1	0.709	0.181	43.6	No	21	21	< 50°C
CuI2	9	12	0.650	0.336	23.6	No	136	136	100°C - 200°C
GeF4	4	5	0.660	0.310	1.3	Yes	234	234	200°C - 300°C
TiF4	4	5	0.638	0.352	3.1	No	243	243	200°C - 300°C
MnCl4	2	3	0.660	0.308	0.0	No	256	256	200°C - 300°C
KBr1	1	2	0.638	0.344	4.6	No	92	92	50°C - 100°C
LaF3	8	9	0.631	0.352	35.2	No	591	591	450°C - 600°C
CaI2	4	6	0.662	0.289	9.4	No	124	124	100°C - 200°C
YCl3	2	3	0.643	0.326	12.5	Yes	283	283	200°C - 300°C
VI4	2	4	0.692	0.192	39.9	No	139	143	100°C - 200°C
VCl2	6	8	0.597	0.397	28.1	No	88	88	50°C - 100°C
PbBr2	7	9	0.671	0.247	33.1	No	60	291	Wide Temp. Window
BeI2	9	12	0.624	0.345	9.7	Yes	105	105	100°C - 200°C
GaBr3	0	1	0.682	0.208	13.6	Yes	195	195	100°C - 200°C
KI1	3	4	0.630	0.331	28.5	No	267	267	200°C - 300°C

CoI2	4	6	0.671	0.236	40.2	No	67	67	50°C - 100°C
PbI2	9	12	0.645	0.298	21.1	No	188	188	100°C - 200°C
FeCl3	8	9	0.600	0.380	41.2	No	572	572	450°C - 600°C
ScCl3	8	9	0.578	0.410	19.7	Yes	608	608	> 600°C
GaBr3	1	2	0.666	0.224	13.6	Yes	256	256	200°C - 300°C
BaI2	4	6	0.660	0.238	2.4	No	133	133	100°C - 200°C
CaBr2	6	8	0.598	0.366	12.1	No	48	268	Wide Temp. Window
VCl3	0	1	0.647	0.266	41.6	No	47	47	< 50°C
MoF4	4	5	0.637	0.288	27.6	No	244	244	200°C - 300°C
AlBr3	8	9	0.620	0.319	25.6	No	665	665	> 600°C
ZrF4	4	5	0.627	0.304	19.2	Yes	262	262	200°C - 300°C
SnF4	4	5	0.642	0.269	2.4	No	252	252	200°C - 300°C
PbBr4	3	5	0.667	0.191	40.3	No	115	146	100°C - 200°C
GeI2	6	9	0.633	0.279	31.9	Yes	-32	178	Wide Temp. Window
GaI3	1	3	0.656	0.206	5.1	Yes	83	83	50°C - 100°C
FeCl2	9	12	0.566	0.388	28.4	No	31	31	< 50°C
YI3	7	10	0.638	0.254	2.9	Yes	31	181	Wide Temp. Window
LaBr3	7	10	0.629	0.269	7.6	No	-35	213	Wide Temp. Window
SrI2	7	9	0.629	0.267	9.0	No	139	235	100°C - 200°C
HfF4	4	5	0.641	0.229	12.0	Yes	267	267	200°C - 300°C
GaCl3	1	2	0.619	0.282	4.5	Yes	137	137	100°C - 200°C
BaBr2	2	4	0.634	0.234	18.7	No	23	23	< 50°C
BaBr2	1	2	0.650	0.184	0.0	No	146	146	100°C - 200°C
WBr4	0	2	0.658	0.152	44.6	No	7	7	< 50°C
BeBr2	9	12	0.568	0.363	11.7	Yes	46	46	< 50°C
ScCl3	0	1	0.615	0.274	46.3	Yes	45	45	< 50°C
LaCl3	1	2	0.642	0.200	22.8	No	113	113	100°C - 200°C
BaBr2	7	9	0.613	0.275	18.1	No	91	228	Wide Temp. Window
GeF2	6	8	0.583	0.334	42.6	Yes	-1	37	< 50°C
VBr3	8	9	0.598	0.304	40.8	No	671	671	> 600°C
PbI2	7	9	0.632	0.217	38.1	No	124	254	100°C - 200°C
SnCl2	0	1	0.629	0.221	37.9	No	41	41	< 50°C
SnI2	7	9	0.620	0.245	39.3	No	42	309	Wide Temp. Window
CaI2	1	2	0.628	0.222	4.0	No	229	229	200°C - 300°C
VCl4	2	3	0.600	0.288	22.0	No	214	214	200°C - 300°C
YBr3	1	2	0.631	0.211	36.6	Yes	253	253	200°C - 300°C
LiI1	2	3	0.612	0.260	7.9	No	61	61	50°C - 100°C
LaBr3	6	9	0.595	0.296	1.6	No	30	213	Wide Temp. Window
BaI2	9	12	0.584	0.315	4.6	No	164	164	100°C - 200°C
LaI3	2	4	0.633	0.197	29.9	No	67	184	100°C - 200°C
GaI3	8	9	0.612	0.250	36.5	Yes	775	775	> 600°C
SrI2	1	2	0.637	0.172	0.0	No	171	171	100°C - 200°C
VI4	0	2	0.640	0.157	31.3	No	47	47	< 50°C
LaCl3	0	1	0.628	0.196	18.6	No	80	80	50°C - 100°C
MoCl4	2	3	0.603	0.254	30.4	No	235	235	200°C - 300°C
LaBr3	2	3	0.627	0.186	14.3	No	278	278	200°C - 300°C
RbBr1	3	4	0.583	0.294	21.0	Yes	205	205	200°C - 300°C
TiI3	7	9	0.597	0.263	34.1	No	86	434	Wide Temp. Window

SnI4	2	4	0.627	0.170	47.6	No	93	175	100°C - 200°C
MoI3	6	9	0.600	0.246	39.7	No	86	86	50°C - 100°C
PbBr2	0	1	0.633	0.141	18.8	No	98	98	50°C - 100°C
CaF2	7	8	0.538	0.363	37.0	No	279	279	200°C - 300°C
ZnCl2	6	8	0.551	0.339	18.1	No	53	53	50°C - 100°C
YBr3	2	3	0.605	0.224	20.5	Yes	314	314	300°C - 450°C
VI3	7	9	0.593	0.252	35.2	No	-5	485	Wide Temp. Window
NiBr3	6	9	0.590	0.257	19.9	No	-3	-3	< 50°C
WI4	3	5	0.621	0.151	36.9	No	132	132	100°C - 200°C
SnCl4	2	3	0.591	0.240	14.2	No	244	244	200°C - 300°C
RbI1	3	4	0.580	0.263	32.3	Yes	240	240	200°C - 300°C
CoBr3	7	9	0.574	0.269	22.0	No	151	151	100°C - 200°C
CuCl2	4	6	0.567	0.281	19.5	No	-40	-40	< 50°C
GeBr2	0	1	0.608	0.176	40.1	Yes	29	29	< 50°C
RbI1	0	1	0.596	0.211	9.6	Yes	60	60	50°C - 100°C
ScI3	7	9	0.573	0.256	7.7	Yes	180	305	Wide Temp. Window
FeI3	6	9	0.580	0.235	21.3	No	49	49	< 50°C
ZnI2	4	6	0.589	0.208	19.7	No	32	32	< 50°C
RbBr1	1	2	0.569	0.258	5.8	Yes	82	82	50°C - 100°C
MoI4	3	5	0.602	0.166	21.0	No	94	147	100°C - 200°C
NiI2	4	6	0.589	0.204	29.2	No	21	21	< 50°C
BaI2	7	9	0.577	0.235	11.7	No	99	247	Wide Temp. Window
YCl3	6	8	0.546	0.302	9.6	Yes	22	134	Wide Temp. Window
CrBr3	8	9	0.558	0.278	22.3	No	590	590	450°C - 600°C
YBr3	6	8	0.572	0.247	3.7	Yes	96	157	100°C - 200°C
CoI3	7	9	0.578	0.230	49.5	No	200	200	200°C - 300°C
PbF4	4	5	0.590	0.194	48.6	No	223	223	200°C - 300°C
YI3	6	8	0.579	0.218	0.0	Yes	181	189	100°C - 200°C
BeCl2	7	9	0.509	0.351	18.6	Yes	-21	58	< 50°C
TiBr3	8	9	0.547	0.287	15.0	No	611	611	> 600°C
VI4	3	5	0.593	0.171	26.6	No	71	143	100°C - 200°C
ZrCl4	2	3	0.561	0.255	43.9	Yes	228	228	200°C - 300°C
GaCl3	2	3	0.557	0.261	16.9	Yes	138	138	100°C - 200°C
SnCl2	7	9	0.540	0.295	33.1	No	49	114	Wide Temp. Window
LiBr1	3	4	0.538	0.295	6.9	No	48	48	< 50°C
LaBr3	0	1	0.596	0.143	16.4	No	114	114	100°C - 200°C
MoBr3	8	9	0.552	0.264	38.6	No	626	626	> 600°C
YBr3	7	9	0.542	0.282	3.9	Yes	157	245	200°C - 300°C
KI1	1	2	0.557	0.251	5.7	No	74	74	50°C - 100°C
GaBr3	8	9	0.545	0.262	23.2	Yes	573	573	450°C - 600°C
NiCl2	6	8	0.510	0.313	40.0	No	20	20	< 50°C
CaI2	6	8	0.528	0.276	11.7	No	115	167	100°C - 200°C
SnBr2	0	1	0.574	0.158	26.0	No	48	48	< 50°C
CuBr2	8	9	0.538	0.251	33.3	No	391	391	300°C - 450°C
YBr3	0	1	0.573	0.151	36.6	Yes	85	85	50°C - 100°C
CuCl2	8	9	0.515	0.293	30.1	No	323	323	300°C - 450°C
BaI2	1	2	0.574	0.139	0.0	No	135	135	100°C - 200°C
PbI4	1	3	0.575	0.133	36.6	No	76	76	50°C - 100°C

LaBr3	1	2	0.568	0.158	16.4	No	177	177	100°C - 200°C
MnBr3	8	9	0.529	0.258	31.9	No	533	533	450°C - 600°C
WCl4	3	4	0.551	0.190	38.2	No	244	244	200°C - 300°C
LaI3	7	9	0.545	0.203	7.7	No	155	247	200°C - 300°C
VCl4	3	4	0.518	0.260	19.3	No	199	199	100°C - 200°C
MoCl4	3	4	0.529	0.235	30.4	No	225	225	200°C - 300°C
YF3	6	8	0.511	0.268	30.7	Yes	-22	8	< 50°C
SnI2	1	2	0.557	0.143	20.6	No	127	127	100°C - 200°C
CoBr2	8	9	0.516	0.245	30.7	No	367	367	300°C - 450°C
SrF2	8	9	0.500	0.274	27.7	No	267	267	200°C - 300°C
PbCl4	2	3	0.541	0.178	20.8	No	218	218	200°C - 300°C
SnI4	3	5	0.546	0.151	28.7	No	93	101	50°C - 100°C
NaI1	3	4	0.513	0.238	16.7	No	89	89	50°C - 100°C
SnF2	7	8	0.506	0.240	29.0	No	222	222	200°C - 300°C
TiCl4	3	4	0.494	0.257	48.7	No	188	188	100°C - 200°C
PbI2	1	2	0.540	0.117	32.6	No	124	124	100°C - 200°C
WBr4	2	3	0.532	0.134	44.6	No	237	237	200°C - 300°C
YI3	2	3	0.522	0.166	32.3	Yes	322	322	300°C - 450°C
ZnI2	6	8	0.500	0.212	20.3	No	63	63	50°C - 100°C
CuCl2	7	8	0.467	0.275	30.1	No	252	252	200°C - 300°C
ZrCl4	3	4	0.488	0.230	26.5	Yes	207	207	200°C - 300°C
SrI2	6	8	0.496	0.209	8.9	No	9	139	Wide Temp. Window
VBr3	3	4	0.506	0.181	19.9	No	176	176	100°C - 200°C
ScI3	6	8	0.500	0.192	6.3	Yes	25	180	Wide Temp. Window
MgCl2	8	9	0.443	0.299	12.2	No	254	254	200°C - 300°C
YI3	7	9	0.499	0.191	0.0	Yes	100	181	100°C - 200°C
HfCl4	3	4	0.500	0.181	40.3	Yes	212	212	200°C - 300°C
SnCl4	3	4	0.489	0.208	5.1	No	202	202	200°C - 300°C
MgBr2	8	9	0.465	0.248	8.9	No	314	314	300°C - 450°C
MoBr4	2	3	0.505	0.151	27.8	No	211	211	200°C - 300°C
NiBr2	8	9	0.474	0.226	43.8	No	316	316	300°C - 450°C
VBr4	2	3	0.499	0.159	20.2	No	188	188	100°C - 200°C
CrBr3	0	1	0.503	0.139	46.0	No	22	22	< 50°C
GaCl3	3	4	0.472	0.220	21.0	Yes	100	100	100°C - 200°C
ZnBr2	8	9	0.470	0.224	21.6	No	320	320	300°C - 450°C
RbI1	1	2	0.481	0.189	14.0	Yes	48	48	< 50°C
SnBr4	2	3	0.494	0.147	25.4	No	223	223	200°C - 300°C
PbF2	7	8	0.483	0.179	30.1	No	204	204	200°C - 300°C
3-Feb	8	9	0.463	0.223	33.2	No	427	427	300°C - 450°C
PbCl2	4	6	0.480	0.182	19.3	No	-32	-32	< 50°C
ScBr3	8	9	0.453	0.241	13.8	Yes	463	463	450°C - 600°C
NaBr1	2	3	0.455	0.236	19.0	No	-20	-20	< 50°C
YF3	3	4	0.475	0.190	20.4	Yes	11	11	< 50°C
ScCl3	3	4	0.447	0.247	9.9	Yes	105	105	100°C - 200°C
PbI4	5	9	0.481	0.156	33.1	No	-45	-21	< 50°C
GaI3	0	1	0.485	0.133	2.7	Yes	153	153	100°C - 200°C
ZnBr2	7	8	0.449	0.224	34.7	No	294	294	200°C - 300°C
CoF3	7	8	0.445	0.229	44.6	No	134	134	100°C - 200°C

SnBr2	6	8	0.459	0.196	25.8	No	10	10	< 50°C
BaF2	8	9	0.449	0.215	23.7	No	224	224	200°C - 300°C
ZrBr4	2	3	0.472	0.151	46.6	Yes	207	207	200°C - 300°C
GeBr2	7	8	0.447	0.209	49.1	Yes	265	265	200°C - 300°C
GeCl2	7	8	0.426	0.240	49.1	Yes	200	200	100°C - 200°C
LaI3	1	2	0.471	0.120	35.7	No	185	185	100°C - 200°C
CoI2	8	9	0.448	0.188	33.2	No	340	340	300°C - 450°C
TiCl4	4	5	0.427	0.230	36.7	No	167	167	100°C - 200°C
CrCl4	4	5	0.429	0.222	44.9	No	158	158	100°C - 200°C
VBr3	0	1	0.465	0.130	41.1	No	2	2	< 50°C
NiCl2	8	9	0.416	0.243	40.0	No	213	213	200°C - 300°C
VCl4	4	5	0.426	0.223	19.3	No	158	158	100°C - 200°C
LaBr3	7	9	0.430	0.214	4.2	No	34	213	Wide Temp. Window
LaBr3	8	10	0.442	0.189	7.6	No	-35	213	Wide Temp. Window
GeCl4	4	5	0.432	0.209	41.4	Yes	164	164	100°C - 200°C
SrCl2	7	8	0.419	0.232	23.6	No	209	209	200°C - 300°C
VBr4	3	4	0.454	0.153	12.8	No	189	189	100°C - 200°C
GeF2	8	9	0.420	0.229	41.7	Yes	156	156	100°C - 200°C
VI3	8	9	0.438	0.186	37.6	No	485	485	450°C - 600°C
MoBr4	3	4	0.452	0.142	27.8	No	202	202	200°C - 300°C
ZnCl2	8	9	0.410	0.238	18.1	No	214	214	200°C - 300°C
ZrCl4	4	5	0.426	0.206	16.9	Yes	183	183	100°C - 200°C
PbCl4	3	4	0.446	0.157	10.4	No	178	178	100°C - 200°C
HfCl4	4	5	0.439	0.166	27.8	Yes	192	192	100°C - 200°C
LaI3	2	3	0.453	0.116	29.8	No	184	184	100°C - 200°C
LaI3	0	1	0.456	0.099	35.7	No	90	90	50°C - 100°C
AlBr3	7	8	0.424	0.195	34.3	No	277	277	200°C - 300°C
LaI3	6	8	0.439	0.159	5.9	No	22	155	Wide Temp. Window
YCl3	8	9	0.388	0.257	9.6	Yes	357	357	300°C - 450°C
AlI3	8	9	0.428	0.182	15.8	No	438	438	300°C - 450°C
SnI2	0	1	0.451	0.111	20.6	No	24	24	< 50°C
VI2	7	8	0.425	0.187	49.0	No	302	302	300°C - 450°C
FeI2	9	12	0.413	0.210	41.5	No	-20	-20	< 50°C
SnCl4	4	5	0.424	0.187	2.6	No	177	177	100°C - 200°C
MoCl4	4	5	0.419	0.194	23.8	No	162	162	100°C - 200°C
CuI2	8	9	0.426	0.176	37.7	No	306	306	300°C - 450°C
NiI2	8	9	0.424	0.177	24.1	No	302	302	300°C - 450°C
NaI1	2	3	0.419	0.186	16.7	No	-13	-13	< 50°C
ScBr3	3	4	0.428	0.164	17.8	Yes	128	128	100°C - 200°C
VCl2	8	9	0.389	0.241	47.9	No	195	195	100°C - 200°C
LiI1	3	4	0.414	0.195	12.9	No	2	2	< 50°C
PbI4	4	5	0.440	0.122	40.8	No	399	399	300°C - 450°C
TiBr4	3	4	0.428	0.148	49.7	No	173	173	100°C - 200°C
VI2	8	9	0.413	0.180	49.0	No	303	303	300°C - 450°C
PbBr2	8	9	0.422	0.156	31.3	No	291	291	200°C - 300°C
LaBr3	6	8	0.416	0.170	0.0	No	30	34	< 50°C
SnI2	7	8	0.417	0.164	39.3	No	309	309	300°C - 450°C
WCl4	4	5	0.421	0.152	38.2	No	161	161	100°C - 200°C

ZrBr4	3	4	0.424	0.141	31.1	Yes	193	193	100°C - 200°C
CoBr2	6	8	0.397	0.201	42.2	No	-23	-23	< 50°C
PbCl2	8	9	0.409	0.170	28.7	No	238	238	200°C - 300°C
AlCl3	7	8	0.376	0.233	34.6	No	169	169	100°C - 200°C
ZnI2	8	9	0.408	0.169	20.3	No	286	286	200°C - 300°C
CaBr2	7	8	0.375	0.229	18.3	No	268	268	200°C - 300°C
PbBr2	4	6	0.417	0.139	20.6	No	-47	-47	< 50°C
NiBr2	7	8	0.392	0.194	43.8	No	209	209	200°C - 300°C
PbF2	8	9	0.407	0.156	20.8	No	163	163	100°C - 200°C
CoI2	6	8	0.400	0.171	40.2	No	-6	-6	< 50°C
MgI2	8	9	0.395	0.179	2.9	No	267	267	200°C - 300°C
TiI3	8	9	0.396	0.175	31.2	No	434	434	300°C - 450°C
NiI2	6	8	0.399	0.167	29.2	No	-12	-12	< 50°C
BeF2	7	8	0.355	0.247	14.2	Yes	50	50	< 50°C
BaCl2	6	8	0.386	0.193	21.8	No	-40	-40	< 50°C
SnBr4	3	4	0.407	0.127	9.8	No	171	171	100°C - 200°C
CaI2	8	9	0.383	0.182	11.7	No	296	296	200°C - 300°C
YCl3	3	4	0.377	0.190	12.8	Yes	75	75	50°C - 100°C
SrBr2	8	9	0.381	0.181	14.9	No	234	234	200°C - 300°C
CrI3	8	9	0.388	0.162	14.1	No	385	385	300°C - 450°C
BeF2	8	9	0.342	0.238	14.2	Yes	68	68	50°C - 100°C
PbCl4	4	5	0.390	0.142	7.1	No	155	155	100°C - 200°C
YI3	8	10	0.382	0.152	2.9	Yes	31	100	50°C - 100°C
PbI4	5	8	0.392	0.116	30.2	No	-45	-45	< 50°C
CrBr3	6	8	0.373	0.165	48.8	No	-43	-11	< 50°C
ScI3	3	4	0.387	0.127	27.6	Yes	159	159	100°C - 200°C
CrI3	6	8	0.378	0.145	14.1	No	13	13	< 50°C
GaCl3	7	8	0.355	0.194	31.1	Yes	151	151	100°C - 200°C
BaF2	7	8	0.363	0.170	27.2	No	99	99	50°C - 100°C
RbBr1	2	3	0.366	0.158	21.0	Yes	-35	-35	< 50°C
YBr3	3	4	0.374	0.139	14.1	Yes	110	110	100°C - 200°C
BaCl2	8	9	0.352	0.185	21.8	No	197	197	100°C - 200°C
PbI2	7	8	0.376	0.127	38.1	No	254	254	200°C - 300°C
ScCl3	7	8	0.340	0.203	19.7	Yes	138	138	100°C - 200°C
LaCl3	8	9	0.337	0.206	12.2	No	302	302	300°C - 450°C
SrCl2	8	9	0.341	0.194	17.1	No	153	153	100°C - 200°C
SrF2	7	8	0.348	0.180	29.1	No	59	59	50°C - 100°C
HfBr4	4	5	0.375	0.109	41.0	Yes	164	164	100°C - 200°C
BaBr2	8	9	0.355	0.159	17.6	No	228	228	200°C - 300°C
GaBr3	2	3	0.368	0.127	10.2	Yes	43	43	< 50°C
BeBr2	8	9	0.334	0.192	9.5	Yes	162	162	100°C - 200°C
GeI2	6	8	0.355	0.149	38.8	Yes	-32	-32	< 50°C
PbBr4	3	4	0.369	0.102	40.3	No	146	146	100°C - 200°C
PbI2	0	1	0.374	0.078	32.6	No	-16	-16	< 50°C
CuI2	6	8	0.352	0.149	37.7	No	-38	-38	< 50°C
VI4	2	3	0.367	0.098	31.3	No	139	139	100°C - 200°C
ZrBr4	4	5	0.359	0.123	22.0	Yes	150	150	100°C - 200°C
TiBr4	4	5	0.357	0.128	38.9	No	128	128	100°C - 200°C

CaBr2	8	9	0.332	0.183	11.4	No	180	180	100°C - 200°C
SrI2	8	9	0.348	0.147	8.9	No	235	235	200°C - 300°C
SnI4	2	3	0.364	0.096	47.6	No	175	175	100°C - 200°C
SnF2	6	7	0.341	0.156	29.0	No	29	29	< 50°C
SnBr4	4	5	0.356	0.115	4.0	No	144	144	100°C - 200°C
GeCl2	8	9	0.318	0.192	39.1	Yes	129	129	100°C - 200°C
SrBr2	7	8	0.333	0.155	16.4	No	144	144	100°C - 200°C
VBr4	4	5	0.346	0.122	8.9	No	111	111	100°C - 200°C
MnBr4	4	5	0.346	0.120	49.1	No	109	109	100°C - 200°C
BaI2	8	9	0.336	0.137	11.6	No	247	247	200°C - 300°C
ScBr3	7	8	0.331	0.149	15.7	Yes	165	165	100°C - 200°C
MoBr4	4	5	0.345	0.112	25.9	No	116	116	100°C - 200°C
YCl3	7	8	0.316	0.175	9.6	Yes	134	134	100°C - 200°C
VI4	3	4	0.348	0.096	39.9	No	143	143	100°C - 200°C
GeF2	6	7	0.317	0.168	43.5	Yes	-1	-1	< 50°C
GeF2	7	8	0.311	0.178	43.5	Yes	37	37	< 50°C
MoI4	3	4	0.341	0.091	32.2	No	147	147	100°C - 200°C
ScI3	8	9	0.321	0.144	6.3	Yes	305	305	300°C - 450°C
BeCl2	8	9	0.289	0.199	18.6	Yes	58	58	50°C - 100°C
CaI2	6	7	0.321	0.135	12.2	No	115	115	100°C - 200°C
HfF4	3	4	0.330	0.109	12.0	Yes	-29	-29	< 50°C
BeI2	7	8	0.314	0.146	2.4	Yes	135	135	100°C - 200°C
YI3	3	4	0.327	0.105	18.4	Yes	117	117	100°C - 200°C
GeBr2	8	9	0.307	0.153	35.6	Yes	140	140	100°C - 200°C
AlI3	7	8	0.318	0.126	21.0	No	203	203	200°C - 300°C
PbCl2	7	8	0.318	0.124	31.6	No	86	86	50°C - 100°C
YI3	6	7	0.317	0.113	0.0	Yes	189	189	100°C - 200°C
SnCl2	8	9	0.294	0.161	31.7	No	114	114	100°C - 200°C
YF3	6	7	0.300	0.151	26.2	Yes	8	8	< 50°C
CaCl2	8	9	0.276	0.190	15.7	No	83	83	50°C - 100°C
YBr3	7	8	0.307	0.133	3.9	Yes	157	157	100°C - 200°C
GeI2	8	9	0.306	0.135	38.8	Yes	178	178	100°C - 200°C
YBr3	8	9	0.296	0.154	3.7	Yes	245	245	200°C - 300°C
PbBr4	4	5	0.321	0.092	28.8	No	115	115	100°C - 200°C
CaBr2	6	7	0.297	0.144	18.3	No	48	48	< 50°C
GaBr3	7	8	0.302	0.128	24.6	Yes	125	125	100°C - 200°C
SnBr2	8	9	0.298	0.130	25.8	No	119	119	100°C - 200°C
ScI3	7	8	0.302	0.116	7.7	Yes	180	180	100°C - 200°C
LaI3	8	9	0.299	0.111	5.9	No	247	247	200°C - 300°C
SrI2	7	8	0.294	0.124	9.0	No	139	139	100°C - 200°C
SnCl2	7	8	0.286	0.141	33.1	No	49	49	< 50°C
NiF2	8	9	0.279	0.155	40.8	No	1	1	< 50°C
CaI2	7	8	0.280	0.147	12.2	No	167	167	100°C - 200°C
YBr3	6	7	0.290	0.119	3.9	Yes	96	96	50°C - 100°C
MoBr3	7	8	0.288	0.119	41.1	No	119	119	100°C - 200°C
YI3	7	8	0.287	0.108	0.0	Yes	181	181	100°C - 200°C
MgF2	8	9	0.253	0.163	29.2	No	-22	-22	< 50°C
BaBr2	7	8	0.275	0.120	18.1	No	91	91	50°C - 100°C

ScF3	7	8	0.261	0.147	43.9	Yes	-25	-25	< 50°C
CaF2	8	9	0.253	0.157	26.3	No	-15	-15	< 50°C
TiBr3	7	8	0.270	0.119	41.0	No	78	78	50°C - 100°C
LaBr3	8	9	0.264	0.131	1.6	No	213	213	200°C - 300°C
CuF2	8	9	0.258	0.141	27.2	No	-18	-18	< 50°C
ZnF2	8	9	0.257	0.141	25.0	No	-16	-16	< 50°C
SnI4	3	4	0.282	0.076	28.7	No	93	93	50°C - 100°C
MoI4	4	5	0.280	0.077	32.2	No	94	94	50°C - 100°C
YCl3	6	7	0.255	0.134	8.8	Yes	22	22	< 50°C
PbI2	8	9	0.272	0.093	24.2	No	124	124	100°C - 200°C
SnI4	4	5	0.276	0.076	23.6	No	101	101	100°C - 200°C
LaCl3	6	7	0.261	0.117	4.6	No	23	23	< 50°C
BeCl2	7	8	0.234	0.164	17.6	Yes	-21	-21	< 50°C
PbBr2	7	8	0.268	0.095	33.1	No	60	60	50°C - 100°C
LaF3	6	7	0.263	0.105	30.2	No	-41	-41	< 50°C
LaI3	3	4	0.270	0.084	29.9	No	67	67	50°C - 100°C
GaF3	7	8	0.251	0.126	49.9	Yes	-40	-40	< 50°C
VI4	4	5	0.269	0.077	39.9	No	71	71	50°C - 100°C
LaI3	7	8	0.259	0.094	7.7	No	155	155	100°C - 200°C
BaI2	7	8	0.252	0.102	11.7	No	99	99	50°C - 100°C
YF3	7	8	0.241	0.126	30.7	Yes	-22	-22	< 50°C
TiI3	7	8	0.243	0.092	34.1	No	86	86	50°C - 100°C
LaBr3	6	7	0.245	0.088	4.2	No	30	30	< 50°C
YI3	8	9	0.225	0.086	0.0	Yes	100	100	50°C - 100°C
SrI2	6	7	0.221	0.088	9.0	No	9	9	< 50°C
SnI2	8	9	0.218	0.086	23.3	No	42	42	< 50°C
CrBr3	6	7	0.212	0.091	48.8	No	-11	-11	< 50°C
ScI3	6	7	0.214	0.079	7.7	Yes	25	25	< 50°C
LaBr3	7	8	0.209	0.086	4.2	No	34	34	< 50°C
GaI3	7	8	0.204	0.073	36.5	Yes	23	23	< 50°C
LaI3	6	7	0.192	0.067	7.7	No	22	22	< 50°C
VI3	7	8	0.184	0.068	37.6	No	-5	-5	< 50°C
CrBr3	7	8	0.174	0.077	22.3	No	-43	-43	< 50°C
YI3	9	10	0.172	0.068	2.9	Yes	31	31	< 50°C
LaBr3	9	10	0.145	0.062	7.6	No	-35	-35	< 50°C
PbI4	8	9	0.129	0.042	33.1	No	-21	-21	< 50°C

Appendix D. MERITS System Analysis

De-Jong et al. described a numerical model to predict the system volumetric energy density of the MERITS solar-thermal TES prototype system using an optimized design based on $Na_2S•5H_2O$ as the storage medium.[138] This model was adopted to predict the volumetric and gravimetric energy densities of systems that employ the HH identified in the present study. Details regarding the masses for the heat exchanger and evaporator/condenser are not provided in the MERITS model description; hence, for the present analyses, these data were extracted from commercial technologies that are consistent with the module dimensions. Additional details regarding the system analysis are presented below.

Table D.1 System components.

Component	Value	Source
Active Modules	7	Cuypers et al.[49]
Module Volume	0.60 m^3	Cuypers et al.[49]
Volume Active Material/Module	0.27 m^3	De Jong et al.,[138] commercial technology
Volume Stainless Steel/Module	0.11 m^3	Commercial technology
Mass Stainless Steel/Module	200 kg	Commercial technology
Mass Heat Exchanger/Module	16 kg	Commercial technology[198]
Mass (Evaporator/Condenser)/Module	20 kg	Commercial technology[199]

Table D.2 Optimized module component configuration.[138]

Component	Volume Fraction of Module
Reactor	0.67
Evaporator/Condenser	0.28
Insulation	0.05

The optimized system model calls for the reactor to take up two-thirds of the volume of the entire module. The heat exchanger will occupy a non-negligible volume in the reactor, hence the

volume fraction of active material will be less than two-thirds of the module's total volume. The mass/volume of stainless steel is based on a set of assumptions about the surface area of the modular prototypes for the MERITS project. These assumptions are discussed in the sections below.

Table D.3 Related quantities for energy density calculations.[49,138,200]

Symbol	Parameter	Units	Value
VED_{system}	Volumetric energy density of system	GJ/m^3	Material dependent
GED_{system}	Gravimetric energy density of system	MJ/kg	Material dependent
Q_s	Total theoretical available sorption heat	GJ	Material dependent
Q_0	Actual stored heat	GJ	Material dependent
η	Heat loss fraction	-	Material dependent
A_{surf}	Estimated surface area	m^2	3.93 m^2
r	Estimated module radius	m	0.3352 m
h	Estimated module height	m	1.7 m
λ	Insulation thermal conductivity	W/m-K	0.04 W/m-K
T_S	Sorption temperature	°C	Material dependent
T_D	Desorption temperature	°C	Material dependent
T_A	Ambient temperature	°C	25°C
b	Insulation thickness	m	0.02 m
P_o	Power output	W	700 W
V_{mod}	Volume of individual module	m^3	0.6 m^3
V_{water}	Volume of water	m^3	Material dependent
V_{hyd}	Volume of salt hydrate	m^3	0.27 m^3
V_{total}	Total volume	m^3	Material dependent
N_{mod}	Number of modules	-	7
M_{total}	Total mass	kg	Material dependent
M_{salt}	Mass of salt	kg	Material dependent
M_{EC}	Mass of evaporator/condenser per module	kg	20 kg
M_{HX}	Mass of heat exchanger per module	kg	16 kg
M_{SS}	Mass of stainless steel per module	kg	200 kg
M_{insul}	Mass of insulation per module	kg	3.54 kg
v_{hyd}	Molar volume of salt hydrate	cm^3/mol hyd	Material dependent
n	Moles of water transferred per mole of salt	mol H_2O/mol hyd	Material dependent
ΔH	Enthalpy of dehydration	kJ/mol H_2O	Material dependent

The following set of equations solve for the system volumetric and gravimetric energy densities of the optimized MERITS system. They include equations described in De Jong et al,[138] but also take into account information needed to estimate the system gravimetric energy density. To more accurately represent the geometry of the experimental prototype used by Cuypers et al.,[49]

the modules were modeled as cylinders rather than cubes. The surface area, module height, and module radius were estimated from pictures provided in the literature. However, the system volumetric and gravimetric energy densities were not very sensitive to changes in the height to radius ratio, assuming a constant module volume. An optimization for the insulation thickness was also outlined in De Jong et al.[138] The power of the system was 600-700 W in the experimental results from Cuypers et al;[49] the high end of this range, 700 W, was used for the present system model.

$$Q_S = \frac{V_{hyd} n \Delta \mathrm{H}}{\mathrm{v}_{hyd}} \quad (D1)$$

$$Q_0 = \frac{Q_S}{1+\eta} \quad (D2)$$

$$A_{surf} = 2\pi r^2 + 2\pi r h \quad (D3)$$

$$\eta = \frac{A_{surf} \lambda (T_S - T_A)}{b P_o} \quad (D4)$$

$$V_{total} = N_{mod}(V_{mod} + V_{water}) \quad (D5)$$

$$M_{total} = N_{mod}(M_{salt} + M_{EC} + M_{HX} + M_{SS} + M_{insul}) \quad (\mathrm{D6})$$

$$VED_{system} = \frac{Q_0}{V_{total}} \quad (D7)$$

$$GED_{system} = \frac{Q_0}{M_{total}} \quad (D8)$$

Improving the energy density in the model also includes optimizing the packing of the material with the heat exchanger in the reactor. The volume fraction of specific components is shown in Table D.2. Ideally for this specific system, the reactor should take up two-thirds of the entire module volume. Within the reactor, it was assumed that the heat exchanger would take up about one-third of the volume while the rest of the volume could be used for active heat storage

material. Based on these assumptions and the equations listed above, the system volumetric and gravimetric energy density is found for all materials solely based on the system geometry and the thermodynamics for each specific material. A 2-dimensional grid search was performed for each material to evaluate the effect that the height of the module (h) and the insulation thickness (b) have on the system energy density. The value for h was varied between 1.4 and 2.0 meters in 0.05-meter intervals, and b was varied between 0.02 and 0.12 meters in 0.01-meter intervals. The radius of the module was changed with h in order to ensure a constant module volume of 0.6 m^3.

Appendix E. Computed Database of Hypothetical Chalcogenide and Complex Anion Salt Hydration Reactions

Table E.1 19 hypothetical chalcogenide salt (de)hydration reactions that are predicted to lie on the convex hull are characterized by the number of water molecules per formula unit in the dehydrated (n_{low}) and hydrated (n_{high}) states, volumetric (VED) and gravimetric (GED) energy densities, maximum distance to the convex hull (E_{hull}), whether the hydrate contains an expensive metal, minimum ($T_{turn,min}$) and maximum ($T_{turn,max}$) turning temperatures of the (de)hydration reaction(s), and temperature category. Reactions are ordered by descending $ED_{RMS} = \sqrt{VED^2 + GED^2}$.

Salt	n_{low}	n_{high}	VED (GJ/m^3)	GED (MJ/kg)	E_{hull} (meV/at)	Expensive Metal	$T_{turn,min}$ (°C)	$T_{turn,max}$ (°C)	Temp. Categ.
Li2S	0	9	3.559	2.642	0.0	No	131	131	100°C - 200°C
Na2S	0	9	3.531	2.670	0.0	No	154	180	100°C - 200°C
Li2Se	0	9	3.513	2.221	0.0	No	121	154	100°C - 200°C
Na2Se	0	9	3.385	2.203	0.0	No	152	184	100°C - 200°C
Na2S	0	5	3.148	2.276	0.0	No	180	180	100°C - 200°C
Li2Se	0	7	3.259	2.056	0.0	No	154	154	100°C - 200°C
K2Se	0	9	2.889	2.046	0.0	No	161	166	100°C - 200°C
Na2Se	0	5	2.983	1.738	0.0	No	184	184	100°C - 200°C
Rb2S	0	9	2.812	2.000	0.0	Yes	153	153	100°C - 200°C
Rb2Se	0	9	2.672	1.708	0.0	Yes	152	152	100°C - 200°C
HfSe2	0	12	2.980	0.982	0.0	Yes	125	125	100°C - 200°C
K2Se	0	5	2.344	1.522	0.0	No	161	161	100°C - 200°C
SrSe	0	4	2.348	0.679	0.0	No	96	96	50°C - 100°C
BaSe	0	4	2.128	0.585	0.0	No	95	95	50°C - 100°C
Na2S	5	9	1.519	1.149	0.0	No	154	154	100°C - 200°C
Na2Se	5	9	1.443	0.939	0.0	No	152	152	100°C - 200°C
K2Se	5	9	1.293	0.915	0.0	No	166	166	100°C - 200°C
MnSe2	0	1	1.012	0.145	0.0	No	114	114	100°C - 200°C
Li2Se	7	9	0.733	0.463	0.0	No	121	121	100°C - 200°C

Table E.2 32 hypothetical chalcogenide salt (de)hydration reactions that are predicted to lie within 10 meV/atom of the convex hull are characterized by the number of water molecules per formula unit in the dehydrated (n_{low}) and hydrated (n_{high}) states, volumetric (VED) and gravimetric (GED) energy densities, maximum distance to the convex hull (E_{hull}), whether the hydrate contains an expensive metal, minimum ($T_{turn,min}$) and maximum ($T_{turn,max}$) turning

temperatures of the (de)hydration reaction(s), and temperature category. Reactions are ordered by descending $ED_{RMS} = \sqrt{VED^2 + GED^2}$.

Salt	n_{low}	n_{high}	VED (GJ/m^3)	GED (MJ/kg)	E_{hull} (meV/at)	Expensive Metal	$T_{turn,min}$ (°C)	$T_{turn,max}$ (°C)	Temp. Categ.
Li2S	0	9	3.559	2.642	0.0	No	119	135	100°C - 200°C
Na2S	0	9	3.531	2.670	0.0	No	154	180	100°C - 200°C
Li2S	0	7	3.315	2.524	1.1	No	134	135	100°C - 200°C
Li2Se	0	9	3.513	2.221	0.0	No	121	154	100°C - 200°C
Na2Se	0	9	3.385	2.203	0.0	No	152	184	100°C - 200°C
Li2S	0	5	3.293	2.308	9.1	No	135	135	100°C - 200°C
K2S	0	9	3.049	2.467	2.2	No	165	165	100°C - 200°C
Na2S	0	5	3.148	2.276	0.0	No	180	180	100°C - 200°C
Li2Se	0	7	3.259	2.056	0.0	No	153	154	100°C - 200°C
Li2Se	0	5	3.211	1.771	0.7	No	154	154	100°C - 200°C
K2Se	0	9	2.889	2.046	0.0	No	161	166	100°C - 200°C
Na2Se	0	5	2.983	1.738	0.0	No	184	184	100°C - 200°C
Rb2S	0	9	2.812	2.000	0.0	Yes	153	153	100°C - 200°C
Rb2Se	0	9	2.672	1.708	0.0	Yes	144	161	100°C - 200°C
HfSe2	0	12	2.980	0.982	0.0	Yes	125	125	100°C - 200°C
K2Se	0	5	2.344	1.522	0.0	No	161	161	100°C - 200°C
CaSe	0	4	2.484	0.778	5.9	No	87	87	50°C - 100°C
Rb2Se	0	5	2.223	1.195	3.0	Yes	144	144	100°C - 200°C
BaS	0	4	2.318	0.809	5.8	No	106	106	100°C - 200°C
SrSe	0	4	2.348	0.679	0.0	No	96	96	50°C - 100°C
BaSe	0	4	2.128	0.585	0.0	No	95	95	50°C - 100°C
Li2S	5	9	1.563	1.160	9.1	No	119	134	100°C - 200°C
Na2S	5	9	1.519	1.149	0.0	No	154	154	100°C - 200°C
Li2Se	5	9	1.526	0.965	0.7	No	121	153	100°C - 200°C
Na2Se	5	9	1.443	0.939	0.0	No	152	152	100°C - 200°C
K2Se	5	9	1.293	0.915	0.0	No	166	166	100°C - 200°C
Rb2Se	5	9	1.215	0.777	3.0	Yes	161	161	100°C - 200°C
Li2S	5	7	0.945	0.720	9.1	No	134	134	100°C - 200°C
Li2Se	5	7	0.929	0.586	0.7	No	153	153	100°C - 200°C
MnSe2	0	1	1.012	0.145	0.0	No	114	114	100°C - 200°C
Li2S	7	9	0.767	0.569	1.1	No	119	119	100°C - 200°C
Li2Se	7	9	0.733	0.463	0.0	No	121	121	100°C - 200°C

Table E.3 149 hypothetical complex anion salt (de)hydration reactions that are predicted to lie on the convex hull are characterized by the number of water molecules per formula unit in the dehydrated (n_{low}) and hydrated (n_{high}) states, volumetric (VED) and gravimetric (GED) energy densities, maximum distance to the convex hull (E_{hull}), whether the

hydrate contains an expensive metal, minimum ($T_{turn,min}$) and maximum ($T_{turn,max}$) turning temperatures of the (de)hydration reaction(s), and temperature category. Reactions are ordered by descending $ED_{RMS} = \sqrt{VED^2 + GED^2}$.

Salt	n_{low}	n_{high}	VED (GJ/m^3)	GED (MJ/kg)	E_{hull} (meV/at)	Expensive Metal	$T_{turn,min}$ (°C)	$T_{turn,max}$ (°C)	Temp. Categ.
NaOH	0	7	3.739	2.746	0.0	No	173	173	100°C - 200°C
LiOH	0	7	3.616	2.742	0.0	No	117	207	100°C - 200°C
CoPO4	0	11	3.857	2.024	0.0	No	93	188	100°C - 200°C
CoPO4	0	9	3.828	1.916	0.0	No	188	188	100°C - 200°C
Ca(OH)2	0	8	3.637	2.207	0.0	No	139	139	100°C - 200°C
AlPO4	0	11	3.551	2.083	0.0	No	131	145	100°C - 200°C
Ba(OH)2	0	8	3.661	1.758	0.0	No	202	202	200°C - 300°C
VPO4	0	11	3.537	1.984	0.0	No	134	335	Wide Temp. Window
NiSO4	0	11	3.445	2.026	0.0	No	172	172	100°C - 200°C
AlAsO4	0	11	3.505	1.881	0.0	No	118	199	100°C - 200°C
AlPO4	0	9	3.438	1.933	0.0	No	145	145	100°C - 200°C
CrPO4	0	9	3.479	1.834	0.0	No	140	261	200°C - 300°C
Na2CO3	0	10	3.251	2.160	0.0	No	150	150	100°C - 200°C
CrAsO4	0	11	3.426	1.751	0.0	No	109	252	100°C - 200°C
AlAsO4	0	9	3.408	1.740	0.0	No	151	199	100°C - 200°C
FePO4	0	11	3.346	1.825	0.0	No	124	124	100°C - 200°C
LiOH	1	7	2.999	2.274	0.0	No	117	117	100°C - 200°C
CrAsO4	0	9	3.342	1.614	0.0	No	135	252	100°C - 200°C
Li2CO3	0	10	3.046	2.090	0.0	No	91	91	50°C - 100°C
FeAsO4	0	9	3.247	1.585	0.0	No	130	376	Wide Temp. Window
VPO4	1	11	3.077	1.726	0.0	No	134	134	100°C - 200°C
Na2HPO4	0	12	2.962	1.899	0.0	No	93	131	100°C - 200°C
MgCO3	0	5	3.019	1.781	0.0	No	152	152	100°C - 200°C
CaSO4	0	11	2.869	1.947	0.0	No	132	132	100°C - 200°C
Na2SO4	0	10	2.847	1.905	0.0	No	147	147	100°C - 200°C
K2CO3	0	10	2.806	1.911	0.0	No	135	219	100°C - 200°C
CrPO4	1	9	3.001	1.582	0.0	No	140	187	100°C - 200°C
Na3PO4	0	8	2.958	1.619	0.0	No	154	154	100°C - 200°C
FeCO3	0	5	2.873	1.466	0.0	No	140	140	100°C - 200°C
AlAsO4	2	11	2.800	1.503	0.0	No	118	151	100°C - 200°C
CaCO3	0	5	2.703	1.657	0.0	No	159	159	100°C - 200°C
MnCO3	0	5	2.752	1.444	0.0	No	132	132	100°C - 200°C
SrCO3	0	6	2.783	1.317	0.0	No	112	112	100°C - 200°C
Ca3(PO4)2	0	11	2.745	1.352	0.0	No	155	155	100°C - 200°C
Na2HPO4	0	7	2.642	1.542	0.0	No	131	131	100°C - 200°C

LiOH	0	1	2.508	1.671	0.0	No	207	207	200°C - 300°C
FeAsO4	1	9	2.703	1.319	0.0	No	130	130	100°C - 200°C
CuHPO4	0	7	2.670	1.384	0.0	No	114	114	100°C - 200°C
NaIO3	0	6	2.729	1.235	0.0	No	158	158	100°C - 200°C
K2CO3	1	10	2.474	1.685	0.0	No	135	135	100°C - 200°C
CrAsO4	2	11	2.655	1.357	0.0	No	109	135	100°C - 200°C
Ni3(PO4)2	0	8	2.798	1.025	0.0	No	156	193	100°C - 200°C
LiIO3	0	6	2.716	1.207	0.0	No	121	151	100°C - 200°C
CrPO4	2	9	2.589	1.365	0.0	No	140	140	100°C - 200°C
CaHPO4	0	7	2.481	1.550	0.0	No	118	141	100°C - 200°C
Ca2SiO4	0	7	2.584	1.329	0.0	No	115	115	100°C - 200°C
AlAsO4	2	9	2.585	1.320	0.0	No	151	151	100°C - 200°C
PbCO3	0	6	2.749	0.895	0.0	No	111	111	100°C - 200°C
Mg3(AsO4)2	0	8	2.668	1.083	0.0	No	186	186	100°C - 200°C
Ni2P2O7	0	6	2.692	1.013	0.0	No	173	220	100°C - 200°C
K3AsO4	0	8	2.547	1.315	0.0	No	178	178	100°C - 200°C
KOH	0	1	2.534	1.336	0.0	No	405	405	300°C - 450°C
LiNO3	0	3	2.380	1.496	0.0	No	147	147	100°C - 200°C
NaBrO3	0	6	2.456	1.297	0.0	No	110	110	100°C - 200°C
Ni3(AsO4)2	0	8	2.621	0.861	0.0	No	168	168	100°C - 200°C
CrAsO4	2	9	2.443	1.180	0.0	No	135	135	100°C - 200°C
K2HPO4	0	6	2.355	1.344	0.0	No	160	160	100°C - 200°C
BaCO3	0	6	2.482	1.060	0.0	No	96	96	50°C - 100°C
Zn(IO3)2	0	6	2.503	0.797	0.0	No	203	203	200°C - 300°C
Sr3(PO4)2	0	11	2.409	0.992	0.0	No	125	165	100°C - 200°C
SrHPO4	0	7	2.288	1.242	0.0	No	103	103	100°C - 200°C
Sr3(AsO4)2	0	11	2.419	0.930	0.0	No	151	190	100°C - 200°C
KIO3	0	6	2.315	1.102	0.0	No	132	132	100°C - 200°C
Ca(NO3)2	0	6	2.199	1.305	0.0	No	132	132	100°C - 200°C
Ba(ClO4)2	0	9	2.313	1.056	0.0	No	127	127	100°C - 200°C
Zn3(AsO4)2	0	8	2.400	0.789	0.0	No	114	175	100°C - 200°C
Co3(AsO4)2	0	8	2.381	0.764	0.0	No	57	129	50°C - 100°C
CaHPO4	1	7	2.112	1.320	0.0	No	118	131	100°C - 200°C
PbHPO4	0	7	2.303	0.896	0.0	No	103	103	100°C - 200°C
Mg(IO3)2	0	6	2.327	0.804	0.0	No	170	170	100°C - 200°C
LiIO3	1	6	2.236	0.994	0.0	No	121	124	100°C - 200°C
Mn3(PO4)2	0	8	2.262	0.917	0.0	No	118	120	100°C - 200°C
KBrO3	0	6	2.134	1.177	0.0	No	97	97	50°C - 100°C
Al(IO3)3	0	9	2.293	0.805	0.0	No	165	165	100°C - 200°C
Mn3(AsO4)2	0	8	2.280	0.825	0.0	No	142	142	100°C - 200°C

Sr3(PO4)2	1	11	2.170	0.894	0.0	No	125	125	100°C - 200°C
Ba3(PO4)2	0	11	2.199	0.793	0.0	No	122	122	100°C - 200°C
Sr3(AsO4)2	1	11	2.181	0.838	0.0	No	151	151	100°C - 200°C
Pb3(PO4)2	0	11	2.247	0.611	0.0	No	111	111	100°C - 200°C
CrPO4	0	2	2.159	0.793	0.0	No	187	261	200°C - 300°C
Pb3(AsO4)2	0	11	2.209	0.579	0.0	No	123	123	100°C - 200°C
Ba3(AsO4)2	0	11	2.155	0.737	0.0	No	134	134	100°C - 200°C
PbHAsO4	0	7	2.127	0.806	0.0	No	100	100	100°C - 200°C
NaNO3	0	3	1.894	1.214	0.0	No	112	112	100°C - 200°C
Co3(AsO4)2	1	8	2.130	0.683	0.0	No	125	129	100°C - 200°C
CrAsO4	0	2	2.125	0.675	0.0	No	252	252	200°C - 300°C
Ni3(PO4)2	0	4	2.137	0.622	0.0	No	193	193	100°C - 200°C
Cu(IO3)2	0	4	2.080	0.583	0.0	No	212	212	200°C - 300°C
AlAsO4	0	2	1.993	0.683	0.0	No	199	199	100°C - 200°C
CaHPO4	0	3	1.857	0.938	0.0	No	131	141	100°C - 200°C
Fe3(PO4)2	0	4	1.947	0.627	0.0	No	188	188	100°C - 200°C
Ca(IO3)2	0	6	1.902	0.689	0.0	No	112	149	100°C - 200°C
Zn3(PO4)2	0	4	1.887	0.585	0.0	No	186	186	100°C - 200°C
LiIO3	2	6	1.786	0.794	0.0	No	121	121	100°C - 200°C
Cu3(PO4)2	0	4	1.830	0.557	0.0	No	159	159	100°C - 200°C
Ni2P2O7	2	6	1.734	0.653	0.0	No	173	173	100°C - 200°C
Zn3(AsO4)2	0	4	1.712	0.479	0.0	No	175	175	100°C - 200°C
Cu3(AsO4)2	0	4	1.692	0.461	0.0	No	153	153	100°C - 200°C
VPO4	0	1	1.654	0.542	0.0	No	335	335	300°C - 450°C
LiIO3	0	2	1.607	0.550	0.0	No	124	151	100°C - 200°C
Pb(NO3)2	0	4	1.599	0.535	0.0	No	96	96	50°C - 100°C
FeAsO4	0	1	1.605	0.446	0.0	No	376	376	300°C - 450°C
Ca(IO3)2	1	6	1.560	0.565	0.0	No	112	112	100°C - 200°C
CaHPO4	3	7	1.393	0.870	0.0	No	118	118	100°C - 200°C
Co3(AsO4)2	0	4	1.581	0.422	0.0	No	57	125	50°C - 100°C
Mn(OH)2	0	1	1.490	0.615	0.0	No	178	178	100°C - 200°C
CrPO4	0	1	1.522	0.472	0.0	No	261	261	200°C - 300°C
Ni2P2O7	0	2	1.492	0.440	0.0	No	220	220	200°C - 300°C
Mn3(PO4)2	3	8	1.411	0.572	0.0	No	118	118	100°C - 200°C
LaPO4	0	2	1.385	0.407	0.0	No	103	103	100°C - 200°C
Ni3(PO4)2	4	8	1.340	0.491	0.0	No	156	156	100°C - 200°C
LaAsO4	0	2	1.356	0.367	0.0	No	122	122	100°C - 200°C
Mn3(PO4)2	0	3	1.321	0.421	0.0	No	120	120	100°C - 200°C
Na2HPO4	7	12	1.162	0.745	0.0	No	93	93	50°C - 100°C
LiClO4	0	1	1.254	0.568	0.0	No	211	211	200°C - 300°C

CaHPO4	1	3	1.227	0.620	0.0	No	131	131	100°C - 200°C
Co3(AsO4)2	4	8	1.223	0.393	0.0	No	129	129	100°C - 200°C
Co3(AsO4)2	1	4	1.239	0.331	0.0	No	125	125	100°C - 200°C
Ca(H2PO4)2	1	4	1.108	0.577	0.0	No	112	167	100°C - 200°C
NiCO3	3	5	1.091	0.529	0.0	No	105	105	100°C - 200°C
Zn3(AsO4)2	4	8	1.111	0.365	0.0	No	114	114	100°C - 200°C
LaAsO3	0	1	1.063	0.236	0.0	No	179	179	100°C - 200°C
K2CO3	0	1	0.978	0.460	0.0	No	219	219	200°C - 300°C
CrPO4	1	2	1.000	0.367	0.0	No	187	187	100°C - 200°C
LiIO3	0	1	1.005	0.309	0.0	No	151	151	100°C - 200°C
CaHPO4	0	1	0.951	0.392	0.0	No	141	141	100°C - 200°C
Sr(BrO3)2	0	2	0.928	0.292	0.0	No	107	107	100°C - 200°C
Co2SiO4	0	1	0.897	0.267	0.0	No	144	144	100°C - 200°C
Mn(H2PO4)2	2	4	0.755	0.352	0.0	No	114	114	100°C - 200°C
LiIO3	1	2	0.777	0.266	0.0	No	124	124	100°C - 200°C
BaHPO4	0	1	0.779	0.226	0.0	No	115	115	100°C - 200°C
Ca(H2PO4)2	2	4	0.705	0.367	0.0	No	112	112	100°C - 200°C
Mg2As2O7	0	1	0.754	0.249	0.0	No	287	287	200°C - 300°C
La(IO3)3	0	2	0.743	0.169	0.0	No	109	155	100°C - 200°C
Zn2As2O7	0	1	0.710	0.190	0.0	No	262	262	200°C - 300°C
AlPO4	9	11	0.627	0.368	0.0	No	131	131	100°C - 200°C
AlAsO4	9	11	0.584	0.313	0.0	No	118	118	100°C - 200°C
CoPO4	9	11	0.579	0.304	0.0	No	93	93	50°C - 100°C
Ca(IO3)2	0	1	0.618	0.151	0.0	No	149	149	100°C - 200°C
CrAsO4	9	11	0.560	0.286	0.0	No	109	109	100°C - 200°C
Co2P2O7	0	1	0.564	0.178	0.0	No	106	106	100°C - 200°C
Ca(H2PO4)2	1	2	0.499	0.238	0.0	No	167	167	100°C - 200°C
Ba(H2PO4)2	0	1	0.503	0.189	0.0	No	179	179	100°C - 200°C
Sr3(PO4)2	0	1	0.489	0.136	0.0	No	165	165	100°C - 200°C
Sr3(AsO4)2	0	1	0.480	0.121	0.0	No	190	190	100°C - 200°C
Co3(AsO4)2	0	1	0.455	0.102	0.0	No	57	57	50°C - 100°C
La(IO3)3	0	1	0.407	0.092	0.0	No	155	155	100°C - 200°C
Ni(ClO4)2	5	6	0.327	0.161	0.0	No	130	130	100°C - 200°C
La(IO3)3	1	2	0.350	0.080	0.0	No	109	109	100°C - 200°C

Table E.4 820 hypothetical complex anion salt (de)hydration reactions that are predicted to lie within 10 meV/atom of the convex hull are characterized by the number of water molecules per formula unit in the dehydrated (n_{low}) and hydrated (n_{high}) states, volumetric (VED) and gravimetric (GED) energy densities, maximum distance to the convex hull (E_{hull}), whether the hydrate contains an expensive metal, minimum ($T_{turn,min}$) and maximum ($T_{turn,max}$) turning

temperatures of the (de)hydration reaction(s), and temperature category. Reactions are ordered by descending $ED_{RMS} = \sqrt{VED^2 + GED^2}$.

Salt	n_{low}	n_{high}	VED (GJ/m^3)	GED (MJ/kg)	E_{hull} (meV/at)	Expensive Metal	$T_{turn,min}$ (°C)	$T_{turn,max}$ (°C)	Temp. Categ.
NaOH	0	7	3.739	2.746	0.0	No	120	275	100°C - 200°C
LiOH	0	7	3.616	2.742	0.0	No	86	207	Wide Temp. Window
NaOH	0	4	3.576	2.537	0.7	No	193	275	200°C - 300°C
CoPO4	0	11	3.857	2.024	0.0	No	93	201	Wide Temp. Window
CoPO4	0	9	3.828	1.916	0.0	No	141	201	100°C - 200°C
Ca(OH)2	0	8	3.637	2.207	0.0	No	139	139	100°C - 200°C
Sr(OH)2	0	8	3.741	1.986	0.2	No	169	183	100°C - 200°C
CoPO4	0	7	3.775	1.700	5.4	No	141	201	100°C - 200°C
KOH	0	4	3.453	2.272	0.5	No	160	405	Wide Temp. Window
LiOH	0	4	3.305	2.455	4.3	No	86	207	Wide Temp. Window
AlPO4	0	11	3.551	2.083	0.0	No	127	206	100°C - 200°C
KOH	0	7	3.296	2.434	2.0	No	75	405	Wide Temp. Window
Ba(OH)2	0	8	3.661	1.758	0.0	No	184	282	200°C - 300°C
VPO4	0	11	3.537	1.984	0.0	No	80	335	Wide Temp. Window
CoPO4	0	6	3.676	1.586	7.2	No	201	201	200°C - 300°C
NiSO4	0	11	3.445	2.026	0.0	No	127	194	100°C - 200°C
AlAsO4	0	11	3.505	1.881	0.0	No	92	219	Wide Temp. Window
AlPO4	0	9	3.438	1.933	0.0	No	127	206	100°C - 200°C
CrPO4	0	9	3.479	1.834	0.0	No	103	261	100°C - 200°C
Na2CO3	0	10	3.251	2.160	0.0	No	146	193	100°C - 200°C
NiSO4	0	9	3.379	1.888	3.1	No	142	194	100°C - 200°C
VPO4	0	9	3.393	1.822	0.4	No	80	335	Wide Temp. Window
CrAsO4	0	11	3.426	1.751	0.0	No	92	252	Wide Temp. Window
AlAsO4	0	9	3.408	1.740	0.0	No	92	219	Wide Temp. Window
NaOH	1	7	3.083	2.265	4.9	No	120	193	100°C - 200°C
FePO4	0	11	3.346	1.825	0.0	No	57	193	100°C - 200°C
LiOH	1	7	2.999	2.274	0.0	No	86	143	100°C - 200°C
NiSO4	0	7	3.354	1.698	8.5	No	194	194	100°C - 200°C
CrAsO4	0	9	3.342	1.614	0.0	No	92	252	Wide Temp. Window

KOH	0	3	3.083	2.053	3.1	No	160	405	Wide Temp. Window
Sr(OH)2	1	8	3.271	1.737	2.6	No	169	183	100°C - 200°C
Li2CO3	0	10	3.046	2.090	0.0	No	91	91	50°C - 100°C
CaCO3	0	6	3.198	1.740	2.3	No	50	160	100°C - 200°C
CrPO4	0	7	3.264	1.569	7.7	No	103	261	100°C - 200°C
FeAsO4	0	9	3.247	1.585	0.0	No	130	376	Wide Temp. Window
VPO4	0	7	3.245	1.565	6.1	No	80	335	Wide Temp. Window
AlPO4	0	7	3.190	1.649	8.0	No	127	127	100°C - 200°C
MnSO4	0	9	3.081	1.814	0.2	No	158	160	100°C - 200°C
MnAsO4	0	11	3.150	1.620	3.8	No	93	293	Wide Temp. Window
VPO4	1	11	3.077	1.726	0.0	No	80	192	100°C - 200°C
FePO4	0	9	3.141	1.600	9.4	No	57	117	50°C - 100°C
FePO4	1	11	3.094	1.687	8.8	No	97	193	100°C - 200°C
KOH	0	2	3.049	1.761	2.1	No	160	405	Wide Temp. Window
Na2HPO4	0	12	2.962	1.899	0.0	No	93	166	100°C - 200°C
AlAsO4	0	7	3.191	1.463	7.8	No	92	199	100°C - 200°C
MgCO3	0	5	3.019	1.781	0.0	No	137	176	100°C - 200°C
MgCO3	0	6	2.979	1.802	7.4	No	-26	176	Wide Temp. Window
Na2CO3	1	10	2.893	1.922	1.2	No	146	146	100°C - 200°C
CaSO4	0	11	2.869	1.947	0.0	No	126	160	100°C - 200°C
Ba(OH)2	1	8	3.126	1.501	0.6	No	184	207	100°C - 200°C
Li2SO4	0	10	2.858	1.948	3.1	No	114	114	100°C - 200°C
Na2SO4	0	10	2.847	1.905	0.0	No	140	165	100°C - 200°C
CrAsO4	0	7	3.123	1.349	9.0	No	92	252	Wide Temp. Window
FeSO4	0	7	3.021	1.565	8.9	No	153	153	100°C - 200°C
MnAsO4	0	9	3.056	1.483	3.8	No	108	293	200°C - 300°C
K2CO3	0	10	2.806	1.911	0.0	No	108	219	100°C - 200°C
CrPO4	1	9	3.001	1.582	0.0	No	103	202	100°C - 200°C
Na3PO4	0	8	2.958	1.619	0.0	No	154	154	100°C - 200°C
MnSO4	0	7	2.959	1.595	8.0	No	160	160	100°C - 200°C
CrPO4	0	5	3.055	1.306	7.5	No	103	261	100°C - 200°C
AlAsO4	0	6	3.032	1.326	9.9	No	92	199	100°C - 200°C
LiOH	0	3	2.427	2.242	8.5	No	86	207	Wide Temp. Window
VPO4	0	5	3.015	1.323	5.5	No	80	335	Wide Temp. Window

NiCO3	0	5	2.948	1.428	7.5	No	105	156	100°C - 200°C
VPO4	1	9	2.857	1.534	0.4	No	80	192	100°C - 200°C
Na2HPO4	1	12	2.716	1.741	9.0	No	93	166	100°C - 200°C
FeCO3	0	5	2.873	1.466	0.0	No	140	140	100°C - 200°C
FeSO4	0	9	2.792	1.609	2.2	No	-32	153	Wide Temp. Window
CaSO4	0	9	2.696	1.759	5.6	No	126	126	100°C - 200°C
FePO4	2	11	2.810	1.532	3.7	No	117	193	100°C - 200°C
VPO4	2	11	2.789	1.565	2.5	No	80	192	100°C - 200°C
AlAsO4	0	5	2.953	1.202	7.5	No	92	199	100°C - 200°C
FePO4	1	9	2.839	1.447	9.4	No	97	117	100°C - 200°C
KOH	1	7	2.561	1.891	2.0	No	75	172	100°C - 200°C
AlAsO4	2	11	2.800	1.503	0.0	No	92	219	Wide Temp. Window
CaCO3	0	5	2.703	1.657	0.0	No	158	160	100°C - 200°C
NaOH	1	4	2.570	1.823	4.9	No	193	193	100°C - 200°C
MnCO3	0	6	2.768	1.480	8.2	No	-40	160	Wide Temp. Window
LiClO4	0	9	2.581	1.779	9.5	No	-19	211	Wide Temp. Window
SrSO4	0	11	2.659	1.642	8.1	No	117	117	100°C - 200°C
CrAsO4	0	5	2.919	1.115	8.2	No	92	252	Wide Temp. Window
MnCO3	0	5	2.752	1.444	0.0	No	114	160	100°C - 200°C
NaClO4	0	11	2.550	1.773	6.6	No	61	143	100°C - 200°C
MnAsO4	1	11	2.740	1.409	3.6	No	93	108	100°C - 200°C
SrCO3	0	6	2.783	1.317	0.0	No	100	171	100°C - 200°C
Ca3(PO4)2	0	11	2.745	1.352	0.0	No	103	220	100°C - 200°C
Na2HPO4	0	7	2.642	1.542	0.0	No	115	166	100°C - 200°C
PbSO4	0	11	2.759	1.291	5.4	No	130	130	100°C - 200°C
LiOH	0	1	2.508	1.671	0.0	No	207	207	200°C - 300°C
FeAsO4	1	9	2.703	1.319	0.0	No	130	130	100°C - 200°C
CuHPO4	0	7	2.670	1.384	0.0	No	114	114	100°C - 200°C
NaIO3	0	6	2.729	1.235	0.0	No	158	158	100°C - 200°C
K2CO3	1	10	2.474	1.685	0.0	No	108	143	100°C - 200°C
Ni(NO3)2	0	6	2.687	1.305	0.7	No	160	162	100°C - 200°C
CrAsO4	2	11	2.655	1.357	0.0	No	92	213	Wide Temp. Window
Ni3(PO4)2	0	8	2.798	1.025	0.0	No	71	410	Wide Temp. Window
LiIO3	0	6	2.716	1.207	0.0	No	121	151	100°C - 200°C
Ba(OH)2	0	3	2.803	0.982	0.7	No	207	282	200°C - 300°C

CrPO4	1	7	2.670	1.284	7.7	No	103	187	100°C - 200°C
Sr(OH)2	0	3	2.742	1.112	3.9	No	169	181	100°C - 200°C
VPO4	0	4	2.732	1.136	9.5	No	80	335	Wide Temp. Window
Ca3(PO4)2	0	10	2.668	1.268	2.5	No	103	220	100°C - 200°C
Na2SO4	0	7	2.484	1.574	8.3	No	140	140	100°C - 200°C
CrPO4	2	9	2.589	1.365	0.0	No	103	202	100°C - 200°C
CaHPO4	0	7	2.481	1.550	0.0	No	59	178	100°C - 200°C
Ca2SiO4	0	7	2.584	1.329	0.0	No	107	126	100°C - 200°C
AlAsO4	2	9	2.585	1.320	0.0	No	92	219	Wide Temp. Window
LiOH	1	4	2.321	1.724	4.3	No	86	143	100°C - 200°C
PbCO3	0	6	2.749	0.895	0.0	No	85	170	100°C - 200°C
NiCO3	0	3	2.673	1.087	7.5	No	156	156	100°C - 200°C
Mg3(AsO4)2	0	8	2.668	1.083	0.0	No	163	254	200°C - 300°C
LaPO4	0	11	2.570	1.298	8.6	No	70	103	50°C - 100°C
K2SO4	0	10	2.370	1.631	0.4	No	113	146	100°C - 200°C
Ni2P2O7	0	6	2.692	1.013	0.0	No	173	263	200°C - 300°C
Na2HPO4	0	6	2.505	1.397	2.6	No	115	128	100°C - 200°C
K3AsO4	0	8	2.547	1.315	0.0	No	178	178	100°C - 200°C
MnAsO4	1	9	2.577	1.251	3.6	No	108	108	100°C - 200°C
KOH	0	1	2.534	1.336	0.0	No	405	405	300°C - 450°C
Ca(ClO4)2	0	9	2.545	1.315	1.9	No	-7	272	Wide Temp. Window
VPO4	2	9	2.521	1.354	2.5	No	80	192	100°C - 200°C
NaOH	0	1	2.502	1.379	4.9	No	275	275	200°C - 300°C
Li3AsO4	0	8	2.507	1.362	0.4	No	81	81	50°C - 100°C
AlAsO4	0	4	2.661	1.027	9.8	No	92	199	100°C - 200°C
VPO4	1	7	2.568	1.239	6.1	No	80	171	100°C - 200°C
LaAsO4	0	11	2.566	1.230	3.5	No	71	148	100°C - 200°C
Mg3(PO4)2	0	8	2.557	1.198	7.8	No	145	145	100°C - 200°C
MgCO3	0	3	2.507	1.298	8.8	No	137	137	100°C - 200°C
K3PO4	0	8	2.459	1.370	6.9	No	145	145	100°C - 200°C
LiNO3	0	3	2.380	1.496	0.0	No	126	177	100°C - 200°C
FePO4	2	9	2.501	1.274	9.4	No	117	117	100°C - 200°C
NaBrO3	0	6	2.456	1.297	0.0	No	83	129	100°C - 200°C
NaClO4	1	11	2.278	1.583	6.6	No	61	84	50°C - 100°C
Ni3(AsO4)2	0	8	2.621	0.861	0.0	No	37	195	Wide Temp. Window
Na4P2O7	0	10	2.422	1.316	5.9	No	129	129	100°C - 200°C
KOH	1	4	2.279	1.499	1.6	No	160	172	100°C - 200°C

CrAsO4	2	9	2.443	1.180	0.0	No	92	213	Wide Temp. Window
K2HPO4	0	6	2.355	1.344	0.0	No	113	195	100°C - 200°C
BaCO3	0	6	2.482	1.060	0.0	No	75	206	Wide Temp. Window
Mg2P2O7	0	6	2.433	1.132	3.1	No	127	214	100°C - 200°C
LiClO4	1	9	2.199	1.516	9.5	No	-19	154	Wide Temp. Window
Sr(OH)2	3	8	2.357	1.251	3.9	No	183	183	100°C - 200°C
Zn3(PO4)2	0	8	2.481	0.903	1.7	No	39	312	Wide Temp. Window
Na2HPO4	1	7	2.280	1.331	9.0	No	128	166	100°C - 200°C
Zn(IO3)2	0	6	2.503	0.797	0.0	No	136	313	Wide Temp. Window
Ni3(PO4)2	1	8	2.464	0.903	1.0	No	71	410	Wide Temp. Window
Li4P2O7	0	10	2.269	1.319	7.9	No	72	72	50°C - 100°C
LiOH	3	7	2.079	1.576	8.5	No	128	143	100°C - 200°C
Sr3(PO4)2	0	11	2.409	0.992	0.0	No	119	165	100°C - 200°C
SrHPO4	0	7	2.288	1.242	0.0	No	70	129	50°C - 100°C
KOH	2	7	2.091	1.544	2.1	No	75	172	100°C - 200°C
Zn2P2O7	0	6	2.428	0.912	3.2	No	122	331	Wide Temp. Window
Sr3(AsO4)2	0	11	2.419	0.930	0.0	No	32	190	Wide Temp. Window
VPO4	4	11	2.255	1.265	9.5	No	115	192	100°C - 200°C
LaAsO4	1	11	2.331	1.117	5.6	No	71	148	100°C - 200°C
LaAsO4	0	9	2.349	1.061	7.5	No	71	148	100°C - 200°C
Na4As2O7	0	10	2.314	1.116	5.8	No	135	135	100°C - 200°C
KIO3	0	6	2.315	1.102	0.0	No	111	136	100°C - 200°C
AlAsO4	4	11	2.255	1.210	9.8	No	109	219	100°C - 200°C
Ca(NO3)2	0	6	2.199	1.305	0.0	No	118	167	100°C - 200°C
Ca(ClO4)2	1	9	2.269	1.172	7.1	No	-7	272	Wide Temp. Window
Ni3(PO4)2	0	7	2.398	0.860	8.9	No	71	246	Wide Temp. Window
LiClO4	0	3	2.256	1.177	1.4	No	109	211	100°C - 200°C
Ba(ClO4)2	0	9	2.313	1.056	0.0	No	20	183	Wide Temp. Window
NaNO3	0	5	2.077	1.461	9.0	No	25	112	Wide Temp. Window
Mg(ClO4)2	1	8	2.217	1.212	8.0	No	49	237	Wide Temp. Window
Zn3(AsO4)2	0	8	2.400	0.789	0.0	No	37	344	Wide Temp. Window

Ni3(AsO4)2	1	8	2.390	0.785	3.6	No	161	195	100°C - 200°C
Co3(AsO4)2	0	8	2.381	0.764	0.0	No	17	341	Wide Temp. Window
CaHPO4	1	7	2.112	1.320	0.0	No	59	178	100°C - 200°C
NaClO4	2	11	2.044	1.421	6.6	No	61	75	50°C - 100°C
Ni(NO3)2	0	4	2.280	0.992	7.4	No	160	160	100°C - 200°C
CrPO4	1	5	2.286	0.978	7.5	No	103	187	100°C - 200°C
Sr3(PO4)2	0	10	2.298	0.929	0.0	No	126	165	100°C - 200°C
CaCO3	0	3	2.154	1.224	7.2	No	158	158	100°C - 200°C
PbHPO4	0	7	2.303	0.896	0.0	No	57	141	50°C - 100°C
Sr3(AsO4)2	0	10	2.310	0.861	1.1	No	32	190	Wide Temp. Window
Mg(IO3)2	0	6	2.327	0.804	0.0	No	156	177	100°C - 200°C
SrCO3	0	5	2.174	1.145	5.4	No	100	100	50°C - 100°C
Cu3(PO4)2	0	8	2.300	0.850	7.4	No	59	159	100°C - 200°C
LiIO3	1	6	2.236	0.994	0.0	No	121	124	100°C - 200°C
Ba(OH)2	3	8	2.200	1.057	0.7	No	184	184	100°C - 200°C
Mn3(PO4)2	0	8	2.262	0.917	0.0	No	118	120	100°C - 200°C
KBrO3	0	6	2.134	1.177	0.0	No	76	114	50°C - 100°C
Al(IO3)3	0	9	2.293	0.805	0.0	No	142	344	Wide Temp. Window
KClO4	0	7	2.034	1.321	9.2	No	69	69	50°C - 100°C
Mn3(AsO4)2	0	8	2.280	0.825	0.0	No	78	221	Wide Temp. Window
Cu(IO3)2	0	6	2.306	0.730	6.3	No	60	326	Wide Temp. Window
Ni2P2O7	1	6	2.255	0.849	9.5	No	173	263	200°C - 300°C
Na2HPO4	1	6	2.099	1.170	9.0	No	128	128	100°C - 200°C
CrPO4	2	7	2.158	1.037	7.7	No	103	134	100°C - 200°C
Mg2As2O7	0	6	2.220	0.881	5.9	No	104	287	100°C - 200°C
VPO4	2	7	2.145	1.034	6.1	No	80	171	100°C - 200°C
Mn2P2O7	0	6	2.198	0.910	3.0	No	115	196	100°C - 200°C
AlAsO4	2	7	2.162	0.991	7.8	No	92	165	100°C - 200°C
Ca(ClO4)2	0	8	2.066	1.169	9.5	No	-7	203	Wide Temp. Window
K2CO3	3	10	1.962	1.336	8.6	No	143	143	100°C - 200°C
CaHAsO4	1	7	2.066	1.166	3.4	No	78	177	100°C - 200°C
K2SO4	0	7	1.974	1.314	9.1	No	113	113	100°C - 200°C
SnHPO4	0	7	2.121	1.045	6.5	No	76	76	50°C - 100°C
VPO4	1	5	2.158	0.947	5.5	No	80	171	100°C - 200°C
MnCO3	0	3	2.125	1.003	8.0	No	114	114	100°C - 200°C
Co3(PO4)2	0	7	2.204	0.807	1.1	No	116	117	100°C - 200°C

Sr3(PO4)2	1	11	2.170	0.894	0.0	No	119	126	100°C - 200°C
Zn3(PO4)2	0	7	2.205	0.790	7.4	No	39	312	Wide Temp. Window
CaHPO4	0	4	2.072	1.090	5.0	No	59	178	100°C - 200°C
BaHPO4	0	7	2.111	1.006	5.3	No	49	115	Wide Temp. Window
Ba3(PO4)2	0	11	2.199	0.793	0.0	No	83	260	Wide Temp. Window
Sr3(AsO4)2	1	11	2.181	0.838	0.0	No	32	180	Wide Temp. Window
Co2As2O7	0	6	2.206	0.745	9.1	No	-20	405	Wide Temp. Window
Pb3(PO4)2	0	11	2.247	0.611	0.0	No	111	111	100°C - 200°C
LaPO4	2	11	2.067	1.044	8.6	No	70	70	50°C - 100°C
K2HPO4	1	6	2.005	1.144	6.2	No	163	195	100°C - 200°C
Ni2SiO4	0	4	2.193	0.722	7.0	No	75	75	50°C - 100°C
LiClO4	2	9	1.898	1.308	9.5	No	-19	154	Wide Temp. Window
CrPO4	0	2	2.159	0.793	0.0	No	187	261	200°C - 300°C
Mg(ClO4)2	1	6	2.062	1.016	8.0	No	77	237	Wide Temp. Window
Pb(IO3)2	0	10	2.178	0.725	9.4	No	57	335	Wide Temp. Window
PbCO3	0	5	2.164	0.759	4.9	No	85	120	100°C - 200°C
Ni3(PO4)2	2	8	2.150	0.788	7.1	No	71	410	Wide Temp. Window
Ca(ClO4)2	0	7	2.005	1.105	8.2	No	-7	203	Wide Temp. Window
Ca3(PO4)2	0	7	2.060	0.999	7.6	No	103	220	100°C - 200°C
LaAsO4	2	11	2.061	0.988	3.5	No	71	132	100°C - 200°C
Pb3(AsO4)2	0	11	2.209	0.579	0.0	No	79	133	100°C - 200°C
BaHAsO4	0	7	2.082	0.934	1.9	No	37	148	Wide Temp. Window
LaAsO4	1	9	2.078	0.939	7.5	No	71	148	100°C - 200°C
Ba3(AsO4)2	0	11	2.155	0.737	0.0	No	124	236	100°C - 200°C
PbHAsO4	0	7	2.127	0.806	0.0	No	75	123	50°C - 100°C
Ba(BrO3)2	0	10	2.070	0.924	2.2	No	85	127	100°C - 200°C
SrHPO4	1	7	1.990	1.080	4.9	No	71	129	100°C - 200°C
Ba(ClO4)2	1	9	2.056	0.938	1.4	No	20	183	Wide Temp. Window
Sr(BrO3)2	0	10	2.036	0.971	6.8	No	67	116	50°C - 100°C
Mg(ClO4)2	1	7	1.969	1.098	8.0	No	49	237	Wide Temp. Window
NaNO3	0	3	1.894	1.214	0.0	No	112	112	100°C - 200°C

Co3(AsO4)2	1	8	2.130	0.683	0.0	No	17	341	Wide Temp. Window
Ca(NO3)2	0	4	1.989	1.021	3.3	No	129	167	100°C - 200°C
CrAsO4	0	2	2.125	0.675	0.0	No	252	252	200°C - 300°C
VPO4	0	2	2.084	0.794	2.5	No	108	335	Wide Temp. Window
Ni3(PO4)2	0	4	2.137	0.622	0.0	No	129	246	100°C - 200°C
NaClO4	3	11	1.825	1.269	6.6	No	75	75	50°C - 100°C
Al(IO3)3	0	8	2.109	0.697	7.6	No	142	142	100°C - 200°C
Sr3(PO4)2	1	10	2.048	0.828	0.0	No	126	126	100°C - 200°C
LiClO4	0	4	1.811	1.266	9.8	No	-19	211	Wide Temp. Window
Co2SiO4	0	4	2.090	0.709	7.2	No	45	144	Wide Temp. Window
VPO4	5	11	1.919	1.077	5.5	No	115	192	100°C - 200°C
Ca(ClO4)2	0	6	1.960	0.999	9.8	No	-7	203	Wide Temp. Window
Sr3(AsO4)2	1	10	2.058	0.768	1.1	No	32	163	Wide Temp. Window
AlAsO4	5	11	1.931	1.036	7.5	No	109	219	100°C - 200°C
AlAsO4	4	9	1.949	0.995	9.8	No	109	219	100°C - 200°C
Zn(IO3)2	0	4	2.105	0.596	3.2	No	136	313	Wide Temp. Window
CrAsO4	2	7	2.005	0.866	9.0	No	92	119	100°C - 200°C
Zn2As2O7	0	6	2.066	0.688	4.9	No	92	262	Wide Temp. Window
Ca2SiO4	0	4	1.978	0.909	4.4	No	107	107	100°C - 200°C
Ni3(AsO4)2	2	8	2.068	0.679	7.1	No	182	195	100°C - 200°C
Mg2P2O7	1	6	1.970	0.917	7.1	No	127	146	100°C - 200°C
Ni3(PO4)2	1	7	2.045	0.733	8.9	No	71	246	Wide Temp. Window
Zn3(PO4)2	1	8	2.038	0.742	5.1	No	39	235	Wide Temp. Window
Sr3(AsO4)2	2	11	2.024	0.778	9.6	No	163	180	100°C - 200°C
Cu(IO3)2	0	4	2.080	0.583	0.0	No	98	326	Wide Temp. Window
Zn3(AsO4)2	1	8	2.051	0.674	0.5	No	37	344	Wide Temp. Window
KIO3	1	6	1.949	0.928	2.7	No	136	136	100°C - 200°C
Mn3(AsO4)2	0	7	2.030	0.729	3.4	No	78	221	Wide Temp. Window
VPO4	4	9	1.897	1.019	9.5	No	115	192	100°C - 200°C
Zn3(AsO4)2	0	7	2.023	0.662	9.8	No	37	212	Wide Temp. Window
PbHPO4	1	7	1.983	0.771	0.7	No	57	141	50°C - 100°C

LiNO3	0	2	1.804	1.126	3.5	No	126	138	100°C - 200°C
CaHPO4	2	7	1.794	1.121	6.0	No	59	178	100°C - 200°C
Ba3(PO4)2	0	10	1.986	0.711	5.0	No	83	125	100°C - 200°C
BaCO3	0	5	1.915	0.883	9.3	No	75	75	50°C - 100°C
AlAsO4	0	2	1.993	0.683	0.0	No	199	199	100°C - 200°C
Ca3(PO4)2	3	11	1.882	0.927	9.3	No	103	175	100°C - 200°C
SrHAsO4	1	7	1.865	0.960	1.1	No	64	136	50°C - 100°C
Ca(NO3)2	1	6	1.802	1.069	1.7	No	118	134	100°C - 200°C
Co3(AsO4)2	0	7	1.986	0.660	6.7	No	17	341	Wide Temp. Window
KOH	1	3	1.733	1.155	3.1	No	160	165	100°C - 200°C
CaHPO4	0	3	1.857	0.938	0.0	No	83	178	100°C - 200°C
CrAsO4	5	11	1.851	0.946	8.2	No	109	213	100°C - 200°C
Ba3(AsO4)2	0	10	1.968	0.667	3.7	No	124	124	100°C - 200°C
Mn2As2O7	0	6	1.952	0.706	3.5	No	90	232	Wide Temp. Window
Ca(ClO4)2	1	8	1.803	1.020	9.5	No	-7	203	Wide Temp. Window
AlAsO4	2	6	1.882	0.823	9.9	No	92	160	100°C - 200°C
Mg3(AsO4)2	2	8	1.903	0.773	9.0	No	163	163	100°C - 200°C
K2CO3	0	3	1.816	0.952	8.6	No	108	219	100°C - 200°C
Fe3(PO4)2	0	4	1.947	0.627	0.0	No	188	188	100°C - 200°C
KBrO3	1	6	1.788	0.986	3.2	No	76	114	50°C - 100°C
Sr(NO3)2	0	6	1.797	0.955	6.0	No	52	115	50°C - 100°C
CaHAsO4	2	7	1.769	0.998	8.8	No	137	177	100°C - 200°C
Ca(ClO4)2	0	5	1.804	0.925	7.4	No	-7	203	Wide Temp. Window
Pb(NO3)2	0	6	1.902	0.692	6.1	No	30	120	Wide Temp. Window
Ca(IO3)2	0	6	1.902	0.689	0.0	No	38	164	Wide Temp. Window
Sr3(AsO4)2	2	10	1.892	0.706	9.6	No	163	163	100°C - 200°C
Ba(BrO3)2	1	10	1.841	0.822	2.3	No	85	85	50°C - 100°C
Co3(PO4)2	1	7	1.888	0.691	8.9	No	116	116	100°C - 200°C
KOH	3	7	1.615	1.193	3.1	No	75	172	100°C - 200°C
Sr(BrO3)2	1	10	1.809	0.862	6.8	No	67	98	50°C - 100°C
LiClO4	0	2	1.794	0.888	3.9	No	109	211	100°C - 200°C
Ca(ClO4)2	0	4	1.799	0.854	2.2	No	118	203	100°C - 200°C
Mg(IO3)2	0	4	1.899	0.588	6.8	No	177	177	100°C - 200°C
Zn2P2O7	1	6	1.860	0.699	9.8	No	122	122	100°C - 200°C
LiOH	1	3	1.454	1.343	8.5	No	86	86	50°C - 100°C

Zn3(PO4)2	0	4	1.887	0.585	0.0	No	141	312	Wide Temp. Window
BaHPO4	1	7	1.780	0.848	5.3	No	49	80	50°C - 100°C
PbHAsO4	1	7	1.843	0.698	8.3	No	75	123	50°C - 100°C
Ca(ClO4)2	1	7	1.722	0.949	8.2	No	-7	203	Wide Temp. Window
LiIO3	2	6	1.786	0.794	0.0	No	121	121	100°C - 200°C
Sr(OH)2	1	3	1.811	0.734	3.9	No	169	169	100°C - 200°C
Mg(ClO4)2	1	5	1.724	0.911	8.0	No	152	237	100°C - 200°C
LaAsO4	2	9	1.769	0.799	7.5	No	71	71	50°C - 100°C
LiOH	4	7	1.544	1.171	4.3	No	128	128	100°C - 200°C
NaClO4	0	3	1.706	0.915	6.1	No	61	143	100°C - 200°C
Ca3(PO4)2	3	10	1.741	0.828	9.3	No	103	152	100°C - 200°C
Mn2P2O7	1	6	1.776	0.735	4.9	No	115	123	100°C - 200°C
NaBrO3	2	6	1.695	0.895	9.0	No	108	129	100°C - 200°C
Pb3(AsO4)2	2	11	1.853	0.486	8.3	No	133	133	100°C - 200°C
Pb(IO3)2	1	10	1.816	0.604	9.4	No	57	95	50°C - 100°C
Cu3(PO4)2	0	4	1.830	0.557	0.0	No	159	159	100°C - 200°C
BaHAsO4	1	7	1.742	0.781	1.9	No	37	113	Wide Temp. Window
Fe2SiO4	0	4	1.788	0.643	5.7	No	31	31	< 50°C
Pb(IO3)2	0	6	1.829	0.514	5.9	No	68	335	Wide Temp. Window
VPO4	1	4	1.752	0.728	9.5	No	80	108	50°C - 100°C
LiClO4	3	9	1.561	1.076	9.5	No	-19	72	< 50°C
LiNO3	1	3	1.604	1.008	1.6	No	126	177	100°C - 200°C
Ba(OH)2	1	3	1.776	0.622	0.7	No	207	207	200°C - 300°C
NaBrO3	0	3	1.708	0.780	6.7	No	83	108	50°C - 100°C
AlAsO4	6	11	1.646	0.883	9.9	No	118	219	100°C - 200°C
SrHPO4	2	7	1.640	0.890	0.3	No	71	113	50°C - 100°C
Zn3(AsO4)2	2	8	1.766	0.581	4.6	No	37	344	Wide Temp. Window
Mg2As2O7	1	6	1.727	0.685	5.9	No	104	124	100°C - 200°C
Ni2P2O7	2	6	1.734	0.653	0.0	No	173	173	100°C - 200°C
Zn3(PO4)2	1	7	1.740	0.623	7.4	No	39	146	Wide Temp. Window
PbHPO4	0	4	1.759	0.542	8.4	No	57	93	50°C - 100°C
Ca(ClO4)2	1	6	1.637	0.835	9.8	No	-7	203	Wide Temp. Window
Ni3(AsO4)2	0	4	1.779	0.459	2.7	No	37	182	Wide Temp. Window
Zn3(PO4)2	2	8	1.725	0.628	1.9	No	39	235	Wide Temp. Window

KOH	2	4	1.529	1.006	2.1	No	165	172	100°C - 200°C
Sr(BrO3)2	0	6	1.697	0.686	4.8	No	68	116	50°C - 100°C
Co3(AsO4)2	1	7	1.737	0.577	6.7	No	17	341	Wide Temp. Window
K2HPO4	2	6	1.581	0.902	2.8	No	163	163	100°C - 200°C
Ni3(PO4)2	2	7	1.713	0.614	8.9	No	71	246	Wide Temp. Window
CoPO4	6	11	1.607	0.843	7.2	No	93	170	100°C - 200°C
PbHPO4	2	7	1.689	0.657	4.9	No	57	141	50°C - 100°C
Ca(H2PO4)2	0	4	1.594	0.829	5.8	No	112	257	100°C - 200°C
CrPO4	5	9	1.579	0.833	7.5	No	134	202	100°C - 200°C
Sr(NO3)2	0	4	1.617	0.742	1.7	No	60	115	50°C - 100°C
Zn3(AsO4)2	0	4	1.712	0.479	0.0	No	123	212	100°C - 200°C
Co3(AsO4)2	3	8	1.690	0.542	8.6	No	94	341	Wide Temp. Window
VPO4	2	5	1.621	0.712	5.5	No	80	171	100°C - 200°C
Ba(ClO4)2	0	6	1.609	0.735	8.3	No	20	139	Wide Temp. Window
CrPO4	2	5	1.624	0.694	7.5	No	103	103	100°C - 200°C
AlAsO4	5	9	1.571	0.802	7.5	No	109	219	100°C - 200°C
Sr(BrO3)2	2	10	1.592	0.759	6.8	No	67	68	50°C - 100°C
PbHAsO4	0	4	1.689	0.496	6.8	No	75	95	50°C - 100°C
AlAsO4	2	5	1.630	0.663	7.5	No	92	160	100°C - 200°C
Mg2P2O7	2	6	1.591	0.740	6.3	No	146	146	100°C - 200°C
Cu3(AsO4)2	0	4	1.692	0.461	0.0	No	147	174	100°C - 200°C
Zn3(AsO4)2	1	7	1.663	0.544	9.8	No	37	183	Wide Temp. Window
NaOH	4	7	1.409	1.035	0.7	No	120	120	100°C - 200°C
CaCO3	3	6	1.532	0.834	7.2	No	50	160	100°C - 200°C
VPO4	0	1	1.654	0.542	0.0	No	335	335	300°C - 450°C
SrHAsO4	2	7	1.544	0.795	1.0	No	64	136	50°C - 100°C
PbCO3	0	3	1.649	0.488	9.0	No	85	85	50°C - 100°C
CaHPO4	1	4	1.520	0.799	5.0	No	59	178	100°C - 200°C
Ni3(PO4)2	1	4	1.648	0.479	1.0	No	129	246	100°C - 200°C
Ca2P2O7	0	4	1.562	0.703	8.6	No	86	154	100°C - 200°C
Na2HPO4	6	12	1.441	0.924	2.6	No	93	166	100°C - 200°C
VPO4	5	9	1.506	0.809	5.5	No	115	192	100°C - 200°C
BaHAsO4	0	4	1.598	0.594	8.0	No	37	148	Wide Temp. Window
Ba(ClO4)2	3	9	1.550	0.708	1.7	No	20	183	Wide Temp. Window
Mn3(AsO4)2	2	8	1.601	0.579	3.3	No	78	202	Wide Temp. Window

LiIO3	0	2	1.607	0.550	0.0	No	124	151	100°C - 200°C
Co2As2O7	1	6	1.606	0.542	1.6	No	-20	117	Wide Temp. Window
Mn3(AsO4)2	0	4	1.623	0.479	3.0	No	78	221	Wide Temp. Window
Ba(ClO4)2	0	5	1.561	0.648	6.9	No	20	139	Wide Temp. Window
Pb(NO3)2	0	4	1.599	0.535	0.0	No	72	120	50°C - 100°C
Zn2As2O7	1	6	1.598	0.532	4.9	No	92	92	50°C - 100°C
Pb(IO3)2	2	10	1.597	0.532	9.4	No	57	68	50°C - 100°C
Mg(ClO4)2	1	4	1.501	0.756	8.0	No	237	237	200°C - 300°C
CaHAsO4	1	4	1.528	0.701	3.4	No	78	177	100°C - 200°C
La(IO3)3	0	9	1.588	0.548	9.7	No	49	155	Wide Temp. Window
MgCO3	3	6	1.436	0.869	8.8	No	-26	176	Wide Temp. Window
NaH2PO4	0	2	1.488	0.771	1.5	No	121	157	100°C - 200°C
CrAsO4	5	9	1.505	0.727	8.2	No	119	213	100°C - 200°C
Cu(IO3)2	0	2	1.623	0.389	1.2	No	326	326	300°C - 450°C
BaHPO4	2	7	1.505	0.717	5.3	No	80	80	50°C - 100°C
Ca(NO3)2	2	6	1.433	0.851	1.9	No	118	129	100°C - 200°C
SrHPO4	0	3	1.526	0.670	3.3	No	70	129	50°C - 100°C
FeAsO4	0	1	1.605	0.446	0.0	No	376	376	300°C - 450°C
Ca(IO3)2	1	6	1.560	0.565	0.0	No	38	164	Wide Temp. Window
PbHAsO4	2	7	1.550	0.587	7.4	No	75	123	50°C - 100°C
LiClO4	4	9	1.361	0.938	9.8	No	72	72	50°C - 100°C
Ca(ClO4)2	1	5	1.466	0.751	7.4	No	-7	203	Wide Temp. Window
CaHPO4	0	2	1.508	0.654	6.0	No	83	141	100°C - 200°C
CaHPO4	3	7	1.393	0.870	0.0	No	59	137	50°C - 100°C
Ca(NO3)2	1	4	1.459	0.749	3.3	No	129	134	100°C - 200°C
Zn(IO3)2	0	2	1.594	0.379	5.1	No	313	313	300°C - 450°C
Co3(AsO4)2	0	4	1.581	0.422	0.0	No	17	341	Wide Temp. Window
BaHAsO4	2	7	1.492	0.669	6.6	No	72	113	50°C - 100°C
Mn2As2O7	1	6	1.527	0.552	7.2	No	90	90	50°C - 100°C
La(IO3)3	0	8	1.544	0.496	9.8	No	49	155	Wide Temp. Window
Mn(OH)2	0	1	1.490	0.615	0.0	No	178	178	100°C - 200°C
CrAsO4	2	5	1.491	0.569	8.2	No	92	92	50°C - 100°C
CaHAsO4	3	7	1.389	0.784	2.3	No	137	138	100°C - 200°C
CrPO4	0	1	1.522	0.472	0.0	No	261	261	200°C - 300°C

LiClO4	1	3	1.411	0.736	1.4	No	109	154	100°C - 200°C
AlPO4	7	11	1.372	0.805	8.0	No	131	206	100°C - 200°C
NaClO4	0	2	1.415	0.712	3.9	No	84	143	100°C - 200°C
Ba(OH)2	0	1	1.520	0.428	0.6	No	282	282	200°C - 300°C
Ca3(PO4)2	0	3	1.462	0.593	9.3	No	220	220	200°C - 300°C
Ba3(PO4)2	4	11	1.479	0.533	9.0	No	125	260	100°C - 200°C
Ca(ClO4)2	1	4	1.412	0.670	7.1	No	203	203	200°C - 300°C
Ni2P2O7	0	2	1.492	0.440	0.0	No	177	263	200°C - 300°C
Zn(IO3)2	2	6	1.475	0.469	5.1	No	136	160	100°C - 200°C
Mn2P2O7	2	6	1.427	0.591	4.9	No	123	123	100°C - 200°C
KBrO3	0	3	1.376	0.698	5.6	No	76	86	50°C - 100°C
PbCO3	3	6	1.467	0.478	9.0	No	120	170	100°C - 200°C
PbHPO4	0	3	1.480	0.435	5.2	No	64	93	50°C - 100°C
Co2SiO4	1	4	1.454	0.494	7.2	No	45	45	< 50°C
MnCO3	3	6	1.347	0.720	8.2	No	-40	160	Wide Temp. Window
VPO4	7	11	1.332	0.747	6.1	No	143	192	100°C - 200°C
SrHPO4	3	7	1.341	0.728	3.3	No	113	113	100°C - 200°C
Mn3(PO4)2	3	8	1.411	0.572	0.0	No	118	118	100°C - 200°C
LiClO4	1	4	1.244	0.869	9.8	No	-19	154	Wide Temp. Window
Ba(ClO4)2	0	4	1.397	0.572	0.7	No	121	139	100°C - 200°C
VPO4	4	7	1.358	0.655	9.5	No	115	171	100°C - 200°C
AlAsO4	4	7	1.366	0.626	9.8	No	109	165	100°C - 200°C
Sr(OH)2	0	1	1.425	0.475	2.6	No	181	181	100°C - 200°C
Mg2As2O7	2	6	1.395	0.554	5.9	No	124	124	100°C - 200°C
Zn3(PO4)2	2	7	1.410	0.505	7.4	No	39	146	Wide Temp. Window
AlAsO4	7	11	1.319	0.708	7.8	No	118	219	100°C - 200°C
Sr(BrO3)2	1	6	1.386	0.561	4.8	No	68	98	50°C - 100°C
Ni2As2O7	2	6	1.417	0.470	6.9	No	119	119	100°C - 200°C
Ni3(AsO4)2	1	4	1.445	0.373	3.6	No	161	182	100°C - 200°C
Ca(IO3)2	0	4	1.407	0.466	7.1	No	38	149	Wide Temp. Window
Co(OH)2	0	1	1.388	0.516	8.9	No	119	119	100°C - 200°C
MgCO3	3	5	1.274	0.751	8.8	No	176	176	100°C - 200°C
FePO4	0	2	1.373	0.547	3.7	No	57	97	50°C - 100°C
PbHPO4	3	7	1.373	0.534	5.2	No	57	141	50°C - 100°C
Ni3(AsO4)2	4	8	1.392	0.457	2.7	No	195	195	100°C - 200°C
PbHAsO4	0	3	1.411	0.392	5.7	No	76	95	50°C - 100°C
Ba(IO3)2	0	6	1.372	0.498	9.9	No	64	67	50°C - 100°C

Co2As2O7	2	6	1.381	0.466	9.9	No	117	117	100°C - 200°C
CaSiF6	0	2	1.362	0.517	8.9	No	113	113	100°C - 200°C
NaBrO3	3	6	1.288	0.680	6.7	No	129	129	100°C - 200°C
Ba(ClO4)2	1	6	1.320	0.603	8.3	No	20	139	Wide Temp. Window
La(IO3)3	1	9	1.369	0.472	9.7	No	49	109	Wide Temp. Window
SrHAsO4	1	4	1.335	0.558	2.9	No	64	136	50°C - 100°C
CoPO4	7	11	1.280	0.671	5.4	No	93	170	100°C - 200°C
LaPO4	0	2	1.385	0.407	0.0	No	103	103	100°C - 200°C
LiH2PO4	0	2	1.275	0.672	7.1	No	49	49	< 50°C
Zn3(AsO4)2	2	7	1.368	0.448	9.8	No	37	183	Wide Temp. Window
MnAsO4	0	1	1.383	0.390	3.8	No	293	293	200°C - 300°C
SrHAsO4	3	7	1.274	0.655	5.4	No	120	136	100°C - 200°C
CrAsO4	7	11	1.274	0.651	9.0	No	109	213	100°C - 200°C
Ni3(PO4)2	4	8	1.340	0.491	0.0	No	71	410	Wide Temp. Window
Ca(ClO4)2	4	9	1.263	0.653	2.2	No	-7	272	Wide Temp. Window
SrHPO4	0	2	1.328	0.496	0.3	No	70	129	50°C - 100°C
Cr3(PO4)2	1	4	1.335	0.466	9.9	No	171	171	100°C - 200°C
Ba(ClO4)2	4	9	1.286	0.587	0.7	No	20	183	Wide Temp. Window
Sr(BrO3)2	0	4	1.320	0.506	3.1	No	68	116	50°C - 100°C
KOH	4	7	1.133	0.836	2.0	No	75	75	50°C - 100°C
Mn3(AsO4)2	2	7	1.325	0.476	3.4	No	78	111	50°C - 100°C
Pb(IO3)2	1	6	1.354	0.380	5.9	No	68	95	50°C - 100°C
Mg2P2O7	0	2	1.314	0.501	6.3	No	127	214	100°C - 200°C
LaAsO4	0	2	1.356	0.367	0.0	No	96	148	100°C - 200°C
Ca(NO3)2	0	2	1.257	0.618	1.9	No	134	167	100°C - 200°C
LiNO3	0	1	1.218	0.690	1.6	No	138	138	100°C - 200°C
Ca(IO3)2	2	6	1.308	0.474	7.3	No	97	164	100°C - 200°C
AlAsO4	6	9	1.239	0.632	9.9	No	165	219	100°C - 200°C
Mn3(PO4)2	0	3	1.321	0.421	0.0	No	120	120	100°C - 200°C
Sr(NO3)2	2	6	1.224	0.650	7.9	No	52	115	50°C - 100°C
Na2HPO4	7	12	1.162	0.745	0.0	No	93	93	50°C - 100°C
K2HPO4	0	2	1.244	0.593	2.8	No	113	195	100°C - 200°C
LiClO4	0	1	1.254	0.568	0.0	No	211	211	200°C - 300°C
CaHPO4	1	3	1.227	0.620	0.0	No	83	178	100°C - 200°C
Na2CO3	0	1	1.260	0.549	1.2	No	193	193	100°C - 200°C
KOH	1	2	1.188	0.686	2.1	No	160	160	100°C - 200°C

La(IO3)3	1	8	1.303	0.418	9.8	No	49	109	Wide Temp. Window
Co3(AsO4)2	3	7	1.299	0.431	8.6	No	94	341	Wide Temp. Window
PbHPO4	1	4	1.297	0.400	8.4	No	57	88	50°C - 100°C
NaBrO3	0	2	1.237	0.557	9.0	No	83	83	50°C - 100°C
Pb(NO3)2	2	6	1.271	0.463	6.1	No	30	120	Wide Temp. Window
Sn(H2PO4)2	0	4	1.245	0.521	5.7	No	26	99	50°C - 100°C
Zn3(PO4)2	1	4	1.286	0.399	5.1	No	141	146	100°C - 200°C
CoPO4	6	9	1.200	0.601	7.2	No	141	170	100°C - 200°C
Mg3(AsO4)2	0	2	1.280	0.398	9.0	No	254	254	200°C - 300°C
PbHAsO4	3	7	1.251	0.474	5.7	No	75	123	50°C - 100°C
Ba(ClO4)2	1	5	1.231	0.511	6.9	No	20	139	Wide Temp. Window
NiSO4	7	11	1.147	0.674	8.5	No	127	142	100°C - 200°C
PbHAsO4	1	4	1.276	0.375	8.3	No	75	95	50°C - 100°C
MnCO3	3	5	1.176	0.617	8.0	No	160	160	100°C - 200°C
Ba3(PO4)2	4	10	1.245	0.446	9.0	No	125	125	100°C - 200°C
Sr(BrO3)2	4	10	1.193	0.569	6.8	No	67	68	50°C - 100°C
Mg2As2O7	0	2	1.260	0.395	2.8	No	104	287	100°C - 200°C
Cu(IO3)2	2	6	1.247	0.395	6.3	No	60	98	50°C - 100°C
Co2As2O7	0	2	1.260	0.327	9.9	No	-20	405	Wide Temp. Window
Zn3(AsO4)2	1	4	1.249	0.350	0.5	No	123	183	100°C - 200°C
Cu3(AsO4)2	1	4	1.249	0.340	3.0	No	147	147	100°C - 200°C
CaHPO4	4	7	1.097	0.685	5.0	No	137	137	100°C - 200°C
Co3(AsO4)2	4	8	1.223	0.393	0.0	No	94	235	Wide Temp. Window
Co3(AsO4)2	1	4	1.239	0.331	0.0	No	17	341	Wide Temp. Window
Ca2SiO4	4	7	1.138	0.585	4.4	No	126	126	100°C - 200°C
KBrO3	3	6	1.117	0.616	5.6	No	114	114	100°C - 200°C
CaCO3	3	5	1.085	0.665	7.2	No	160	160	100°C - 200°C
PbHPO4	0	2	1.232	0.302	4.9	No	64	93	50°C - 100°C
Ba(H2PO4)2	0	4	1.157	0.512	7.2	No	47	179	Wide Temp. Window
Ba(ClO4)2	0	3	1.179	0.444	1.7	No	121	128	100°C - 200°C
Mg(ClO4)2	4	8	1.105	0.604	5.2	No	49	152	Wide Temp. Window
Ca(H2PO4)2	1	4	1.108	0.577	0.0	No	112	167	100°C - 200°C
CaHAsO4	1	3	1.141	0.500	3.4	No	78	177	100°C - 200°C
Mn2P2O7	0	2	1.182	0.391	4.9	No	115	196	100°C - 200°C

K2CO3	1	3	1.102	0.578	8.6	No	108	108	100°C - 200°C
AlAsO4	2	4	1.160	0.448	9.8	No	92	92	50°C - 100°C
La(IO3)3	2	9	1.173	0.405	9.7	No	49	82	50°C - 100°C
Ni3(PO4)2	2	4	1.188	0.346	7.1	No	246	246	200°C - 300°C
VPO4	2	4	1.138	0.473	9.5	No	80	80	50°C - 100°C
Ca(H2PO4)2	0	2	1.100	0.524	5.8	No	167	257	200°C - 300°C
Ba(IO3)2	1	6	1.145	0.416	9.9	No	64	67	50°C - 100°C
NiCO3	3	5	1.091	0.529	0.0	No	105	105	100°C - 200°C
Ca(ClO4)2	5	9	1.076	0.556	7.4	No	18	272	Wide Temp. Window
BaHPO4	0	2	1.147	0.385	4.4	No	49	115	Wide Temp. Window
NaClO4	1	3	1.065	0.571	6.1	No	61	84	50°C - 100°C
Ba(ClO4)2	5	9	1.098	0.501	6.9	No	70	183	100°C - 200°C
Zn3(PO4)2	0	2	1.152	0.345	1.9	No	141	312	Wide Temp. Window
BaHAsO4	1	4	1.125	0.418	8.0	No	37	72	50°C - 100°C
CaHAsO4	4	7	1.042	0.588	1.8	No	138	138	100°C - 200°C
KH2PO4	0	2	1.041	0.590	3.6	No	68	82	50°C - 100°C
CaHAsO4	2	4	1.085	0.498	8.8	No	137	177	100°C - 200°C
Pb(IO3)2	0	2	1.168	0.240	2.0	No	95	335	Wide Temp. Window
PbHAsO4	0	2	1.160	0.270	7.4	No	76	87	50°C - 100°C
Mn3(AsO4)2	4	8	1.118	0.405	3.0	No	111	202	100°C - 200°C
Ni(ClO4)2	4	8	1.053	0.545	1.4	No	19	198	Wide Temp. Window
CaHPO4	2	4	1.044	0.549	6.0	No	59	178	100°C - 200°C
Fe(IO3)3	6	9	1.116	0.369	0.1	No	339	360	300°C - 450°C
Sr(BrO3)2	2	6	1.089	0.441	4.8	No	68	68	50°C - 100°C
Zn3(AsO4)2	4	8	1.111	0.365	0.0	No	37	344	Wide Temp. Window
Ca2P2O7	0	2	1.087	0.429	3.7	No	154	154	100°C - 200°C
PbHPO4	4	7	1.085	0.422	8.4	No	141	141	100°C - 200°C
Zn3(PO4)2	4	8	1.091	0.397	1.7	No	39	235	Wide Temp. Window
Ni3(PO4)2	0	2	1.122	0.301	7.1	No	129	154	100°C - 200°C
Ca3(PO4)2	3	7	1.039	0.504	9.3	No	103	103	100°C - 200°C
Mn3(AsO4)2	0	2	1.113	0.301	3.3	No	221	221	200°C - 300°C
BaHAsO4	0	2	1.099	0.341	6.6	No	37	148	Wide Temp. Window
La(IO3)3	2	8	1.088	0.349	9.8	No	49	49	< 50°C
SrHPO4	1	3	1.045	0.459	4.9	No	71	129	100°C - 200°C
Ba(ClO4)2	1	4	1.047	0.429	1.4	No	121	139	100°C - 200°C

Ca3(PO4)2	7	11	1.004	0.495	7.6	No	152	175	100°C - 200°C
Pb(IO3)2	2	6	1.066	0.299	5.9	No	68	68	50°C - 100°C
Ba3(PO4)2	0	4	1.050	0.308	9.0	No	83	83	50°C - 100°C
LaAsO3	0	1	1.063	0.236	0.0	No	179	179	100°C - 200°C
Ca(NO3)2	2	4	0.969	0.497	3.3	No	129	129	100°C - 200°C
AlAsO4	4	6	0.993	0.434	9.9	No	109	160	100°C - 200°C
K2CO3	0	1	0.978	0.460	0.0	No	219	219	200°C - 300°C
Na2SO4	7	10	0.890	0.596	8.3	No	165	165	100°C - 200°C
Zn3(AsO4)2	0	2	1.040	0.252	4.6	No	123	212	100°C - 200°C
Cu3(PO4)2	4	8	1.000	0.370	7.4	No	59	59	50°C - 100°C
CrPO4	1	2	1.000	0.367	0.0	No	187	187	100°C - 200°C
SrHAsO4	4	7	0.946	0.487	2.9	No	120	120	100°C - 200°C
LiOH	3	4	0.853	0.633	8.5	No	143	143	100°C - 200°C
SrHAsO4	1	3	0.987	0.382	5.4	No	64	127	50°C - 100°C
Ca(IO3)2	1	4	1.004	0.332	7.1	No	38	97	50°C - 100°C
Sn(H2PO4)2	1	4	0.973	0.407	7.0	No	78	99	50°C - 100°C
LiIO3	0	1	1.005	0.309	0.0	No	151	151	100°C - 200°C
Co3(AsO4)2	0	3	1.018	0.261	8.6	No	17	57	< 50°C
KOH	2	3	0.872	0.581	3.1	No	165	165	100°C - 200°C
LiNO3	1	2	0.888	0.554	3.5	No	126	126	100°C - 200°C
NaClO4	0	1	0.951	0.432	4.7	No	143	143	100°C - 200°C
PbHAsO4	4	7	0.967	0.366	6.8	No	123	123	100°C - 200°C
Sr(BrO3)2	1	4	0.964	0.370	3.1	No	68	98	50°C - 100°C
Ni(ClO4)2	4	7	0.922	0.460	0.7	No	62	198	100°C - 200°C
CaHPO4	0	1	0.951	0.392	0.0	No	141	141	100°C - 200°C
BaHAsO4	4	7	0.935	0.419	8.0	No	113	113	100°C - 200°C
KBrO3	1	3	0.908	0.461	5.6	No	76	76	50°C - 100°C
PbHPO4	1	3	0.971	0.285	5.2	No	64	88	50°C - 100°C
Ni3(AsO4)2	2	4	0.979	0.253	7.1	No	182	182	100°C - 200°C
Sr(H2PO4)2	1	4	0.910	0.435	2.0	No	8	113	Wide Temp. Window
LiNO3	2	3	0.851	0.535	3.5	No	177	177	100°C - 200°C
AlPO4	7	9	0.876	0.492	8.0	No	206	206	200°C - 300°C
CrPO4	5	7	0.904	0.435	7.7	No	134	134	100°C - 200°C
Pb(NO3)2	0	2	0.964	0.275	6.1	No	72	72	50°C - 100°C
Ni(NO3)2	4	6	0.899	0.436	7.4	No	162	162	100°C - 200°C
Sr(NO3)2	0	2	0.918	0.393	7.9	No	60	60	50°C - 100°C
PbHAsO4	1	3	0.954	0.265	8.3	No	87	95	50°C - 100°C
AlAsO4	5	7	0.893	0.410	7.8	No	109	165	100°C - 200°C
Ca(ClO4)2	6	9	0.871	0.450	9.8	No	31	272	Wide Temp. Window

Ca(IO3)2	0	2	0.945	0.251	7.3	No	38	149	Wide Temp. Window
Ba(IO3)2	2	6	0.917	0.333	9.9	No	67	67	50°C - 100°C
Sr(BrO3)2	0	2	0.928	0.292	0.0	No	98	116	100°C - 200°C
LiClO4	2	4	0.797	0.557	9.8	No	-19	154	Wide Temp. Window
PbCO3	3	5	0.914	0.321	9.0	No	120	120	100°C - 200°C
Pb(H2PO4)2	1	4	0.912	0.323	2.2	No	69	79	50°C - 100°C
Ca(ClO4)2	4	8	0.841	0.476	9.5	No	-7	115	Wide Temp. Window
Ba(ClO4)2	6	9	0.878	0.401	8.3	No	183	183	100°C - 200°C
NaH2PO4	0	1	0.868	0.417	4.5	No	121	121	100°C - 200°C
AlAsO4	7	9	0.857	0.438	7.8	No	219	219	200°C - 300°C
CrPO4	7	9	0.851	0.449	7.7	No	202	202	200°C - 300°C
VPO4	5	7	0.864	0.417	6.1	No	115	115	100°C - 200°C
Pb2P2O7	0	2	0.939	0.196	4.3	No	145	145	100°C - 200°C
Sr(NO3)2	2	4	0.870	0.399	7.9	No	115	115	100°C - 200°C
Co2As2O7	0	1	0.919	0.249	9.1	No	405	405	300°C - 450°C
Ni3(AsO4)2	0	2	0.924	0.222	7.1	No	37	161	Wide Temp. Window
SrHAsO4	2	4	0.869	0.363	2.9	No	64	136	50°C - 100°C
Mg(ClO4)2	4	7	0.822	0.459	5.2	No	49	152	Wide Temp. Window
Co2SiO4	0	1	0.897	0.267	0.0	No	144	144	100°C - 200°C
VPO4	7	9	0.820	0.441	6.1	No	192	192	100°C - 200°C
CrAsO4	7	9	0.833	0.402	9.0	No	213	213	200°C - 300°C
Zn2P2O7	0	1	0.883	0.273	9.8	No	331	331	300°C - 450°C
KOH	3	4	0.771	0.507	3.1	No	172	172	100°C - 200°C
Na2HPO4	0	1	0.846	0.354	9.0	No	115	115	100°C - 200°C
CoPO4	7	9	0.818	0.410	5.4	No	170	170	100°C - 200°C
K2SO4	7	10	0.752	0.518	9.1	No	146	146	100°C - 200°C
PbHPO4	2	4	0.872	0.269	8.4	No	57	88	50°C - 100°C
CrAsO4	5	7	0.837	0.361	9.0	No	119	119	100°C - 200°C
Ni3(PO4)2	4	7	0.855	0.307	8.9	No	71	71	50°C - 100°C
Mg(ClO4)2	5	8	0.795	0.435	1.4	No	49	149	Wide Temp. Window
Zn3(AsO4)2	2	4	0.871	0.244	4.6	No	183	183	100°C - 200°C
Sr2P2O7	0	2	0.858	0.284	7.7	No	102	102	100°C - 200°C
Sr2As2O7	0	2	0.866	0.252	3.9	No	136	136	100°C - 200°C
Zn3(PO4)2	2	4	0.861	0.267	1.9	No	146	146	100°C - 200°C
Zn(IO3)2	2	4	0.865	0.245	5.1	No	136	136	100°C - 200°C
Pb(NO3)2	2	4	0.851	0.285	6.1	No	120	120	100°C - 200°C

PbHAsO4	2	4	0.849	0.249	7.4	No	75	95	50°C - 100°C
Ca3(PO4)2	7	10	0.798	0.379	7.6	No	152	152	100°C - 200°C
LiClO4	1	2	0.791	0.392	3.9	No	109	109	100°C - 200°C
Sr(BrO3)2	6	10	0.795	0.379	6.8	No	67	67	50°C - 100°C
Co3(AsO4)2	4	7	0.834	0.277	6.7	No	94	94	50°C - 100°C
NaH2PO4	1	2	0.776	0.402	4.5	No	157	157	100°C - 200°C
Mn3(AsO4)2	4	7	0.823	0.296	3.4	No	111	111	100°C - 200°C
NaNO3	3	5	0.707	0.498	9.0	No	25	25	< 50°C
Ba(H2PO4)2	1	4	0.787	0.348	7.2	No	47	47	< 50°C
VPO4	1	2	0.802	0.305	2.5	No	108	108	100°C - 200°C
Mn(NO3)2	4	6	0.758	0.391	7.6	No	111	111	100°C - 200°C
Fe(IO3)3	6	8	0.810	0.255	8.2	No	360	360	300°C - 450°C
FePO4	0	1	0.797	0.285	8.8	No	57	57	50°C - 100°C
Ni2P2O7	1	2	0.811	0.239	9.5	No	263	263	200°C - 300°C
LiClO4	2	3	0.744	0.388	3.9	No	154	154	100°C - 200°C
Pb(IO3)2	0	1	0.824	0.154	3.6	No	335	335	300°C - 450°C
Ba(ClO4)2	1	3	0.781	0.295	1.7	No	121	121	100°C - 200°C
Mn(H2PO4)2	2	4	0.755	0.352	0.0	No	114	114	100°C - 200°C
Ba(ClO4)2	3	6	0.754	0.344	8.3	No	20	139	Wide Temp. Window
Pb(IO3)2	6	10	0.785	0.261	9.4	No	57	57	50°C - 100°C
BaHAsO4	2	4	0.776	0.288	8.0	No	72	72	50°C - 100°C
Cu(IO3)2	2	4	0.796	0.223	1.2	No	98	98	50°C - 100°C
LiIO3	1	2	0.777	0.266	0.0	No	124	124	100°C - 200°C
Ca(NO3)2	4	6	0.707	0.419	3.3	No	118	118	100°C - 200°C
Ca(NO3)2	0	1	0.742	0.353	1.7	No	167	167	100°C - 200°C
BaHAsO4	0	1	0.789	0.208	1.0	No	148	148	100°C - 200°C
FePO4	9	11	0.715	0.390	9.4	No	193	193	100°C - 200°C
Ni(ClO4)2	5	8	0.723	0.374	1.4	No	19	130	Wide Temp. Window
BaHPO4	0	1	0.779	0.226	0.0	No	115	115	100°C - 200°C
Zn3(PO4)2	0	1	0.775	0.211	5.1	No	312	312	300°C - 450°C
Zn(IO3)2	4	6	0.759	0.241	3.2	No	160	160	100°C - 200°C
Mg(IO3)2	4	6	0.751	0.260	6.8	No	156	156	100°C - 200°C
Ca(H2PO4)2	2	4	0.705	0.367	0.0	No	112	112	100°C - 200°C
Mg2As2O7	0	1	0.754	0.249	0.0	No	287	287	200°C - 300°C
MnSO4	7	9	0.683	0.402	8.0	No	158	158	100°C - 200°C
Zn3(PO4)2	4	7	0.744	0.266	7.4	No	39	39	< 50°C
Ni(ClO4)2	4	6	0.709	0.349	0.7	No	130	198	100°C - 200°C
NiSO4	7	9	0.685	0.383	8.5	No	142	142	100°C - 200°C
Mg2P2O7	0	1	0.726	0.296	7.1	No	214	214	200°C - 300°C

PbHPO4	0	1	0.766	0.166	0.7	No	93	93	50°C - 100°C
Ca(ClO4)2	4	7	0.686	0.378	8.2	No	-7	115	Wide Temp. Window
Ca2P2O7	2	4	0.714	0.321	8.6	No	86	86	50°C - 100°C
Sn(H2PO4)2	0	2	0.729	0.281	5.7	No	26	99	50°C - 100°C
FePO4	1	2	0.726	0.289	8.8	No	97	97	50°C - 100°C
KIO3	0	1	0.739	0.242	2.7	No	111	111	100°C - 200°C
Mg(ClO4)2	4	6	0.693	0.341	5.2	No	77	152	100°C - 200°C
Ba(IO3)2	0	2	0.749	0.188	8.1	No	64	64	50°C - 100°C
SrHPO4	0	1	0.730	0.249	4.9	No	70	70	50°C - 100°C
CaHPO4	2	3	0.685	0.346	6.0	No	178	178	100°C - 200°C
SrHPO4	1	2	0.716	0.267	4.9	No	129	129	100°C - 200°C
La(IO3)3	0	2	0.743	0.169	0.0	No	109	155	100°C - 200°C
Ca(ClO4)2	5	8	0.662	0.375	9.5	No	18	115	Wide Temp. Window
CaHPO4	1	2	0.697	0.302	6.0	No	83	83	50°C - 100°C
K2HPO4	1	2	0.682	0.325	6.2	No	195	195	100°C - 200°C
KBrO3	0	1	0.700	0.284	3.2	No	86	86	50°C - 100°C
Ca(IO3)2	4	6	0.708	0.257	7.1	No	164	164	100°C - 200°C
Sr3(AsO4)2	0	2	0.726	0.195	9.6	No	32	190	Wide Temp. Window
LaAsO4	1	2	0.723	0.196	5.6	No	148	148	100°C - 200°C
Ca(IO3)2	2	4	0.707	0.234	7.3	No	97	97	50°C - 100°C
Ca(H2PO4)2	0	1	0.674	0.307	5.8	No	257	257	200°C - 300°C
TiPO4	9	11	0.641	0.369	9.6	No	158	158	100°C - 200°C
Sr(H2PO4)2	2	4	0.667	0.319	6.3	No	113	113	100°C - 200°C
Zn2As2O7	0	1	0.710	0.190	0.0	No	262	262	200°C - 300°C
KH2PO4	0	1	0.651	0.336	1.6	No	82	82	50°C - 100°C
NaClO4	1	2	0.653	0.329	4.7	No	84	84	50°C - 100°C
AlPO4	9	11	0.627	0.368	0.0	No	131	131	100°C - 200°C
Zn3(AsO4)2	4	7	0.690	0.226	9.8	No	37	37	< 50°C
Ni2P2O7	0	1	0.695	0.212	9.5	No	177	177	100°C - 200°C
PbHAsO4	0	1	0.709	0.139	8.3	No	76	76	50°C - 100°C
VPO4	9	11	0.629	0.353	0.4	No	143	143	100°C - 200°C
LaAsO4	0	1	0.692	0.182	5.6	No	96	96	50°C - 100°C
K2HPO4	0	1	0.649	0.293	6.2	No	113	113	100°C - 200°C
Mn3(AsO4)2	2	4	0.675	0.199	3.3	No	78	78	50°C - 100°C
SrHAsO4	1	2	0.666	0.222	1.1	No	127	127	100°C - 200°C
CaHAsO4	2	3	0.641	0.281	8.8	No	177	177	100°C - 200°C
Sn(H2PO4)2	2	4	0.636	0.266	5.7	No	78	78	50°C - 100°C
Mn2P2O7	0	1	0.650	0.227	4.9	No	196	196	100°C - 200°C

VPO4	4	5	0.625	0.275	9.5	No	171	171	100°C - 200°C
CaHAsO4	1	2	0.640	0.237	8.8	No	78	78	50°C - 100°C
Ca(NO3)2	1	2	0.605	0.297	1.9	No	134	134	100°C - 200°C
CaSO4	9	11	0.557	0.378	5.6	No	160	160	100°C - 200°C
Ca(ClO4)2	7	9	0.598	0.309	8.2	No	31	272	Wide Temp. Window
Ni3(PO4)2	0	1	0.651	0.162	1.0	No	154	154	100°C - 200°C
Co3(AsO4)2	1	3	0.649	0.166	8.6	No	17	17	< 50°C
Sr(BrO3)2	2	4	0.624	0.239	3.1	No	68	68	50°C - 100°C
Mn2As2O7	0	1	0.638	0.189	7.2	No	232	232	200°C - 300°C
AlAsO4	9	11	0.584	0.313	0.0	No	118	118	100°C - 200°C
Co3(AsO4)2	3	4	0.637	0.170	8.6	No	341	341	300°C - 450°C
AlAsO4	4	5	0.607	0.247	9.8	No	160	160	100°C - 200°C
NaBrO3	2	3	0.595	0.272	9.0	No	108	108	100°C - 200°C
Pb3(AsO4)2	0	2	0.645	0.110	8.3	No	79	79	50°C - 100°C
CoPO4	9	11	0.579	0.304	0.0	No	93	93	50°C - 100°C
NiSO4	9	11	0.563	0.331	3.1	No	127	127	100°C - 200°C
Pb(H2PO4)2	2	4	0.613	0.217	2.2	No	79	79	50°C - 100°C
Ca(IO3)2	0	1	0.618	0.151	0.0	No	149	149	100°C - 200°C
Mg2P2O7	1	2	0.592	0.226	7.1	No	127	127	100°C - 200°C
Sr(NO3)2	4	6	0.558	0.297	6.0	No	52	52	50°C - 100°C
Ba(ClO4)2	3	5	0.581	0.241	6.9	No	20	139	Wide Temp. Window
CrAsO4	9	11	0.560	0.286	0.0	No	109	109	100°C - 200°C
Ni(ClO4)2	5	7	0.563	0.281	0.5	No	62	130	50°C - 100°C
Cu(IO3)2	4	6	0.590	0.187	6.3	No	60	60	50°C - 100°C
Mg(ClO4)2	6	8	0.541	0.296	1.1	No	49	149	Wide Temp. Window
Zn3(AsO4)2	0	1	0.592	0.144	0.5	No	212	212	200°C - 300°C
PbHPO4	1	2	0.590	0.145	4.9	No	64	64	50°C - 100°C
PbHAsO4	1	2	0.589	0.137	8.3	No	87	87	50°C - 100°C
MnAsO4	9	11	0.530	0.273	0.4	No	93	93	50°C - 100°C
Cu3(AsO4)2	0	1	0.579	0.134	3.0	No	174	174	100°C - 200°C
SrCO3	5	6	0.535	0.253	5.4	No	171	171	100°C - 200°C
Co2P2O7	0	1	0.564	0.178	0.0	No	106	106	100°C - 200°C
Pb(NO3)2	4	6	0.554	0.201	6.1	No	30	30	< 50°C
Sr(BrO3)2	4	6	0.545	0.220	4.8	No	68	68	50°C - 100°C
KH2PO4	1	2	0.510	0.289	3.6	No	68	68	50°C - 100°C
NaClO4	2	3	0.515	0.276	6.1	No	61	61	50°C - 100°C
BaCO3	5	6	0.536	0.229	9.3	No	206	206	200°C - 300°C
Mg(ClO4)2	5	7	0.503	0.281	3.4	No	49	77	50°C - 100°C

LaAsO4	9	11	0.519	0.249	7.5	No	132	132	100°C - 200°C
Ca(ClO4)2	0	1	0.525	0.222	7.1	No	118	118	100°C - 200°C
CaHAsO4	3	4	0.517	0.238	2.3	No	137	137	100°C - 200°C
Ni3(PO4)2	7	8	0.534	0.196	8.9	No	410	410	300°C - 450°C
Mn2P2O7	1	2	0.535	0.177	4.9	No	115	115	100°C - 200°C
Ni3(PO4)2	1	2	0.543	0.146	7.1	No	129	129	100°C - 200°C
Ca(ClO4)2	5	7	0.493	0.272	8.2	No	18	115	Wide Temp. Window
Ba(BrO3)2	0	1	0.542	0.142	2.3	No	127	127	100°C - 200°C
PbCO3	5	6	0.530	0.173	4.9	No	170	170	100°C - 200°C
Sr(BrO3)2	0	1	0.532	0.157	1.2	No	116	116	100°C - 200°C
Ni3(AsO4)2	1	2	0.539	0.129	7.1	No	161	161	100°C - 200°C
Ca(H2PO4)2	1	2	0.499	0.238	0.0	No	167	167	100°C - 200°C
BaHPO4	1	2	0.520	0.175	4.4	No	49	49	< 50°C
Co3(PO4)2	0	1	0.527	0.148	8.9	No	117	117	100°C - 200°C
Ba(H2PO4)2	0	1	0.503	0.189	0.0	No	179	179	100°C - 200°C
Ca(ClO4)2	6	8	0.466	0.264	9.8	No	31	115	Wide Temp. Window
Mg2As2O7	1	2	0.507	0.159	2.8	No	104	104	100°C - 200°C
SrHPO4	2	3	0.482	0.212	3.3	No	71	71	50°C - 100°C
CoPO4	6	7	0.479	0.216	7.2	No	141	141	100°C - 200°C
AlAsO4	6	7	0.477	0.219	9.9	No	165	165	100°C - 200°C
PbHPO4	2	3	0.502	0.148	5.2	No	88	88	50°C - 100°C
Ba(ClO4)2	0	1	0.492	0.165	1.4	No	128	128	100°C - 200°C
SrHAsO4	3	4	0.476	0.199	5.4	No	136	136	100°C - 200°C
Ca(ClO4)2	4	6	0.459	0.234	9.8	No	-7	18	< 50°C
Sr3(PO4)2	0	1	0.489	0.136	0.0	No	165	165	100°C - 200°C
AlAsO4	5	6	0.465	0.203	9.9	No	109	109	100°C - 200°C
Ba(ClO4)2	4	6	0.457	0.209	8.3	No	20	70	< 50°C
PbHAsO4	2	3	0.483	0.134	7.4	No	95	95	50°C - 100°C
CaHPO4	3	4	0.443	0.233	5.0	No	59	59	50°C - 100°C
Zn3(PO4)2	1	2	0.477	0.143	5.1	No	141	141	100°C - 200°C
Ni(ClO4)2	6	8	0.440	0.228	1.4	No	19	62	< 50°C
Sr3(AsO4)2	0	1	0.480	0.121	0.0	No	190	190	100°C - 200°C
BaHAsO4	1	2	0.466	0.145	6.6	No	37	37	< 50°C
SrHAsO4	2	3	0.451	0.175	5.4	No	64	64	50°C - 100°C
Zn3(AsO4)2	1	2	0.468	0.113	4.6	No	123	123	100°C - 200°C
Sr(BrO3)2	1	2	0.453	0.143	1.2	No	98	98	50°C - 100°C
CaCO3	5	6	0.416	0.227	2.3	No	50	50	50°C - 100°C
Na2HPO4	6	7	0.409	0.239	2.6	No	166	166	100°C - 200°C
Ni(ClO4)2	4	5	0.426	0.198	0.7	No	198	198	100°C - 200°C

Zn3(AsO4)2	7	8	0.443	0.146	9.8	No	344	344	300°C - 450°C
Co3(AsO4)2	0	1	0.455	0.102	0.0	No	57	57	50°C - 100°C
Ba(IO3)2	0	1	0.442	0.097	5.9	No	64	64	50°C - 100°C
Pb(IO3)2	1	2	0.440	0.091	3.6	No	95	95	50°C - 100°C
FeSO4	7	9	0.389	0.224	8.9	No	-32	-32	< 50°C
Ni3(AsO4)2	0	1	0.433	0.096	3.6	No	37	37	< 50°C
PbHPO4	3	4	0.416	0.128	8.4	No	57	57	50°C - 100°C
Sn(H2PO4)2	1	2	0.404	0.156	7.0	No	99	99	50°C - 100°C
Ca(ClO4)2	8	9	0.384	0.198	9.5	No	272	272	200°C - 300°C
PbHAsO4	3	4	0.413	0.121	6.8	No	75	75	50°C - 100°C
Mg(ClO4)2	4	5	0.375	0.198	5.2	No	152	152	100°C - 200°C
La(IO3)3	0	1	0.407	0.092	0.0	No	155	155	100°C - 200°C
Ca(IO3)2	1	2	0.401	0.107	7.3	No	38	38	< 50°C
Zn3(PO4)2	7	8	0.384	0.140	7.4	No	235	235	200°C - 300°C
Co3(AsO4)2	7	8	0.386	0.124	6.7	No	235	235	200°C - 300°C
Ba(ClO4)2	3	4	0.359	0.147	1.7	No	139	139	100°C - 200°C
Ba(IO3)2	1	2	0.375	0.094	8.1	No	64	64	50°C - 100°C
Pb(H2PO4)2	1	2	0.367	0.114	1.4	No	69	69	50°C - 100°C
Fe(IO3)3	8	9	0.364	0.120	8.2	No	339	339	300°C - 450°C
Al(IO3)3	8	9	0.359	0.126	7.6	No	344	344	300°C - 450°C
Sn(H2PO4)2	0	1	0.352	0.132	7.0	No	26	26	< 50°C
Ni(ClO4)2	5	6	0.327	0.161	0.0	No	130	130	100°C - 200°C
LiClO4	3	4	0.298	0.208	9.8	No	-19	-19	< 50°C
MgCO3	5	6	0.310	0.188	7.4	No	-26	-26	< 50°C
La(IO3)3	1	2	0.350	0.080	0.0	No	109	109	100°C - 200°C
Co2As2O7	1	2	0.343	0.089	9.9	No	-20	-20	< 50°C
Mg(ClO4)2	7	8	0.307	0.168	3.4	No	149	149	100°C - 200°C
Mg(ClO4)2	5	6	0.313	0.154	1.4	No	77	77	50°C - 100°C
Mn3(AsO4)2	7	8	0.327	0.118	3.4	No	202	202	200°C - 300°C
Sr(H2PO4)2	1	2	0.301	0.129	6.3	No	8	8	< 50°C
MnCO3	5	6	0.286	0.153	8.2	No	-40	-40	< 50°C
Ca(ClO4)2	6	7	0.282	0.155	9.8	No	115	115	100°C - 200°C
Sr3(AsO4)2	1	2	0.288	0.077	9.6	No	32	32	< 50°C
Ca3(PO4)2	10	11	0.261	0.129	2.5	No	175	175	100°C - 200°C
Ba3(PO4)2	10	11	0.270	0.097	5.0	No	260	260	200°C - 300°C
Ni(ClO4)2	6	7	0.255	0.127	0.5	No	62	62	50°C - 100°C
Mg(ClO4)2	6	7	0.242	0.135	3.4	No	49	49	< 50°C
Ba(ClO4)2	5	6	0.247	0.113	8.3	No	70	70	50°C - 100°C
Ca(ClO4)2	5	6	0.240	0.122	9.8	No	18	18	< 50°C
Ba(ClO4)2	4	5	0.242	0.100	6.9	No	20	20	< 50°C

Ca(ClO4)2	4	5	0.230	0.118	7.4	No	-7	-7	< 50°C
Ba3(AsO4)2	10	11	0.245	0.084	3.7	No	236	236	200°C - 300°C
Sr3(AsO4)2	10	11	0.233	0.090	1.1	No	180	180	100°C - 200°C
Ca(ClO4)2	7	8	0.205	0.116	9.5	No	31	31	< 50°C
Sr3(PO4)2	10	11	0.214	0.088	0.0	No	119	119	100°C - 200°C
Ni(ClO4)2	7	8	0.205	0.106	1.4	No	19	19	< 50°C
La(IO3)3	8	9	0.182	0.063	9.8	No	82	82	50°C - 100°C

Appendix F. Mixed Metal Salt Hydrate Templates from the ICSD

Table F.1 List of 311 mixed metal salt hydrates extracted from the Inorganic Crystal Structure Database (ICSD).[103]

Ag2SrI4*8H2O	CdSb2F12*6H2O	CuSiF6*4H2O	LaRb3Cl6*2H2O
AgMnF4*4H2O	CdSn2F6*6H2O	CuSiF6*6H2O	LaRbCl4*4H2O
AgNaI2*3H2O	CdSrI4*8H2O	CuTiF6*4H2O	LaTh4F19*H2O
AgSbF6*2H2O	CdTa6Br16*18H2O	CuZrF6*4H2O	Li2SnF6*2H2O
Al2MgF8*2H2O	Ce2CsF9*H2O	Er2ThF10*H2O	Li2TiF6*2H2O
Al3K3F12*2H2O	CoCsCl3*2H2O	Fe2Sr2F10*H2O	Li2ZnCl4*2H2O
Al3K3F12*H2O	CoGeF6*6H2O	FeGeF6*6H2O	Li3RuCl6*12H2O
AlCa2F7*H2O	CoMgCl4*8H2O	FeHgF5*2H2O	LiMgCl3*7H2O
AlCoF5*7H2O	CoNp2F10*8H2O	FeK2Cl5*H2O	LiMnF4*H2O
AlCsF4*2H2O	CoNpF6*3H2O	FeK2F5*H2O	Mg2MnCl6*12H2O
AlHg2F5*2H2O	CoRbCl3*2H2O	FeMnF5*2H2O	MgMn2Br6*12H2O
AlK2F5*H2O	CoSiF6*6H2O	FeMnF5*7H2O	MgRbBr3*6H2O
AlMgF5*2H2O	CoSn2F6*6H2O	FePtCl6*6H2O	MgRbCl3*6H2O
AlPb3F9*H2O	CoSnF6*6H2O	FeRb2Cl5*H2O	MgSiF6*6H2O
AlRb2F5*H2O	Cr2Cu3F12*12H2O	FeRb2F5*H2O	MgTeBr6*6H2O
AlRuCl6*10H2O	CrCs2Cl5*4H2O	FeSbCl8*8H2O	MgTeCl6*6H2O
AlTl2F5*H2O	CrCs2Cl5*H2O	FeSiF6*6H2O	MgTeI6*6H2O
AlZnF5*2H2O	CrK2Cl5*H2O	FeSnF6*6H2O	MgZn2Br6*6H2O
AlZnF5*7H2O	CrK2F5*H2O	FeZnF5*2H2O	MgZnBr4*7H2O
Au2ZnCl8*2H2O	CrRb2Cl5*H2O	GaMnF5*2H2O	MgZnCl4*6H2O
AuKBr4*2H2O	CrRb2F5*H2O	GeMgF6*6H2O	MgZrF6*2H2O
AuKCl4*2H2O	CrSiF6*4H2O	GeNiF6*6H2O	MgZrF6*5H2O
AuNaBr4*2H2O	CrSiF6*6H2O	GeZnF6*6H2O	Mn2ZrF8*6H2O
AuNaCl4*2H2O	CrTl2F5*H2O	Hf3K5F17*H2O	MnNaF4*3H2O
Ba7Fe6F32*2H2O	Cs12Pd9Cl30*2H2O	HfKF5*H2O	MnRb2Cl4*2H2O
BaCd2Cl6*5H2O	Cs2EuBr5*10H2O	HfNiF6*6H2O	MnRb2F5*H2O
BaCdCl4*4H2O	Cs2FeCl5*H2O	Hg2SiF6*2H2O	MnRbCl3*2H2O
BaFeF5*H2O	Cs2FeF5*H2O	Hg3MgCl8*6H2O	MnRbF4*H2O
BaGaF5*2H2O	Cs2Hg3I8*H2O	HgK2Cl4*H2O	MnSb2F8*2H2O
BaMnF5*H2O	Cs2InCl5*H2O	HgK2I4*3H2O	MnSiF6*6H2O
BaZr2F10*2H2O	Cs2IrCl5*H2O	HgKBr3*H2O	MnSrF5*H2O
BeCuF4*5H2O	Cs2MnCl4*2H2O	HgKI3*H2O	MnTiF6*6H2O

Bi2MgI8*8H2O	Cs2MnF5*H2O	HgNaCl3*2H2O	MnTl2F5*H2O
Bi2MnI8*8H2O	Cs2Mo6Cl14*3H2O	HgNb6Br16*18H2O	MnTlF4*H2O
Bi3Na7Br16*18H2O	Cs2Re2Cl8*H2O	HgSrI4*8H2O	MnVF5*2H2O
BiK2Br5*2H2O	Cs2RhCl5*H2O	HgTa6Br16*18H2O	MnZnBr4*6H2O
BiK2Cl5*2H2O	Cs2RuCl5*H2O	InK2Br5*H2O	MnZrF6*5H2O
BiKI4*H2O	Cs2TiCl5*4H2O	InK2Cl5*H2O	Mo6Rb2Cl14*H2O
BiLaI6*13H2O	Cs2TiF5*H2O	InK3Cl6*H2O	Na2PtCl6*6H2O
BiLiI4*5H2O	Cs2TlCl5*H2O	InKBr4*2H2O	Na2ReCl6*6H2O
BiRb5I10*2H2O	Cs2VBr5*4H2O	InRb2Cl5*H2O	Na2TeBr6*6H2O
BiSrBr5*8H2O	Cs2VCl5*4H2O	InRbF4*2H2O	Na2ZnCl4*3H2O
Ca2Cd3Cl10*18H2O	Cs3Cu2Cl7*2H2O	InZnF5*7H2O	Na3TlCl6*12H2O
Ca2CdBr6*12H2O	Cs3FeCl6*H2O	IrK2Cl5*H2O	NaNiF3*3H2O
Ca2CdCl6*12H2O	Cs3LaCl6*3H2O	IrK3Cl6*H2O	NaSb2F7*H2O
Ca2Hg11Cl26*16H2O	Cs3VCl6*4H2O	IrRb3Br6*H2O	NaZnBr3*5H2O
CaCd2Br6*7H2O	Cs5PuCl8*6H2O	IrSrF6*2H2O	NiSb2F8*6H2O
CaCd2Cl6*6H2O	Cs5Zr4F21*3H2O	K2MnCl4*2H2O	NiSiF6*6H2O
CaCdI4*8H2O	Cs6Hf5F26*4H2O	K2MnF5*H2O	NiSn2F6*6H2O
CaCs2Cl4*2H2O	Cs6Pd5Cl16*2H2O	K2Mo6Cl14*H2O	NiSnCl6*6H2O
CaHgBr4*8H2O	CsInF4*2H2O	K2MoCl4*H2O	NiSnF6*6H2O
CaHgI4*8H2O	CsLaCl4*3H2O	K2PbBr4*H2O	NiTiF6*6H2O
CaIrF6*2H2O	CsMgBr3*6H2O	K2PtBr4*2H2O	NiZrF6*6H2O
CaMg2Cl6*12H2O	CsMgCl3*6H2O	K2PtI4*2H2O	Pb2SrBr6*5H2O
CaMnBr4*8H2O	CsMnCl3*2H2O	K2PtI5*2H2O	Pb2SrI6*7H2O
CaSiF6*2H2O	CsMnF4*2H2O	K2RhCl5*H2O	PbSiF6*2H2O
CaTlCl5*7H2O	CsNa2Cl3*2H2O	K2RuCl5*H2O	PdSb2F12*8H2O
CaZn2Br6*6H2O	CsNdCl4*4H2O	K2SnCl4*H2O	PtRb2Br4*H2O
CaZnBr4*5H2O	CsPuCl4*4H2O	K2SnF6*H2O	PtRb2I5*2H2O
Cd2MgCl6*12H2O	CsTa6Br15*12H2O	K2TlCl5*2H2O	PtSb2F12*4H2O
Cd2NiCl6*12H2O	CsUCl4*3H2O	K3Pb3Cl9*H2O	Rb2TiF5*H2O
Cd2SrBr6*8H2O	CsZrF5*H2O	K3RhCl6*H2O	Rb2TlCl5*H2O
Cd2SrCl6*8H2O	Cu18Rb11Cl30*2H2O	K3Tc2Cl8*2H2O	Rb2VF5*H2O
Cd2ZrF8*6H2O	Cu2Rb2I4*H2O	K3TlCl6*2H2O	RbTlBr4*H2O
Cd3KCl7*4H2O	Cu2ZrF8*12H2O	KCl2I*H2O	RbTlI4*2H2O
Cd3YbCl9*15H2O	Cu3Fe2F12*12H2O	KMgCl3*6H2O	RbVF4*2H2O
Cd4CeCl11*13H2O	Cu3Mn2F12*12H2O	KMnCl3*2H2O	SiSrF6*2H2O
Cd4NiCl10*10H2O	Cu3SmCl3*6H2O	KMnF4*H2O	SiZnF6*6H2O
CdCsI3*H2O	Cu3V2F12*12H2O	KPbBr3*H2O	Sn2SrBr6*5H2O
CdCuCl4*4H2O	Cu3Zr2F14*16H2O	KPbI3*2H2O	Sn2SrCl6*5H2O
CdGaF5*7H2O	CuFe2F8*2H2O	KReCl4*H2O	Sn2ZnF6*6H2O
CdKCl3*H2O	CuIn2F8*10H2O	KTlBr4*2H2O	SrTiF6*2H2O

CdMg2Br6*12H2O	CuK2Cl4*2H2O	KYb3F10*H2O	Ta6ZnBr16*18H2O
CdMg2Cl6*12H2O	CuLiCl3*2H2O	KZnBr3*2H2O	Tc2YCl8*9H2O
CdNa2Cl4*3H2O	CuNaI2*4H2O	KZnCl3*2H2O	TiZnF6*6H2O
CdNb6Br16*18H2O	CuNp2F10*6H2O	KZnCl3*H2O	Tl2VF5*H2O
CdNi2Cl6*12H2O	CuRb2Cl4*2H2O	KZnI3*2H2O	Zn2ZrF8*12H2O
CdRbI3*H2O	CuSb2F8*6H2O	KZrF5*H2O	

Bibliography

(1) Lawrence Livermore National Laboratory. *Estimated U.S. Energy Consumption in 2019: 100.2 Quads*; Livermore, CA. https://flowcharts.llnl.gov/ (Accessed on 18 January 2021), 2020.

(2) Tatsidjodoung, P.; Le Pierrès, N.; Luo, L. A Review of Potential Materials for Thermal Energy Storage in Building Applications. *Renew. Sustain. Energy Rev.* **2013**, *18*, 327–349. https://doi.org/10.1016/j.rser.2012.10.025.

(3) N'Tsoukpoe, K. E.; Schmidt, T.; Rammelberg, H. U.; Watts, B. A.; Ruck, W. K. L. A Systematic Multi-Step Screening of Numerous Salt Hydrates for Low Temperature Thermochemical Energy Storage. *Appl. Energy* **2014**, *124*, 1–16. https://doi.org/10.1016/j.apenergy.2014.02.053.

(4) Sharma, A.; Tyagi, V. V.; Chen, C. R.; Buddhi, D. Review on Thermal Energy Storage with Phase Change Materials and Applications. *Renew. Sustain. Energy Rev.* **2009**, *13* (2), 318–345. https://doi.org/10.1016/j.rser.2007.10.005.

(5) Sun, Y.; Wang, S.; Xiao, F.; Gao, D. Peak Load Shifting Control Using Different Cold Thermal Energy Storage Facilities in Commercial Buildings: A Review. *Energy Convers. Manag.* **2013**, *71*, 101–114. https://doi.org/10.1016/j.enconman.2013.03.026.

(6) Pielichowska, K.; Pielichowski, K. Phase Change Materials for Thermal Energy Storage. *Prog. Mater. Sci.* **2014**, *65* (0), 67–123. https://doi.org/10.1016/j.pmatsci.2014.03.005.

(7) Mondal, S. Phase Change Materials for Smart Textiles – An Overview. *Appl. Therm. Eng.* **2008**, *28*, 1536–1550. https://doi.org/10.1016/j.applthermaleng.2007.08.009.

(8) Sharma, R. K.; Ganesan, P.; Tyagi, V. V.; Metselaar, H. S. C.; Sandaran, S. C. Developments in Organic Solid–Liquid Phase Change Materials and Their Applications in Thermal Energy Storage. *Energy Convers. Manag.* **2015**, *95*, 193–228. https://doi.org/10.1016/j.enconman.2015.01.084.

(9) Krishnan, S.; Garimella, S. V. Thermal Management of Transient Power Spikes in Electronics - Phase Change Energy Storage or Copper Heat Sinks? In *International Electronic Packaging Technical Conference and Exhibition*; Maui, Hawaii, 2003; pp 1–12.

(10) Fleming, E.; Wen, S.; Shi, L.; Da Silva, A. K. Thermodynamic Model of a Thermal Storage Air Conditioning System with Dynamic Behavior. *Appl. Energy* **2013**, *112*, 160–169. https://doi.org/10.1016/j.apenergy.2013.05.058.

(11) Narayanan, S.; Li, X.; Yang, S.; Kim, H.; Umans, A.; McKay, I. S.; Wang, E. N. Thermal Battery for Portable Climate Control. *Appl. Energy* **2015**, *149*, 104–116. https://doi.org/10.1016/j.apenergy.2015.03.101.

(12) Kato, Y.; Takahashi, R.; Sekiguchi, T.; Ryu, J. Study on Medium-Temperature Chemical Heat Storage Using Mixed Hydroxides. *Int. J. Refrig.* **2009**, *32* (4), 661–666. https://doi.org/10.1016/j.ijrefrig.2009.01.032.

(13) Myagmarjav, O.; Ryu, J.; Kato, Y. Waste Heat Recovery from Iron Production by Using Magnesium Oxide / Water Chemical Heat Pump as Thermal Energy Storage. *ISIJ Int.* **2015**,

55 (2), 464–472. https://doi.org/http://dx.doi.org/10.2355/isijinternational.55.464.
(14) Pardo, P.; Deydier, A.; Anxionnaz-Minvielle, Z.; Rougé, S.; Cabassud, M.; Cognet, P. A Review on High Temperature Thermochemical Heat Energy Storage. *Renew. Sustain. Energy Rev.* **2014**, *32*, 591–610. https://doi.org/10.1016/j.rser.2013.12.014.
(15) N'Tsoukpoe, K. E.; Liu, H.; Le Pierrès, N.; Luo, L. A Review on Long-Term Sorption Solar Energy Storage. *Renew. Sustain. Energy Rev.* **2009**, *13* (9), 2385–2396. https://doi.org/10.1016/j.rser.2009.05.008.
(16) Tian, Y.; Zhao, C. Y. A Review of Solar Collectors and Thermal Energy Storage in Solar Thermal Applications. *Appl. Energy* **2013**, *104*, 538–553. https://doi.org/10.1016/j.apenergy.2012.11.051.
(17) Odukomaiya, A.; Woods, J.; James, N.; Kaur, S.; Gluesenkamp, K. R.; Kumar, N.; Mumme, S.; Jackson, R.; Prasher, R. Addressing Energy Storage Needs at Lower Cost via On-Site Thermal Energy Storage in Buildings. *Energy Environ. Sci.* **2021**, *14* (10), 5315–5329. https://doi.org/10.1039/d1ee01992a.
(18) Aftab, W.; Usman, A.; Shi, J.; Yuan, K.; Qin, M.; Zou, R. Phase Change Material-Integrated Latent Heat Storage Systems for Sustainable Energy Solutions. *Energy Environ. Sci.* **2021**, *14* (8), 4268–4291. https://doi.org/10.1039/d1ee00527h.
(19) Chen, X.; Gao, H.; Tang, Z.; Dong, W.; Li, A.; Wang, G. Optimization Strategies of Composite Phase Change Materials for Thermal Energy Storage, Transfer, Conversion and Utilization. *Energy Environ. Sci.* **2020**, *13* (12), 4498–4535. https://doi.org/10.1039/d0ee01355b.
(20) Arce, P.; Medrano, M.; Gil, A.; Oró, E.; Cabeza, L. F. Overview of Thermal Energy Storage (TES) Potential Energy Savings and Climate Change Mitigation in Spain and Europe. *Appl. Energy* **2011**, *88*, 2764–2774. https://doi.org/10.1016/j.apenergy.2011.01.067.
(21) DeForest, N.; Mendes, G.; Stadler, M.; Feng, W.; Lai, J.; Marnay, C. Optimal Deployment of Thermal Energy Storage under Diverse Economic and Climate Conditions. *Appl. Energy* **2014**, *119*, 488–496. https://doi.org/10.1016/j.apenergy.2014.01.047.
(22) Wagner, S. J.; Rubin, E. S. Economic Implications of Thermal Energy Storage for Concentrated Solar Thermal Power. *Renew. Energy* **2014**, *61*, 81–95. https://doi.org/10.1016/j.renene.2012.08.013.
(23) Henry, A.; Prasher, R.; Majumdar, A. Five Thermal Energy Grand Challenges for Decarbonization. *Nature Energy*. Nature Research September 2020, pp 635–637. https://doi.org/10.1038/s41560-020-0675-9.
(24) Wang, Q.; Wu, R.; Wu, Y.; Zhao, C. Y. Parametric Analysis of Using PCM Walls for Heating Loads Reduction. *Energy Build.* **2018**, *172*, 328–336. https://doi.org/10.1016/j.enbuild.2018.05.012.
(25) Coldchain Technology Services. Greenbox https://coldchain-tech.com/consulting/thermal-systems/greenbox.html (accessed Sep 16, 2021).
(26) Jankowski, N. R.; McCluskey, F. P. A Review of Phase Change Materials for Vehicle Component Thermal Buffering. *Appl. Energy* **2014**, *113*, 1525–1561. https://doi.org/10.1016/j.apenergy.2013.08.026.
(27) Gumus, M. Reducing Cold-Start Emission from Internal Combustion Engines by Means of Thermal Energy Storage System. *Appl. Therm. Eng.* **2009**, *29* (4), 652–660. https://doi.org/10.1016/j.applthermaleng.2008.03.044.
(28) Romaní, J.; Gasia, J.; Solé, A.; Takasu, H.; Kato, Y.; Cabeza, L. F. Evaluation of Energy Density as Performance Indicator for Thermal Energy Storage at Material and System

Levels. *Appl. Energy* **2019**, *235*, 954–962. https://doi.org/10.1016/j.apenergy.2018.11.029.
(29) Zalba, B.; Marín, J. M.; Cabeza, L. F.; Mehling, H. Review on Thermal Energy Storage with Phase Change: Materials, Heat Transfer Analysis and Applications. *Appl. Therm. Eng.* **2003**, *23* (3), 251–283. https://doi.org/10.1016/S1359-4311(02)00192-8.
(30) Aydin, D.; Casey, S. P.; Riffat, S. The Latest Advancements on Thermochemical Heat Storage Systems. *Renew. Sustain. Energy Rev.* **2015**, *41*, 356–367. https://doi.org/10.1016/j.rser.2014.08.054.
(31) Herrmann, U.; Kearney, D. W. Survey of Thermal Energy Storage for Parabolic Trough Power Plants. *J. Sol. Energy Eng.* **2002**, *124* (2), 145–152. https://doi.org/10.1115/1.1467601.
(32) van Essen, V. M.; Cot Gores, J.; Bleijendaal, L. P. J.; Zondag, H. a.; Schuitema, R.; Bakker, M.; van Helden, W. G. J. Characterization of Salt Hydrates for Compact Seasonal Thermochemical Storage. *ASME 2009 3rd Int. Conf. Energy Sustain. Vol. 2* **2009**, *2*, 825–830. https://doi.org/10.1115/ES2009-90289.
(33) Wentworth, W. E.; Chen, E. Simple Thermal Decomposition Reactions for Storage of Solar Thermal Energy. *Sol. Energy* **1976**, *18*, 205–214. https://doi.org/https://doi.org/10.1016/0038-092X(76)90019-0.
(34) Garg, H. P.; Mullick, S. C.; Bhargava, A. K. Chemical Energy Storage. In *Solar Thermal Energy Storage*; D. Reidel Publishing Company: Dordrecht, Holland, 1985; pp 292–427.
(35) Deutsch, M.; Müller, D.; Aumeyr, C.; Jordan, C.; Gierl-mayer, C.; Weinberger, P.; Winter, F.; Werner, A. Systematic Search Algorithm for Potential Thermochemical Energy Storage Systems. *Appl. Energy* **2016**, *183*, 113–120. https://doi.org/10.1016/j.apenergy.2016.08.142.
(36) Visscher, K.; Veldhuis, J. B. J.; Oonk, H. a. J.; Ekeren, P. J. Van; Blok, J. G. *Compact Chemical Seasonal Storage of Solar Heat*; 2004.
(37) Kiyabu, S.; Lowe, J. S.; Ahmed, A.; Siegel, D. J. Computational Screening of Hydration Reactions for Thermal Energy Storage: New Materials and Design Rules. *Chem. Mater.* **2018**, *30* (6). https://doi.org/10.1021/acs.chemmater.7b05230.
(38) Sögütoglu, L. C.; Donkers, P. A. J.; Fischer, H. R.; Huinink, H. P.; Adan, O. C. G. In-Depth Investigation of Thermochemical Performance in a Heat Battery: Cyclic Analysis of K2CO3 , MgCl2 and Na2S. *Appl. Energy* **2018**, *215*, 159–173. https://doi.org/10.1016/j.apenergy.2018.01.083.
(39) Gaeini, M.; Shaik, S. A.; Rindt, C. C. M. Characterization of Potassium Carbonate Salt Hydrate for Thermochemical Energy Storage in Buildings. *Energy Build.* **2019**, *196*, 178–193. https://doi.org/10.1016/j.enbuild.2019.05.029.
(40) Müller, D.; Knoll, C.; Gravogl, G.; Jordan, C.; Eitenberger, E.; Friedbacher, G.; Artner, W.; Welch, J. M.; Werner, A.; Harasek, M.; Miletich, R.; Weinberger, P. Medium-Temperature Thermochemical Energy Storage with Transition Metal Ammoniates – A Systematic Material Comparison. *Appl. Energy* **2021**, *285*, 116470. https://doi.org/10.1016/j.apenergy.2021.116470.
(41) Yan, T.; Wang, R. Z.; Li, T. X. Experimental Investigation on Thermochemical Heat Storage Using Manganese Chloride/Ammonia. *Energy* **2018**, *143*, 562–574. https://doi.org/10.1016/j.energy.2017.11.030.
(42) Neumann, K.; Wiegand, M.; Opel, O.; Korhammer, K. Solid Sorption Refrigeration With Calcium Chloride Methanolates on Technical Scale. *Proc. 14th Int. Renew. Energy Storage Conf. 2020 (IRES 2020)* **2021**, *6*, 142–149. https://doi.org/10.2991/ahe.k.210202.022.

(43) Korhammer, K.; Neumann, K.; Opel, O.; Ruck, W. K. L. Thermodynamic and Kinetic Study of CaCl2-CH3OH Adducts for Solid Sorption Refrigeration by TGA/DSC. *Appl. Energy* **2018**, *230*, 1255–1278. https://doi.org/10.1016/j.apenergy.2018.08.100.
(44) Deshmukh, H.; Maiya, M. P.; Srinivasa Murthy, S. Study of Sorption Based Energy Storage System with Silica Gel for Heating Application. *Appl. Therm. Eng.* **2017**, *111*, 1640–1646. https://doi.org/10.1016/j.applthermaleng.2016.07.069.
(45) Johannes, K.; Kuznik, F.; Hubert, J.-L.; Durier, F.; Obrecht, C. Design and Characterisation of a High Powered Energy Dense Zeolite Thermal Energy Storage System for Buildings. *Appl. Energy* **2015**, *159*, 80–86. https://doi.org/10.1016/j.apenergy.2015.08.109.
(46) Ehrenmann, J.; Henninger, S. K.; Janiak, C. Water Adsorption Characteristics of MIL-101 for Heat-Transformation Applications of MOFs. *Eur. J. Inorg. Chem.* **2011**, No. 4, 471–474. https://doi.org/10.1002/ejic.201001156.
(47) Yu, N.; Wang, R. Z.; Lu, Z. S.; Wang, L. W.; Ishugah, T. F. Evaluation of a Three-Phase Sorption Cycle for Thermal Energy Storage. *Energy* **2014**, *67*, 468–478. https://doi.org/10.1016/j.energy.2013.12.044.
(48) Zhang, X.; Li, M.; Shi, W.; Wang, B.; Li, X. Experimental Investigation on Charging and Discharging Performance of Absorption Thermal Energy Storage System. *Energy Convers. Manag.* **2014**, *85*, 425–434. https://doi.org/10.1016/j.enconman.2014.05.100.
(49) Cuypers, R.; Anastasopol, A.; De Jong, A.-J.; Oversloot, H.; Van Vliet, L.; Bodis, P.; Hoegaerts, C. A Novel Heat Battery to Save Energy & Reduce CO2 Production. In *International Solar Energy Society*; Palma de Mallorca, Spain, 2016; pp 1–7. https://doi.org/10.18086/eurosun.2016.03.08.
(50) Sharma, R.; Anil Kumar, E.; Dutta, P.; Srinivasa Murthy, S.; Aristov, Y. I.; Tokrev, M. M.; Li, T. X.; Wang, R. Z. Ammoniated Salt Based Solid Sorption Thermal Batteries: A Comparative Study. *Appl. Therm. Eng.* **2021**, *191*, 116875. https://doi.org/10.1016/j.applthermaleng.2021.116875.
(51) Critoph, R. E. Performance Limitations of Adsorption Cycles for Solar Cooling. *Sol. Energy* **1988**, *41* (1), 21–31.
(52) Vasta, S.; Brancato, V.; La Rosa, D.; Palomba, V.; Restuccia, G.; Sapienza, A.; Frazzica, A. Adsorption Heat Storage: State-of-the-Art and Future Perspectives. *Nanomater. (Basel, Switzerland)* **2018**, *8* (7), 522. https://doi.org/10.3390/nano8070522.
(53) Burtch, N. C.; Jasuja, H.; Walton, K. S. Water Stability and Adsorption in Metal–Organic Frameworks. *Chem. Rev.* **2014**, *114* (20), 10575–10612. https://doi.org/10.1021/cr5002589.
(54) Smeets, B.; Iype, E.; Nedea, S. V.; Zondag, H. a.; Rindt, C. C. M. A DFT Based Equilibrium Study on the Hydrolysis and the Dehydration Reactions of MgCl2 Hydrates. *J. Chem. Phys.* **2013**, *139* (12), 124312. https://doi.org/10.1063/1.4822001.
(55) Donkers, P. A. J.; Sögütoglu, L. C.; Huinink, H. P.; Fischer, H. R.; Adan, O. C. G. A Review of Salt Hydrates for Seasonal Heat Storage in Domestic Applications. *Appl. Energy* **2017**, *199*, 45–68. https://doi.org/10.1016/j.apenergy.2017.04.080.
(56) Weck, P. F.; Kim, E. Solar Energy Storage in Phase Change Materials: First-Principles Thermodynamic Modeling of Magnesium Chloride Hydrates. *J. Phys. Chem. C* **2014**, *118* (9), 4618–4625. https://doi.org/10.1021/jp411461m.
(57) Glasser, L.; Jones, F. Systematic Thermodynamics of Hydration (and of Solvation) of Inorganic Solids. *Inorg. Chem.* **2009**, *48* (4), 1661–1665. https://doi.org/10.1021/ic802101g.
(58) Mercury, L.; Vieillard, P.; Tardy, Y. Thermodynamics of Ice Polymorphs and “ice-like”

Water in Hydrates and Hydroxides. *Appl. Geochemistry* **2001**, *16*, 161–181.
(59) Shkatulov, A.; Aristov, Y. Modification of Magnesium and Calcium Hydroxides with Salts: An Efficient Way to Advanced Materials for Storage of Middle-Temperature Heat. *Energy* **2015**, *85*, 667–676. https://doi.org/10.1016/j.energy.2015.04.004.
(60) Dicaire, D.; Tezel, F. H. Use of Adsorbents for Thermal Energy Storage of Solar or Excess Heat: Improvement of Energy Density. *Int. J. Energy Res.* **2013**, *37*, 1059–1068. https://doi.org/10.1002/er.
(61) Hongois, S.; Kuznik, F.; Stevens, P.; Roux, J.-J. Developement and Characterisation of a New MgSO4-Zeolite Composite for Long-Term Thermal Energy Storage. *Sol. Energy Mater. Sol. Cells* **2011**, *95*, 1831–1837.
(62) Lefebvre, D.; Tezel, F. H. A Review of Energy Storage Technologies with a Focus on Adsorption Thermal Energy Storage Processes for Heating Applications. *Renew. Sustain. Energy Rev.* **2017**, *67*, 116–125. https://doi.org/10.1016/j.rser.2016.08.019.
(63) Henninger, S. K.; Habib, H. A.; Janiak, C. MOFs as Adsorbents for Low Temperature Heating and Cooling Applications. *J. Am. Chem. Soc.* **2009**, *131* (8), 2776–2777. https://doi.org/10.1021/ja808444z.
(64) Wickenheisser, M.; Janiak, C. Hierarchical Embedding of Micro-Mesoporous MIL-101(Cr) in Macroporous Poly(2-Hydroxyethyl Methacrylate) High Internal Phase Emulsions with Monolithic Shape for Vapor Adsorption Applications. *Microporous Mesoporous Mater.* **2015**, *204*, 242–250. https://doi.org/10.1016/j.micromeso.2014.11.025.
(65) Elsayed, A.; Elsayed, E.; Al-dadah, R.; Mahmoud, S.; Elshaer, A.; Kaialy, W. Thermal Energy Storage Using Metal – Organic Framework Materials. *Appl. Energy* **2017**, *186*, 509–519. https://doi.org/10.1016/j.apenergy.2016.03.113.
(66) Roine, A. HSC Chemistry 7.0. Outotec 2006.
(67) Glasser, L. Thermodynamics of Inorganic Hydration and of Humidity Control, with an Extensive Database of Salt Hydrate Pairs. *J. Chem. Eng. Data* **2014**, *59* (2), 526–530. https://doi.org/10.1021/je401077x.
(68) West, C. J.; Washburn, E. W.; Dorsey, N. E.; National Research Council (U.S.); National Academy of Sciences (U.S.); International Research Council; Knovel. *International Critical Tables of Numerical Data, Physics, Chemistry, and Technology*, 1st electr.; Knovel: Norwich, NY, 2003.
(69) Richter, M.; Habermann, E.-M.; Siebecke, E.; Linder, M. A Systematic Screening of Salt Hydrates as Materials for a Thermochemical Heat Transformer. *Thermochim. Acta* **2018**, *659*, 136–150. https://doi.org/10.1016/j.tca.2017.06.011.
(70) Wagmen, D. D.; Evans, W. H. The NBS Tables of Chemical Thermodynamic Properties. *J. Phys. Chem. Ref. Data* **1982**, *11*.
(71) Patnaik, P. *Handbook of Inorganic Chemicals*; McGraw-Hill: New York, 2003.
(72) Vieillard, P.; Tardy, Y. Thermochemical Properties of Phosphates. In *Phosphate Minerals*; Nriagu, J. O., Moore, P. B., Eds.; Springer-Verlag Berlin Heidelberg, 1984; pp 171–198.
(73) Afflerbach, S.; Trettin, R. A Systematic Screening Approach for New Materials for Thermochemical Energy Storage and Conversion Based on the Strunz Mineral Classification System. *Thermochim. Acta* **2019**, *674*, 82–94. https://doi.org/10.1016/j.tca.2019.02.010.
(74) Clark, R.-J.; Gholamibozanjani, G.; Woods, J.; Kaur, S.; Odukomaiya, A.; Al-Hallaj, S.; Farid, M. Experimental Screening of Salt Hydrates for Thermochemical Energy Storage for Building Heating Application. *J. Energy Storage* **2022**, *51*, 104415.

https://doi.org/10.1016/j.est.2022.104415.
(75) Jenkins, H. D. B.; Glasser, L. Ionic Hydrates , MpXq•nH2O: Lattice Energy and Standard Enthalpy of Formation Estimation. *Inorg. Chem.* **2002**, *41* (17), 4378–4388.
(76) Jenkins, H. D. B.; Glasser, L. Difference Rule - A New Thermodynamic Principle: Prediction of Standard Thermodynamic Data for Inorganic Solvates. *J. Am. Chem. Soc.* **2004**, *126*, 15809–15817.
(77) Glasser, L.; Jenkins, H. D. B. The Thermodynamic Solvate Difference Rule: Solvation Parameters and Their Use in Interpretation of the Role of Bound Solvent in Condensed-Phase Solvates. *Inorg. Chem.* **2007**, *46* (23), 9768–9778.
(78) Born, M.; Oppenheimer, R. Zur Quantentheorie Der Molekeln. *Ann. Phys.* **1927**, *389* (20), 457–484.
(79) Sholl, D. S.; Steckel, J. A. What Is Density Functional Theory? In *Density Functional Theory A Practical Introduction*; John Wiley & Sons Inc.: Hoboken, New Jersey, 2009; pp 1–34.
(80) Hohenberg, P.; Kohn, W. Inhomogeneous Electron Gas. *Phys. Rev.* **1964**, *136* (3B), B864–B871. https://doi.org/https://doi.org/10.1103/PhysRev.136.B864.
(81) Kohn, W.; Sham, L. J. Self-Consistent Equations Including Exchange and Correlation Effects. *Phys. Rev.* **1965**, *140* (4A), A1133–A1138.
(82) Perdew, J. P.; Burke, K.; Ernzerhof, M. Generalized Gradient Approximation Made Simple. *Phys. Rev. Lett.* **1996**, *77* (18), 3865–3868.
(83) Perdew, J. P.; Wang, Y. Accurate and Simple Analytic Representation of the Electron-Gas Correlation Energy. *Phys. Rev. B* **1992**, *45* (23), 244–249.
(84) Dion, M.; Rydberg, H.; Schröder, E.; Langreth, D. C.; Lundqvist, B. I. Van Der Waals Density Functional for General Geometries. *Phys. Rev. Lett.* **2004**, *92*, 246401. https://doi.org/10.1103/PhysRevLett.92.246401.
(85) Klimeš, J.; Bowler, D. R.; Michaelides, A. Chemical Accuracy for the van Der Waals Density Functional. *J. Phys. Condens. Matter* **2010**, *22*, 022201.
(86) Román-Pérez, G.; Soler, J. M. Efficient Implementation of a van Der Waals Density Functional : Application to Double-Wall Carbon Nanotubes. *Phys. Rev. Lett.* **2009**, *103*, 096102. https://doi.org/10.1103/PhysRevLett.103.096102.
(87) Lee, K.; Murray, É. D.; Kong, L.; Lundqvist, B. I.; Langreth, D. C. Higher-Accuracy van Der Waals Density Functional. *Phys. Rev. B* **2010**, *82*, 081101.
(88) Klimeš, J.; Bowler, D. R.; Michaelides, A. Van Der Waals Density Functionals Applied to Solids. *Phys. Rev. B* **2011**, *83*, 195131.
(89) Thonhauser, T.; Cooper, V. R.; Li, S.; Puzder, A.; Hyldgaard, P.; Langreth, D. C. Van Der Waals Density Functional: Self-Consistent Potential and the Nature of the van Der Waals Bond. *Phys. Rev. B* **2007**, *76*, 125112. https://doi.org/10.1103/PhysRevB.76.125112.
(90) Grimme, S.; Antony, J.; Ehrlich, S.; Krieg, H. A Consistent and Accurate Ab Initio Parametrization of Density Functional Dispersion Correction (DFT-D) for the 94 Elements H-Pu. *J. Chem. Phys.* **2010**, *132*, 154104. https://doi.org/10.1063/1.3382344.
(91) Grimme, S. Semiempirical GGA-Type Density Functional Constructed with a Long-Range Dispersion Correction. *J. Comput. Chem.* **2006**, *27* (15), 1787–1799. https://doi.org/10.1002/jcc.20495.
(92) Tkatchenko, A.; Scheffler, M. Accurate Molecular Van Der Waals Interactions from Ground-State Electron Density and Free-Atom Reference Data. *Phys. Rev. Lett.* **2009**, *102*, 073005. https://doi.org/10.1103/PhysRevLett.102.073005.

(93) Kresse, G.; Furthmüller, J. Efficient Iterative Schemes for Ab Initio Total-Energy Calculations Using a Plane-Wave Basis Set. *Phys. Rev. B* **1996**, *54* (16), 169–186.
(94) Blöchl, P. E. Projector Augmented-Wave Method. *Phys. Rev. B* **1994**, *50* (24), 17953–17979.
(95) Kresse, G.; Joubert, D. From Ultrasoft Pseudopotentials to the Projector Augmented-Wave Method. *Phys. Rev. B* **1999**, *59* (3), 1758–1775.
(96) Monkhorst, H. J.; Pack, J. D. Special Points for Brillouin-Zone Integrations. *Phys. Rev. B* **1976**, *13* (12), 5188–5192.
(97) Fushiki, T. Estimation of Prediction Error by Using K-Fold Cross-Validation. *Stat. Comput.* **2011**, *21* (2), 137–146. https://doi.org/10.1007/s11222-009-9153-8.
(98) Hoerl, A. E.; Kennard, R. W. Ridge Regression: Biased Estimation for Nonorthogonal Problems. *Technometrics* **1970**, *12* (1), 55–67. https://doi.org/10.1080/00401706.1970.10488634.
(99) Hastie, T.; Tibshirani, R.; Friedman, J. *The Elements of Statistical Learning: Data Mining, Inference, and Prediction*, 2nd ed.; Springer, 2009. https://doi.org/10.1007/978-0-387-84858-7.
(100) Drucker, H.; Burges, C. J. C.; Kaufman, L.; Smola, A.; Vapnik, V. Support Vector Regression Machines. In *Advances in Neural Information Processing Systems*; 1996; pp 155–161.
(101) Breiman, L. Random Forests. *Mach. Learn.* **2001**, *45*, 5–32. https://doi.org/10.3390/rs10060911.
(102) Geurts, P.; Ernst, D.; Wehenkel, L. Extremely Randomized Trees. *Mach. Learn.* **2006**, *63* (1), 3–42. https://doi.org/10.1007/s10994-006-6226-1.
(103) Hellenbrandt, M. The Inorganic Crystal Structure Database (ICSD) - Present and Future. *Crystallogr. Rev.* **2004**, *10* (1), 17–22. https://doi.org/10.1080/08893110410001664882.
(104) Pathak, A. D.; Nedea, S.; Zondag, H.; Rindt, C.; Smeulders, D. A DFT-Based Comparative Equilibrium Study of Thermal Dehydration and Hydrolysis of CaCl2 Hydrates and MgCl2 Hydrates for Seasonal Heat Storage. *Phys. Chem. Chem. Phys.* **2016**, *18*, 10059–10069. https://doi.org/10.1039/C6CP00926C.
(105) Pathak, A. D.; Nedea, S.; Duin, A. C. T. Van; Zondag, H.; Rindt, C.; Smeulders, D. Reactive Force Field Development for Magnesium Chloride Hydrates and Its Application for Seasonal Heat Storage. *Phys. Chem. Chem. Phys.* **2016**, *18*, 15838–15847. https://doi.org/10.1039/C6CP02762H.
(106) Yan, J.; Zhao, C. Y. First-Principle Study of CaO/Ca(OH)2 Thermochemical Energy Storage System by Li or Mg Cation Doping. *Chem. Eng. Sci.* **2014**, *117*, 293–300. https://doi.org/10.1016/j.ces.2014.07.007.
(107) Madelung, O.; Rssler, U.; Schulz, M. The Landolt-Börnstein Database. Springer Materials: Heidelberg 2017.
(108) Kirkpatrick, S.; Gelatt Jr., C. D.; Vecchi, M. P. Optimization by Simulated Annealing. *Science (80-.).* **1983**, *220* (4598), 671–680.
(109) Materials Studio 8.0. Dassault Systèmes BIOVA: San Diego 2014.
(110) Rappe, A. K.; Casewit, C. J.; Colwell, K. S.; Goddard, W. A.; Skiff, W. M. UFF, a Full Periodic Table Force Field for Molecular Mechanics and Molecular Dynamics Simulations. *J. Am. Chem. Soc.* **1992**, *114* (25), 10024–10035. https://doi.org/10.1021/ja00051a040.
(111) Fischer, M. Structure and Bonding of Water Molecules in Zeolite Hosts: Benchmarking Plane-Wave DFT against Crystal Structure Data. *J. Crystallogr.* **2015**, *230* (5), 325–336.

https://doi.org/10.1515/zkri-2014-1809.
(112) Kato, Y.; Yamashita, N.; Kobayashi, K.; Yoshio, Y. Kinetic Study of the Hydration of Magnesium Oxide for a Chemical Heat Pump. *Appl. Therm. Eng.* **1996**, *16* (11), 853–862. https://doi.org/10.1016/1359-4311(96)00009-9.
(113) Sugimoto, K.; Dinnebier, R. E.; Hanson, J. C. Structures of Three Dehydration Products of Bischofite from in Situ Synchrotron Powder Diffraction Data (MgCl2•nH2O; n = 1, 2, 4). *Acta. Cryst.* **2007**, *B63*, 235–242. https://doi.org/10.1107/S0108768107002558.
(114) Partin, D. E.; O'Keeffe, M. The Structures and Crystal Chemistry of Magnesium Chloride and Cadmium Chloride. *J. Solid State Chem.* **1991**, *95*, 176–183.
(115) Černý, R.; Valvoda, V.; Chládek, M. Empirical Texture Corrections for Asymmetric Diffraction and Inclined Textures. *J. Appl. Crystallogr.* **1995**, *28*, 247–253. https://doi.org/10.1107/S002188989400960X.
(116) Hazen, R. M. Effects of Temperature and Pressure on the Cell Dimension and X-Ray Temperature Factors of Periclase. *Am. Mineral.* **1976**, *61*, 266–271.
(117) Chase Jr., M. W.; Davies, C. A.; Downey Jr., J. R.; Frurip, D. J.; McDonald, R. A.; Syverud, A. N. *NIST-JANAF Thermochemical Tables*; Gaithersburg, MD, 1985.
(118) Cerqueira, T. F. T.; Pailhès, S.; Debord, R.; Giordano, V. M.; Viennois, R.; Shi, J.; Botti, S.; Marques, M. A. L. Prediction and Synthesis of a Non-Zintl Silicon Clathrate. *Chem. Mater.* **2016**, *28*, 3711–3717. https://doi.org/10.1021/acs.chemmater.6b00392.
(119) Gautier, R.; Zhang, X.; Hu, L.; Yu, L.; Lin, Y.; Sunde, T. O. L.; Chon, D.; Poeppelmeier, K. R.; Zunger, A. Prediction and Accelerated Laboratory Discovery of Previously Unknown 18-Electron ABX Compounds. *Nat. Chem.* **2015**, *7*, 308–316. https://doi.org/10.1038/nchem.2207.
(120) Hautier, G.; Jain, A.; Ong, S. P.; Kang, B.; Moore, C.; Doe, R.; Ceder, G. Phosphates as Lithium-Ion Battery Cathodes: An Evaluation Based on High-Throughput Ab Initio Calculations. *Chem. Mater.* **2011**, *23*, 3495–3508.
(121) Schmidt, J.; Shi, J.; Borlido, P.; Chen, L.; Botti, S.; Marques, M. A. L. Predicting the Thermodynamic Stability of Solids Combining Density Functional Theory and Machine Learning. *Chem. Mater.* **2017**, *29*, 5090–5103. https://doi.org/10.1021/acs.chemmater.7b00156.
(122) Armiento, R.; Kozinsky, B.; Hautier, G.; Fornari, M.; Ceder, G. High-Throughput Screening of Perovskite Alloys for Piezoelectric Performance and Thermodynamic Stability. *Phys. Rev. B* **2014**, *89*, 134103. https://doi.org/10.1103/PhysRevB.89.134103.
(123) U.S. Geological Survey. *Metal Prices in the United States Through 2010*; Reston, Virginia, 2013.
(124) Mckinney, W. Data Structures for Statistical Computing in Python. In *Proceedings of the 9th Python in Science Conference*; van der Walt, S., Millman, J., Eds.; 2010; pp 51–56.
(125) Wolverton, C.; Siegel, D. J.; Akbarzadeh, A. R.; Ozoliņš, V. Discovery of Novel Hydrogen Storage Materials: An Atomic Scale Computational Approach. *J. Phys. Condens. Matter* **2008**, *20* (6), 064228. https://doi.org/10.1088/0953-8984/20/6/064228.
(126) Jenkins, H. D. B.; Ponikvar-Svet, M.; Liebman, J. F. Relative Packing Efficiencies in Hydrates. *J. Chem. Eng. Data* **2009**, *54*, 2722–2728.
(127) Ahmed, A.; Liu, Y.; Purewal, J.; Tran, L. D.; Veenstra, M.; Wong-Foy, A.; Matzger, A.; Siegel, D. Balancing Gravimetric and Volumetric Hydrogen Density in MOFs. *Energy Environ. Sci.* **2017**, *10*, 2459–2471. https://doi.org/10.1039/C7EE02477K.
(128) Goldsmith, J.; Wong-Foy, A. G.; Cafarella, M. J.; Siegel, D. J. Theoretical Limits of

Hydrogen Storage in Metal–Organic Frameworks: Opportunities and Trade-Offs. *Chem. Mater.* **2013**, *25* (16), 3373–3382. https://doi.org/10.1021/cm401978e.
(129) Panella, B.; Hirscher, M.; Roth, S. Hydrogen Adsorption in Different Carbon Nanostructures. *Carbon N. Y.* **2005**, *43* (10), 2209–2214. https://doi.org/10.1016/j.carbon.2005.03.037.
(130) Fajans, K.; Joos, G. Molefraction of Ions and Molecules in the Light of Atomic Structure. *J. Phys.* **1924**, *23*, 1–46. https://doi.org/10.1007/BF01327574.
(131) Fajans, K. Deformation of Ions and Molecules Based on Refractometric Data. *J. Electrochem.* **1928**, *34*, 502–520.
(132) Ceder, G. Opportunities and Challenges for First-Principles Materials Design and Applications to Li Battery Materials. *MRS Bull.* **2010**, *35* (9), 693–701. https://doi.org/10.1557/mrs2010.681.
(133) Ahmed, A.; Siegel, D. J. Predicting Hydrogen Storage in MOFs via Machine Learning. *Patterns* **2021**, *2* (7), 100291. https://doi.org/10.1016/j.patter.2021.100291.
(134) Lodziana, Z.; Vegge, T. Structural Stability of Complex Hydrides: LiBH4 Revisited. *Phys. Rev. Lett.* **2004**, *93* (14), 145501. https://doi.org/10.1103/PhysRevLett.93.145501.
(135) Kim, K.; Siegel, D. J. Correlating Lattice Distortions, Ion Migration Barriers, and Stability in Solid Electrolytes. *J. Mater. Chem. A* **2019**, *7* (7), 3216–3227. https://doi.org/10.1039/C8TA10989C.
(136) Koh, H. S.; Rana, M. K.; Hwang, J.; Siegel, D. J. Thermodynamic Screening of Metal-Substituted MOFs for Carbon Capture. *Phys. Chem. Chem. Phys.* **2013**, *15*, 4573–4581. https://doi.org/10.1039/c3cp50622c.
(137) Rana, M. K.; Koh, H. S.; Zuberi, H.; Siegel, D. J. Methane Storage in Metal-Substituted Metal-Organic Frameworks: Thermodynamics, Usable Capacity, and the Impact of Enhanced Binding Sites. *J. Phys. Chem. C* **2014**, *118*, 2929–2942. https://doi.org/10.1021/jp4104273.
(138) De Jong, A.-J.; Van Vliet, L.; Hoegaerts, C.; Roelands, M.; Cuypers, R. Thermochemical Heat Storage - From Reaction Storage Density to System Storage Density. *Energy Procedia* **2016**, *91*, 128–137. https://doi.org/10.1016/j.egypro.2016.06.187.
(139) De Jong, A.-J.; Trausel, F.; Finck, C.; Van Vliet, L.; Cuypers, R. Thermochemical Heat Storage - System Design Issues. *Energy Procedia* **2014**, *48*, 309–319. https://doi.org/10.1016/j.egypro.2014.02.036.
(140) Nemtzow, D.; Sawyer, K.; Mumme, S.; James, N. Novel Materials in Thermal Energy Storage for Buildings. *Thermal Energy Storage Webinar Series*. U.S. Department of Energy Office of Energy Efficiency & Renewable Energy 2020.
(141) Kebede, G.; Mitev, P. D.; Broqvist, P.; Eriksson, A.; Hermansson, K. Fifty Shades of Water: Benchmarking DFT Functionals against Experimental Data for Ionic Crystalline Hydrates. *J. Chem. Theory Comput.* **2019**, *15*, 584–594. https://doi.org/10.1021/acs.jctc.8b00423.
(142) Ong, S. P.; Richards, W. D.; Jain, A.; Hautier, G.; Kocher, M.; Cholia, S.; Gunter, D.; Chevrier, V. L.; Persson, K. A.; Ceder, G. Python Materials Genomics (Pymatgen): A Robust, Open-Source Python Library for Materials Analysis. *Comput. Mater. Sci.* **2013**, *68*, 314–319.
(143) Jain, A.; Ong, S. P.; Hautier, G.; Chen, W.; Richards, W. D.; Dacek, S.; Cholia, S.; Gunter, D.; Skinner, D.; Ceder, G.; Persson, K. A. Commentary: The Materials Project: A Materials Genome Approach to Accelerating Materials Innovation. *APL Mater.* **2013**, *1*, 011002. https://doi.org/10.1063/1.4812323.

(144) Hummelshøj, J. S.; Blomqvist, J.; Datta, S.; Vegge, T.; Rossmeisl, J.; Thygesen, K. S.; Luntz, A. C.; Jacobsen, K. W.; Nørskov, J. K. Communications: Elementary Oxygen Electrode Reactions in the Aprotic Li-Air Battery. *J. Chem. Phys.* **2010**, *132* (7), 071101. https://doi.org/10.1063/1.3298994.
(145) National Institute of Standards and Technology. *NIST Chemistry WebBook, NIST Standard Reference Database Number 69*; Linstrom, P. J., Mallard, W. G., Eds.; Gaithersburg MD. https://doi.org/10.18434/T4D303.
(146) Mathworks Inc. Matlab Statistics and Machine Learning Toolbox https://www.mathworks.com/help/stats/ (accessed Oct 10, 2019).
(147) Ward, L.; Dunn, A.; Faghaninia, A.; Zimmermann, N. E. R.; Bajaj, S.; Wang, Q.; Montoya, J.; Chen, J.; Bystrom, K.; Dylla, M.; Chard, K.; Asta, M.; Persson, K. A.; Snyder, G. J.; Foster, I.; Jain, A. Matminer: An Open Source Toolkit for Materials Data Mining. *Comput. Mater. Sci.* **2018**, *152*, 60–69. https://doi.org/10.1016/j.commatsci.2018.05.018.
(148) Wolfram Research Inc. Mathematica. Champaign, IL 2016.
(149) Shannon, R. D. Revised Effective Ionic Radii and Systematic Studies of Interatomic Distances in Halides and Chalcogenides. *Acta. Cryst.* **1976**, *32*, 751–767.
(150) Dudev, M.; Wang, J.; Dudev, T.; Lim, C. Factors Governing the Metal Coordination Number in Metal Complexes from Cambridge Structural Database Analyses. *J. Phys. Chem. B* **2006**, *110*, 1889–1895. https://doi.org/10.1021/jp054975n.
(151) Wold, S.; Esbensen, K.; Geladi, P. Principal Component Analysis. *Chemom. Intell. Lab. Syst.* **1987**, *2*, 37–52. https://doi.org/10.1007/SpringerReference_205537.
(152) Kramer, O. *Genetic Algorithm Essentials*; Kacprzyk, J., Ed.; Springer Nature, 2017.
(153) Chipperfield, A. J.; Fleming, P. J.; Pohlheim, H.; Fonseca, C. M. A Genetic Algorithm Toolbox for Matlab. In *Tenth International Conference on Systems Engineering*; Coventry, UK, 1994; pp 200–207.
(154) Ayodeji, A.; Liu, Y. SVR Optimization with Soft Computing Algorithms for Incipient SGTR Diagnosis. *Ann. Nucl. Energy* **2018**, *121*, 89–100. https://doi.org/10.1016/j.anucene.2018.07.011.
(155) Ghareb, A. S.; Bakar, A. A.; Hamdan, A. R. Hybrid Feature Selection Based on Enhanced Genetic Algorithm for Text Categorization. *Expert Syst. Appl.* **2016**, *49*, 31–47. https://doi.org/10.1016/j.eswa.2015.12.004.
(156) Wang, A.; Kingsbury, R.; McDermott, M.; Horton, M.; Jain, A.; Ong, S. P.; Dwaraknath, S.; Persson, K. A. A Framework for Quantifying Uncertainty in DFT Energy Corrections. *Sci. Rep.* **2021**, *11*, 15496. https://doi.org/10.1038/s41598-021-94550-5.
(157) Hagen, M.; Hanselmann, D.; Ahlbrecht, K.; Maça, R.; Gerber, D.; Tübke, J. Lithium-Sulfur Cells: The Gap between the State-of-the-Art and the Requirements for High Energy Battery Cells. *Adv. Energy Mater.* **2015**, *5*, 1401986. https://doi.org/10.1002/aenm.201401986.
(158) Jaziri, N.; Boughamoura, A.; Müller, J.; Mezghani, B.; Tounsi, F.; Ismail, M. A Comprehensive Review of Thermoelectric Generators: Technologies and Common Applications. *Energy Reports* **2020**, *6*, 264–287. https://doi.org/10.1016/j.egyr.2019.12.011.
(159) Enescu, D. Thermoelectric Energy Harvesting: Basic Principles and Applications. In *Green Energy Advances*; Enescu, D., Ed.; 2019; pp 1–37. https://doi.org/10.5772/intechopen.77501.
(160) Togo, A.; Tanaka, I. First Principles Phonon Calculations in Materials Science. *Scr. Mater.* **2015**, *108*, 1–5. https://doi.org/10.1016/j.scriptamat.2015.07.021.

(161) Togo, A.; Chaput, L.; Tanaka, I.; Hug, G. First-Principles Phonon Calculations of Thermal Expansion in Ti3SiC2, Ti3AlC2, and Ti3GeC2. *Phys. Rev. B - Condens. Matter Mater. Phys.* **2010**, *81*, 174301. https://doi.org/10.1103/PhysRevB.81.174301.
(162) Parlinski, K.; Li, Z. Q.; Kawazoe, Y. First-Principles Determination of the Soft Mode in Cubic ZrO2. *Phys. Rev. Lett.* **1997**, *78* (21), 4063–4066. https://doi.org/10.1103/PhysRevLett.78.4063.
(163) Wagner, W.; Pruß, A. The IAPWS Formulation 1995 for the Thermodynamic Properties of Ordinary Water Substance for General and Scientific Use. *J. Phys. Chem. Ref. Data* **2002**, *31* (2), 387–535. https://doi.org/10.1063/1.1461829.
(164) Albertus, P.; Babinec, S.; Litzelman, S.; Newman, A. Status and Challenges in Enabling the Lithium Metal Electrode for High-Energy and Low-Cost Rechargeable Batteries. *Nat. Energy* **2018**, *3*, 16–21. https://doi.org/10.1038/s41560-017-0047-2.
(165) Chen, C.; Ye, W.; Zuo, Y.; Zheng, C.; Ong, S. P. Graph Networks as a Universal Machine Learning Framework for Molecules and Crystals. *Chem. Mater.* **2019**, *31* (9), 3564–3572. https://doi.org/10.1021/acs.chemmater.9b01294.
(166) Ward, L.; Liu, R.; Krishna, A.; Hegde, V. I.; Agrawal, A.; Choudhary, A.; Wolverton, C. Including Crystal Structure Attributes in Machine Learning Models of Formation Energies via Voronoi Tessellations. *Phys. Rev. B* **2017**, *96*, 024104. https://doi.org/10.1103/PhysRevB.96.024104.
(167) Lam Pham, T.; Kino, H.; Terakura, K.; Miyake, T.; Tsuda, K.; Takigawa, I.; Chi Dam, H. Machine Learning Reveals Orbital Interaction in Materials. *Sci. Technol. Adv. Mater.* **2017**, *18* (1), 756–765. https://doi.org/10.1080/14686996.2017.1378060.
(168) Behler, J. Atom-Centered Symmetry Functions for Constructing High-Dimensional Neural Network Potentials. *J. Chem. Phys.* **2011**, *134*, 074106. https://doi.org/10.1063/1.3553717.
(169) Khorshidi, A.; Peterson, A. A. Amp: A Modular Approach to Machine Learning in Atomistic Simulations. *Comput. Phys. Commun.* **2016**, *207*, 310–324. https://doi.org/10.1016/j.cpc.2016.05.010.
(170) Ward, L.; Agrawal, A.; Choudhary, A.; Wolverton, C. A General-Purpose Machine Learning Framework for Predicting Properties of Inorganic Materials. *npj Comput. Mater.* **2016**, *2* (1), 16028. https://doi.org/10.1038/npjcompumats.2016.28.
(171) Weston, L.; Tshitoyan, V.; Dagdelen, J.; Kononova, O.; Trewartha, A.; Persson, K. A.; Ceder, G.; Jain, A. Named Entity Recognition and Normalization Applied to Large-Scale Information Extraction from the Materials Science Literature. *J. Chem. Inf. Model.* **2019**, *59* (9), 3692–3702. https://doi.org/10.1021/acs.jcim.9b00470.
(172) Hansen, K.; Biegler, F.; Ramakrishnan, R.; Pronobis, W.; Von Lilienfeld, O. A.; Müller, K.-R.; Tkatchenko, A. Machine Learning Predictions of Molecular Properties: Accurate Many-Body Potentials and Nonlocality in Chemical Space. *J. Phys. Chem. Lett.* **2015**, *6* (12), 2326–2331. https://doi.org/10.1021/acs.jpclett.5b00831.
(173) Umehara, M.; Stein, H. S.; Guevarra, D.; Newhouse, P. F.; Boyd, D. A.; Gregoire, J. M. Analyzing Machine Learning Models to Accelerate Generation of Fundamental Materials Insights. *npj Comput. Mater.* **2019**, *5* (34), 1–9. https://doi.org/10.1038/s41524-019-0172-5.
(174) Friedman, J. H. Greedy Function Approximation: A Gradient Boosting Machine. *Ann. Stat.* **2001**, *29* (5), 1189–1232.
(175) De Jong, M.; Chen, W.; Notestine, R.; Persson, K.; Ceder, G.; Jain, A.; Asta, M.; Gamst, A. A Statistical Learning Framework for Materials Science: Application to Elastic Moduli

of k-Nary Inorganic Polycrystalline Compounds. *Sci. Rep.* **2016**, *6* (34256), 1–11. https://doi.org/10.1038/srep34256.
(176) Isayev, O.; Oses, C.; Toher, C.; Gossett, E.; Curtarolo, S.; Tropsha, A. Universal Fragment Descriptors for Predicting Properties of Inorganic Crystals. *Nat. Commun.* **2017**, *8* (15679), 1–12. https://doi.org/10.1038/ncomms15679.
(177) Ferchaud, C. J.; Scherpenborg, R. a. a.; Zondag, H. a.; de Boer, R. Thermochemical Seasonal Solar Heat Storage in Salt Hydrates for Residential Applications – Influence of the Water Vapor Pressure on the Desorption Kinetics of MgSO4.7H2O. *Energy Procedia* **2014**, *57*, 2436–2440. https://doi.org/10.1016/j.egypro.2014.10.252.
(178) Sögütoglu, L.-C.; Birkelbach, F.; Werner, A.; Fischer, H.; Huinink, H.; Adan, O. Hydration of Salts as a Two-Step Process: Water Adsorption and Hydrate Formation. *Thermochim. Acta* **2021**, *695*, 178819. https://doi.org/10.1016/j.tca.2020.178819.
(179) Pedregosa, F.; Varoquaux, G.; Gramfort, A.; Michel, V.; Thirion, B.; Grisel, O.; Blondel, M.; Prettenhofer, P.; Weiss, R.; Dubourg, V.; Vanderplas, J.; Passos, A.; Cournapeau, D.; Brucher, M.; Perrot, M.; Duchesnay, É. Scikit-Learn: Machine Learning in Python. *J. Mach. Learn. Res.* **2011**, *12*, 2825–2830.
(180) Ward, L.; Agrawal, A.; Choudhary, A.; Wolverton, C. A General-Purpose Machine Learning Framework for Predicting Properties of Inorganic Materials. *npj Comput. Mater.* **2016**, *2*, 16028. https://doi.org/10.1038/npjcompumats.2016.28.
(181) Choudhary, K.; DeCost, B.; Tavazza, F. Machine Learning with Force-Field-Inspired Descriptors for Materials: Fast Screening and Mapping Energy Landscape. *Phys. Rev. Mater.* **2018**, *2* (8), 083801. https://doi.org/10.1103/PhysRevMaterials.2.083801.
(182) Rammelberg, H. U.; Osterland, T.; Priehs, B.; Opel, O.; Ruck, W. K. L. Thermochemical Heat Storage Materials – Performance of Mixed Salt Hydrates. *Sol. Energy* **2016**, *136*, 571–589. https://doi.org/10.1016/j.solener.2016.07.016.
(183) Rehman, A. U.; Khan, M.; Maosheng, Z. Hydration Behavior of MgSO4–ZnSO4 Composites for Long-Term Thermochemical Heat Storage Application. *J. Energy Storage* **2019**, *26*, 101026. https://doi.org/10.1016/j.est.2019.101026.
(184) Li, W.; Zeng, M.; Wang, Q. Development and Performance Investigation of MgSO4/SrCl2 Composite Salt Hydrate for Mid-Low Temperature Thermochemical Heat Storage. *Sol. Energy Mater. Sol. Cells* **2020**, *210*, 110509. https://doi.org/10.1016/j.solmat.2020.110509.
(185) Heijmans, K.; Tranca, I. C.; Gaastra-Nedea, S. V.; Smeulders, D. M. J. Exploring the Electronic Structure of New Doped Salt Hydrates, Mg1- XCa XCl2· NH2O, for Thermochemical Energy Storage. *J. Phys. Chem. C* **2020**, *124* (45), 24580–24591. https://doi.org/10.1021/acs.jpcc.0c05799.
(186) Galwey, A. K.; Laverty, G. M. The Thermal Decomposition of Magnesium Chloride Dihydrate. *Thermochim. Acta* **1989**, *138*, 115–127. https://doi.org/10.1016/0040-6031(89)87246-6.
(187) Huinink, H. P.; Sansotta, S.; Zahn, D. Defect-Driven Water Migration in MgCl2 Tetra- and Hexahydrates. *J. Solid State Chem.* **2019**, *277*, 221–228. https://doi.org/10.1016/j.jssc.2019.06.010.
(188) Sutton, R.; Jewell, E.; Searle, J.; Elvins, J. Discharge Performance of Blended Salt in Matrix Materials for Low Enthalpy Thermochemical Storage. *Appl. Therm. Eng.* **2018**, *145*, 483–493. https://doi.org/10.1016/j.applthermaleng.2018.09.052.
(189) Settles, B. *Active Learning Literature Survey*; Madison, Wisconsin, 2009. https://doi.org/10.1.1.167.4245.

(190) Zhang, H.; Iype, E.; Nedea, S. V.; Rindt, C. C. M. Molecular Dynamics Study on Thermal Dehydration Process of Epsomite (MgSO4·7H2O). *Mol. Simul.* **2014**, *40* (14), 1157–1166. https://doi.org/10.1080/08927022.2013.854891.
(191) Iype, E.; Ahmed Khalfay, Z. S.; Ghosh Chaudhuri, R.; Prakash Kumar, B. G. Epsomite Dehydration: A Molecular Dynamics Study. *J. Energy Storage* **2018**, *20*, 337–343. https://doi.org/10.1016/j.est.2018.10.005.
(192) Kresse, G.; Hafner, J. Ab Initio Molecular Dynamics for Liquid Metals. *Phys. Rev. B* **1993**, *47* (1), 558–561. https://doi.org/10.1103/PhysRevB.47.558.
(193) Henkelman, G.; Uberuaga, B. P.; Jónsson, H. A Climbing Image Nudged Elastic Band Method for Finding Saddle Points and Minimum Energy Paths. *J. Chem. Phys.* **2000**, *113* (22), 9901–9904. https://doi.org/10.1063/1.1329672.
(194) Sögütoglu, L.-C.; Steiger, M.; Houben, J.; Biemans, D.; Fischer, H. R.; Donkers, P.; Huinink, H.; Adan, O. C. G. Understanding the Hydration Process of Salts: The Impact of a Nucleation Barrier. *Cryst. Growth Des.* **2019**, *19* (4), 2279–2288. https://doi.org/10.1021/acs.cgd.8b01908.
(195) Willems, T. F.; Rycroft, C. H.; Kazi, M.; Meza, J. C.; Haranczyk, M. Algorithms and Tools for High-Throughput Geometry-Based Analysis of Crystalline Porous Materials. *Microporous Mesoporous Mater.* **2012**, *149* (1), 134–141. https://doi.org/10.1016/j.micromeso.2011.08.020.
(196) Martin, R. L.; Smit, B.; Haranczyk, M. Addressing Challenges of Identifying Geometrically Diverse Sets of Crystalline Porous Materials. *J. Chem. Inf. Model.* **2012**, *52*, 308–318.
(197) Pinheiro, M.; Martin, R. L.; Rycroft, C. H.; Jones, A.; Iglesia, E.; Haranczyk, M. Characterization and Comparison of Pore Landscapes in Crystalline Porous Materials. *J. Mol. Graph. Model.* **2013**, *44*, 208–219.
(198) Grainger https://www.grainger.com/product/BEACON-MORRIS-Steam-Hydronic-Heater-Element-5E305?ef_id=EAIaIQobChMIvdidhuGB6wIVisDACh1PewqFEAAYASAAEgLaIfD_BwE:G:s&s_kwcid=AL!2966!3!431945874416!b!!g.
(199) Guanyu Tube https://tubingchina.com/Corrugated-Seamless-Stainless-Steel-Pipe-Tube.htm.
(200) Solé, A.; Miró, L.; Barreneche, C.; Martorell, I.; Cabeza, L. F. Corrosion of Metals and Salt Hydrates Used for Thermochemical Energy Storage. *Renew. Energy* **2015**, *75*, 519–523. https://doi.org/10.1016/j.renene.2014.09.059.